

City Research Online

City St George's, University of London

Citation: Driels, M. R. (1973). 'Valve stroking' with separated flow. (Unpublished Doctoral thesis, The City University)

This is the accepted version of the paper.

This version of the publication may differ from the final published version. To cite this item please consult the publisher's version.

Permanent repository link: https://openaccess.city.ac.uk/id/eprint/38351/

Copyright and Reuse: Copyright and Moral Rights remain with the author(s) and/or copyright holders. Copies of full items can be used for personal research or study, educational, or not-for-profit purposes without prior permission or charge, unless otherwise indicated, provided that the authors, title and full bibliographic details are credited, a hyperlink and/or URL is given for the original metadata page and the content is not changed in any way. For full details of reuse please refer to City Research Online policy.

City Research Online: http://openaccess.city.ac.uk/ publications@citystgeorges.ac.uk

T5 07144

'VALVE STROKING' WITH SEPARATED FLOW

by Morris Robert Driels

A thesis submitted for the Degree of Doctor of Philosophy

THE CITY UNIVERSITY LIBRARY,
ST. JOHN STREET, LONDON, E.C.1.

Department of Mechanical Engineering
The City University, London.

September 1973.

Summary.

The phenomenon of column separation downstream of a closing valve in an aviation kerosene pipeline was investigated both theoretically and experimentally. The experimental work involved the recording of pressure transients immediately downstream of the valve, during and after the valve is closed by a pneumatic actuator moving with a constant speed. The results were compared with the output of a computer program, PTP1, which involved the method of characteristics for the numerical analysis of the governing differential equations. The boundary condition at the valve-end of the pipeline was determined using the steady state and transient processes associated with air release from a liquid.

Once the model was working correctly, it was used in an investigation of valve stroking techniques (Ref. 80) applied to separated flow. It was found that conventional methods were impracticable in such cases and as a result, alternative proceedures for minimising the magnitude of pressure fluctuations were postulated. All of these methods involved controlling the pressure just downstream of the closing valve and it was assumed at this stage that the required pressure-time history at this location could be achieved. To fulfil this function, a closed loop servo system seemed the obvious choice and an initial attempt with a mechanical/pneumatic system was made. This did not have the necessary performance and the final design was an electrohydraulic servo system utilising pressure feedback. The components of the servo system were simulated both in linear and non-linear modes and this enabled

a program VSP2 to be written which was able to predict the degree of success of the proposed methods of valve-stroking.

The servo system was constructed and used to operate the valve in accordance with the criteria proposed in the valve-stroking methods, allowing a comparison with program VSP2 to be made. Only one of the two proposed methods was investigated experimentally and in this case a reduction of 40% of the total pressure fluction about the steady state pressure was easily achieved for all the flow cases tested. For the other method, reductions of the order of 90% were predicted although the method appeared to be sensitive to parameter changes. It was concluded that the former method would be useful for almost any flow situation while the latter would find use in systems where the initial flow conditions were well defined and preferably invariant.

Acknowledgment.

The author wishes to record his thanks to all the members of The City University staff who have given support and advice throughout the project, and to the University Senate for the provision of a studentship grant.

In particular, the assistance of the following staff members was most valuable: [redacted] Department of Mechanical Engineering; [redacted], Department of Systems and Automation; [redacted], Department of Mathematics; [redacted], Mechanical Engineering Workshop and all the staff of the City University Computer Unit.

Finally, for permission to reproduce various figures and diagrams, the author wishes to thank: [redacted] of Dowty Servos Ltd., (figs 90 & 91), [redacted] of Rolls Royce (1971) Ltd., (fig 22) and [redacted] of The Polytechnic of the South Bank (fig 19).

List of Contents.

Summary.

Acknowledgment.

Contents.

Summary of computer programs developed.

List of Figures and Tables.

Nomenclature.

1. Introduction. 20

2. Literature Survey. 22

2.1. Early Work.

2.2. Modelling Techniques.

2.3. Air Release and Column Separation.

2.4. Controlled Valve Closure - theoretical and experimental.

PART 1

3. Development of Equations of Motion. 48

3.1. Equation of continuity.

3.2. Equation of momentum conservation.

3.3. Approximate forms of equations of motion-wave analysis.

3.4. Conversion from partial to total differential equations.

3.5. Finite difference approximations and characteristics.

4. Mechanism of Air Release. 78

4.1. Use of Henry's Law.

5. Boundary conditions at downstream valve face. 84

5.1. With air release.

5.2. No air release.

6. Mathematical Modelling. 97

6.1. Program philosophy and development.

6.2. Description of Master Segment.

6.2.1. Standard print out format.

6.2.2. Subroutine VALVE.

6.2.3. Subroutine ANGLE.

6.2.4. Subroutine CHAR.

6.2.5. Subroutine CHANGE.

6.3. Program PTP3 - Subroutine VALVE.

6.4. Numerical stability of method of solution.

6.4.1. Mimmisation of run time.

7. Description of Test Rig. 110

7.1. Preliminary experimental work.

7.2. Use of manometers on the test rig.

7.3. Pressure - flow characteristics of valves for steady state condition.

7.4. Determination of the $\Psi - \theta$ characteristics of the spherical ball valves.

7.5. Determination of acoustic speed.

7.6. Measurement and observation of pressure transients.

8. Discussion and Conclusions of Part 1. 133

PART 2.

9. Introduction to valve stroking. 138

9.1. Valve stroking without either friction or separation.

9.2. Valve stroking with friction but no separation.

9.3. Parameter limitations for high friction systems.

9.4. Time criterion and linear closure.

10. Valve stroking with cavity formation. 152

11. The nature of pressure transients for approximate analysis. 157

12. Alternative methods of valve stroking - Proposed method No.1. 159

13. Proposed method No.2. 163

14. Proposed method No.3. 169

PART 3.

15. Valve actuator design Philosophy. 172

16. Initial servo design. 179

16.1. Design of pneumatic servo system.

16.2. Testing and evaluation of pneumatic servo.

17. Block diagram notation (using Laplace transformations) 188

18. Modified servo design. 192

18.1. Electrohydraulic servo system.

18.2. Electrohydraulic servo valve.

18.3. Transducer and feedback amplifier.

18.4. Hydraulic actuator.

18.5. Signal generator and servo amplifier.

19. Dynamic analysis. 207

19.1. Analysis of linear system components.

19.2. Simulation of servo components.

20. Development of valve stroking program VSP2. 213

20.1. Master segment of VSP2.

20.2. Subroutine VALVE.

20.3. Subroutine GEN.

20.4. Subroutine INTSTP.

20.5. Subroutine DIFEQN.

20.6. Subroutine LOOKUP.

21. Design and construction of hydraulic system. 224

21.1. Hydraulic power source.

21.2. Hydraulic power regulation.

21.3. Transient flow requirements.

21.4. Filtration and cooling.

21.5. Working pressure and pipe sizes.

21.6. Choice of hydraulic actuator.

21.7. Overall system configuration.

PART 4.

22.1. Theoretical investigations with Program VSP2. 233

22.1.1. Performance variation for variable servo parameters.

22.1.2. Typical parameter plots from VSP2.

22.1.3. Gain setting and gain switching.

22.1.4. Determination of signal generator function.

22.1.5. Theoretical investigation of valve stroking method No. 3.

22.1.6. Theoretical investigation of valve stroking method No. 2.

22.1.7. Maximum valve performance limits - method 3.

22.1.8. Investigation into the effects of fluid inertia on the servo response.

22.2. Second stage experimental work and scope of results. 252

22.2.1. Operation of test rig.

22.2.2. Scope and presentation of results.

23. Summary of research. 258

23.1. Discussion of Results.

23.1.1. Discussion of part 1.

23.1.2. Discussion of part 2.

23.1.3. Discussion of part 3.

23.1.4. Discussion of part 4.

23.2. Conclusions.

23.3. Further work.

24. Biblography. 282

Figures and Tables. 289

Appendices.

1. Measurement of air release from kerosene.

2. Solution of Boundary condition equations.

2a While valve is closing.

2b Valve shut, air release continuing.

2c After air release ceases.

2d Cavity collapse while valve still closing.

2e Valve closing - no separated flow (PTP3)

3. Program PTP1 description and listing.

4a. Simulation of a first order feedback lag element.

4b. Program VSP3 description and listing.

5. Program PTP6 description and listing.

6. Program PTP7 description and listing.

7. Program VSP2 description and listing.

8. Derivation of the Bode diagram for a dynamic system.

9. The design construction and testing of a servo amplifier and signal generator.

Summary of Computer programs developed.

PTP1 Basic pressure transients program for prediction of unsteady flow with column separation and air release following linear valve closure.

PTP2 As PTP1 but producing a line printer graph of PP(2,1) against time in addition to the numerical output.

PTP3 As PTP1 but not simulating air release from kerosene. Instead, a vapour cavity is assured to exist should the pressure fall sufficiently.

PTP4 As PTP1, incorporating a facility for dividing the step size by five should the cavity volume change by more than 34% in one time step.

PTP5 As PTP1 but printing out only the time of occurance and magnitude of the first pressure peak. The program may also be run several times for different initial flow conditions. Since the program is very similar to PTP1, no listing is included.

PTP6 Pressure transients program which simulates the rigid column system shown in fig 60. Following valve closure, air release or absorbtion is neglected; the cavity containing a constant mass of gas.

PTP7 An algorithm to solve the differential equations developed in Section 13 for the implementation of valve stroking method No. 2.

VSP2 Principle valve stroking program which simulates the valve servo system components in addition to the unsteady nature of the flowing kerosene. Fig. 89 illustrates the components modelled in VSP2.

VSP3 A program to predict the overall valve closure time needed for the valve stroking criteria employed by Streeter (80), for given initial flow conditions.

PAGE A program which using any other program as data, lists it in any orientation on the line printer paper. This is used to obtain listing for photocopying and presentation purposes.

List of Figures and Tables.

Fig No.

1. Control volume used to derive the equation of continuity.
2. a. External forces acting on a system.
   b. Momentum transfer across control surfaces.
3. Rich's solution of the wave equation.
4. Wave interpretation of pressure transients following instantaneous valve closure.
5. Wave analysis of transients in a downstream pipe system.
6. Method of characteristics (geometric interpretation).
7. Alternative forms of the method of characteristics.
8. Method of characteristics applied to a downstream pipe system.
9. Variation of cavity parameters with time.
10. Exponential cavity growth during one time step.
11. Boundary condition at valve.
12. Comparison between isothermal and adiabatic cavity processes predicted by the computer model.
13. Steady state valve characteristics showing the data points used in array TANG.
14. Valve linkage geometry.
15. Numerical oscillation in iteration.
16. Overlapping ranges of two variables.
17. Schematic diagram of test rig.
18. Schematic diagram of full transient test facilities available.

19. External view of Saunders E60F16 fuel valve.

20. Sectioned view of Saunders E60F16 fuel valve.

21. External view of sleeve valve used for acoustic speed tests.

22. Sectioned " " " " " " " " "

23. View of downstream end of test rig showing mainly:

    a) Downstream reservoir and air charging apparatus.

    b) Pipework and return line pump.

24. View of upstream end of test rig showing mainly:

    a) Pipe bends, junctions and control valves.

    b) Reservoir air pressure equipment and pipe supports.

25. View of valve linkage, limit switches and transducer near valve.

26. Location of pressure transducer stations (14mm thread)

27. Drawing of fuel valve transition sections and transducer housing.

28. Venturi meter calibration curve.

29. Pressure drop - flow rate for plug valve (steady state).

30. Pressure drop - flow rate for disc (gate) valve (steady state).

31. Experimentally derived, steady state, ball valve characteristic.

32. View of oscilloscope, charge amplifier and demodulator.

33. Valve static head calibration curve.

34. Pressure changes along main pipeline (steady flow)

35. Typical results from acoustic wave speed tests.

36. Definition of time interval used to determine the acoustic speed.

37. Time ratio - No. of characteristic sections for program PTP1.

38. Kerr's derivation of 'Equivalent valve closure time'.

39. Linear displacement transducer and ancilliary equipment.

40. Valve linkage limit switch arrangement.

41. View of two axis travelling microscope arrangement.

42. Typical oscilloscope trace.

43. Trace illustrating the repeatability of experimental results.

44-51. Pressure-time traces for the first stage of experimental work.

52. Comparison of output from programs PTP1, PTP3 and experimental results.

53. Definition of valve stroking parameters.

54. Wave diagram used in graphical analysis of valve stroking.

55. Graphical analysis (P-V plane) of frictionless valve stroking.

56. Free-body diagram of incompressible column.

57. Results obtained from program VSP3.

58. Computer plot of P-V diagram for 'forced' valve stroking with column separation.

59. Cavity interface velocities to produce phase 3 of ideal valve stroking.

60. Assumed system for proposed valve stroking method No.1.

61. Comparison of mass oscillation and waterhammer effects.

62. Parameter transients for system of method No.1.

63. Desired P-V trajectory for method No.1.

64. Limitations on P-V trajectory for method No.1.

65. Assumed system for proposed valve stroking method No.2.

66. Desired P-V trajectory for method No. 2.

67. Pressure and velocity variation with time for method No. 2.

68. Integration path for equation 64.

69. Results obtained from program PTP7.

70. Reduction of basic feedback servo system.

71. Simple closed loop pressure control system.

72. Pneumatic/mechanical feedback control system.

73. Flapper valve geometry.

74. Static performance of flapper valve.

75. Block diagram of pneumatic/mechanical servo system.

76. Experimental characteristics of Munro metal bellows.

77. Amplification characteristics for a built-in beam.

78. Experimental characteristics of opposed flapper valves.

79. Two views of the pneumatic/mechanical servo system.

80-84. Results from pneumatic/mechanical servo frequency response tests.

85. Functions used to determine the total amplitude of clipped sine waves.

86. Open loop frequency response of pneumatic servo mechanism.

87. Mechanical suspension.

88. Response of mechanical suspension for variable damping factor.

89. Electro-hydraulic pressure control servo system.

90. Cut away view of Dowty servo valve.

91. Functional diagram of Dowty servo valve.

92. Servo valve torque motor and connections.

93. Servo valve torque motor characteristics.

94. Servo valve baffle - flapper valve characteristics.

95. Flow - pressure drop for servo valve (steady state).

96. Flow gain of servo valve.

97. Effect of spool lap on servo valve flow gain in the null region.

98. Pressure gain of servo valve for blocked load.

99. Servo valve leakage curve.

100. Oil flow-time curve predicted by program VSP2.

101. Bode diagram for Dowty 4551.262 servo valve.

102. Flow diagram for the variable DISPL in program VSP2.

103. Typical function specification by subroutine GEN.

104. Accumulator chart - H. P. range.

105. Accumulator chart - L. P. range.

106. Schematic diagram of hydraulic circuit.

107. View of servo valve installation showing hydraulic actuator and valve linkage.

108. View of hydraulic power supply and ancilliary equipment.

109. Servo performance for variable loop gain.

110. System performance for variable servo valve bandwidth.

111. Servo performance for variable actuator bore diameter.

112. Representative control loop parameters forcast by program VSP2.

113. Predicted rate of pressure drop for linear closure.

114. Suggested method for gain switching the servo amplifier by a factor N.

115. Effect of gain switching on pressure control system.

116. Response of system to various inputs.

117. Method No. 3. for $G_2 = 0 \cdot 2$ and $P_{min} = 34 \cdot 3$ kN/m^2.

118. Method No. 3. for $G_2 = 0 \cdot 2$ and $P_{min} = 103$ kN/m^2.

119. Method No. 3. for $G_2 = 0 \cdot 6$ and $P_{min} = 103$ kN/m^2.

120. Predicted effect on $\emptyset$ of varying Pmin only (method No. 3).

121. Predicted effect on $\emptyset$ of varying G_2 only (method No. 3).

122. Predicted effect of gain switching on method No. 3.

123. Pressure-time for method No. 2 as predicted by program VSP2.

124. Predicted pressure-velocity diagram for method No. 2.

125. Theoretical investigation of method No. 2. ($\emptyset = 0 \cdot 067$).

126. " " " " " ($\emptyset = 0 \cdot 030$).

127-192. Presentation of 2nd stage experimental results for method 3. (see tables 5-7 for further details).

193-198. Results of method No. 3 for variation in Pmin.

199. Predicted effect of changing Pmin for method No. 3.

200. Servo system hydraulic pressure calibration chart.

201. View of transient air release apparatus.

202. Detailed view of agitator and container of transient air release apparatus.

203. Typical output of program PTP6.

204. Predicted flow reduction for method No. 3.

205. View of steady state air release equipment.

206. General view of rig operating area.

207. View of the electronic equipment associated with the servo system.

208. General view of the test rig looking towards the downstream end.

209. Different rates of valve closure - Ref. 76.

210. Determination of solubility coefficient for t_{sat} = 100 mins.

211. " " " " " t_{sat} = 15 mins.

Tables.

1. Steady state pressure drops for full flow conditions on test rig.

2. Results from steady state ball valve characteristics test.

3. Results from air release test (steady state) for t_{sat} = 100 mins.

4. " " " " " " " " " = 15 mins.

5. Summary of test cases employed for the 2nd stage of experimental work.

6. List of results of the experimental investigation of valve stroking method No. 3.

7. Summary of results for method No. 3, measured directly from the oscilloscope.

8. Results from the acoustic velocity determination tests.

Nomenclature.

A	Pipe internal area.
B	Initial saturation pressure.
c	Acoustic velocity.
C	Solubility coefficient (% Vol/unit of pressure).
D	Pipe internal diameter.
DT, dt	Time step.
E	Youngs Modulus.
f	Fanning friction factor.
F	External force.
g	Acceleration due to gravity.
K	Solubility coefficient (mass/unit of pressure).
L	Pipe length.
m	Mass of gas.
n	Cavity process index.
N	General extensive property.
P	Pressure.
P_o	Initial pressure at downstream valve face.
ΔP_o	" " drop across valve.
P_{min}	Minimum control pressure.
R	Gas constant for air.
s	Laplace operator.
T, t	Time.
Te	Temperature.
Δt, ΔT	Time step.

T-1	Subscript for the previous time step.
t_{sat}	Time of liquid saturation.
Tr	Computer time ratio.
T_{CLOS}	Overall valve closure time.
V	Velocity.
Vo	Initial steady state velocity.
VOL	Cavity volume.
VOL_F	Volume of kerosene evolving air.
VOL_G	Steady state cavity volume.
VOL_T	Actual cavity volume at time T.
VAP	Vapour pressure of kerosene.
X	Constants used in characteristic equations.
Δx	Space increment.
α	Time constant used in rate of air release equation.
α'	Constant used in an equation of Set 1.
β	Constant used in rate calculation = $1 - e^{-\alpha t}$
Υ	Steady state valve characteristic.
ρ	Fluid density.
$\forall$	Cavity volume

Pipe notation.

The dependant variables, P and V, are usually accompanied by two figures in brackets to indicate the location of the point to which the variables refer. The first figure is the pipe number; pipe No.1. being upstream of the valve, No.2. downstream of the valve. The second figure refers to the section number in the pipe. Since the number of sections may vary, it is denoted by N1 for the upstream pipe and N2 for the downstream pipe. Section numbering begins at the upstream end of each pipe so that the flow passes points (1,1), (1,N1+1), (2,1) and (2,N2+1) in that order. Time notation is accomplished by double characters for the time step in question i.e. PP or VV, and a single character for the previous step, P or V.

Symbols not found in this list may be included in appendices 3 and 7 which list parameters chiefly found in programs PTP1 and VSP2.

Introduction.

The recent introduction of computer techniques has enabled a variety of complex and non-linear problems associated with hydraulic transients to be investigated. One such area, which traditional graphical methods are unsuited to solve is that known as column separation. Column separation is usually associated with vapour pressure conditions causing the flowing liquid to change state and hence the remaining liquid may then move independantly. However for the work reported here, column separation may occur when any gas (in particular air) forms a full bore cavity between either a solid boundary and a liquid column or between two liquid columns.

The inclusion of such phenomena is particularly relevent when transients in petro-chemical fluids are under investigation since they dissolve, and subsequently evolve, relatively large quantities of air. In certain cases this process may not manifest itself, for example the pressure rise on the upstream side of a closing valve will preclude any air evolution and hence the maximum system pressure may be calculated without reference to cavity formation. On the downstream side of the same valve, the pressure will initially fall and air evolution is a distinct possibility, and because of this the research undertaken has been directed to the region downstream of a closing valve. Since aviation kerosene was used for the liquid in the pipe, the influence of released air has been maximised. The first part of the work has been the determination of a mathematical model which predicts, with reasonable accuracy, the transient flow parameters associated with the system just described; the model being tested against data obtained from an experimental rig.

The procedure known as 'valve stroking' has received attention from many people but most of the experimental verification has been performed by observing transient flow in upstream pipe systems. Valve stroking may be defined as the predetermined closure mode of a valve such that the transients present in a system are minimised or eliminated. It would seem that in the work conducted so far by other researchers, insufficient attention has been paid to the relevance of the valve actuator dynamics on the method of transient attenuation adopted. However exact the theory of valve stroking may be, its successful implementation depends on a fast response, high resolution actuator as at one of the boundary conditions.

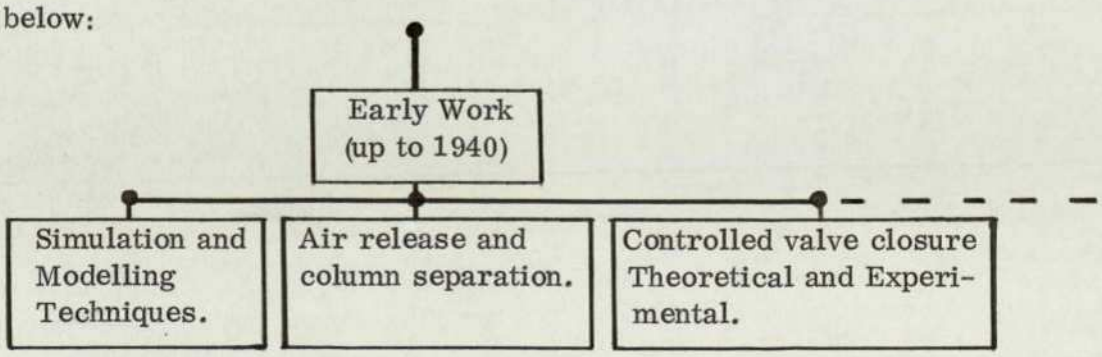
Such valve and actuator dynamics are quantified and simulated, and together with the equations describing the transients within the fluids, allow a program to be written which illustrates the relationship between the two mechanisms. This will enable an assessment to be made as to the usefulness of the existing theories regarding valve stroking, when applied to separated flow. If such methods are proved to be inadequate then the model may be used to test any alternative propositions that are designed to reduce the transient pressure changes downstream of a valve.

2. Literature Survey.

The amount of published work associated with pressure transients is both extensive and diverse. It would be inappropriate in this work to attempt to review all the aspects of the subject since not only has it been done before (8, 37,) but for the work covered by this thesis, the majority of the various aspects would be of minor interest only.

Much of the theoretical work concerning water hammer had been developed by 1930 although it must be realised that it was of a fundamental nature and left many engineering phenomena unexplained. Since the advent of the electronic computer, interest has been aroused in a wide variety of subjects which encompass not only the need to simulate complex hydraulic systems but also into the numerical proceedures that enable non-linear effects to be studied in detail.

Thus the work reviewed in this section will begin by covering the early years of development in the fundamental concepts concerning transients and going on to cover only those areas of the subject which are needed to pursue the research objectives of this thesis. This approach may be summarised by means of the diagram shown below:



2.1. Early Work.

The origins of pressure transient theory lie in the eighteenth century when the problem of sound wave propogation both in air and vibrating strings was of interest to mathematicians and physicists alike. Much of the present theory was to be developed before the problem began to be investigated by engineers.

Eulers first article (1) on the propogation of sound marks the earliest work that can be considered to have significantly contributed towards modern theory. This involved a cylindrical column of air, horizontal and within a rigid container. The air, when subjected to a disturbance at some point, transmitted the disturbance in both directions such that the equation

$$\frac{\partial^2 y}{\partial t^2} = a^2 \frac{\partial^2 y}{\partial x^2} \qquad a^2 = gh$$

describes the response of the air to the disturbance. Here x is the equilibrum position of a particle suspended in the air, y is its position at time t and h defined by Euler as "the height of a column of air of constant density which exerts atmospheric pressure at its base". It is easy to combine the expression for a^2 with the isothermal equation of state for an ideal gas

$$PV = \text{constant}$$

to arrive at the expression

$$a = \sqrt{\frac{kg}{\gamma}}$$

where γ = specific weight of the fluid and k = its bulk modulus. This expression is still widely used to obtain a first approximation to the speed of wave propogation in a fluid.

Euler went on to develop a solution to his one dimensional wave equation of the form

$$y = F(x + at) + f(x - at)$$

Where the general functions F and f are arbitary.

The difference between the speed of propagation in confined and unconfined fluids was explained first by Helmholtz in 1848, by stating that this was due to the elasticity of the pipe wall in which the confined fluid existed. However the first analytic study which included the pipe wall elasticity was published by Weber (2) in 1865. In this study, use is made of two equations; those of continuity and momentum, namely

$$\frac{\partial v}{\partial x} = -\frac{2}{r}\frac{\partial r}{\partial t}$$

$$\frac{\partial v}{\partial t} = -\frac{1}{\rho}\frac{\partial P}{\partial x}$$

which leads to the equation

$$\frac{\partial^2 r}{\partial t^2} = \frac{r}{2k\rho}\frac{\partial^2 r}{\partial x^2}$$

where k is defined as the elastic modulus

v is the fluid velocity

P is the fluid Pressure

r = radius of the pipe.

from which the wave propagation speed = a = $\sqrt{\frac{K_p g}{\gamma}}$

where K_p = bulk modulus = $r / 2k$

Weber attempted to measure the wavespeed in water in a rubber hose and his theoretical and experimental valves differed by 12%,a large proportion of which is attributable to the measuring equipment used. Since Weber's theory assumed an incompressible fluid in an elastic pipe, no combined theory was yet available for both elastic fluid in an elastic pipe. This combined theory was published by Kortweg (3) in 1878 which also included the effects of pipe wall radial acceleration. Although Korteweg's analysis includes the majority of those factors used in present day analysis, the object of the study was still the determination of the wave propagation and no mention of pressure rise is to be found. His analysis led to the expression

$$\frac{\partial^2 u}{\partial x^2} = \frac{\gamma}{g}\left\{\frac{1}{K} + \frac{2r}{bE}\right\}\frac{\partial^2 u}{\partial t^2}$$

with the relationship for the wavespeed as

$$a = \sqrt{\frac{\frac{Kg}{\gamma}}{\left\{1 + \frac{2Kr}{bE}\right\}}}$$

This is in complete agreement with present day theory, although his equations of motion etc. do not include either frictional effects or longitudinal stresses produced in the pipe walls.

In 1878 Lamb (4) took into account for the first time, the effects of longitudinal stress in the pipe wall and this led to the result that two wave velocities were associated with the system although it would be some years before these two waves were investigated in any detail by Skalak and Thorley.

Interest in parameters other than wave propagation velocity began in 1878 when Michaud (5) published a paper concerned with surge suppression devices such as relief valves and types of surge tanks. Unfortunately Michaud did not use the analytic techniques developed by his predecessors to evaluate the magnitude of such pressure and velocity fluctuations. It was not until almost twenty years later that Frizell (6) in 1897 published a paper which gave quantitatively the expected change of pressure for a known change of velocity. As the solution to his equations developed, he calculated the wave velocity to be given by a formulae identical to that derived by Korteweg, and he went on to produce the following result

$$P = \frac{a \gamma V}{g}$$

where P = pressure rise

a = wave speed

γ = specific wt. of fluid

V = change of velocity

Frizell went on further to explain the variation of wave propagation velocity in restricted and unrestricted fluids using his equation for wave speed, and also considered more complex piping systems including junctions and branches along with the concept of wave reflection.

At about the same time that Frizell was developing his ideas, a Russian engineer Joukowsky (7) was working on the same problem of evaluating pressure fluctuations and in 1898 he published his results. Joukowsky was considering both elastic fluid and pipe but pipe elasticity only in a radial direction. There was still no

attempt to include frictional effects in the system. He had three separate pipework loops on which to test his theories and was able to study, as well as the pressure change, the effects of branches, dead ends and the response of various valves and air chambers. Joukowsky's theoretical work agrees identically with that of Frizell and Korteweg and further explains the functional solution of Eulers wave equation with the physical phenomenon of wave reflection which he was able to measure. He also concluded that the pressure rise at a closing valve was maximised if the valve was closed in a time less than 2L/a where L is the pipe length.

As Wood (8) writes in his "History of Waterhammer" the work of Frizell and Joukowsky was a milestone in the development of waterhammer theory. From this point onwards the problem was studied by engineers with a particular interest to the applications aspect of the fundamental theory. The topic no doubt lost most of its appeal to theoreticians, and although the theory has been continually refined since 1897, the basic concepts have remained unchanged. A summary of the then existing theory was published by Allievi (9) (10) between 1904 and 1913 as well as reworking the basic equations himself. He obtained for the equation of motion, however, a more accurate expression which included the variation of velocity with distance i.e. using the total differential of the velocity. This gave

$$-\frac{\partial P}{\partial x} = \frac{\rho}{g}\left\{\frac{\partial v}{\partial t} + v\frac{\partial v}{\partial x}\right\} = \frac{\rho}{g}\frac{dv}{dt}$$

Allievi's work was a comprehensive one including relationships for slow as well as rapid valve closure. His expression for the wave speed was the same as that due to his predecessors, as the extra term in his equation of motion, above, was shown to

be negligible with respect to other terms. Other major aspects of his work included the first attempt at a graphical solution to the waterhammer equations although it proved difficult to use. The graphical procedure enable him to compile several charts to enable engineers to calculate pressure change for various flow rates and valve closure rates.

Although Allievi's work was comprehensive, it did not enable a wide variety of complex systems to be analysed and work was published between 1900 and 1925 which appeared to specialise in one or more aspects of pressure transients. For example in 1915 Johnson (11) looked at the assessment of pressure rises for slow valve closure as did Gibson (12). Gibson (13) also published work on an approximate calculation of pressures in an elastic liquid column. Difficulty was also encountered in representing boundary conditions in anything other than linearised form. Warren (14) assumed a linear pressure rise at the valve during closure while Gibson (12) proposed a linear reduction in gate area with time although a later paper by Strowger and Kerr (15) did take into account the possible non-linear gate movement associated with turbine speed regulation.

The tool used for most of the pre-war waterhammer calculations, the graphical method, was first proposed as such by Lowy (16) in 1928 although it was seven years before he was recognised for it. Perhaps it was due to the rapid publication of work by Schnyder in 1929 (17) and Bergeron in 1931 (18) that Lowy's work was overshadowed. The use of the graphical method diverted interest away from single elements such as surge tanks or pipes that exhibited transients, and enabled a study of systems of components to be made. Of the three original workers mentioned above, Bergerons

contribution was perhaps the most significant as he not only developed the graphical method from the functional solution of the wave equation, but proposed what is in effect a characteristics type of solution in the pressure - flow plane. In 1932 Schnyder (19 included friction in his graphical analysis although a publication by Gibson (12) did include a V^2 friction term in a numerical method of solution. The inclusion of friction in the graphical method took the form of lumping the effect at one end of the pipe and regarding the flow in the remainder of the pipe as frictionless. This enabled the lines in the P-V plane to remain straight. It can be assumed that friction may be more accurately simulated by means of a series of orifices in the pipe since the more orifices are present then the more the lumped model approaches that of a distributed model. However for more than 4 orifices, the diagram that results is complex and draughting inaccuracies are significant. Many applications of the graphical method were to be found in the A. S. M. E. meetings in 1933 (20) and 1937 (21). In 1937 (22) and 1938 (23), Angus presented the graphical analysis of various engineering systems including the effects of boundary conditions and branched pipes. The graphical solution remained the best method for analysing transients until the advent of the digital computer, although attempts to simplify or linearise the basic equations did have limited success. These methods will be described in the next section.

2.2. Modelling Techniques.

The type of work reviewed in this section may be classified into the two major areas of analytical and numerical methods. This classification clearly indicates the divergence between the two aims of:

a) Simplifying the basic equations of momentum and continuity to derive an analytic solution which may be used by engineers in simple systems, and:

b) Attempting a numerical solution, usually using a computer, of the overall equations with a view of achieving accurate results when compared to an experimental system. This procedure usually involves refinements to the fundamental theory to simulate non-linear effects with greater accuracy.

The work of Harding (Ref. 94) was a computer solution to the graphical method described earlier. In this work the equations of continuity and equilibrium are modified so that the friction term is ignored by considering such effects to be lumped at various points, thus reducing to the familiar

$$dH/dV = \pm c/g \qquad \text{for} \quad dx/dt = \mp c$$

Hence by using first order finite difference approximations to the differentials a simple algorithm is available for determining the changes in head and velocity. This method is particularly favoured by B. H. R. A. (Refs. 24, 25, 26) and other authors have used it successfully.

Operational calculus is an elegant method of analysing transient systems although it suffers from its inability to cope with non-linear aspects of the subject. The

two main works on the topic are those by Wood (27) and Rich (28). The solutions obtained were complex expressions relating to simple systems and relied on the assumptions of instantaneous valve closure and a friction term proportional to the velocity of flow. Rich's solution is discussed in more detail later on. The advantage of such solutions is that it is easy to express the results in transfer function form so that where the fluid dynamics of a system is just one of the overall system features under investigation, a compatable interface with other sub-systems is easily effected. This may be of importance in the type of work reported by Zielke (29) where control components are also simulated.

Enever (30) re-stated that a liquid column may be considered rigid and developed the equation

$$H = \frac{L}{g} \frac{dV}{dt}$$

by considering the free body diagram of such a column experiencing a head rise H due to a retardation to a velocity V, ignoring friction. This simplification enables a more efficient program to be written but is constrained by the fact that any disturbance must occur in a time much greater than one pipe period. Macagno and Macagno (31) proceed one stage further to consider the liquid compressibility but still ignore fluid friction. The two equations that result are relatively simple differential (total) equations which enable simple systems to be analysed. The resultant expression for the pressure at a closing valve is of the form

$$P = P_0 + \alpha \left\{ 1 - \cos 2\pi t / (4L/c) \right\}$$

whereas direct integration of the wave equation subject to the same initial and boundary conditions is

$$P = P_0 + \alpha \left\{ 1 - \overset{\Delta}{\cos} 2\pi t / (4L/c) \right\}$$

where $\Delta\cos$ is the triangular cosine function. Thus the pressure fluctuation magnitude is identical but the period of oscillation is not.

Although system simplification, and subsequent analytical solution, may provide an insight into the behaviour of the system, it rarely provides sufficiently accurate results to be of direct use to the design engineer. Thus techniques had to be and have been developed to scrutinise any particular system via a numerical approach. The two factors enabling this to be done are the availability of proceedures for converting the partial differential equations of momentum and continuity into total differential equations and a more accurate assessment of frictional effects. The equation conversion proceeded may be obtained from several references, Lister (32) and H.M.S.O. (33) being the more prominent. The accurate assessment of friction is closely related to the development of the method of characteristics. This method first described in 1860 by Riemann is the cornerstone of much of the numerical approach to transient analysis, although it was almost a hundred years until Lamaen (34) and Gray (35) were to use the method to investigate waterhammer.

The foremost exponent of the characteristics method has been Streeter who along with Lai (36), and Wylie (37) lumped friction at several discrete sections in a pipe. Computer application enabled the number of these sections to be as large as possible, although computer run time will be the limiting parameter. The friction term itself is proportional to the square of the velocity and utilises a friction factor based upon the velocity of the previous time step in the program. It is possible, as illustrated later to use a mean velocity for the determination of the friction factor but this leads

to an increased complexity of the problem and the necessity to use a further iterative proceedure. Lai's work also showed instabilities in the solution if the friction term was based on velocity not on the characteristic curve. The Courant condition imposes a necessary but not sufficient condition on the step sizes to give a stable solution. The condition is

$$\Delta t \leq \Delta x / c$$

and may, in some instances, impose a serious limitation. This may be overcome in systems where the inertia forces are small compared to the friction term by the use of Yow's (38) inertial multiplier α . This effectively increases the time step by a factor of α which is useful for the analysis of slow transients in long pipelines. Streeter (39) has developed another numerical method known as an Implicit method for pipe transient evaluation. In this method the pressure and velocity at four points in a grid in the x - t plane are related by the continuity and equilibrium equations expressed in finite difference form. This enables a simultaneous solution of the equations without the restrictions imposed by the Courant condition, although of course, the larger the steps in the x direction, the less accurate will be the simulation of friction.

A significant contribution by Zielke (40) has recognised the fact that while the wall shear stress is dynamically in phase with and proportional to the pressure gradient, the mean velocity may be out of phase with both due to the inertia of the fluid. Zielke's work uses a history of the transient to determine the phase shift and hence model the shear stress accurately. Unfortunately the theory only considers laminar flow cases although Hirose (41) has developed a semi-empirical method for turbulent cases. The experimental work of Holmbe (42) has verified thats Zielke's proposals result in a very close agreement between theory and practice.

The analogue computer has made little impact in the solution of problems involving pressure transients although it has several attractive features. Due to its ability to analyse linear differential equations Thomasson (43) uses an analogue solution to a simple mass oscillation problem. Friction and fluid compressibility implies a more complex solution and a lumped system model is usually adopted. Since analogue computers will run out of computing elements long before digital computers have used all their storage capacity, the number of sections or nodes that a system may be divided into is limited to typically, eight. Even so the paper by Morris and Morgan (44) achieves results compatable with the Schneyder - Bergeron graphical solution while maintaining the important advantage of being able to change various system parameters easily. The same authors also use a hybrid computer to solve the problem of limited nodes by storing in the digital section those parameters used by a basic computing analogue circuit, so that the same circuit may be used to evaluate parameters in the next element. Since this involves several analogue digital convertors, it is difficult to justify the proceedure for most problems.

2.3. Air release from liquids and Column Separation.

The earliest recorded work dealing with column separation is that published by LeConte in 1937 (45) and concerned column separation on the upstream side of a valve which closes in less than one pipe period. After the first wave returns and is reflected from the valve, LeConte observed that the column of liquid broke away from the valve leaving a "vacuous" space behind. Although no mention of air release or vapour formation was mentioned, LeConte's observations enabled him to assess the phenomenon and to proceed to develop theoretical expressions for the time interval between the high pressure peaks recorded at the valve. Although his calculations were based on an imcompressible liquid column, he achieved reasonable results in the calculation of the resurge periods but no attempt was made to determine the magnitude of the pressure rise.

The first investigation of column separation downstream of a closing valve is due to Bunt (46) although Binnie and Thackrah (47) observed the phenomenon while simulating pump shut down by the use of a rapidly closing valve. In ref.47 account is taken of the compressibility of the water column allowing the development of an expression for the pressure rise to be calculated. It is also recognised that the cavity pressure is non-zero. Careful measurement of the cavity pressure showed that its magnitude was three times that of the expected vapour pressure of the liquid and the difference was attributed, for the first time, to the liberation of dissolved air from the liquid. Binnie and Thackrah also analysed the superimposed effects of column separation and classical waterhammer waves.

In 1959 Gayed and Kamal (48) extended the work of Binnie and Thackrah by explaining separation downstream of the valve. Mention is made of the cavity

contents in terms of liberated air, vapour and a combination of the two. It is also observed that the air released does not re-dissolve when the water column moves towards the valve and compresses the cavity and a cushioning effect is explained. The paper goes on to explain the resurge interval in terms of classical waterhammer theory.

Investigators concerned with pumping systems also worked on column separation effects and the publications of De Haller and Bedue (49) and Richards (50) is prominent. J. Duc (51) in 1965 observed the phenomenon of separation (or cavitation) in a 1 Km pipeline with a short, elevated test section. He used piezo-electric transducers with an oscilloscope to record the pressure time history and observed that the pressure in the cavity formed following valve closure fell to almost absolute vacuum and that the pressure rise produced on cavity collapse was of very short duration. He also states that the nature of the cavity appeared to be a true void and suggest that the inclusion of air inlet valves will eliminate the high pressure transient.

In his 1963 paper Li (52) presented a mathematical treatment of column separation downstream of an instantaneously closing valve. He assumed that the cavity formed was at the vapour pressure of the liquid and developed an equation of motion for the separated column ignoring gravitational effects acting on the liquid/vapour interface. He further went on to study such gravitational effects in an inclined pipe by the use of open channel flow theory. He concluded that it was not necessary to consider the non-linear cavity geometry to estimate pressures encountered on the re-joining of the column. In Li's second paper (published a year later, jointly with Walsh (53)), experimental evidence of column separation is presented in the form of a

series of photographs of cavity formation downstream of a closing valve. In these photographs, gravity does affect the cavity dynamics although no mention of the pipe period is made so the result may be expected in long pipelines. It is also acknowledged that bubbles of liberated gas also form in the vicinity of the low head region of the pipe adjacent to the closing valve. The paper also deals with a method of predicting the duration of the cavity by analysing the equations of motion and continuity via a Laplace transform approach. Another of Li's papers (54) is of interest only to those studying cavity thermal processes and will not be discussed in this section.

It was in the mid-sixties that two schools of thought developed concerning column separation and air release. Up to this point it had been assumed that if separation and/or air release occurred, the voids formed could be treated as discrete cavities effectively enabling the original system to be replaced by two systems where the cavity formed the boundary condition. Problems were encountered in analysing systems where the air release took the form of a uniform distribution of gas bubbles throughout the liquid. This was not so straightforward to analyse and the common method proposed to handle such situations followed from a paper by Pearsall (55). In this work, the effect of various parameters such as pressure variation, temperature, gas content etc. on the acoustic velocity were determined. It was realised that a small amount of gas evenly distributed, throughout the liquid would reduce the wave speed considerably. For example, the presence of 1% of air in water by volume resulted in a reduction in wave velocity to 7% of the original. This phenomenon had already been investigated by several researchers the most prominent being Ripken and Olsen (56) Silkerman (57) and Spitzer (58). Unfortunately not all hydraulic systems exhibiting air release or column separation may be easily classified into the 'distributed' or 'lumped' cavity category and care must be exercised in applying one method of analysis, or the other to any system.

The graphical method attributed to Schnyder and Bergeron has been adopted for use with flow separation but only under the assumption of vapour only occupying the cavity. Bergeron (95) and Lupton (59) include this effect while the work of Marples (60) shows that with the inclusion of an air valve to limit the pressure drop in a pipeline will result in significant pressure fluctuations a short time later. It will be shown in the computer analysis of transient systems that the accurate determination of interface velocities is essential to the accurate prediction of pressures. This proves a major disadvantage in the graphical method as the interface velocities cannot be known very accurately due to the large time steps involved in the calculation. This limitation does not necessarily apply to the 'computerised graphical method' proposed by Harding.

Balzer (61) investigated column separation in a pipe upstream of a closing valve and also used a plexiglass pipe to observe the growth of cavities. Although Balzer's analysis was based on open channel flow and the cavities observed were not full bore but lay at the tope of the pipe, he also observed the formation of bubbly liquid throughout the pipe. The higher than anticipated energy dissipation of his experimental results is attributed to this two phase mixture within the pipe. Using the same test rig as Balzer, Weyler, and Larsen (62) investigated the formation of the bubbles observed previously and attempted to explain that these bubbles would require energy to expand and contract them. This would, explain the additional energy loss needed to bring Balzer's results in line with experimental evidence. The viscous dissipation is interpreted as an equivalent shear stress on the pipe wall but the work is, in the authors opinion, degraded by the inclusion of a factor C which "contains all the numerical factors and unknown constants" which effectively renders the

investigation empirical in nature. The results are good for suitable valves of C but no indication is given regarding the dependence of the theoretical results on the factor C.

Since 1967, column separation has received wide attention from research workers and their results may be suitably presented by discussing some papers presented at the International Conference on Pressure Surges, held at Canterbury in September 1972. Fox (63) presented a paper dealing with a global computer program for the simulation of general hydraulic systems exhibiting pressure transients and air release. Fox's method is to calculate the actual wave speed in any particular section based on the amount of free gas in suspension in the liquid, in the particular section. The work of Pearsall (55) is used to calculate the wave speed. Work on developing a program similar to that of Fox, led Apelt (64) to consider a lumped model for inclusion of flow separation in his program. If the pressure at any section falls to vapour pressure, then the system is divided into two sub-systems with the cavity forming a common constant pressure boundary condition. The two papers described above clearly indicate the two distinct methods of analysing flow separation and air release. It would be instructive to compare the two programs described for a common experimental test case. Enever (65) dissatisfied with the over estimate of pressure given by liquid theory and the under-estimate given by an appropriate reduction of wave velocity, applies the theories of gas dynamics to determine the pressure change across a shock wave in gas-liquid mixtures. Although it assumes instantaneous valve closure, the theory bridges the two extreme theories mentioned above. The theory was built into a computer program and the results compared favourably with an analytical solution although it is unfortunate that comparison with an experimental case was not available. Swaffield (66) presented a paper on column separation

in aircraft fuel system. Since the authors work is closely allied with that of Swaffield the work will be discussed in detail at the end of this survey.

The existance of a shock front in a falling column of liquid was demonstrated by Vaidyaraman and Anderson (67). Here, a vertical pipe with a valve at the top was passing water to a lower level. It was found that abrupt pressure changes occurred at some point in the pipe where the mixture appeared to be a homogeneous mixture of water vapour and water liquid. Since the shock-front is stationary in the liquid column the phenomenon is one of steady rather than transient flow.

The paper published by Kranenburg (68) deals with cavitation and air release accompanying transient flow. This paper, along with the authors work are the only instances found where the gas solubility pressure is considered to be the point at which air release begins. Once again the analysis begins by considering bubble dynamics and interprets the subsequent fluid motion as a combination of separation and classical waterhammer ih the separated column. The bibliography accompanying this paper contains several interesting articles on the distributed bubble theory of flow separation, the most notable being Kalkwijk and Kranenburg (69), Tanahashi and Kasahara (70) and Hsieh and Plesset (71).

Safwat and de Kluyver (72) described a computer program developed to simulatean experimental test rig which exhibits flow separation in water pipes. The program uses the method of characteristics for the analysis of the governing equations and assumes, like the author and Swaffield, that the voids formed are full

bore. The paper further assumes that the cavity contains only vapour, and air release is not considered. Further work by Safwat and Van der Polder (73) uses similar theory but includes the resistance due to valve closure. The correlation between experiment and theory is good. Safwat also presented a paper (74) which gave experimental evidence of flow separation inside a head box of a condenser in a cooling water system. It was claimed that pressure measurements in the vicinity of the void indicated vapour pressure of water.

Condenser cooling water systems also received the attention of Atzeni. Cao and Piga (75). They investigated column separation in a vertical loop pipe rig and attempted to relate theoretical and experimental results for the condenser located in the upward-going, downward-going and horizontal top sections of the rig. Separation was observed in all three cases but only in one case did the theory predict with any accuracy what was observed in practice. It was found that the theoretical results given by simple rigid column theory were more accurate than those which included the compressibility of the liquid. The paper contains an extensive bibliography on cooling system transients.

2.4. Controlled valve closure - Theoretical and Experimental.

a. Theoretical.

Traditionally, the analysis of pressure transients has been one of a method of analysis rather than synthesis so that if pressure fluctuations of dangerous magnitude occur, means are sought to eliminate or reduce them. This is usually accomplished by including in the system components such as air vessels, surge tanks, reflux valves etc. The literature on the various design criteria associated has been reviewed extensively and as a result will not be duplicated in this work. The publications that will be reviewed here are those dealing with attempts to reduce the magnitude of pressure transients by using the available equipment in a manner to be determined either by mathematical synthesis or observation.

This work has origins in experimental observation of the fact that the majority of valves are highly non linear in their operation. Kerr (76) presented work in 1950 which investigated the reduction of flow of several valves for linear valve operation. The result is shown as curve B in fig. 38 whereas linear flow reduction is represented by curve A. This rapid reduction of flow leads to a higher head developed and an approximate method of calculating this head was also proposed by Kerr. This involved the 'equivalent closure time' as illustrated by point C in fig. 38 which is 40% of the actual closing time. This gave an estimate accurate to 7% in the maximum pressure developed when compared with a graphical analysis of the non-linear valve closure. In a further publication Kerr (77) develops his ideas further and provides experimental evidence of the validity of his 'equivalent closure time' proceedure.

In 1963 Streeter (78) presented his first paper on valve stroking, analysing systems with and without friction as well as considering flow establishment as well as reduction. The paper clearly illustrates the first practical method of limiting the pressure fluctuation during valve closure and subsequent elimination of transients after the valve has closed. While it is obvious from the characteristics viewpoint, and is in fact demonstrated by the graphical method, that the system works, no mention is made as to the origin of the theory in terms of the shape of the lines drawn in the P-V plane. In the absence of such an explanation it may be assumed that the method was derived from 'experimenting' with the graphical method of solution for non-linear valve closure.

Streeter presented another paper in 1965 (79) in which his work to date was summarised and included the conversion of any arbitary hydraulic gradeline shape to one corresponding to uniform flow. In 1967 Streeter (80) developed his ideas to more complex (parallel) pipe systems and included the use of systems and included the use of special boundary conditions. He also presented some experimental verification of his theories by considering the pressure rise up-stream of a closing valve. These results were also presented in his book, written jointly with Wylie (37). Still investigating valve characteristics, Livingston and Wilson (81) proposed a two stage method of closure to reduce the effects of transients. This involved an initial closure from 0° to 55° in one pipe period followed by 55° to 90° in seven pipe periods, which reduced the maximum head by 50%. This method has been investigated by Enever (82) who varied both the percentage closure of the first phase and the time interval ratio of the two phases. In ref 81, the writers state that optimum valve closure is achieved when the initial increase in pressure achieves the maximum pre-determined valve and subsequent

valve operation is to maintain it at this value. They also conclude that this corresponds to almost linear reduction of flow. The first section of their conclusions ties in exactly with the proposals of Streeter.

Valve stroking has also been applied to the control of natural gas transients by Stoner (83) who instead of specifying the desired conditions in terms of a pressure distribution in the space axis, specified conditions in the time axis. This enabled the correct valve manipulation to be made to produce the flow of gas best suited to the consumer needs, predicted in advance. Further work has been done on valve stroking in hydraulic systems by Propson (84) who also recognised that time axis definition at the boundary of a system was sufficient to determine the overall nature of transient flow. Propson went further to use this fact in determining the required valve manipulation necessary to achieve an absence of pressure transients after valve closure is complete, in frictionless flows. In their paper presented in 1972, Wood and Jones (85) investigate two proposed methods of valve stroking. One is that attributable to Streeter while the other consists of increasing the pressure to its maximum value and holding it constant until valve closure is complete. This method is very similar to that used by the author in this thesis. Wood and Jones also investigated the use of six types of valve to achieve their aims, although no mention of the mechanism used to operate the valves is made. The authors work is the only one known which deals with practical valve stroking downstream of a valve.

b. Experimental.

This section will review the publications dealing with the practical aspects of valve stroking along with the work needed to design and build the authors servo system.

The only documents found which describe the valve operating mechanism are those by Streeter and Wylie (37) and Propson (84). Streeters mechanism is an open loop pneumatic device which uses input data in the form of a card profile fitted to a rotatable drum. When the drum rotates the profile is used to position the valve according to the height of the card profile. The mechanism requires overall calibration before a meaningful profile can be cut. The arrangement used by Propson (84) is identical to that described above.

Once a hydraulic control system was decided upon is became necessary to choose a servo valve. In addition to the wide range of literature published by various manufactures, the paper by Walters (86) enabled the design criteria associated with such devices to be easily identified. This article was followed by a list and description of the various valves available in this country in 1969. After the individual components have been selected, overall system performance has to be assessed and a guide to such performance standards is discussed by both Powell (87) and Zellor (88). The latter is particularly interesting since it optimises the servo actuator area to be consistant with maximum valve acceleration, a problem encountered by the author in his work. Powell's work is based on the use of electrohydraulic servo valves in closed loop configuration and deals with the choice of individual component specification based on overall performance. Digital simulation of the proposed system was aided by Thaler's (89) publication which gives the appropriate transfer function for the range of servo valves manufactured by the Dowty company. The procedure for the practical construction of a hydraulic servo system was unfamiliar to the author but the works of Guillon (90), Merrit (91) and Walters (92) contained most of the information required to construct a

successful system. The knowledge of electronics needed for the servo system is fairly elementary, most topics being covered in the book by Sutcliffe (93) and various technical data sheets available from the manufactures of components.

The work of J. Swaffield.

Swaffields work, which may be summarised by his thesis (96), was concerned with the development of a mathematical model for the accurate prediction of pressure transients in separated flow due to linear valve closure. The authors work contains many features that appear in Swaffields thesis particularly in the analysis of the mathematical model used to predict transient pressures. This is not surprising since the two test rigs used are of similar geometry, but different size, and exhibit common physical phenomena. The main area of divergence between the two models is in the assessment of the air release mechanism initiated by pressure reduction in the flowing liquid. Since this feature forms a boundary condition critical to obtaining an accurate model, a difference in such boundary conditions implies a distinct difference in the derived model. Finally, the author acknowledges the fact that Swaffields work provided a 'launching point' for his own research, and hopes that the work presented in subsequent chapters helps to give a better insight into the mechanism of air release from a liquid.

3. Development of Equations of Motion.

This section will develop the equations of motion of a fluid element in a pipe, in terms of the two independant variables; distance x and time t. The equations will relate the two dependant variables of the fluid flow namely the pressure P and velocity V. Thus two independant equations will be needed and these may be obtained by considering both continuity and momentum conditions for the element of fluid in the pipe. This will result in a pair of quasi-linear hyperbolic partial differential equations.

Before these equations are modified, various approximations will be made so that the equations may be simplified. The solutions to such equations will illustrate not only how other investigators have obtained their results, but will allow a more quantitive analysis of pressure transient systems. This will introduce the concept of wave theory in fluids and will give an initial insight into the type of flow pattern to be expected. Finally a pair of total differential equations will be derived and direct use of these will be made in the computer simulation of unsteady flows.

3.1. Equation of continuity.

Using the equation relating the changes in an extensive property N for a system and control volume, namely

$$\frac{DN}{Dt} = \oiint_{c.s.} \eta(\rho \bar{V}.d\bar{A}) + \frac{\partial}{\partial t} \iiint_{c.v.} \eta(\rho dV) \qquad a$$

where η = N/m and m = mass

We may use the relationship to derive the equation of continuity for the control volume shown in fig.1 by letting the property N be mass. Recognising that for a system

$$Dm / Dt = 0$$

we have

$$\oiint_{c.s.} (\rho \bar{V}.d\bar{A}) = -\frac{\partial}{\partial t} \iiint_{c.v.} \rho \, dV \qquad b$$

or: The net efflux rate of mass across the control surface equals the rate of decrease of mass inside the control volume.

This, applied to fig.1 gives

$$\dot{m}_2 + \dot{m}_3 - \dot{m}_1 = -\frac{\partial}{\partial t} \left\{ \rho dx \left(A + \frac{1}{2} \frac{\partial A}{\partial x} dx \right) \right\} \qquad c$$

which, ignoring 2nd order differential quantities gives

$$\dot{m}_2 + \dot{m}_3 - \dot{m}_1 = -\frac{\partial}{\partial t} (\rho A dx) \qquad d$$

Now for the L. H. S. of equation (d) we may write

$$\dot{m}_1 = \rho A V$$

$$\dot{m}_3 = \rho A V + \frac{\partial}{\partial x}(\rho A V)\, dx$$

$\dot{m}_2$ = radial mass efflux.

Thus in a time δt the amount of radial mass efflux is:

$$\begin{aligned} \delta t . \dot{m}_2 &= (\rho . \text{ Volume of fluid}) \\ &= (\rho . \text{ Change of internal pipe volume}) \\ &= \Big\{ \rho . \Big\{ \Big(A + \tfrac{1}{2} \frac{\partial A}{\partial x} dx\Big) dx \\ &\qquad + \frac{\partial}{\partial t} \Big[\Big(A + \tfrac{1}{2} \frac{\partial A}{\partial x} dx\Big) dx \Big] \delta t \\ &\qquad - \Big(A + \tfrac{1}{2} \frac{\partial A}{\partial x} dx\Big) dx \Big\} \Big\} \end{aligned}$$

which neglecting second order differential quantities gives

$$\begin{aligned} \dot{m}_2 &= \rho \frac{\partial}{\partial t}(A\, dx) \\ &= \rho\, dx \frac{\partial A}{\partial t} \end{aligned}$$

Thus substituting for $\dot{m}_1$, $\dot{m}_2$ and $\dot{m}_3$ in equation (d)

we have

$$\rho A V + \frac{\partial}{\partial x}(\rho A V)\, dx - \rho A V + \rho\, dx \frac{\partial A}{\partial t} = -\frac{\partial}{\partial t}(\rho A\, dx)$$

i.e. $$dx\left\{\rho A\frac{\partial V}{\partial x}+\rho V\frac{\partial A}{\partial x}+AV\frac{\partial \rho}{\partial x}\right\}+\rho\,dx\frac{\partial A}{\partial t}=-A\,dx\frac{\partial \rho}{\partial t}$$

dividing by $\rho A dx$

$$\frac{\partial V}{\partial x}+\frac{V}{A}\frac{\partial A}{\partial x}+\frac{V}{\rho}\frac{\partial \rho}{\partial x}+\frac{1}{A}\frac{\partial A}{\partial t}=-\frac{1}{\rho}\frac{\partial \rho}{\partial t}$$

or

$$\frac{\partial V}{\partial x}+\frac{1}{A}\left\{V\frac{\partial A}{\partial x}+\frac{\partial A}{\partial t}\right\}+\frac{1}{\rho}\left\{V\frac{\partial \rho}{\partial x}+\frac{\partial \rho}{\partial t}\right\}=0$$

which, if $\theta = f(x, t)$ we may use the relationship:

$$\frac{d\theta}{dt}=\frac{\partial \theta}{\partial t}+\frac{\partial \theta}{\partial x}\frac{dx}{dt}$$

to write

$$\frac{\partial V}{\partial x}+\frac{1}{A}\frac{dA}{dt}+\frac{1}{\rho}\frac{d\rho}{dt}=0 \qquad 1$$

The three terms in equation (1) may be interpreted as:

(1) The change of velocity along the control volume at a given time.

(2) Rate of change of pipe area with time.

(3) Compressibility of the liquid.

The equation is not of direct use as it stands since we need an equation involving P, V, x and t only. Thus the last two terms in the equation will have to be expressed in these parameters.

Compressibility of the liquid.

The bulk modulus of the liquid is defined mathematically as:

$$K=\frac{\rho\, dP/dt}{d\rho/dt}$$

thus $$\frac{1}{\rho}\frac{d\rho}{dt} = \frac{1}{K}\frac{dP}{dt} \qquad 2a$$

Rate of change of pipe area with time.

Assuming that ε_2 is the circumferential strain, the increase in the radius of the pipe, dr is related to ε_2

$$\varepsilon_2 = \frac{2\pi(r+dr) - 2\pi r}{2\pi r} = \frac{dr}{r}$$

or

$$dr = r\varepsilon_2$$

hence the increase in pipe area dA is

$$dA = \pi(r+dr)^2 - \pi r^2$$

$$= \pi(r^2 + dr^2 + 2r\,dr) - \pi r^2$$

which, ignoring the product of small quantities gives:

$$dA = 2\pi r\,dr$$

$$= 2\pi r^2 \varepsilon_2$$

hence

$$\frac{1}{A}\frac{dA}{dt} = \frac{1}{\pi r^2}\frac{d\varepsilon_2}{dt}\,2\pi r^2 = 2\frac{d\varepsilon_2}{dt}$$

Now the circumferential strain ε_2 and axial strain ε_1 are related to the circumferential stress σ_2 and axial stress σ_1 by:

$$\varepsilon_1 = \frac{1}{E}(\sigma_1 - \mu\sigma_2)$$

$$\varepsilon_2 = \frac{1}{E}(\sigma_2 - \mu\sigma_1)$$

where μ = Poissons ratio for the pipe material.

Thin walled tube theory gives for a pressurised cylinder, the principle stresses:

$$\sigma_1 = PD/4e \,, \qquad \sigma_2 = PD/2e$$

where P = internal pressure and e = wall thickness.

hence

$$\frac{1}{A}\frac{dA}{dt} = 2\frac{d\varepsilon_2}{dt}$$

$$\therefore \frac{1}{A}\frac{dA}{dt} = \frac{2}{E}\left(\frac{d\sigma_2}{dt} - \mu\frac{d\sigma_1}{dt}\right) \qquad 2b$$

The complete evaluation of equation (2b) will depend upon the assumptions made about the manner in which the pipe is constrained. The stresses σ_1 and σ_2 will be eliminated from the above expression and replaced by equations derived from thin walled tube theory i.e.

$$\frac{d\sigma_1}{dt} = \frac{D}{4e}\frac{dP}{dt} \,, \qquad \frac{d\sigma_2}{dt} = \frac{D}{2e}\frac{dP}{dt} \qquad 2c$$

Three common modes of pipe restrain will be considered, beginning with the case where the pipe is supported axially so both circumferential and axial stresses are present. Thus substituting (2c) into (2b) gives

$$\frac{1}{A}\frac{dA}{dt} = \frac{2}{E}\frac{dP}{dt}\left(\frac{D}{2e} - \frac{\mu D}{4e}\right)$$

$$\therefore \frac{1}{A}\frac{dA}{dt} = \frac{D}{Ee}\frac{dP}{dt}\left(1 - \mu/2\right) \qquad 2d$$

If however the pipe is incapable of axial movement then

$$\frac{d\varepsilon_1}{dt} = 0$$

hence

$$\frac{d\sigma_1}{dt} = \mu \frac{d\sigma_2}{dt}$$

hence substituting into equation (2b)

$$\frac{1}{A}\frac{dA}{dt} = \frac{2}{E}\left(\frac{d\sigma_2}{dt} - \mu^2 \frac{d\sigma_2}{dt}\right)$$

$$= \frac{2}{E}\frac{dP}{dt}\frac{D}{2e}(1-\mu^2)$$

$$\therefore \frac{1}{A}\frac{dA}{dt} = \frac{D}{Ee}\frac{dP}{dt}(1-\mu^2) \qquad 2e$$

Finally if expansion joints are fitted throughout the pipe so that axial stress cannot be sustained then

$$\varepsilon_1 = \sigma_1 = 0$$

thus

$$\frac{1}{A}\frac{dA}{dt} = \frac{2}{E}\frac{d\sigma_2}{dt} = \frac{2}{E}\frac{dP}{dt}\frac{D}{2e}$$

$$\therefore \frac{1}{A}\frac{dA}{dt} = \frac{dP}{dt}\frac{D}{Ee} \qquad 2f$$

Substituting equations 2a, 2d, 2e and 2f into equation 1 results in three expressions for the continuity equation depending upon the assumptions made about pipe constraint.

They are:

$$\left.\begin{aligned} \frac{\partial V}{\partial x} + \frac{dP}{dt}\left\{ 1/K + \frac{D}{Ee}(1-\mu/2)\right\} &= 0 \\ \frac{\partial V}{\partial x} + \frac{dP}{dt}\left\{ 1/K + \frac{D}{Ee}(1-\mu^2)\right\} &= 0 \\ \frac{\partial V}{\partial x} + \frac{dP}{dt}\left\{ 1/K + \frac{D}{Ee}\right\} &= 0 \end{aligned}\right\} \quad 2g$$

Velocity of transient propagation.

In an unconfined expanse of liquid, the transient propagation speed, c, is related to the physical properties of the fluid by the expression:

$$c^2 = K^1/\rho$$

where K^1 = K = the bulk modulus of the liquid. If the liquid is now constrained, say within a pipe, K^1 will no longer be a function of just fluid properties but dependent upon pipe parameters, restraint mode etc. For the three cases of pipe restraint outlined previously we may define an equivalent bulk modulus (of both liquid and pipe) K^1 such that

a) $$1/K^1 = 1/K + \frac{D}{Ee}(1-\mu/2)$$

b) $$1/K^1 = 1/K + \frac{D}{Ee}(1-\mu^2)$$

c) $$1/K^1 = 1/K + \frac{D}{Ee}$$

Thus the expression for wave speed given above may still be used providing the correct

expression is used for the equivalent bulk modulus. Thus the set of equations represented by the set (2g) may all be written as:

$$\frac{\partial v}{\partial x} + \frac{1}{\rho c^2}\frac{dp}{dt} = 0$$

and since*

$$\frac{dp}{dt} = \frac{\partial p}{\partial x}\frac{dx}{dt} + \frac{\partial p}{\partial t}$$

we get for the final form of the continuity equation:

$$\frac{\partial p}{\partial t} + v\frac{\partial p}{\partial x} + \rho c^2\frac{\partial v}{\partial x} = 0 \qquad (3)$$

*In the expression shown it may seem confusing to write

$$dx/dt = v$$

since x is the coordinate defining the inflow face of the control volume and hence has nothing to do with the velocity of a fluid particle passing through that face. The explanation is that the equation is derived from equation (a) which relates the change in a property N in a system and a control volume which at time t are instantaneously coincident. Thus at this time the coordinate x also defines the position of a fluid system and hence the location of a fluid particle. It thus seems reasonable to interpret the rate of change of x with time as a definition of fluid velocity.

3.2. Equation of Momentum conservation.

If the control volume shown in fig.1 is considered to be identical with a system of fluid at time t, then the forces acting on such a system may be represented by those forces shown in fig. 2a. The Euler equation of motion is obtained by considering the relationship between changes of momentum in a system and control volume. Thus substituting linear momentum for the property N in equation (a) and noting that

$$\eta = N/m = mV/m = V$$

we get

$$\frac{D(m\bar{V})}{Dt} = \oiint_{c.s.} \bar{v}\,(\rho \bar{v}.d\bar{A}) + \frac{\partial}{\partial t} \iiint_{c.v.} \bar{v}\rho\, d\forall \qquad e$$

Further, Newtons 2nd law may be applied to the system by equating the time rate of change of linear momentum to the sum of the applied forces i.e.

$$\Sigma \bar{F} = \frac{D(m\bar{V})}{Dt} \qquad f$$

Equation (e) is best described in words as: The total rate of change of linear momentum in a system at time t is equal to the time rate of change of linear monentum within a corresponding control volume plus the net efflux of linear momentum across the surface of the control volume. Using this definition and equation (f), equation (e) may be re-written as

$$\Sigma \bar{F} = \oiint_{c.s.} \rho \bar{v}(\bar{v}.d\bar{A}) + \frac{\partial}{\partial t}\left(\rho \bar{v}\, dx\,(A + \tfrac{1}{2}\frac{\partial A}{\partial x}\, dx)\right)$$

which, using the fact that for a control volume

$$\frac{\partial A}{\partial t} = \frac{\partial (dx)}{\partial t} = 0$$

and that second order differential terms may be neglected we get

$$\Sigma \bar{F} = \iint_{c.s.} \rho \bar{v} (\bar{v}. d\bar{A}) + A dx \frac{\partial}{\partial t} (\rho \bar{v})$$

To determine the net efflux of linear momentum across the control surface, the mass flow rates illustrated in fig. 1 may be used. Fig. 2b shows the momentum transfers across the control surface. The net efflux across the end faces of the control volume is:

$$= -\rho A v^2 + \left\{ \rho A v^2 + \frac{\partial}{\partial x} (\rho A v^2) dx \right\}$$

$$= \frac{\partial}{\partial x} (\rho A v^2) dx$$

The mass flow rate across the transverse faces of the control volume is obtained from equation (d) and is

$$\dot{m}_2 = \dot{m}_1 - \dot{m}_3 - \frac{\partial}{\partial t} (\rho A dx)$$

$$= \rho A v - \left\{ \rho A v + \frac{\partial}{\partial x} (\rho A v) dx \right\} - \frac{\partial}{\partial t} (\rho A dx)$$

$$= -\frac{\partial}{\partial x} (\rho A v) dx - \frac{\partial}{\partial t} (\rho A dx)$$

hence the linear momentum efflux across these faces is

$$- \left\{ v + \tfrac{1}{2} \frac{\partial v}{\partial x} dx \right\} \left\{ \frac{\partial}{\partial x} (\rho A v) dx + \frac{\partial}{\partial t} (\rho A dx) \right\}$$

which, by making the usual approximations with regard to products of small quantities reduces to:

$$-V\left\{\frac{\partial}{\partial x}(\rho AV)\,dx + \frac{\partial}{\partial t}(\rho A\,dx)\right\}$$

and giving the total linear momentum efflux from the control volume as

$$\frac{\partial}{\partial x}(\rho AV^2)\,dx - V\left\{\frac{\partial}{\partial x}(\rho AV)\,dx + \frac{\partial}{\partial t}(\rho A\,dx)\right\}$$

Thus the equation of motion is given by

$$\Sigma\bar{F} = A\,dx\,\frac{\partial}{\partial t}(\rho\bar{V}) + \frac{\partial}{\partial x}(\rho A\bar{V}^2)\,dx - \bar{V}\left\{\frac{\partial}{\partial x}(\rho A\bar{V})\,dx + \frac{\partial}{\partial t}(\rho A\,dx)\right\}$$

From Fig. 2a we get that if m = mass of fluid in control volume at time t

$$\Sigma\bar{F} = pA - \left(p+\frac{\partial p}{\partial x}\,dx\right)\left(A+\frac{\partial A}{\partial x}\,dx\right) - \tau_0\,\pi\,dx\left(D+\frac{\partial D}{\partial x}\,dx\right)$$

$$+\left(p+\tfrac{1}{2}\frac{\partial p}{\partial x}\,dx\right)\frac{\partial A}{\partial x}\,dx + mg\,\sin\alpha$$

Again ignoring the product of small quantities we get:

$$\Sigma\bar{F} = -\frac{\partial p}{\partial x}A\,dx - \tau_0\,\pi D\,dx + mg\,\sin\alpha$$

Thus substituting for $\Sigma\bar{F}$ in the equation of motion results in:

$$-\frac{\partial p}{\partial x}A\,dx - \tau_0\,\pi D\,dx + mg\,\sin\alpha = A\,dx\,\frac{\partial}{\partial t}(\rho V) + \frac{\partial}{\partial x}(\rho AV^2)\,dx$$

$$-V\left\{\frac{\partial}{\partial x}(\rho AV)\,dx + \frac{\partial}{\partial t}(\rho A\,dx)\right\}$$

Now the mass of the fluid within the control volume, m, is dependant upon the density which in turn is a function of x and t. Thus

$$m = \left\{ \rho + \tfrac{1}{2}\left(\frac{\partial \rho}{\partial t}\,dt + \frac{\partial \rho}{\partial x}\,dx\right)\right\}\left\{ A + \tfrac{1}{2}\frac{\partial A}{\partial x}\,dx \right\} dx$$

$$\simeq \rho A\,dx$$

Thus expanding the equation of motion gives:

$$-\frac{\partial p}{\partial x} A\,dx - \tau_0 \pi D\,dx + \rho A\,dx\, g \sin\alpha = A\,dx\left(\rho\frac{\partial V}{\partial t} + V\frac{\partial \rho}{\partial t}\right)$$

$$+ dx\left\{\rho A \frac{\partial (V^2)}{\partial x} + \rho V^2 \frac{\partial A}{\partial x} + A V^2 \frac{\partial \rho}{\partial x}\right\}$$

$$- V\left\{dx\left(\rho A \frac{\partial V}{\partial x} + AV\frac{\partial \rho}{\partial x} + \rho V \frac{\partial A}{\partial x}\right) + A\,dx\,\frac{\partial \rho}{\partial t}\right\}$$

which reduces to, after dividing by $\rho A dx$

$$\frac{1}{\rho}\frac{\partial P}{\partial x} + \frac{\partial V}{\partial t} + V\frac{\partial V}{\partial x} + \frac{4\tau_0}{\rho D} - g\sin\alpha = 0 \qquad (4)$$

3.3. Approximate forms of Equations of Motion - Wave Analysis.

To illustrate some of the early work done in the field of pressure transients and to introduce some useful concepts, the two derived equations 3 and 4 are simplified by making the assumption that the rate of change of the dependant variables with respect to x is negligible compared to the rate of change with respect to time t. This reduces the equations to the form:

Equilibrium $$\frac{1}{\rho}\frac{\partial P}{\partial x} + \frac{\partial V}{\partial t} = 0$$

Continuity $$\frac{1}{\rho c^2}\frac{\partial P}{\partial t} + \frac{\partial V}{\partial x} = 0$$

These equations apply to a horizontal, frictionless pipe. If the first equation is differentiated, , partially, with respect to x and the second with respect to t we get

$$\frac{1}{\rho}\frac{\partial^2 P}{\partial x^2} + \frac{\partial^2 V}{\partial x\,\partial t} = 0$$

$$\frac{1}{\rho c^2}\frac{\partial^2 P}{\partial t^2} + \frac{\partial^2 V}{\partial x\,\partial t} = 0$$

hence subtracting these equations leads to

$$\frac{\partial^2 P}{\partial x^2} = \frac{1}{c^2}\frac{\partial^2 P}{\partial t^2} \qquad 5$$

by changing the variables of differentiation an alternative result obtained is;

$$\frac{\partial^2 V}{\partial x^2} = \frac{1}{c^2}\frac{\partial^2 V}{\partial t^2} \qquad 6$$

Both 5 and 6 are forms of the one dimensional wave equation which have been studied by mathematicians and scientists for many years. The solution to 5 and 6 may be written as

$$P - P_o = F(t + x/c) + f(t - x/c) \qquad 7$$

and

$$V - V_o = \frac{-1}{\rho c}\left\{ F(t + x/c) - f(t - x/c) \right\} \qquad 8$$

Where the functions F and f are arbitary functions that must be differentiable at least twice. The two functions may be thought of as two waves moving in opposite directions, the F wave moving in the -x direction and the f wave in the +x direction. If a system involving a reservoir of constant pressure, a long pipe and a valve is considered, it will be seen that if the valve is closed instantaneously thus shutting off a steady flow of velocity V_o at pressure P_o, then only one of the waves will initially be propagated, depending upon the sign convention used. If this wave is an F type wave then equations 7 and 8 may be written as

$$P - P_o = F(t + x/c)$$

$$V - V_o = \frac{-1}{\rho c} F(t + x/c)$$

which after eliminating the function F gives

$$P - P_o = -\rho c (V - V_o)$$

or generally

$$\Delta P = \rho c \Delta V \qquad 9$$

Equation 9 was first demonstrated by Zhukowsky in 1897 and the pressure rise ΔP due to a velocity change ΔV is known as the Zhukowsky pressure rise. Note that equation 9 was derived using the assumption that only an F type wave was present during the rise of the pressure from P_0 to P. Thus the equation may be used not only for pressure rises due to instantaneous valve closure but closure that occurs in less than one pipe period i.e. before an f type wave is also present. One pipe period has a duration of t_c where

$$t_c = 2L/c$$

where L is the pipe length and c = wave speed.

It is worthwhile to point out that the method of solution of the wave equation just outlined is not the only solution. As pointed out in section 2, operational calculus has been used to advantage with this form of equation and in particular Rich (Ref. 28) has derived solutions for instantaneous valve closure. The form of these solutions is:

$$H = H_0 + \frac{cV_0}{g} \sum_{n=1}^{\infty} (-1)^{n+1} \left\{ 1_{t > \frac{(2n-1)L-x}{c}} - 1_{t > \frac{(2n-1)L+x}{c}} \right\}$$

and

$$V = V_0 \left\{ 1 - \sum_{n=1}^{\infty} (-1)^{n+1} \left\{ 1_{t > \frac{(2n-1)L-x}{c}} - 1_{t > \frac{(2n-1)L+x}{c}} \right\} \right\}$$

where H and V are the transient head and velocity at the valve and H_0 and V_0 are the steady state values.

These equations were obtained using pipe boundary conditions of V = O at x = L (i.e. instantaneous valve closure) and H = a constant at x = O. Thus the pipe line configuration and form of the above equations is shown in Fig. 3a, b and c respectively. Rich also obtained a solution to the equilibriumand continuity equations with a first order* friction term included. The form of solution was complex and only the graph of the solution is shown in fig. 3d. It thus becomes apparent that any direct analytical solution of equations 3 and 4 will be difficult.

To illustrate the relative simplicity of the wave approach, the same system as shown in Fig. 3a will be discussed in detail to show that it yields the same results as those obtained in figs. 3b and 3c. The text is illustrated by Fig. 4.

Initially the flow velocity is V_o and line pressure P_o when instantaneous closure of the valve occurs (Fig. 4a). Just after valve closure, the liquid next to the valve is brought to rest, loses its kinetic energy and increases its pressure. This stretches the pipe wall. The pressure rise may be calculated from equation 9. As other sections of the fluid are brought to rest, the pressure increases in more and more of the fluid and a wave is visualised moving away from the valve, towards the reservoir. Since the wave is moving in the negative x direction it is designated an F type wave. Eventually conditions shown in fig. 4b will be achieved when all the fluid velocity is zero, the fluid is at a high pressure and all the pipe is stretched. This occurs after an interval L/c after valve closure. This is however an unstable situation since the fluid next to the reservoir is at a higher pressure than the fluid in the reservoir and thus fluid will flow out of the pipe at a rate such that the two

*A frictional force proportional to the velocity to the power 1.

pressures are equalised. This velocity is seen to be V_o and conditionsachieve the state shown in fig.4c where the fluid is beginning to move with velocity V_o out of the pipe and the pressure is reducing to the initial pressure Po. As section after section of fluid begins to do this the effect is like that of another wave being transmitted towards the valve, an f type wave this time. Thus in terms of the waves approaching and leaving the reservoir end, both pressure and velocity have been reduced towards negative values and hence the reservoir is attributed with a -1 reflection coefficient.

To return to the situation in fig.4c, the f type wave proceeds towards the valve until it reaches it in a time $t = 2L/c$ as shown in fig.4d. At this instant, the pressure everywhere in the pipe is the steady state pressure Po and the velocity is Vo towards the reservoir. Again an unstable situation occurs since immediately, the liquid column will begin to move away from the valve face and if it does so it will produce a low pressure region in this area. Thus conditions shown in fig.4e will hold where the velocity is zero (since if the liquid did move, a vacuum would be formed) and the pressure adjacent to the valve is reduced causing a contraction of the pipe. This effect 'moves' towards the reservoir end, as shown in fig.4e, as visualised by an F type wave. Since a pressure reduction wave approached the valve, and another pressure reduction wave left it, the valve has effectively reflected the wave without changing its sign and for this reason has a +1 reflection coefficient as far as pressure waves are concerned. After an interval $3L/c$ has elapsed, this F type wave arrives back at the reservoir as shown in fig.4f. At this instant, the velocity everywhere is zero but the pressure is less than the steady state pressure Po. Thus fluid is able to flow from the reservoir into the pipe and will do so at a rate such that the pressures in the reservoir and pipe are equal. This velocity is again Vo and

conditions shown in Fig. 4g are achieved where after the fluid has begun to flow with velocity Vo, the pressure is restored to the steady state value of Po. Once again an f type wave is propagates towards the valve. It will be seen that the reservoir maintains its -1 pressure reflection coefficient since it was a negative pressure wave approaching the reservoir, and a positive pressure wave leaving it. The f type wave illustrated in fig. 4g continues towards the valve and reaches it after an overall interval of $4L/c$ (see fig. 4h). At this instant the velocity everywhere in the pipe is Vo and the pressure is Po. Hence conditions are exactly the same as those at the instant of valve closure. The effect is to reproduce the events described every $4L/c$ seconds and in the case considered the pressure would indefinitely change in accordance with fig. 3b. However pipe friction will gradually dissipate energy and the amplitude of the pressure peaks will diminish until no detectable fluctuation about the mean pressure Po will be observed. It is noteworthy that the pressure drop at the valve end shown in fig. 4e is subject to the limitation of vapour pressure conditions. If the pressure change is sufficient to reduce the pressure to vapour conditions, then the liquid in this region will vapourise, as will the whole column of fluid as the F type wave propagates towards the reservoir.

Using the travelling wave concept and the reflection coefficients derived for a valve and reservoir in the previous example, we can analyse the pressure &flow variations to be expected in a system shown in fig. 5a. This is the case of a flow of fluid down-stream of a valve in a pipe leading to a constant pressure reservoir. Again the initial steady state flow velocity is Vo and head Ho, and the valve closure is assumed to be instantaneous. Positive x is taken to be in the direction of the initial steady flow.

Upon valve closure the fluid must be brought to rest otherwise a vacuum would form at the down-stream face of the valve; in addition the pressure would reduce and the pipe contract. Again the minimum pressure is assumed to be greater than the vapour pressure of the liquid. It will be noted that the instant valve closure occurs conditions in the pipe are precisely those shown in fig. 4d and a short time later as those in 4e. All subsequent flow and pressure fluctuations may be explained in terms of fig. 4 beginning at fig.4d and proceeding through the cycle already described back to the conditions illustrated in fig. 4e. The head and velocity at the valve will thus vary in the manner shown in figs. 5b and 5c respectively.

Although the development of equations 3 and 4 into the wave equation and its subsequent solution has been instructive, it is not a realistic attempt to model the overall system. To do this, frictional effects must be taken into account as well as the terms of the equations which contain x as independant variable. The solutions of equations 3 and 4 are not easy to obtain directly since far fewer standard methods are available for handling partial differential equations as there are for total differential equations. For this reason an attempt will be made to convert equations 3 and 4 into total differential equations which may not lead to a direct analytic solution, but will at least enable a numerical procedure to be applied to them. This conversion is described in the next section.

3.4. Conversion from Partial to Total differential Equations.

Equations (3) and (4) can be combined with the relationship:

$$d\theta = \frac{\partial \theta}{\partial a} da + \frac{\partial \theta}{\partial b} db + \frac{\partial \theta}{\partial c} dc + \ldots\ldots$$

which expresses a relationship between partial and total differential operators, to give the following set of equations.

$$\frac{\partial P}{\partial t} + V\frac{\partial P}{\partial x} + \rho c^2 \frac{\partial V}{\partial x} = 0$$

$$\frac{\partial P}{\partial x} + \rho\left\{\frac{\partial V}{\partial t} + V\frac{\partial V}{\partial x}\right\} + 2\rho\frac{f V|V|}{D} = 0$$

$$\frac{dP}{dt} = \frac{\partial P}{\partial x}\frac{dx}{dt} + \frac{\partial P}{\partial t}$$

$$\frac{dV}{dt} = \frac{\partial V}{\partial x}\frac{dx}{dt} + \frac{\partial V}{\partial t}$$

This set can be written in matrix notation and assuming the unknowns to be the partial differential operators we get:

$$\begin{bmatrix} 1 & 0 & \rho V & \rho \\ V & 1 & \rho c^2 & 0 \\ dx & dt & 0 & 0 \\ 0 & 0 & dx & dt \end{bmatrix} \cdot \begin{bmatrix} \partial P/\partial x \\ \partial P/\partial t \\ \partial V/\partial x \\ \partial V/\partial t \end{bmatrix} = \begin{bmatrix} -2\rho f V|V|/D \\ 0 \\ dP \\ dV \end{bmatrix}$$

or more simply

$$A\,\underline{x} = B \qquad 10$$

This gives the augmented matrix, C.

$$C = \begin{bmatrix} 1 & 0 & \rho V & \rho & -2\rho f V|V|/D \\ V & 1 & \rho c^2 & 0 & 0 \\ dx & dt & 0 & 0 & dP \\ 0 & 0 & dx & dt & dV \end{bmatrix}$$

If we pre-multiply 10 by A^{-1} we get

$$\underline{x} = A^{-1} B$$

which will give a unique solution for $\underline{x}$ if

$$|A| \neq 0$$

since

$$A^{-1} = \frac{Adj\ A}{|A|}$$

However since it is possible for the above inequality not to be true, for a solution still to exist the rank of A must equal the rank of B, which in this case both equal 3. So from the theory of linear equations for Rank A to be 3

$$\begin{vmatrix} -2\rho f V|V|/D & 0 & \rho V & \rho \\ 0 & 1 & \rho c^2 & 0 \\ dP & dt & 0 & 0 \\ dV & 0 & dx & dt \end{vmatrix} = 0 \qquad 11$$

which must hold for the condition when

$$|A| = 0 \qquad 12$$

Expanding (11) gives

$$-\rho c^2 dt^2 + \rho v(v\,dt^2 - dx\,dt) - \rho(v\,dt\,dx - dx^2) = 0$$

$$-\rho c + \rho v^2 - 2\rho v\frac{dx}{dt} - \rho\left(\frac{dx}{dt}\right)^2 = 0$$

$$\rho\left\{\left(\frac{dx}{dt}\right)^2 - 2v\frac{dx}{dt} + (v^2 - c^2)\right\} = 0$$

$$\therefore \frac{dx}{dt} = \frac{2v \pm \sqrt{4v^2 - 4v^2 + 4c^2}}{2}$$

$$\therefore \frac{dx}{dt} = v \pm c \qquad 13$$

Expanding equation (12) gives:

$$\frac{2\rho^2 f v|v| (dt)^2}{D} - \rho v dP dt - \rho(-dP dx - \rho c^2 dv dt) = 0$$

using equation (13)

$$\frac{2\rho^2 f v|v| (dt)^2}{D} - \rho v dP dt + \rho dP dt (v \pm c) + \rho^2 c^2 dv dt = 0$$

$$\rho dt\left\{\frac{2\rho f|v| v c^2}{D} \pm c\frac{dP}{dt} + \rho c^2\frac{dv}{dt}\right\} = 0$$

$$\therefore \rho c^2\frac{dv}{dt} \pm c\frac{dP}{dt} + \frac{2\rho f v|v| c^2}{D} = 0 \qquad 14$$

Thus the two partial differential equations have been transformed into four equations represented by equations (13) and (14). There will be four equations since a positive or negative sign may be taken in both equations 13 and 14. All four equations are shown below,

$$\left.\begin{aligned} &\frac{dV}{dt} + \frac{1}{\rho c}\frac{dP}{dt} + \frac{2f\,V|V|}{D} = 0 \\ &\frac{dx}{dt} = V + C \end{aligned}\right\} \quad + \text{ sign} \qquad 15$$

$$\left.\begin{aligned} &\frac{dV}{dt} - \frac{1}{\rho c}\frac{dP}{dt} + \frac{2f\,V|V|}{D} = 0 \\ &\frac{dx}{dt} = V - c \end{aligned}\right\} \quad - \text{ sign} \qquad 16$$

Finite difference approximations and Characteristics.

In the system set up in the laboratory it was found that the minimum value of c/V was found to be of the order of 500. This implies that equation 13 may be written as

$$\frac{dx}{dt} = c \qquad 17$$

and

$$\frac{dx}{dt} = -c \qquad 18$$

Thus for four equations used to describe the system are (15)→(18). Equations (17) and (18), which must be satisfied if (15) and (16) are true, have a simple interpretation in terms of the x - t plane. They are both straight lines in this plane, equation (17) having a slope of +c and equation (18) a slope of -c. If the conditions at a time t_o are known for all values of x then in the x - t plane this implies that, say, pressure and velocity values are known all along the line L, shown in fig. 6, and in particular the points A and B. Thus if we draw a pair of lines through these points to represent equations (17) and (18) we see that they intersect at point C. The significance of this fact may be understood if equations (15)→(18) are written in finite difference form namely:

$$\frac{\Delta V}{\Delta t} + \frac{1}{\rho c}\frac{\Delta P}{\Delta t} + \frac{2f V|V|}{D} = 0 \qquad 19$$

$$\frac{\Delta x}{\Delta t} = c \qquad 20$$

$$\frac{\Delta V}{\Delta t} - \frac{1}{\rho c}\frac{\Delta P}{\Delta t} + \frac{2f V|V|}{D} = 0 \qquad 21$$

$$\frac{\Delta x}{\Delta t} = -c \qquad 22$$

The above equations may be interpreted as follows. Equation (19) represents the change of the flow parameters (P and V) along the line represented by equation (20). Similarly equation (21) represents a similar change of flow parameters along the line expressed by equation (22). The lines in the x - t plane are defined as characteristics and represents the only paths in this plane along which changes of flow parameters may be calculated. Thus in terms of points shown in fig. 6, equations (19) → (22) may be multiplied through by Δt and written as:

$$V_c - V_A = \frac{-1}{\rho c}(P_c - P_A) - \frac{2f V_A |V_A|}{D} \qquad 23$$

$$V_c - V_B = \frac{1}{\rho c}(P_c - P_B) - \frac{2f V_B |V_B|}{D} \qquad 24$$

Valid only along

$$x_c - x_A = c(t_c - t_A) \qquad 25$$

$$x_c - x_B = -c(t_c - t_A) \qquad 26$$

The friction term in equations (23) and (24) may present some difficulty. This arises since the frictional effects are velocity dependent and since the velocity will in general change along the characteristics, it may be argued that some other velocity may be used to accurately assess frictional losses. In fact a better approximation may be to write the friction term as

$$-\frac{2f}{D}\ \frac{1}{4}(V_A + V_c)|(V_A + V_c)|$$

which averages the velocity between the points A and C in fig. 6. Unfortunately a modification of this nature results in a characteristics type of program being not only larger, but taking more time to run. This will be illustrated after the next stage of the analysis. Subtracting equations (23) and (24) gives

$$V_B - V_A = \frac{-1}{\rho c}\left\{P_c - P_A + P_c - P_B\right\} + \frac{2f}{D}\left\{V_B|V_B| - V_A|V_A|\right\}$$

or $$\frac{1}{\rho c}\,2P_c = (V_A - V_B) + \frac{1}{\rho c}(P_A + P_B) + \frac{2f}{D}\left\{V_B|V_B| - V_A|V_A|\right\}$$

$$\therefore\ P_c = \frac{\rho c}{2}(V_A - V_B) + \frac{(P_A + P_B)}{2} + \frac{f}{D}\left\{V_B|V_B| - V_A|V_A|\right\}\rho c \qquad 27$$

Since all the conditions at points A and B are known, P_c may be determined directly from equation (27) and V_c from either equation (23) or (24) once P_c has been determined. Thus it is possible to determine at all the points along the line L_2 in Fig. 6 the values of pressure and velocity. Thus the solution has been advanced in the x - t plane for a time increment of Δt and consequently the cycle may be repeated indefinitely until sufficient information regarding the flow pattern has been obtained. Returning to the problem of correctly assigning a friction velocity, it will be appreciated that if a mean velocity over the step Δt were used, the R. H. S. of equation 27 would contain the quantity V_c which is, of course, unknown. Thus an iterative procedure would be required to achieve a simultaneous solution for both P_c and V_c. Unless very precise simulation of frictional effects is required, it is generally not necessary to use a mean

velocity for the friction term and this will not be done in this work. Also since the author will be using a value of Δt of the order of 0·001 seconds or less, it is thought that the error involved in neglecting velocity changes over such an interval will not be as great as, say, assuming a steady state friction factor f to be used for unsteady flow.

In the analysis so far, it has been assumed that all the initial conditions are known. This is not, however, all that is needed to proceed with a characteristics type of solution since it will be seen that conditions at the boundaries of the x - t plane have also to be known. This is illustrated in fig. 6 where to obtain conditions at point E, the pressure and flow velocity need to be known at point D, connected to E by a C^+ characteristic. Thus a boundary condition is necessary at time $t = \Delta t$ and it will be seen that knowledge of the boundary conditions are necessary to allow the solution to proceed. Although this aspect of the work will be dealt with fully in section 5, it will be useful to re-write equations (23) and (24) in a simple form that may be used in that section. It will be seen that such a form is

$$V_c = X_1 - X_2 P_c \qquad 28$$

$$V_c = X_3 + X_4 P_c \qquad 29$$

Where the X's are not only a collection of constants, but are a function of the dependant variables of the previous time step which are known. Equations (28) and (29) will thus be used to calculate the dependant variables at internal sections of the x - t plane, advancing the solution in increments of a pre-determined time step Δt

It is apparent from the characteristics shown in Fig. 6 that once a physical system is analysed, the slope of the characteristics in the x - t plane is

also fixed. Also we probably will not need to know the values of the flow variables at all points at a fixed time i.e. all the points along L_2, only some of them. These two factors introduce the idea that there are at least two common ways of proceeding with a characteristics type of solution. The first is that shown in fig. 7a where a number of locations in the x direction are chosen such that the characteristics will give the solution at the next location along in the x direction. This is a technique that may be simply and efficiently programmed but does not have sufficient flexibility to make the method attractive enough. This is due to equations 20 and 22 which expresses the relationship between the time and space intervals as

$$\frac{\Delta x}{\Delta t} = \pm c$$

In fact Streeter (Ref. 79) has shown that for a stable solution to the characteristics equation

$$\Delta x \geqslant \pm c \, \Delta t$$

Thus if the choice of the number of stations at which values of P and V are required is to be changed, then a corresponding change in the time step has to be made to preserve stability of solution. It will be shown in later sections, however, that certain numerical techniques do not lend themselves to a frequent change in integration step length (in time) and such a change may cause instabilities in other equations needed to simulate the boundary conditions. It is also apparent that it is convenient to specify the time step size beforehand since if it is calculated using a prespecified Δx then it may turn out to be something like 0·011967 seconds. This type of result will not make the interpretation or plotting of a programs output easy since it is usual to have time as the major independent variable.

A better method than the exact grid proceedure described above is to interpolate the results to intermediate points as shown in fig. 7b. Thus if conditions are known at points A and B then any quantity 'q' required at P may be linearly interpolated using the expression

$$q_P = q_A + \frac{(\Delta x - \alpha)}{\Delta x}(q_B - q_A)$$

where

$$\alpha = c\Delta t$$

Note that if $\alpha = \Delta x$ then this method is identical with the exact grid method described previously. This method requires more programming since interpolation equations, such as the one shown above, have to be solved for each quantity that has to be known but the system does provide more freedom in the choice of the overall number of computing sections that are needed in the x direction. As an example, in the program eventually developed, the number of computing sections was able to be halved without invalidating the stability criterion mentioned previously. This saved a lot of computing time and the proceedure will be described fully in a later section.

The method using interpolation procedures was adopted for the model developed and a schematic diagram of the procedure is shown in fig. 8. This diagram also shows the downstream pipeline studied along with the pipe notation used and the two types of boundary conditions considered.

4.1. Mechanism of Air Release - Use of Henry's Law.

The object of this section is to derive an expression relating the volume and pressure of a quantity of air that is released from kerosene. The fundamental concept associated with this process is known as Henry's Law and it states "The mass of gas dissolved in a liquid is proportional to the partial pressure of the space above the liquid with which the solution is in equilibrium". Partial pressure being defined as the pressure of the gas if it, and it alone, could occupy the space above the liquid. If the constant of proportionality in Henry's Law is defined as the solubility coefficient, we have:

$$m = K VOL_F \; P$$

If it is assumed that air and kerosene obey Henry's Law then the mass of air dissolved at an initial pressure B will be given by

$$m_1 = K \, VOL_F \, (B - VAP) \qquad 30$$

Supposing the pressure of the kerosene is now lowered to a value P so that some air is released from the kerosene, then the amount remaining in solution is

$$m_2 = K \, VOL_F \, (P - VAP) \qquad 31$$

Thus the total amount of air released, and occupying the space above the kerosene is given by the difference of (30) and (31)

Hence

$$m_R = m_1 - m_2 = K VOL_F \, (B - P) \qquad 32$$

If it is further assumed that the released air obeys the ideal gas equation we can write

$$P . VOL_G = m_R \, R \, T_e \qquad 33$$

and after substituting (33) into (32) we get

$$\frac{P.\,VOL_G}{R\,T_e} = K\,VOL_F\,(B-P)$$

or

$$VOL_G = VOL_F\,K\,R\,T_e\,(B/P - 1) \qquad 34$$

Thus equation (34) could be used to determine K experimentally, as defined on page 78 This would be achieved by noting the volume of air released as a known quantity of kerosene is subjected to a reducing pressure; and plotting VOL_G against (B/P -1). The solubility coefficient is then available from the slope, in units of mass/unit of pressure, per unit vol. of fuel.

It is usual however to define the solubility coefficient in terms of % volumes at N. T. P. /unit of pressure (Ref. 103) and so to achieve this, we need to find a relationship between

K (mass/unit of pressure, unit vol. of fuel)

and C (% Vol. at N. T. P. /unit of pressure)

So if we consider conditions at N. T. P. denoted by subscript o we may write:

$$mR = P_o \forall_o / T_o$$

i.e. $$m = \alpha_1 \forall_o \qquad (\alpha_1 = P_o / R T_o)$$

Now, percentage volume of free air at N. T. P. is given by:

$$\frac{VOL\ (at\ N.T.P)}{VOL_F} \cdot 100$$

$$= \forall_o\ 100 / VOL_F$$

$$= \frac{m T_o R \cdot 100}{P_o\ VOL_F}$$

hence

$$C = \frac{m T_o R\ 100}{P P_o VOL_F} = \frac{K T_o\ 100\ R}{P_o}$$

and substituting into (34) gives

$$VOL_G = VOL_F \cdot \frac{R T_e P_o C}{100\ R T_o} (B/P - 1)$$

$$\therefore \frac{100\ VOL_G\ T_o}{VOL_F\ T_e\ P_o} = C(B/P - 1)$$

if temperature is measured in ^{o}R and pressure in mm of Hg then P_o and T_o can be given values and we get

$$\frac{64{\cdot}74\ VOL_G}{T_e\ VOL_F} = C(B/P - 1) \qquad 35$$

Equation (35) is that derived in Ref. 103 and it is the one which is used to derive the solubility coefficient C. This procedure is described in Appendix 1. This results in a value of

C = 12·3% at atmospheric pressure.

Equation (35) shows that the volume of released air is dependent on

1. Volume of kerosene to give up its air.
2. A solubility coefficient.
3. An assumed constant pressure existing through out the volume of kerosene considered.
4. The prevailing temperature.
5. The pressure at which the fuel was initially saturated.

Factors not taken into account of in the equation are

1. Whether the air has sufficient time to dissolve in the kerosene to fully saturate it.

2. If sufficient agitation was applied to the kerosene at reduced pressure to release all the air.

This being the case, the colume of released air VOL_G, can be regarded as a steady state volume i.e. the volume of air released if the kerosene were subjected to a step decrease in pressure and then agitated for a long time. However, as the scale of hydraulic systems decreases the process of air evolution is required to be investigated over smaller intervals of time. It seems likely that the volume VOL_G will not be reached over one such interval and it requires the study of how fast the air is released for a step change of pressure.

The work published by Szebehely and Schweitzer (Ref. 97) shows the actual volume of air release to be an exponential function of time and also publishes values of the time constant of this exponential process, typically $0{\cdot}2\ \text{sec}^{-1}$ for kerosene.

Thus for a step change in pressure:

$$VOL(t) = VOL_G\,(1 - e^{-\alpha t}) \qquad 36$$

Other figures published by Szebehely and Schweitzer are time constants for the solution process and these are shown to be about 10 times those for air evolution

for aviation fuels. As this implies that it is more difficult to dissolve air in kerosene than to extract it, the fact may help to explain the observations of other workers on this topic. J. Swaffield (Ref. 96) states that when all transients had subsided, the air evolved did not go back into solution. It is possible that when the cavity was subjected to a high pressure, the air began to dissolve in the kerosene at a very slow rate and did not complete its solution, or even really get started, before the high pressure transient had gone.

It was decided to model the rate of air evolution process but difficulty was encountered when attempting to decide when air release should stop. Logically, as long as the pressure of the kerosene remains below that of the initial saturation pressure B, air release would occur. However if the kerosene is subject to a step decrease in pressure from B to P_1 and then left sufficiently long, then equilibrium will be achieved with P_1 as the new saturation pressure. Since the model will proceed with a step change of pressure at each time interval, it is probable that the saturation pressure will effectively decrease and so prevent further air release at a pressure below B.

Due to the nature of the step response features of equation 36 it seemed reasonable to think of the relationship between VOL(t) and VOL_G as

$$VOL(t) = VOL_G / (1 + \tau s) \qquad 37$$

where $\tau = 1/\alpha$ and s is the Laplace operator. This being so, it is possible to use equations (36) and (37) to show what happens to VOL_G and VOL as the pressure P varies. As suggested by (37) VOL is just a lagged version of VOL_G, the degree of lag determined by the time constant τ, see Fig. 9. At point A in Fig. 9, $VOL_G \leq$

VOL_T which indicates the point at which air release stops and re-solution begins. Due to the time scale of the transient events, it was not considered worthwhile at this stage to consider resolution and for the remainder of the model from this time onwards the cavity is assumed to be one of a constant mass of gas undergoing adiabatic compression and expansion.

Returning to the phase in which air release occurs, if the air volume at time $T - \Delta t$ is VOL_{T-1} and at time T, VOL_T, and the pressure of the system decreases in the interval,

$$(T-\Delta t) \leq t < T$$

then air release will occur and the cavity volume will increase as shown in Fig. 10. The maximum theoretical cavity volume will be given by equation (35) but when the rate process of equation (36) is considered, the final volume at the end of the interval will be given by

$$VOL_T = VOL_{T-1} + (VOL_G - VOL_{T-1})(1 - e^{-\alpha \Delta t})$$

This assumes a step decrease in pressure over the time interval, occuring at the beginning of the interval, since the program will proceed with a constant time step we can write the above equation in the form

$$VOL_T = VOL_{T-1} + \beta (VOL_G - VOL_{T-1}) \qquad 38$$

Providing, of course

$$VOL_G \gg VOL_{T-1}$$

and

$$\beta = 1 - e^{-\alpha \Delta t}$$

5.1. Valve Boundary condition - including air release.

The type of system shown in fig. 8 may be investigated using the method of characteristics already described. Since this system will derive the values of the unsteady flow parameters at internal pipe sections only, the variation of the two boundary conditions will have to be expressed mathematically if an overall solution is to be derived. The reservoir end may be defined as a constant pressure source of value PR2 and if this is a known quantity, then the velocity at the end of the pipeline may be calculated from the appropriate characteristic equation. In this case a C^+ characteristic is suitable giving from equation 29

$$V_{RES} = X_3 + X_4 PR2$$

or in terms of the pipe notation used:

$$VV(2,N2+1) = X_3 + X_4 PP(2,N2+1)$$

The valve boundary condition is not so simple since the following sequence of events is assumed to take place. If the system is pressurised then the liquid will dissolve air, in accordance with Henry's Law, at the system pressure. Thus the assumption will be made that the solubility equilibrium pressure is that to which the system is pressurised at the upstream reservoir. Thus it follows that any pressure reduction that the kerosene experiences will be accompanied by air release, again in accordance with Henry's Law. This process will be subject to the rate of release process described in the previous section. It has been suggested (Ref. 97) that for such an air release to occur, microscopic nucleation bubbles must be present, and agitation of the liquid occur. Once the kerosene leaves the upstream tank, it will experience a pressure drop due to friction losses in the upstream pipe which will initiate the process of air release. Also when passing through the ball valve, it will be agitated since the flow pattern is

substantially disturbed particularly for larger angles of valve closure. Thus as the valve closes, the pressure drop across it increases, implying that the pressure at the downstream face of the valve (PP(2,1)) falls. This will again cause a release of air, the amount evolved being dependent upon the magnitude of the pressure drop, and other factors including the volume of liquid considered to release this air. Aspects of air release have been discussed by several research workers in this field, Refs. 66, 63, 73, and the associated phenomenon of fluid vaporisation is usually discussed with it. If no air is released from the kerosene, or any other liquid, the pressure will continue to fall until the pressure equals that of the liquids vapour pressure. When this happens, the liquid will become vapour and the remaining liquid has effectively become separated from the valve body. This phenomenon is called column separation. A similar mechanism may be considered to be in operation when air release occurs. If sufficient air is evolved, then an air pocket or cavity may be considered to exist in the vicinity of the valve, again causing column separation. There is evidence (Ref. 96) that this occurs and implies that the process happens with sufficient rapidity to ignore the gravitational forces tending to make the cavity lie above the liquid.

It must be recognised that if a system is considered over a long time interval then bubbles or cavities will rise through the liquid and such dynamic effects will have to be assessed. In systems exhibiting air or gaseous release, it is commonly assumed that the cavities formed contain not only gas, but the liquid vapour. While it is true that a vapour is always present with a liquid a distinction has to be made between this effect and total vaporisation of a liquid. It may be that to allow for both of these effects that usually the total cavity pressure is assumed to be the sum of the liquid

vapour pressure and the partial pressure of any released gas i.e.

$$P_{CAV} = VAP + \text{partial pressure of air}$$

It will be seen from the above equation, however that if any air is released then the total cavity pressure will never drop to the liquid vapour pressure since the released air must have some pressure. Thus large scale vapourisation of the liquid cannot occur. Whilst some vapour will be present in any cavities formed, as stated above, this effect is considered to be of secondary magnitude when compared with liquid vapourisation and in the subsequent analysis, only air is considered to occupy the cavity formed by subjecting kerosene to a pressure drop.

With the above points in mind, it is possible to summarise the assumptions made concerning the valve end boundary condition. They may be read in conjunction with fig.11 which shows diagramatically, the situation at the downstream face of the valve.

a) No air release occurs in the upstream pipeline.

b) The steady state valve characteristics adequately describe the dynamic valve characteristics.

c) No flow separation occurs, and no cavities are formed, inside the valve body itself.

d) The amount of fuel considered to give up its air is that which has passed through the valve from the time at which valve closure began.

e) Maximum agitation is experienced by the kerosene as it passes through the valve, and the air is released at the valve exit.

f) The released air forms a discrete cavity at the downstream valve face, the various cavity parameters being given by equations (35) and (38).

g) Only air occupies the cavity space at the valve, the effects of kerosene vapour being ignored.

h) The pneumatic ram which closes the valve via a slider linkage, does so with a constant velocity.

i) The cavity volume is small compared with a characteristic volume (Area X Δx) and that the cavity remains stationary.

From fig. 11, we may obtain a continuity equation by considering the cavity namely

$$\text{change in volume} = \Delta VOL = A \int_{T-\Delta t}^{T} (V_{down} - V_{up})\, dt$$

where V_{down} = mean velocity of downstream face of the cavity

$$= \tfrac{1}{2} (VV(2,1) + V(2,1))$$

Similarly

$$V_{up} = \tfrac{1}{2} (VV(1, N1+1) + V(1, N1+1))$$

hence we get for the new cavity volume at time T.

$$VOL_T = VOL_{T-\Delta t} + \tfrac{1}{2} A \Delta t \left\{ VV(2,1) + V(2,1) - VV(1, N1+1) - V(1, N1+1) \right\} \qquad 39$$

Now we can express mathematically the conditions at the valve downstream face while the pressure is falling and the valve is closing. To do this we use assumptions (b) and

(d) along with equations (28), (29), (35), (38) and (39). This gives the following set

$$
\left.
\begin{aligned}
VV(1,N1+1) &= X_1 - X_2\, PP(1,N1+1) \\
VV(2,1) &= X_3 + X_4\, PP(2,1) \\
VOL_G &= \alpha' VOL_{F,T}\,(P_0 / PP(2,1) - 1) \\
VOL_T &= VOL_{T-1} + \beta\,(VOL_G - VOL_{T-1}) \\
VOL_T &= VOL_{T-1} + \tfrac{1}{2} A D t \left\{ VV(2,1) + V(2,1) - VV(1,N1+1) - V(1,N1+1) \right\} \\
Y &= \frac{VV(1,N1+1)}{V_0} \sqrt{\frac{\Delta P_0}{PP(1,N1+1) - PP(2,1)}} \\
VOL_{F,T} &= VOL_{F,T-1} + A\, Dt\, V(1,N1+1)
\end{aligned}
\right\} \text{Set 1}
$$

Thus the seven equations of set 1 above may be solved for the seven unknowns: PP(1,N(1)+1), VV(1,N(1)+1), VV(2,1), PP(2,1), VOLF,T, VOL_T and VOL_G. This is performed at each time step and makes available not only the upstream boundary condition for the downstream pipe, but the downstream boundary condition of the upstream pipe. Thus using the characteristics method and the constant pressure condition for upstream boundary of the upstream pipe (see fig.17). Then the overall flow for both pipes may be calculated.

The above set of equations describe the flow system until such time as the valve is fully closed. If it is further assumed that all column separation effect are ignored in the upstream pipe, then we can see that

$$VV(1,N1+1) = 0$$

while the valve is shut

also $\tau = 0$

Thus the equations of set 1 may be considerably simplified for this phase of the transient, and we may describe the system as:

$$\left.\begin{aligned} VV(1,N1+1) &= X_3 + X_4\, PP(2,1) \\ VOL_T &= VOL_{T-1} + \tfrac{1}{2} A\, DT \{ VV(2,1) + V(2,1) \} \\ VOL_G &= \alpha' (P_0 / PP(2,1) - 1) \\ VOL_T &= VOL_{T-1} + \beta (VOL_G - VOL_{T-1}) \end{aligned}\right\} \text{Set 2}$$

Although the downstream system is of primary interests, the pressure fluctuations at the valve upstream face may be monitored by use of

$$PP(1, N1+1) = X_1 / X_2 \qquad 40$$

This will give the valve-end boundary condition for the upstream pipe and will enable the flow in that pipe to be calculated as the analysis proceeds.

As can be seen from fig. 9, a point comes when air release may be considered to have ceased (point A on fig. 9). Once this point has been reached, no air is either released from, or redissolved in the kerosene. Thus the cavity contains a constant mass of air which will be compressed or expanded depending upon the prevailing pressure gradient and liquid column velocity. The condition for cessation of air release is that

$$VOL_G \leq VOL_{T-1} \qquad 41$$

The air in the cavity undergoes compression and expansion as explained earlier, and the type of process that the expansion and compression assume, are of the form

$$PP(2,1) . (VOL_T)^n = \text{constant} \qquad 42$$

Three typical cases are listed below for the process

n = 1·0 - Isothermal process.

n = 1·2 - Polytropic process.

n = 1·4 - Adiabatic process.

Fig.12 shows the difference in extreme values of n i.e. for an isothermal and adiabatic process. The difference is of the order of 10% in the assessment of the maximum peak pressure, and a negligible amount in the time of occurance of these peaks. It would seem appropriate to assume an adiabatic process for the cavity since no account of heat transfer is taken in the analysis, however the program is written so that any value of n may be used.

Hence once air release has ceased, and the valve is shut, the valve-end boundary conditions for the downstream pipe may be written as:

$$\left.\begin{aligned} PP(2,1)\,(VOL_T)^n &= RTM \\ VV(2,1) &= X_3 + X_4\,PP(2,1) \\ VOL_T &= VOL_{T-1} + \tfrac{1}{2}\,ADt\left\{VV(2,1) + V(2,1)\right\} \end{aligned}\right\} \text{Set 3}$$

Once more the valve-end boundary condition for the upstream pipe is given by equation (40). Note that RTM is a single variable and is constant. Once the condition shown as equation (41) is found to be true, RTM is calculated from the values of pressure and velocity at the previous time step i.e.

$$RTM = P(2,1)\left\{VOL_{T-1}\right\}^n$$

This precludes the calculation of the mass of air in the cavity as well as reading in data to obtain the gas constant for air and the temperature.

Once the physical situation achieves the conditions expressed by the equations of Set 3, no further modifications to the program are assumed to be necessary. The cavity is expanded and compressed and "waterhammer type" pressure transients are propagated within the continuous column of liquid.

Although it will not occur for transient flows with linear valve closure, a fourth case will be considered for completeness. This situation will arise in work with valve stroking programs and studies the situation when cavity collapse occurs while the valve is still open. This pressure rise is assumed to occur with sufficient magnitude that air release ceases. In addition this will complete the set of possible flow conditions due to valve position and air release. This is set out in the table shown below:

Valve Open		Valve Closed
Air evolution	Set 1	Set 2
No air evolution	Set 4	Set 3

For the case of valve open and no air release; the same assumptions as before apply and the equations may be written directly as

$$PP(2,1)\left\{VOL_T\right\}^n = RTM$$

$$\tau = \frac{VV(1,N1+1)}{V_0}\sqrt{\frac{\Delta P_0}{PP(1,N1+1) - PP(2,1)}}$$

$$VV(1,N1+1) = X_1 - X_2\, PP(1,N1+1)$$

$$VV(2,1) = X_3 + X_4\, PP(2,1)$$

$$VOL_T = VOL_{T-1} + \tfrac{1}{2} A\, Dt \left\{ VV(2,1) + V(2,1) - VV(1,N1+1) - V(1,N1+1) \right\}$$

} Set 4

Sets 1, 2, 3 and 4 are solved in Appendices 2a, 2b, 2c and 2d respectively.

5.2. Valve Boundary condition - No air release.

It may be useful in the future to have available a program which does not simulate air release from a quantity of kerosene subject to a pressure drop. It will also be instructive to compare the output of such a program with the output of one which does simulate air release so that the differences may be noted. This will, in fact provide a good test of the benefits of using resources in the investigation of pressure transients including air release mechanisms.

The nature of the two programs is virtually identical; the main difference occurring in the definition of the valve end boundary condition. While the valve is closing and the pressure is falling, no flow separation will occur providing the pressure everywhere in the pipe remains above vapour pressure. Once vapour pressure has been reached at the valve downstream face, the liquid becomes vapour and the remainder of the liquid then moves in a manner determined by the pressure gradient and its initial motion. The vapour cavity forms a constant pressure boundary at the valve end of the liquid column. Since the downstream reservoir pressure will be greater than the vapour pressure acting on the other end of the liquid, the column will experience an acceleration towards the valve. Once flow reversal has occurred, the vapour cavity will decrease in volume as the separated column moves towards the valve. Eventually the vapour cavity will be zero when the column reaches the valve and since it will have a finite velocity at this point, very rapid compression of the liquid will occur and this produces an equally rapid rise of pressure. Once the magnitude of this pressure is greater than that of the downstream reservoir, the column

will be accelerated away from the valve causing column separation once more with a vapour cavity next to the valve. The procedure is repeated until sufficient energy is dissipated by viscous friction and the steady state pressure of the downstream reservoir is achieved.

The above mode of flow may be described mathematically by two sets of equations representing first of all the situation when the valve is closing and the pressure PP(2,1) is above vapour pressure. The same assumptions (except those relating to air evolution) apply and the set of equations may be written directly as:

$$\left.\begin{aligned} VV(1,N1+1) &= X_1 - X_2\, PP(1,N1+1) \\ VV(2,1) &= X_3 + X_4\, PP(2,1) \\ \tau &= \frac{VV(1,N1+1)}{V_0}\sqrt{\frac{\Delta P_0}{PP(1,N1+1) - PP(2,1)}} \\ VV(1,N1+1) &= VV(2,1) \end{aligned}\right\} \text{Set 5}$$

The last equation of set 5 is simply a continuity equation for the control volume around the valve and assumes that the inflow pipe area is equal to the outflow area which is indeed the case in the valve considered. Thus set 5 is a set of four equations in four unknowns VV(1,N(1)+1), PP(1,N(1)+1), VV(2,1), and PP(2,1). Note that in this case, and those preceding cases which considered air release, τ, the valve characteristic is not an unknown. This is due to assumption (h) in the initial set of assumptions; and the fact that the valve is closed in a pre-determined time T_{CLOS}. Thus at any time t the ram has moved a distance x where

$$x = \frac{t}{T_{CLOS}} \cdot \text{Stroke of ram}$$

This is essentially the mathematical representation of assumption (h). We also have the functional relationship between x and the valve angle θ .

$$\theta = f(x)$$

where the nature of the function depends upon the mechanical linkage between the actuator and valve arm. It will be shown in section 7 that we can write

$$\tau = g(\theta)$$

thus

$$\tau = g(\theta) = h(x) = j(t)$$

where f, g, h and j represent "functions of". Thus since t is the master independant variable, τ may be allocated a value for every value of t providing the function j is known.

Returning to the problem of column separation with no air release, we may write down the set of equations that may be considered to apply if the pressure adjacent to the valve downstream face should fall to vapour pressure. The set is:

$$\left.\begin{aligned} VV(1,N1+1) &= X_1 - X_2\, PP(1,N1+1) \\ VV(2,1) &= X_3 + X_4\, VAP \\ \tau &= \frac{VV(1,N1+1)}{V_0}\sqrt{\frac{\Delta P_0}{PP(1,N1+1) - VAP}} \\ VOL_T &= VOL_{T-1} + \tfrac{1}{2} A\, Dt\{VV(2,1)+V(2,1) - VV(1,N1+1) - V(1,N1+1)\} \end{aligned}\right\} \text{Set 6}$$

where VAP is the vapour pressure of the kerosene.

Again four equations in four unknowns VV(1,N(1)+1), PP(1,N(1)+1), VV(2,1) and VOL_T. The solution of the equations is simple and consists of obtaining VV(2,1) directly from the second equation. Eliminating VV(1,N(1)+1) from the first and third equations results in a quadratic in PP(1,N(1)+1) which may be solved directly. The remaining unknown VOL_T is obtained by direct substitution in the last equation.

Once the valve is fully closed the two possibilities outlined above may occur again. If the column is separated then we may write set 6 as:

$$\left.\begin{aligned} PP(1,N1+1) &= X_1 / X_2 \\ VV(2,1) &= X_3 + X_4\ VAP \\ VOL_T &= VOL_{T-1} + \tfrac{1}{2} A\, Dt \left\{ VV(2,1) + V(2,1) \right\} \end{aligned}\right\} \text{Set 7}$$

which is a set of three equations in three unknowns. The method of solution of set 7 is obvious. In this case, no upstream separation is assumed to occur hence VV(1,N(1)+1) = 0.

If there is no separation, and hence the pressure PP(2,1) is above vapour pressure then the fluid velocity adjacent to the downstream face of the valve is zero. Hence we have:

$$PP(1,N1+1) = X_1 / X_2$$

$$PP(2,1) = -X_3 / X_4$$

which enables all the variables to be determined directly. Set 5 is solved in Appendix 2e.

6. Mathematical Modelling.

6.1. Program Philosophy and Development.

The object of developing a program to simulate pressure transient effects was to predict as accurately as possible the magnitude and time of occurrence of the largest pressure likely to be transmitted through the system. It was also felt desirable to reproduce the essential features of unsteady flow and that the collapse and expansion modes of cavities other than that producing the largest pressure rise, should be featured in the model. This requirement becomes dominant in future work when the model will be used in a study of valve-stroking techniques where the mode of flow simulation is more important than predicting the magnitude of pressure peaks.

The model, which takes the form of a digital computer program written in FØRTRAN, was developed specifically for the test rig described in the introduction, but the subroutines can easily be combined with other boundary conditions to simulate most flow systems. Flow separation and air release were modelled using the boundary conditions described in section 3, and the program is known as PTP1 (Pressure Transients Program No.1). The description of each subroutine and its associated flow diagram is given in this section, while appendix 3 gives the program listings along with a record of the most important parameters used in the program, their notation and some values of the data input.

Once PTP1 was developed and working satisfactorily, several other programs were developed from it. The only other one that will be described in this

section is PTP3. PTP3 is a program that simulates separated flow in hydraulic systems, but does not take into account air release. When the pressure falls to vapour pressure at a certain section, separation occurs but the pressure remains at vapour pressure while a cavity exists. Since the major distinguishing features of PTP3 are contained in the subroutine VALVE, only this is described, but a full program listing is included in appendix 3.

6.2. Program Description - Master Segment.

The master segment has two functions. The first is to set up the initial conditions for the variables of the problem either by direct assignment statements, or by reading in their values. The first section of the Master reads in all the data necessary to solve the problem, a full list of input parameters is given with the program listing in Appendix 3. The program then calculates pipe areas, time steps, section lengths and the pressure drop across the two disc valves protecting the pipeline, at the extreme ends. The input data is then written out to identify the run and ensure that it has been read in correctly. The next section calculates the steady state friction drop along the pipeline, for each characteristic length, and assigns the line pressure to the array P; the initial conditions along the pipe are then written out.

The second function of the master segment is to set up a loop in which the time is incremented by DT. The first statement in this loop is labelled 8, and the loop is stopped when TIME is greater than TMAX. A variable TRAT is made equal to the amount of valve closure and several variables are initialised. The next section of program interpolates the arrays PU, VU, PD and VD from the arrays V and P. This enables the correct points to be chosen for the beginning of the characteristic (see Fig. 8). Subroutine CHAR is called which results in the determination of all internal points at the new step, the only remaining one being that at the valve boundary condition. Providing the valve is still open (TIME $>$ T_{CLOS}), subroutine ANGLE is called which results in the determination of THETA and TAU1, needed for valve boundary condition. Subroutine VALVE evaluates the remaining unknowns, and

in the label 7 loop, the V, VV, P and PP arrays are updated in preparation for the next time step. The next section of program determines whether a line of results is to be printed or not, the controlling variable being ICOUNT. The program will print out every ICOUNT time steps, and since this variable is not read in as data, it has to be re-set by an assignment card.

Two forms of print out are available, depending upon whether the valve is open or closed. Since after valve closure occurs only the downstream side of the valve is of interest, only those variables relating to the downstream pipe are displayed. If the valve is still open, however, then both upstream and downstream parameters are printed out. At the end of the loop there is a statement which decides whether TIME is greater than TMAX; if not, control reverts to statement labelled 8 and the loop is repeated. If TIME is greater than TMAX then the run is completed and the program terminated.

6.2.1. Standard Print-out Format.

As explained in the previous section there are two types of format in use. While the valve is closing, the variables are arranged as shown below at each time step that is printed out.

TIME	TAU	THETA	CAVITY VOLUME	VELOCITY U.S.	VELOCITY D.S.
	ITCOUNT	MARKER		PRESSURE U.S.	PRESSURE D.S.

Most of the variables are self explanatory. ITCOUNT is the total number of iterations performed by the various numerical proceedures used in subroutine VALVE, required to obtain an accuracy in the solution better than 0·005%. MARKER indicates which section of VALVE control has been switched to. This depends upon whether the valve is open or closed and if air release is occurring or not. After valve closure, the cavity volume is multiplied by a factor of 1000 to provide greater accuracy for observing the process of cavity collapse.

After total valve closure, the printout format takes the form:

TIME ITCOUNT MARKER CAVITY VOL. VELOCITY D.S. PRESSURE U.S.

6.2.2. Subroutine VALVE.

This subroutine contains the logic and proceedures necessary to solve the valve-end boundary condition, subject to the equations and assumptions described in section 5.1. This subroutine is called once every time step and begins by initialising several variables but only on the first occasion that VALVE is called. Then, variables that will be needed in the subsequent analysis are determined along with a linearly interpolated value of the new pressure PP(2,1) obtained from previous values. This variable is PG. There then follows a logical GOTO statement, the point to which control is transferred depends upon the value of MARKER. There are three possible points to

go to, described by Sets 1, 2 and 3 in section 5.1. The particular means of evaluation of these sets is described in Appendix 2. All of these paths produce the same result, the value of PP(2,1); and each of these paths return control to statement labelled 2. Here, the remaining variables are evaluated and a check made to see whether the cavity is opening or closing. The value of M2 is O when the cavity is opening and 1 when closing. Before control is returned to MASTER, variables needed in VALVE during the next time step are updated.

6.2.3. Subroutine ANGLE.

The object of this subroutine is to calculate, from a given value of TIME, the value of THETA and TAU1 using the information obtained in section 7.4, in particular Fig.13. This valve characteristic is incorporated in an array TANG. This lists values of θ for increments in τ of 0·05. However in the range of τ from 0 to 0·05, the slope of the curve is steep and a linear interpolation between these extreme values will give appreciable error. For this reason this first section is divided into 10 sections to give a closer approximation to the true curve. The values of θ associated with each value of τ is shown in Fig.13. The geometry of the valve linkage is also simulated in this subroutine, the essential features of this geometry are shown in Fig.14. The subroutine begins by calculating the initial angle that the link arm makes with the reference line. This angle is THETAO. Then using the relationship

$$\text{TIME}/T_{CLOS} = \text{DIST}/\text{STROKE}$$

which implies the linear closure, the angle the link arm makes with the datum (PHI) is calculated. From these two angles, THETA the actual valve angle can be determined.

Note that when TAU = 1, THETA = 90 and when TAU = O, THETA = O. The final section of ANGLE sorts through the array TANG until a value of TAU corresponding to THETA is found. This is made difficult due to the non-linear distribution of the values of TAU in TANG due to reasons described previously.

6.2.4. Subroutine CHAR.

CHAR determines the values of flow velocity and pressure at all internal sections of both pipes from information available from the previous time step. The equations that govern the calculation are 23 and 24. The subroutine may be considered to consist of three separate sub-functions. The first is to determine the friction term occurring in equation 14. In this process, the velocity is checked at each section to determine whether the flow is stationary, laminar or turbulent before the appropriate value of the friction factor is calculated from the Reynolds number. Once the friction factor is available, the remainder of the calculation in this section is straightforward. Note that at each characteristic section there are two values of the friction effect to be calculated, one for the upstream interpolation position, and one for the downstream position (see Fig. 8)

The next section of CHAR uses equations 23 and 24, the results from the first portion of CHAR along with the arrays PU, PD, VU and VD interpolated from the previous time step to determine conditions at all sections of the two pipes at the new time step, except of course the boundary conditions. If the pressure at any section should fall to vapour pressure, then that pressure is held at vapour pressure until it increases once more.

The final section of CHAR calculates the boundary conditions of the two pipes at the reservoirs. This is achieved by substituting a constant value of the reservoir pressure into either of equations 23 or 24, to give the flow velocity at that section. By using the "Trace statement numbers" facility of the CDC 6600 computer, it was found that most of the time taken in the running of the program is in fact used up in this subroutine, particularly the first section, in which the frictional effects are calculated. To reduce the time spent in this subroutine, a facility is included which only performs the calculations described for the down-stream pipe only. It is further suggested that if a user wi shes to modify or improve the program with regard to its running economy, then the best results may be achieved by the modification of this subprogram.

6.2.5. Subroutine CHANGE.

Subroutine CHANGE is basically a subprogram which performs Metric - British and British - Metric data conversions. The program PTP1 was intended for use in either metric or British units and so the following procedure was adopted. The program would calculate everything in terms of British units while the input data and the results would be in metric units. Although this may appear inefficient it does provide the facility of enabling the program to be used with either system simply by the removal of a few cards.

Subroutine CHANGE has three sections, the variable ICH deciding where control is placed. Since all input data is in metric units, and the program works in British units, it is necessary to convert the majority of the input data. To do this

CHANGE is called with the control variable ICH equal to 1. This uses the section of subprogram beginning with label 1 and upon completion a return to the master segment is made. To write out data in metric units it is also required that the variables to be printed out are changed to metric units. The second part of CHANGE accomplishes this providing ICH = 2. Once the data of that particular step has been written, it is re-converted to British units so that the subsequent calculations may proceed with consistant units. Thus CHANGE is called once more this time with ICH = 3.

To operate the program in British units all the time it is only necessary to feed in the data in British units and remove all three 'call' statements referring to subroutine CHANGE. The subroutine itself may be removed from the program deck if it is required to economise on core storage.

6.3. Subroutine VALVE - Program PTP3.

As mentioned before, this subroutine models the boundary conditions likely to be experienced at the downstream face of the valve for continuous or separated flow of a liquid which does not absorb or release air. The subprogram begins by calculating various variables which will be used later in the analysis. If the valve is shut when VALVE is called, control is transferred to label 1 which models the system expressed mathematically in section 5.2. for the boundary conditions; control then passes to label 2. If the valve is open at the particular instant concerned, PP(2,1) and VV(2,1) are calculated according to set 5 in section 5.2. and upon completion the control is again transferred to label 2. Here the upstream pipe conditions are evaluated and a check made as to whether PP(2,1) is less than the vapour pressure of the liquid. Providing this pressure is greater than VAP, a return is made to the master segment.

If the pressure is less than or equal to vapour pressure, control is passed to label 3. In this section use is made of set 6 in section 5.2. In this, PP(2,1) is assigned vapour pressure and using this to calculate the values of the remaining variables, including the cavity volume. It was found necessary to determine the exact time at which the pressure at the downstream valve face reached vapour pressure and the section of the program headed by label 6 does this. It also performs a linear interpolation inside the arrays PP and VV so that all of these quantities are referred back to the instant at which vapour pressure appeared. A similar procedure is followed when the vapour cavity collapses and PP(2,1) no longer has the value of vapour pressure.

6.4. Numerical stability of Method of Solution.

When considering the set of equations shown in section 3.1, it might be expected that the method of solving such a set will suffer from numerical instability due to the changing values of the various coefficients in the set. In practice, instability of this nature was not frequently found but problems were encountered in solving the equation; the problems being attributable to the form of the equations rather than the value of some of the coefficients. The trouble invariably occurred at the very beginning of the run and the equation causing the trouble was found to be:

$$\Upsilon = \frac{VV(1,N1+1)}{V_0} \sqrt{\frac{\Delta P_0}{PP(1,N1+1) - PP(2,1)}}$$

belonging to Set.1. The problems occur in the denominator of the square root where, in the case of the spherical plug valve, the pressure drop is relatively small.

In an iterative procedure, each variable has associated with it, a certain range of values within which the variable takes values before converging to a steady solution. This range usually lies on both sides of the actual root, as shown in Fig.15. The problems associated with the above equation are that the ranges of solution for the two variables in the denominator overlap, as shown in Fig.16, so that if at some time in the iteration procedure the variables take the values θ_1 and θ_2 then the result is the square root of a negative number.

So far the cause and effect are easily definable but if the above equation is squared and incorporated into other equations, as described in Appendix 2(a), it would

appear to solve the problem. This is not so, in fact, as the result of squaring such an equation is to render the roots of an equation containing the squared equation very sensitive to parameter change, or changes in the value of the estimated variable. Once this occurs, it is very difficult to work back to find the cause of such sensitivity. This problem may be overcome by some of the methods listed below.

1. Increase the time step of the program so that the changes in the variables become greater in a single step.
2. Begin the iteration with the best guess possible so that the resulting errors are minimal.
3. Use 'double precision' arithmetic to solve the sets of equations for the first few time steps.
4. Modify the method of combining equations to eliminating variables since a different polynomial will have different sensitivity to the guessed value of the variables. This method is rather hit and miss.
5. Use an iterative proceedure which converges from one side of the solution only. This will ensure stability at the expense of longer running time and core store usage.

Once this region of instability does not present problems, convergence to the required root is very rapid for the proceedures employed. It rarely takes more than 3 iterations to produce a root accurate to within 0·005%. Although the iterations performed in the program are done so on a polynomial in the variable, there is another method that is worth consideration. This is "equation iteration" in which the initial guess is substituted directly into one of the equations of, say, Set 1 (section 3.1) to obtain

another variable, rather than combining the equations of the set to form a polynomial in a single unknown. While this method is longer and uses more core, it does give an idea of how all the other unknowns are varying during the iteration and will help to expose whether any of the variables are particularly sensitive to parameter changes. If one is iterating on a polynomial, the changing values of the coefficients is little guide to parameter sensitivity.

6.4.1. Minimisation of run time.

It was found by investigation that the total running time of the program is almost proportional to the number of pipe sections in the downstream pipe. This had the nominal value of 50 but the run time of the program is cut drastically if the number of sections is reduced (see Fig. 37). There is however a tendency to produce less accurate results. The time ratio Tr is defined as the number of seconds of run time needed to produce 1 second of results.

7.1. Description of test rig - Preliminary experimental work.

The facilities for investigating pressure transients on an experimental basis consisted basically of two pipelines; a short and a long one. The majority of the work described was performed using the long pipeline section, a diagram of which appears in fig.17. The overall rig is shown in schematic form in fig.18. The long line is about 65m long and is downstream of a Saunders type E60F16 aircraft fuel valve, shown in figs.19 and 20. The pipe is standard 2" (50·8mm) internal diameter galvanised steel pipe made up in sections of 20' (6·1m). The sections are joined either by flanges or external collars. The short line is of the same pipe as the long line, this time however the object is to study upstream effects so the test valve is situated at the downstream end. The valve for this line is a one-shot quick acting sleeve valve shown in figs. 21 and 22. The main object of the short pipe was to perform tests on items that were to be subject to the passage of pressure waves of a transient nature. The details of this work may be found in Ref. 98. The purpose of including this pipeline in the authors work was to measure the acoustic velocity in kerosene in this type of pipe. The rig was ideally suited for this objective since the quick-acting valve generated a wave front of steep slope. This work will be fully described in section 7.5.

To achieve a long run of pipe in the laboratory, the long pipeline had to be looped. In this fashion four straight runs together with the bends provided about 65m downstream of the Saunders Valve. The upstream pipe was about 5m length. It was realised that any pressure transients travelling along the pipe may be attenuated and reflected at these bends. Swaffield (Ref. 99) found however that providing the radius

of curvature of such bends is greater than about 0·5m then these effects may be neglected. The radius of curvature of the bends in the test rig were of the order of 1·2m. In both long and short pipelines, 14mm tapped tranducer housings were constructed at suitable points. The precise locations are shown in fig. 26.

Both pipelines used the same end reservoirs and to achieve this the short pipe was connected to the long pipe via "swept T" pipe junctions. These may be seen in figs. 23 and 24. The upstream reservoir has a total capacity of $0{\cdot}9m^3$ and pressure tested to 500 KN/m^2. The downstream reservoir was also pressure tested to 500 KN/m^2 although its capacity is $0{\cdot}2m^3$. The downstream reservoir may be seen in fig. 23 along with the two disc valves installed in both pipelines so that when one line is in operation, the other may be protected from an transients generated. In addition the short pipe has to be isolated as it would otherwise form a "short circuit" when the long pipeline needed to be used. These disc valves will, of course affect the steady state conditions in the pipe and this problem is investigated fully in section 7.3. Also to be seen in fig. 23 are the bends in the long pipe configuration together with a pressure transducer location Fig. 24 showing the upstream end of the pipeline includes views of the swept T junctions and shut off valves, transducer locations and pressure control equipment for the upstream reservoir. This reservoir is located outside the laboratory wall and the main inlet and outlet to this tank are shown in Fig. 24. On the same figure are two items of further interest. Firstly the manometer which is connected to the return line. This is located near to valve number 2 so that the effects of throttling the return pump outlet may be observed in terms of the flow circulation. Secondly, simple screw jacks may be observed acting as longitudinal pipe restraints.

Re-cycling of the fuel is achieved by drawing kerosene from the downstream reservoir by means of a Saunders Safran three phase pump and using this to replenish the upstream reservoir. The venturi meter used for flow measurement is located in this return line. Although steady flow tests to determine the characteristics of the four disc valves was considered necessary, it was not thought that significant transients would be reflected, from them due to the passage of a wave. This is due to the fact that they are located very close to the constant pressure reservoirs and will not experience rapid fluctuations in pressure anyway.

The mounting arrangement of the spherical ball valve is shown in fig. 25. The valve support is braced into the floor of the laboratory to provide a restraint against the longitudinal movement of the valve-pipe assembly. The valve actuation mechanism is mounted separately from the valve base plate and pipe so that any impact effect of the actuator is isolated from the pipeline. This means that the pressure transducer located in the vicinity of the valve will not pick up such vibration and interpret them as pressure signals. The actuation mechanism consisted of a double acting pneumatic actuator of 25mm bore, operating a slotted crank on the valve stem similar to that shown in fig.25. A linear displacement transducer was also screwed into the end of the piston rod so that the actuator displacement could be monitored. Although the ball valve is designed for use with 50·8mm bore pipe, its internal bore is less than this (about 49·5mm) and to achieve a connection to the pipe with a minimum of pressure loss, a pair of adaptor rings were manufactured. Fig. 27 shows a dimensioned sketch of the valve, pipe and adaptor rings assembled, together with the location of the two pressure tapping points on either side of the valve. The diameters at these points are indicated since any pressure measurements made at those locations must take into account that the tappings are at different diameters.

The preliminary experimental work may be summarised as follows:-

1. Flow velocity assessment is achieved by determining the venturi meter - manometer characteristic. Fig. 28 shows the velocity plotted against manometer height for the theoretical analysis presented. It also shows the results of an experimental test performed by Swaffied in June 1969. For the work reported here, the theoretical curve is used.
2. The steady state pressure - flow characteristics of the Saunders ball valve were determined experimentally. The results are shown in Fig. 29.
3. The steady state pressure - flow characteristics of the pipeline protection disc valves were measured and the results shown in Fig. 30. Both figs. 29 and 30 are used in the determination of steady state pressures in the mathematical model.
4. The Tau - valve angle characteristic of the Saunders ball valve was determined and the result shown in fig. 31. Since the pressure tappings used in this determination are actually located on the adaptor rings, the rings will have an effect on fig. 31 which, strictly, is not just for the valve but for part of the adaptor rings as well.

7.2. The Use of Manometers on the Test Rig.

Manometers are used for determining differential pressures on the test rig; their main functions being as follows:-

1. A manometer is required to measure the pressure difference across the venturi meter located in the pump return line. This is to determine the steady state flow velocity in the system.
2. A manometer will be used in the determination of the steady state characteristics of the Saunders ball or plug valve.

For the first of these functions, a theoretical relationship between flow velocity and manometer height will be derived. This will enable a working chart to be drawn which will be kept on the test rig itself. The most suitable manometer that was available was graduated in inches of mercury and to ensure a direct comparison of flow velocity with manometer height, the unit of pressure will be considered as a height of mercury in inches.

The general equation for a venturi meter may be written as:

$$V = C_d \sqrt{\frac{2g\,\Delta P}{W(1-a_r^2)}} \qquad 43$$

where V = throat velocity of the fluid.

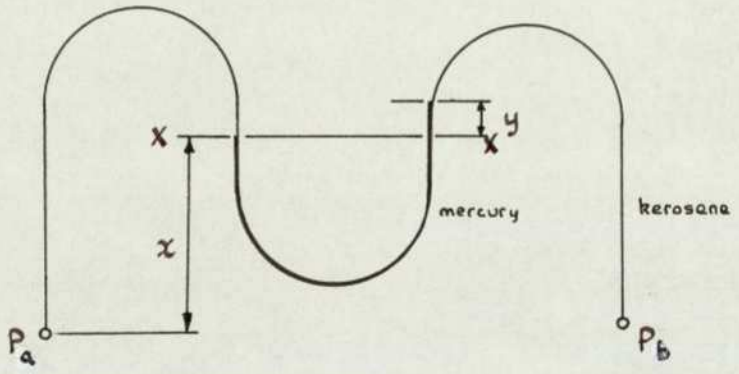
W = specific weight of the fluid.

ΔP = pressure drop between throat and full bore.

a_r = Area ratio of throat to full bore.

C_d = discharge coefficient (supplied by manufactures).

If a simple mercury manometer is connected between the throat and full bore tappings of the venturi meter, then the manometer configuration may be represented by the figure shown below



Thus equating pressures at the level of X - X we get

$$P_a - W_k x - W_k y + W_k y = P_b - W_k x - W_k y + W_m y$$

where W_k = specific weight of kerosene.

and W_m = specific weight of mercury.

thus

$$P_a - P_b = y(W_m - W_k)$$

however $P_a - P_b$ is the same as the pressure ΔP in equation (43) and further, if this pressure is expressed as a head of kerosene we may write

$$\frac{P_a - P_b}{W_k} = \frac{\Delta P}{W_k} = y\left\{\frac{W_m}{W_k} - 1\right\}$$

Since we require the column of mercury to be expressed in inches we have

$$\frac{\Delta P}{W_k} = \frac{y}{12}\left\{\frac{W_m}{W_k} - 1\right\} \qquad 44$$

Now the manufactures supply data on the venturi meter to give

$$\frac{\text{Throat diameter}}{\text{full bore dia}} = \frac{2{\cdot}28}{3{\cdot}81} = 0{\cdot}597.$$

and $C_d = 0{\cdot}975.$

Thus for convenience, maintaining the British system of units we get by substituting (44) into (43).

$$V = 0.975 \sqrt{\frac{y\,(13.6/0.8 - 1)\,64.4}{12\,(1 - (0.597)^4)}}$$

and for the velocity in m/s we obtain:

$$V = 0.3048 \cdot 0.975 \sqrt{\frac{y\,(13.6/0.8 - 1)\,64.4}{12\,(1 - (0.597)^4)}}$$

$$\therefore \quad V = 2.96\sqrt{y} \qquad 45$$

where V = fluid velocity at venturi throat (m/s)

y = manometer height (inches of mercury)

It will be convenient to relate this velocity to the velocity at the Saunders valve by using the continuity relationship:

$$V \cdot \frac{\pi}{4} (2.28)^2 = V^1 \cdot \frac{\pi}{4} (5.1)^2$$

where V^1 = velocity at the valve where the pipe dia = 5·1 cms.

thus the venturi equation may finally be written as:

$$V^1 = 0.2\,V$$

$$\therefore \quad V^1 = 0.2 \cdot 2.96\sqrt{y}$$

$$V^1 = 0.592\sqrt{y} \qquad 46$$

This curve is plotted in fig. 28 and a copy of this graph may be found on the test rig itself.

The second section of manometer theory deals with the measurement of pressures across the Saunders ball valve. As can be seen from fig. 20, the bore of the valve is smaller than the bore of the pipe to which the valve is fitted. To ensure a smooth flow pattern, a pair of transition pieces were manufactured so that a gradual change of effective flow area was accomplished. The two pressure tapping points used in the valve tests are located as near to the valve body as is practical and this meant that these points occurred on the transition sections. Since the inside of the transition sections are tapered, the pressure tapping points are located at different diameters which will affect the static pressure readings obtained at them. This is due to a re-distribution of kinetic energy of the fluid passing these sections so a direct comparison of the measured pressure is impossible. The pipe diameter at the upstream tapping is 48·4 mm while that of the downstream tapping is 53·2 mm. To achieve compatable pressure measurements, it will be necessary to convert the total head at one tapping to an equivalent static and dynamic head at the diameter of the other tapping. This will enable the true difference in static head to be assessed. Using incompressible flow theory we may write

$$\frac{P_1}{\rho} + \frac{V_1^2}{2} = \frac{P_2}{\rho} + \frac{V_2^2}{2}$$

and for continuity:

$$V_1 A_1 = V_2 A_2$$

If we define conditions at section 1 as those in a pipe of diameter 48·4 mm while conditions at 2 refer to a pipe of diameter 53·2 mm we may substitute the continuity equation into the total head equation to obtain

$$\frac{P_1}{\rho} + V_2^2 \frac{A_2^2}{A_1^2} = \frac{P_2}{\rho} + \frac{V_2^2}{2}$$

$$\text{or} \quad P_2 = P_1 + \tfrac{1}{2} \rho V_2^2 \left\{ \left(\frac{d_2}{d_1} \right)^4 - 1 \right\} \qquad 47$$

where ρ is the density of kerosene

and d is the particular pipe diameter.

Thus conditions have all been referred to a pipe of 53·2 mm diameter. Unfortunately the velocity V_2 is unknown, all that is known is the velocity in a pipe of 51·0 mm diameter since this is available from the venturi-manometer equipment described in the previous section.

Thus if conditions at 3 refer to a pipe of 51·0 mm diameter then from the continuity equation we may write

$$V_2 A_2 = V_3 A_3$$

$$\therefore V_2 = V_3 \frac{A_3}{A_2} = V_3 \left(\frac{d_3}{d_2}\right)^2 = V_3 \left(\frac{51.0}{53.2}\right)^2$$

$$\therefore V_2 = 0.91 V_3 \qquad 48$$

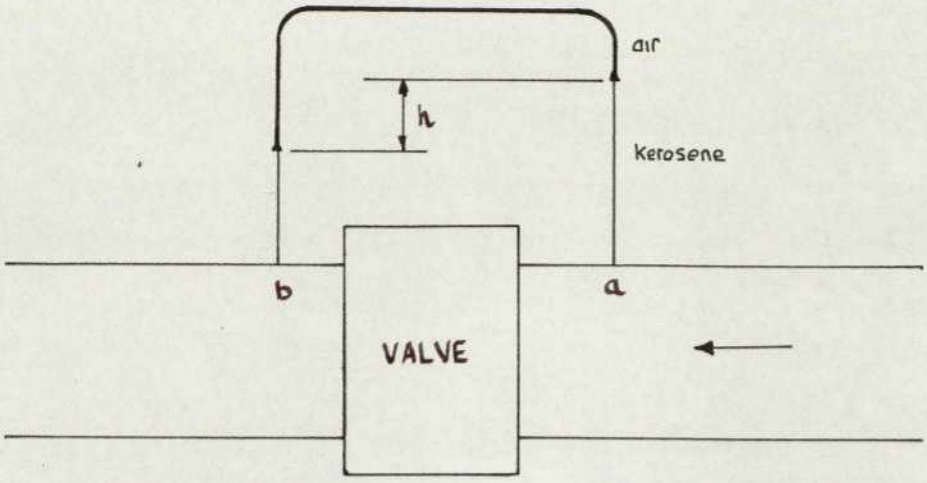
Thus substituting (48) into (47) we get

$$P_2 = P_1 + \tfrac{1}{2}\rho (0.91 V_3)^2 \left\{ \left(\frac{53.2}{48.4}\right)^4 - 1 \right\}$$

$$\therefore P_2 = P_1 + 0.191 \rho V_3^2 \qquad 49$$

i.e. Static pressure in 53·2 mm dia pipe = Static pressure in 48·4 mm pipe + $0.191 \rho V_3^2$

Thus if an inverted manometer is used to measure the pressure drop across the ball valve, as shown below



then we can write

$$h = (P_a - P_b)/\rho_K g \qquad 50$$

where a and b are at different diameters

since $P_a \equiv P_1$ in the preceding analysis, we may write the actual pressure at 'a' as an equivalent pressure P_a' referred to the diameter at 'b'. Thus using equation (49) we have

$$P_a' = P_a + 0{\cdot}191 \rho_K V_3^2$$

thus substituting in (50) above gives

$$h = \frac{P_a' - P_b - 0{\cdot}191 \rho_K V_3^2}{\rho_K g}$$

which may be re-written to evaluate the total static head loss across the valve as:

$$\frac{P_a' - P_b}{\rho_K g} = h + \frac{0{\cdot}191 V_3^2}{g} \qquad 51$$

The second term of equation (51) may be plotted against V_3 as this will provide an easy way of finding the additional quantity to be added onto the measured manometer height. This graph is shown in fig. (33).

7.3. Pressure - flow characteristics of valves for steady state conditions.

As explained in section 3.4, to obtain an accurate characteristics-type solution from a mathematical model, full knowledge of both boundary and initial conditions is necessary. Thus an assessment of all the pressure losses due to friction and changes of sectional area needs to be made of the rig in its steady state condition. Figure 34 shows another schematic diagram of the test rig operating with the long pipe. The figure shows the pressure losses that will occur in the rig when the fluid is circulating, as well as the parameters that were measured to determine the value of the pressure losses illustrated.

With both end reservoirs pressurised and steady flow within the system, the air pressure above the kerosene in the reservoirs was noted. This was measured by using an open ended mercury manometer and the result will thus be a pressure above atmospheric pressure. This gave pressures P_1 and P_2. Also, the static head of kerosene in the reservoirs was recorded giving h_1 and h_2. The pressure drop across the ball valve Δp_1 was measured using the inverted manometer arrangement described and analysed in the previous section. Finally, the steady state flow velocity was obtained using the venturi meter in the pump return line. Table 1, columns 1 → 6 show the results taken from the test rig while columns 7 → 12 list the derived data which will be used in the mathematical model. To obtain greater sensitivity in pressure measurements, the inverted manometer recording the pressure drop across the ball valve was inclined at about 1 in 15 to the horizontal. The analysis of the data is as follows:-

1. Convert all recorded pressures and pressure changes in consistent units such as cms of mercury.
2. Calculate total pressures in the end reservoirs by summing the recorded air pressure and the static head of kerosene.
3. Find the actual measured pressure drop across the ball valve using the slope of the inclined manometer.
4. Correct (3) by the use of equation (51) and fig. 33. This will require a knowledge of the flow velocity obtained from the venturi meter.
5. Using the data supplied by the kerosene manufactures for the kinematic viscosity of the liquid, calculate the Reynolds number for the particular flow.
6. With a knowledge of the Reynolds Number, it can be decided whether the flow is turbulent or laminar and an appropriate friction factor may be used.
7. By measuring the pipe lengths (i.e. both upstream and downstream) the frictional loss in each may be derived providing the friction factor is known and the loss in each pipe is assumed to be proportional to the square of the velocity of the fluid.
8. Add together both pipe losses and the pressure loss through the ball valve and subtract this figure from the difference in total head between the upstream and downstream reservoirs. This figure represents the pressure loss through the two shut off (disc) valves. It is assumed that these two valves are identical and other minor losses due to the pipe bend, flanges and couplings may be neglected.

The analysis outlined above enables figs. 29 and 30 to be drawn. These show the pressure loss, in centimetres of mercury, through both ball and disc valves for a variety of flow conditions. The graphs are in fact plotted against the square of the velocity so that a single steady state valve characteristic may be calculated and used in the mathematical model.

7.4. To determine the τ-θ characteristic of the Spherical Ball Valve.

The series of tests described in section 7.3. derived a steady state flow characteristic for the Saunders ball valve while in the fully open position. The tests described in this section deal with the characteristics of the same valve for varying degrees of valve closure. The valve characteristic may be defined as

$$\tau = \frac{V}{V_0}\sqrt{\frac{\Delta P_0}{\Delta P}}$$

where V and ΔP are the flow velocity through the valve and the pressure drop across it for any valve angle. Vo and ΔP_0 refer to conditions when the valve is fully open. Flow velocity measurement was made using the venturi meter and a manometer was used for pressure measurement. Although it could be argued that since the pressure tapping points are only about 50mm from the valve faces that flow distortion will produce an erroneous manometer reading, it should be remembered that the characteristic sections used in the analysis begin and end at the valve faces themselves. It is for this reason that the valve characteristic is required between the end of the last upstream section and the beginning of the first downstream section, in spite of it being good practice to have pressure measurements some way away from the distorted flow in the region of the valve.

The valve was closed in steps of 5° from the fully open position and after altering the valve position, the rig was left for a few minutes to achieve a steady state. As the valve became closed, the pressure drop across it increased and the inverted manometer which was used for small angles of valve closure had to be replaced by a

mercury manometer. At the valve position at which the change - over occurred, the valve characteristic was calculated for both types of manometer so that it could be checked if the rig had been disturbed in any way. The two values obtained were 0·165 and 0·161 which indicated that the change over had not caused any error in the measurement. At valve angles less than 35° (90° corresponds to fully open, 0° fully shut) insufficient kerosene was flowing through the valve to maintain steady conditions on the downstream side, hence the pressure tapping at this point produced a fluctuating reading. Thus reading were not available for $\theta < 35^{o}$.

All pressure measurements recorded were corrected using fig. 33 and thus allowed for the venturi effect due to the different diameters at which the pressure measurements were taken. Table 2 shows the results of the test and fig. 31 illustrates them together with the extrapolated curve for angles of valve closure less than 35°.

7.5. Determination of Acoustic Speed.

The determination of the wave speed of pressure transients was performed in the short pipeline shown in fig.18. The method consisted of generating a pressure wave of minimum rise time, and observing the passage of such a wave between two transducers located in the pipe. Thus if the time interval between the wave passing two locations can be determined and the distance between the locations is measured, then the wave speed may be calculated directly.

It will be noted that air release and column separation will not influence the values obtained since in the pipeline configuration used, a pressure wave of increasing magnitude will be generated as the pipeline in question is upstream of the quick-acting valve. Also it is this first wave that will be used to determine the wave speed so any negative reflections at the upstream reservoir causing flow separation at the valve end will be of no consequence.

The valve shown in figs. 21 and 22 is used to generate the pressure rise and it is known that it can achieve a closing time of the order of 0·005 seconds. Since the valve has to be closed in less than one pipe period, it is checked to see whether this time is less than a pipe period. The pipe is approximately 12 m in length and a wave speed of 1150 m/s is estimated. Thus a pipe period τ' is give by

$$\tau' = 2L/c = 24/1150 = 0{\cdot}021 \text{ s}$$

Thus the valve will close in less than a single pipe period. The precise nature of the recording of the pressure waves is described in detail in section 8 but basically transducers

measure the pressure which is displayed on an osilloscope. Photographs are taken of the trace and fig. 35 shows two typical results. The time interval measured is the distance between the two points on the photograph where the pressure wave has risen to one half of its maximum rise. This is illustrated in fig. 36. Figs. 35a, and 35b correspond to tests 5 and 8 in Table 8. This table gives the results of 10 tests carried out in the manner described and a mean time of travel for the wave is calculated and found to be 0·0086 seconds. The measured distance between the two transducer was 10·53 m and this gives a wave speed of

$$c = \Delta x / \Delta t = 10{\cdot}53/0{\cdot}0086 = 1228 \text{ m/s}$$

It will be useful to compare this figure with two other theoretical values for the acoustic velocity. The first will be the wave speed in an unconfined expanse of kerosene and the second will be for the actual test rig theoretical wave speed.

The general expression for wave speed is

$$c^2 = K^1/\rho \qquad \text{(Section 3.1.)}$$

for an unconfined fluid $K^1 = K$ = bulk modulus of kerosene, for fluid in a pipeline

$$\frac{1}{K^1} = \frac{1}{K} + \frac{D}{eE}$$

from the test rig

$D = 51{\cdot}0$ mm

$E = 207{\cdot}10^6 \text{KN/m}^2$

$e = 4{\cdot}83$ mm

$\rho = 819{\cdot}0 \text{ Kg/m}^3$

$K = 1{\cdot}26\ 10^6 \text{KN/m}^2$

Thus for an unconfined fluid

$$c = \sqrt{\frac{1{\cdot}26 \cdot 10^9}{819}} = \sqrt{1{\cdot}54 \cdot 10^6} = 1242 \text{ m/s}$$

and for a fluid confined to a pipe specified above we get for the equivalent bulk modulus.

$$\frac{1}{K^1} = \frac{1}{K} + \frac{D}{eE}$$

$$\therefore K^1 = \frac{KeE}{eE + KD}$$

$$= \frac{1{\cdot}26 \cdot 10^9 \cdot 0{\cdot}00483 \cdot 207 \cdot 10^9}{0{\cdot}00483 \cdot 207 \cdot 10^9 + 1{\cdot}26 \cdot 10^9 \cdot 0{\cdot}051}$$

$$= \frac{10^{18} \cdot 1{\cdot}26}{10^9 (1{\cdot}0 + 0{\cdot}0643)}$$

$$= 1{\cdot}182 \cdot 10^9$$

thus

$$c = \sqrt{\frac{1{\cdot}182 \cdot 10^9}{819}} = \sqrt{1{\cdot}445 \cdot 10^6}$$

$$\therefore c = 1207 \text{ m/s}$$

Thus the error between the predicted and measured wave speed is 1·7% which is considered tolerable.

7.6. Measurement and Observation of Pressure Transients.

The Vibro-meter 12QP250 quartz crystal pressure transducer and the Vibrometer TA3C charge amplifier serve a dual function in this research. As well as allowing observations of the pressure transients in the kerosene to be made, they also form an integral part of the servo system to be described later. For this reason the complete specification of these components is left until section 19.5. where their relevance to servo applications is discussed. All that need be said at this stage is that the transducer produces an electrostatic charge when subject to an external pressure and the amplifier converts this charge into a voltage proportional to the measured pressure. The other components used for the measurement of transient pressures due to linear closure will now be outlined.

Linear displacement transducer.

The L. D. T. shown connected to the pneumatic actuator in fig. 25 is a Honeywell LD10 series instrument. The principle of operation is shown in fig. 39 and consists of a four element A. C. bridge circuit; two of the coils being mounted inside the body of the transducer in which a soft iron core is free to move. If this core does move, it will change the relative inductance of the two coils producing an imbalance in the bridge and hence an output signal. The magnitude of this signal will be proportional to the displacement of the core. An oscillator/demodulator unit has to be used with the transducer since the coils must be supplied with a constant frequency input signal. Also since the output will still be of A. C. form it requires demodulation

so that the corresponding D. C. signal may be used to drive a suitable recording device. The oscillator/demodulator used for this purpose is a Honeywell OD31 instrument.

Actuator Limit switches.

It was thought that an accurate assessment of the overall valve closure time could be made by the use of a switching arrangement to detect the extreme positions of the pneumatic actuator. This was accomplished by mounting a pair of lever operated limit switches above the valve linkage mechanism (see fig. 25). Thus by suitable connection of a small D. C. voltage source to these switches, the result of the valve closing would be a square wave voltage output from the switches, the duration of which indicates the valve closure time. The circuit diagram associated with this arrangement is shown in fig. 40.

Tektronix 564 Oscilloscope.

The voltage signals from the linear displacement transducer, limit switches and pressure transducer charge amplifiers were all connected to the 564 storage oscilloscope for observation. While a detailed description of this unit would be inappropriate, a brief description of its operating features would be instructive. The display mechanism may be in storage or non-storage made, the former allowing permanent records to be made with the use of a polaroid camera arrangement. The oscilloscope may be used with a range of amplifier and time base units, depending

upon the application and use of various transducers. The 3A74 four channel amplifier unit was used for all the work reported here; the unit being calibrated regularly by means of a stabilised voltage source available on the oscilloscope itself. The time base used was a type 3B3 which allowed a choice of 20 calibrated sweep rates ranging from 0·5 sec to 1·0 sec per graticule division. The time base unit allowed the trace to be initiated by a change in any of the recorded variables and this feature was particularly useful in achieving consistant traces. Fig. 32 shows a collection of the instruments used to measure the parameters described.

System Calibration.

The linear displacement transducer is simply checked by manually closing the valve so that the actuator moves in constant increments. The corresponding deflection of the oscilloscope trace (run in non-storage mode at a sweep rate of 0·001 sec/graticule div.) showed that the instrument was linear within the measuring capability of the test.

With regard to pressure calibration of the quartz crystal transducer and amplifier, there are three possibilities. Firstly, the manufactures of the amplifier claim that external calibration is rendered unnecessary since a knowledge of the transducers transfer function enables a sensitivity value to be chosen to give any desired calibration factor for the amplifier. This was found to be generally true although factors external to the amplifier such as dampness or bad wiring connectors occasionally altered the effective gain. Secondly, the 'TEST' facility of the charge amplifier, an accurate charge is applied to the input (hence simulating a transducer reading) and enables the

screen deflection of the oscilloscope to be observed. This will provide a check on the overall calibration factor from pressure to oscilloscope screen deflection. Finally, the transducer may be calibrated statically by using a dead-weight testing machine. This method was used several times particularly when the transducers were changed but the results obtained in all the tests corresponded to the figures predicted by the choice of sensitivity value on the charge amplifier.

Test procedure.

The chosen flow velocity and initial line pressure we set by means of the return pump line throttle valve and reservoir air-side inlet valve respectively. The electronics were switched on and checked to be in working order. The rig was left for several minutes to let the electronics become stable and to allow the kerosene to dissolve air at the pressure of the upstream reservoir. During this period the pump was shut down and the pressure of the air supplying the pneumatic actuator adjusted until the required closing time had been achieved. When this had been done, the pump was restarted and the system left to settle.

The oscilloscope was set in triggered mode with the channels of the amplifier unit being allocated to the linear displacement transducer, limit switches and pressure recorded at the downstream face of the valve. The remaining channel was sometimes used to record the pressure at some mid point in the pipe but as this trace is very similar to that recorded at the valve, it was omitted from the traces to aid the reading of the traces already present. The valve was closed by switching a solenoid operated valve which controls the supply of air to the actuator. Simultaneously, the

pump was switched off, since, as some of the transients were observed over a period of about two seconds, the pump may have taken sufficient kerosene from the downstream tank to change the boundary condition. As soon as the oscilloscope sweep was completed the pump was re-started and valve opened so that the fuel could continue to re-circulate.

The traces appearing on the oscilloscope were photographed using a polaroid camera and film, the results being in the form of 10·5 cm x 8·5 cm black and white prints. Most cases considered enabled the reading of the prints with a pair of dividers and a diagonal scale reading to 0·01". If further accuracy is required, the print can be mounted between a piece of perspex and plywood, placed on the crossslide of a lathe and observed through a microscope clamped in the tool holder (see fig.41). Thus by reading the travel of the tool holder using the micrometer dials, accuracy of 0·001" may be achieved.

Although three variables are associated with the experimental work namely flow velocity, line pressure and valve closure time, only the first two were varied in the tests conducted and the valve closure time was held constant at 0·4 s. The type of trace obtained is shown in fig.42 using three channels of the amplifier unit, while fig.43 indicates the repeatability of the experimental results. The results of the tests are shown in figs.44-51. These have been obtained by re-plotting the pressure - time functions from the photographs and superimposing the results from program PTP1 using the same initial conditions and valve closure time. The range of flow parameters used in these test were as wide as possible for the test rig.

8. Discussion and Conclusions.

In the majority of engineering applications of transient flow theory, the occurrence of the first pressure peak is of primary interest since it is the one which will impose the most severe loads on the system considered. The computer model predicts the major peak in the cases considered, which were those approaching the maximum and minimum values of line pressure and flow available on the experimental rig. The absolute values of the maximum error involved were 10% in the prediction of the maximum pressures and 2% in the prediction of the time of occurrence of the peak.

It will be noted that the accuracy, for some cases, is not so good for predicting the behaviour of flow for the remaining peaks and this may be attributed to several factors some of which are listed and discussed below:

1. The assumption that once air release stops, the mass of gas in the system remains constant, is an approximation. Obviously during a high pressure region in the vicinity of the cavity some air must dissolve, even though this region is of short duration, and re-emerge when the pressure begins to fall once more. A direct result of this is to realise that the process that the cavity undergoes will not be strictly of an adiabatic form, however if any sort of process is to be assumed, the adiabatic one does seem the most logical. There is a mechanical analogy with the type of pressure time function obtained from transient work. This is the fact that similar traces are obtained for the response to changing boundary conditions for a second order mechanical system such as a spring-mass-damper combination, where a measure of the energy dissipation per cycle of oscillation is given by the "logrithmic decrement". This is the equation of the exponential envelope curve that encloses the maximum amplitude locus.

A similar curve is obtained if the maximum pressures in a transient graph are joined up; the time constant associated with this curve being a measure of energy dissipation. As can be seen from the predicted/experimental curves (Figs.44-51), the main source of error would appear to be in the assessment of this energy dissipation. This error may be attributed to two main areas; the first is that due to out of phase pipe friction and will be discussed in the next paragraph. The other form of energy transfer not taken into account is that during the expansion and compression of the cavity. Perhaps if the heat transfer effects of the compression could be quantified, then more accurate work would result.

2. The work quoted by Zeilke (Ref.40) would appear to include several features desirable in an accurate model of the frictional effects in unsteady pipe flow. The additional modulation, particularly of the secondary peaks, would no doubt increase the accuracy of the authors work. Unfortunately, no theory could be found to cope adequately with turbulent flow, and as the interval in which the flow was found to be laminar was relatively small, it was not considered economical to include this effect.

3. The program assumes that the actuator closing the valve moves with a linear motion, This assumption stems from a requirement for the application of the program to investigate valve stroking techniques in separated flow. As can be seen from Fig.43 this linear closure is not accurately achieved due to the mechanical response of the piston and rod assembly when the air is suddenly introduced into the cylinder.

4. The assumption made in the Analysis section which states that the air released occurs only as the kerosene passes through the valve, is an approximation. It has been shown (Ref.47) that air release from a liquid subject to a decrease in pressure, is a function of the agitation it experiences. In practical applications, it is difficult even

to define agitation, let alone measure it, and for this reason the value of the time constant for the gas evolution may not be accurate for this type of fuel subject to the degree of agitation it experiences when passing through the valve. Also, with reference to practical systems, air may be released from the liquid before it reaches the valve, by encountering disturbances in the pipe due to flanges, other valves, or junctions. Theoretically it is possible for air release to occur before the liquid reaches the valve due to the pressure drop attributed to friction.

5. There are reasonable grounds for assuming that the air released will coalesce into a discrete cavity at the downstream face of the valve. Swaffield (Ref. 96) performed flow visualisation tests which consisted of a glass section of pipe at the valve downstream section and it appeared that all air released formed a cavity in this region. This is further demonstrated by the authors work which showed a transducer located approximately midway between the valve and downstrem reservoir producing a trace from which the acoustic velocity may be determined. This matched the theoretical wave speed (to within 3%) for that in kerosene with a negligible gas content.

6. A model was developed which included the assumption that the cavity contained vapour as well as air. This model gave results that deviated very little from those of the model just described and so it was decided to modify the assumption to consider air only, as then the model could be operated with more economy. This was also confirmed by discussions with a Chemistry department lecturer who suggested that although vapour always exists in a region next to a liquid the effect increases as the pressure of the liquid approaches its vapour pressure. In all the tests performed with the model, the minimum pressure was never less than about 25 times the vapour pressure of the liquid, at room temperature.

7. It is commonly thought that the more air introduced into a system, the smaller the resulting transient is likely to be. This may not be strictly true since it will depend on when the air is released. For example if more air is released during valve closure then from equation 39 the cavity's downstream face velocity will be a lot larger which effectively means that the valve is not decreasing the momentum of the separated column and a higher pressure peak will result when the column returns, compressing the cavity.

8. As the degree of air release gets smaller, the theory approaches that of the direct analysis of the continuity and equilibrium equations only. The limitations on the program are those imposed by equation 39 which is only an approximation to an integral equation. This tends to become unstable if large changes of cavity volume occur over a single time increment. If this occurs, there are two alternatives. Firstly, a higher order approximation to the integral becomes necessary, the author has found that a Simpsons 3/8 rule is adequate in most cases. If this does not prove successful there is a second feature of the program which effectively divides the time step by 5 while the rate of change of cavity volume exceeds a certain value. This is not generally used when kerosene is being considered due to the large amounts of air released but the study of liquids such as distilled water may make the use of this subroutine necessary.

9. The need for a program to simulate separated flow with air release is shown in Fig. 52. This compares the output from programs PTP1, and PTP3 along with the experimentally derived results for a typical case. It will be seen that the vapour only program grossly over estimates the pressure rise occurring upon cavity collapse, and the time at which the peak occurs is incorrect also by a large degree. Thus in systems where an accurate estimation of pressure transients is required, the problems associated with air release need to be studied.

10. The program PTP1 consists of about 300 cards (including data and control cards), requires about 7,000 words of store and takes 60 seconds (real time) to perform 3000 time increment steps, and produce a line-printer graph of the pressure at the valve against time. The above figures refer only to the CDC 6600 computer. Program PTP3 is somewhat smaller in physical size to PTP1 (about 230 cards) but requires the same amount of core store and running time. The following programs are also available.

a) A program which plots with the line-printer a graph of PP(2,1) against time. This takes negligible extra core but about 3 seconds to produce the graph. This is program PTP2.

b) The time step division mentioned previously adds about 500 words of core but uses a lot more time, depending upon when the subprogram is used, and for how long. This particular subprogram is useful for very rapidly changing boundary conditions or for the simulation of flows of liquids which do not release large quantities of air. This is program PTP4.

9. Introduction to Valve Stroking.

The possibility of controlling the mode of flow in a particular hydraulic system is apparent from a characteristics method approach to it. Since the boundary conditions to a system have to be specified in terms of the other parameters of the system, suitable specification of one or more of the boundary conditions will influence the resulting flow pattern, providing the other remaining boundary conditions are known. Before saying whether the resulting flow is better or worse than the original flow pattern, criteria have to be established and a technique applied to optimise these criteria. In pressure transient work, a criterion is apparent for a single system such as pipe downstream of a valve, feeding a large reservoir, namely to minimise the pressure fluctuation in the pipe when the valve is closed. However, taken in a wider view this may not be the "best" criterion when it is learnt that as the pressure fluctuation in the pipe is reduced, by closing the valve in a certain manner, the time taken to close the valve will increase. Also the transients propagated in the upstream pipe may be substantially worse due to valve stroking for the downstream pipe. Eventually both these conditions will have to be quantified, included with the pressure fluctuation condition, and this will be the criterion to optimise.

However we shall initially consider the pressure change minimisation in a single pipe to be of prime importance. By way of an introduction to the analysis of valve stroking a case such as that shown in Fig. 53 will be considered and friction will be neglected. Most cases of valve stroking considered have the following basic underlying principles (Ref. 37).

1. During 1 round trip wave travel time in the pipe considered, the flow is organised so that the flow velocity is constant throughout the pipe and the hydraulic gradient is straight.
2. During the second, or central phase, the fluid is decelerated, keeping the flow substantially constant throughout the pipe in the pipe.
3. Finally in 1 round trip wave travel time, the flow velocity is brought to zero and the hydraulic gradient is horizontal and at its steady-state value.

If these conditions are achieved successfully then once the valve motion ceases the flow will be zero everywhere in the pipe and there will be no pressure gradients present. Thus there will be no transient flow.

9.1. Valve Stroking Without friction and separation.

The case considered is that shown in Fig. 53. As no friction is present the head Ho is constant along the pipe, Hmin being the minimum head that it is desired should be present at any time in the pipe. In this analysis dimensionless variablesare used, these being defined thus:

$$B = cV_o / gH_o$$

$$h_m = H_{min} / H_o$$

$$t' = \frac{t}{2L/c}$$

$$V = \text{Velocity at time } t / V_o$$

$$h = H / H_o$$

where c = speed of sound in fluid and pipe considered.

g = acceleration due to gravity.

Vo = Initial flow velocity.

Ho = Initial static head.

t = time.

L = Pipe length.

For this analysis, a graphical solution will be drawn as this demonstrates the technique clearly. Fig. 54 shows the wave traversing the pipe whilst Fig. 55 shows the head - velocity diagram. If for the 1st phase the head at the valve is reduced linearly from 1

to hm in 1 unit of dimensionless time we can see from Fig. 55 that the hydraulic gradient is straight, between the two limits of 1 and hm, and the velocity is uniform at V_1.

Since $$B = dh / dV$$

and the velocity is uniform in the pipe

$$V_1 = V_{01} - (h_m - 1) / B \qquad \text{at } t' = 1$$

Since the head and hence velocity change was linear with time we can derive the required valve motion, since

$$\tau = \frac{V}{\sqrt{h}} = \frac{V_{01} - (V_{01} - V_1) t'}{\sqrt{1 - (1 - h_m) t'}}$$

for

$$0 \leq t' < 1$$

Now for the second phase, the head at the valve is kept constant at its minimum value hm, and the water column is decelerated. This is shown by the fact that when a wave travels from A1 to E1$\frac{1}{2}$ in Fig. 55, the velocity change is

$$dV = -(1 - h_m) / B$$

This takes place in $\frac{1}{2}$ dimensionless unit of time, hence the deceleration is given by

$$dV/dt' = -2(1 - h_m) / B$$

which is the uniform deceleration of the water column. This equation can be integrated using the initial condition

$$V = V_1 \qquad \text{when} \qquad t' = 1$$

hence $$\int_{V_1}^{V} dV = \int_{1}^{t'} -2(1-h_m)/B \; dt'$$

$$V - V_1 = -2(1-h_m)(t'-1)/B$$

$$\therefore \; V = V_1 - 2(1-h_m)(t'-1)/B$$

Once again we can determine the required valve motion to produce this flow as:

$$\tau = \frac{V}{\sqrt{h}} = \frac{1}{\sqrt{h_m}} \left\{ V_1 - 2(1-h_m)(t'-1)/B \right\}$$

It is apparent that the flow is decelerating and the valve closing during the central phase if the physical situation is investigated closely. When the valve begins to close, a pressure wave is propagated down the pipe while the pressure at the valve falls. The pressure wave reflects from the downstream reservoir as a pressure rise wave and arrives back at the valve after 1 unit of dimensionless time. At this time the pressure at the valve has fallen to the minimum required and at which value it is required to be kept. If the valve motion continued as in the first phase, the pressure at the valve would rise due to the returning wave, hence the valve is now closed at a greater rate which produced a further pressure drop equal in magnitude to the pressure rise of the returning wave. The algebraic sum of pressures at the valve reveals that it is still at the required minimum even though the valve is still closing and hence reducing the flow velocity.

The second or central phase is continued until such time as the flow has been reduced to a state that can be returned to the original head and zero velocity in one pipe period. This flow velocity is V_2 on Fig. 55. During the final phase, the head at A is increased from its minimum value of hm at $t^1 = t^1_c - 1$ to its steady state value of 1 at $t^1 = t^1_c$. From Fig. 55 it can be seen that at the end of the final phase all points in the pipeline are back to the original head and the velocity is zero everywhere. There are no transients. We can now determine the valve motion over this final period.

$$V_2 = 0 + (1 - h_m)/B$$
$$= (1 - h_m)/B$$

Since the velocity at A reduces linearly with time:

$$\tau = \frac{V}{\sqrt{h}} = \frac{V_2 (t_c' - t_1')}{\sqrt{1 - (1-h_m)(t_c' - t')}}$$

during the period

$$(t_c' - 1) \leq t' \leq t_c'$$

The total closing time (dimensionless) is two plus the time for the central phase or:

$$t_c' = 1 + BV_{01}/2(1-h_m)$$

9.2. Valve Stroking with Friction.

The main problem at this stage appears to be relating this technique to real systems i.e. those including friction since the graphical procedure just described is no longer accurate. This leads to difficulties in determining the time for the central phase. In the analysis that follows the fluid is considered incompressable and the resulting free-body diagram of the water column downstream of the valve appears in Fig. 56 with the prevailing forces on it shown.

where P = Pressure on downstream side of valve.

This is to vary in the manner described in the previous section

Po = Constant reservoir pressure acting on downstream face of fluid column.

P_F = Total pressure loss due to pipe friction.

V = Instantaneous real (not nodimensional) velocity of water column.

V_o = Initial fluid velocity.

A = Cross-sectional area of pipe and fluid considered:

We can now apply Newtons' second law to the liquid column

$$A\{P - P_F - P_o\} = \frac{d}{dt}(\rho A L V)$$

$$= \rho A L \frac{dV}{dt}$$

Now the friction loss term is a function of velocity namely

$$P_F = 4 f L V^2 / 2 d g$$

The P term is a function of time as shown by the frictionless case considered previously.

The term Po is constant. Hence we can write

$$\frac{dV}{dt} = \frac{1}{\rho L}\left\{ P(t) - 4fLV^2/2dg - P_o \right\}$$

which is a non-linear 1st order differential equation not lending itself to simple integration. The pressure just down-stream of the valve is expressible for the three stages of valve stroking, as follows:

for Stage 1 $$P = P_o\left\{1 - (P_o - P_{min})t/\alpha\right\}$$

for Stage 2 $$P = P_{min}$$

for Stage 3 $$P = P_o\left\{1 - (P_o - P_{min})t/\alpha\right\}$$

where $$\alpha = 2L/c$$

Thus for stages 1 and 3 the correct expression for P can be inserted in the differential equation above and a numerical Runge - Kutta method used to integrate the expression from known initial conditions. For example in stage 1, when $t = 0$ $V = Vo$. The variable t is incremented in steps and the procedure enables the velocity V at that time to be determined. Since the first phase lasts for 1 pipe period, the velocity at the end of the first phase can be determined i.e. V_1 (corresponding to V_1 in Fig. 55). Note that for stage 3 the final condition, and not the initial condition is known i.e. $V = O$ when $t = t_c$. In this case the solution may proceeds backwards in time from an initial condition $V = O$ when $t = O$ and calculates the velocity after a total negative time increment of 1 pipe period. This enables V_2 to be found.

For stage two however an exact solution can be found since the differential equation reduces to a linear one with one dependent variable V

$$\frac{dV}{dt} = \frac{1}{\rho L}\left\{ P_{min} - 4fLV^2/2dg - P_o \right\}$$

which is of the form

$$\frac{dV}{dt} = -A(D + EV^2)$$

where A, D and E are constants (since P_{min} is constant)

i.e.

$$\frac{dV}{dt} = -EA\left\{ \frac{D}{E} + V^2 \right\}$$

$$\therefore \quad dt = \frac{-1}{EA}\left\{ \frac{dV}{B^2 + V^2} \right\}$$

where

$$B^2 = D/E$$

This can now be integrated over the central phase to find the duration of it since during the central phase the velocity change is from V_1 to V_2 i.e.

$$\int_{t_1}^{t_2} dt = \frac{-1}{EA} \int_{V_1}^{V_2} \frac{dV}{(B^2 + V^2)}$$

$$\therefore \Delta t_{Phase\ 2} = -\frac{1}{AEB} \left| \tan^{-1} \frac{V}{A} \right|_{V_1}^{V_2}$$

A program was written which performs all these functions, namely:

1. Given initial and final conditions, a numerical integration technique is employed to give the velocity at the end of phase 1, and the velocity at the beginning of phase 3.

2. Using the two velocities, calculates the time needed during phase 2 and hence calculates the total required time to close the valve.

The program (called VSP3) is fully described and listed in appendix 4b at the end of the work reported. The results of the program are shown in Fig. 57. A range of flow rates was supplied as data along with the initial line pressure and the required minimum line pressure. The time required to close the valve was found to be dependant only on the overall pressure change from initial line pressure to minimum line pressure, for the same velocity. For example, at a line velocity of 1 m/s, the valve will be closed in the same time if the pressure variation is from 180 to 100 KN/m^2 or if the variation is form 150 to 70 Kn/m^2. This is apparent from the free-body diagram Fig. 56, since Po is dependant on the initial line pressure and velocity; the column of liquid being retarded by the effective pressure difference between its two ends.

Ths use of this analysis may be demonstrated by modifying slightly Program PTP1. If, in Subroutine VALVE, the pressure just downstream of the valve is forced to take values in accordance with the theory outlined then the overall valve closure time may be evaluated using the results from program VSP3. This enables an investigation to be made into the effectiveness of valve stroking principles via a theoretical model. This was done and the results, shown in fig. 58, are presented in the pressure velocity plane. The results are the variation in pressure and flow just downstream of the closing valve. It is apparent that the method works even though small transients may still be observed once valve closure is complete. This indicates that the theory is valid providing the required pressure time function at the boundary can be achieved.

9.3. Parameter limitations for High Friction Systems.

The previous analysis including friction gives good results for the elimination of pressure transients (within 5%) for low friction systems. The study of high friction systems, i.e. long pipes or high flow rates, leads to certain limitations on the assumptions made and upon the use of valve stroking as a means of eliminating pressure surges. The consideration of air release in the region of controlled pressure leads to an almost impossible situation with regard to exact pressure control.

Neglecting the air release for the moment, the major limitation on valve stroking as applied to high friction systems is the ability to retard the liquid column during the central phase. The three basic criteria (page 39) are still applied and the solution can be made more accurate by taking better approximations for the head loss due to friction. During the central phase however, the liquid column has to retard and this implies that

$$P_{min} > P_F + P_o$$

since $P_F = f(V)$ the above equation is assumed to be valid at $V = V_1$ in the notation of Fig. 55. If the equation is not satisfied, the liquid column will not decelerate but will accelerate until the frictional resistance equals the net accelerating force. Since P_F will be small compared to PR2 at $V = V_1$ we can make the approximation that valve stroking can occur only if

$$P_{min} > P_o$$

In low friction cases the pressure drop along the pipe may only be small and hence the above condition is likely to be true. To give an example, consider a flow of 2·75 m/s

through a 51 mm dia pipe with an upstream tank pressure of 275 KN/m^2 and variable length pipe, downstream of a valve situated about 5·5 m from the upstream tank. For a 9·1 m downstream pipe, the pressure at the end will have dropped to 247 Kn/m^2 hence the minimum pressure during the central phase cannot be between 247 Kn/m^2 and 275 KN/m^2. Obviously this leaves plenty of choice. If the pipe is 55 m long however, the downstream pressure will have dropped to something like 178 KN/m^2 and this means that the minimum value of the pressure during the central phase will have to be less than 178 KN/m^2 which is a relatively severe limitation.

9.4. Time criterion and Linear Closure.

As has already been stated, some concept will have to be derived which, when tested, will decide whether a particular mode of valve closure is good or bad. From the work described in sections 7 and 8 on the operation of the model for pressure transients in the pipe system considered,a situation exists which defines a standard closure as one in which the actuator closing the valve moves with constant velocity. Thus a controlled valve closure is considered to be worthwhile if the pressure fluctuation in the pipe before and after the valve has shut, is less than a linear or standard valve closure from the same initial flow parameters, and occuring in the same interval of time. This criterion will be used to judge all the methods of valve stroking proposed but will be redefined in terms of a function which is measurable.

A function, ϕ, may be defined as the ratio of the pressure fluctuation (about the pressure of the downstream reservoir) for controlled valve closure, to the fluctuation about the same pressure produced by a linear closure in the same time interval i.e.

$$\phi = (\hat{P}_c - P_0) / (\hat{P}_L - P_0)$$

The function ϕ is an easy indication as to whether controlled valve closure is a worthwhile proposition under any given circumstances. Ideally ϕ requires minimisation and if ϕ is always greater than unity then less damage will occur in the system if linear closure is used. Realising that controlled closure is more expensive than ordinary linear closure, the evaluation of ϕ for a particular system may enable a decision to be

made upon the value of valve stroking. For ideal valve stroking $\emptyset = O$, but it should be emphasised that this function will provide an indication of the merit of the method of valve closure, independant of that method.

10. Valve stroking with cavity formation.

Once air release is considered to influence pressure transients, the exact solution of valve stroking requirements and equations becomes difficult. This is mainly due to the fact that the cavity parameter equations (for pressure and volume) are not only dependent on time, but on several other initial conditions such as liquid saturation pressure and rate of air release coefficient etc. which have, as yet, not been included in the analysis. Thus while it may be possible to obtain an exact solution to the equations specifying the first phase, it will not be possible to do the same for phase 3 since the solution will depend upon the cavity volume at the beginning of phase 3, this in turn being dependant upon the duration of phase 2. As this is not known an exact solution cannot be found, and implies that conditions of phases 1 and 3 cannot be achieved simultaneously.

Since the major work of other authors (Refs. 80, 84) was concerned only with pressure rise on the upstream side of a closing valve, air release would not appear to be significant since there would be no cavity formation if valve stroking principles could be achieved. However since the valve closing mechanism performance will become a significant effect in systems with pipe periods sufficiently small, exact valve stroking will probably not be achieved even on upstream side pipelines, and the question of air release will arise in these systems.

Returning to the case of a pipe downstream of a valve, it is possible to check the effectiveness of valve stroking in systems with cavity formation by effectively

"forcing" the pressure adjacent to the downstream valve face to be equal to any desired value. It will be recalled from section 5.1. that the set of equations defining the upstream boundary condition, at the valve, is:

$$VV(1, N1+1) = X_1 - X_2\, PP(1, N1+1)$$

$$VV(2,1) = X_3 + X_4\, PP(2,1)$$

$$VOL_G = \alpha' \left(P_0 / PP(2,1) - 1 \right)$$

$$VOL_T = VOL_{T-1} + \beta \left(VOL_G - VOL_{T-1} \right)$$

$$VOL_T = VOL_{T-1} + \tfrac{1}{2} A D t \left\{ VV(2,1) + V(2,1) - VV(1,N1+1) - V(1,N1+1) \right\}$$

$$\Upsilon = \frac{VV(1,N1+1)}{V_0} \sqrt{\frac{\Delta P_0}{PP(1,N1+1) - PP(2,1)}}$$

$$VOL_{F,T} = VOL_{F,T-1} + A D t\, V(1,N1+1)$$

Thus we can define PP(2,1) in the second equation above at each time step in accordance with classical valve stroking principles outlined in section 9.1. Since the above set of 7 equations can be solved for the seven unknowns, defining PP(2,1) will make one variable redundant. This variable is Υ, the valve characteristic. Once the other variables have been calculated, Υ will also be determined so that an indication of the mode of valve closure will be available even though this parameter will have no effect on other parameters in the subsequent flow.

It is easy to modify program PTP1 so that the pressure PP(2,1) is defined for all intervals of time up to valve closure. The majority of the program is identical to that of PTP1, the differences being in subroutine VALVE.

When the program is run it appears that if pressure PP(2,1) can by some means be made to follow the time history demanded by classical valve stroking,

then again the elimination of pressure transients is complete. There are two features, however which are available from the printout which indicate that for real systems, this will be impossible. The first feature is the rapid valve closure to produce the linear drop in pressure in one pipe period. In the case considered, the valve has to rotate about 30° in 10 m secs which is an almost impossible performance standard for a low power servo system. This feature will of course depend upon the type of valve used to control the flow; in this case it may be possible to begin with the valve partially closed instead of fully open to ease the large angular accelerations required.

A point of more significance is encountered when the pressure in the cavity has to increase at a fixed rate, to fulfil phase 3 of valve stroking principles. It can be seen from the program output (Fig. 59) that at this point, the velocity of the upstream column of fluid increases instantaneously to a large value. This effect is best understood from consideration of the equation of the cavity volume and its relationship to its interface velocities namely

$$d\forall / dt = A (V_{ds} - V_{us})$$

where $\forall$ = cavity volume, A = area of pipe.

V_{ds} = velocity of downstream liquid/cavity interface.

V_{us} = velocity of upstream liquid/cavity interface.

Since phase 3 requires dp/dt = a constant

and it may be assumed that $p.\forall$ = a constant = a_1

then

$$\frac{dp}{dt} = \frac{dp}{d\forall} \cdot \frac{d\forall}{dt}$$

$$\therefore \frac{dp}{dt} = \frac{-a_1}{\forall^2} \left\{ A (V_{ds} - V_{us}) \right\}$$

thus $V_{us} > V_{ds}$ for dp/dt to be greater than zero. However generally, while the valve is closing, the cavity is growing in volume and hence $V_{ds} > V_{us}$ This accounts for the rapid acceleration observed in the theoretical model. In physical terms, classical valve stroking achieves a pressure rise in the continuous column of fluid by means of a change of velocity induced by either partial valve opening or a reduction in the rate of closing. This follows from the equation

$$\Delta P = B \Delta V$$

where the constant, B, is a function of the bulk modulus of the liquid flowing. However if a cavity exists in the region of controlled pressure then the bulk modulus will be that of the cavity contents and not the liquid in the rest of the system; since it is assumed that the cavity content is air, then the pressure rise the air experiences due to a change of velocity compressing the cavity, will be less than that experienced by liquid. Since the pressure rise is predetermined (as dp/dt in phase 3) then the velocity changes associated with cavity compression will be far higher than those encountered in non-separated flow, to produce the required pressure rise.

It will be impossible to produce such a rapid acceleration of the upstream column since the valve can only open fully and produce conditions for maximum acceleration of the upstream column. The magnitude of the acceleration will largely depend upon the pressure difference across the column at the instant of valve re-opening, but it will invariably be less than the acceleration required. Thus it would seem impossible to reproduce exactly the precise requirements of all three phases of classical valve stroking as proposed by Streeter. It will not be possible to investigate how the deviations from the ideal method will effect the overall concept of controlled flow, until the valve operating servo system is modelled also. This will enable an investigation into the maximum

acceleration of the upstream column (hence the rate of increase in pressure) to be undertaken, including the effects of the dynamic lags involved in opening the valve.

11. The Nature of Pressure transients for Approximate Analysis.

The estimation of pressure transients in separated flow has been shown to be difficult even for the most elementary cases. It has also been shown that the assumption of cavity formation at the valve will produce the type of flow pattern, if not exact in magnitude and frequency, to be found after valve closure (see Figs. 44→51). This would indicate that the total transient pressure function is the summation of two distinct patterns. The first is due to the traditional "waterhammer" waves propagated in the fluid due to the fluctuation of boundary conditions. The second pattern is that produced by repeatedly compressing and expanding a pocket of air at one end of the fluid column. The magnitude of this pressure will depend upon the initial conditions in the pipe, such as fluid velocity, and cavity volume, at the instant of valve closure.

It has been shown that of the two undesirable features arising from the previous section, the accurate achievement of Phase 3 will cause most trouble. Since this phase occurs at fluid velocities less than those at the commencement of valve operation, it could be argued that to a first approximation it may be possible to ignore the transient pattern due to classical waterhammer since the magnitude of this effect will be dependant upon the velocity distribution in the downstream column. This implies that the transients model used in the discussion and derivation of alternative valve stroking techniques will have the essential features of the system shown in Fig. 60, although any computer model will of course include both effects unless otherwise stated.

The approximation mode above is further justified when the results from the computer model PTP1 are studied. Fig. 61 shows the pressure time traces from a point in the pipeline for a typical flow case and valve closure. The graph shows the

pressure fluctuation at a point approximately half way between the valve and the downstream reservoir. Thus the trace may be assumed to show pressure fluctuations in the separated column. Experimental observations confirm the form of fig. 61. Noting that the pipe period is about 0·11 seconds, it is obvious that the peaks shown are not a feature of classical waterhammer since the interval between them is so long compared to one pipe period. They are more attributable to a mass-oscillation theory. Waterhammer type pressure fluctuations are observed in the lower trace as expected but this effect is very much dominated by the pressure changes induced by cavity expansion and compression. Note that the peak pressure generated at the valve by cavity compression is transmitted through the separated column which would not be expected if the column were assumed rigid. Thus the phenomenon shown in fig. 61 is best described as mass-oscillation with compressible liquid.

12. Alternative Methods of Valve Stroking - Proposed Method 1.

From the arguments of the previous sections, it is apparent that some other forms of valve stroking should be put forward for dealing with separated flow conditions. Although it is not suggested that the methods proposed are in any way exact, it will be seen that they all attempt to reduce the effect of pressure transients based on the linear closure criterion defined in section 9.4.

Method 1.

The first method will be more clear if the equations of motion for the system shown in fig. 60 are written down and solved. The solution will be in the pressure velocity plane as this will give a better understanding of what is trying to be achieved in the physical situation.

Newtons 2nd law gives:

$$\frac{d}{dt}(\rho A L V) = A(P - P_o) \qquad \text{neglecting friction.}$$

leading to

$$\frac{dV}{dt} = a_1 (P - P_o) \qquad 52$$

Equation of state for an ideal gas gives

$$P . \forall . = a_2 \qquad 53$$

Equation of continuity for the cavity gives

$$\frac{d\forall}{dt} = A V \qquad 54$$

from equation 53

$$\forall = a_2 / P$$

$$\therefore \frac{dA}{dt} = \frac{dA}{dP} \cdot \frac{dP}{dt}$$

$$= \frac{a_2}{P^2} \frac{dP}{dt} = a_3 V \qquad \text{if } A = a_3$$

$$\therefore \frac{dP}{dt} = -\frac{a_3}{a_2} V P^2$$

Since

$$\frac{dV}{dt} = \frac{dV}{dP} \cdot \frac{dP}{dt}$$

and from equation (1)

$$\frac{dV}{dt} = a_1 (P - P_0)$$

we get

$$\frac{dV}{dP} = \frac{a_1 a_2}{a_3} \left\{ \frac{P_0}{P} - 1 \right\} \frac{1}{PV} \qquad 55$$

Reconsidering the physical situation shown in Fig. 60, it will be found that if the initial conditions are Pa, and zero velocity, the resulting mode of flow will be as shown in fig. 62. This will be illustrated by considering the four regions R1, R2, R3 and R4. In R1, if $P > P_0$ the liquid column will accelerate in a positive direction, causing the cavity to expand and its pressure P to fall. When P = Po, dv/dt = O, from equation 52 and when $P < P_0$, the column will decelerate since dv/dt $<$ O from equation 52 again. This is region R2; the velocity is still positive so the cavity volume is increasing. Eventually the fluid velocity will become zero, the pressure a minimum. Since dv/dt is stillnegative (from 52) the column will accelerate towards the closed valve increasing the cavity pressure and reducing its volume, region R3. This continues until $P > P_0$ when dv/dt is +ve , V is -ve and P is increasing. The cycle ends when V = O indicating minimum cavity volume and maximum pressure, region R4. Then the cycle repeats itself indefinitely. Note a $\frac{\pi}{2}$ phase shift between the curves for P and V. Equation 55 may be solved by separating variables and integrating, thus if

$$\frac{dV}{dP} = a_5\left\{\frac{P_0}{P^2} - \frac{1}{P}\right\}\frac{1}{V}$$

then

$$\int_1^2 V\,dV = a_5\left\{\int_1^2 \frac{P_0}{P^2}\,dP - \int_1^2 \frac{1}{P}\,dP\right\}$$

$$\frac{1}{2}(V_2^2 - V_1^2) = a_5\left\{\left(-\frac{P_0}{P}\right)_1^2 - \left(\log P\right)_1^2\right\}$$

$$= a_5\left\{P_0\left[-\frac{1}{P_2} + \frac{1}{P_1}\right] - \left[\log P_2 - \log P_1\right]\right\}$$

$$\therefore \frac{1}{2}(V_2^2 - V_1^2) = a_5\left\{\frac{P_0}{P_1 P_2}(P_2 - P_1) - \log\frac{P_2}{P_1}\right\} \qquad 56$$

Method 1 consists of using equation 56 to arrange the flow so that as the valve is shut the subsequent flow may be organised such that at a particular instant the velocity of flow is zero when the cavity pressure equals the reservoir pressure, Po. This is illustrated in Fig. 63 which shows what is hoped to be the solution in the pressure-velocity plane. The focus F is the point through which we want the trajectory to pass. At point A, valve closure is complete and the system is described by the three equations 52, 53, 54, and hence the solution 56. We wish to determine the velocity V_1 at which valve closure should be complete. Thus if in equation 56 we can represent conditions at F as point 2 and those at A as point 1 we have

$$V_2 = 0, \quad P_2 = P_0 \quad \& \quad P_1 = P_{min}, \quad V_1 = ?$$

where V_1 is the unknown variable we have:

$$-\frac{V_1^2}{2} = a_5\left\{\frac{P_0 - P_1}{P_1} - \log\frac{P_0}{P_1}\right\}$$

So far the solution seems reasonable, but we see that if the velocity V_1 is not to be complex we have

$$\log (P_o/P_1) > (P_o - P_1)/P_1$$

or

$$\log P_r > P_r - 1 \qquad 57$$

where Pr = pressure ratio Po/P_1.

From Fig. 63 we see that Pr > 1 but it is easily shown that condition 57 is true only when Pr < 1. These two conflicting requirements lead to the conclusion that this form of valve stroking will not work and it is useful to investigate why this is so by consideration of the physical situation along with equation 55. Fig. 63 is correct up to point B where V = O and dv/dp = ∞ and this is confirmed by equation 55. However in quadrant Q_1 where P < Po and V < O we get from 55 that dv/dp is negative and that when dv/dp = O, P = Po hence point C cannot exist. These conditions define the trajectory in quadrant Q_1 and it will be of the form shown in fig. 64 and hence will never pass through point F.

13. Proposed Method 2.

Although the method 1 just described did not lead to a successful conclusion, an extension of classical valve stroking where the upstream column is used to increase the cavity pressure might be adequate. It may be well at this point to remember that the transients being discussed are those solely due to cavity compression and that even if both ends of the fluid column downstream of the valve were at equal pressures when the valve-end velocity is zero, there is no guarantee that there will be no transients. There may be a one-dimensional velocity distribution along the fluid column which will cause transients to be propagated although it is expected that these will be small compared to 'linear closure' induced transients.

Since Method 2 incorporates the dynamics of both upstream and downstream fluid columns (both assumed incompressible and invisid) it is tending towards a solution for a particular system rather than a general method, however these effects will be discussed in a later section. Although it will be impossible to solve the equations of Method 2 exactly, a development of the analysis will process the equations into a form that is helpful to study, both with regard to boundary condition substitution, and the convenient pressure - velocity plane solution. The physical system is shown in Fig. 65 while the objective in terms of pressure - velocity representation is shown in Fig. 66. At some velocity $V = V_t$, the valve is opened instantaneously, allowing column Cu to accelerate towards the cavity and compressing it. Assuming the mass of column Cu is less than that of Cd the pressures and velocities sketched against time will be as shown in Fig. 67. It is assumed that initially the rate of change of cavity

volume is negligible i.e. $V_o \simeq V_{o1}$. Since friction has been neglected, the two reservoir pressures are equal and Cu will accelerate faster than Cd because $L_u < L_d$ and the accelerating pressure gradient is equal to $P_o - P$, thus P will increase. As Cu accelerates towards the valve, so does Cd, its velocity gradually reducing as the cavity pressure increases. Ideally P will equal P_o when V = O. At this point dV_1/dt will be zero and the column Cu will have its maximum kinetic energy and hence dP/dt will not be zero, so the valve is closed completely at the instant $P = P_o$ thus isolating the two systems. Again any analysis using the assumptions of incompressible, fluid with no friction losses as depicted in Fig. 65 will not be a serious attempt at an accurate solution but it is hoped that any flaws in the method's philosophy will be brought to light. Using Newtons 2nd law again we get for the equations of motion of the two liquid columns.

$$dV/dt = a_1 (P - P_o) \qquad 58$$

$$dV_1/dt = a_4 (P_o - P) \qquad 59$$

And the equation of state for the air in the cavity is

$$P.\forall = a_2 \qquad 60$$

And continuity of the cavity gives

$$d\forall/dt = a_3 (V - V_1) \qquad 61$$

from equation 61.

$$V_1 = V - \frac{1}{a_3} \frac{d\forall}{dt}$$

$$\therefore \quad \frac{dV_1}{dt} = \frac{dV}{dt} - \frac{1}{a_3} \frac{d^2\forall}{dt^2} = a_4 (P_o - P) \qquad \text{from 59}$$

$$\therefore\ a_4(P_0 - P) = \frac{dV}{dt} - \frac{1}{a_3}\frac{d^2}{dt^2}\left\{\frac{a_2}{P}\right\}$$

$$= \frac{dV}{dt} - \frac{a_2}{a_3}\frac{d^2}{dt^2}\left\{\frac{1}{P}\right\}$$

$$\therefore\ a_4(P_0-P) = \frac{dV}{dt} - \frac{a_2}{a_3}\left\{\frac{2}{P^3}\left(\frac{dP}{dt}\right)^2 - \frac{1}{P^2}\frac{d^2P}{dt^2}\right\} \qquad 62$$

we can eliminate dV/dt from equation (58) and other time dependant terms using

$$\frac{dP}{dt} = \frac{dP}{dV}\cdot\frac{dV}{dt} = \frac{dP}{dV}\cdot a_1(P-P_0)$$

and

$$\frac{d^2P}{dt^2} = \frac{d^2P}{dV^2}\,a_1^2(P-P_0)^2 + a_1^2(P-P_0)\left(\frac{dP}{dV}\right)^2$$

and substituting into (62) gives

$$a_4(P_0-P) = a_1(P-P_0) - \frac{a_2}{a_3}\left\{\frac{2}{P^3}\left(\frac{dP}{dV}\right)^2 a_1^2(P-P_0)^2 - \frac{1}{P^2}a_1^2(P-P_0)\left(\frac{dP}{dV}\right)^2 - \frac{a_1^2}{P^2}(P-P_0)^2\frac{d^2P}{dV^2}\right\}$$

$$a_4(P_0-P) = a_1(P-P_0) - a_2a_1^2\left\{\left(\frac{dP}{dV}\right)^2\frac{1}{P^3}(P-P_0)(P-2P_0) - \frac{(P-P_0)}{P^2}\frac{d^2P}{dV^2}\right\}$$

$$a_1 + a_4 - \frac{a_2 a_1^2}{a_3}\left\{\frac{(P-2P_0)}{P^3}\left(\frac{dP}{dV}\right)^2 - \frac{(P-P_0)}{P^2}\frac{d^2P}{dV^2}\right\} = 0$$

if $W = dP/dV$ then $\frac{d^2P}{dV^2} = \frac{dW}{dV} = \frac{dW}{dP}\cdot\frac{dP}{dV} = W\frac{dW}{dP}$

$$\therefore \frac{(P-2P_0)W^2}{P^3} - \frac{(P-P_0)}{P^2} W\frac{dW}{dP} = \frac{(a_1+a_4)a_3}{a_2 a_1^2}$$

$$= K$$

where $K > 0$

or $$\frac{2(P-2P_0)W^2}{P^3} - \frac{2(P-P_0)}{P^2} W\frac{dW}{dP} = 2K$$

$$-\frac{2(P-2P_0)W^2}{P^3} + \frac{(P-P_0)}{P^2}\frac{d(W^2)}{dP} = -2K$$

$$\frac{dW^2}{dP} - \frac{2}{P}\left\{\frac{P-2P_0}{P-P_0}\right\}W^2 = -\frac{2KP^2}{P-P_0} \qquad 63$$

Equation 63 is a first order linear differential equation in W^2 which may be made integrable by evaluation of the integrating factor (I.F.) where

$$\text{I.F.} = \text{EXP}\left\{\int -\frac{2}{P}\left\{\frac{P-2P_0}{P-P_0}\right\} dP\right\}$$

$$= \text{EXP}\left\{\int -\frac{4}{P}\,dP - \int\frac{2}{P-P_0}\,dP\right\}$$

$$= \text{EXP}\left\{ -4\log P + 2\log(P_o - P) \right\}$$

$$= (P_o - P)^2 / P^4$$

Thus multiplying (63) through by the integrating factor.

$$\frac{d}{dP}\left\{ \frac{(P_o-P)^2 W^2}{P^4} \right\} = -\frac{2KP^2 (P_o - P)^2}{(P_o - P)\ P^4}$$

$$= 2K (P_o - P) / P^2$$

$$\therefore \frac{d}{dP}\left\{ \frac{(P_o-P)^2 W^2}{P^4} \right\} = \frac{d}{dP}\left\{ -2K \frac{P_o}{P} - 2K \log P \right\}$$

and forming the indefinite integral with respect to P

$$(P_o - P)^2 W^2 / P^4 = -2K \left(\frac{P_o}{P} + \log P + \alpha \right)$$

where α = a constant of integration depending on boundary conditions.

When $P = P_{min}$, $W \left(= \frac{dP}{dV}\right) = 0$

$$\therefore \alpha = -P_o / P_{min} - \log P_{min}$$

thus substituting for α we get

$$(P_o - P)^2 W^2 / P^4 = -2K \left\{ \frac{P_o}{P} - \frac{P_o}{P_{min}} + \log \frac{P}{P_{min}} \right\}$$

$$\therefore W^2 = \left(\frac{dP}{dV}\right)^2 = \frac{P^4}{(P_o - P)^2}\ 2K \left\{ \frac{P_o}{P} - \frac{P_o}{P_{min}} - \log \frac{P}{P_{min}} \right\}$$

$$\therefore \frac{dP}{dV} = \frac{P^2}{P_o - P} \sqrt{2K \left\{ \frac{P_o}{P} - \frac{P_o}{P_{min}} - \log \frac{P}{P_{min}} \right\}} \qquad 64$$

which is equation of the form

$$dP/dV = f(P)$$

and may be numerically integrated by either Simpson or Runge-Kutta methods between the points F and A on Fig. 68. Equation 64 fits the boundary condition at A in that when $P = P_{min}$, $dP/dV = O$ (which is not surprising as this was used to determine α) and at point F we have $P = Po$ and $dP/dV = \infty$. Also since along the path from A to F dP/dV is negative and $P < Po$, the negative sign from the square root must be taken. Since the numerical integration will begin at F and work towards A, difficulties of a computing nature will be encountered at the first point F since most integration methods use an estimate of the slope, this will work out to ∞. To overcome this we invert the equation to get:

$$\frac{dV}{dP} = \frac{Po - P}{P^2\sqrt{2K\left\{\frac{Po}{P_{min}} - \frac{Po}{P} - \log\frac{P}{P_{min}}\right\}}} \qquad 65$$

and the integration is performed on (65) using steps of ΔP from F to an arbitary point D. At this point integration of (64) will continue the solution from D to A in steps of ΔV since (65) will become infinite at A. Point D has been chosen to be the point where the slope = -1. Although the positive quantity K is constant, it is unknown since it will be proportional to the mass of air in the cavity. As this will be generally unknown, the equation will have to be solved several times with different values of K, the true solution curve being determined after information on cavity parameters is available.

The program developed to solve equations 64 and 65 is described in appendix 6 and the program is known as PTP7. Typical output from program PTP7 is shown in fig. 69. These results are for a variable value of K but for the same initial flow conditions.

14. Proposed Method 3.

This method is based upon a quasi-empirical method of optimising or minimising the function ϕ. It will be noted from the sets of results obtained from both experiment and program PTP1 that the magnitude of the pressure peak due to the first cavity compression increases with increased flow velocity. This suggests that if the flow velocity can be reduced at a rate faster than it is reduced during a linear valve closure then the transients resulting following complete valve closure will be less than those for linear closure in the same time. The rapid deceleration of the liquid column is achieved by maintaining the pressure at the valve end of the column at a constant value which is as small as can be obtained using the valve operating mechanism. This enforces an almost linear deceleration on the liquid column, its value depending upon the pressure drop across the ends of the column. Then after a certain time t has elapsed, the valve is shut fully at its maximum rate, the value of the maximum pressure recorded, and the function ϕ calculated. Time t is varied and a plot of ϕ against t is obtained. This shows the minimum value of ϕ and hence the total valve closing time which makes the most use of this method of closure. It will also indicate whether or not this method is worth employing if the total valve closure time is determined by other system constraints. There is no guarantee that the minimum value of ϕ will be less than unity for any given set of initial flow conditions, although a value of ϕ can be assessed for the two extreme values of time. If the minimum valve closure time is t_o then it will be closed in that time by saturating the driving amplifier with a large signal whether the intention was to close it in a controlled or linear manner. Thus at this point the value of ϕ must be unity and since due to rapid flow reduction,

the value of ϕ should be less than unity for some times greater than t_o, it is reasonable to suppose that a minimum value of ϕ, less than unity, may be found. Similarly, if infinite time is taken to close the valve then the pressure fluctuation measured is the same for both linear and controlled closure and equal to zero. Thus again ϕ is unity and a minimum value is to be expected somewhere between the two extremes.

There are two other methods of transient reduction based upon Method 3 just described. The first involves maintaining the pressure at the valve end of the downstream column at a constant value until the flow velocity is zero. Then the valve is shut quickly so that the column will be subject to a pressure gradient along it, the magnitude of which depends upon the downstream reservoir pressure and the minimum valve-end pressure. This pressure gradient will accelerate the liquid column towards the valve, compressing the cavity and increasing the cavity pressure. The resulting transient pressures may be of smaller amplitude than that due to linear closure. The second method is an extension of the first in that the constant pre-determined value of PP(2,1) is made equal to the pressure of the downstream reservoir. Thus when the flow has stopped, there will be no pressure gradient acting on the column and its velocity will be zero. This would appear to be an ideal method except for the value of ϕ corresponding to this type of closure. Since during the retardation of the column, there is no net decelerating pressure gradient, then only friction between the fluid and the pipe wall will provide any means of retarding the flow. This indicates that infinite time will be required to halt the column of fluid since the frictional resistance is a direct function of velocity. Hence even ignoring the probable time constraints on the system,

a linear closure in the same time would also produce no transients so the factor ϕ is equal to unity.

Before the methods proposed for a modified form of valve stroking can be tested, consideration has to be given to the type of mechanism that will operate the valve to produce the specified pressure-time functions. This will enable a mathematical model to be formed which may then be subject to methods proposed in previous sections. The study of such mechanism is the purpose of the next part of this thesis.

15. Valve Actuator Design Philosophy.

The theoretical work described up to this point assumes a mechanism is available to manipulate the valve in such a way as to produce the required pressure in the required place at the required time. Several authors (Refs. 80 and 84) have investigated valve stroking without devoting resources to the problem of designing a good valve actuator, which may account for some discrepancies between their theoretical and experimental results, although how much of the error is attributable to actuator performance is rarely considered. Most work on valve stroking has employed an open loop actuator control system using computer programs or lengthy hand calculation to determine the required input or forcing function. These functions were inevitably complex and had to be drawn on and cut out of cardboard (as in Ref. 84) to produce a mechanical signal generator.

The author does not wish to criticise these methods since, as will be explained later, the quality of results from any servo system operating upon a fluid system depends largely upon the ratio of the frequency responses of the servo of fluid systems concerned. This means for instance if a mechanical servo has a cycle of operation of 1 second duration ($\omega = 1$ Hz) then the use of such a servo may well be adequate in controlling transients in a system with pipe periods of the order of minutes.

However, as smaller systems are considered, the performance requirements of a servo system become more rigourous and have to be taken into account when overall system performance is analysed. If the system is a feedback control system then the following advantages should be gained:

1. Greater operating accuracy to reduce effects of machining, setting and environment.

2. Faster response of servo system (see section 17)
3. The control signal can be made independant of a large proportion of the system hardware.

The basic control system for the application considered may be drawn as in fig. 70. The four groups of elements are:

1. The signal generator denoted by A.
2. The servo control system which responds to an error signal. This is shown as B.
3. The plant or manipulated process which in this case is basically the fluid dynamics of pressure transients shown as D.
4. The feedback element or transducer which measures the desired output variable from the process. The transducer is shown as box C.

The servo usually requires a power input, and various disturbances or non-linearities impare the accurate measurement of the output process variable. Usual block diagram reduction produces the equivalent diagram C which gives the desired input/output relationship as

$$\theta_1 = \theta_i \, ABD / (1 + BCD)$$

Since θ_1 is known from theory and as yet the required signal is unknown, the equation is written as

$$\theta_i = \theta_1 (1 + BCD) / ABD$$

Now if the servo loop gain is made sufficiently high so that

$$BCD \gg 1$$

we get

$$\theta_1 = \theta_2 \, C/A$$

This equation indicates a total independance of the performance characteristics of components B and D which comprise about 90% of the system hardware; the overall performance being dependant upon the feedback transducer and signal generator. This analysis assumes, of course, that the performance of each component is frequency independant which is hardly likely to be true but this analysis may be useful in optimising high gain servo systems which are not subject to high frequency inputs.

The essential design requirements of the servo system may be set into two groups. The first is to perform a logic function to determine whether the actual system output is greater or smaller than the desired value and to determine the magnitude and sign of the error. The second requirement of the servo is that it should provide sufficient power amplification to enable the error signal to influence the plant or process in a manner which will tend to reduce the error involved. The requirements may be accomplished by employing, for this particular case, any combination of the following sub-systems

1. Electronic.
2. Pneumatic/Hydraulic.
3. Mechanical.

Some parts of the servo system lend themselves to construction by one of the methods listed above more easily than others, but even with other system constraints the choice is not automatic. The logic function may be best performed by either electronic or mechanical means, depending upon the speed of response required. An electronic system may be expected to respond in the order of micro seconds but

suffers from the disadvantage of operating at relatively low power levels and since this requires some form of amplification the initial advantage would be lost. It is important to realise that in a system of several dynamic components, the overall frequency response is determined largely by the component with the slowest response. This means that it is of no use employing electronics working to an accuracy in time of micro seconds if further along in the loop a large solenoid has a response of a few Hertz. Mechanical items suffer largely from inertia and non-linearities such as gear backlash or dry friction. Although no detailed analysis of the effect of non-linear elements will be given in this work, such effects can seriously degrade the operating performance of a servo causing instability or even immobility of certain components.

The use of pneumatic or hydraulic components would appear to have several advantages, They are readily available and usually of sound and robust design. Pneumatic elements are not expensive and systems may be built up in a "bread-board" manner without the use of great skill. Power sources are usually available in the laboratory and pneumatic elements interface easily with mechanical and electrical systems. Problems may be encountered if high power levels are required at the same time as high performance since the use of a compressible working fluid will inevitably cause a slower response than a relatively incompressible fluid. It may also be dangerous to use large high pressure gas containers in the construction of such a system. A hydraulic system tends to be expensive and requires attention to details such as filtration and cavitation which either do not occur, or are of minor importance in pneumatic systems. The system is also (generally) closed cycle which makes it more complex as well as increasing pipe losses; the returning fluid may also need cooling if

large power levels are employed. Hydraulics do offer a great advantage in being able to supply large amounts of power from relatively small units and again the interface between hydraulic and other systems is straightforward.

The possibility of using a fluidic method of control was considered and whilst it would seem well suited to perform the logic servo function, there did not appear to be any means available of converting the error signal into one of much higher power. Several commercially available items for power amplification were available and while the amplification appeared to be suitable the linearity of such devices did not put them into catagory of "linear power amplifiers" that may be required for this work. It was realised at an early stage that one of the major problems would be the accurate amplification of the error signal to a sufficiently high power level without appreciably degrading the frequency response of the system. Thus an electrical actuator would not be used since the size of solenoid required to move the valve would be such that the core would be sluggish in response simply due to its inertia. Similarly electric motors would not seem suitable since to increase the torque, gear reduction would be employed and this would in turn slow down the speed of response, increasing the effective inertia of the motor by a factor of N^2 if the gear ratio is N. The possibility of using a Stepper motor was considered although such items with their ancillary equipment are expensive to buy and require a relatively stable environment.

To illustrate the concept of a closed loop servo system, that shown in fig. 71 is intended as a first attempt, and the operation is as follows. Compressed air is introduced into the centre of the double spool valve. This valve performs the function of differencing the desired and actual output signals. The actual output signal, pressure, is measured on the outside of the righthand spool by connection to the location in the

kerosene pipe at which pressure regulation is required. The desired pressure time history is in the form of a cam profile. When this cam rotates the piston and cylinder arrangement cause the constant mass of gas in chamber A to expand and contract;the profile is such that gas in A has a pressure - time function equal to the one required in the pipe. Thus the signal generator unit is also mechanical. The difference between the two pressures causes the spool to move allowing air to enter the larger actuator chamber. The movement of this actuator causes the valve to move. For example, suppose the feedback pressure is less than the desired pressure. The 1st stage spool would move to the right causing the main stage to move to the left. This would cause the valve to open which would produce a pressure rise in the kerosene,this pressure rise returning the first stage spool to the central or null position. Note that when both signal generator and fluid system are in accordance, the servo unit does nothing.

If constructed this servo would probably suffer mainly from leakage problems around the first stage spool and power amplification may well be a problem although higher pressure oil instead of air could be used. The problem of accurately machining the cam profile may be difficult as well as the analysis of the system in chamber 'A' including various thermodynamic and heat transfer aspects. In spite of these defects the system does illustrate the relationship between physical elements and the various components shown in Fig. 70. It also shows the fundamental reason for the choice of a closed loop rather than an open loop system. The mechanism shown can be operated in open loop mode by disconnecting and sealing the connection between the servo and the kerosene pipe. However this would need a computer program to determine the correct cam profile, if worked in this mode, since the relationship between output pressure and cam profile includes all of the hardware transfer functions as well as a knowledge of

the transfer function between valve rotation and output pressure - a complex piece of analysis. If closed loop mode is used, however, only a knowledge of the gas laws is required (theoretically) to determine the correct cam profile. The system is known as a 'force balanced' system since the error actuator provides a signal due to an imbalance of two forces acting on the spool.

16. Initial Servo Design.

16.1. Design of Pneumatic Servo System.

Since the author had no previous experience in servo construction and at the beginning of the work no theoretical model for the fluid mechanics was available, it was thought that the construction of an inexpensive servo should be undertaken if only to investigate two of the primary design constraints. These were the speed of operation of the logic subsystem in the form of the difference unit; and the dynamic response at higher power levels of the actuator unit. It was felt that if the primary design could be improved upon then a reliable low cost servo would result although the overall dynamic performance would probably be more accurately determined by the experiment rather than analysis.

The inefficient design points of the first servo outlined in the previous section we modified so as to reduce the types of error mentioned; the final design shown in fig. 72 being a pneumatic/mechanical servo system with hydraulic feedback. Error measurement is achieved by the use of a device known as a flapper valve (see fig. 73) which consists of a tube with a hole in the end (in this case about 0·035 mm dia), a flow restrictor R and an outlet tube, S. A baffle B may restrict the flow out of the valve by being in close proximity to the hole. If the flow is unrestricted, the flow is throttled through the restrictor R so that $P_2 > P_1$ and as the baffle nears the hole P_2 gets larger as the flow rate decreases. When the hole is blocked there is zero flow and $P_2 = P_1$ Thus the instrument is effectively a distance transducer, the output of which is a pressure that may be sensed through tube S. The performance of the flapper valves used are shown in fig. 74 while fig. 78 shows the characteristics of an opposed pair of valves with a common beam.

The overall system is shown in fig. 75, and the operation is as follows. In fig. 72, the cam with a given profile is rotated through an angle θ . The built-in beam cam follower is displaced to the right causing the push rod to move to the right. If the error beam between the two flapper valves A and B is initially central, then the subsequent movement to the right increases the measured pressure in B while decreasing it in A. This pressure difference moves the spool in the diaphragm operated valve which in turn moves the main actuator causing the valve position to change. This produces a change in the pressure of the flowing kerosene; this change being detected by the metal bellows connected to the pipeline at the point where pressure control is required. The deflection of the metal bellows returns the error beam to the central position between the flapper valves. Thus a finite rotation of the cam will produce a finite change of pressure in the kerosene and if the cam is driven at a uniform angular rate by, say, a rack and pinion gear set actuated by another pneumatic cylinder, then correctly profiling the cam will produce any required pressure time history in the kerosene. Fig. 75 shows the system in block diagram notation; note that this system is now a 'displacement balanced' system since the error signal is produced as a result of the difference in actual and required variables expressed in terms of displacements. The mechanical amplifier unit is necessary since the flapper-baffle displacement is usually quite small and if the baffle were moved by the cam directly then the profile would have to be machined very accurately indeed. However the push rod assembly will reproduce the cam profile only at a smaller scale and this eliminates the requirement for accurate machining providing that a relationship is found between the required push rod displacement and cam profile. Since the system is displacement balanced, a knowledge of the desired pressure time history will enable a displacement time function to be determined for the metal bellows providing the characteristics of the bellows are known. These characteristics were determined experimentally by charging the bellows

with air of known pressure and measuring the deflection with a dial gauge. The results, shown in fig. 76 indicate a certain amount of non linear operation in the region around the origin as well as hysteresis.

The determination of the cam profile is based on the fact that the push rod end of the beam is to be displaced an equal and opposite amount and this will enable the push rod displacement - time function to be determined. This function will be used in conjunction with the "mechanical amplifier" characteristic to determine the cam profile. The beam may be regarded as a light elastic beam built in at one end, subject to a deflection at the other. It is required to know the deflection at any point along the beam for the given deflection at the end. This equation is

$$\theta_1 / \theta_2 = 3\left(\frac{x}{L}\right)^2 - \left(\frac{x}{L}\right)^3$$

where the notation and graphical representation of the above equation is shown in fig. 77. Thus the amplification may be determined and so too may the cam profile.

The diaphragm operated spool valve is an item available commercially and is supposed to provide a linear response in that the flow of air from the valve is proportional to the pressure difference between the two diaphragms. The valve actuator is a 25 mm bore jack of 175 mm stroke connected to the valve arm by a pin and slotted crank linkage, although this was replaced for frequency test purposes by an 25 mm bore actuator with a stroke of 100 mm.

16.2. Testing and Evaluation of Pneumatic servo.

The servo system described in section 2 was constructed, and a view of the main components is shown in fig. 79. The testing procedure was intended to investigate the dynamic performance, or frequency response, of the overall system since it is this feature which will determine largely whether it is acceptable or not. Thus some form of sinusoidal driving function was needed and this took the form of an electric motor driving a cam. The cam profile was simply an offset circle, or eccentric although it was realised that this would impart a motion to the beam that is only approximately simple harmonic.

A test cylinder of 25 mm bore and 100 mm stroke was used for the tests although the choice of the test cylinder will have some effect on the overall frequency response of the system. The test cylinder was connected to a linear displacement transducer with an output voltage proportional to the input displacement. This output voltage was displayed on the Tektronic 564 storage oscilloscope and records of the traces made were in the form of polaroid photographs.

The test itself consisted of driving the motor at a constant speed and measuring, for this speed, the amplitude of oscillation of the test actuator and transducer. Naturally as the frequency of the input signal i.e. the speed of the motor, increases, the various components have less time to react to the signal and the amplitude of the output displacement will decrease. The rate of decrease of amplitude will be an indication of the band width of the system. Note that this procedure will not yield the

overall closed loop system response since it is being operated in open mode, but it will provide information on the forward path element shown in Fig. 75 and will thus enable the type of closed loop performance to be estimated.

Typical traces obtained from the test are shown in figs. 80 – 84, for a variety of motor speeds. Note that since the maximum amplitude of the displacement is limited by the stroke of the cylinder, the traces appear to be 'clipped' particularly in the slower speed ranges investigated. This feature also occurs at higher speed ranges since it was found difficult to maintain the oscillation in the mid-stroke of the cylinder. This was thought to be due to the cam profile since as the motion of the error beam was not simple harmonic, then the time when the movement was zero, or dwell period, was different for the two flapper valves. This implies that the actuator would move faster in one direction than in the other.

It will also be noted that the peaks on the trace are not all the same amplitude and so an average value had to be taken. This effect is probably due to the fact that as the amplitude of oscillation decreases, the effects of non-linearities such as friction and dead-space will become more prominent. Since it was not possible to maintain the oscillation about the mid point of the actuator stroke, some of the reduced amplitude traces are also clipped by the stroke limitation. It is difficult under such circumstances to estimate the overall amplitude of oscillation although the frequency will not of course be affected. To overcome this difficulty an approximation is made in that it is assumed the traces are of sinusoidal form. Thus for a trace such as that shown in fig. 83 where the oscillation is limited on its lower region, an indication of the additional travel that would be achieved if the limit

was not there may be made with the use of fig. 85. This illustrates the relationship between the amount of cut-off on the top of a sine wave and additional displacement in the perpendicular direction for such a cut off. Thus the overall peak to peak amplitude may be measured and if this then exceeds the maximum stroke limit then it will be subject to that limit although this will probably not be necessary.

To determine the amplitude of oscillation the procedure is as follows. From the trace determine the frequency ω . Hence determine the period λ from

$$\lambda = 1/\omega \quad \text{secs}$$

Determine the mean cut off time $\bar{\tau}$, and hence calculate α from

$$\bar{\tau} = \alpha\lambda$$

or

$$\alpha = \bar{\tau}/\lambda$$

from fig. 85 find value of y to correspond with α . Thus portion of trace showing above cut off is of magnitude

$$A(1-y) = \bar{x}$$

where $\bar{x}$ = measured mean amplitude above cut off.

Hence the amplitude of oscillation is obtained from

$$A = \bar{x}/(1-y)$$

and it is this value of A which is then subject to the original low frequency cylinder stroke limits.

Results:

Each of the five traces (figs. 80 – 84) was analysed separately.

Fig. 80.

It is apparent from the trace that the stroke limitation of the actuator is encountered on both ends of the stroke and thus the dynamic amplitude performance is the same as for the quasi-static case i.e. the modulus ratio.

$$\frac{\text{dynamic amplitude}}{\text{static amplitude}}$$

is equal to unity. This amplitude corresponds to a scope deflection of 5.8 cms. The frequency is a mean value and obtained by measuring 6 cycles to occur in 8.6 secs giving a frequency of 0·698 HZ.

Fig. 81.

The same comments apply to fig. 81 as to the previous one. The actuator is still saturated so that the modules is again unity. This time the frequency is 8 cycles in 9·1 seconds or 0·880 HZ.

Fig. 82.

Here the lower limit is reached on some peaks but it is only just, so the mean value of the peak amplitudes are found. This gives a value of 5·17 cms which determines the dynamic modulus to be 0·891. The frequency is 8 cycles in 8·6 secs or 0·930 HZ.

Fig. 83.

In this trace the first four peaks are not clipped and so may be considered separately from the other five which are subject to a constraint on the lower part of the trace. Now following the proceedure laid out in the previous part of this section, the frequency was found to be 9 cycles in 9·2 secs i.e.

$$\omega = 0{\cdot}978 \text{ Hz} \quad \therefore \lambda = 1{\cdot}02 \text{ s}$$

The mean interval of the clipped waveform was found to be 0·375 secs and hence

$$\alpha = 0{\cdot}375 / 1{\cdot}02 = 0{\cdot}368$$

and from fig. 85 $y = 0{\cdot}17$.

The mean amplitude of the five clipped peaks was found to be $\bar{x} = 3{\cdot}76$ cms and hence the unrestricted amplitude is

$$A = 3{\cdot}76 / (1 - 0{\cdot}17) = 4{\cdot}52 \text{ cms}$$

This value may then be used in conjunction with the amplitude of the unrestricted peaks to give an overall mean amplitude of 3·94 cms and hence a dynamic modulus of 0·68.

Fig. 84.

The last trace was not restricted by the stroke on any of the peaks and a mean peak to peak amplitude may be calculated directly as 1·8 cms giving a dynamic modulus of 0·310. The frequency of oscillation being 9 cycles in 8·7 seconds or 1·035 HZ.

To summerise the results, a Bode type diagram showing the dynamic amplitude plotted against excitation frequency was drawn and this is found in fig. 86.

Conclusions of Test.

The servo appears to have a band width of approximately 1·0 HZ. This would not be sufficiently fast for the type of application for which the servo was designed and it would seem that the inadequate response time is a result of the system operating with a working fluid which is compressible to a large degree. This implies that the servo takes a long time to respond not because it cannot supply air to valves and actuators sufficiently fast, but that it needs some time to compress the air to a pressure sufficiently high to enable useful work to be done. This factor is directly measurable by the fluids bulk modulus and the advantages of a hydraulic system over a pneumatic system become immediately apparent.

Although the redesign of the servo will not include the set up just outlined it is worthwhile to remember that the system may be adequate for pipelines of significantly longer pipe period where such rapid valve movement, and hence servo response, may not be required.

At this stage it was only suspected that the pneumatic servo performance was inadequate. Once the mathematical model of the generalised system has been written, a more quantative analysis could be undertaken.

17. Block Diagram Notation. (Using Laplace transformations).

Block diagram notation in conjunction with operational calculus will be used for the study of dynamic characteristics as it offers a standard and straightforward method of determining both stability and performance characteristics. As an example, consider the suspension system shown in Fig. 87. The mass M is subject to an external force f, the other forces acting on it are

1. Inertia force = $M\ddot{x}$ = $M\dot{v}$
2. Damping force = $R\dot{x}$ = Rv
3. Spring force = Kx = $K\int v\,dt$

where $\dot{x}$ is x differentiated with respect to time and v = the velocity of the mass.

If we use Newtons 2nd law to write down the equation of motion of the mass we get

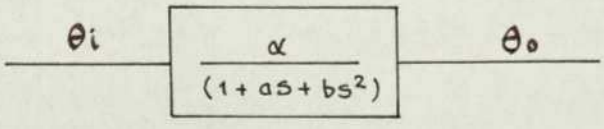
$$f = M\dot{v} + Rv + K\int v\,dt$$

Taking the Laplace transform of this equation

$$F = MsV + RV + \frac{KV}{s} \qquad \text{where } V = L(v) \text{ etc.}$$

$$\therefore V = \frac{F}{(Ms^2 + Rs + K)} = \frac{F/K}{(s^2M/K + sR/K + 1)}$$

hence the suspension system may be represented in block diagram form using operational calculus as



where θ_i = an input parameter (in this case force f)

θ_o = an output parameter (in this case velocity v)

α = steady state gain of system

a, b are physical properties of the system which will determine the transient response for any given input.

Advantages of Closed loop Systems.

Consider the equation of the system just described i.e.

$$\theta_o = \theta_i \alpha / (1 + as + bs^2)$$

if the input is a unit step change then $L(\theta_i) = 1/s$

and $$\theta_o = \alpha / s(1 + as + bs^2) \qquad 66$$

This may be compared to the standard second order system described by the equation

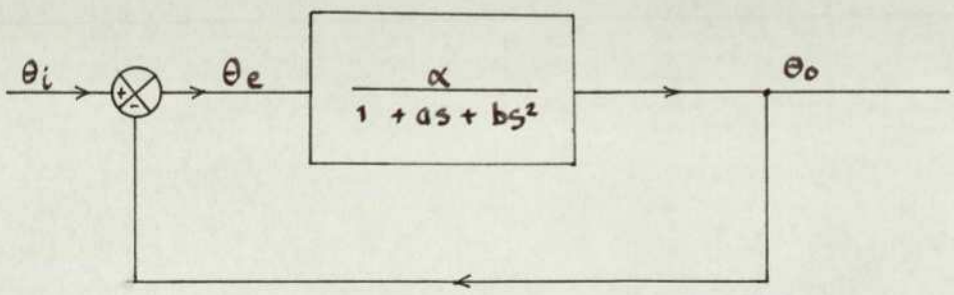
$$\theta_o = \frac{\alpha}{s(1 + 2\eta s/w_n + s^2/w_n^2)} \qquad 67$$

where η = a damping ratio.

and w_n = undamped natural frequency.

The inverse transform (hence the solution in the time domain) will be overdamped, critically damped or oscillatory depending upon whether η is greater than, equal to or less than unity respectively. The time response for several values of η is given in fig. 88. The point worth noting is that when a system is operated in open loop mode, the transient performance is fixed by the physical parameters of the system (a and b) since altering α, the steady state gain, will not change the transient response only the steady state response. Thus if the damping in a system should be negative the system will beunstable, but nothing can be done about it without changing the system itself.

If we now consider a negative feedback closed loop system.



we can state that $\theta_o = \theta_e \alpha / (1 + as + bs^2)$

and $\theta_e = \theta_i - \theta_o$

thus if $G(s) = 1 + as + bs^2$

$$\therefore \theta_o \left\{ 1 + \frac{\alpha}{G(s)} \right\} = \frac{\theta_i \alpha}{G(s)}$$

$$\theta_o = \frac{\theta_i \alpha}{G(s)} \Big/ \left\{ 1 + \frac{\alpha}{G(s)} \right\}$$

$$= \frac{\theta_i \alpha}{G(s) + \alpha}$$

and if θ_i is again a unit step input as before

$$\theta_o = \frac{\alpha}{s\{(\alpha+1) + as + bs^2\}}$$

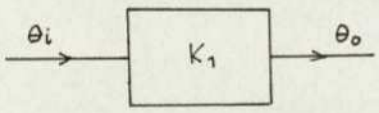
$$= \frac{\alpha/(\alpha+1)}{s\left\{ 1 + \frac{a}{\alpha+1} s + \frac{b}{\alpha+1} s^2 \right\}} \qquad 68$$

Now equation (68) is essentially of the same form as (66) or (67) for the open loop system except that the parameters that effect both the stability and total response of the system in question i.e. W_n and η are now both a function of α , the steady state gain i.e.

$$2\eta / W_n = a/\alpha+1 \qquad \& \quad 1/W_n^2 = b/\alpha+1$$

thus the performance of the system may be defined and specified in terms of parameters that may be altered easily to give that performance. Note that this is done at the expense of the steady state gain which is now $\alpha/\alpha+1$ but this rarely presents problems since amplifiers with a varible gain in series with this element will restore the gain to any desired value.

A further advantage of closed loop control lies in its ability to perform the control function even after a substantial system failure. For example, suppose it is required to control an output variable θ_o such that it follows an input variable θ_i in magnitude. The two control systems, open and closed loop are compared below.



$$\theta_o = K_1 \theta_i$$

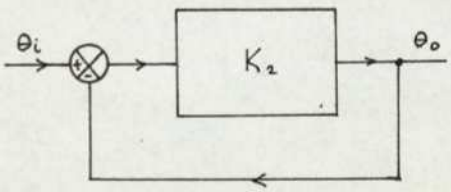
hence for direct linear control

$$K_1 = 1.0$$

At this point, each amplifier suffers a loss of gain of 90%

$$\theta_o = 0.1 \theta_i$$

Hence the loss of gain results in a loss of 90% of the system output



$$\theta_o = K_2(\theta_i - \theta_o)$$

$$\theta_o = K_2 \theta_i \; / \; 1+K_2$$

hence for direct linear control

(to within 1%) $K_2 = 100$

thus $\theta_o = 100 \theta_i/101$

$$\theta_o = 10 \theta_i/11 = 0.91 \theta_i$$

Hence the loss of gain results in a loss of less than 9% of the system output.

18. Modified Servo design.

18.1. Electrohydraulic Servo System.

It is obvious from the previous section that the nature of a pneumatic system would not be acceptable for the requirements of high frequency response (of the order 50 HZ bandwidth) while maintaining a reasonable power level. Electro-hydraulic servo systems are capable of achieving these two goals in a manner superior to any other type of servo. The basic component of such a servo system is an electro-hydraulic servo valve which may at this stage be considered an instrument which delivers a flow of hydraulic oil proportional to a input of electric current; this servo valve will be discussed in detail in a later section.

The electrohydraulic servo system is a relatively new concept, only receiving world wide attention in the 1960's. This is due mainly to the fact that the manufacturing processes required to construct servo valves to the close tolerences that are necessary have only recently been available to a commercial market. Initial development was chiefly for aerospace applications. The advantage of electrohydraulic servo systems is that it is a very flexible system. It combines the rapid response at high power levels to be found in the hydraulic system with the relatively instantaneous operation of the electrical logic system working at low power levels thus maximizing overall response. The electronic portion enables almost any quantity to be used as the feed back parameter since almost any quantity may be measured with a transducer. In addition to this, arithmetic operations may easily be performed with the signals, including simple compensation networks, which will be discussed later. Electronic amplifiers

which drive the servo valve provide an easy manner by which the forward path gain of the servo system may be changed to account for variations in the plant or controlled process.

Since servo systems are usually classified by the name of the quantity being controlled, the system being designed is known as an electrohydraulic pressure control servo system, and is shown in block diagram form in fig. 89. The system itself is straight forward enough but the provision of power supplies and signal generator in fact requires more attention than the system itself. The signal generator will provide a voltage which, subject to a suitable scaling factor, is in proportion to the desired pressure-time function. A pressure transducer records the pressure in the kerosene at the point where pressure control is required and this voltage is subtracted from the signal generator voltage to produce an error signal. This signal is amplified to a level suitable for acceptance by the electrohydraulic servo valve which then produces a flow of oil proportional to the error signal. The oil moves a hydraulic jack which in turn alters the valve angle producing a pressure change in the flowing kerosene. This change is monitored by the pressure transducer and the loop may be so arranged that overall a negative feedback signal reduces the error signal. Although this describes the servo system operation, each component will be described in detail.

18.2. Electrohydraulic Servo-valve.

The servo valve chosen was the Dowty series 4551/262 model which is shown in section in fig. 90 and diagramatically in fig. 91. Since the servo valve is the heart of the system it will be described at length. The valve consists of three basic parts; the electric torque motor, the first hydraulic stage and the second hydraulic stage. Fig. 92 shows in more detail the layout of a torque motor which consists of a fixed permanent magnet framework and a coil and armature assembly which is free to rotate but is kept in the null position by means of a torsion spring. Supposing the coils are connected in series as shown in fig. 92c, and a small current I_o is passed through the coils. The effect is to induce a magnetic field into the armature which will then rotate since it is located in a magnetic field. Equilibrium is reached when the magnetic torque on the armature is balanced by the torque exerted by the torsion spring. If the current is increased further, the magnetic torque will increase until equilibium is again reached following a further rotation. Ideally the rotation θ is related linearly to the current flowing, i, i.e.

$$\theta = Ki$$

where the constant K depends upon the stiffness of the torsion spring and the strength of the permanent magnetic field. Typical plots of the above equation are shown in fig. 93. Connected to the armature is a baffle which together with a pair of opposed nozzles form the first stage hydraulic amplifier. The mode of operation of the flapper-nozzle valve has already been described in Section 16 and will thus need no further discussion except to state that the stage is usually designed to give linear operation over as wide an operating domain as possible. Thus the deflection of the baffle x is related to the output pressure P_L by $P_L = Gx$ for $x \leq 0.7\hat{x}$

A typical curve for a flapper-nozzle valve is shown in fig. 94 illustrating linearity over about 60% of the total allowable deflection of x. Since the maximum values of x are small, then it can be linearly related to the rotation of the armature by the equation

$$x = r\theta$$

where r is the effective radius and θ is measured in radians

thus

$$P_L = GrKi = c_1 i$$

which preserves the overall linearity of the valve so far.

The pressure difference output from the first stage flapper-nozzle valve is then applied to the second stage spool. The spool is maintained in the central position by means of the central spring shown, although this has another function which will be described shortly. The effect of a pressure difference across the ends of the spool is to cause a deflection until the spring force balances the pressure differences force. This deflection enables one of the piston ports to be connected to drain while the other is connected to supply. The flow and hence the total pressure drop will be determined by the amount of opening of the ports. Since this effect will be, for round ports at least, non-linear, the restoring spring characteristic has also to be made non-linear to produce the overall linear relationship between the pressure difference, P_L, across the spool ends, and the flow of oil supplied, Q.

$$Q = c_2 P_L$$

which may be combined with the previous equation to yield

$$Q = c_3 i \qquad (c_3 = c_2 c_1)$$

which is the approximate equation of the servo valve operated under steady state conditions. Note that the spring which keeps the spool centred is in fact a form of internal

force feedback in that if the flapper is deflected to the left, say, the spool will move to the right tending to restore the flapper to the central position. This increases the internal "stiffness" of the process with a consequent reduction of response time.

The preceeding description of the Dowty valve does not encompass all varieties to be found available on a commercial basis. A radically different design, known as a jet pipe valve has a tube as the armature, enabling fluid to be directed into one outlet port or the other depending upon the rotation of the tube. However only one such valve is marketed in this country by Abex Denison and the remainder follow the construction described for the Dowty valve. Large flow servo valves accomplish their aims by either incorporating a third stage with a large spool or have a single spool which is moved by means of an electric motor. Although the motor reduces considerably the performance of the servo it is unusual to need high response (above 10 HZ) with simultaneous high flows (above 20 litres/min).

The process of determining which servo valve is suitable for the proposed pressure control system is to specify a general servo valve and incorporate this into the model. Then constraints corresponding to manufactures figures are introduced one at a time until either a constraint degrades the servo operation to an unacceptable degree, in which case the valve is rejected or the performance is adequate in which case the valve is considered as a candidate. Such constraints are, typically, the flow-current steady state gain, or the maximum current available from the servo amplifier, or the open loop bandwidth of the servo valve. Since the specification is determined in terms of flows, gains and bandwidths etc., the figures have to be related to the standard

specification characteristics for any particular valve before the choice may be made. These are defined here and assigned values for the particular valve chosen.

Rated Flow (Q_R) is defined as the flow through the servo valve when maximum current is applied to the torque motor and pressure drop across the valve of 1000 lbf/in^2 (6860 Kn/m^2). The stated pressure is standard since maximum power transferred to the load occurs with this valve pressure drop when the supply pressure is 3000 lbf/in^2, a common figure for electrohydraulic servo systems. Q_R = 10 litres/min for the Dowty valve (9·6 m^3/s) when $i = i_{max}$. This enables a pressure drop-flow rate curve to be drawn for the valve, as shown in fig. 95. This is the envelope of performance since a smaller current will produce a curve inside that for maximum current.

Flow Gain is an important parameter since it is a measure of the steady state gain of the servo valve and will thus determine the stability and performance of the overall servo system. This parameter is usually expressed graphically, as shown in fig. 96, the flow being measured at the standard 1000 lbf/in^2 pressure drop. Unfortunately the precise characteristics around the null position are not easily determined since it depends upon the fit of the spool with the sleeve. Even with modern production methods, the fit cannot be controlled to sufficiently fine limits to enable performance to be predicted. The slope of the flow gain curve in the region of the origin also depends upon the 'lap' of the spool in its sleeve. This effect is shown in Figs. 97 which also implies that a critical centre or ideal valve lap is required for a precisely linear characteristic in the region of the origin. The valve lap may be used to incidate the quality of manufacture of a valve. Since servo valves may be fitted with a variety of coils rated at different current values, the flow gain depends upon the individual valve chosen. The

one used in this work had a maximum current input from the servo amplifier of 7·5 mA when the coils are in series, giving a flow gain of 1·34 litres/min per m.amp.

Pressure Gain, or pressure sensitivity is measured by blocking the load lines and passing a small current through the torque motor. The ratio between the measured load pressure and the supply pressure gives the Pressure Gain. The characteristic is shown in fig. 98. Ideally the curve should have a steep slope and rapidly achieve the supply pressure since no flow is possible. The ability to achieve a high pressure gain indicates an ability to overcome stiction type forces and will also tend to improve stability by reducing other non-linear effects. For the valve chosen the pressure gain is quoted as between 30% and 80% of supply pressure for a current of 1% of that rated for the valve.

Leakage Characteristic Leakage is totally internal, a result of employing a flapper nozzle type of valve on the first stage which produces a leakage Q_{Po} and the leakage between the spool and sleeve Q_l . A graph of total leakage for variable input current is shown in fig. 99. Note that maximum leakage occurs in the null position since the minimum resistance of the port-spool system occurs in this position, and as a result, the null leakage is usually specified by the manufacture. It is important to know the leakage particularly in the application of the valve to a pressure control servo since the model indicated that the flow - time requirement of the actuator would be typically that shown in fig. 100. This indicates that a large flow is required for a relatively short duration. Obviously the servo valve has to be able to pass such a flow but if the pump unit is also expected to do so then the unit will be greatly under used during the rest of

the time. To eliminate the need for a large pump, an accumulator or other energy storage device may be used to provide the high flow for a short duration, however the pump unit will still have to provide a flow greater than the leakage flow or the accumulator will not become pressurised. The servo valve chosen has a leakage of 3% of the rated flow (0·3 litres/min) while the pump unit delivers 4·4 litres/min.

Null Shift, is defined as the current required to re-centre the second stage spool after it has been disturbed by a pressure or temperature variation. It is usually defined in terms of a percentage of the maximum current that may be passed through the servo valve, and typically is in the region of 2%.

Valve Threshold is a measure of the valves ability to respond to a change in input signal. It is usually the smallest change in current which produces a detectable change in flow and is of the order of 0·5% of the maximum rated current for the servo valve.

Frequency Response may be the most important dynamic characteristic governing the choice of a servo valve. It is defined as the response of a component to a sinusoidal input signal. All machinery which may be classified in terms of input and output variables do not usually respond to high frequency signals due to friction and inertial effects and so the performance for a steady state signal does not indicate the performance to be expected if a dynamic signal is applied to the input. It is conventional to plot the ratio of the input amplitude to the output amplitude i.e.

$$A_r = x_{out} / x_{in}$$

at a given frequency, for varying frequency. If the quantity

$$20 \log_e A_r$$

is plotted in the y - axis and log frequency is plotted along the x - axis then a diagram

known as a Bode diagram is produced. The units of the y axis variable is decibels (db). Also, as the frequency of excitation is increased, the phase angle between input and output increases and this is usually plotted on the same diagram. A full explanation of these effects is demonstrated by a simple example in Appendix 8. Fig.101 shows the Bode diagram for the Dowty valve. Since the majority of servo valves are priced within 25% of each other it was thought that one with a good frequency response was desirable although a wide range was available to choose from with bandwidths (see appendix 8) from 5 up to 250 HZ specified by the manufactures. It should be remembered that a servo loop is only as fast in response to a signal as the response of the slowest component. Thus in the determination of the frequency response it is important to realise that figures given in Ref. 89 are for a negligible load. However it is obvious that to measure the output some form of actuator and transducer must be connected to the servo valve which implies that the open-loop or no-load performance would be better than that provided by the manufactures.

Although the description of the servo-valve parameters implies that the overall servo performance is dependant upon these parameters, it is not a practical proposition to measure them. This is because the testing proceedure itself is lengthy and complex (see ref. 89). It is for this reason that the manufactures figures are used for the simulation of the servo valve and once the model is complete then it may be possible to investigate the effect of varying some of the more important parameters of the servo valve. There are also several factors to consider with regard to the installation of the servo valve into a hydraulic circuit but this aspect of the work will be dealt with in a later section.

Servo Valve Simulation, The function of the servo valve in the context of the pressure control loop described is to provide a flow of oil to the actuator which is proportional to the magnitude and sign of a given input current. Thus the steady state transfer function is given by

$$\frac{Q}{i} = \frac{\hat{Q}_R}{\hat{i}_r} = \frac{10}{7.5} = 1.34 \text{ l/min / mA}$$

However the dynamic response of the servo valve cannot be ignored due to the inertia of the spool, and the transient response transfer function may be written as

$$1 / \left\{ 1 + \frac{2\eta s}{W_n} + \frac{s^2}{W_n^2} \right\}$$

Where W_n is the apparent natural frequency of the servo valve and η is a damping factor. Thus the overall transfer function is written as

$$Q/i = G_3 / \{ 1 + as + bs^2 \} \qquad 68a$$

where G_3 = 1·34 litres/min per m amp.

$a = 2\eta/W_n$

$b = 1/W_n 2$

Equation (68a) is used in the simulation of the servo valve.

18.3. Transducer and Feedback Amplifier.

The transducer, located approximately 40 mm downstream of the spherical plug valve, is a Vibrometer 12QP quartz crystal pressure transducer. A quartz crystal inside the transducer is deformed by the action of pressure on a diaphragm. This produces a piezo- electric charge on the crystal, the detection and measurement of which will indicate the magnitude of the pressure being registered. The quartz module is functionally separated from the transducer housing hence eliminating the effects of temperature and spurious stressing conditions.

The amplifier unit converts the charge from the pressure transducer into a voltage which is proportional to the pressure registered by the transducer. It also has a variable output current to operate a wide range of recorders or analogue circuits. Since the manufactures specify that the frequency response (Bode Diagram) of the amplifier and transducer is flat up to 50,000 HZ and the bandwidth as 150,000 HZ then the dynamic response may be neglected. Thus the pressure transducer and amplifier unit may be considered to be a simple gain or scaling factor, in block diagram terms, which converts a pressure signal into a voltage, independant of the dynamic changes associated with the pressure signal. The problem of amplifier sensitivity is solved, for experimental methods at least, by arranging the scaling factor of the amplifier to be variable. The maximum output signal is limited to ±10V and so an estimate of the pressure fluctuations expected has to be made. This enables the correct scaling factor to be chosen so that any pressures recorded are not cut off above or below the 10V limit. This scaling feature has further implications when the servo system gains are considered in relation to the model specification, but this point will be dealt with in another section of this work.

18.4. Hydraulic actuator.

The hydraulic actuator specification is relatively simple in that there are two conflicting restraints. The stroke of the actuator is fixed at 100 mm. From a frequency response point of view it is necessary to use an actuator with minimum piston area since this will correspond to minimum swept volume to complete one stroke. It will be apparent that the swept volume of the actuator is proportional to the frequency response of the actuator providing the flow of oil available from the servo valve remains constant. Contradicting this requirement, we see that for high flow rates of oil from the servo valve, the pressure loss also is high (fig. 95). Thus the oil may be at a pressure appreciably less than the delivery pressure of the pump. If the friction loss between the servo valve and actuator is also considered, the pressure of the oil in the actuator chambers may be so low, and the effective piston area so small, that the force exerted by the oil on the piston is not sufficient to close the valve with sufficient speed.

It is also instructive to realise that the actuator is an element which performs an integration function with regard to its input and output variables. This is because a constant input variable i.e. flow of oil produces in the output variable, ram displacement, a value which is approximately linear with time. Thus we may write for an approximate transfer function

$$x = G_4 Q / s$$

where s = Laplace operator. When the dynamic response of the mechanical components are taken into account, the general expression is

$$x = \frac{G_4 Q}{s\left\{1 + \frac{2\eta s}{w_n} + \frac{s^2}{w_n^2}\right\}}$$

where η is a damping coefficient and

W_n = natural frequency of the mechanical components.

This may be written as

$$x = G_4 Q / \{s(1 + cs + ds^2)\}$$

Note that the steady state gain G_4 is a function of the effective piston area A_p which depends upon the type of actuator used. If, for example, a double acting actuator with a single piston rod is considered, the effective piston areas are different for movement of the piston in both directions. This effect will have to be considered when the model is in operation.

18.5. Signal generator and Servo amplifier.

The work associated with these two items has been published as an internal research memorandum (100) in The City University and a copy of this is included as appendix 9. This report deals fully with both practical and theoretical aspects of the components so that only a brief resume will be given in this section.

It should be realised that as the work on the electro-hydraulic servo system was progressing, the development of the mathematic model was also proceeding in parallel. Thus information available from the mathematical model was used in the design of the servo amplifier. For example, it was apparent from the model of the servo system that a forward path gain of 0·2 between flow of oil and error voltage was a figure which gave good transient response and a wide stability margin, so this figure was used to set the amplifier gain for the static tests even though the mathematical model of the servo system has not been discussed yet.

The unit constructed fulfils three functions. The first is the generation of voltage waveforms which, when associated with a suitable constant scaling factor display the two pressure - time functions associated with Methods 2 and 3 described in sections 13 and 14. These functions are shown in fig. 9 of appendix 9. Note that V_1 represents the minimum pressure required at the cavity and is variable whereas the other levels are large voltages to drive the servo valve fully in one direction or the other.

The second function is to compare the command signal from the signal generator with the actual cavity pressure as registered by the transducer. The difference between the two is the error voltage used to drive the servo valve and implies that for a meaningful subtraction to occur, the scaling factor of the signal generator should equal that of the charge amplifier.

The final function of the unit is to process the signal from the difference unit to a suitable level to be accepted by the servo valve. This usually implies a form of voltage amplification while preserving the linearity of the process. This voltage amplification, or gain, of the servo amplifier is a critical parameter in the operation of the servo system as a whole and appendix 9 explains how this gain is related to the theoretically predicted gain from the computer model. The signal generator/servo amplifier and ancillary equipment are illustrated in fig. 207.

19. Dynamic Analysis.

19.1. Analysis of linear system components.

The basic system decided upon, shown diagramatically in Fig. 89, consists of several basic types of element. The first may be classed as non-linear and describable. Items in this catagory are the function or signal generator, the amplifier saturation limits and the actuator - valve linkage assembly. Each of these can be described mathematically or logically with relative ease. This cannot be said of the next class which will be termed non-linear indescribable. The box marked "Fluid Dynamics" in fig. 89 is in this group since it is not easy to specify what equations fit into this box without knowing a lot of other things beforehand, indeed the first part of this research was to develop and solve the problems encountered in "Fluid Dynamics". More will be said of this transfer function later.

The final class of system component is linear and whilst no component is precisely linear, it is easy to appreciate that for the purposes of this analysis the linear approximation is justified. As an example the feedback transducer is supposed to give a signal (voltage) proportional to the measured pressure. If the measured pressure happens to fluctuate with a frequency greater than a few thousand cycles a certain amount of linearity is lost but in this particular application of the instrument, fluctuations of such frequency will have a very low amplitude. Thus a totally linear relationship between input and output may safely be assumed.

Although components may be described as linear, the relationship between the input and output may be a complex differential equation which does not lend itself to

an easy solution. It becomes necessary, therefore, to outline the method used to tackle such equations and this will follow closely the proceedure given in ref. 101 and begins by considering the nth order differential equation.

$$\sum_{j=1}^{n} a_j \frac{d^j z}{dx^j} = \phi(x)$$

where $\phi(x)$ is an input function. This may be expanded to give

$$a_1 \frac{dz}{dx} + a_2 \frac{d^2 z}{dx^2} + a_3 \frac{d^3 z}{dx^3} + \ldots + a_n \frac{d^n z}{dx^n} = \phi(x)$$

if we introduce a new set of variables y such that

$$y_1 = z$$

$$y_2 = \frac{dy_1}{dx} = \frac{dz}{dx}$$

$$y_3 = \frac{dy_2}{dx} = \frac{d^2 z}{dx^2}$$

$$\vdots \qquad \vdots \qquad \vdots$$

$$y_n = \frac{dy_{n-1}}{dx} = \frac{d^{n-1} z}{dx^{n-1}}$$

then we may write the nth order differential equation for z in terms of the variable set y i.e.

$$\left.\begin{aligned} \frac{dy_1}{dx} &= y_2 \\ \frac{dy_2}{dx} &= y_3 \end{aligned}\right\}$$

$$\left.\begin{aligned} \frac{dy_3}{dx} &= y_4 \\ &\vdots \\ \frac{dy_{n-1}}{dx} &= y_n \\ \frac{dy_n}{dx} &= \frac{1}{a_n}\left\{\phi(x) - \sum_{j=1}^{n} a_j y_j\right\} \end{aligned}\right\} \quad 69$$

Equations denoted by (69) are a set of n first order linear differential equations which replace the single n^{th} order differential equation. There are many subroutines in existance which will solve a set of equations such as those shown above, but the use of the method just described will best be understood after consideration of the next section which analyses the various dynamic system components.

19.2. Simulation of servo components.

As mentioned in a previous section, the insensitivity of many components to signal frequencies below 1K HZ enables them to regarded as pure gains. This means that they exhibit no transient response. The only two components (apart from the fluid dynamics) that will have a transient response are the servo valve and the hydraulic actuator. The transfer function for these elements may be written in Laplace transform notation as

$$Q = \frac{G_3 i}{(1 + as + bs^2)} \qquad \text{servo valve}$$

$$x = \frac{G_4 Q}{s(1 + cs + ds^2)} \qquad \text{hydraulic actuator}$$

giving for the overall transfer function from flow of oil to ram displacement.

$$\frac{x}{i} = \frac{G_3 G_4}{s(bs^2 + as + 1)(ds^2 + cs + 1)}$$

$$= \frac{G_3 G_4}{c_5 s^5 + c_4 s^4 + c_3 s^3 + c_2 s^2 + c_1 s}$$

where

$$c_1 = 1$$

$$c_2 = a + c$$

$$c_3 = b + d + ac$$

$$c_4 = bc + ad$$

$$c_5 = bd$$

hence multiplying across and writing in ordinary differential form

$$c_5 \frac{d^5x}{dt^5} + c_4 \frac{d^4x}{dt^4} + c_3 \frac{d^3x}{dt^3} + c_2 \frac{d^2x}{dt^2} + c_1 \frac{dx}{dt} = G_3 G_4 i$$

If we now let

$$y_1 = x$$
$$y_2 = \dot{y}_1 = dx/dt$$
$$y_3 = \dot{y}_2 = d^2x/dt^2$$
$$y_4 = \dot{y}_3 = d^3x/dt^3$$
$$y_5 = \dot{y}_4 = d^4x/dt^4$$

Then we may write the fifth order differential equation as a set of five first order differential equations in the new variable y, i.e.

$$\left.\begin{aligned} \dot{y}_1 &= y_2 \\ \dot{y}_2 &= y_3 \\ \dot{y}_3 &= y_4 \\ \dot{y}_4 &= y_5 \\ \dot{y}_5 &= \frac{1}{c_5}\left\{G_3 G_4 i - c_4 y_5 - c_3 y_4 - c_2 y_3 - c_1 y_2\right\} \end{aligned}\right\} \quad 70$$

A standard library subroutine was available to solve the set of equations denoted by (70), providing the initial conditions are known, over a small increment in time Δt. This subroutine and its use will be described in a later section. At the end of a particular time step all the y's will be known and hence the actuator displacement, x, may be found directly from y_1. It may be of interest, from a design point of view, to observe the predicted flow of oil Q from the servo valve. To achieve this it will be most convenient to work back from x through the actuator via the inverse transfer function

$$Q = \frac{1}{G_4}\left\{sx + cs^2x + ds^3x\right\}$$

$$= \frac{1}{G_4} \left\{ \frac{dx}{dt} + c\frac{d^2x}{dt^2} + d\frac{d^3x}{dt^3} \right\}$$

$$\therefore Q = \frac{1}{G_4} \left\{ y_2 + c y_3 + d y_4 \right\}$$

hence the flow rate at the end of the time step may be determined from the values of y_2, y_3, and y_4 which are available.

20. Development of valve stroking program - VSP2.

The object of program VSP2 is to simulate the closed loop pressure control system shown in fig. 89. As explained in the previous sections, all but one of the components shown comprising the system may be reduced to linear form. The box denoted as 'fluid dynamics' represents, in effect, the simulation of pressure variation in unsteady flow. Thus this element may be represented by program PTP1. It should be noted that if a model were chosen such that fluid transient effects could be described by linear differential equations then the closed loop pressure control system incorporating such a model would be easily dealt with using an analogue computer. This would provide the best possible man - machine relationship to investigate the influence of parameter variations upon the effectiveness of any proposed pressure reduction methods and would, in fact, make the derivation of such methods considerably more simple. However, since flow separation is dominant feature of the investigation undertaken,a totally analogue solution will not be possible. It would be possible to use a hybrid computer for the solution of transient problems by allocating program PTP1 to the digital section while the analogue section deals with the differential equations of the servo system. Theoretically this is the best way of solving the problem but in practice the availability of a hybrid computer to the user is far less than that of a purely digital machine. Thus the program developed will be digital although it is worth remembering that as the number of system components increases, so will the number of differential equations that are handled and another form of solution may become more appropriate.

The use of digital techniques enables the simulation of non-linearities in the system to be easily undertaken. These include limits imposed on ram displacement, oil flow and servo valve input current as well as the $Q - \theta$ relationship for the valve. Program PTP1 is, for the purposes of analysis, considered simply as a transducer which converts a certain input variable (valve arm movement) into an output variable (pressure at the downstream face of the valve) via a transfer function. This transfer function is program PTP1 which when provided with the correct initial conditions and input data may be represented by a transducer.

The additional blocks of program necessary to achieve the system simulation are presented in the following sections while appendix 7 gives a full listing of the program along with flow diagrams of subroutines and a list of variables used in the program. The subroutines necessary to convert PTP1 to VSP2 are outlined in the following sections.

20.1. Master Segment VSP2.

The dual function of the Master segment of PTP1 is preserved in VSP2, namely to set up the initial conditions and then to initiate a loop in which time is incremented at the beginning of the loop and the required parameters are evaluated. The segment begins by reading in the necessary data for the solution of the problem and assigning all variables appearing on the right hand side of equations their initial values, zero being the initial value for the majority of the quantities. Although this proceedure is not necessary on many machines, it causes execution errors on others and is generally considered good practice to do this. The initial valve angle THETA need not be 90° so subroutine LOOKUP is called to find a value of TAU corresponding to the initial value of THETA. This is then used to calculate the initial value of actuator displacement DISPL. Once this is done the input data is written out along with the relevant parameters derived up to this point. Then, subroutine CHANGE is called which converts the data to British units and writes them out again. The output headings are written out at this stage. The steady state gain of the hydraulic actuator G4, has two values G4A and G4B depending upon which direction the actuator is moving. Initially G4 is given the value of G4A until the motion of the actuator can be determined after the first time interval. The initial friction losses are then determined for the given flow parameters and the pressure distribution along the pipeline is stored in array P. This section ends at Label 23. The next section deals with the formulation of coefficients and initial conditions for the analysis of the differential equations describing the servo system components (see section 19.2). The dummy variable y used in section 19.2 is also used in the program i.e. Y(1) = DISPL, so the initial values of array Y are assigned zero except Y(1) which may have a non-zero initial condition depending upon the initial valve angle. The

feedback signal FB is also assigned its steady state value, followed by the pressure and flow initial conditions in the arrays used for characteristics interpolation. This ends the 'initial conditions' section of the Master Segment.

Statement No. 8 begins the overall time loop of the program by incrementing TIME by the step size DT. The six points (X and Y) used do determine the shape of the function provided by the signal generator are now specified followed by the call statement to subroutine GEN which will linearly interpolate between these points. The result is a value of POUT which is the pressure demand signal. This is then converted to an equivalent voltage by means of the scaling factor G_1. A facility is incorporated in the pressure feedback path to use a simple lag filter should any high frequency signals appear. The derivation of the equation of this filter is demonstrated in appendix 4. The input variable to the filter is FBIN and the output variable FB, but if the bandwidth of the filter is above 990 HZ, the effect of the filter is ignored. This bandwidth is read in as data for the variable W1. The error voltage VER is calculated and the corresponding current CURRENT from the servo-amplifier is determined, subject to an overload limit specified as BIMIT. This provides all the variables needed to solve the linear differential equations for the servo valve and actuator as described in section 19.2. Subroutine INTSTP is called to perform this function and the result is that the values of array Y are provided at the end of the time step. This enables the actuator displacement to be determined directly and consideration may now be given to the mechanical limits imposed on this variable. It is not sufficient to limit this variable in the same manner as CURRENT was limited since the direction of velocity has also to be considered. The logic flow diagram for this section of program is shown in fig.102, while the outcome is a value of DISPL. This is used, together with the value

of the same variable at the previous time step, to determine the sign of the velocity during the time step. This will enable a choice of the correct value of G4 to be made and consequently the flow of oil from the servo valve during the interval. Next, the valve angle may be determined using a knowledge of the linkage geometry (see fig. 14) and the calling of subroutine LOOKUP once more provides the corresponding value of the valve characteristic. The next logic statement is merely to decide whether valve closure is complete. This ends the main section of the program associated with the servo system and so working around the control loop shown in fig. 89 the 'fluid dynamics' element is reached. This begins by linearly interpolating the values of pressure and velocity at the grid points to give internal values at the beginning of the characteristics. Subroutine CHAR determines the values of flow parameters at all the internal grid points at the end of the time step as well as the flow velocity at the downstream reservoir end, the pressure assumed to remain constant. If the valve is shut, the valve upstream velocities are allocated the value zero and subroutine VALVE is called. This result is the remaining flow parameters to be evaluated and the new values of the pressure and velocity PP and VV are re-written into the array P and V. After this, logical statements decide whether any output should be written this time step, the choice depending on the value of ICOUNT as printing occurs every ICOUNT time steps. Subroutine CHANGE converts all the output parameters to metric and the results are written out. CHANGE is called once more to convert back to British units in preparation for the next time step. There then follows an updating of some servo parameters and providing TIME < TMAX, control is transferred back to statement 8 and and loop executed once more.

Standard Print-out format.

As with program PTP1, there are two different print-out formats used; one before the valve is completely closed, the other following valve closure. Before the valve is fully shut, each print out line corresponds to one time interval and the variables incorporated in it are (from left to right) Time, Signal, feedback, error, current, flow, travel, theta, tau, volume, downstream velocity, upstream velocity, downstream pressure, iterations, marker. Most of the variables are self explanatory, both 'signal' and 'feedback' are the voltages corresponding to the demand and achieved pressures although since the scaling factors used are usually unity, they also correspond to the pressures. "Travel" is the ram displacement and 'volume' is the cavity volume. The pressure and velocities printed are those in the immediate vicinity of the valve while 'iterations' denotes how many times a numerical procedure had to be used in VALVE to achieve an accurate result; the section of VALVE in which this was done is indicated by 'marker'.

Once valve closure has been completed then all of the parameters associated with the servo system in addition to the flow parameters of the upstream pipe become of no interest. Thus for the remainder of the program, the output is of the form shown below:

TIME ITCOUNT MARKER CAVITY VOL. VELOCITY D.S. PRESSURE D.S.

20.2. Subroutine VALVE

Subroutine VALVE is essentially the same as in program PTP1. The only difference is that in PTP1 it was not found necessary to consider a solution to the boundary conditions for the case when the valve was still open but air release had effectively ceased. This was because while valve closure was taking place, the cavity continued to expand and air was released.

With program VSP2, however, the motion of the valve is unpredictable and it may occur that the pressure of the cavity fluctuates in such a manner that air release does stop while the valve is still open. This involves additional logic to identify such an occurrence although the proceedure for processing the necessary equations already exists within the subroutine. A flow chart for the modified subroutine would not provide much more information than that of VALVE in PTP1 but a full listing of this subroutine is given in appendix 7. Due to the slow variation of many flow parameters in the first few time intervals, the logic statements associated with the allocation of a value to MARKER may give unpredictable results so a statement is included which holds the initial value of MARKER constant over the first fifty time steps. If, however, the pressure fluctuates by more than $\frac{1}{2}\%$ during this interval, the constraint is overridden and the true value of MARKER is used.

20.3. Subroutine GEN.

Subroutine GEN was written to simulate the signal generator function in the servo system. It was intended to generate a wide range of straight line functions and may easily be extended to give any complex function that can be represented as a series of straight lines. The program is supplied with six pairs of data points X_i , Y_i and an input variable X. The program linearly interpolates the given values of X_i to provide a value of Y corresponding to the input variable X. This is demonstrated in fig.103. If the input variable is outside the range of the last data value i.e. X_6 , then the function is assumed horizontal after this value resulting in $Y = Y_6$ being returned to the Master segment. The program works by checking which values of X_i the input variable lies between, beginning with X_1 and X_2. Having determined this, the output variable is calculated from

$$Y = Y_{n-1} + \left\{ \frac{X - X_{n-1}}{X_n - X_{n-1}} \right\} (Y_n - Y_{n-1})$$

where

$$X_{n-1} < X \leq X_n$$

20.4. Subroutine INTSTP.

This subprogram solves a set of first order linear differential equations over a specified interval of the independant variable. The subroutine is a standard library subroutine, number D203 from the CERN scientific package and uses an ordinary Runge - Kutta numerical proceedure to solve the equations. The information needed by the subroutine are the number of equations to be solved, (limited to twenty), the starting value of the independant variable, the step size and the initial values of the dependant variables. The output is an updated value of the independant variable together with the new values of the dependant variables at the end of the step. The subroutine calls an external subprogram (EXTERN or DIFEQN) during the solution process; this subprogram will now be described.

20.5. Subroutine DIFEQN.

DIFEQN is called from INTSTP and is the means by which the form of the differential equations to be solved, are stated. The equations, denoted by equation (70) in section 19.2, are merely listed in DIFEQN using the array F to represent the differential of the dependant variable Y. Since DIFEQN is called from another subroutine, it requires an EXTERNAL declaration in the Master Segment.

20.6. Subroutine LOOKUP.

This subroutine uses an input variable, THETA, with a data array, TANG, to derive an output variable TAU1. This relates the steady state valve characteristic to the valve angle as shown in fig.13. This proceedure is the same as that used in subroutine ANGLE in section 6.2.3. except that LOOKUP has the value of THETA already available whereas ANGLE has to calculate it. The reader is referred to section 6.2.3. for more details of the method employed.

21. Design and Construction of Hydraulic System.

The primary function of the hydraulic system is to supply the servo valve with oil of a specified quality, pressure and in sufficient quantity to enable the linear characteristics of the valve to be utilized with respect to its input/output variables. The design of the system is orthodox provided the various system parameters are based upon the specification of the servo valve itself. These parameters have already been discussed in section 18.2. and the relevant design features associated with these figures will be outlined in the following sections.

21.1. Hydraulic Power Source.

The two main parameters connected with this unit are the pressure and flow rate capabilities. The value of the delivery pressure is the least relevant since the servo valve manufactures claim that the response of the valve does not deteriorate significantly from the quoted figures at 21 000 KN/m^2 (3000 lbf/in^2) when the unit is worked at a pressure as low as 1750 KN/m^2 (250 lbf/in^2). Most power sources available appear to fall into two major price catagories; those that have a delivery pressure below 14000 KN/m^2 (2000 lbf/in^2) and those above this figure. Thus it was considered adequate to choose a power source with a delivery pressure around 14000 KN/m^2 if a suitable one could be found. The flow rate specification is more critical since the lack of sufficient oil flow to the servo valve will seriously degrade the overall system performance. The maximum flow required by the servo valve was found from the computer model to be 10·0 litres/min. In addition to this, however, oil will be required to compensate for the first stage null leakage which is quoted as 3% of the maximum rated flow and may safely be neglected. Although the figure of 10·0 litres/min is the maximum flow rate required, it is only present in the system for a very short interval of time (see fig.100) Also, the size of the power source will increase with an increase in flow demand (so also will the cost) so alternative methods of providing high flow for short durations were investigated. Since the total swept volume of the actuator was of the order of 17 ml and a typical valve closure time was 0·3 secs, a mean value of flow rate is given as 3·4 litres/min. A reconditioned Power unit, a Pratt Precision Co. type PX700 was considered suitable since this would deliver 4·6 litres/min at a pressure of 12,000 KN/m^2 (1750 lbf/in^2).

If oil was required at a faster rate, for example in the case of a very rapid valve closure, it would have to be supplied by an external energy source. The unit was found to be particularly convenient since it contained pump, motor (1·5 H. P.), reservoir and filter in a single unit. It was realised that additional filtration might be required as that on the power source was to a level of only 74 microns. The resevoir capacity was 67 litres (15 galls).

21.2. Hydraulic Power regulation.

The pump, being a gear pump, delivered a constant flow of oil so the energy output of supply was varied directly by control of the output pressure. The most efficient way of doing this is to use a multi-piston swash plate pump and to alter the angle of the swash plate to regulate the supply pressure. This minimises the energy loss (heat) from the oil supply. The cheapest way of achieving pressure control is to install a relief valve between the supply and return lines of the pump unit. This has several disadvantages, the most important being that it is difficult to alter the system pressure and that substantial power losses occur when the pump is running but the oil is not being used. Above about 3 H. P. this system becomes expensive due to the oil cooling facilities required for energy dissipation in the pump return line. A compromise between the two methods above is to use an off-loading valve instead of the relief valve between the supply and drain lines. This enables the system pressure to be set accurately when required and the overall system may be depressurised when servo valve operation is not needed. Hence avoiding switching off the pump and allowing air and dust to enter the pipework. In addition to this item, an emergency shut off valve and drain down valve were provided in the main delivery line.

21.3. Transient flow requirements.

The problem of providing a relatively high flow rate over a short interval was solved by including a hydraulic accumulator in the supply line. The accumulator was a Greer-Mercier replacable bag type A15 with a fluid capacity of 0·164 litres ($10in^3$) with a maximum working pressure of 35000 KN/m^2 (5000 lbf/in^2). The amount of liquid stored in the accumulator may be calculated by denoting the pressure and volume at charging by P_o and V_o and at any system pressure by P_1 and V_1. If the compression of the initial charge obey PV^n = a constant we have

$$V_1 = V_o \left\{ \frac{P_o}{P_1} \right\}^{1/n}$$

hence the volume of liquid stored

$$= V_o - V_1 = V_o \left\{ 1 - \left(\frac{P_o}{P_1} \right)^{1/n} \right\}$$

This may be plotted for two initial charging pressures and the usual range of values for n (see figs.104 and 105). To enable the charging pressure to be altered, the gas-side of the accumulator was connected to a nitrogen bottle via a charging valve, although once set at the correct pressure, this unit was disconnected to avoid any possible gas leakage. The accumulator was mounted horizontally as near to the servo valve as possible to reduce line friction and fluid inertia, and was surrounded by a 1/4" wall steel tube in case of explosion.

21.4. Filtration and Cooling.

Although the use of an oil cooler was not considered essential, a Bowman counter flow heat exchanger was available and was installed just before the power supply reservoir inlet. Water was used as the coolant. The performance and service life of the servo-valve depends greatly upon the level of filtration of the oil it uses. It is thus advisable to adhere to the manufactures requirements for the minimum level of filtration and if possible attempt better filtration as well. The filter chosen was a Fawcett R70/10 which achieves the 10 micron level recommended by Dowty for their servo valve. The filter was fitted into the return line between the oil cooler and servo valve. Even if the filter were passing the maximum flow rate of 10 litres per minute, the pressure drop across the unit would be of the order of $7KN/m^2$ ($1\ lbf/in^2$) which should not produce any cavitation problems in the return line. Note that the power source has a 72 micron filter as well as a fine strainer for the oil inlet; the servo valve itself being fitted with another 10 micron filter. Although the filter is fitted after the servo valve, measures were taken to clean the system before the servo valve was installed by replacing it with a flushing block. The system was then run under low pressure for eight hours to clean the oilways. All filters have visual indicators showing when they are dirty but after flushing, none of them had changed so the elements were not replaced. When the oil had been cleaned the servo valve was installed.

21.5. Working pressure and pipe sizes.

The only pressure constraint is that when the system is passing its maximum flow rate, the supply pressure should be greater than the total friction losses due to valves, pipes and bends. For the system components chosen this minimum pressure appears to be around 6500 KN/m^2 (900 lbf/in^2) which corresponds to the pressure loss at a flow of 10·0 litres/min. However since the power source may develop 12,000 KN/m^2 the elements fitted within the system should be capable of accepting this pressure. The problem of determining the return line pressure is not an easy one. Provided no blockage of flow occurs, the pressure should not exceed a few atmospheres at most but may be greatly in excess of this if some restriction occurs and the servo valve spool is moving rapidly. The filter may safely take 2100 KN/m and the return line pipework was the same as the supply line so the filter determines the maximum return line pressure. Ermeto high pressure fittings were used for all the pipework and valves. Flexible hose was used from the power unit to the off-loading valve in the supply line and from the servo valve back to the power unit in the return line.

Using a maximum figure of 3 m/s for fluid velocity in the pipe, a pipe diameter of 3/8" O.D. would seem appropriate for the maximum transient flow. This gives, for a pipe bore of 1/4" a maximum velocity of 2·5 m/s which is within the limit stated. Steel pipe of these dimensions have a maximum working pressure of 31,000 KN/m while flexible hose may be operated at 23,000 KN/m^2 both of which are well above the proposed operating range. All pipe fittings will accept similar pressure levels.

21.6. Choice of Actuator.

As mentioned in section 18.4, it is required to use an actuator with a bore as small as possible although if the bore is reduced to give an effective area of less than 0·07 in^2 (see ref 88) the gain in frequency response is more than offset by the actuators inability to move significant inertia. Since this optimum figure is very small and is hardly likely to be reached in practice, the problem reduces to that of choosing an actuator of sufficient stroke and small enough piston area that can withstand the maximum system pressure. The actuator chosen was a Knapp Microhydraulic cylinder type Z11 - 10 which is a double acting device with 10 mm bore, 100 mm stroke, piston rod diameter of 6 mm with a working pressure of 19,500 KN/m^2 (2800 lbf/in^2). This results in an effective piston area of 50 mm^2 and 75 mm^2, and results in a force exerted by the piston of 420 KN/m^2 (60 lbf) to close the valve. Since this may be accomplished manually with a force of about 20 KN/m^2 the piston force appears to be adequate.

21.7. Overall system Layout.

The complete system is shown in fig.106. A none-return valve is included in the pump delivery line to protect the power unit from either flow reversal or pressure transients in the hydraulic system. The line with the pressure gauge attached was bled frequently as air may collect in the region of the gauge when the pump unit is switched off. The accumulator, servo valve and actuator are mounted as close to each other as possible. This reduces not only pipe friction but also fluid inertia and the pipe period, should any transients be propagated within the system. Sharp bends were eliminated as much as possible between the servo valve and actuator (see fig.107) so that friction and other losses are further reduced. Although the pipe-work in this section is longer than that which may be achieved using elbow and banjo fittings, it was thought that the latter would suffer greater flow restriction during intervals of high flow rate. The return line filter is mounted beneath the pressure regulator shown in fig.107, in the return line. Figure 108 shows the power unit and its associated equipment including the shut-off and relief valves, primary filter and oil cooler.

22.1. Theoretical investigations with Program VSP2.

22.1.1. Performance variation for variable servo parameters.

Once the system in which the pressure transients occur has been defined, the ability to control the pressure at any point in that system will be dependant only upon the response of the servomechanism which changes the boundary conditions. Although the servo system previously described has several variables which are initially unknown, the assumption that the servo is substantially linear in operation enables the number of variables to be considerably reduced. This is illustrated in Appendix 9 where the overall forward path gain is assumed to be composed of several fixed (unity) gains together with a single variable gain, namely that of the servo amplifier. Thus once this variable has been determined, then so has the overall gain, which is the critical parameter. Thus the forward path gain of the system is one parameter which has to be investigated. The only frequency sensitive components are the servo valve and hydraulic actuator. The latter will probably cause less trouble than the servo valve since the natural frequency of such a small actuator will be of the order of KHZ and if the fluid lines connecting the servo valve and actuator are kept small then fluid inertia effects may be neglected. The frequency response of the servo valve, apart from influencing system performance, will have a major effect on the cost of the control system. This is because servo valves are manufactured in two main application catagories; aerospace and industrial. The latter has an inferior frequency response but if found to be adequate may cost approximately one half of a high tolerance valve. One variable associated with the actuator is worthy of investigation; that is the effect of the bore diameter. This is because this value cannot be fixed as independantly as others since the items are manufactured only with predeter-

mined piston sizes. Also it is of interest to see how this element, the one which has the slowest response time, degrades the remainder of the servo loop.

Fig.109 shows the response of the pressure control system for a change in servo amplifier (forward path) gain with other fluid flow and control parameters held constant. The problem is to choose a value of gain which is high enough to produce a rapid change from the initial conditions yet low enough to prevent a certain degree of system instability, which may be seen as oscillation in the pressure time curve for the higher values of gain. Although the figures are denoted by a variable value of G_2, this is in fact the overall loop gain from pressure feedback to ram displacement. For the conditions represented by fig.109 the 'best' value appears to be $G_2 = 0.2$ since a reasonable balance between response time and overshoot has been achieved. Further it was found that this value also is suitable for a wide variety of flow rate conditions within the fluid system. Since, for the purposes of this research, it was not considered practical to vary the servo loop gain to get optimum response for each flow condition, the value of $G_2 = 0.2$ was adopted as the nominal figure for all tests. It may be seen that this will not influence the comparison between theoretical and experimental results, but may degrade the methods of pressure attenuation employed.

The change in performance corresponding to a change in servo valve bandwidth is illustrated in fig.110. It will be seen that the overshoot and amplitude of oscillation of pressure are almost identical for a reduction in bandwidth from 150 HZ to 50 HZ, whilst further reduction renders the servo system incapable of following the desired input. It also illustrates clearly how the pneumatic servo with its 1 HZ bandwidth would not be adequate for this application. For the Dowty servo valve used in the tests the bandwidth was in the region of 100 HZ.

Finally, the effect of various actuators may be investigated by changing the values of the constants G4A and G4B in Program VSP2. Fig.111 shows the results of this and demonstrates how significant the actuator bore is upon overall system performance. By changing the bore from 10 mm to 15 mm the servo takes approximately four times as long to reach the demand pressure while increasing the bore further results in totally unacceptable response. Since the actuator bore area is in effect a gain in the forward loop, a change of bore from 10 mm to 15 mm implies a change of loop gain of the order of 2·3. This feature leads to practical difficulties when choosing hydraulic components since the minimum size bore cylinder produced by the majority of manufactures was 25·4 mm (1") and a search for specialist cylinder manufactures had to be made. Also as the bore size decreases it is difficult to maintain a higher working pressure. A cylinder with a bore of 10 mm was chosen as the predicted performance of such a cylinder appeared to be adequate.

22.1.2. Typical parameter plots from VSP2.

Once the various system parameters were fixed, observations of the control loop variables is possible for given initial flow conditions. This will provide information about the ability of the control components to respond to the input signals as well as indicating the order of error involved in holding the pressure constant. The manner in which the variables are plotted is to begin with the measured pressure and proceed around the loop of fig. 89 until the box marked 'fluid dynamics' is reached. These theoretical results are presented in fig.112. Plot (a) shows the response for a change of pressure from 160 KN/m^2 to 48·5 KN/m^2 and the demand pressure is achieved within 100 ms with a maximum overshoot of 4%. The next plot, b, shows the percentage error between the demand and achieved pressures and illustrates the transient nature

of both fluid mechanics and servo system. The reason why the error slowly increases is explained in the next section. The current to the servo amplifier will be a constant multiple of the pressure error, subject to the power capacity of the operational amplifier. This will in fact limit the output current to 7·5 ma in the actual unit. (See appendix 9). The flow of oil, Q, will be approximately proportional to the amplifier delivery current but subject to the dynamic response of the mechanical elements of the servo valve. This is shown in plot C and indicates that shortly after valve operation begins, a large amount of oil is delivered for a period of 100 ms. This corresponds to the time taken for the pressure to achieve the same order as the pressure demand. Once this has been achieved, the servo valve does not deliver more than 5% of its rated flow which implies that it is important to have some idea of the valves operating characteristics in the so-called null-region. Plot d shows the movement of the actuator ram and should approximate to the integral of plot c, the oil flow. This confirms that the most rapid movement of the fuel valve occurs at the beginning which is to be expected when fig.113 is considered. This is the output of program PTP1, the linear closure program, and shows how the pressure downstream of a valve varies if the valve is closed in a linear fashion. Note that in half of the total closure time the pressure is reduced 10% below the initial steady state pressure. Thus if the pressure is required to drop instantaneously then very rapid valve movement is to be expected. In this instance a ram speed of 60 cms/sec is achieved. The corresponding valve angle θ is shown in plot e and shows that if the mechanism is left for sufficient length of time to maintain the pressure at P_{min}, then the valve will eventually be closed. This effect is discussed in a paragraph later in this section. The final diagram, f, shows how the steady state valve characteristic varies for this type of closure. When simulating the operation of certain types of valve (in the fluid system) it may be necessary to consider the reaction of the flowing

fluid on the moving parts of the valve. This will decrease the valves ability to rotate quickly and applies an additional dynamic constraint to the system. For the valve used for this work, the flow forces would not be as great as for, say, a butterfly valve and so this effect was not included in the analysis.

22.1.3. Gain setting and Gain switching.

As explained in Section 22.1.1, a conflict of design criteria exists when the forward path gain is determined. If the gain is set too high, not only is an unacceptable degree of overshoot experienced, but the complete control system may become unstable so that the achieved pressure never settles to the demand level. On the other hand if the gain is too low, the system is sluggish in operation and hence required longer periods to achieve the demanded pressure level. This slow response time may seriously degrade the results predicted by valve stroking method No. 3 which requires a large, decelerating pressure gradient to be implemented as rapidly as possible.

It is with consideration of the two criteria described above that the 'best' gain for the servo is decided upon. Ideally a different value of gain should be associated with a particular flow state so that the optimum servo performance will always be obtained; however for the work undertaken this was not considered to be practical since the constant value of gain chosen did not produce either instability or sluggish response over the whole range of flow states available. So far only the transient servo response has been considered but the steady state performance also has an effect on the ability of the servo to maintain a constant fluid pressure. In this

region it is advantageous to increase the gain since the corresponding 'stiffness' of the control system enables it to hold the fluid pressure at its demanded value with greater accuracy. This is illustrated in fig.109 which shows that as the gain is increased past its nominal value of 0·2 up to 0·4, although the overshoot increases, the system manages to control the pressure a lot closer to P_{min} once the servo transients have diminished.

This leads to the concept of attempting to change the servo loop gain some time after the system has begun functioning. This will enable the transient overshoot to be limited to a reasonable amount whilst the control function in the steady state will be improved. The mechanism for performing the switching may be as shown in fig.114. This device is placed either before or after the servo amplifier and should not cause saturation in either the amplifier or servo valve due to the relatively low level signals encountered in the steady state mode of the control system (see fig.112 b and c). The switching device consists of an operational amplifier arranged to provide unity gain until the change-over relay switches the feedback resistance to a value of NR. Since the gain of the amplifier is equal to the ratio of the feedback to input resistance, we get

$$N = V_{out} / V_{in} \qquad \text{for } t > t_s$$

The switching interval is arranged by connecting the correct values of the external components R_t and C_t to the timing junctions of a monostable. The monostable is triggered by the master switch which initiates the control function.

The effect of gain switching may be illustrated by fig.115. This shows two similar cases for pressure control; in one case no switching occurs while in the

other the servo amplifier gain is multiplied by a factor of 5 after the interval indicated. The better control achieved by gain switching is apparent. Although this proceedure is advantageous in that it gives better control, it does make the practical problem more complex especially in that the interval after which switching occurs does not have a single best value. As a result the feature has only been investigated theoretically and no attempt was made to include the device shown in fig.114 into the system. The proceedure has been described since the fluid dynamics may be difficult to control and a variable forward path gain may be the only method of achieving optimum system performance.

22.1.4. Determination of Signal Generator function.

The proposed methods of valve stroking (methods 2 and 3) were devised after program VSP2 was in operation and so the reasons for choosing a particular pressure-time function had to be left until this section i.e. until after program VSP2 had been described. Classical valve stroking theory requires the pressure at a boundary to vary linearly with time so that in one pipe period the pressure falls from its steady state value to the predetermined minimum pressure P_{min}. Likewise during the final pipe period the pressure rises in a linear fashion.

If this feature of the initial pressure drop demand is modelled in subroutine GEN and used in a typical flow state, the results are as shown in fig.116a. The servo system does its best, but the characteristics of the fluid dynamics involved prevent an accurate approximation to the demanded ramp function shown. It was decided to simulate a step change in demand pressure instead of the ramp function and

if this is programmed then the results are shown in fig.116b. It should be noted that subroutine GEN cannot simulate a ramp with infinite slope since the program uses such a slope in its interpolation proceedure but a change of demand pressure occuring in 0·001 seconds is permissible. The difference between the two pressure-time curves, one for a ramp and the other for a step in demand, is only in the time at which they occur and not substantially in the shape. Thus the step change of pressure is adopted since:

1. The demanded ramp change does not produce a corresponding ramp change in output pressure anyway.
2. The step change is easier to construct electronically.
3. The step change produces a faster drop in pressure, and hence in valve stroking method 3, for a fixed time, the flow will have a lower velocity than for a ramp change in demand.

For valve stroking method 2, it is required to increase the pressure just downstream of the fuel valve. To do this the momentum of the upstream column of fluid is used to compress the air cavity and hence increase its pressure. It was realised that the rate of pressure rise would be determined primarily by the dynamics of the two liquid columns and the cavity and that any form of valve motion would only increase the time taken for the cavity pressure to rise (by interfering with the column movement). Thus the valve is opened fully so the maximum rate of pressure rise is achieved and this is illustrated in fig.116c. The valve is opened fully at $t = 0{\cdot}6$ secs. and it, will be seen that the pressure reaches the reservoir pressure within one pipe period.

22.1.5. Theoretical Investigation of Valve Stroking Method 3.

The successful operation of program VSP2 enabled the theoretical investigation of valve stroking method No. 3. as out lined in section 14, to be undertaken. The proceedure is as follows. The flow parameters such as initial velocity of flow and steady state line pressure are fixed. The various quantities associated with the servo system are assigned their nominal values in the theoretical model and a suitable value of the minimum pressure P_{min} is programmed into subroutine GEN. Also the nominal valve closure time is defined although the actual closure time will be, in general, longer than the nominal value since it will take the servo a finite time to respond to the signal for full valve closure. This delay will depend mainly on how near to the fully closed valve position the valve is when the signal is received.

With all the program variables specified, the program is executed and a note of the maximum transient pressure in the pipe is made together with the overall time to close the valve and the eventual steady state pressure in the pipe following complete valve closure. This proceedure is repeated with a different value of nominal valve closure time until a point is reached when the valve has closed in a time less than the nominal time specified. This time defines a performance boundary for the servo system which will be discussed in a later section. The results are plotted graphically as shown in fig. 117. Also, the results from program PTP1 for identical flow conditions and linear valve closure times are plotted for comparison. This enables the function ϕ, as defined in section 14 as:

$$\phi = \frac{\hat{\Delta P} \text{ for controlled closure}}{\hat{\Delta P} \text{ for linear closure}}$$

to be determined directly since $\hat{\Delta P}$ is determined as the maximum pressure fluctuation about the final steady state pressure. Thus the three curves shown in fig.117. are

1. ϕ - t_{clos} for linear closure.
2. ϕ - t_{clos} for controlled closure.
3. ϕ - t_{clos}

This enables a ready assessment to be made of the usefulness of method 3 for this particular flow case. Note that the curves begin at a minimum valve closure time of 50 m sec. as this figure corresponds to the fastest time that the servo may achieve. The maximum closure time is defined by the performance boundary mentioned previously. It will be seen for the case considered that reduction by one half of the pressure fluctuation is to be expected if the valve closure time is independant of other closure constraints. It should be noted that in fig.117 for $t_{clos} > 0{\cdot}205$ secs, the maximum predicted pressure will be equal to the maximum predicted pressure at the performance boundary. This is because the valve is fully closed at $t = 0{\cdot}205$ secs and will be independant of any control signals after this time unless those signals cause the valve to open again. This means that the line corresponding to the maximum predicted pressure for controlled closure is horizontal after the performance boundary and hence ϕ may be calculated for time of closure in excess of $0{\cdot}205$ secs. Since the curve for maximum pressure corresponding to linear closure continues to fall after the performance boundary, the value of ϕ will increase, exhibiting a discontinuity of the boundary itself. As one of the main purposes of the investigation is to determine the minimum value of ϕ, the curves have not been drawn beyond the performance boundary.

It is possible to determine the effect of changing the values of P_{min} and the servo loop gain while keeping the flow conditions constant. A change of P_{min}

results in the chart shown in fig.118. It will be seen that for $0{\cdot}14 \leq t_{clos} < 0{\cdot}2$ secs we have $\phi > 1$. This may be explained in terms of the initial signal to servo valve which is proportional to the pressure error i.e. $P_{min} - P_o$. Since for fig.118 the value of P_{min} is greater than that for fig.117, the initial signal to the servo amplifier will be smaller which implies a slower closing rate of the Saunders fuel valve. Consequently the pressure of the fluid in the vicinity of the valve will not be in the region of P_{min} for as long as for the case when the servo responds more quickly. This implies that the fluid column may not be retarded as fast as for, say, linear closure and as a result when the signal to close the valve fully arrives, the column may have a greater velocity than for the linear closure case. This will lead to the generation of higher transient pressures and hence a value of ϕ greater than unity. However, once the servo has time to achieve the demanded pressure then sufficient retardation of the liquid column is available to reduce the value of ϕ to less than unity. Note that in fig.118 the performance boundary, as well as the mininum value of ϕ , has changed.

The effects described above may be rectified by changing the servo loop gain. For an increase in P_{min}, it has been explained that the input signal to the servo amplifier is smaller and if the gain of the amplifier is not changed then a slower valve closure rate is obtained. Thus if the servo amplifier gain is increased then the original rapid valve movement should be restored. This may be simulated in program VSP2 and the results for a value of loop gain of $0{\cdot}6$ as opposed to $0{\cdot}2$ is shown in fig.119. Once more the value of ϕ is less than unity everywhere and in fact better results are achieved both in the range of the performance boundary and in the minimum valve of ϕ obtained.

It should now be clear that a precise method of determining the best values of all the variables to derive the optimum value of ϕ is not within the scope of this work. Methods are available which deal with optimising systems of linear equations containing the variables defined but these are not at present capable of dealing with the types of non-linearity and discontinuous functions to be found in the 'fluid dynamics' section of the control loop. Thus the optimisation process must take the form of finding, by repeated running of the model, a best set of values for the control parameters and using these values to compare the overall system performance for a variety of flow conditions in the kerosene pipeline. The parameter variations described in this section may be summarised in figs.120 and 121. Fig.120 shows, for constant flow conditions and loop gain the effect of altering P_{min} while fig.121 shows the variation of servo gain for a constant value of P_{min}. Note the similarity between the curve for $P_{min} = 34{\cdot}3$, $G_2 = 0{\cdot}2$ and that for $P_{min} = 103$ and $G_2 = 0{\cdot}6$.

Finally the effect of gain switching, described in the previous section, may be illustrated (see fig.122). This shows that although the introduction of gain switching achieves better pressure control the end results are inferior to those where such switching is not used. This provides an insight into the two effects which influence the magnitude of the resulting pressure transients. Once the valve is fully closed the liquid column will have a velocity (assuming for the moment a rigid column) and a differential pressure between its ends. Both of these factors will produce transients although it is not apparent which one will be the most significant in any given circumstances. Now, when gain switching is not employed it will be seen from fig.115 that the cavity pressure tends to increase, thus in this instance the pressure differential across the column is decreasing while its velocity is not decreasing as quickly as when

the cavity pressure is accurately maintained at P_{min}. For gain switching cases however, the pressure is maintained more closely to P_{min} so the velocity reduction is greater because the pressure differential is greater. The conclusion to be drawn from fig.122 is that the pressure differential effect is more significant than the residual velocity effect once valve movement has ceased. It can also be seen that since the velocity reduction is faster for cases where gain switching is employed the performance boundary will occur sooner than closure cases not using gain switching. It is interesting to note that the relatively small change in maximum predicted pressure for controlled closure results in a large change in the values of ϕ.

22.1.6. Theoretical investigation of Valve Stroking Method No.2.

Although the work described in this section is termed theoretical it is essentially empirical in nature and consists of 'experimenting' with the mathematical model instead of a test rig. As reported in Section 14 program PTP7 enables values to be obtained for the velocity of the downstream fluid column at which the valve is to be fully opened. There then follows a period of cavity compression which terminates when the velocity everywhere is zero and the pressure differential across the ends of the downstream column is likewise zero. At that instant the valve is closed instantaneously thus isolating the two systems. Unfortunately the difference in assumptions used in formulating programs VSP2 and PTP7 enable the latter to be used only as a rough guide to the magnitude of column velocity at which valve opening begins. The main source of discrepancy lies in the fact that VSP2 simulates the actuator dynamics whereas PTP7 assumes that instantaneous valve operations are possible. Knowing that the minimum time to rotate the valve from a fully open to a fully closed position takes

approximately 50 m.secs, it is possible to estimate the time at which the movements should be initiated. These times are then programmed into subroutine GEN and VSP2 may be run.

The results for a certain initial flow state is shown in fig.123. This is the pressure-time history at the valve face and the figure also illustrates the demand signals and the times at which they occur. The same function ϕ that was used in the previous section may be employed to assess the benefits of this method and the value of ϕ corresponding to fig.123 is 0·067. This indicates a substantial improvement in controlling the pressure fluctuations since it amounts to approximately 7% of that due to linear closure. The process may also be shown on a pressure - flow velocity plane and this is presented in fig.124. The initial pressure overshoot is apparent in the bottom right-hand corner of the diagram. If part of this figure is enlarged i.e. the section relating to the opening and closing of the valve, the locus may be compared to the output of program PTP7 and this is shown in fig.125. For this particular flow case the agreement between the two programs is not as good as might be expected although it improves for other flow cases. Such a case is shown in fig.126 and this has a value of $\phi = 0{\cdot}03$.

Although the theoretical results achieved by method 3 are good, the model predicted that if the time at which the signals for opening and closing the valve were displaced by only 15 m.secs the magnitude of the transient pressure increased rapidly and in certain circumstances produces values of ϕ in excess of 1. This implies that the method is suitable for installations which have predetermined flow conditions

but otherwise the inflexibility of the proceedure detracts from its overall effectiveness. For this reason it was decided to concentrate the practical aspects of this work into method 3, which appeared from the model to provide results which were invariably better than a simple linear closure. More will be said about method 2 in the conclusions of the work.

22.1.7. Maximum valve performance limits - Method 3.

When method 3 is used to attenuate the pressure fluctuations experienced in linear closure, there is found to be a maximum time, t_{max}, of valve closure so that in this time the valve finds itself shut while attempting to maintain the pressure at the valve constant. This may be explained by means of the following sequence of events. When the valve closes through an initial amount, the effect on the fluid flowing through the valve is to propagate a pressure drop wave towards the downstream reservoir. This wave is reflected at the reservoir as a pressure rise wave and arrives back at the valve after one pipe period. Hence if the servo system is to maintain the pressure at a constant value, the valve must be rotated so as to produce another pressure drop of magnitude equal to the pressure rise of the returning wave hence the net pressure fluctuation is zero. Now this second pressure drop wave is propagated down the pipe, reflected and returns to the valve where it again cancelled. The process is repeated in a continuous fashion until the valve is fully closed. It is the time at which this occurs that determines the performance boundary for the pressure control system and any subsequent control signals requiring total closure of the valve will have no effect.

Further, the time t_{max} will be proportional to the initial flow velocity for a constant value of P_{min}. Hence if the pressure is required to drop from P_o to

P_{min} for two different flow velocities then a greater percentage of flow reduction will occur for the low flow case than for the high flow case. This implies that t_{max} will be smaller for the low flow case since the valve will be closed to a greater degree for the initial pressure reduction.

22.1.8. Investigation into the effect of fluid inertia on the servo response.

It was thought that method 2 could be made to work exactly if the servo response were made instantaneous with regard to the fluid response. It was not possible with the present experimental system since the servo required approximately 50 m sec to change the valve position from fully open to fully closed and in this time the pressure of the fluid has time to change appreciably. What is required ideally is for the pressure in the pipe to be uniform (or equal at both ends of the liquid column) at the value of the downstream reservoir pressure while the velocity everywhere (or again at both ends) is zero. When this condition is approached while the valve is fully open, instantaneous closure is required when the condition is reached so as to isolate the two systems. If the valve is not closed instantaneously, pressure changes occur in the interval preceeding valve closure producing transients after valve closure.

It is possible that 'instantaneous' valve operation may be assumed if the pipe period of the kerosene pipe is considered to be very much greater say, of the order of seconds. If this were so, then the frequency response of the servo system would be only a few percent of this 'fluid' response. Thus an enlarged system was simulated in the theoretical model and ideal valve stroking as predicted by Method 2 was attempted.

It failed due to the pressure continuing to change appreciably while the valve was closed as rapidly as possible. This surprising result prompted the following analysis: Considering the system, again, shown in fig. 65 and writting down the equations of motion for the frictionless fluid columns we have

$$\frac{dV}{dt} = a_1(P - P_0) \qquad 71$$

$$P\forall = a_2 \qquad 72$$

$$\frac{d\forall}{dt} = a_3(V - V_1) \qquad 73$$

$$\frac{dV_1}{dt} = a_4(P_0 - P) \qquad 74$$

It is probable (according to the model) that when the valve is fully opened, $V \simeq V_1$ and the graphs shown in Fig. 67 will describe the subsequent fluid motion. Time t_{vo} is when the valve is fully opened and t_{vc} is the time when instantaneous valve closure is required. At time t_{vo} the velocities are equal and the minimum cavity pressure is reached. After this, the pressure rises while V_1 increases as V decreases until $P = P_0$ and from equations 71 and 74 the acceleration of the two columns are zero. Since we are primarily interested in the pressure changes we can write, using equation 73.

$$P = a_2 / \forall$$

and

$$\frac{dP}{dt} = \frac{-a_2}{\forall^2}\frac{d\forall}{dt}$$

$$= \frac{-a_2 a_3}{\forall^2}(V - V_1) \qquad 75$$

also from (71)

$$P = \frac{1}{a_1}\frac{dV}{dt} + P_0 \qquad 76$$

If we now investigate the rate of change pressure at or near the time t_{vc} i.e. when the valve end pressure is equal to the reservoir pressure and the velocity is zero, we can be using equations 75, 76 and 72 obtain

$$\frac{dP}{dt} = -\frac{a_2 a_3 (V-V_1)}{a_2^2} \left\{ \frac{1}{a_1} \frac{dV}{dt} + P_0 \right\}$$

Note that the only term in the above equation which involves the liquid column's length is a_1. Now, around time t_{vc}, $P \rightarrow P_0$ and hence from equation 71

$$\frac{dV}{dt} \rightarrow 0$$

hence at $t = t_{vc}$

$$\frac{dP}{dt} = \frac{-a_3 (V-V_1) P_0}{a_2}$$

and is thus independant of the column length. This helps to explain the results from the model, when the same servo system was used but on a pipe line of about ten times the length of the experimental pipe. For this case the servo could not close fast enough, relative to the rate of change of pressure at the valve, to complete valve closure and maintain the required conditions. It will be seen from the above equation however that the rate of pressure change may be accomplished by reducing the pipe diameter and thus reducing the constant a_3. Also, since the pipe diameter is related to a_3 in the form

$$a_3 = K d^2 \qquad \text{where K is a constant}$$

it is possible to produce large changes in a_3 for relatively small changes in d. Also a_2 is found to be indirectly related to the length of the liquid columns. Since a_2 is a measure of the mass of gas released from the kerosene, and recalling the work dealing with rates of air release, it will be seen from equations 71 and 74 that

for the same initial conditions, it will take longer for a large mass of liquid to retard than a small mass. This extra time for deceleration implies that more air has the opportunity to be released. This increases the value of a_2 and hence reduces the rate of pressure change at time t_{vc}.

A disadvantage of this form of valve stroking also becomes apparent. At time t_{vc} the upstream column of liquid, of which no consideration has been made so far, appears to be at a state of maximum kinetic energy at time $t = t_{vc}$. Thus if the valve is closed instantaneously at this instant, then large pressure transients (caused by liquid compressibility) may be expected in the upstream pipe.

From the preceding arguments, it is shown that the ratio of frequency responses of the servo system to the fluid transient system may be reduced by several means, but not directly by the method of simply lengthening the pipe of the fluid system. Since changing some of the parameters of the model may cause a change in the magnitude of rounding off errors, it was decided to simulate an ideal system in which the actuator could be opened, closed or set to any intermediate position instantaneously. This is easily accomplished in a digital program.

Trouble occurs however, since as the response time of the servo is reduced until it is insignificant then when the valve is 'instantaneously' opened or shut then it will produce pressure transients due to liquid elasticity of the most significant magnitude. If servo performance is considered as that specified by practice, these transients are not so large due to slower valve movement and thus the theory proposed in method 2 will be more precise. The 'instantaneous' valve operation produces transients which invalidate some assumptions used in the development of method 2.

22.2. Second stage experimental work and scope of results.

22.2.1. Operation of test rig.

As outlined in section 22.1, the main object of this phase of the experimental work was to verify the results predicted by program VSP2 due to the implementation of the proposed valve stroking method number 3. The overall apparatus for doing this (shown in fig.207) may be divided into the following groups.

1. Basic kerosene transients loop.
2. Hydraulic servo system for operating the plug valve.
3. Electronics associated with the control function.
4. Equipment for observing the pressure transients.

Elements of the above groups may be seen in the operating area, fig.206.

The initial test proceedure relating to the kerosene loop has been discussed in section 7.6. and the startup methods outlined in that section were followed for this part of the practical work. This involves, briefly, setting the line flow velocity by means of the pump return line throttle valve and the initial pressure by introducing air into the upstream reservoir. The actuator mechanism, however, is completely different from that used in section 7.6. and references to this item should be ignored.

To operate the hydraulic servo, the reservoir level should first be checked and then the oil cooler water supply turned on. The shut off valve should be

fully opened, together with the pressure gauge restrictor valve and the system pressure regulation valve. The drain down valve should be closed. The pump may be started once the mains supply has been switched on. While the system is at a low pressure, the air may be bled from both the branch pipe terminating with the pressure gauge and the actuator. The gauge-pipe junction may be opened slightly to allow the air to escape and closed tightly again once oil is present at the junction. The hydraulic actuator has its own bleed screws which should be left open for a few seconds since the leakage past the spool of the servo valve is low. Once this is done the bleed screws must be closed. It is hoped that air trapped within the main oil loop will be transported by the oil to the sump.

At this stage, an assessment of the total quantity of oil it is necessary to store in the accumulator must be made. The accumulator will contain a maximum of 0·164 ℓ of oil and since the swept volume of the actuator is in the region of 0·003 ℓ then it is not necessary to store a large quantity. Any leakage flow is adequately met by the pump delivery. Having decided on the volume of stored oil, figs.104 and 105 enable the charging pressure of the accumulator to be determined. Charging is achieved by connecting a nitrogen gas bottle via a Fawcett charging valve onto the accumulator. The proceedure for charging is explained fully in the accumulator manufacturers' instructions sheet. Once the correct pressure has been achieved the nitrogen bottle is sealed and disconnected leaving the charging valve on the accumulator. This enables the air-side pressure to be checked periodically since the charging valve has a pressure gauge attached. The checking was found necessary since two accumulators were destroyed due to a sudden pressure loss on the air side while the liquid side was also under pressure

The system pressure can then be set by means of the regulator valve and it was set to such a value that the quantity of oil stored in the accumulator was the quantity calculated from figs.104 or 105. The pressure gauge should be read in conjunction with its calibration chart shown in fig.200. In practice, the working pressure of the servo valve may vary from 350 KN/m^2 to 21,000 KN/m^2 without serious loss of frequency response. It was found that when the servo was worked in the region of 7000 KN/m^2 a high frequency, small amplitude oscillation developed which also caused the actuator to oscillate. While the origins of this instability remain uncertain, it was found to disappear if the working pressure was lowered to the order of 3000 KN/m^2. Since this did not produce a significant degradation of overall system performance, the adjustment was considered worthwhile. The nature of the oscillation suggests that it comes from the signal generator, possibly from the NAND gate/reed relay combination but why this is dependant upon the system pressure is not clear. Thus fig.105 was used mainly to determine the charging pressure of the accumulator.

The control system electronics are fully described in ref.100 which is included as appendix 9 to this report. In appendix 9 a description of the units involved will be found together with the necessary startup and operating proceedures, and so will not need further discussion here. Similarly, the equipment (transducers, amplifiers, oscilloscope etc.) for observing transient pressures in a pipe were described in section 7.6. It was found useful to employ two oscilloscopes since four traces were observed, although one oscilloscope has the capacity to handle all four. One instrument displayed the demanded and achieved pressures downstream of the Saunders valve while the other showed the overall valve closing time and the linear displacement transducer output.

22.2.2. Scope and presentation of results.

For the investigation of valve stroking method No. 3, the following parameters may be considered as independant variables

1. Flow velocity.
2. Initial line pressure.
3. Total valve closure time.
4. Minimum demanded pressure.

Ideally three variables should be held constant while the dependant variable, maximum system pressure, is observed for variations of the fourth independant variable. If the results are plotted and, say, six points are required for each graph this will result in $6 \times 4!$ or 144 experiments. This was considered to be too great for the time available so one of the parameters listed above was held constant. This parameter is P_{min}, the minimum demanded pressure and this was kept constant at 34·3 KN/m^2. A brief discussion of how this parameter influences the results is available in section 22.1.5. based on the theoretical results of program VSP2. To further simplify the experimental work, discrete values for initial flow velocity and line pressure were chosen; two initial pressures and three flow velocities giving six test cases covering the range of flow parameters available on the test rig. The flow conditions associated with the six test cases are summarised in table 5. For each test case, a theoretical diagram for method 3 may be drawn and is similar to that shown in fig.117. The object of the experimental work is to fit points to the curve for the maximum transient pressure for controlled closure, $\hat{P}_c$, while the nominal valve closure time varies. The data from the experiments is presented in two forms for a given flow case. Values of T_{CLOS}

near the extremities of the $\hat{P}_c$ curve are recorded photographically from the oscilloscope traces and where the interval between these two points is large, a mid point is also included. A summary of the photographs and the data obtained from them is presented in table 6. The second form of data is measured directly from the oscilloscope and no visual, permanent record was kept. The results obtained by this proceedure is shown in table 7. For a given flow case the two types of data are combined onto a single graph.

For each nominal value of valve closure time, two photographs are obtained from the two oscilloscopes. These are redrawn using a pantograph arrangement so that they may be compared to the output of program VSP2 for the same initial conditions. The two parameters that are checked in this way are:

1. Pressure-time for the section immediately downstream of the valve.
2. Actuator displacement - time.

The second parameter is of minor importance but does allow a check to be made on the assumptions attributed to the modelling of the servo system. Thus the results are presented in six sections, each one considering a flow case (see table 5). In each section the first graph summarises the results for that particular flow case and compares the theoretical with experimental work. This is followed by the two or three data points for which photographs are available;. each pair of photographs being followed by the redrawn curve along with the theoretical results for the same conditions. The results are shown in figs.127-192.

As time was available after completing the above practical work, a brief investigation was made into the effect of changing the value of the minimum

demanded pressure P_{min}. Six values of this parameter were taken in the range 34.3 KN/m^2 up to 120·0 KN/m^2 in equal steps. The six results for the pressure at the valve end against time are shown in figs.193 - 198 while fig.199 summarises the maximum pressures and illustrates the values predicted by program VSP2. The flow conditions for figs.193-198 are

a) $V_o = 1{\cdot}525$ m/s

b) $P_o = 308$ KN/m^2

c) T_{CLOS} (nominal) = 0·4 s.

23. Summary of Research.

23.1. Discussion of Results.

The work reported has been divided into four main sections since this layout represents the manner in which the subject has been developed. In practice some of the sections were worked in parallel since time did not allow one item to be finished before some attempt had been made on the next. As a result of this division of work some discussion has been included within the main text on the particular topic under investigation. Thus, this section will deal with points that supplement any arguments already raised within the text and if any features are not included in this section then the appropriate chapter in the text should be consulted.

23.1.1. Discussion of Part 1.

The majority of this work was dealt with in section 8, however the following additional points should be added.

a) When obtaining experimental results, a source of inconsistancy may arise if the pump returning the fluid to the upstream reservoir is not shut down at the same time as the valve is closed. As mentioned in section 7.6. if this is not done the pump will remove a quantity of kerosene from the reservoir at the downstream end and allow an expansion of the air above the reservoir level to take place. The inconsistancy arises when the initial volume of air above the kerosene is not constant. For example, if the pump removes one litre of liquid from the tank and the volume of air is large then a small change of pressure, and hence of the boundary condition, will take place. If the air volume is small, the liquid level will drop the same amount

and introduce a relatively large change in the boundary conditions.

b) The rigidity of the valve may be significant in determining the magnitude of the pressure rise at the valve. This is because as the column of separated kerosene returns towards the closed valve it does so very rapidly. In fact in some cases the entire duration of the transient peak is only 10 ms. Thus if the pipe and valve are insufficiently restrained in the longitudinal direction to the order of only 1 mm and movement does occur in 10 ms, then the corresponding velocity of the valve is 0·1 m/s. This effectively reduces the velocity of the returning column by the same amount which is a significant effect.

c) The nature of the pressure-time functions displayed in figs. 44-51 suggest that the mechanism of classical waterhammer waves have only a minor influence on the type of flows produced for this type of valve closure. It will be shown in a later section that the approximations used in section 11 give a good representation of the flows after valve closure is complete. Essentially this reduces the downstream system to a rigid column subject to a driving pressure gradient between the downstream constant pressure reservoir and an upstream air cavity containing a fixed mass of gas. The inclusion of friction will allow energy to be dissipated but the basic form of the pressure time diagrams remain unchanged.

d) The proposed assumptions for the mechanism of air release appear to give satisfactory results although more information regarding the rate of evolution process would be helpful. The author attempted to determine the time constant for the evolution process in a similar manner to that described in ref. 97, without success. The apparatus is shown generally in fig. 201 while a detailed view of the stirring baffle is shown in fig. 202. The apparatus consisted of a sealed vessel containing a specimen of kerosene and a motor driven agitator. The three taps at the top of the vessel were connected to a pressure gauge, a compressed air supply and the third to the atmosphere.

The vessel was filled approximately half full with keorsene and then pressurised to a known pressure. The motor was started which caused the baffle inside the vessel to oscillate and thus agitate the kerosene. This caused the liquid to become saturated with air at the known pressure. After about 10 mins the motor was stopped and the system was left to settle for 1 min. Then, the tap connecting the vessel to atmosphere was carefully cracked so as to produce a super-saturated liquid at atmospheric pressure. The vessel was then sealed. If the motor is now started the liquid will effectively be subject to a step pressure drop from its initial saturation pressure to atmospheric pressure and will evolve air. The rate of air evolution may be assessed by the pressure time function for the space above the kerosene in the vessel. This was recorded using a Honeywell differential pressure transducer, the output being displayed on a storage oscilloscope. Unfortunately an insignificant change of pressure was recorded on several occasions and this was attributed to:

1. The degree of agitation available with the present baffle is insufficient to dissolve large quantities of air in the kerosene.

2. The opening of the tap to atmosphere disturbed the fluid to a degree whereby air evolution took place immediately. Since the time constant quoted by ref. 97 is of the order of 0·2 secs. then the air would be evolved very quickly and as a result of 2 above, all the air may have been released before the vessel was sealed once more.

23.1.2. Discussion of Part 2.

a) The limitations imposed by the consideration of friction (described in section 9.3) may restrict the use of both existing and proposed methods of valve stroking. However it may be argued that in systems with high friction losses, the pressure at the downstream reservoir will be lower, for a fixed flow rate, than for a system with less significant frictional effects. Also, once the column has separated, its velocity will be determined by the pressure drop across the ends and since the minimum pressure in the cavity will be of the order of 10 KN/m^2 then a smaller pressure gradient will exist for a high friction system resulting in lower peak transient pressures. In this way the loss in flexibility in applying valve stroking principles is compensated for by the general decrease in the magnitude of transients to be expected.

b) The definition and use of the function $\emptyset$ has been a valuable aid in comparing both the proposed methods of valve stroking and in the optimisation of valve closure time for given flow conditions. It may tend to give inconsistent results if applied to an experimental situation where the time for complete valve closure is in the region of the upper performance boundary. This occurs when a difference in recorded result of $\hat{P}_c$ for example may vary by 5% causing a variation of something like 15% in $\hat{P}_c - P_0$ and hence in $\emptyset$. This problem does not occur in results obtained theoretically since they are precisely repeatable.

c) The influence of valve and valve-servo dynamics has not been investigated by other research workers interested in valve stroking. Although the main reason for not pursuing the methods proposed by Streeter (80) is due to cavity formation and, hence, is nothing to do with the valve actuator mechanism, it would appear that the initial demand for a ramp decrease in pressure would be highly dependant upon the performance of the valve actuator.

It would, however, seem necessary that the relationship between the valve dynamics and the pressure transient system should be known so that any new method of valve stroking that may be proposed can be assessed by knowing how much of the error in pressure control is attributable to servo performance and how much to the proposed method itself.

d) The approximations made in Section 11 were used to write a computer program to simulate the variation of pressure and velocity in a pipe after valve closure is complete based on the system shown in fig. 60. The program, in the first half of its operation, prior to valve closure, estimates the amount of air released during valve operation so as to arrive at a value of the quantity of air in the cavity when the valve is shut. The program known as PTP6 is listed and described in appendix 5. Typical output of pressure against time for $t > T_{CLOS}$ is shown in fig. 203. If fig. 203 is compared to fig. 163 it will be seen that the model presented in fig. 60 may be regarded as more accurate than a conventional water hammer analysis producing traces similar to those shown in fig. 5. The system shown in fig. 60 may be analysed to form a single differential equation for the transient pressure by considering equations 52, 53 and 54 in section 12.

from 54 $$\frac{dV}{dt} = \frac{1}{A}\frac{d^2\forall}{dt^2} \qquad 77$$

The general form of equation (53) may be written as:

$$P(\forall)^n = \alpha$$

giving $$\forall = \left(\frac{\alpha}{P}\right)^{1/n} = (\alpha P^{-1})^{1/n} = \alpha^{1/n} P^{-1/n}$$

$$\therefore \frac{d\forall}{dt} = \alpha^{1/n}\left\{-\frac{1}{n}(P)^{-\frac{1}{n}-1}\frac{dP}{dt}\right\} = \alpha^{\frac{1}{n}}\frac{dP}{dt}\left(\frac{-1}{n}\right)(P)^{\frac{-1-n}{n}}$$

$$\text{and} \quad \frac{d^2A}{dt^2} = \alpha^{\frac{1}{n}}\left\{\left(-\frac{1}{n}\right)\left(-\frac{1-n}{n}\right)(P)^{-\frac{1-n}{n}-1}\frac{dP}{dt} + \left(-\frac{1}{n}\right)(P)^{-\frac{1-n}{n}}\frac{d^2P}{dt^2}\right\}$$

$$\therefore \quad \frac{d^2A}{dt^2} = \alpha^{\frac{1}{n}}\left\{\frac{1+n}{n^2}P^{-\left(\frac{1+2n}{n}\right)}\frac{dP}{dt} - \frac{1}{n}P^{-\left(\frac{1+n}{n}\right)}\frac{d^2P}{dt^2}\right\} \qquad 78$$

Now substitute (77) and (78) into 52 giving

$$P - P_o = \frac{\rho L}{A}\left\{\alpha^{\frac{1}{n}}\left\{\frac{1+n}{n^2}P^{-\left(\frac{1+2n}{n}\right)}\frac{dP}{dt} - \frac{1}{n}P^{-\left(\frac{1+n}{n}\right)}\frac{d^2P}{dt^2}\right\}\right\}$$

which, assuming n = 1 simplifies to

$$P - P_o = \frac{\alpha\rho L}{A}\left\{2P^{-3}\frac{dP}{dt} - P^{-2}\frac{d^2P}{dt^2}\right\}$$

$$\therefore \quad \frac{1}{P^2}\frac{d^2P}{dt^2} - \frac{2}{P^3}\frac{dP}{dt} - a_1P = a_2 \qquad 79$$

where $a_1 = A/\alpha\rho L$ & $a_2 = P_o/a_1$

Although no attempt has been made to solve equation (79), a comparison with the standard first degree, second order differential equation may suggest the following features of solution.

1. The solution may be periodic.
2. The solution may be damped.
3. The solution will be non-harmonic.

The three characteristics listed above are common to figs.163 and 203 which indicates that equation 79 could be used to describe pressure transients adequately.

23.1.3. Discussion of Part 3.

a) At the beginning of the work on valve stroking, it was thought that the performance requirement of the servo operating the valve would be determined by the size of the system exhibiting the transient pressures. This is because intuition suggests that events occur more rapidly in a small bore pipe sixty metres long than in a hydro-electric station turbine penstock which may be four metres in diameter and a kilometere long. However the theoretical investigation reported in section 22.1.8. suggests that the pipe period of the transients system considered may be a misleading quantity on which to base the servo design. A more important criterion is whether the actuator will produce a change in the physical state of the boundary condition for an insignificant change in pressure. If this can be achieved then the implementation of valve stroking method No. 2. would be very simple. It should be stated that such a servo requirement is desirable though not necessary since the use of a program such as VSP2 allows the interelation between valve dynamics and pressure changes to be investigated and due allowance made.

b) The choice of a closed loop control system would seem to offer several advantages over the methods used for previous investigations into transient pressure control (refs. 80 and 84). These advantages are outlined in section 17. Ultimately, the economics of constructing such a servo will have to be considered in terms of the benefit obtained by a reduction in the magnitude of pressure surges, although this may present some difficulty in installations where a wide range of flow cases and valve closure times occur. It is easier to study a single flow case, such as the rated in flow to a turbine, together with the maximum valve closing rate associated with, say, loss of electrical load. For such a problem a single value of the functions $\emptyset$, may be determined, and hence the advantages associated with controlled valve closure.

c) The control system constructed did not appear to suffer from serious instabilities in both transient and quasi steady state modes of operation. It is possible that when other components within the loop are modelled, or the fluid dynamics of other transient systems are simulated, that system instabilities will occur. It may be of use to briefly discuss some causes and cures of this phenomenon. It should be possible to determine whether the oscillation is originating with the electronics or not, since the instability will persist if the feedback loop is broken. If the instability disappears then it is a feature of the closed loop dynamics and may be attenuated without fully identifying the source. There are three common ways of stabilising a system.

1. Reduce the loop gain, providing the gain value associated with the stable system is consistant with an adequate response rate.
2. Introduce series compensation usually in the form of passive electrical networks which artificially introduce poles or zeros to modify the existing system root locus (ref.102)
3. Introduce parallel compensation in the form of additional feedback loops which essentially increase the overall damping of the system. Thus if the actuator position was fed back in addition to the pressure then the former would be a less rapidly changing variable and would tend to stabilise the system if its effect was more dominant than the pressure feedback.

d) The simulation of the electohydraulic servo valve is only approximate. Although it has been shown that the effect of changing the bandwidth of the unit is not critical, it is possible that the variation in some of the valves non-linearities may introduce significant changes in system performance. Zellor (88) has investigated both linear and non-linear features of servo valves and reference should be made to his paper if the simulation of these effects is considered necessary.

e) The proceedure outlined in section 19.2. for analysing higher order differential equations is a useful technique since a single subroutine may be used for any order equation. Similarly the step size of the integration may be varied to investigate the stability of solution, but it was found for a case where the parameter change were most severe (x and i) that negligible error was involved in the prediction of the output variables. Thus the step size used in program VSP2 was considered to be adequate as was also the integration step size.

23.1.4. Discussion of Part 4.

a) Program VSP2 enables the performance of the pressure control system to be analysed for changes in the linear components. It follows from basic control theory that the servo loop gain is an important parameter since its value will determine both the speed of response of the system as well as the stability boundary. In the present analysis, this could only be achieved by repeated running of the model to optimise the loop gain over as wide a range of flow cases as possible. This is because the control loop contains a complex 'component' which is the fluid dynamics of the transient system and does not lend itself to linearisation. The control system also has non-linear constraints such as a maximum amplifier current, or oil flow delivery and these effects should be investigated to determine their influence on overall performance. The variation in servo loop gain produces the expected effects in the system's ability to maintain a constant pressure. The improved performance obtained by a higher gain leads directly to the method of gain switching to benefit from both reasonable overshoot and good control. It must be remembered, however, that the prime objective is to reduce the magnitude of pressure transients in a kerosene pipeline and not to construct a pressure control system and as a result of the

characteristics shown in fig.122, it would seem that gain switching is not such a desirable feature of the overall system.

b) It is unfortunate that all of the information shown in fig.110 was not available at the time when the servo valve selection was made. Since a valve with a bandwidth of 50 HZ would appear to fulfil the control function as well as a valve with three times the bandwidth, it is possible that a less expensive servo valve could have been employed. It also illustrates how the performance is severely degraded for valves with bandwidths less than 25 HZ. As expected, the biggest influence of performance is due to the choice of actuator. In the particular application described, the actuator response rate is more dominant than its ability to produce a force large enough to close the valve. However it is possible that if the hydraulic control system is operated at a low pressure to avoid the unexplained oscillation mentioned in 23.1.1. then for the high flow rate demand at the beginning of valve closure, most of the oil pressure may be lost in the servo valve itself (see fig.95). If this occurs then the ball valve dynamics will be significant compared to the forces acting upon it and may lead to discrepancies between experimental and predicted results, and will result in a slower valve closure rate than expected. This effect is more pronounced in cases where the upper valve performance limit is short since the high flow demand regime forms a greater proportion of the overall valve closure time and hence the less accurate results around the valve performance limit for test case No.4. (fig.162) than, say, test case No.1 (fig.127).

c) Fig.112 confirms that the most stringent test of the servo occurs within the first 0·1 secs and is essentially the ability of the system to close the valve to about 40% open (see fig.112d) as quickly as possible. In this connection it may be that the valve could be partially closed a few seconds before total valve closure is required, providing of course that it is done slowly enough not to propagate transients

in the system. Theoretically this does constitute a valve closure but reference to fig.113 indicates that for only a reduction of 5% of the steady state pressure, the valve could be closed from $\theta = 90^{\circ}$ to $\theta = 55^{\circ}$. This is the order of magnitude of the initial valve closure demand and implies that further valve movement would produce an immediate response in pressure change instead of the 70 ms delay experienced when closing from the fully open position.

d) Figs.112d or e might suggest a less expensive manner of closed loop control, called position control. Both of these figures could be represented, for the case shown, by a pair of straight lines with a discontinuity around t = o.1s. Thus the linear displacement transducer (or a rotary potentiometer mounted on the valve spindle) could be used to feed back information on the servo performance. Obviously the function generator supplying the amplifier would have to provide the straight line approximations to figs.112d or e and the servo valve would act on the error between say, the desired and actual ram displacement (or valve rotation). This is a closed loop form of the system used by Streeter and Propson (80 and 84) and has the advantage of being relatively cheap to build since theoretically no pressure transducer or ancilliary equipment are needed. However since the pressure in the kerosene will be observed anyway, the transducer and amplifier unit will be available, so use of them in a control loop is not a major undertaking. The pressure control system has the more fundamental advantages of:

1. Actually controlling the variable in which we are interested and:
2. Eliminating the dependance of the analysis on a pressure transients program such as VSP2.

As a consequence of 2 above it is important to realise that with the system used by Streeter, a program was needed to determine a graph such as fig.112d

so that the signal generator function can be derived from it. With the system proposed by the author, no program is necessary and the various valve stroking principles may be implemented directly on the test rig. Program VSP2 was developed to illustrate the effects of parameter variations and the determination of performance boundaries. Note also that the system is independant of the steady state valve characteristic and hence independant of any assumptions made regarding relevance to unsteady flow situations.

e) As far as the experimental investigation of method 3 is concerned, it should be realised that the series of tests conducted do not represent a comprehensive variation in all the parameters involved. This may be justified by claiming that the method of valve stroking was under scrutiny rather than the effects of parameter change upon that method. The six flow cases discussed do cover the maximum and minimum regions of flow velocity and initial line pressure and there is nothing to suggest that any intermediate values will produce discrepancies of greater magnitude than those encountered under test.

f) The upper performance limit was accurately matched, except in flow case No. 2 when the boundary was found to be 0·92 instead of 0·82 seconds. The minimum time for valve closure was determined by scaling factor associated with the pressure transducer/charge amplifier. As explained in appendix 9, this scaling factor is set with regard to two functions.

1. To fulfil a gain within the control loop.
2. To allow observation of the pressure transients occuring within the kerosene.

Since the amplifier has a maximum output of ±10v, function 1 above implies that the maximum linear output of the unit will correspond to the maximum observable pressure. This pressure is in the region of 13000 KN/m^2 and the registering of pressures in excess of this figure is impossible without an internal change of gain within the servo amplifier. If the maximum pressure of 13000 KN/m^2 is not reached then the minimum performance limit depends upon the least time of valve closure that can be achieved by the signal generator. This time is approximately 0·1 s.

g) The minimum predicted valve closure time is approximately 0·050 seconds, so the curve for $\hat{P}_c$ is not drawn for times less than this (see fig.127). Note that $\phi \neq 1$ at this time but, theoretically, only for $T_{CLOS} = O$. This is due to the different rates of valve closure for the controlled and linear valve operations. For linear valve closure, no account is taken of the actuator's ability to produce such a linear closure and so $dx/dt \neq O$ when valve operations begin, while this condition obviously cannot be true for a real situation. The difference between the two initial valve closure rates may be seen by comparing figs.113 and, for example, 135; and will account for the fact that $\phi \neq 1$ at the lower performance boundary.

h) In all six flow cases considered, the maximum error involved between the experimental and predicted values of $\hat{P}_c$ derived by method 3 are not greater than 9%. This leads to the conclusion that the method investigated does reduce the magnitude of pressure transients since the predicted values were computed using a program that incorporates the linear closure program i.e. Prog. VSP2 includes Prog. PTP1. Thus it would not be reasonable to expect the results of VSP2 to contain significantly less error than PTP1. For most cases considered the pressure-time curves for predicted and experimental work correlate well either in terms of magnitude and timing (see fig.152) or in magnitude only (see fig.191). Generally the comments with regard to secondary peaks are the same as those for the linear

closure case (see section 8) although for some cases the predicted times and magnitudes were surprisingly accurate (see fig.165 or 169 compared to fig.130), and appear to apply only to the more rapid valve closure rates. For method 3, the validity of equation 52 may be shown by fig.204 illustrating the quasi linear flow reduction.

i) The predicted and measured actuator displacement against time functions may indicate one of the main causes of discrepancy - friction. Many of the experimental curves presented have the same slopes as the theoretical ones but are displaced vertically which suggests that friction, or possibly inertia, is significant when the signals levels in the servo are small. These effect, not simulated in the model may be due to the following:

1. Friction between the actuator piston and inside cylinder wall.
2. Friction in all moving parts of the valve linkage.
3. Inertia of the oil in the pipes joining the servo valve and the actuator.
4. Inertia of the oil within the hydraulic accumulator.
5. Inertia of the actuator piston, valve linkage components and the Saunders valve.
6. Seals in the Saunders valve exert a frictional torque on the valve spindle. By moving the valve linkage with the link pin removed and by rotating the valve manually, the valve seal friction was not only estimated to be greater than that of the linkage but the "stictional" effects were considerable.
7. Dynamic loading of the Saunders valve by the kerosene flowing through it.

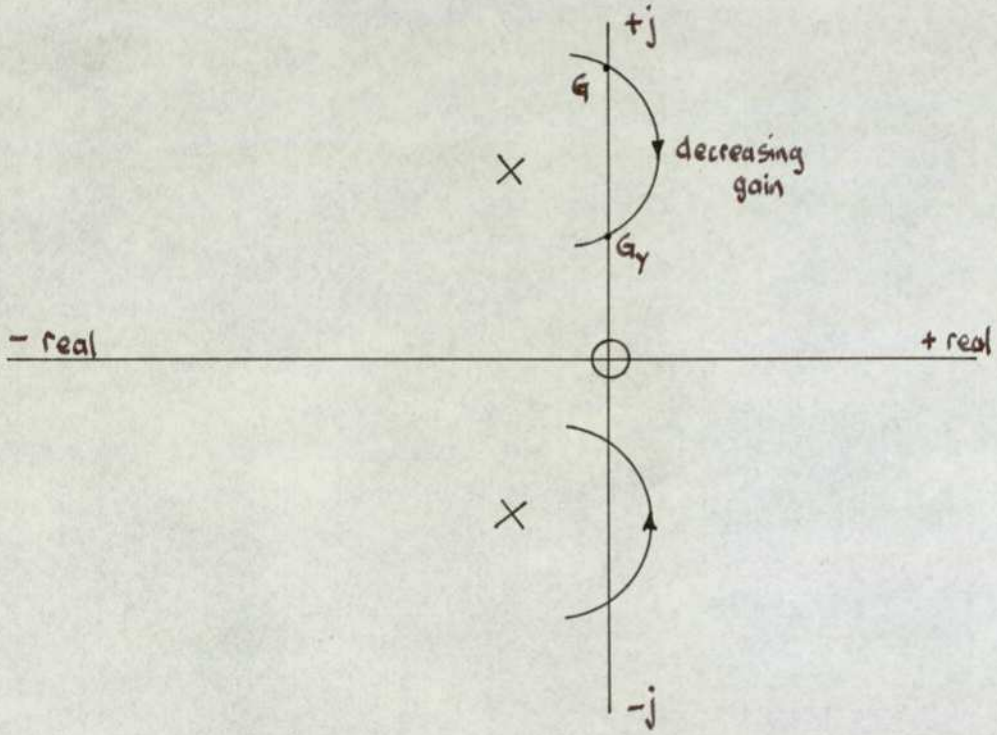
8. Backlash effects in the valve linkage. Could be influential although the valve pin and slider block were both sliding fits and the overall backlash was estimated at 1·0 mm at the pin.

9. The possible occurrence of pressure transients within the hydraulic servo system is illustrated by figs.129, 133, 138, 146 and 151. It would seem however that these transients do not influence the pressure-time traces associated with them. It was thought that the ripple seen on the steep part of actuator displacement curve could also be due to the valve linkage being out of alignment so that when subject to a rapidly moving valve pin, large frictional forces would arise introducing the vibration illustrated. The apparent frequency of the ripple is 0·025 secs. and assuming for the wave speed of oil in a steel pipe 1000 m/s and the pipe length found to be 0·5 m, the pipe period is τ where

$$\tau = 2.\ 0{\cdot}5 / 1000 = 0{\cdot}001\,s$$

k) The work illustrated in figs.193-199 shows the need for an overall optimisation program to calculate the best value of P_{min} and G_2 for a given flow case. For such a case, a further reduction of over 30% in the value of $\hat{P}_c$ may be achieved by changing the value of P_{min} and shutting the valve in the same overall time. There is, however, an unpredictable effect which occurs experimentally and not in the model. As the value of P_{min} is increased, the amplitude of maximum transient pressure decreases but an instability within the control system becomes more pronounced. This instability may be seen on the P_{min} level, growing as the value of P_{min} increases until figs.197 and 198 the fluctuations are of the same order of magnitude as the demanded pressure drop. In fact with a value of $P_{min} = 137{\cdot}2$ KN/m^2 which is the next step on from fig.198, the system oscillations are so large as to be indistinguishable from the transients produced after valve closure. In other words the system hunts.

Using the root locus analysis of control systems (ref.102), it could be argued that a change of P_{min} is effectively a change of gain in the forward path (see section 22.1.5) and would suggest that a pair of complex poles exist in the S - plane such that the dominant section of the system locus crosses the imaginary axis in the fashion of the sketch below:



So that if the equivalent systems gain is reduced below G, a system instability occurs. The locus must re-cross the axis again for a gain of G_y since zero gain renders the servo inoperative and hence stable. This would explain the phenomenon observed. However the period of oscillation is around 5 HZ and it is not clear where such a low frequency instability could arise, since the only suspect source - the electronics unit should be well above this figure. The question also arises as to why this effect is not observed when the system gain is varied by means of the servo amplifier gain, G_2 (see fig.109). The logical answer is that the two methods of varying the system gain are not the same and yet it will be seen that for a linear system it should not make any difference whether one gain is changed or the other. In fact

a non-linearity is found to exist between these two gains in the form of the servo amplifier saturation limit and this is the only element to which the oscillation can be attributed. The analysis of the non-linearities of the system is not within the scope of this work and it must produce a limit cycle type of oscillation within the system.

23.2. Conclusions.

a) The formulation of accurate boundary conditions for the numerical computation of pressure transients is essential. The assumptions made regarding both steady state and transient modes of air release appear to be reasonable in view of the predicted and experimental results.

b) The results obtained experimentally (section 8) would validate the assumptions that:

1. No internal cavities occur within the liquid column.
2. The air released coalesces into a single cavity.
3. Maximum agitation occurs at the valve causing any air release to take place at this point.

c) The effects of kerosene vapour within the cavity may be neglected for the flow cases considered.

d) The method of characteristics can be used to reduce the partial differential equations for continuity and motion to total differential equation suitable for solution in a digital computer program. Further, such a program when subject to the other assumptions stated in Part 1 of this report provides results which are in error by a maximum of 10% in the prediction of the maximum system pressure.

e) To accurately predict the unsteady pipe flow occurring during and after valve closure, the effects of released air from the flowing liquid should be considered.

f) While the method of valve stroking proposed by Streeter may be adequate for fluids experiencing continuous flow, the occurrence of internal cavities within the liquid may render such procedures unworkable.

g) For the flow cases considered, after valve closure was completed, the transient pressures could be more accurately represented in shape by a rigid column analysis than by a compressible liquid column theory.

h) The techniques employed for the simulation of the servo system components were shown to be in general accurate enough although the assessment of some non-linear effects may be improved upon.

i) The development of Program VSP2 confirms that both of the valve stroking methods proposed, Nos. 2 and 3, theoretically attenuate the magnitude of pressure transients occurring in the system such that the factor ϕ is in the region of 0·6. The program also predicts that there is an upper and lower performance boundary of the servo system so that a limited range of total valve closure time is available. Both the performance boundaries and the minimum value of ϕ are dependant upon the choice of the parameters P_{min} and G_2. The author was unable to synthesises the system for the optimum value of ϕ (and the corresponding values of P_{min} and G_2) for a given flow case.

j) The valve and actuator dynamics formed a significant feature in determining the theoretical values of the maximum predicted pressure for controlled closure. From the arguments presented in section 22.1.8. it can be concluded that such dynamic effects are significant even in situations where the geometry of the flow systems suggest otherwise.

k) The ability of the control system to achieve the demanded signal depends largely upon the loop gain, servo-valve bandwidth and the bore of the actuator. Only the first parameter is variable once the components of the loop are specified and it was found that a single value of loop gain provided satisfactory (though not optimum) response.

l) A theoretical investigation into valve stroking method No. 2. indicated that a value of $\phi = 0 \cdot 05$ was not difficult to achieve. Although this means an attenuation of 95% of the pressure fluctuation, the model also proved that the method is sensitive to the timing of the various system inputs and must cast doubt on the method's ability to cope with small fluctuations in individual components.

m) In the comparison between experimental and theoretical work relating to method 3, the maximum error between the two values of the maximum system pressures for controlled closure was found to be 9%. Thus the method may be used to reduce the magnitude of pressure fluctuations within a piping system by approximately 40% about the final steady state line pressure. Also the actuator displacement-time functions obtained were of the same form as those predicted indicating that the method of simulating the servo dynamics was sufficiently accurate.

23.3. Further work.

The numerical proceedures employed in the analysis of hyperbolic partial differential equations appeared to give satisfactory results without any stability problems. The geometrical nature of the "characteristic lines" in the space-time plane would suggest that it is possible to work backwards in time from a known, final quiescent condition to an initial condition, equally steady. The magnitude of pressure transients in the intermediate phase may be assessed and possibly limited while the boundary condition changes necessary for such effects could also be quantified. Problems will arise due to the dissipative nature of viscous friction since energy will have to be "added" to the system if the time direction is reversed, although an initial investigation may be made of frictionless systems. This proceedure could lead to the formulation of several methods of valve stroking.

The work investigating both steady state and transient modes of air release from liquids would benefit from an assessment of the time constant of the rate process. Although the apparatus shown in fig. 201 is inadequate for such a purpose, it is possible that refinement of the valves at the top of the chamber would lead to useful results. Once a figure has been obtained, the effect of agitation could be investigated along with a quantitive analysis of agitation itself via, perhaps, a dimensional analysis. This could then be related to the agitation experienced by the fluid passing through the valve (a function of the valve opening) and the appropriate time constant used. The program PTP1 could, with very little modification, be used to simulate air absorbtion and release during cavity compression and subsequent

re-opening phases, although this would require the use of a solubility rate time constant as well as an evolution rate time constant. This should lead to an improvement in the prediction of the decay rate of the pressure peaks although the author suspects that pipe wall friction and heat transfer effects are equally significant.

The possibility of manufacturing a valve with pressure transient reduction as a dominant design criterion would be interesting. Both classical methods and those proposed in this research share the common feature that the downstream liquid column should be retarded with constant deceleration, or as near constant as the controlling mechanism will allow. A valve which would reduce the flow through it in a manner directly proportional to its degree of closure would achieve similar goals to the valve and actuator mechanism described. The advantage would be that it need only be closed in a linear fashion and would not need the additional expense of a servo control system.

Utilising an on-off type of control system would reduce the cost of the servo control to a fraction of a linear system. In addition the units would be more robust and insensitive to fluctuations in operating conditions although their non-linear nature would make any analysis of the overall control loop difficult. However this aspect of the work could bring about significant improvements in the overall operation of the system and a theoretical investigation using program VSP2 would be recommended, since a single high pressure spool valve would replace the servo valve and servo amplifier.

In retrospect, an electromechanical system could have performed the same function as the system employed. The use of a stepper motor and reduction

gear box would still have the necessary frequency response although the electronics would be more sensitive to the adverse environment (e.g. vibration, vapour and shock) than the hydraulic servo. Mention has only been made of this method in case any on-line computer control of the valve was forseen, perhaps in the process control industry, where the interface between a computer and stepper motor would be more simple than between a computer and a hydraulic valve.

If a test rig was available with sufficient fluid inertia to make the actuator response appear instantaneous, then the design and construction of a series of inexpensive servo controls could be undertaken. These units similar to the pneumatic servo described in section 16, could theoretically be coupled to a power amplifier for use in large hydraulic pipe systems such as hydro-electric station feeders, pump storage projects or long oil pipeline situations. The author feels that in such applications the advantages gained by employing a method of pressure transient reduction are greater than the cost of installing such a system. It is on small scale equipment that the differences between linear closure and controlled closure are not so great.

In the work described, where mass oscillation has been more dominant than waterhammer (see fig. 61), the approximate method of valve stroking where the two ends of the liquid column are brought to the same pressure at the instant that the column is stationary, has proved useful. The study of proposed valve stroking method number 2 has indicated that a unique solution for valve closure does not exist, hence the fluid dynamics could be analysed more accurately to predict valve closure modes for the almost total elimination of transients. In such work, account should be taken of the pressure transients in other parts of the system instead of one pipe taken in

isolation. This could lead to an optimisation analysis of more complex pipe systems where the object is to minimise a transients function which is composed of the weighted individual transient events in each sub-system.

If more work into valve stroking methods is proposed, the author suggests that flow separation is not simulated in any mathematical models developed. This is because such a feature not only makes the analysis of the fluids more complex, but that it makes it non linear and discontinuous. If a mathematical model of the fluid dynamics could be arrived at which consists of linear differential equations, then the whole of the control loop shown in fig. 89 could be synthesised. This would lead to a more elegant mathematical approach to valve stroking and thus be applicable to a larger number of flow cases. In addition the system could be simulated on either an analogue computer or built up in 'bread board' fashion from electronic components. This would enable the design engineer to optimise the servo parameters faster and identify instability regions or system abnormalities.

24. Bibliography

1.	Euler	'De la Propagation du Son' Memoires de l'Acad. d. Wiss. Berlin 1759.
2.	Weber, E.H.	'Propagation of waves through water or other incompressible fluids in elastic pipes' Akad. d. Wiss Leipzig Berichte 1865.
3.	Korteweg, D.J.	'Uber die Fortphlanzungsgeschindigkit des Schalles in elastisches Rohren' Annalen der Physik und Chemie, 5 Floge, Band 5 1878.
4.	Lamb, H.	'Motion of fluids' 1878.
5.	Michand, J.	'Coup de bellier dans les conduites. Etude des moyens pour en attenuer les effects'. Bull. Soc. Vaudoise Eng. Lausanne 1878.
6.	Frizell, J.P.	'Pressures from velocity changes in pipes'. Trans. A.S.C.E. 1898.
7.	Joukowsky, N.	Paper to Polytechnic Soc. of Moscow, 1898 (Translated by Miss O. Simin. Proc. A.W.W.A., 1904).
8.	Wood, F.M.	'History of Waterhammer' Civ. Eng. research report No. 65, Queens University, Kingston, Ontario 1970.
9.	Allievi, L.	'General theory of Pressure variation in Pipes' Ann. d. Ing. et Archct. Italy 1902.
10.	Allievi, L.	'Notes' Atti d. Cole. d. Ing. Milan 1913.
11.	Johnson, R.	'Rigid fluid column waterhammer theory' Trans. A.S.C.E. Vol. 79 1915.
12.	Gibson, N.	'Pressures in penstocks caused by gradual closing of turbine gates' Trans. A.S.C.E. 1920.
13.	Gibson, N.	'Elastic fluid column theory' Trans. A.S.C.E. Vol. 83, 1920.
14.	Warren, M.M.	'Penstock and surge tank problems' Trans. A.S.C.E. 1915.
15.	Strowger & Kerr, S.L.	'Speed changes of Hydraulic Turbines for sudden changes of load' A.S.M.E. 1926.

16. Lowy, R. 'Druckschwankungen in Druckrohrleitungen' Springer 1928.

17. Schnyder, O. 'Druckstosse in Pumpensteigleitungen' Schweizerische Bauzitung, 1929.

18. Bergeron, L. 'Variations de regime dans les conduites d'eau' Comptes Rendus des Travaux de la Soc. Hydrotech. de France, 1931.

19. Schnyder, O. 'Uber druckstosse in Rohrleitungen' Wasserkraft u. Wasserwirtschaft. Heft 5, 1932.

20. A.S.M.E. & A.S.C.E. 'Symposium on Waterhammer', Chicago 1933.

21. A.S.M.E. & A.S.C.E. 'Second Waterhammer Symposium', New York 1937.

22. Angus, R.W. 'Waterhammer in pipes, including those supplied by centrifugal pumps: a graphical treatment' Proc. I. Mech. Eng. Vol. 136, 1937.

23. Angus, R.W. 'Waterhammer in compound and branched pipes' Proc. A.S.C.E. 1938.

24. Enever, K.J. 'The use of the computerized graphical method of surge analysis with particular reference to a water supply problem' Symposium on Pressure Transients City University, London 1970.

25. Harding, D.A. 'Reports on the digital computation of surge pressures: Pumping systems incorporating an air vessel'. B.H.R.A. Paper No. P.R. 782, 1963.

26. Harding, D.A. 'Reports on the digital computation of surge pressures: Systems with several pumps operating in parallel.' B.H.R.A. Paper No. P.R. 802, 1964.

27. Wood, F.M. 'Applications of Heavisides Operational Calculus to the solution of waterhammer problems' Trans. A.S.M.E. 1938.

28. Rich, C.R. 'Waterhammer analysis by the Laplace-Mellin transformation'. Trans. A.S.M.E. 1945.

29. Zeilke, W. 'Digital simulation of Airplane Hydraulic Systems'. Trans. A.S.M.E. 1971.

30. Enever, K.J. 'Rigid column theory & its relation to wave Theory' - Course on Pressure Transients, City Univ. & B.H.R.A., Canterbury 1972.

31. Macagno & Macagno 'Non-Wave approximate analysis of pressure surges' Paper A5 Int. Conf. on Pressure Surges, Cantabury 1972.

32. Lister, M. 'The numerical solution of hyperbolic partial differential equations by the method of characteristics'. Mathematical Methods for Digital Computers. J. Wiley 1960.

33. H.M.S.O. 'Modern Computing Methods' Notes on applied Science, London 1961.

34. Lamoen, J. 'Le coup de belier d'Allievi, compte tenu des partes de charge continues' Bull. Centre de Etudes, Liege 1947.

35. Gray, C. 'Analysis of Waterhammer by Characteristics' Trans. A.S.C.E. 1954.

36. Streeter, V. and Lai, C. 'Waterhammer analysis including fluid friction' J. Hydr. Div. A.S.C.E. Vol. 88 1962.

37. Streeter, V. & Wylie, E. 'Hydraulic Transients' McGraw-Hill 1967.

38. Yow, W. 'Analysis and Control of Transient flow in Natural gas piping systems.' Ph.D. Thesis, Civ. Eng. Dept., Univ. of Michigan 1971.

39. Streeter, V. 'Unsteady flow calculations by Numerical Methods' Trans. A.S.M.E. 1971.

40. Zeilke, W. 'Frequency dependant friction in transient pipe flow' Trans. A.S.M.E. (Basic Eng.) Vol. 90 1968.

41. Hirose, M. 'Frequency dependant wall shear in transient fluid flow simulation of unsteady turbulent flow' Masters thesis, M.I.T. 1971.

42. Holmboe, E. 'Viscous distortion in wave propagation as applied to waterhammer and short pulses' Ph.D. thesis, Carnegie Inst. of Tech. 1964.

43. Thomasson, P. 'Application of analogue computers' Paper C Symposium on Pressure Transients, City Univ., London 1971.

44. Morris, W. & Morgan, N. 'The solution of unsteady pipe flow problems on the analogue and hybrid computers' Symposium on Pressure Transients, City Univ., London 1970.

45. Le Conte, J. 'Experiments and calculations on the resurge phase of Waterhammer. Trans. A.S.M.E. Vol.59 1937.

46. Bunt, E. 'Preliminary study of valve cavitation in a pipeline. Jour. S.A.I. Mech.E. Vol. 2 1953.

47. Binnie, A. & Thackram, M. 'Waterhammer in a pumping main and its prevention' Proc. I. Mech. E. Vol. 165 1951.

48. Gayed, Y. & Kamel, M. 'Mechanics of secondary waterhammer waves.' Proc. I. Mech. E. Vol. 173 1959.

49. Haller & Bedue 'The breakaway of water columns as a result of negative pressure shocks' Water & Water Eng. June 1952.

50. Richards, R. 'Water column separation in pump discharge lines'. Trans. A.S.M.E. Vol. 78 1956.

51. Duc, J. 'Negative pressure phenomena in Pump Pipelines' Int. Symposium on Waterhammer in pumped storage projects A.S.M.E. 1965.

52. Li, W. 'Mechanics of pipe flow following column separation' Trans. A.S.C.E. Vol. 128 1963.

53. Walsh, J. & Li, W. 'Pressure generated by cavitation in a pipe' Procs. A.S.C.E. Vol. 90 1964.

54. Li, W. 'Thermal effects on the growth & collapse of cavities' Paper A1, Symposium on cavitation & Hydraulic Machinery, Int. Assn. for Hydr. Research. 1962.

55. Pearsall, I. 'The velocity of water hammer waves'. Symposium on surges in pipelines. Inst. of Mech. Eng. 1965.

56. Ripken, J. and Olsen, R. 'A study of the gas nuclei on cavitation scale effects in water tunnel tests.' St Anthony Falls Hyd. Lab. Report No. 58, Univ. of Minnesota 1958.

57. Silberman, E. 'Some velocity attenuation in bubbly mixtures measured in standing wave tubes.' Jour. Acoustic Soc. of Am. Vol. 29 1957.

58. Spitzer, L. 'Acoustic properties of gas bubbles in a liquid.' Columbia Univ. OSRD report No. 1705 - 1943.

59. Lupton, H. 'Graphical analysis of pressure surge in pumping systems.' J. Inst. Water Eng. Vol. 7 1953.

60. Marples, E. 'The significance of surge diagrams'. Symposium on surges in pipelines. Inst. of Mech. Eng. 1965.

61. Balzer, R. 'Column separation accompanying liquid transients in pipes'. Trans. A.S.M.E. 1967.

62. Weyler, Streeter & Larsen 'An investigation into the effect of momentum loss in transient pipe flow.' Trans. A.S.M.E. 1970.

References 63 → 75 were presented at the International Conference on Pressure Surges at Canterbury, Sept. 1972 (unless otherwise specified).

63. Fox, J. 'Pressure Transients in pipe-networks - a computer solution' - Paper B1.

64. Apelt, C. 'Analysis of waterhammer in complex pipe systems' Paper B2.

65. Enever, K.J. 'Surge pressures in gas-liquid mixtures with a low gas content' Paper C1.

66. Swaffield, J.A. 'Column separation in an aircraft fuel system' Paper C2.

67. Vaidyaraman, P. & Anderson, A. 'Two phase flow in long vertical pipes' Paper C3.

68. Kranenburg, C. 'The effect of free gas on cavitation in pipelines, induced by waterhammer' Paper C4.

69. Kalkwijk, J. and Kranenburg, C. 'Cavitation in horizontal pipelines due to waterhammer'. A.S.C.E. J. of Hyd. Div. Vol. 97, 1971.

70. Tanahashi, T. and Kasahara, E. 'Comparisons between experimental and theoretical results of the waterhammer with water column separation'. Bull. Jap. Soc. Mech. Engrs., Vol 13 1970.

71. Hsieh, D. & Plesset, M. 'On the propagation of sound in a liquid containing gas bubbles'. Physics of fluids, Vol. 4, 1961.

72. Satwat, H. and de Kluyver, J. 'Digital computations for water hammer - column separation.' Paper C5.

73. Safwat, H. and Van der Polder, J. 'Experimental and Analytic data correlation study of water column separation.' Journal of Fluids Eng. A.S.M.E. March 1973.

74. Safwat, H. 'Experimental studies of pressure surges in condenser cooling water systems. Paper D2.

75. Atzeni, Cao and Piga 'Transients with column separation in cooling water systems for steam power plants.' Paper D3.

76. Kerr, S. 'Surge problems in pipelines - oil & water' Trans. A.S.M.E. July 1950.

77. Kerr, S. 'Effect of valve operation on waterhammer' Journal of A.W.W.A. Jan. 1960.

78. Streeter, V. 'Valve stroking to control waterhammer'. Proc. A.S.C.E. J. Hyd. Div. March 1963.

79. Streeter, V. 'Computer solution of surge problems' Symposium on surges in pipelines, I. Mech. Engrs., 1965.

80. Streeter, V. 'Valve stroking for complex pipe systems' Proc. A.S.C.E. J. Hyd. Div., May 1967.

81. Livingston, A. and Wilson, J. 'Effects of valve operation' Symposium on surges in pipelines, I. Mech. Engrs., 1965.

82. Enever, K.J. 'Grain Power station surge analysis' B.H.R.A. Fluid Eng. research report No. 1187, May 1973.

83. Stoner, M. 'Analysis and control of Natural Gas Piping Systems' A.S.M.E. (J. of Basic Eng.) Vol. 91 Sept. 1969.

84. Propson, T. 'Valve stroking to control Transient flows in liquid piping systems.' Ph.D. thesis, Civ. Eng. Dept. University of Michigan 1970.

85. Wood, D. & Jones, S. 'Prediction & control of pressure surges due to valve closures'. Int. Conf. on Pressure Surges, Canterbury, England. Sept. 1972.

86. Walters, R. 'Electro-hydraulic servo valves' Fluid Power Int. Jan. 1969.

87. Powell, J. 'Integrated electro-hydraulic control systems' Fluid Power Int. July 1972.

88. Zellor, J. 'Fast response electro-hydraulic servo system' Instruments & Control systems, March 1970.

89. Thaler, W. 'Transfer functions for Dowty-Moog servo-valves.' Dowty Rotol Ltd.

90. Guillon, M. 'Hydraulic servo systems: analysis and design' Butterworths 1969.

91. Merritt, H. 'Hydraulic control systems' Wiley 1967.

92. Walters, R. 'Hydraulic and electro-hydraulic servo systems' Iliffe books Ltd., 1967.

93. Sutcliffe, H. 'Electronics for students of Mechanical Engineering' Longmans 1964.

94. Harding, D. 'A method of programming graphical surge analysis for medium speed computers' Symposium on surges in pipelines, Inst. Mech. Engnrs., 1965.

95. Bergeron, L. 'Waterhammer in hydraulics and wave surges in Electricity' Wiley 1961.

96. Swaffield, J. 'A study of column separation accompanying pressure transients in an aviation kerosene pipeline' Ph.D. thesis, City Univ., London 1970.

97. Schweitzer, P. & Szebehely, V. 'Gas evolution in liquids and cavitation' J. App. Physics, Vol. 21. Dec. 1950.

98. Rolls Royce (1971) Ltd. 'Investigations into the effect of various aircraft and engine fuel system components on "water hammer" type pressure transients' City University June 1972.

99. Swaffield, J. 'A study of the influence of bends on fluid transients in pipelines' M. Phil. thesis, City Univ., London 1968.

100. Driels, M. 'The design, construction and testing of a servo amplifier and signal generator' Research Memo ML61, City Univ., London, June 1973.

101. Driels, M. State space analysis notes taken from M.Sc. lectures in Control Engineering, Hatfield Polytechnic, March 1970.

102. Thaler & Brown 'Servo mechanism analysis' McGraw-Hill 1952.

103. Derry, Evans, Faulkner & Jelfs 'Vapour and air release from aviation fuels' Inst. of Petroleum, Vol. 38 July 1952.

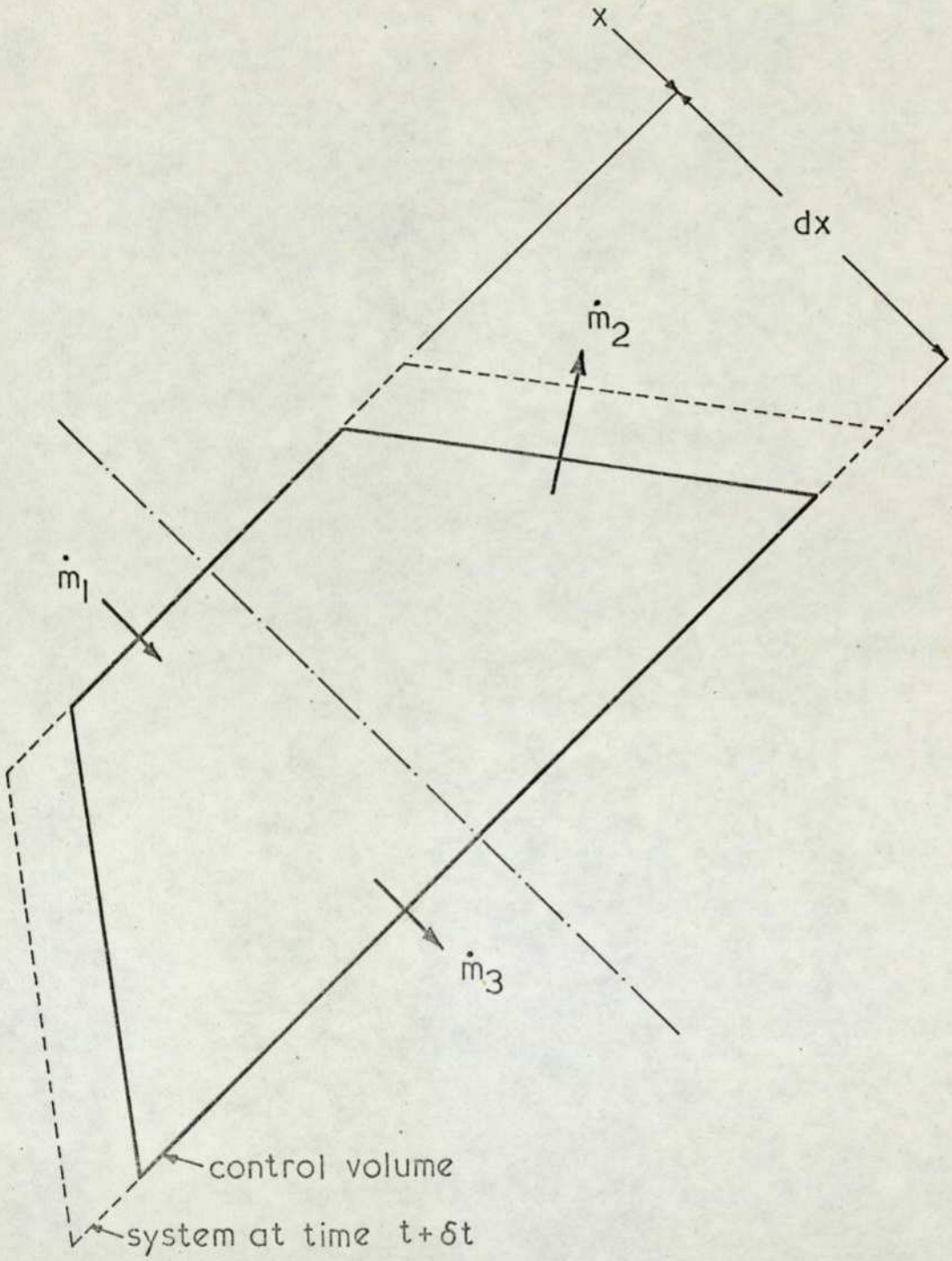


FIG 1 CONTROL VOLUME USED TO DERIVE THE EQUATION OF CONTINUITY

FIG 2a EXTERNAL FORCES ACTING ON SYSTEM

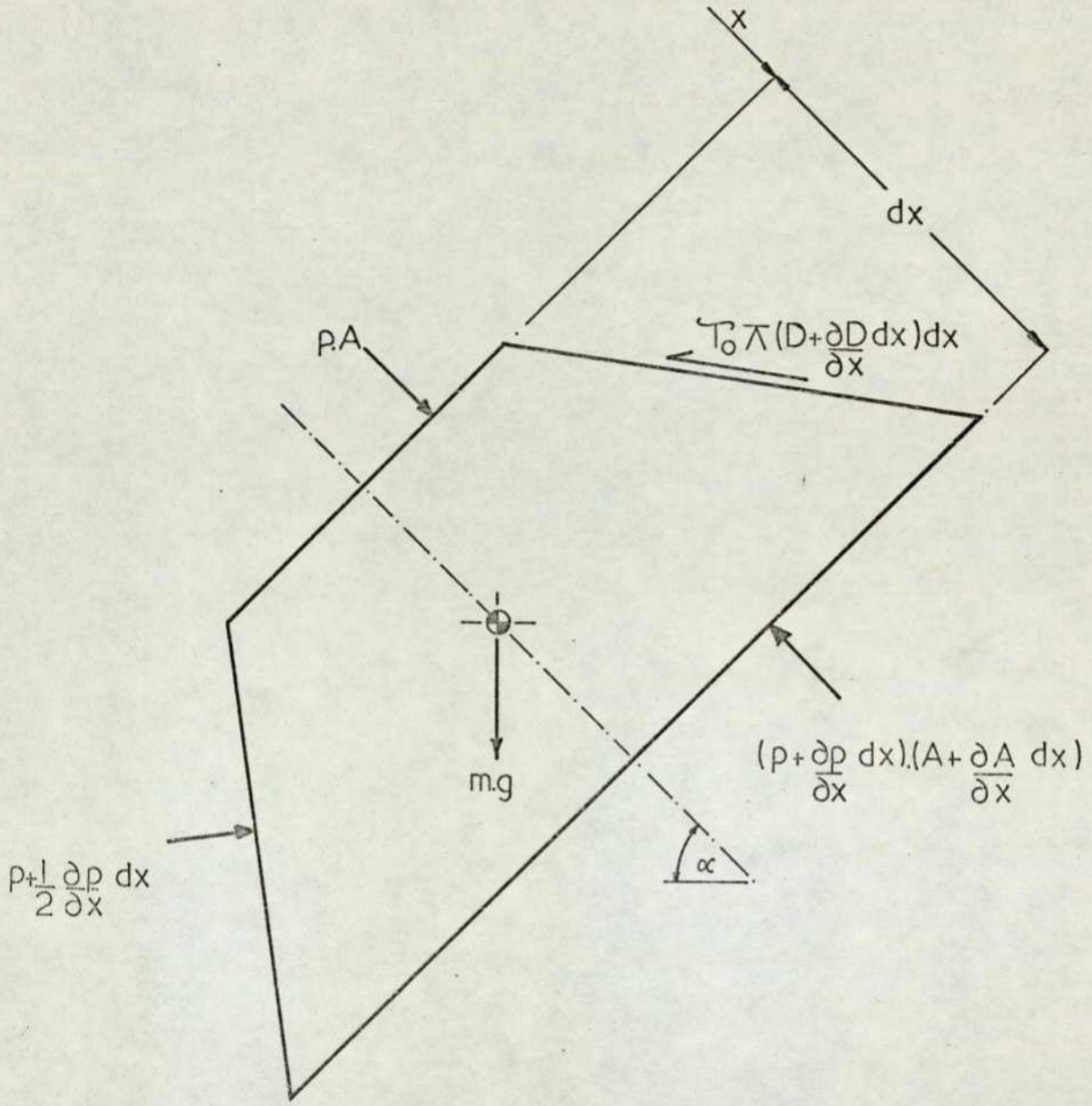
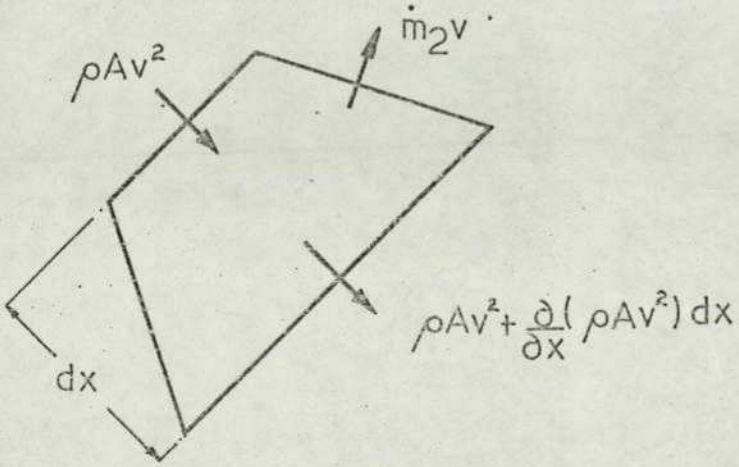


FIG 2b MOMENTUM TRANSFER ACROSS CONTROL SURFACES



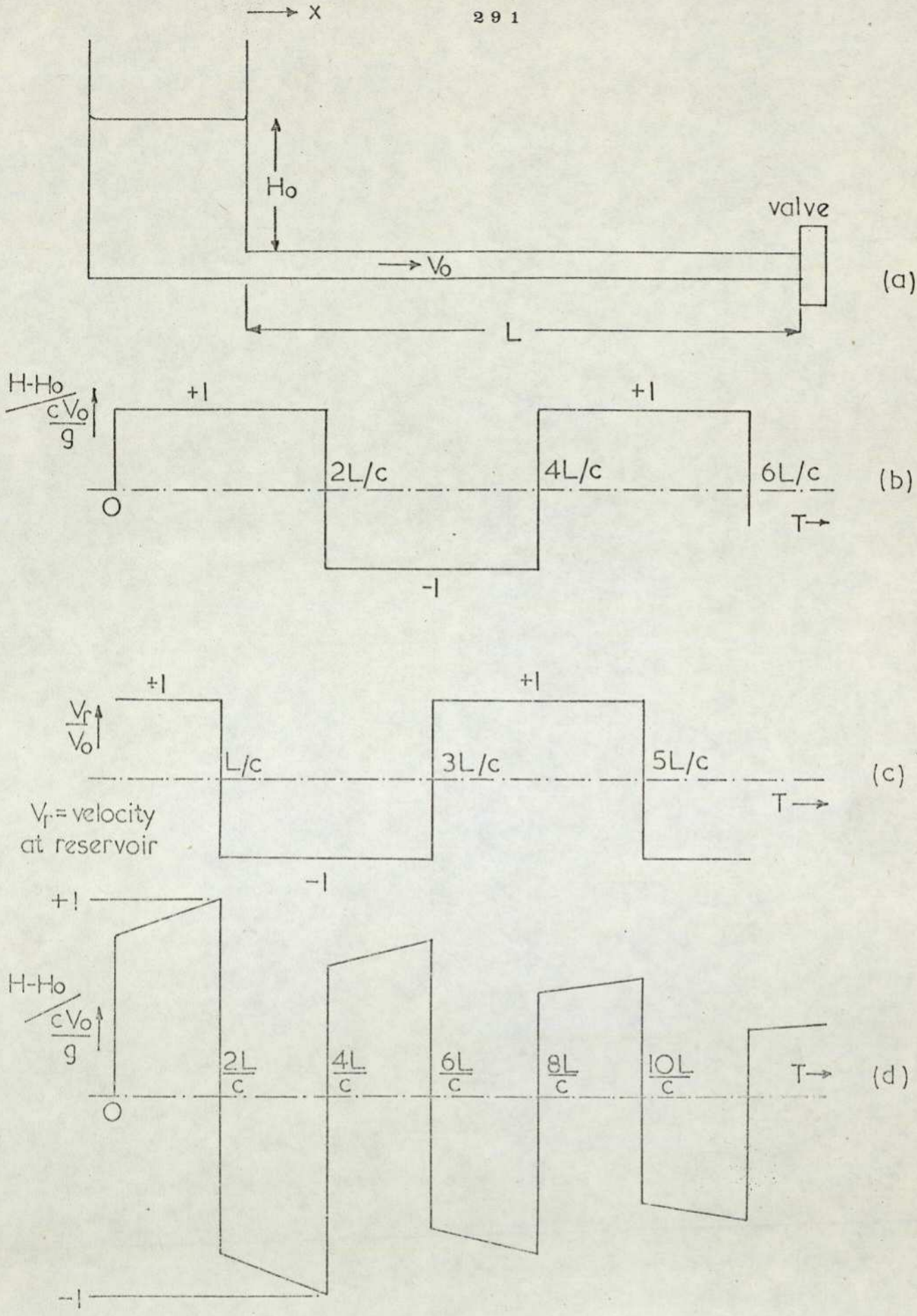


FIG 3 RICH'S SOLUTION OF THE WAVE EQUATION

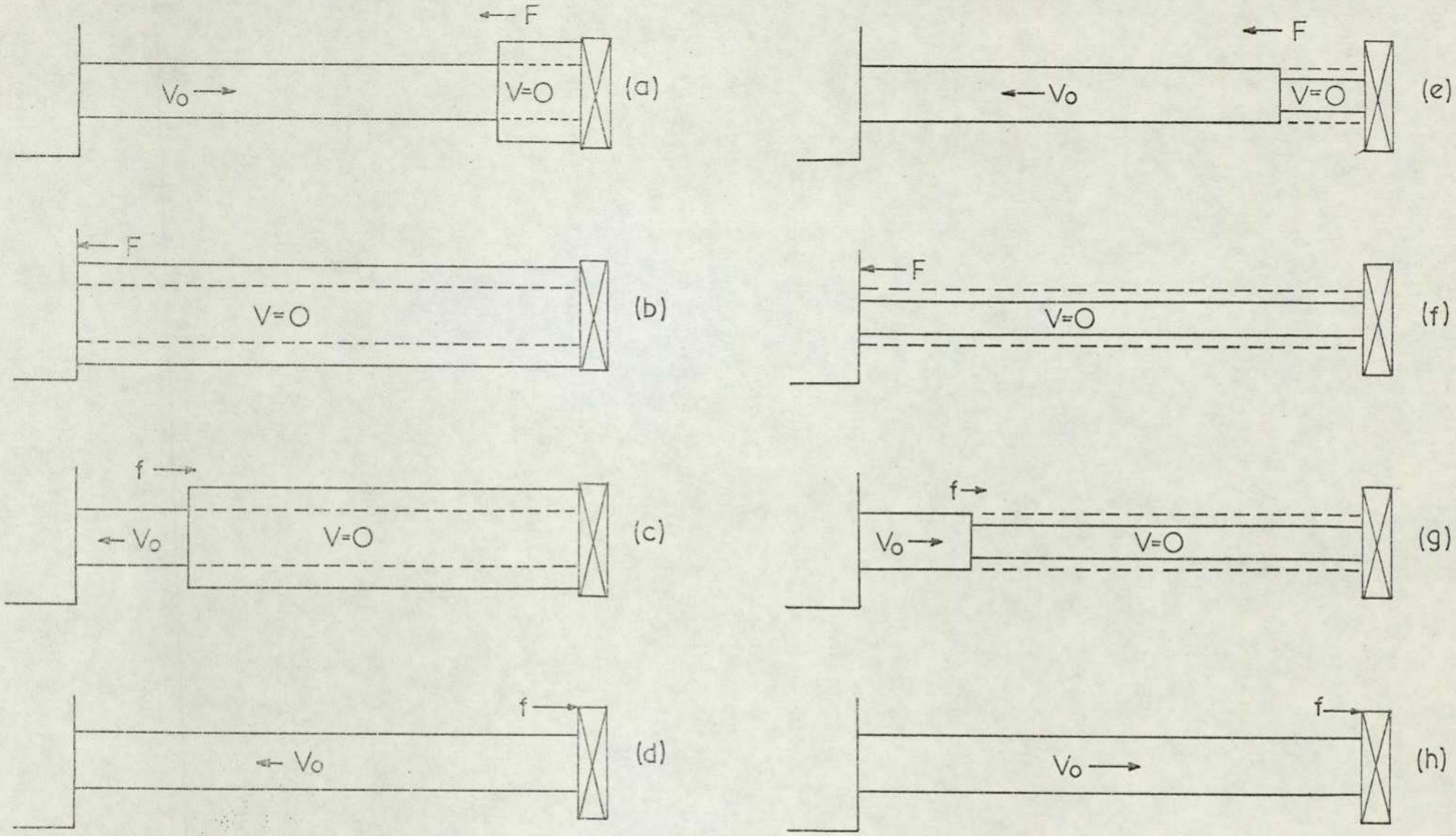


FIG 4 WAVE INTERPRETATION OF PRESSURE TRANSIENTS FOLLOWING INSTANTANEOUS VALVE CLOSURE

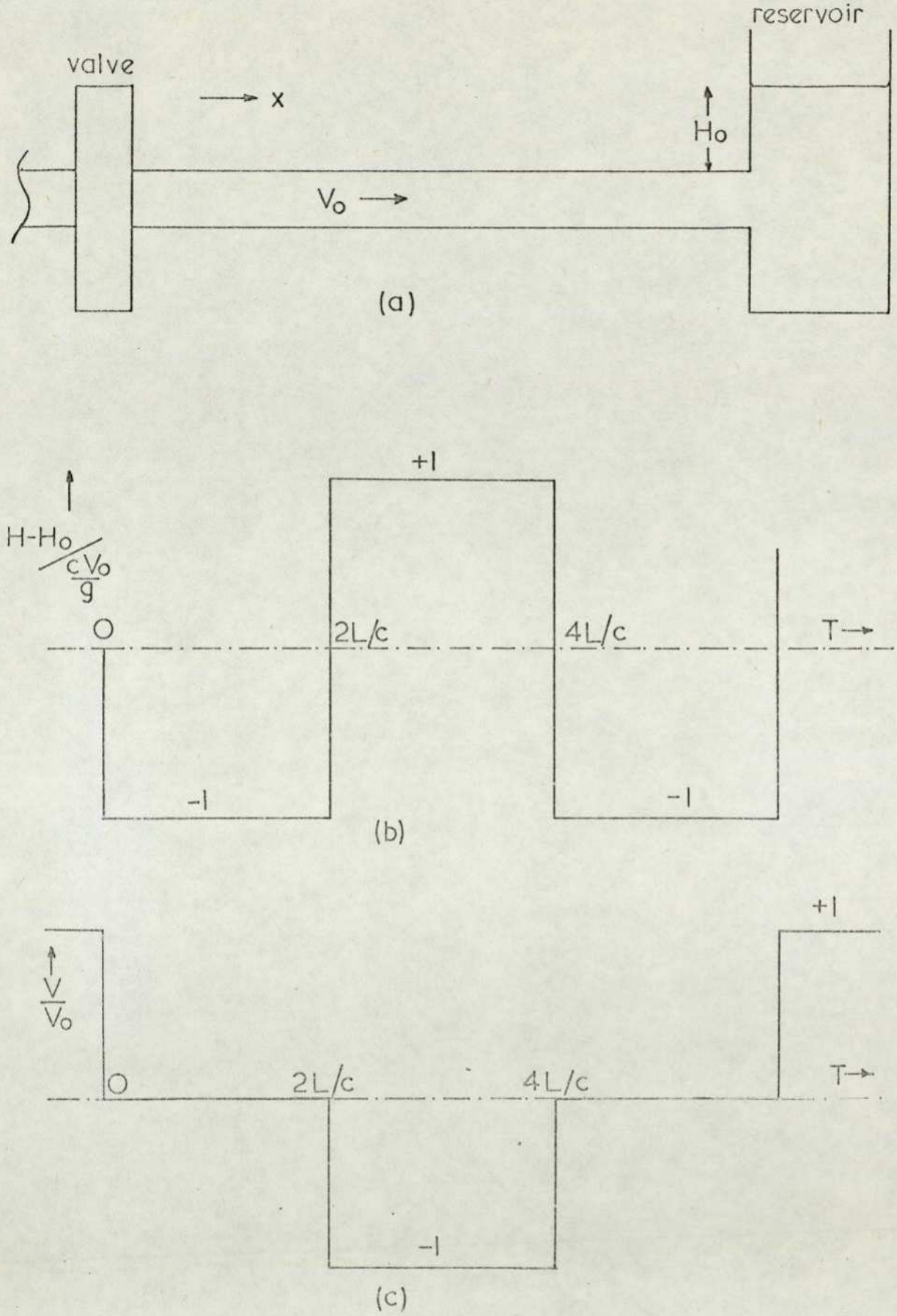


FIG 5 WAVE ANALYSIS OF TRANSIENTS IN A DOWNSTREAM PIPELINE SYSTEM

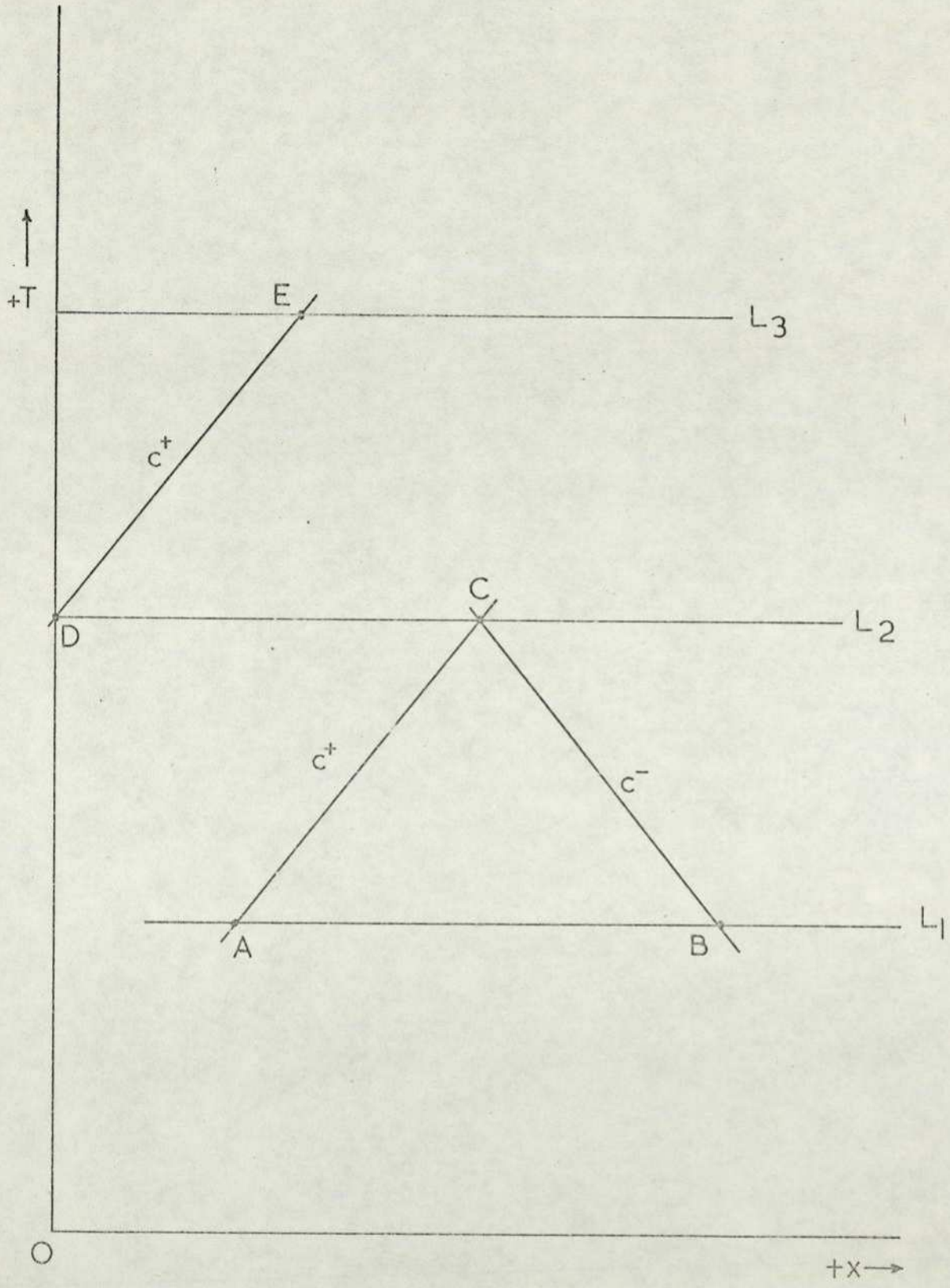
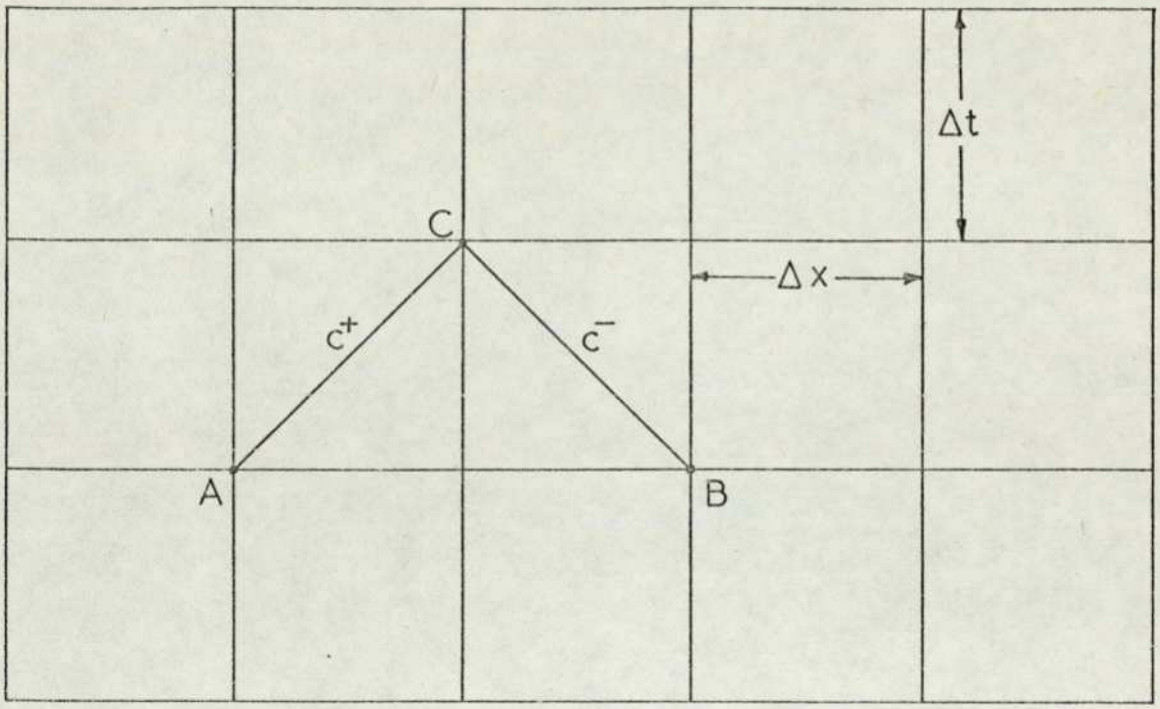


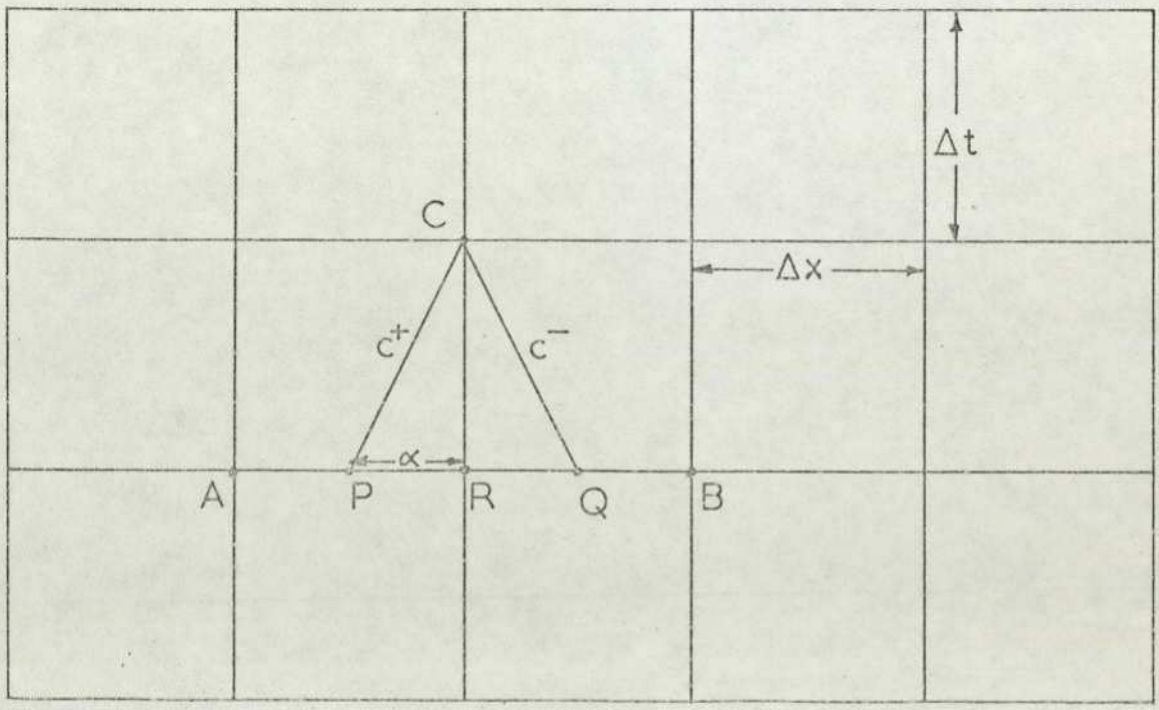
FIG 6 METHOD OF CHARACTERISTICS

Exact method



(a)

interpolated method



(b)

FIG 7 ALTERNATIVE FORMS OF THE METHOD OF CHARACTERISTICS.

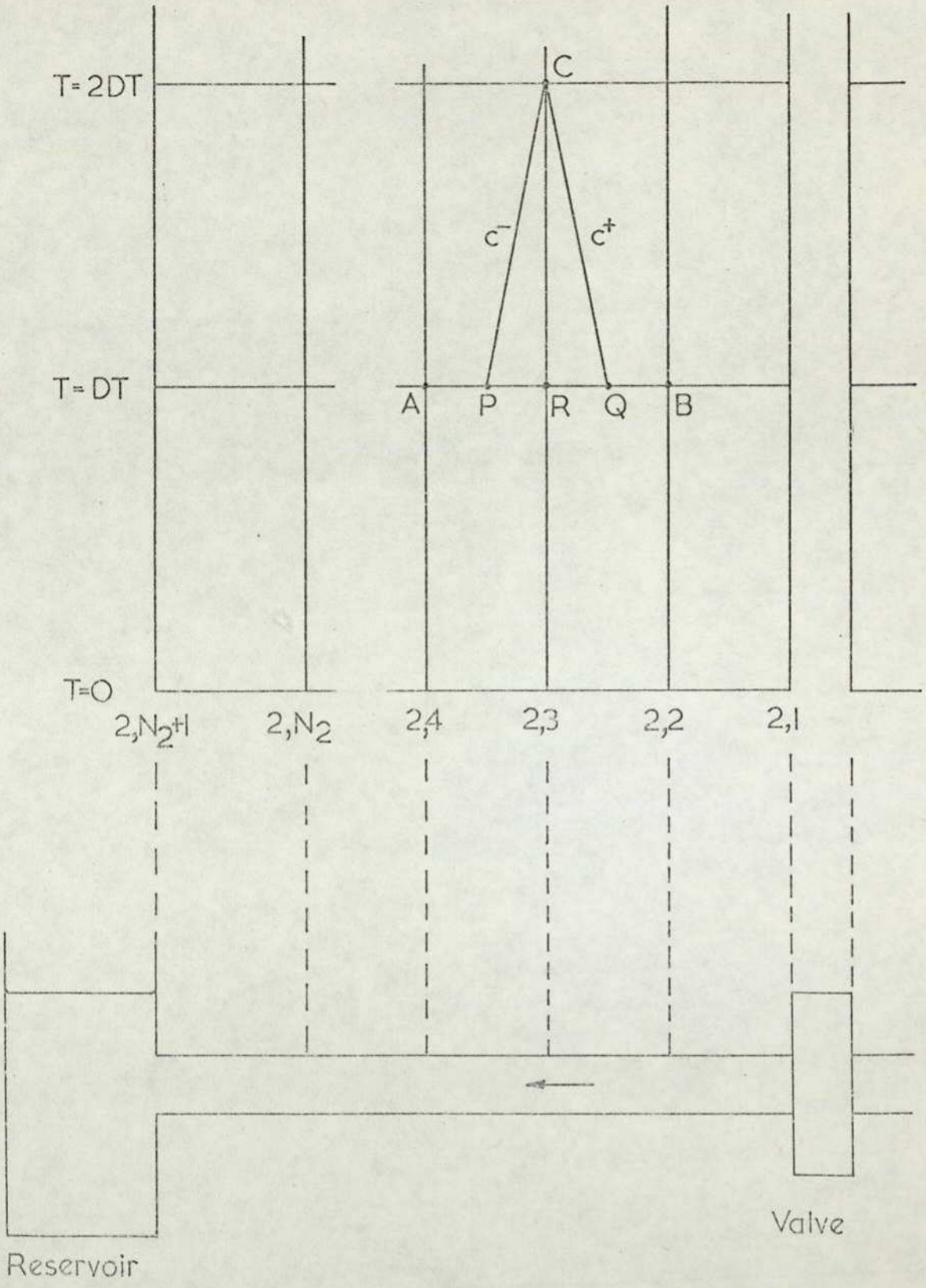


FIG 8 METHOD OF CHARACTERISTICS APPLIED TO A DOWNSTREAM PIPE SYSTEM

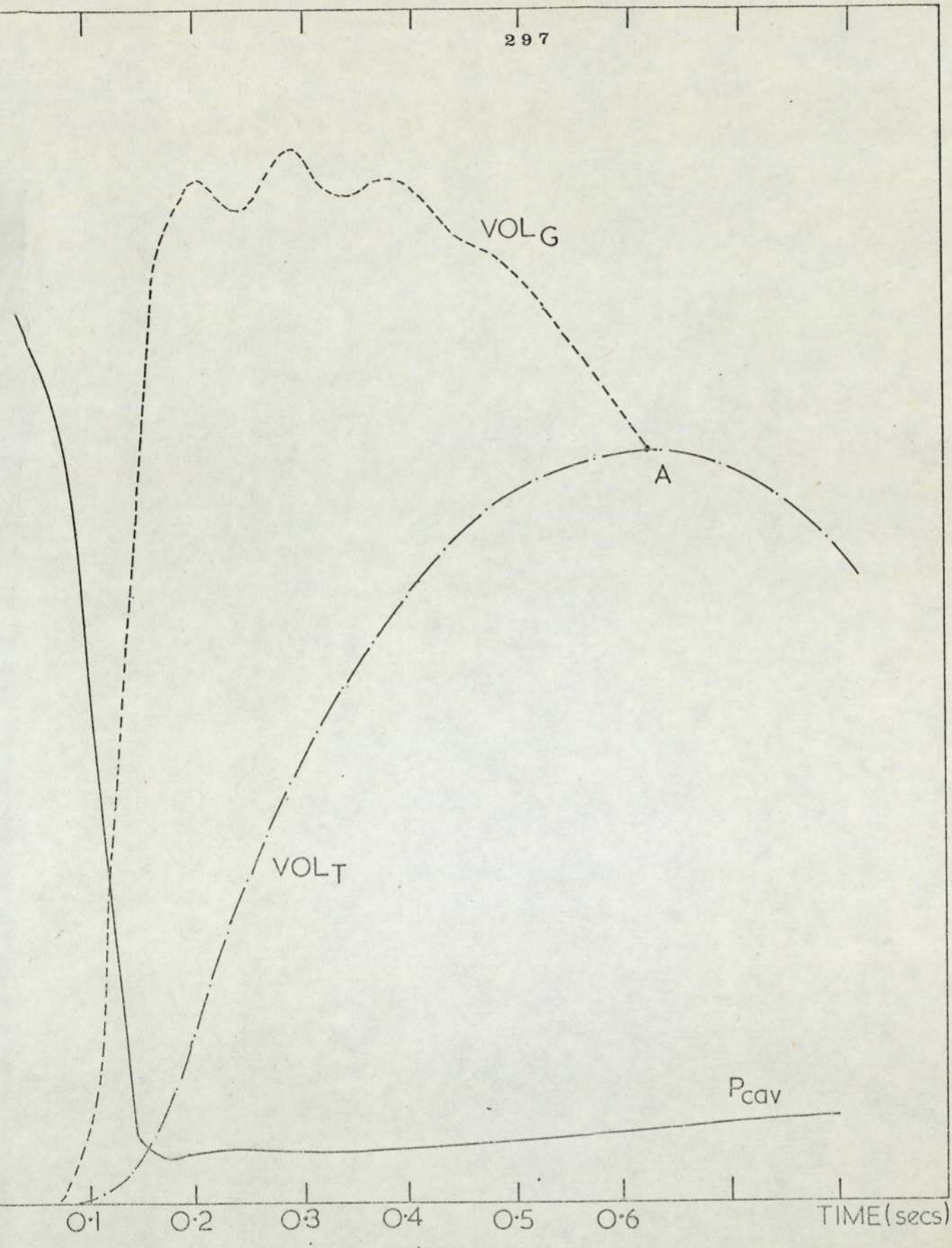


FIG 9 VARIATION OF P_{cav}, VOL_G AND VOL_T WITH TIME

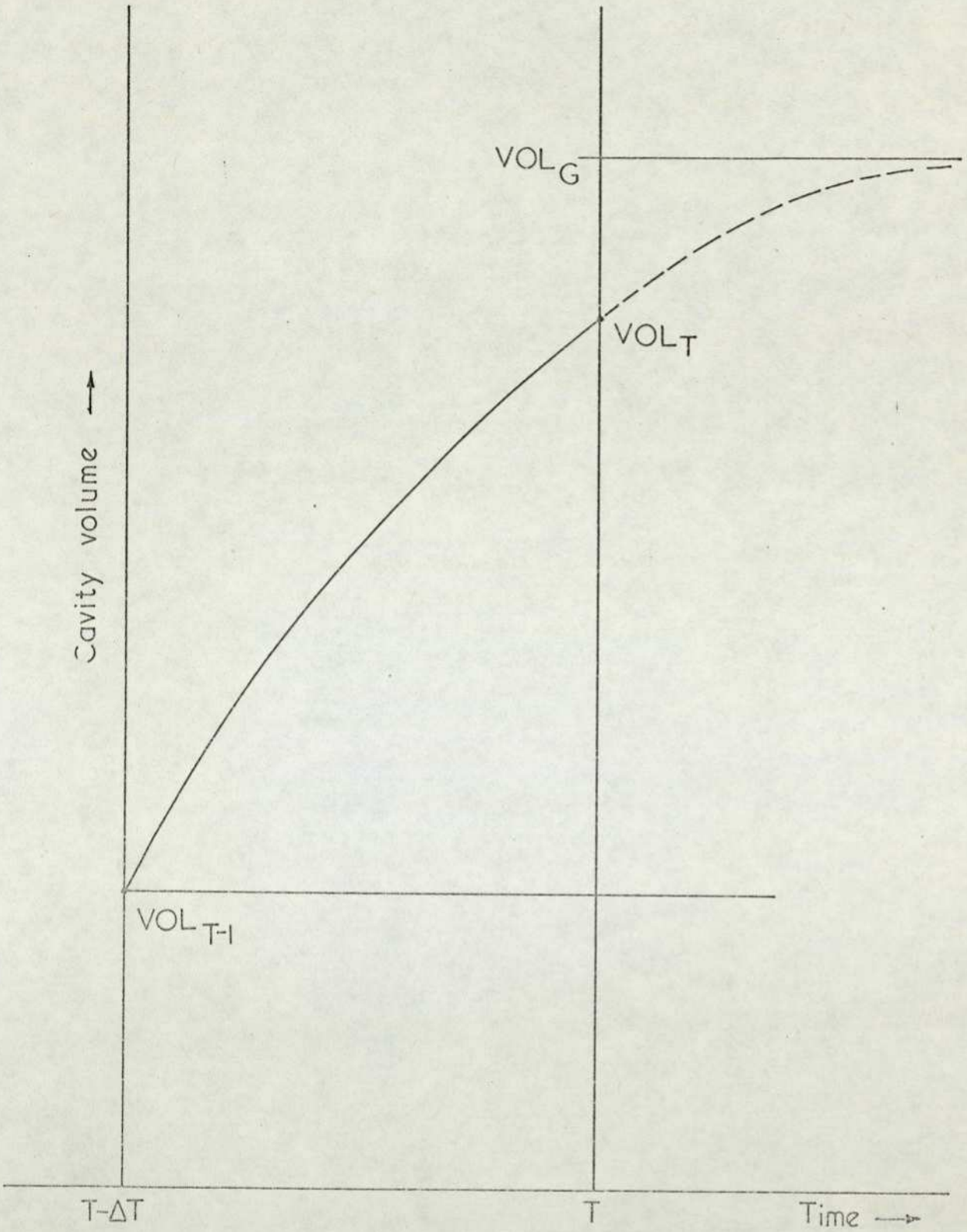


FIG 10 EXPONENTIAL CAVITY GROWTH DURING ONE TIME STEP

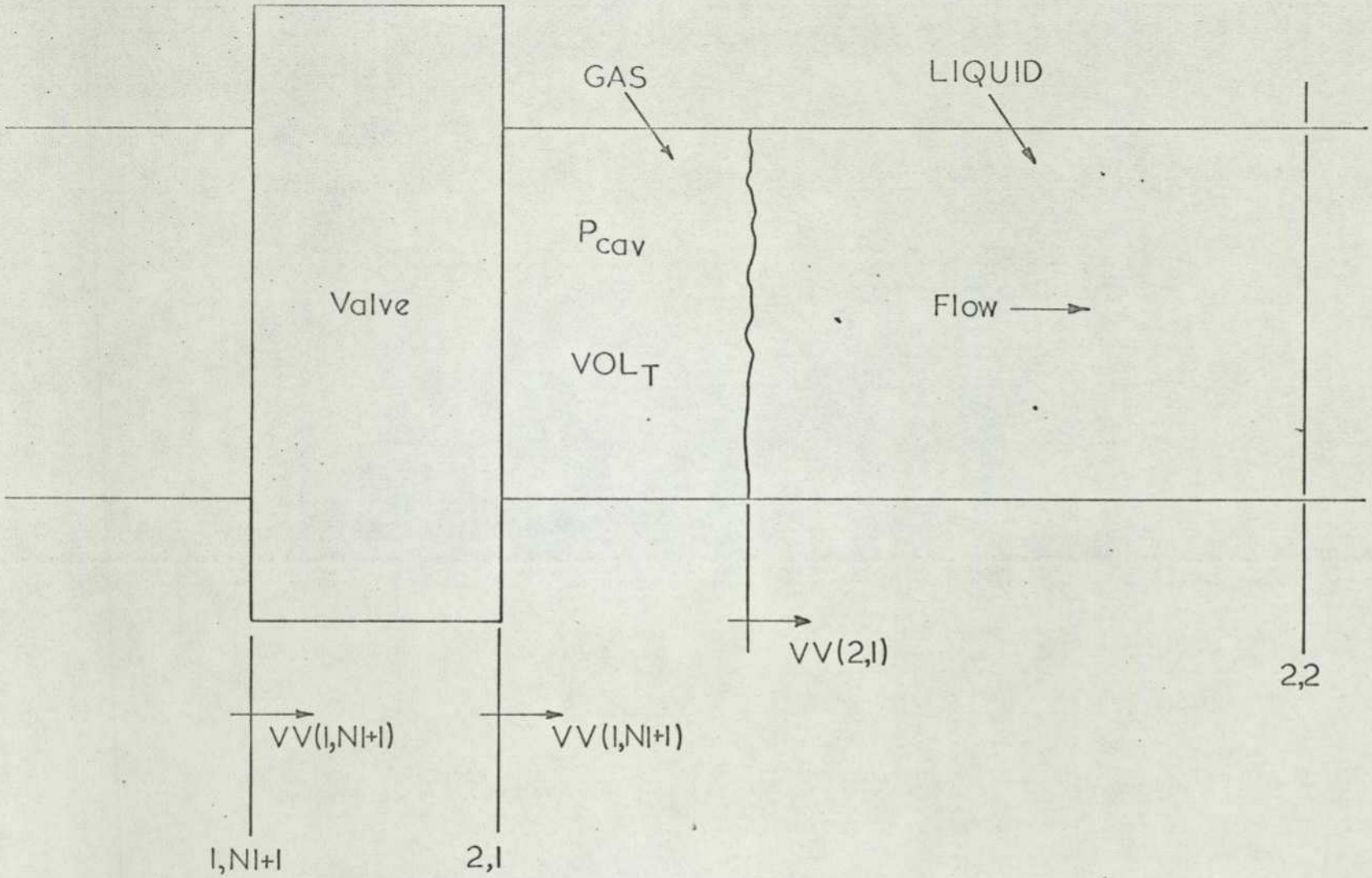
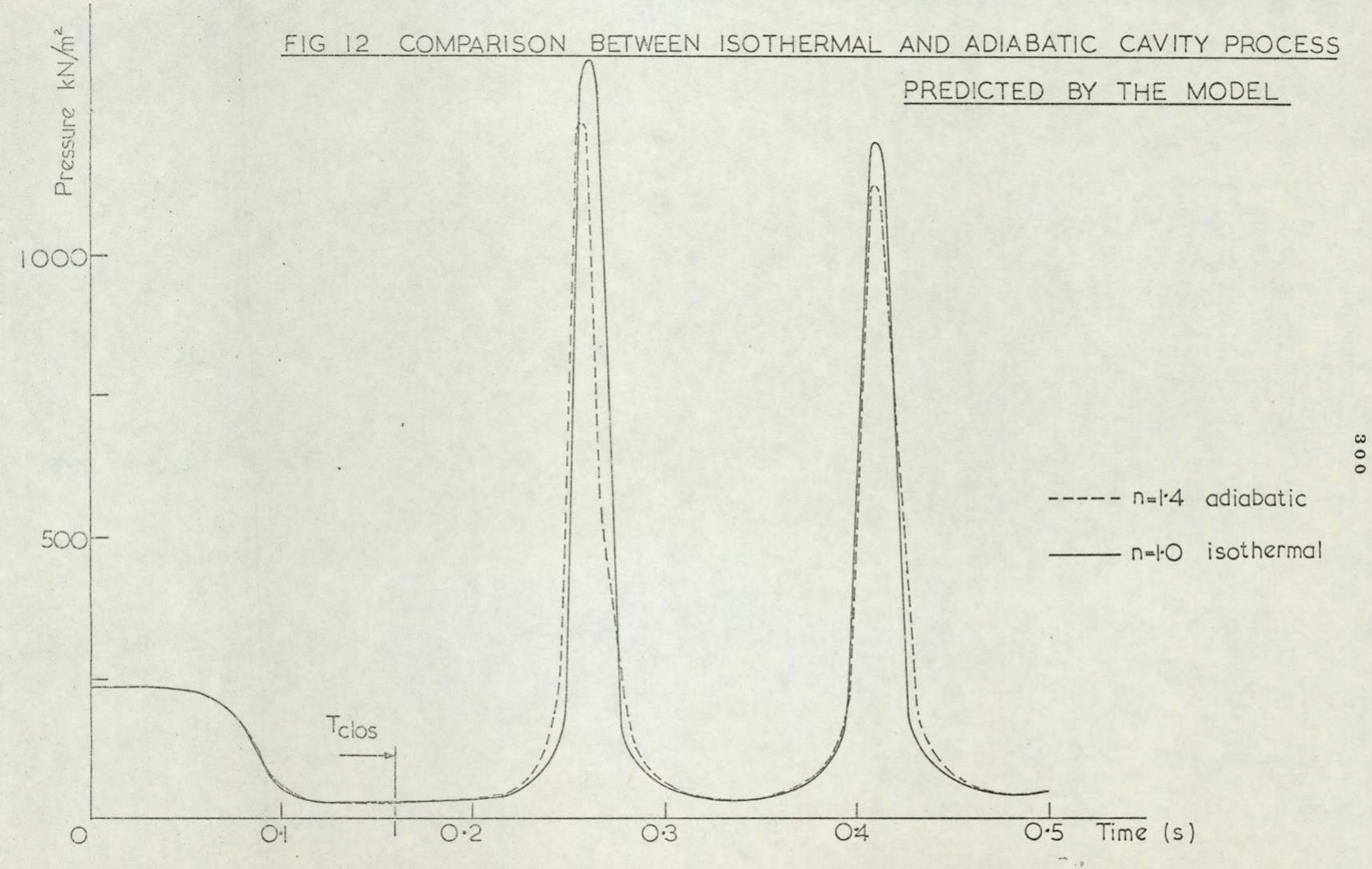


FIG 11 BOUNDARY CONDITION AT VALVE

FIG 12 COMPARISON BETWEEN ISOTHERMAL AND ADIABATIC CAVITY PROCESS PREDICTED BY THE MODEL



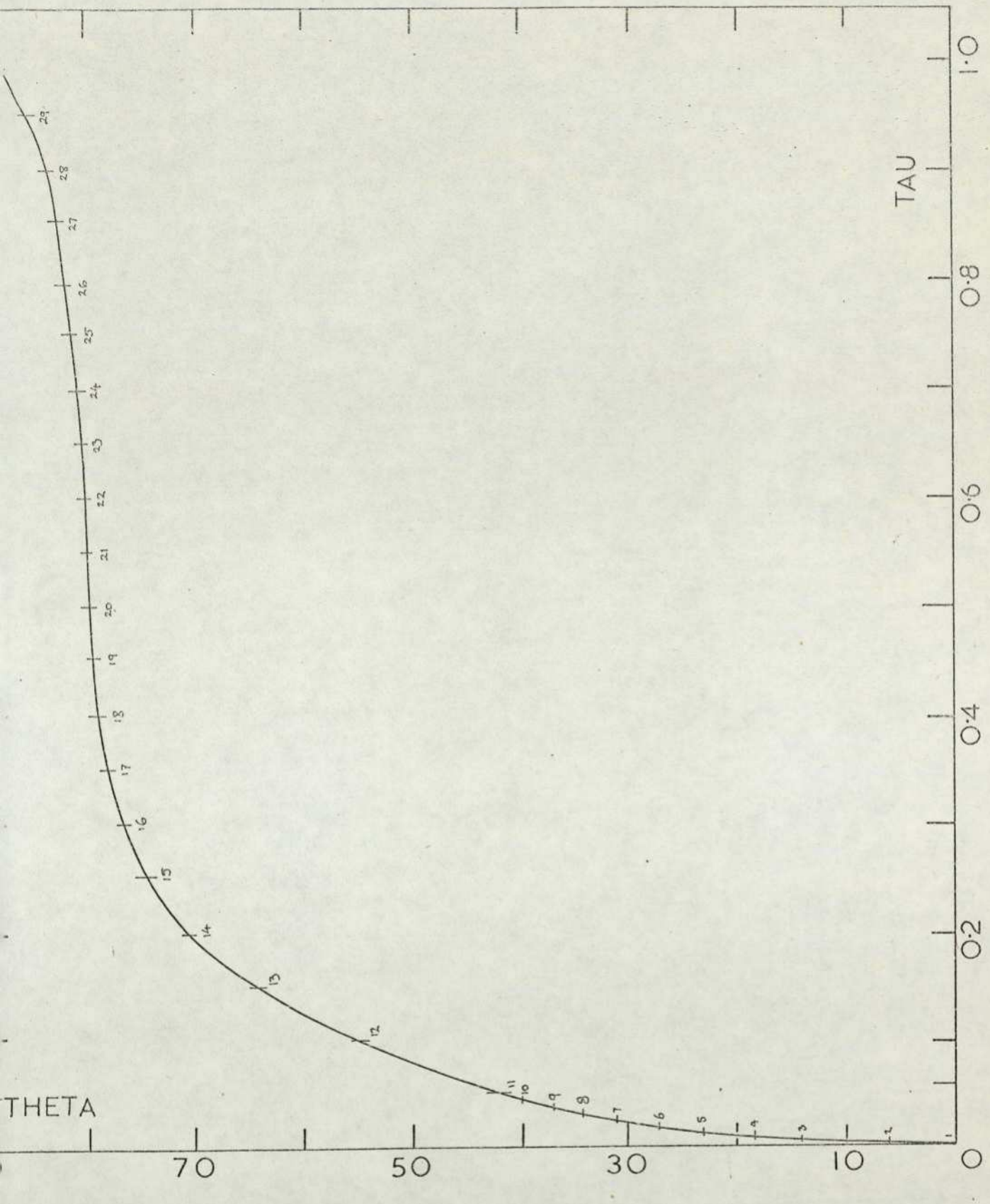


FIG 13 STEADY STATE VALVE CHARACTERISTIC

SHOWING THE DATA POINTS USED IN ARRAY 'TANG'

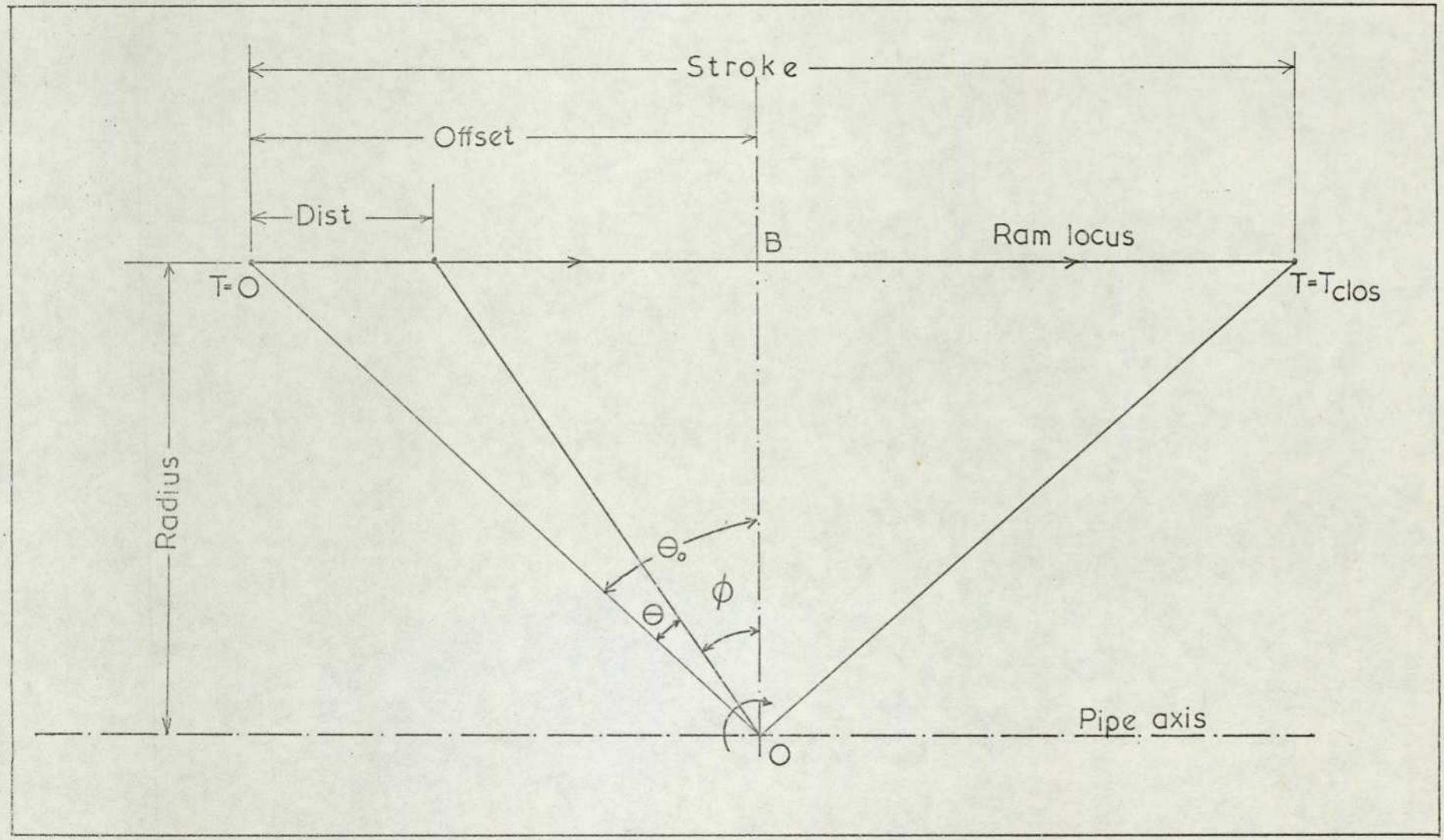


FIG 14 VALVE LINKAGE GEOMETRY

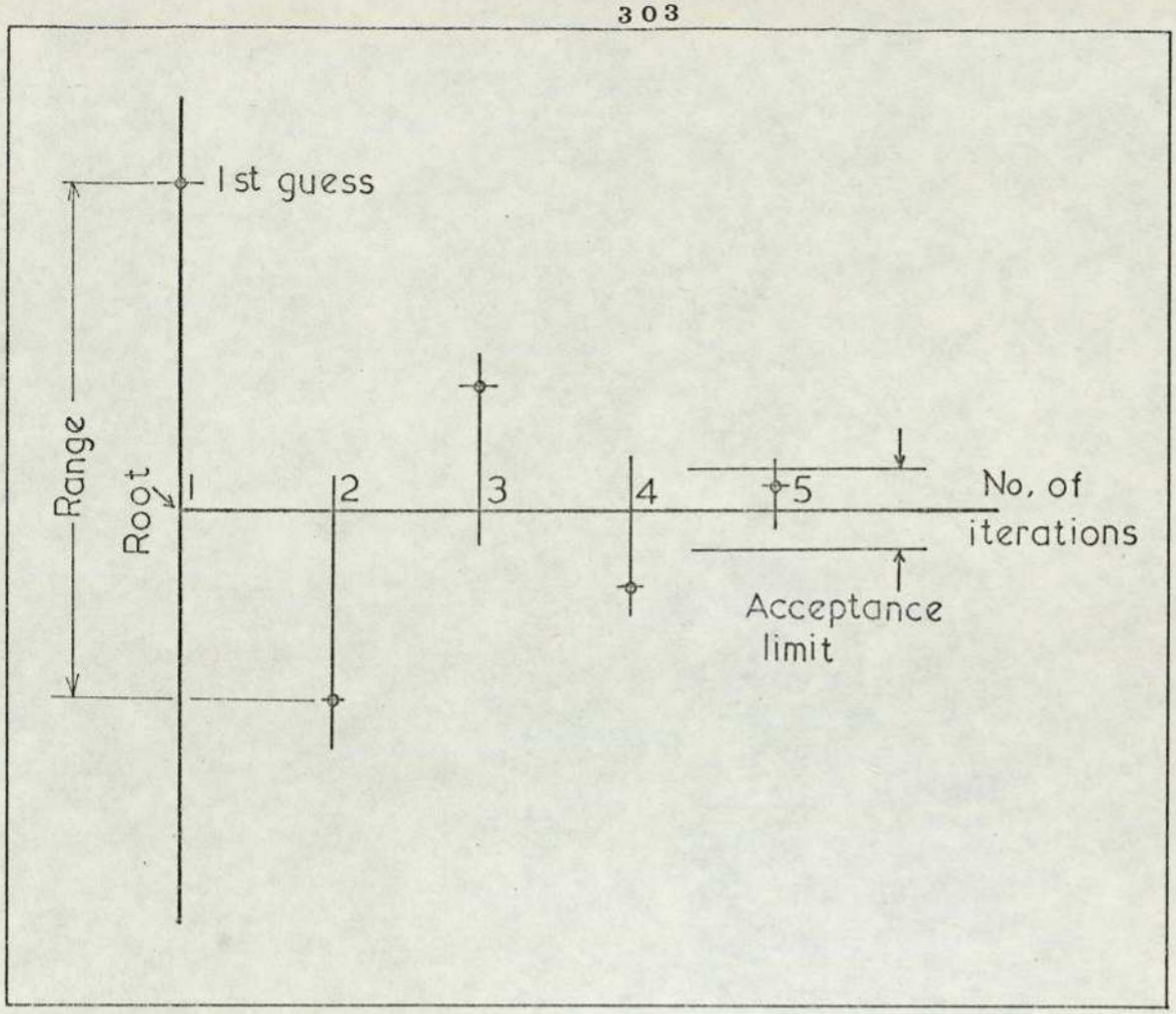


FIG 15 NUMERICAL OSCILLATION IN ITERATION

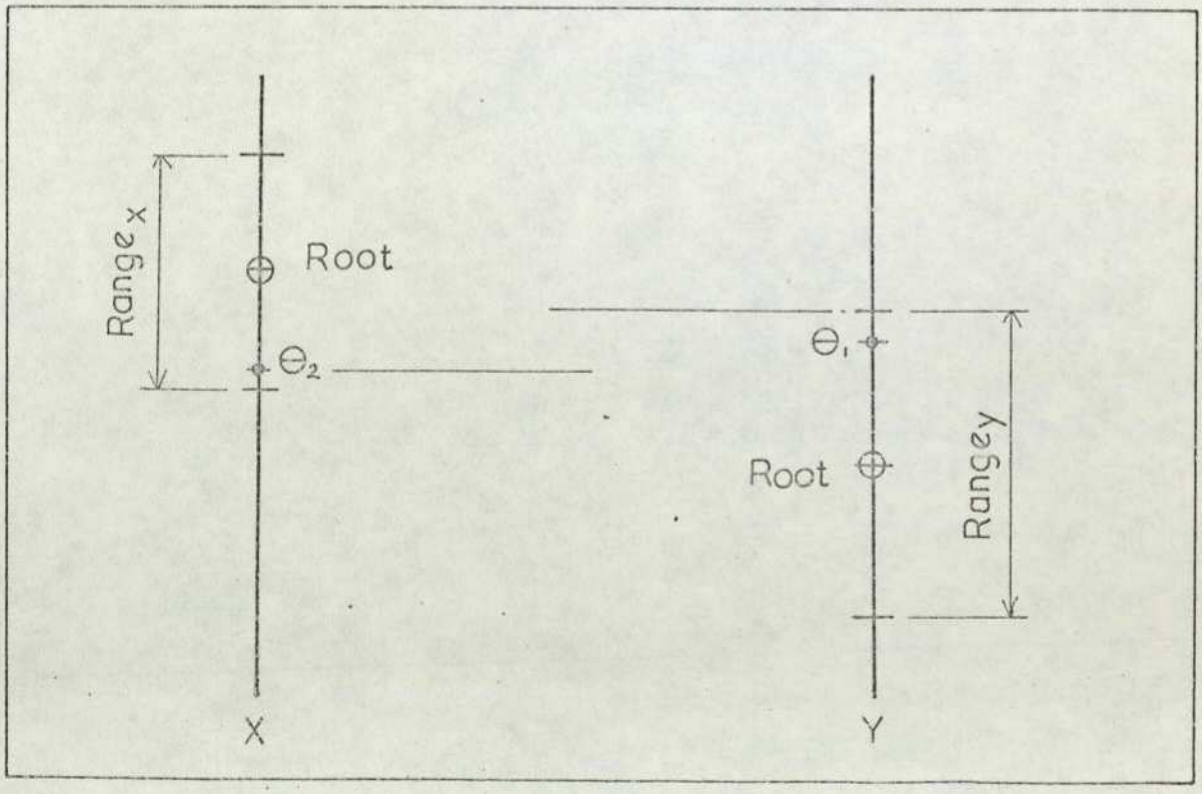


FIG 16 OVERLAPPING RANGES OF TWO VARIABLES

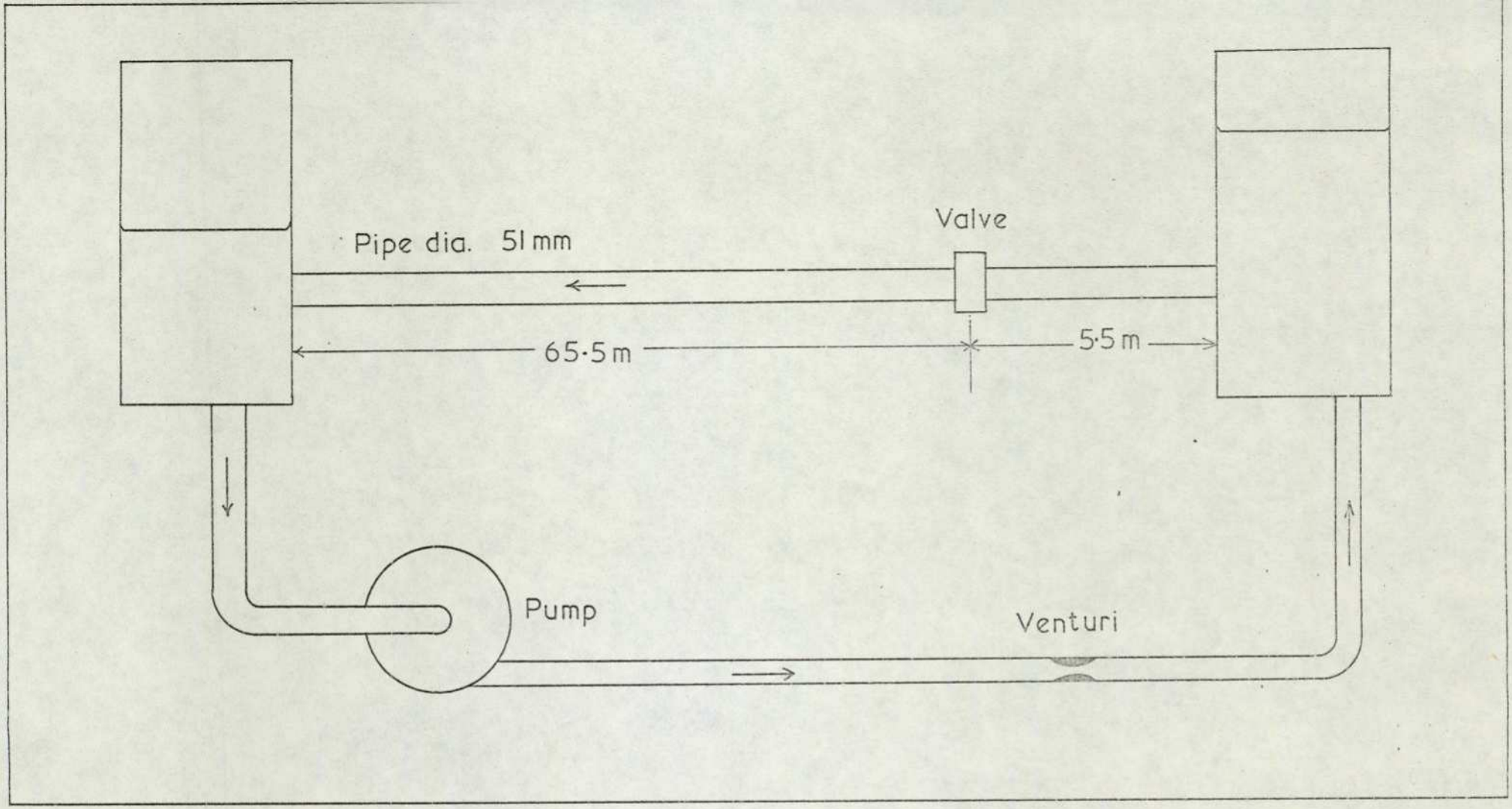


FIG 17 SCHEMATIC DIAGRAM OF TEST RIG

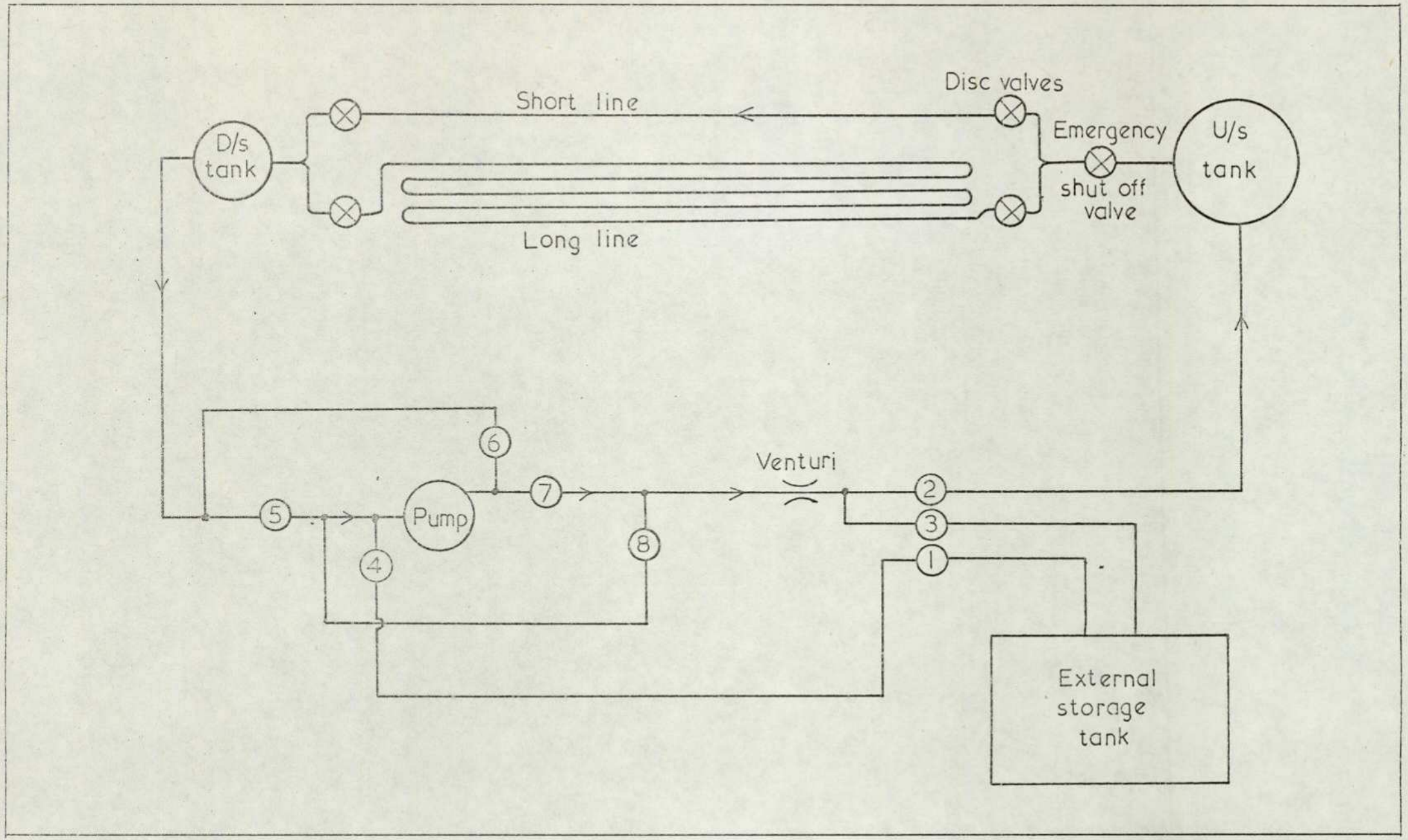
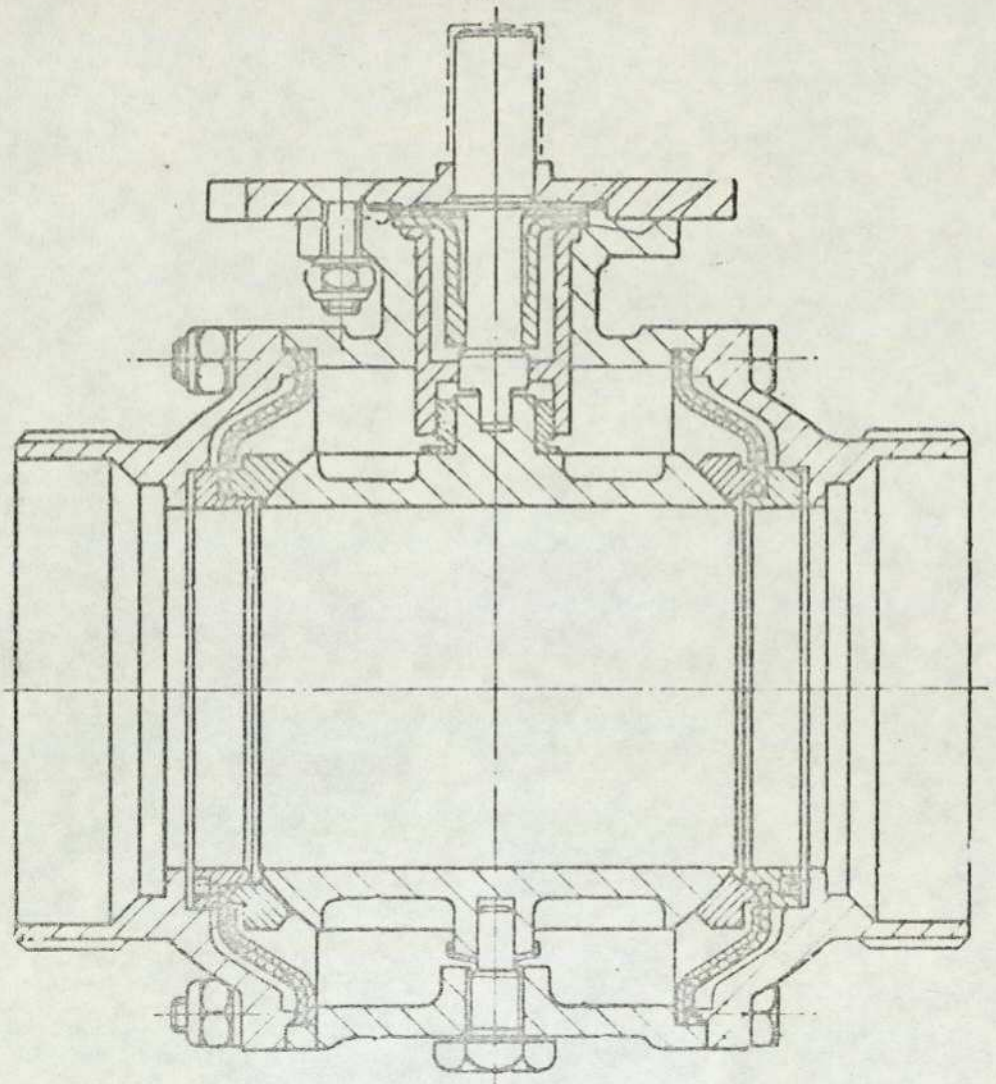


FIG 18 SCHEMATIC DIAGRAM OF FULL TRANSIENT TEST FACILITIES AVAILABLE



FIG 19 EXTERNAL VIEW OF SAUNDERS E6OF16 FUEL VALVE



Scale: Full Size

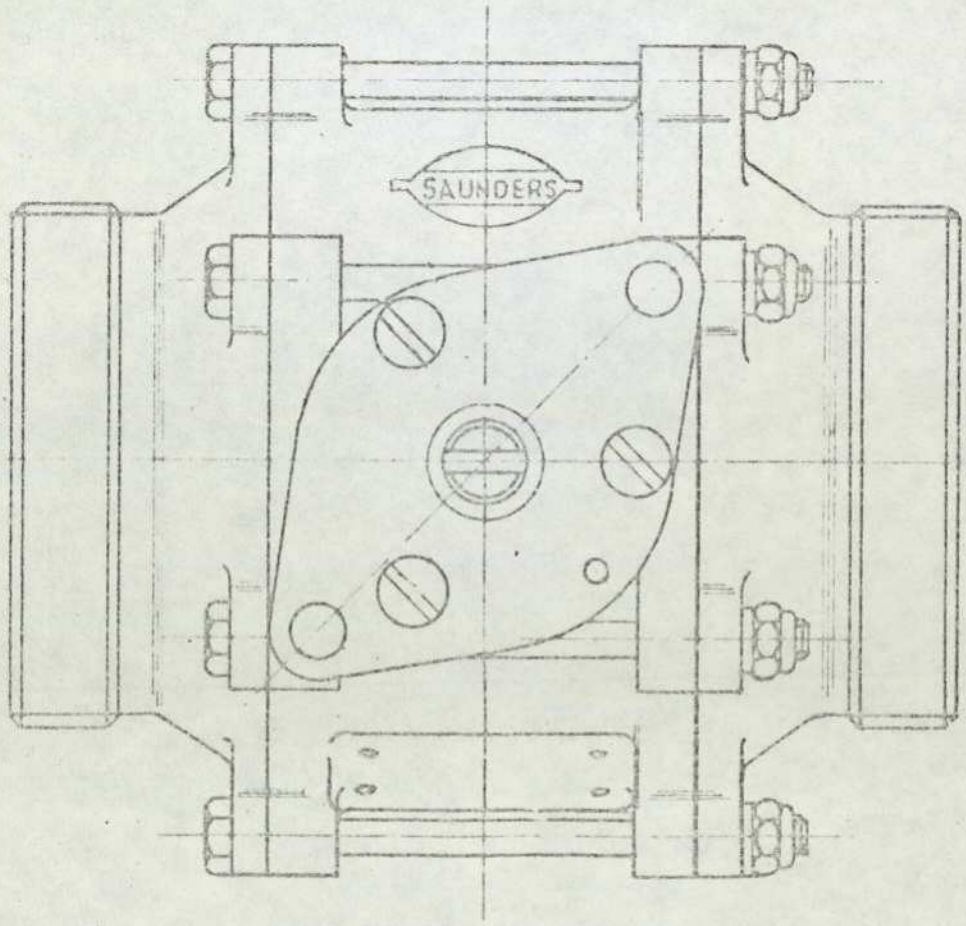


FIG 20 SECTION VIEW OF SAUNDERS E6OF16 VALVE

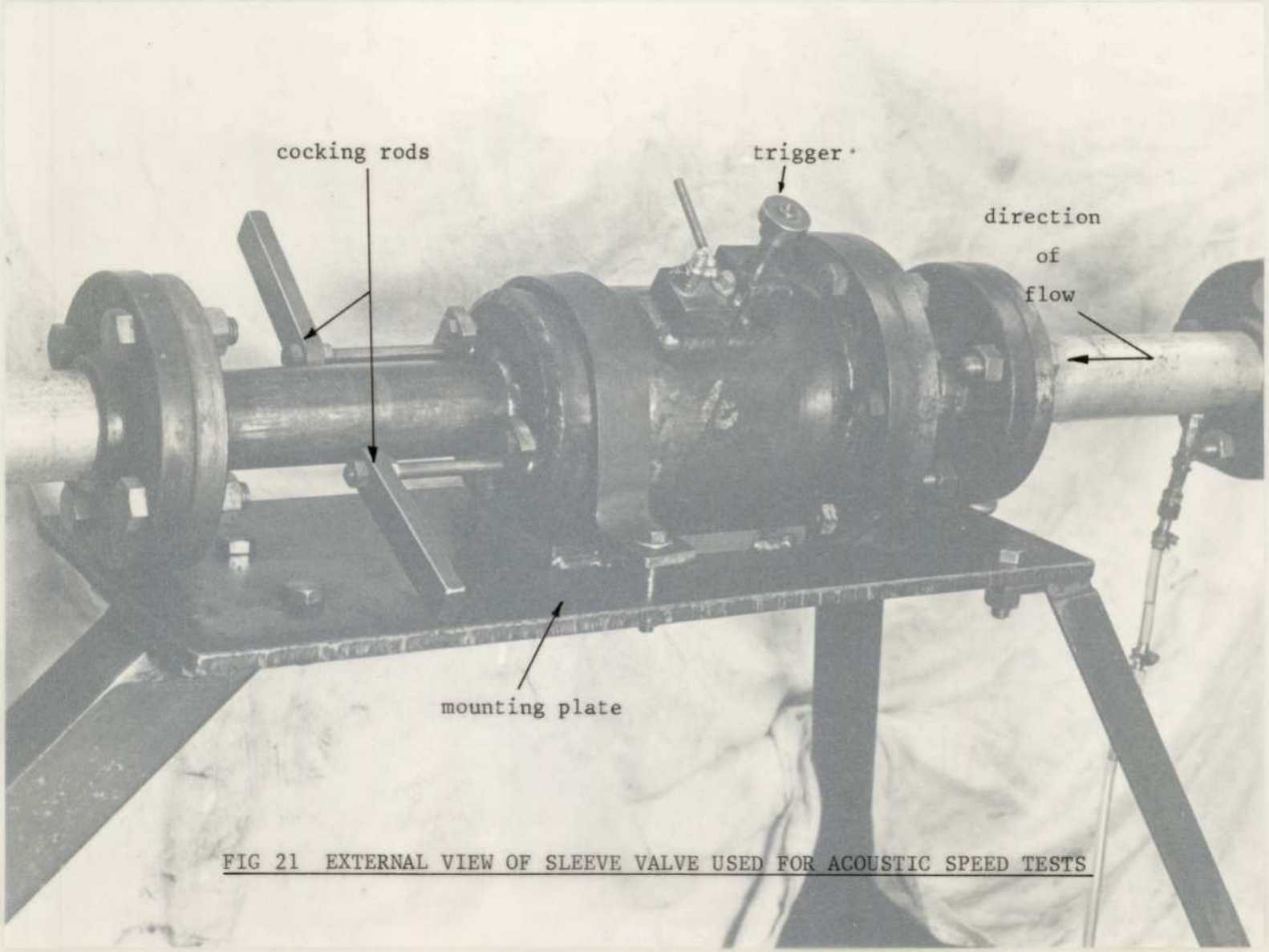
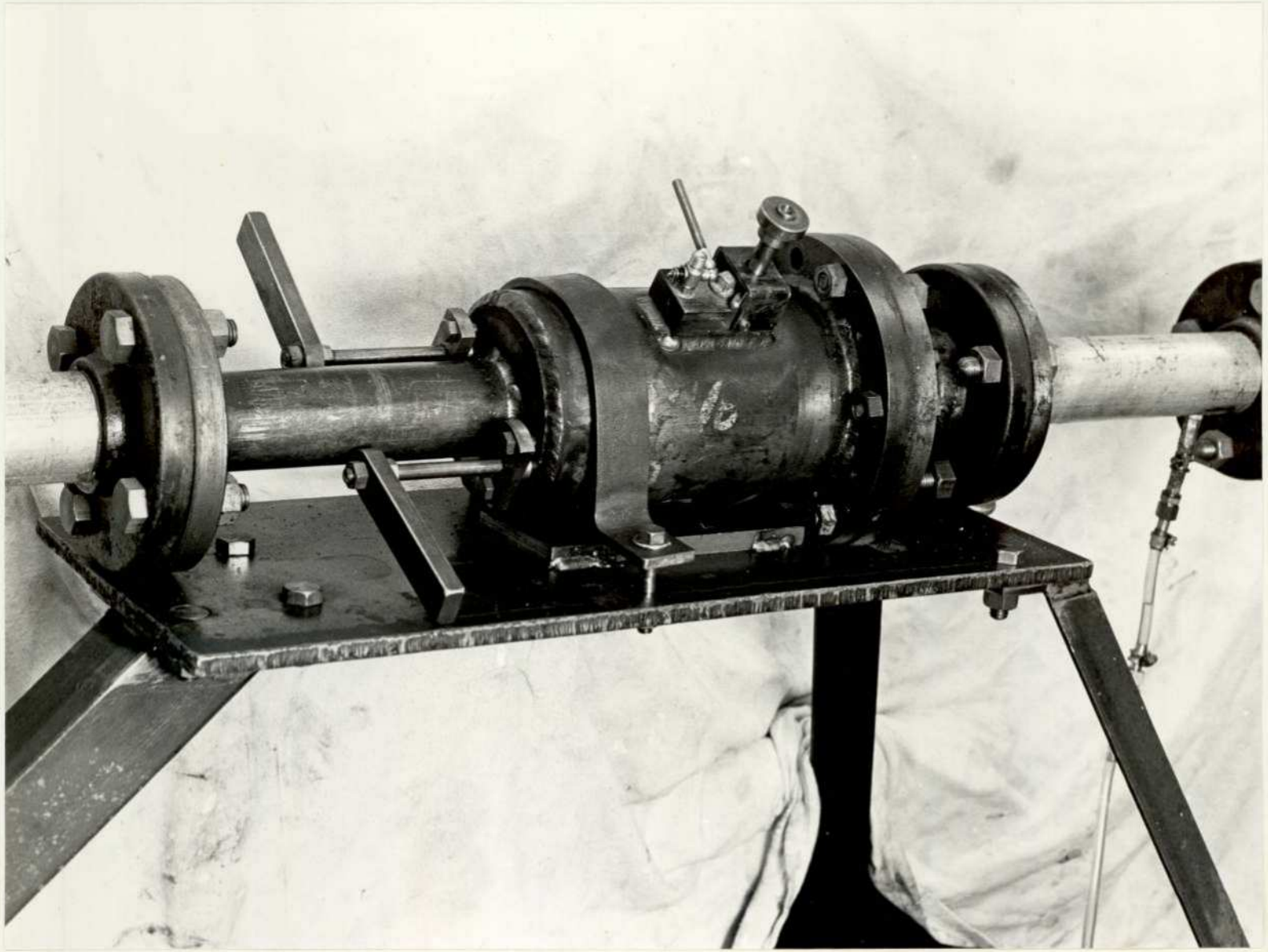


FIG 21 EXTERNAL VIEW OF SLEEVE VALVE USED FOR ACOUSTIC SPEED TESTS



. ROLLS-ROYCE (1971) LIMITED.



FIG 22 ARRGT. OF FAST CLOSING VALVE. (COCKING RODS PARTIALLY DELETED FOR CLARITY)

J.C. McDERMID. MARCH 1972.

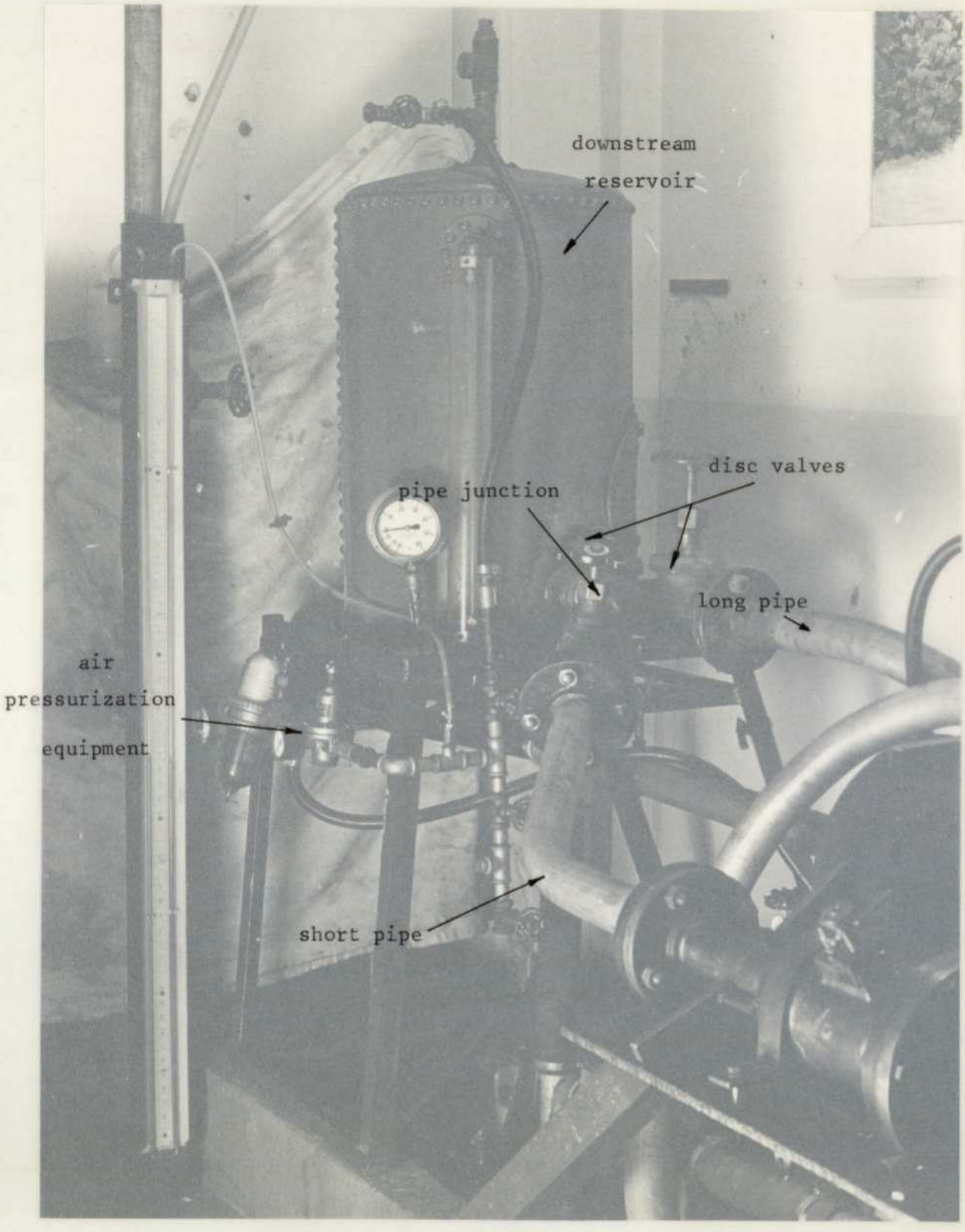


FIG 23a DOWNSTREAM END OF EXPERIMENTAL RIG

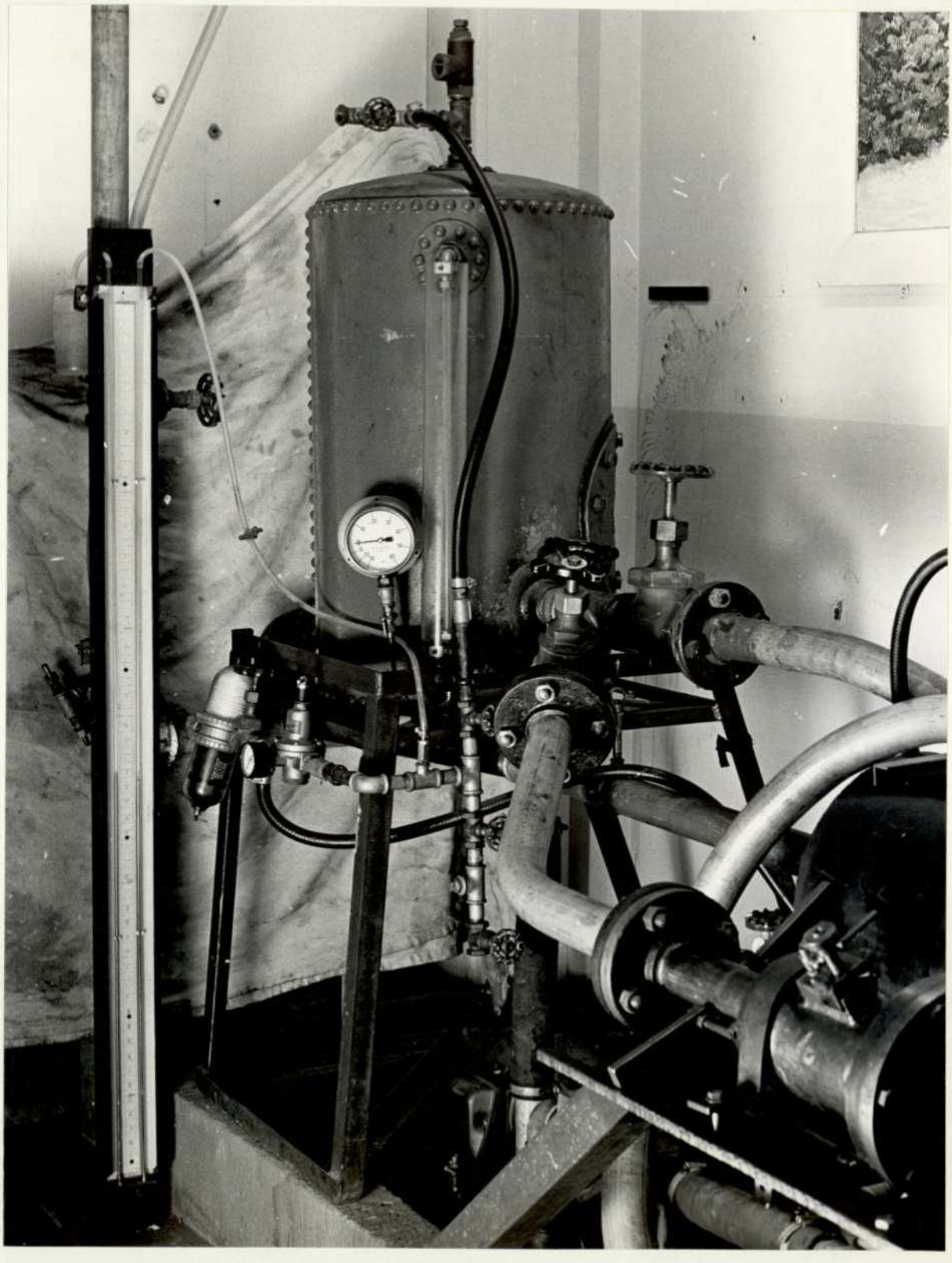
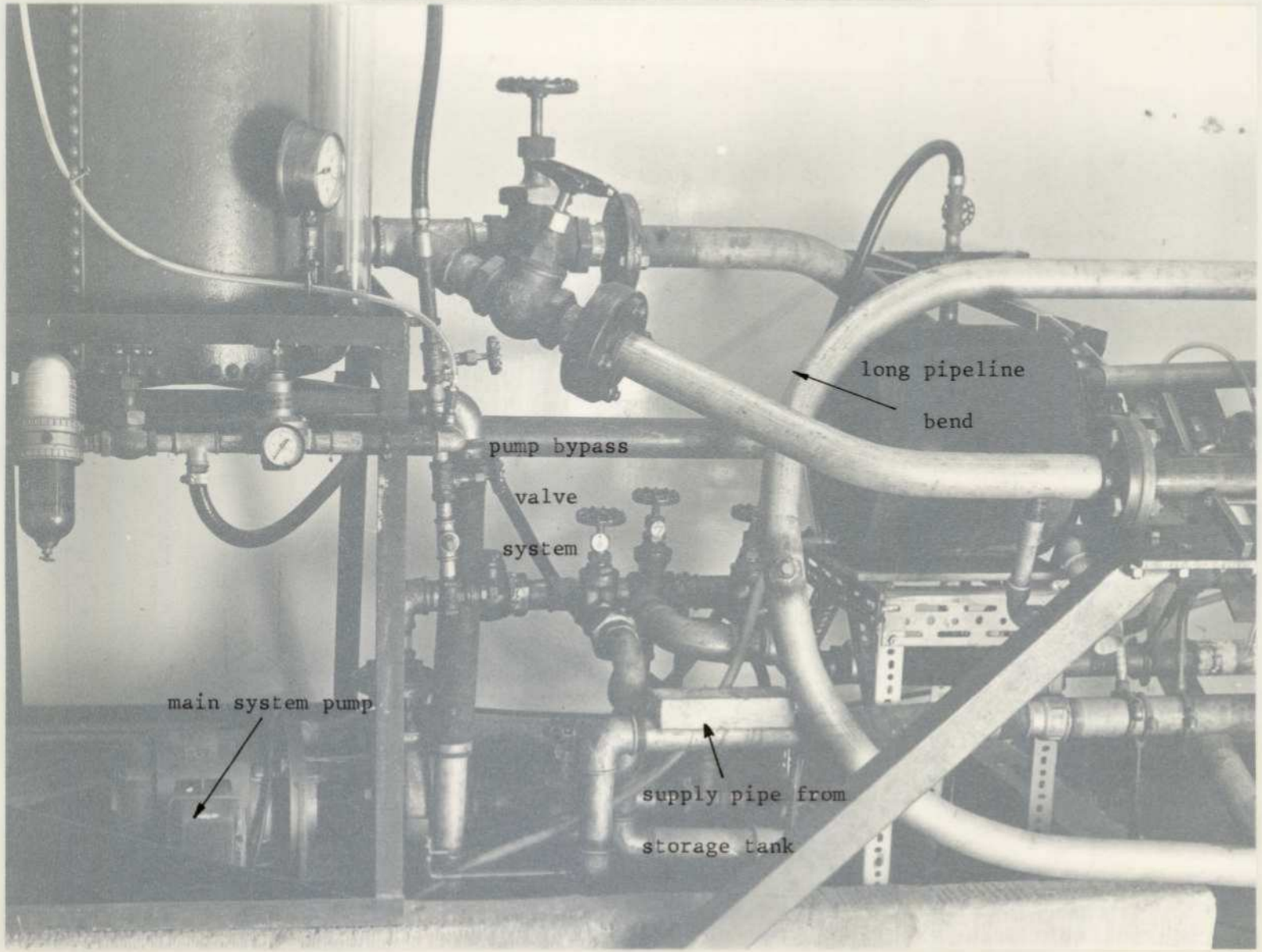


FIG 23b DOWNSTREAM END OF EXPERIMENTAL RIG



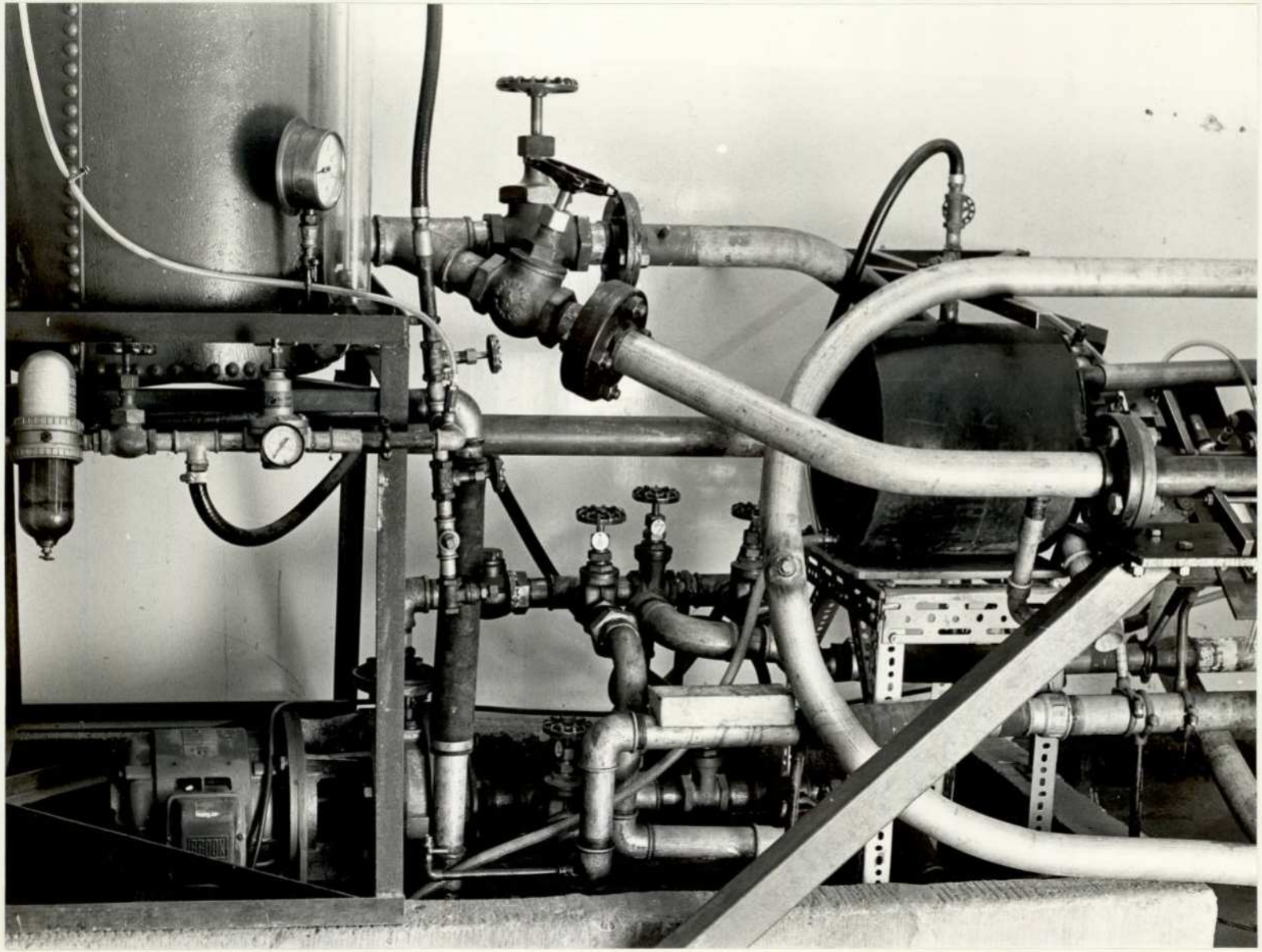
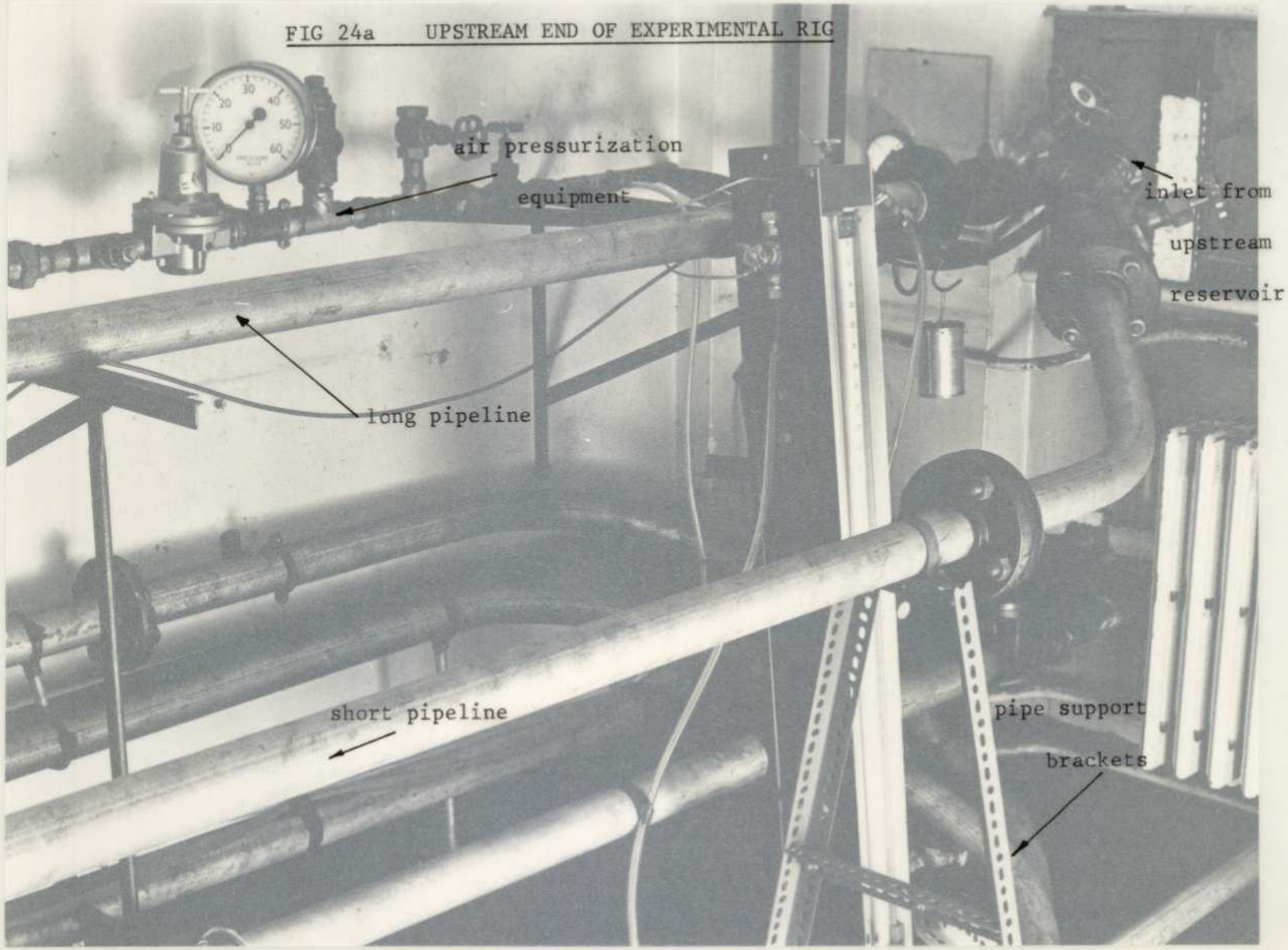
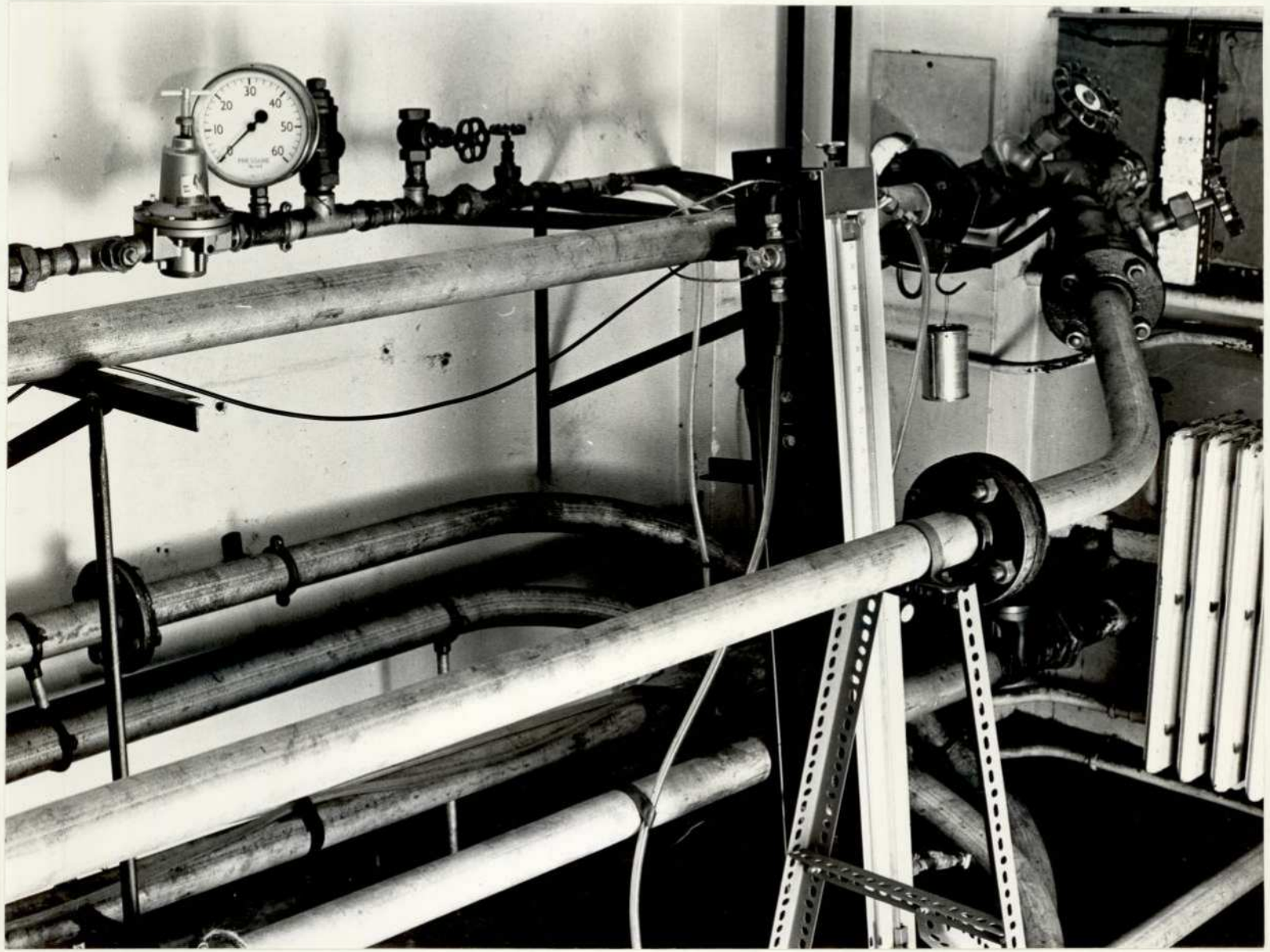


FIG 24a UPSTREAM END OF EXPERIMENTAL RIG




30
20
40
10
50
0
60

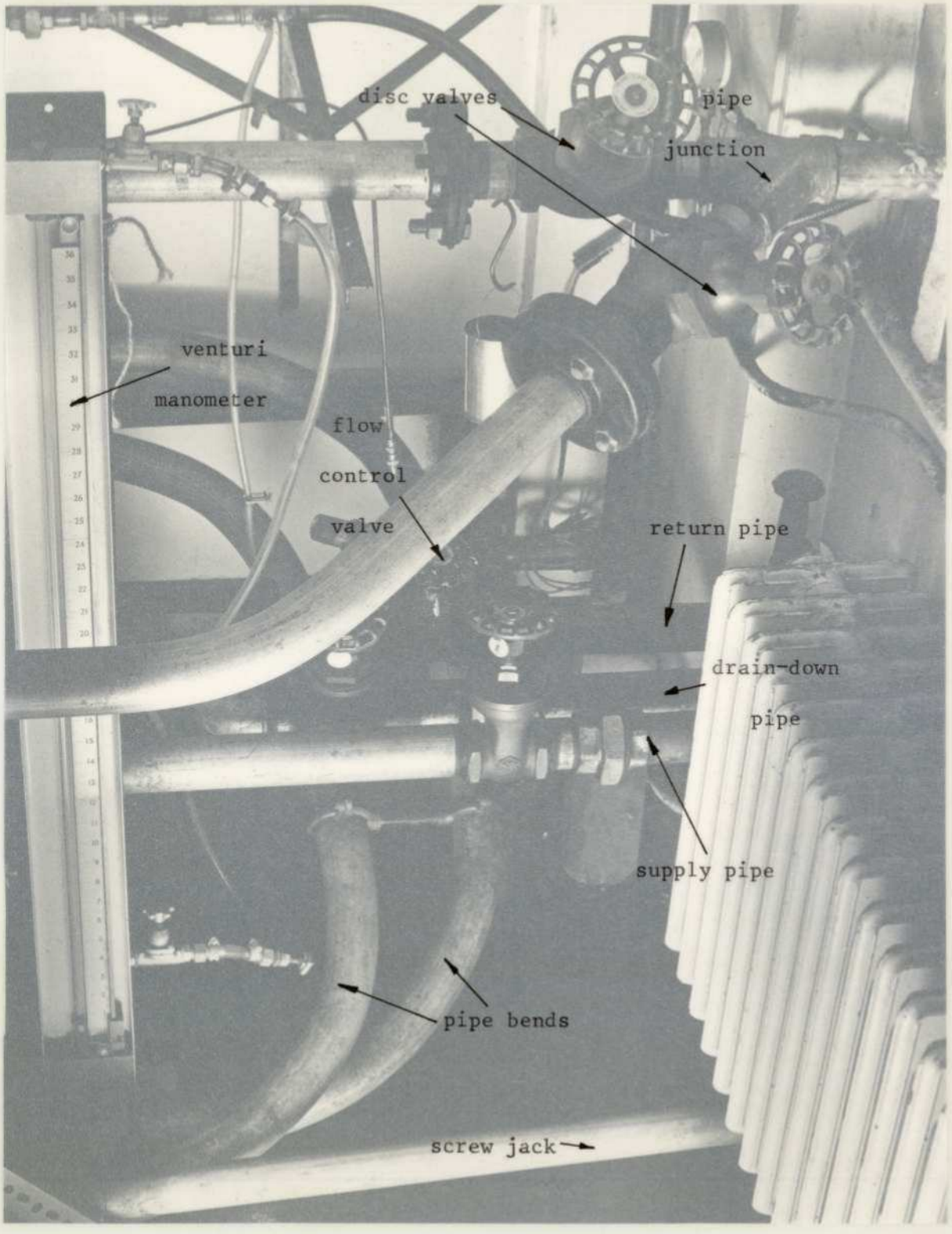


FIG 24b UPSTREAM END OF EXPERIMENTAL RIG

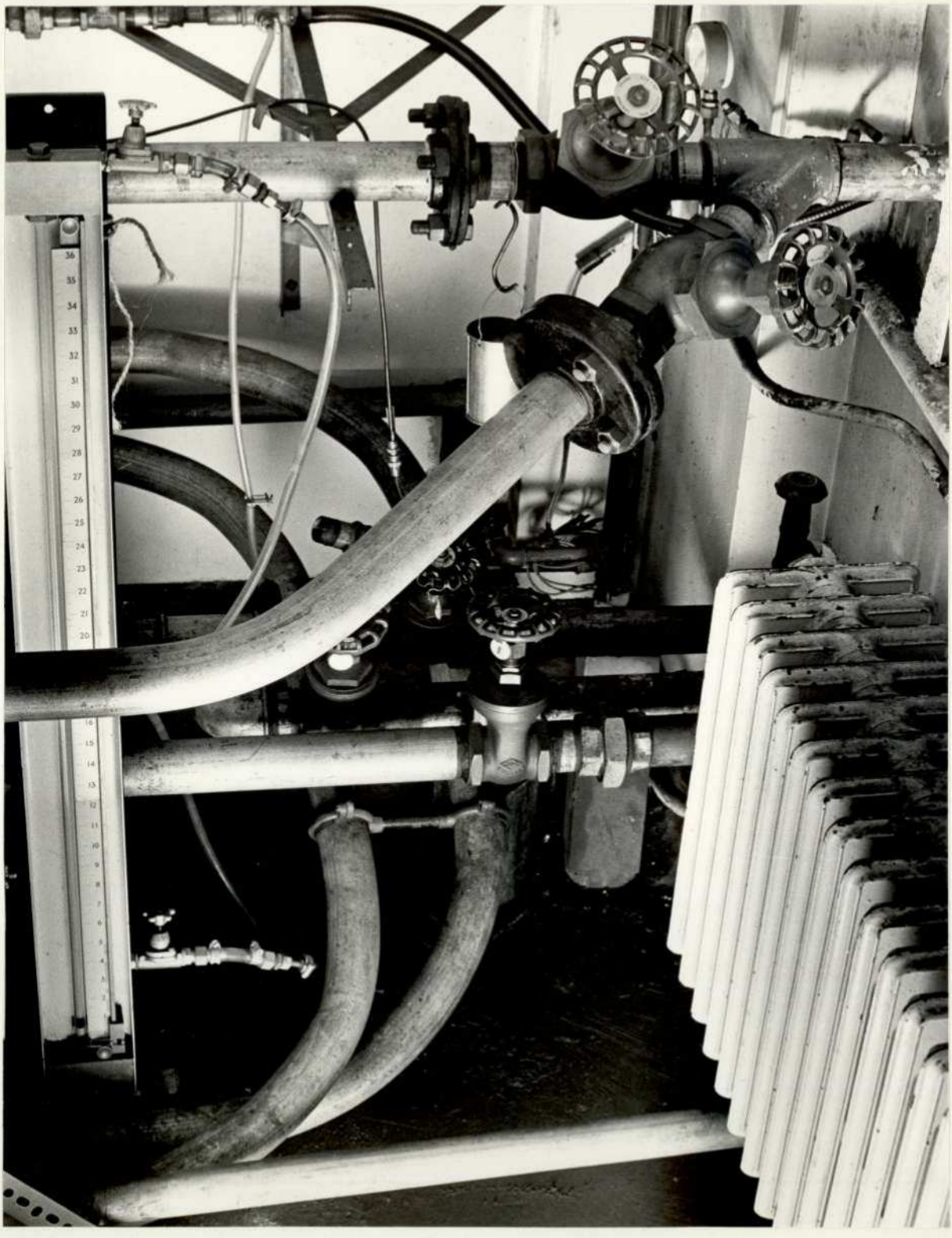
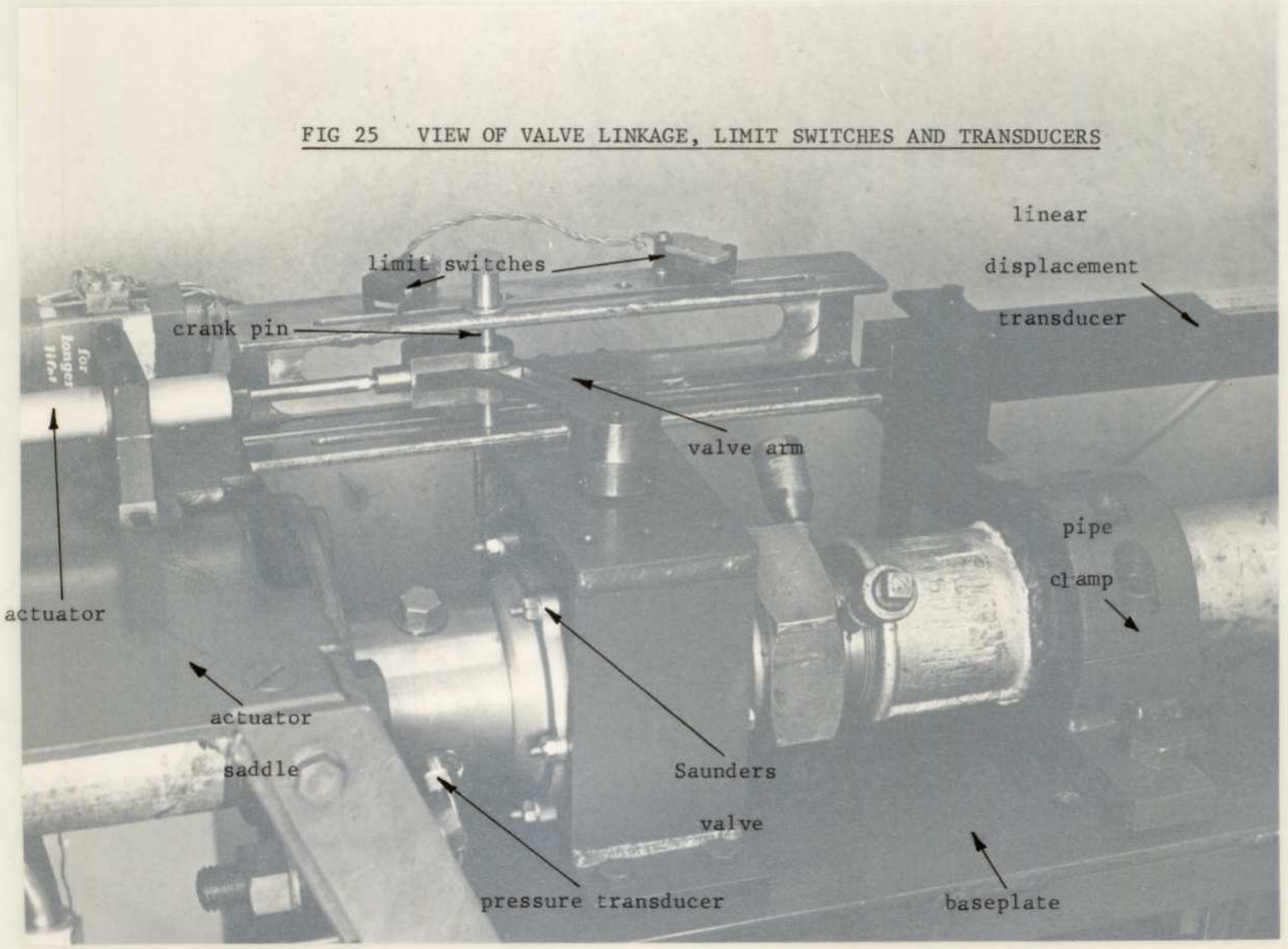
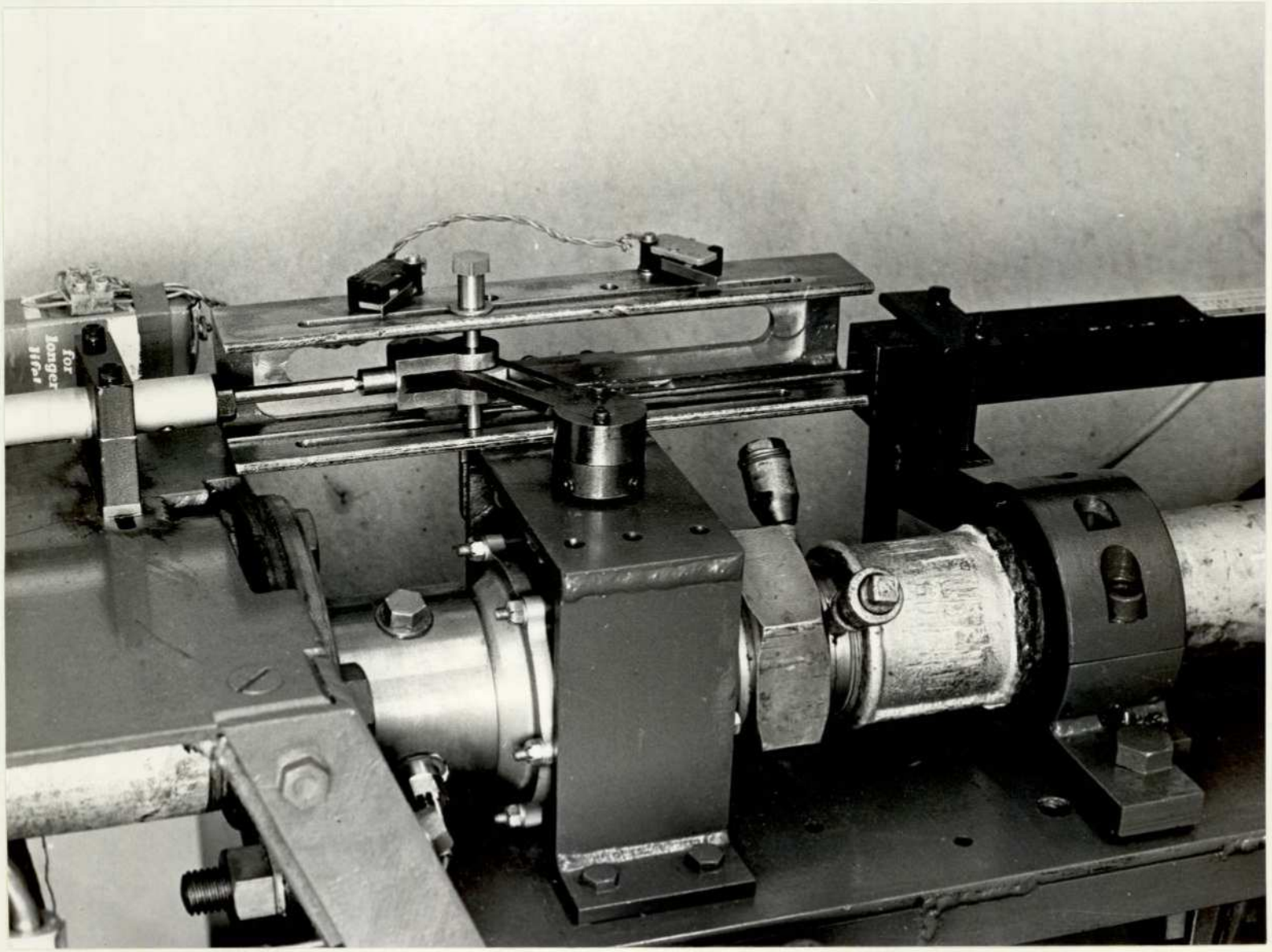


FIG 25 VIEW OF VALVE LINKAGE, LIMIT SWITCHES AND TRANSDUCERS





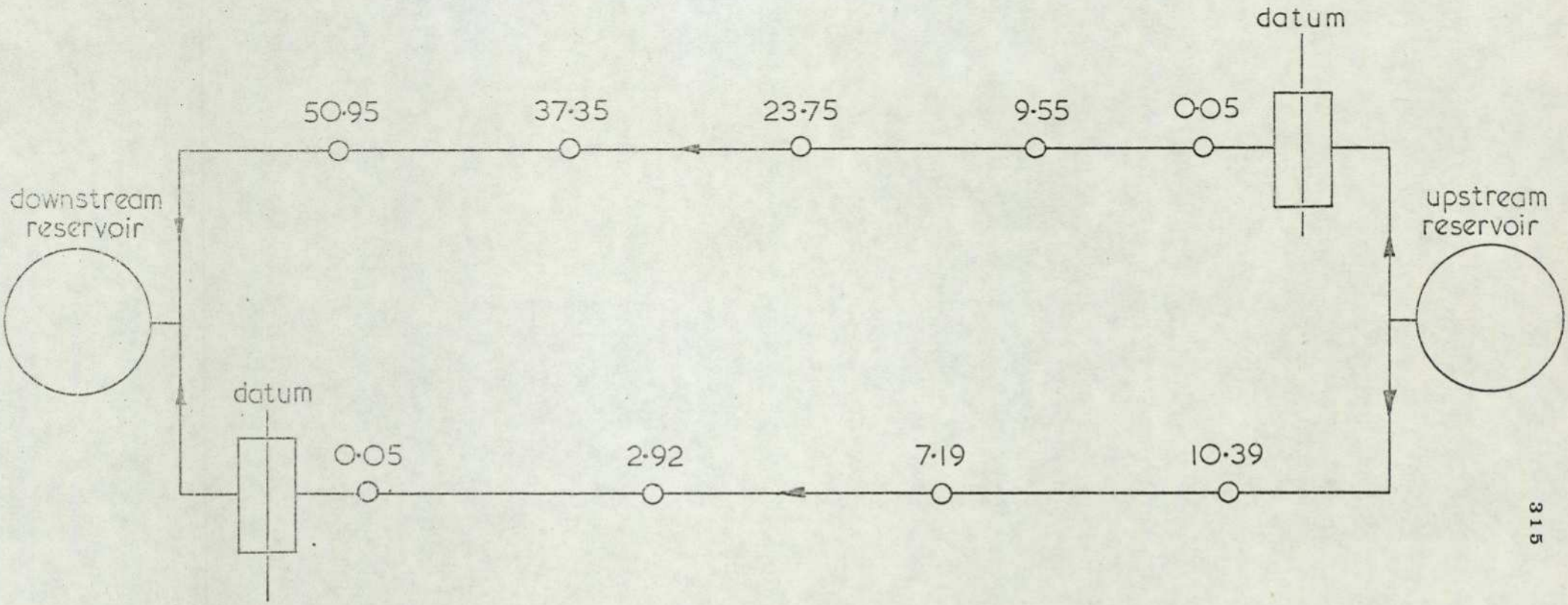


FIG 26 LOCATION (IN m) OF 14mm TRANSDUCER STATIONS REFERRED TO THE VALVE DATUM IN EACH PIPE

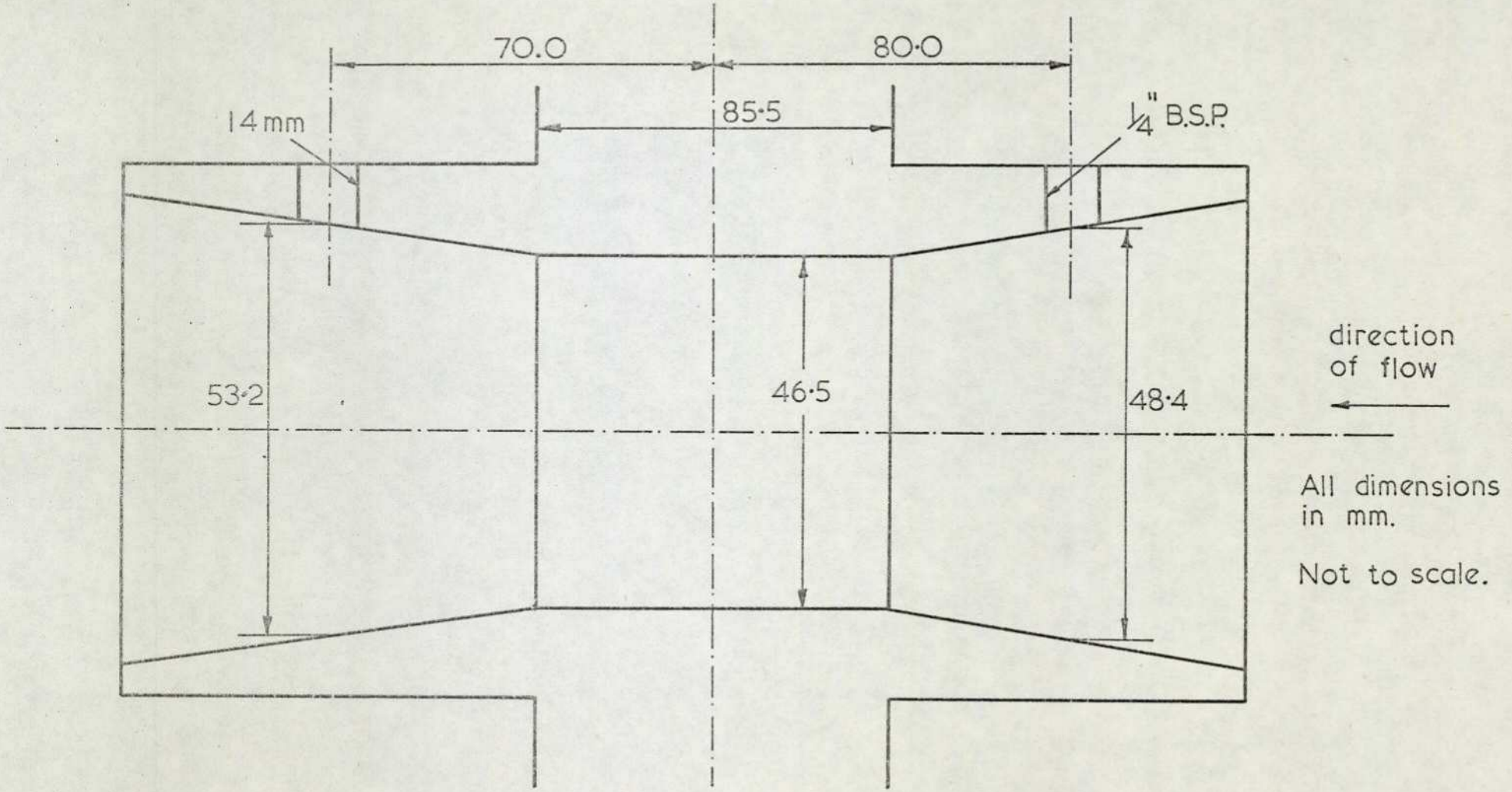


FIG 27 SAUNDERS FUEL VALVE & TRANSITION SECTIONS

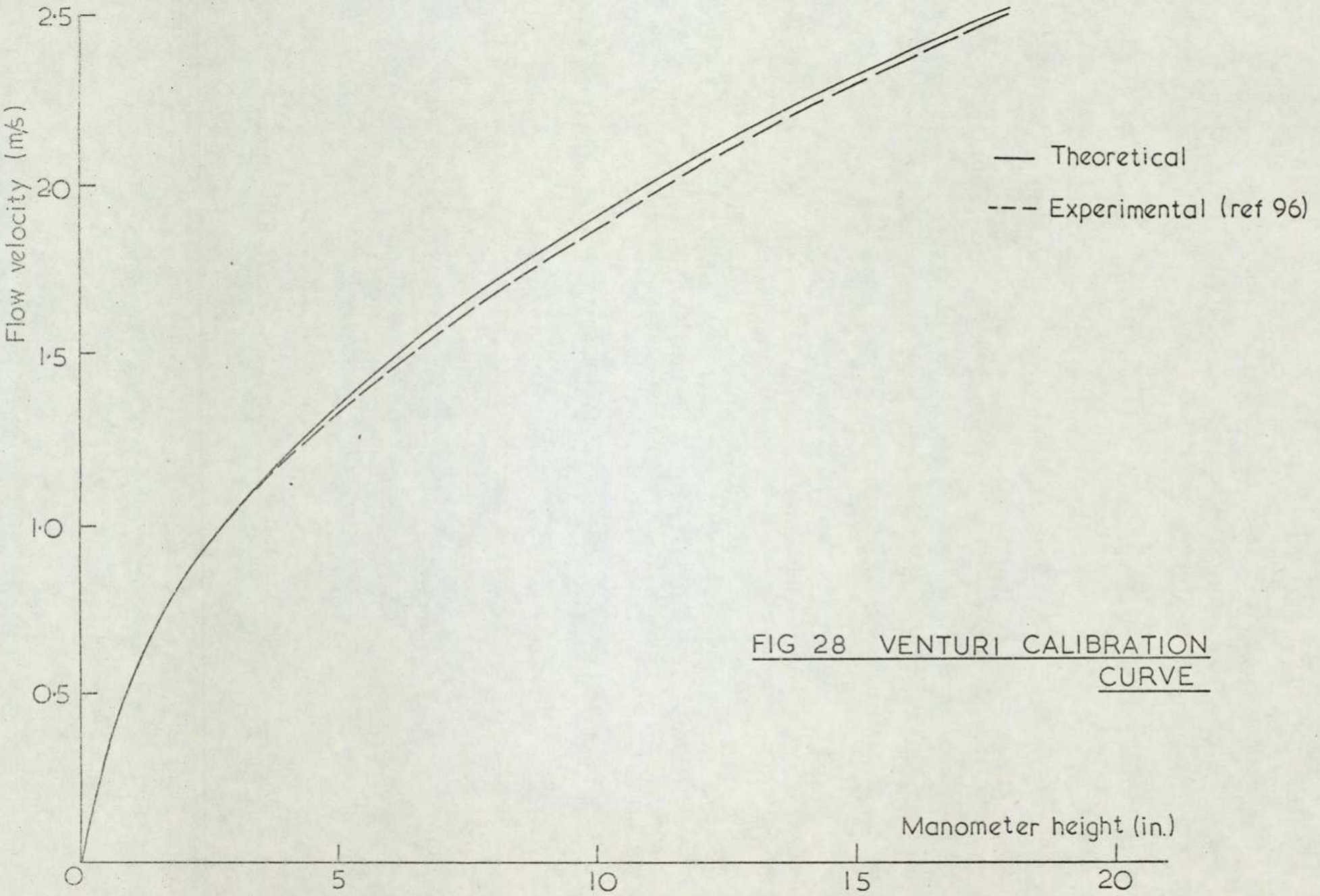


FIG 28 VENTURI CALIBRATION CURVE

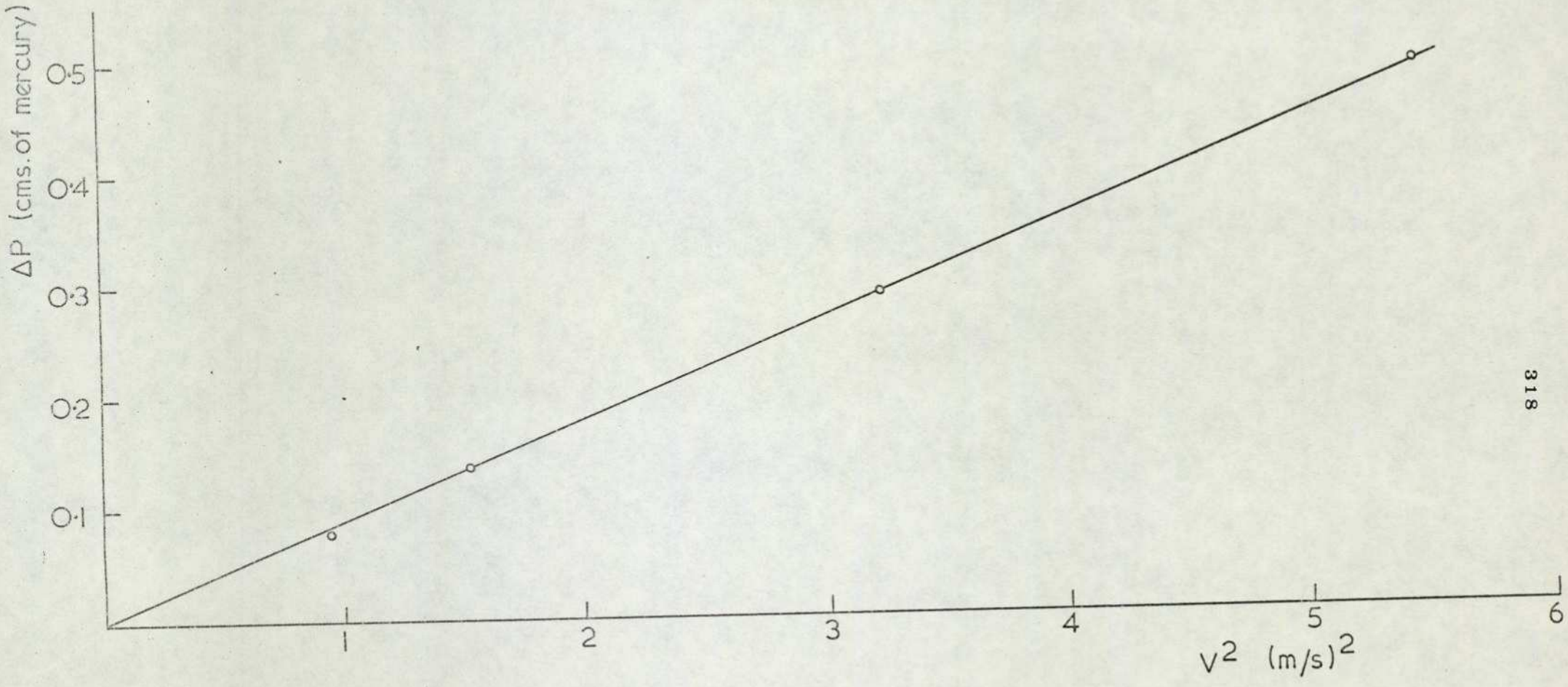


FIG 29 PRESSURE DROP-FLOW RATE FOR PLUG VALVE

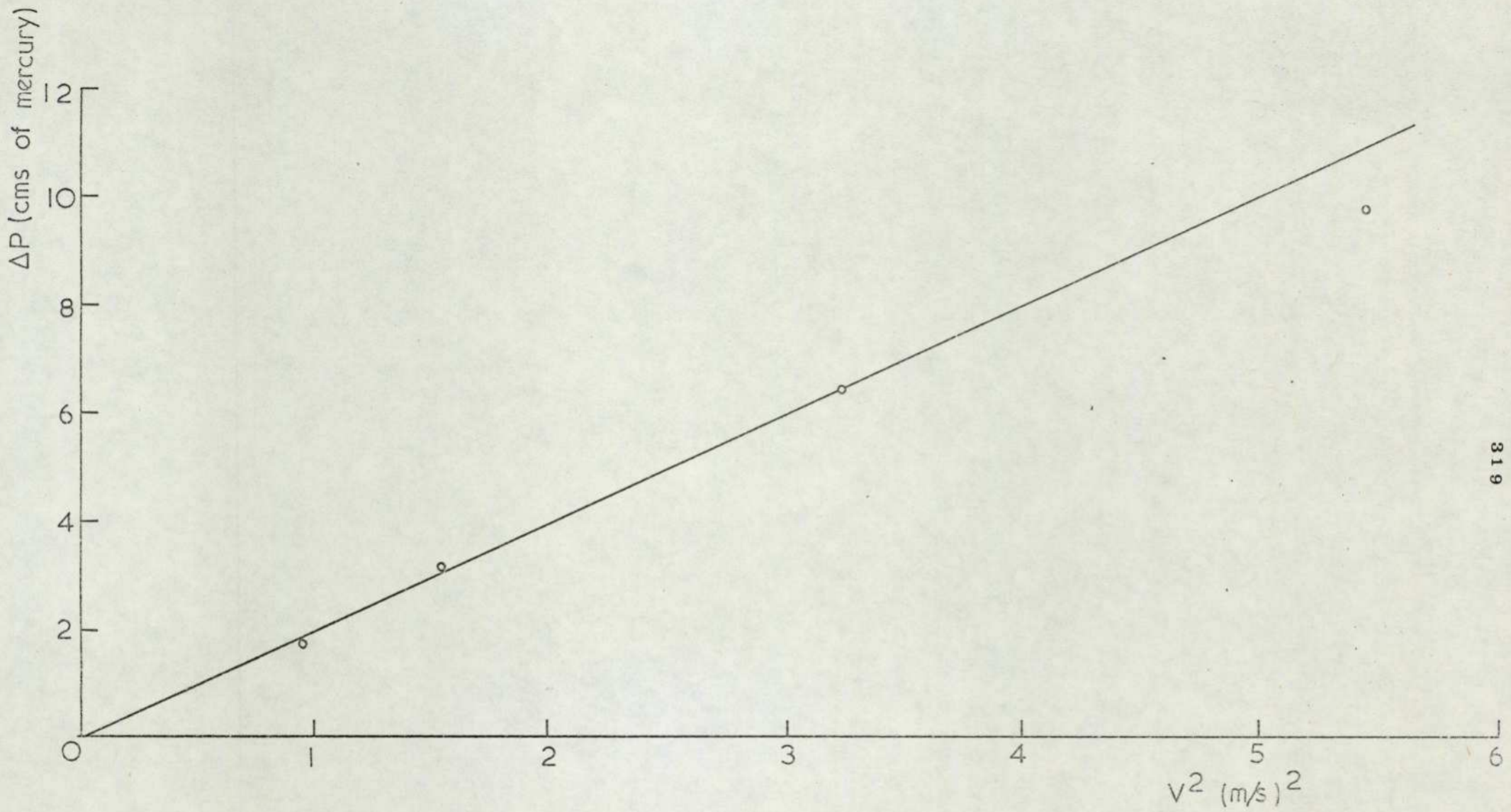


FIG 30 PRESSURE DROP-FLOW RATE FOR DISC VALVE

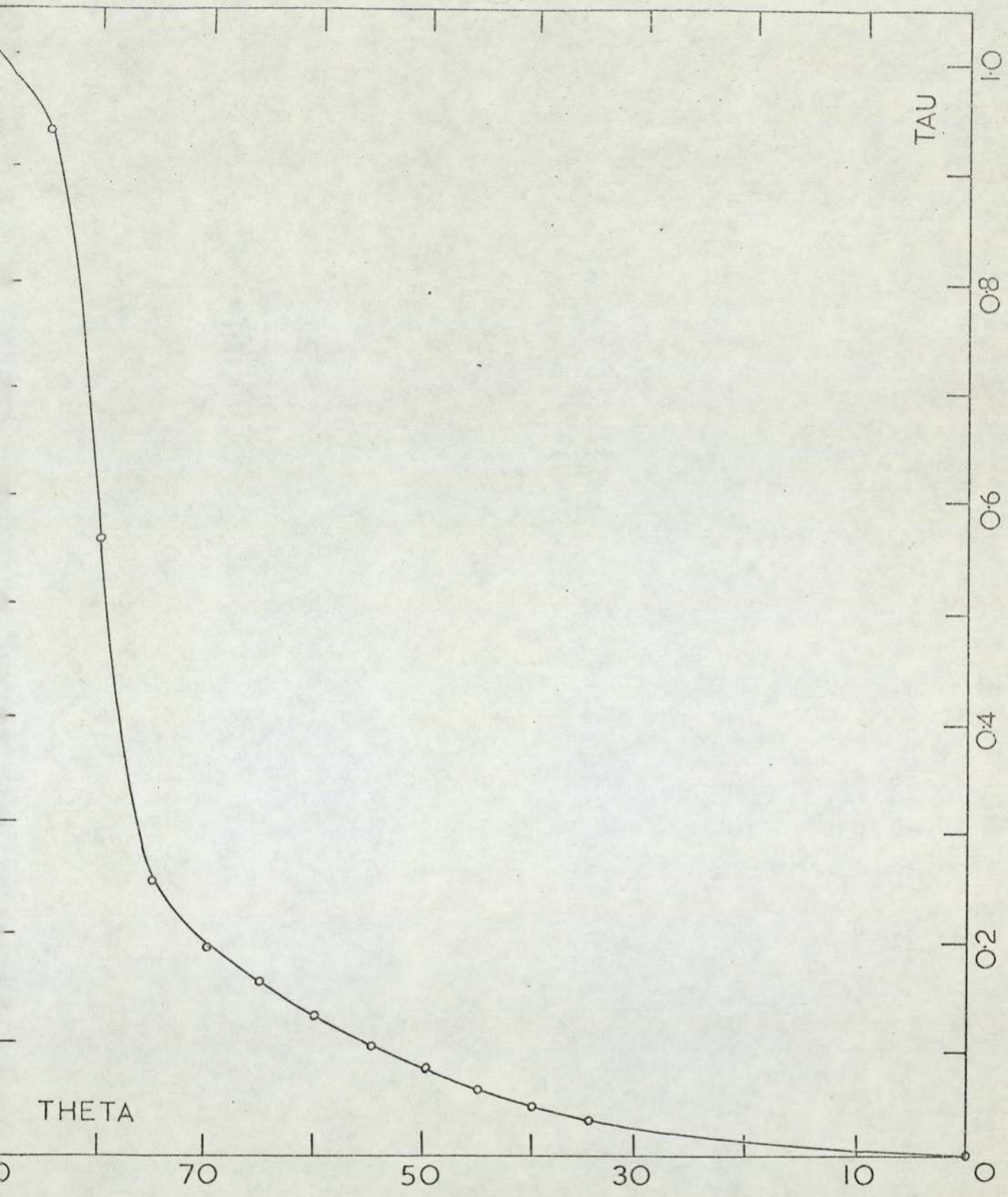
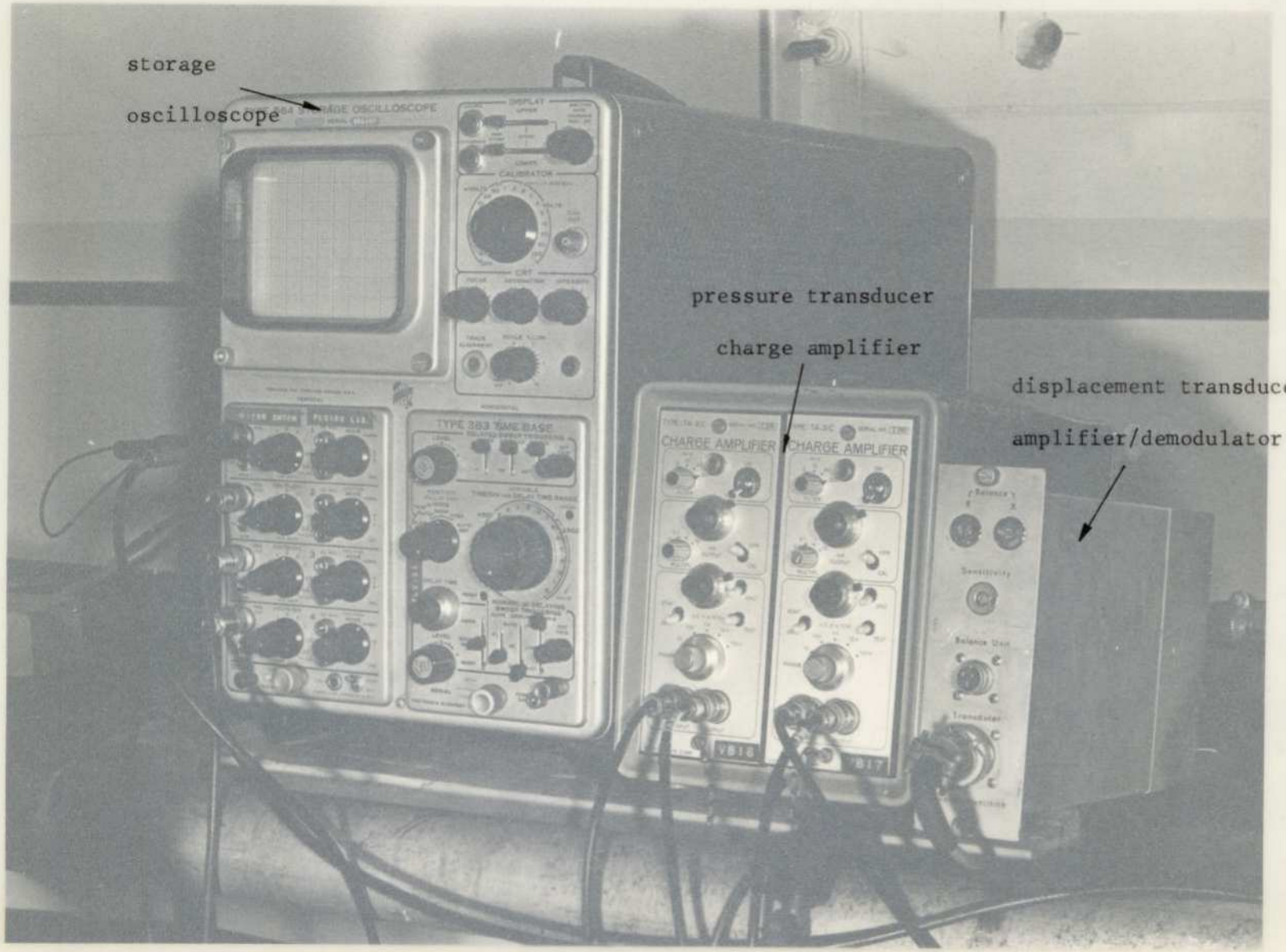


FIG 31. STEADY STATE VALVE CHARACTERISTIC

SHOWING EXPERIMENTAL POINTS ON CURVE

FIG 32 VIEW OF OSCILLOSCOPE, CHARGE AMPLIFIER AND DEMODULATOR



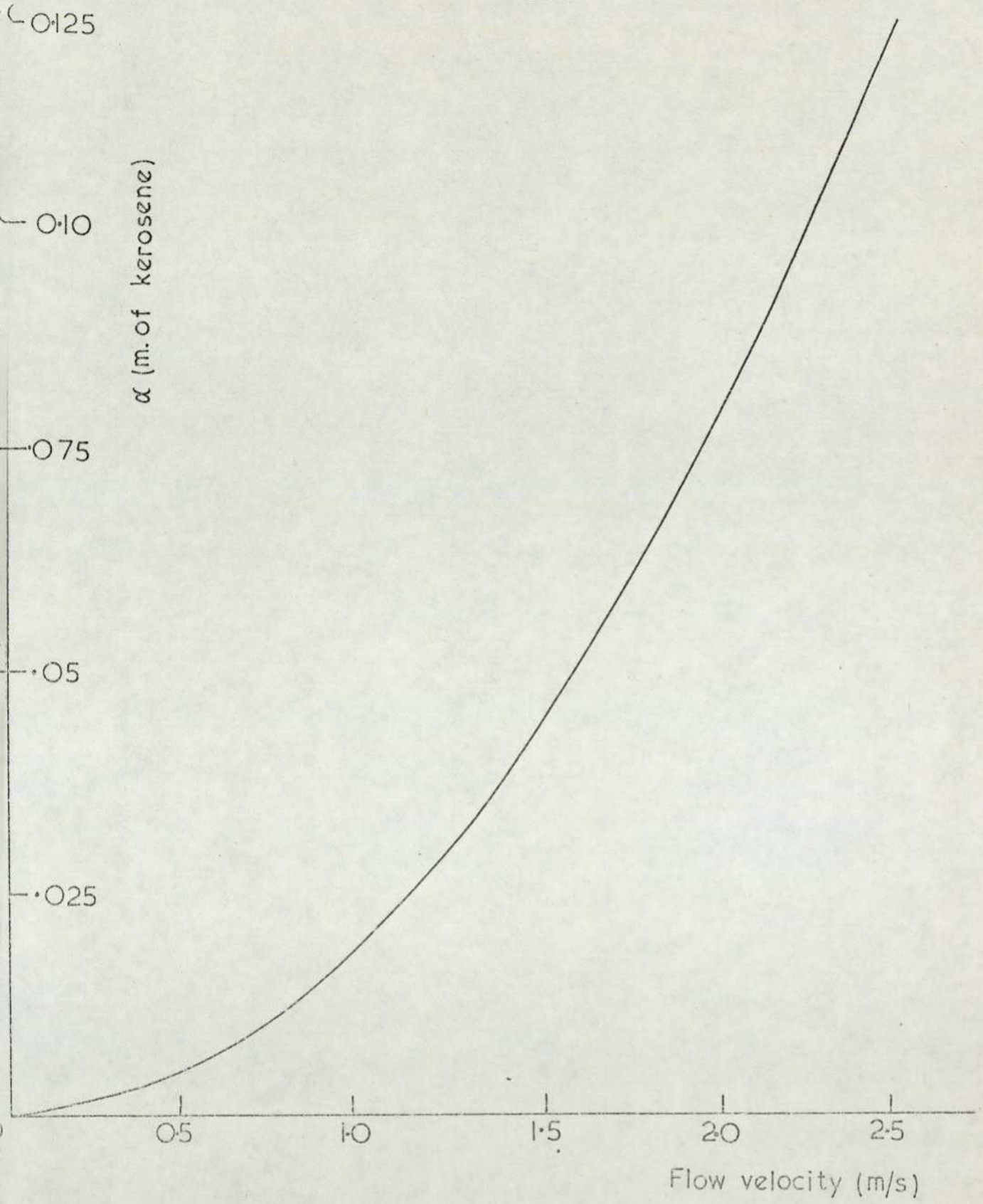


FIG 33 VALVE STATIC HEAD CALIBRATION CURVE

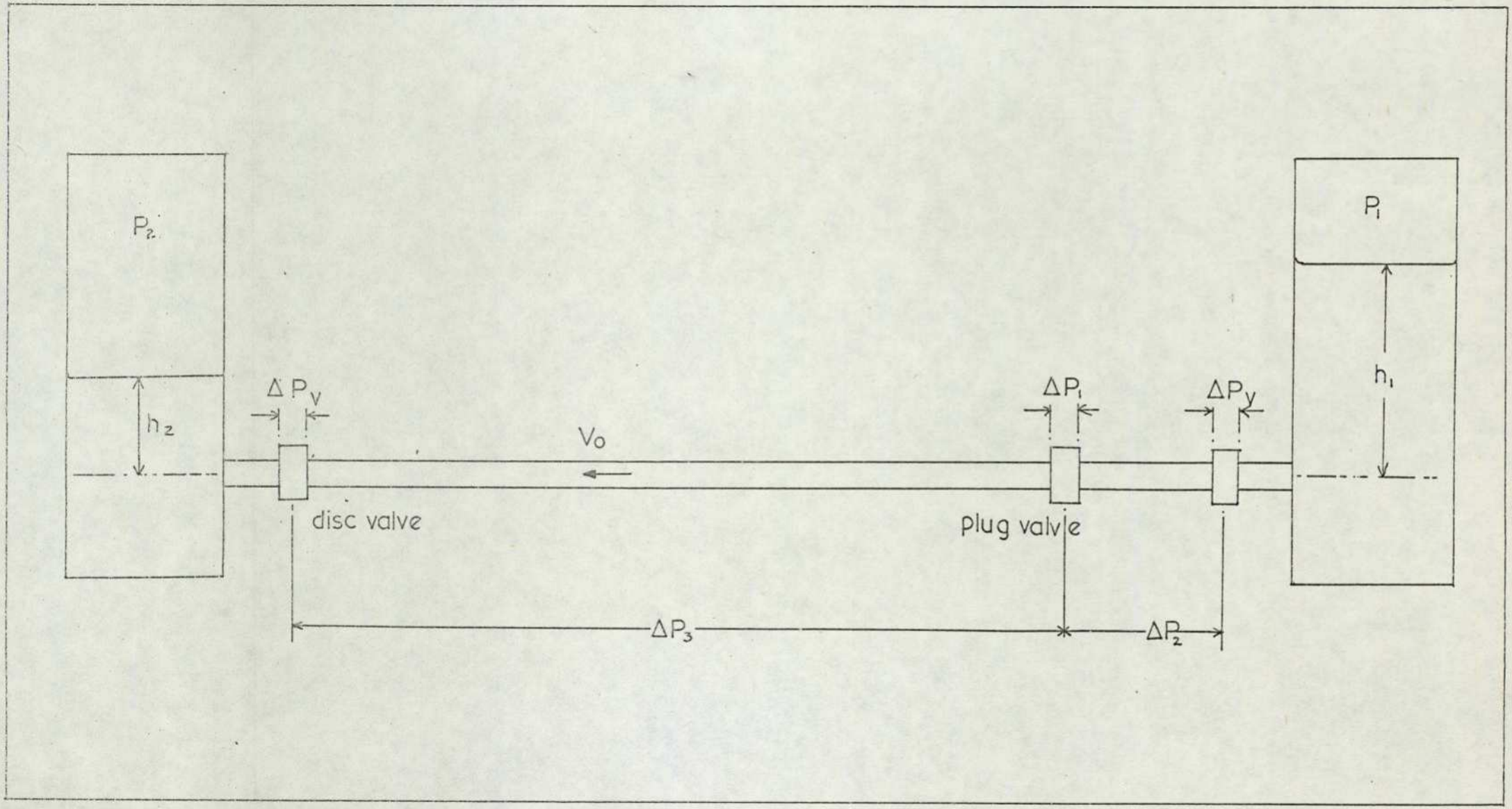
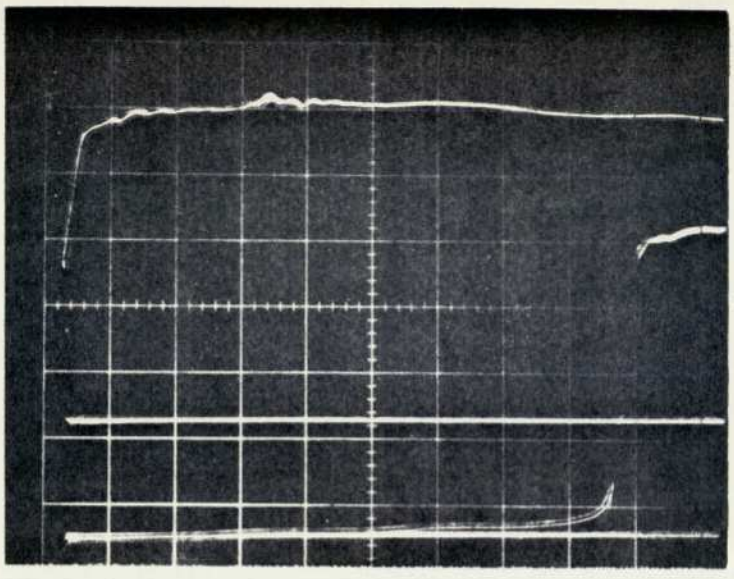
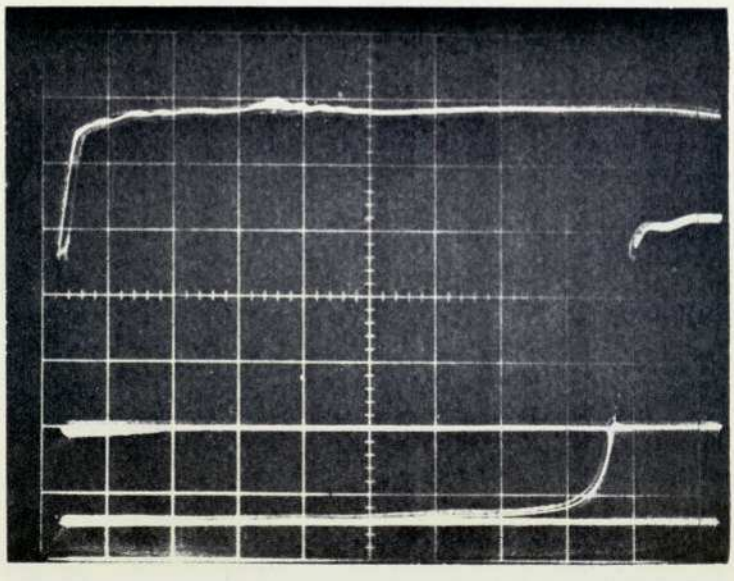


FIG 34 PRESSURE CHANGES ALONG MAIN PIPELINE (STEADY FLOW)



35a. Test No. 5



35b. Test No. 8

FIG 35 TYPICAL RESULTS OF WAVE SPEED TESTS

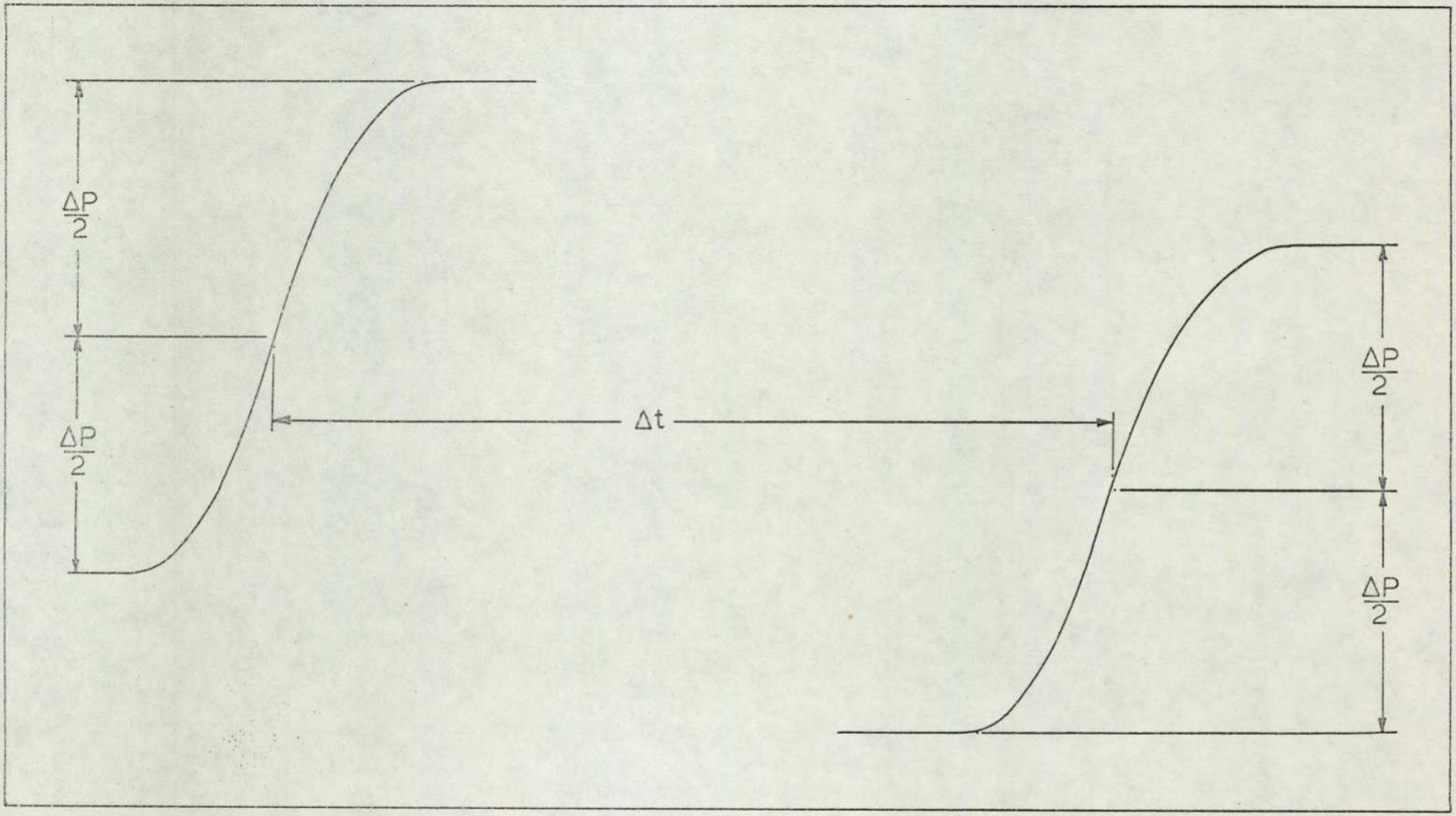


FIG 36 DEFINITION OF TIME INTERVAL, Δt, USED TO DETERMINE THE ACOUSTIC WAVE SPEED

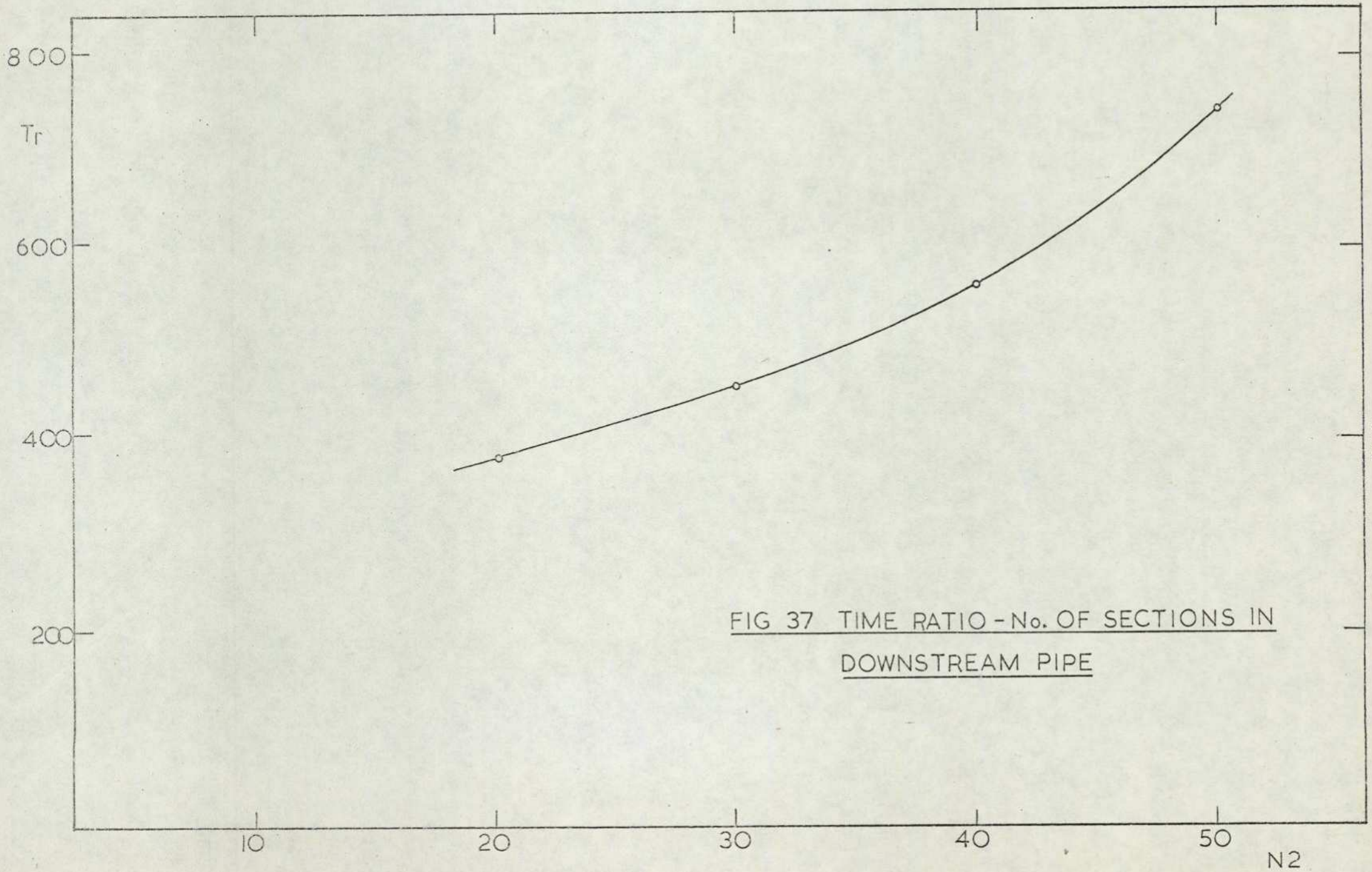


FIG 37 TIME RATIO - No. OF SECTIONS IN DOWNSTREAM PIPE

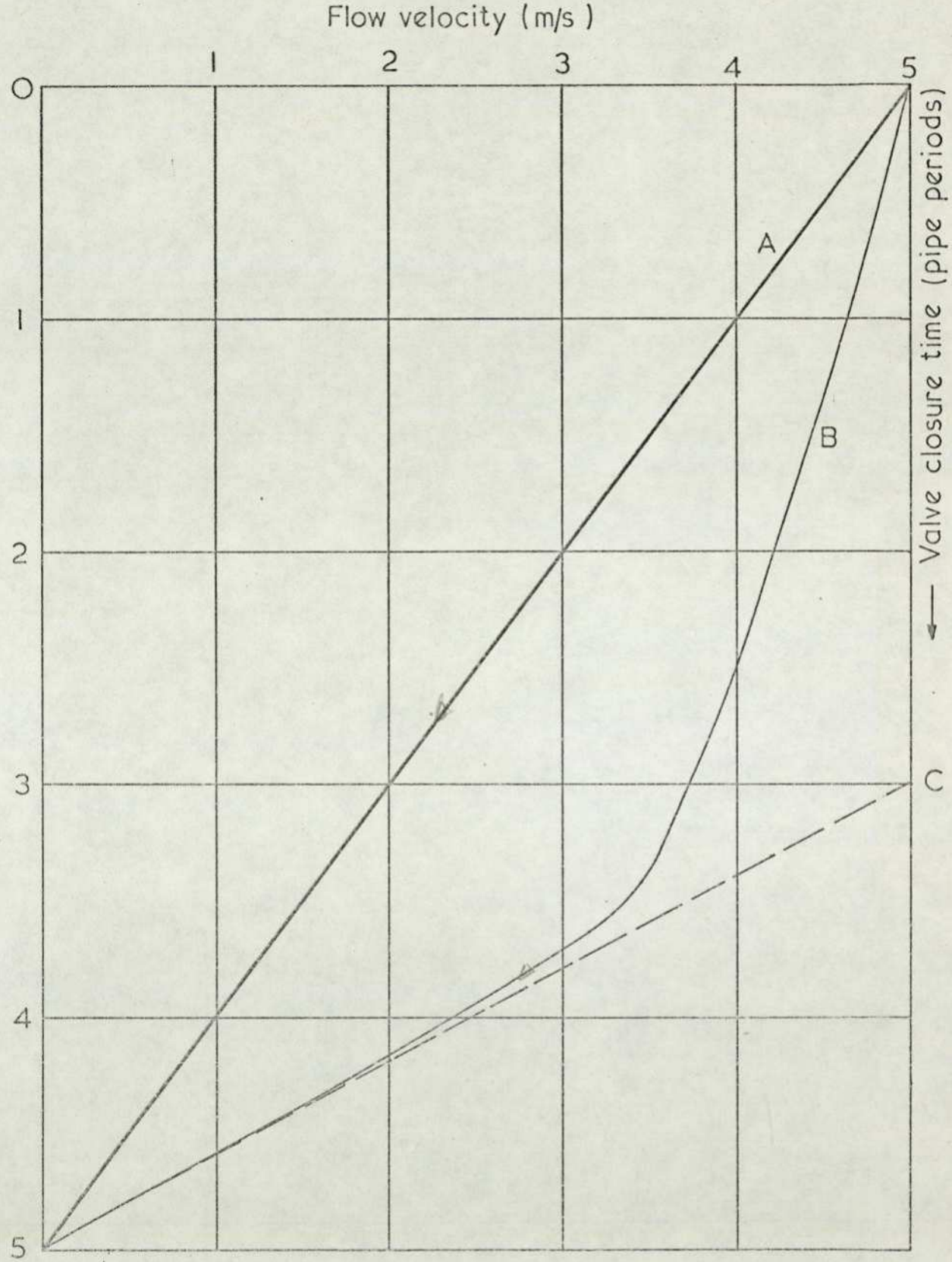


FIG 38 KERR'S DERIVATION OF 'EQUIVALENT VALVE CLOSING TIME'

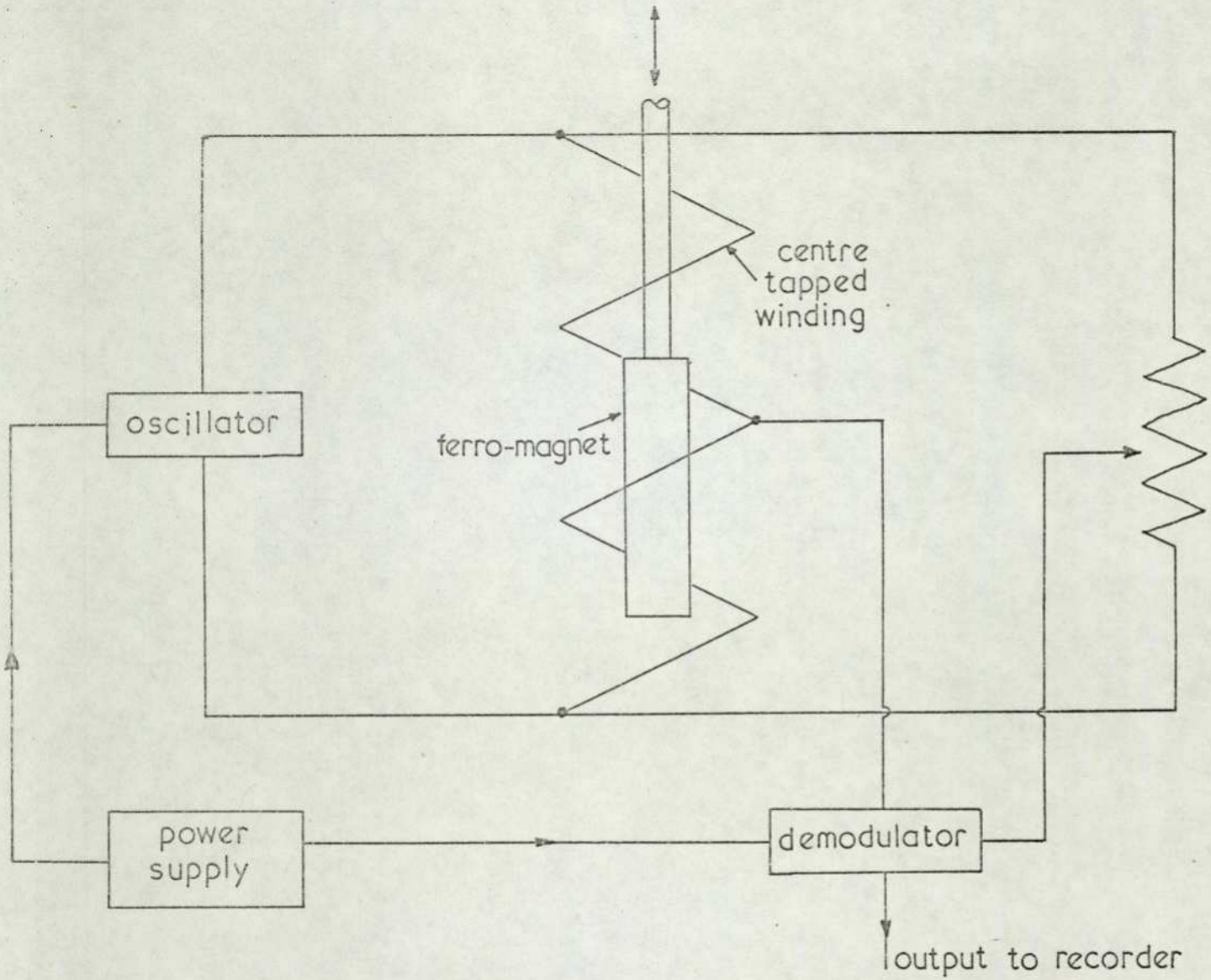


FIG 39 LINEAR DISPLACEMENT TRANSDUCER & ANCILLARY EQUIPMENT

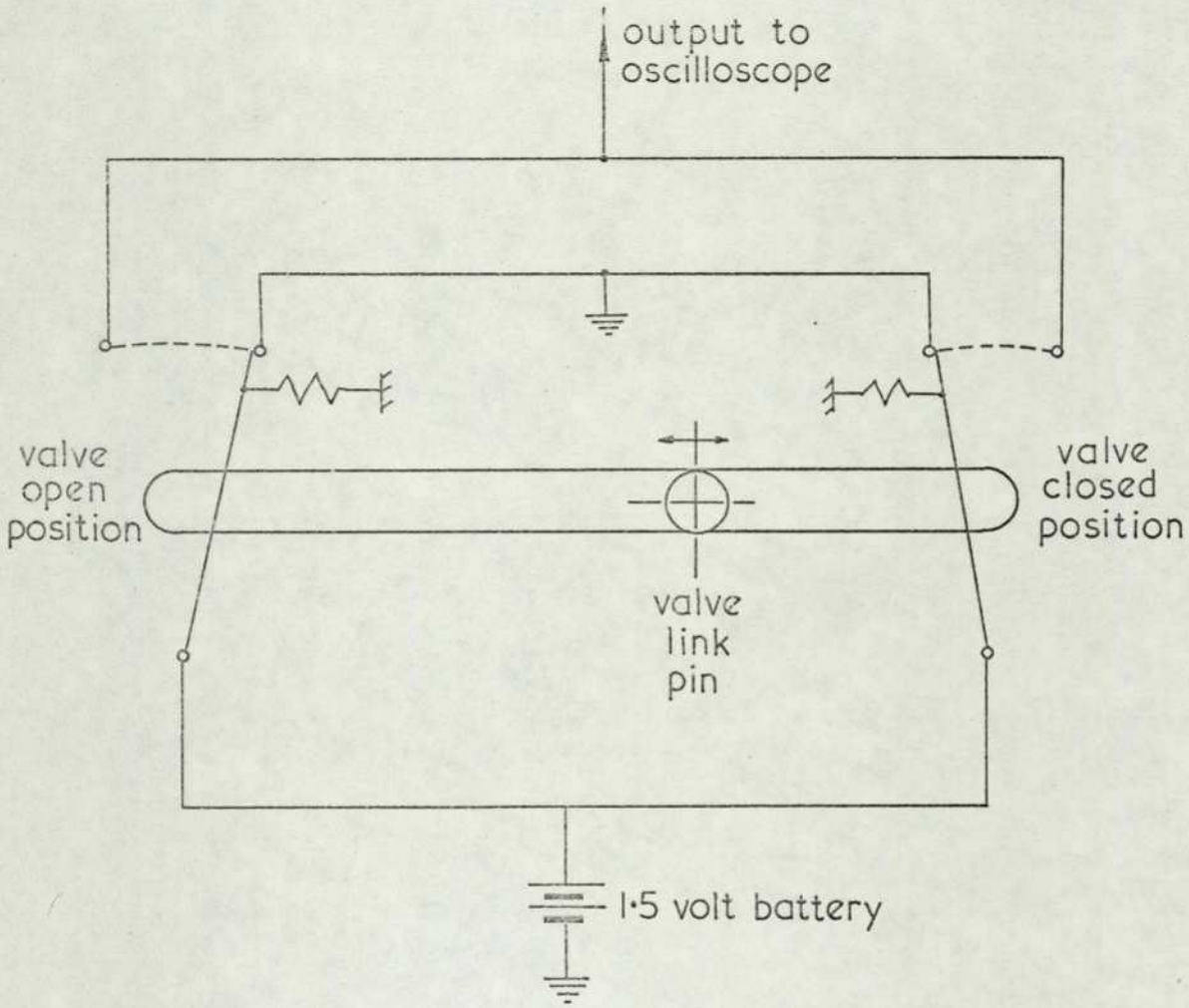


FIG 40 VALVE LINKAGE LIMIT SWITCH ARRANGEMENT

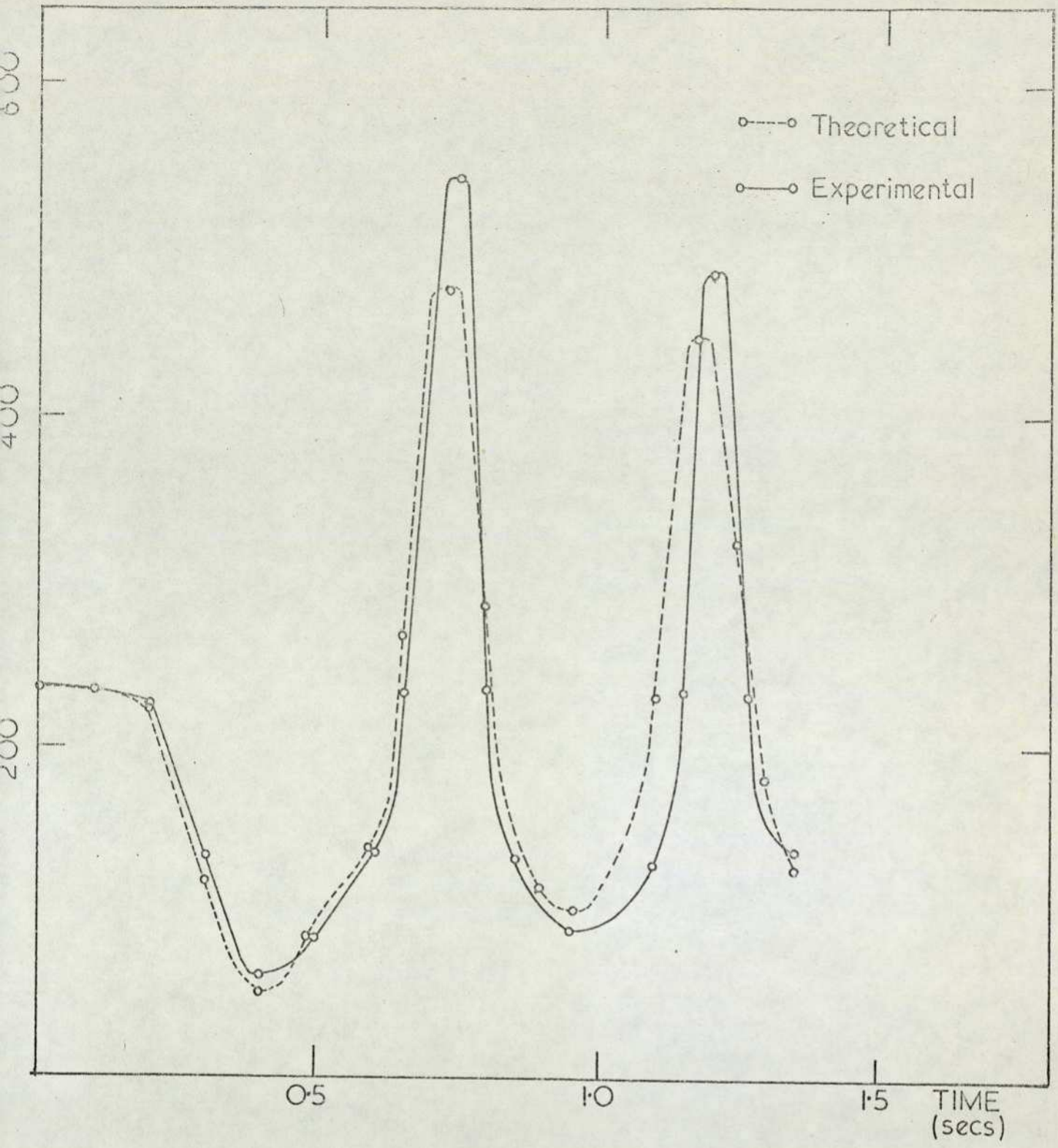


FIG 44 P_{cav} – TIME $V_o = 0{\cdot}76$ m/s $P_o = 237$ kn/m²

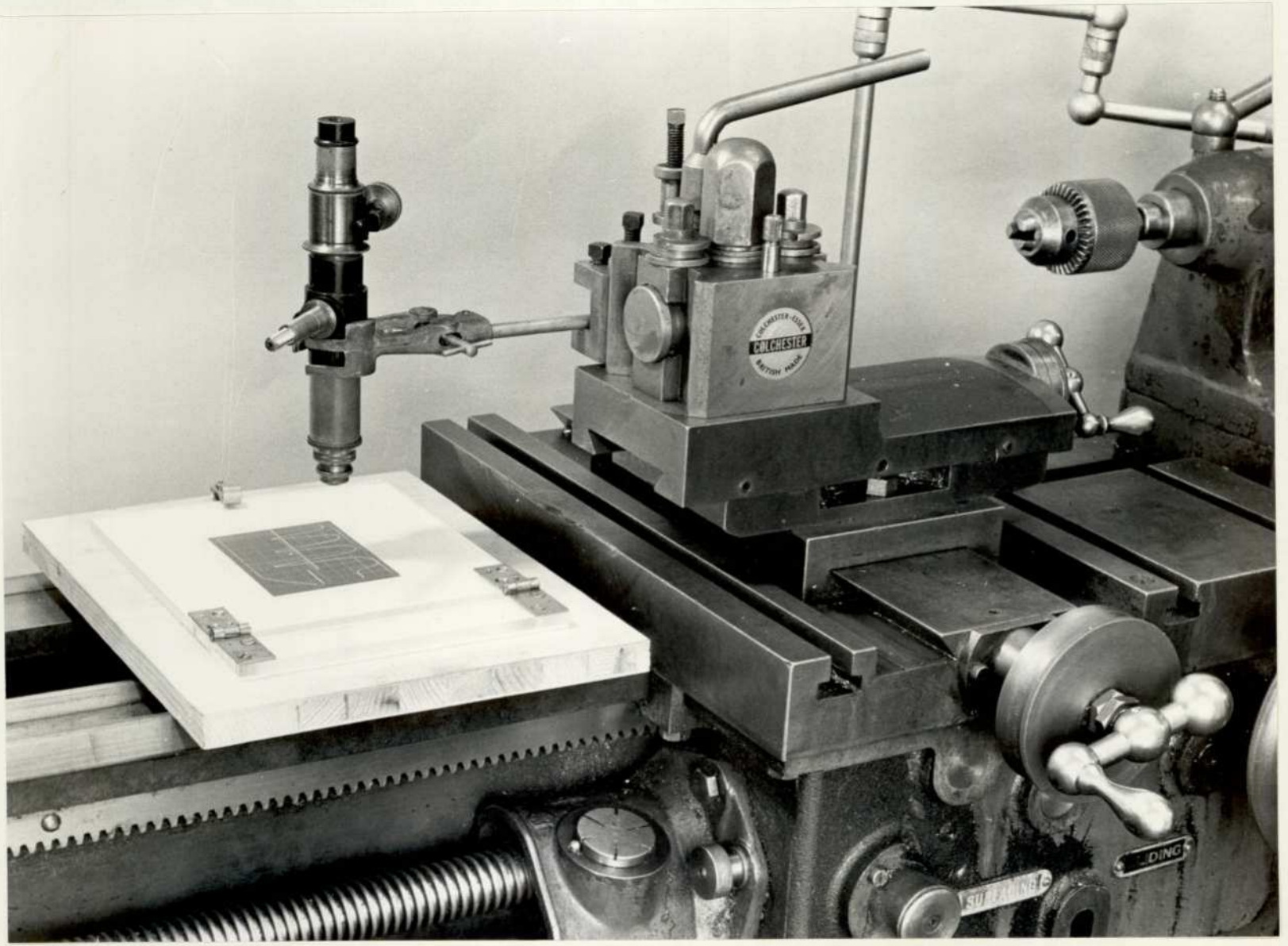


FIG 41 VIEW OF TWO AXIS TRAVELLING MICROSCOPE ARRANGEMENT

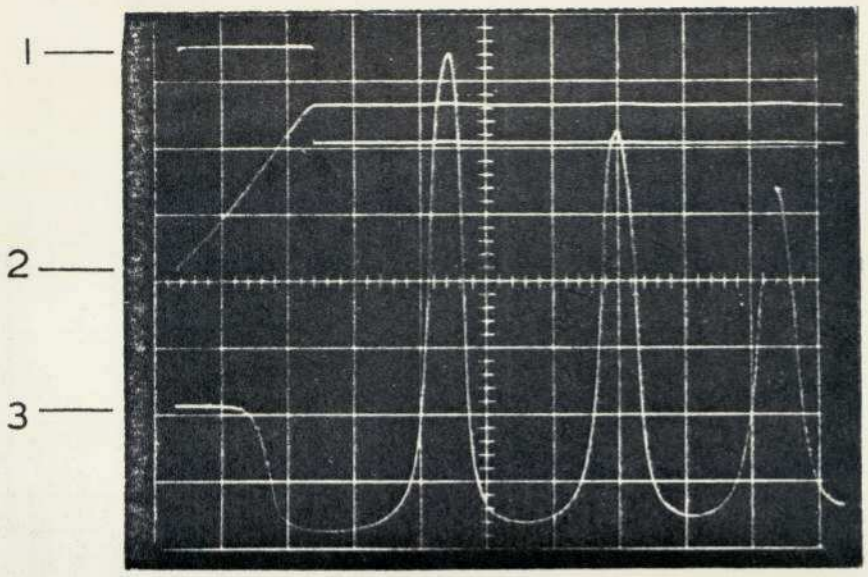


FIG. 42

Typical oscilloscope trace showing:

1. Square wave limit switch signal.
2. Linear displacement transducer.
3. Pressure at valve (P_{cav}) trace.

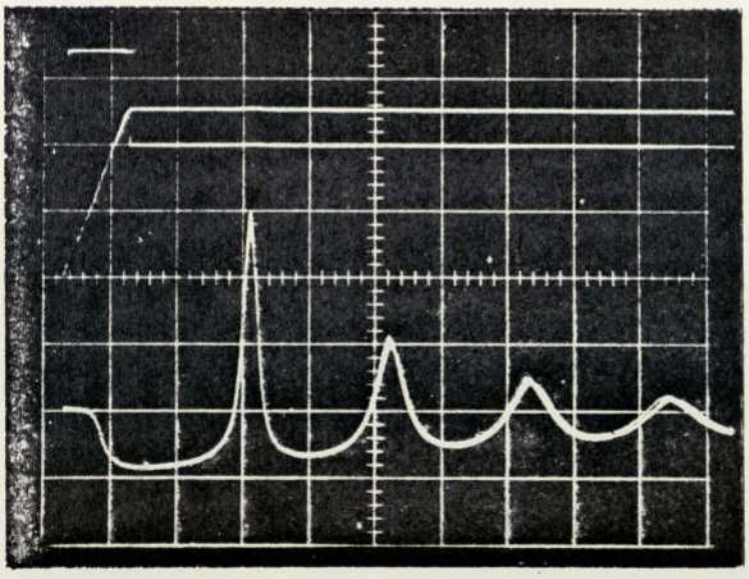


FIG. 43

Trace showing three tests superimposed to illustrate the repeatability of experimental results.

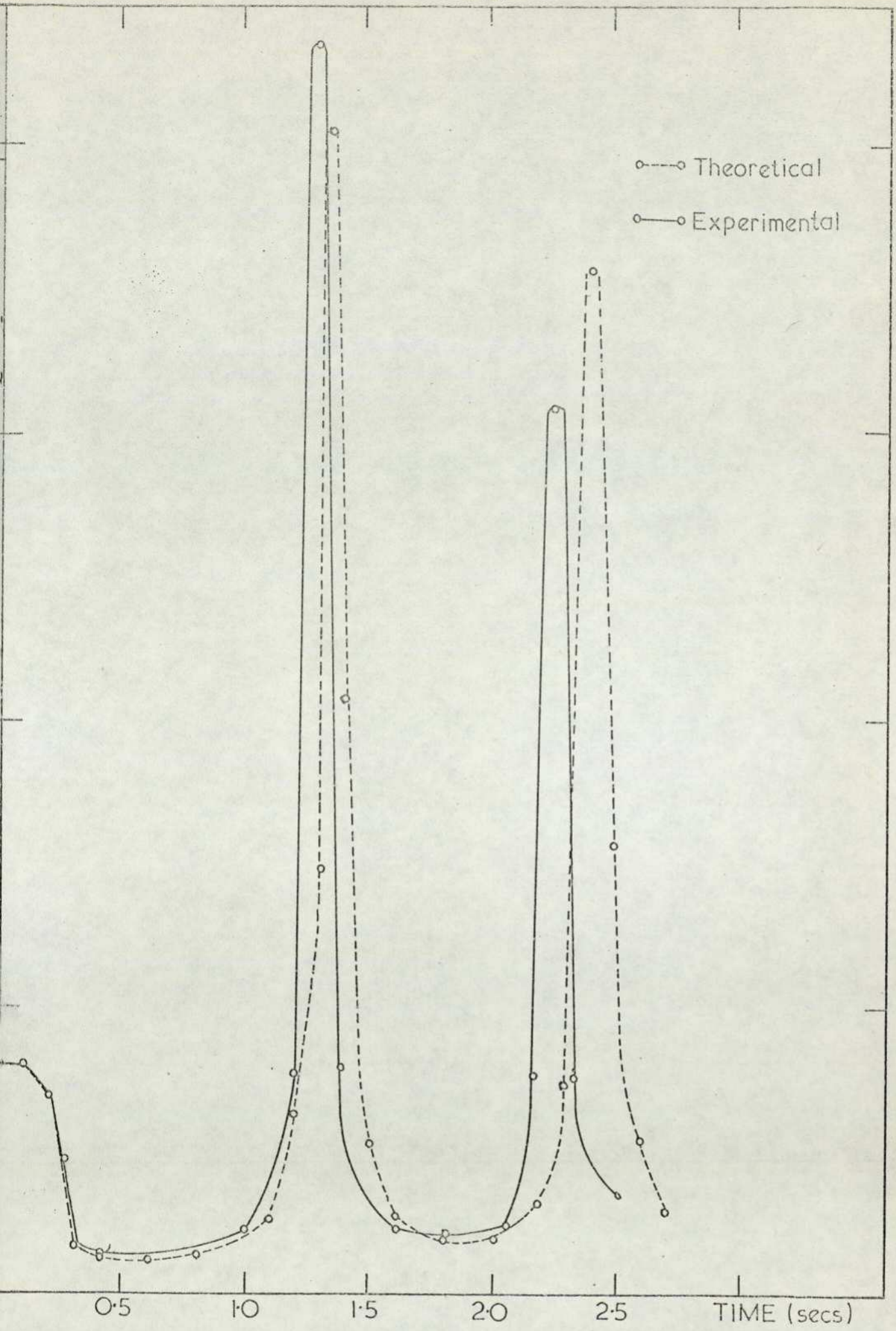


FIG45 P_{cav} –TIME V_o=1·34 m/s P_o=170 kn/m^2

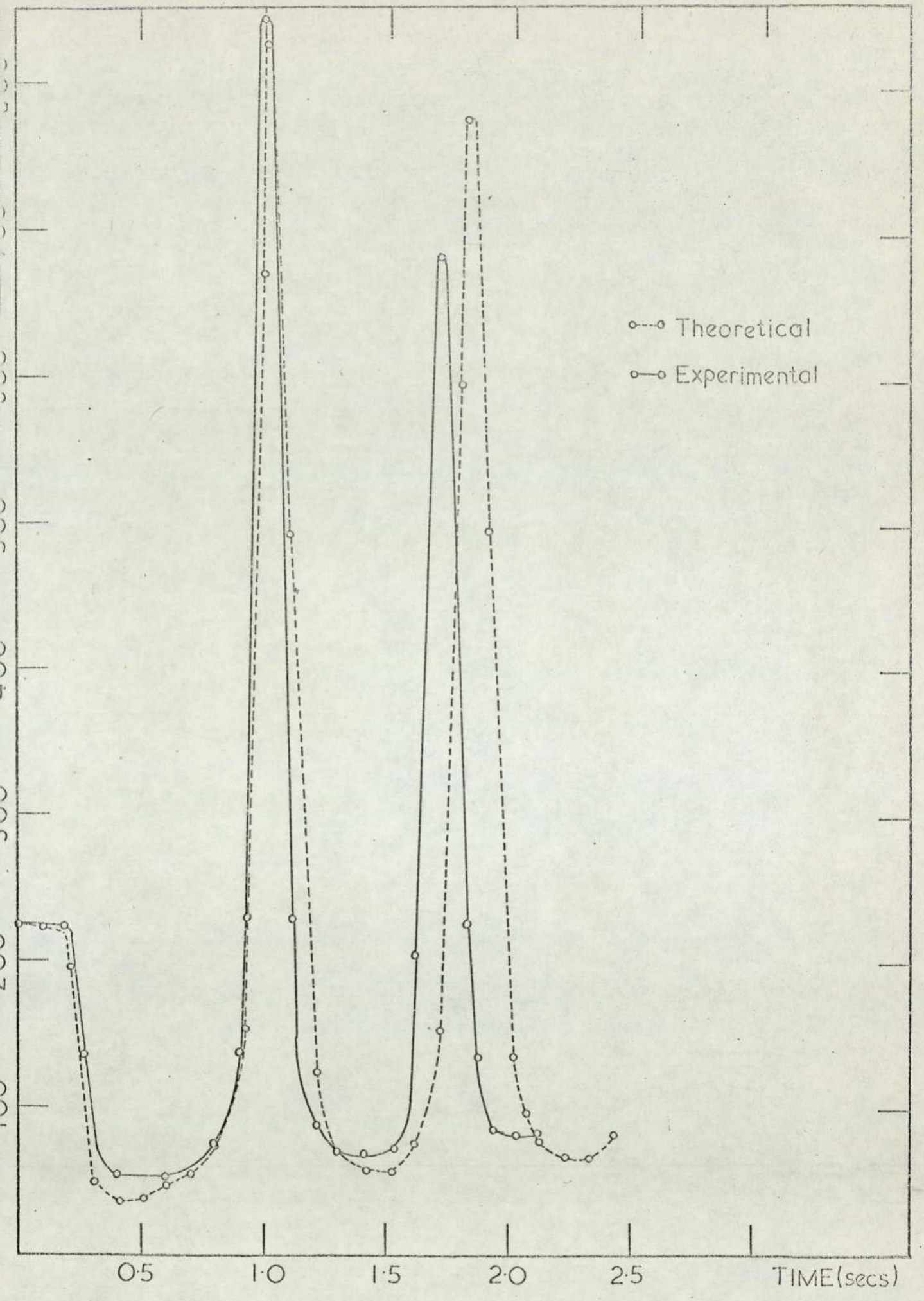
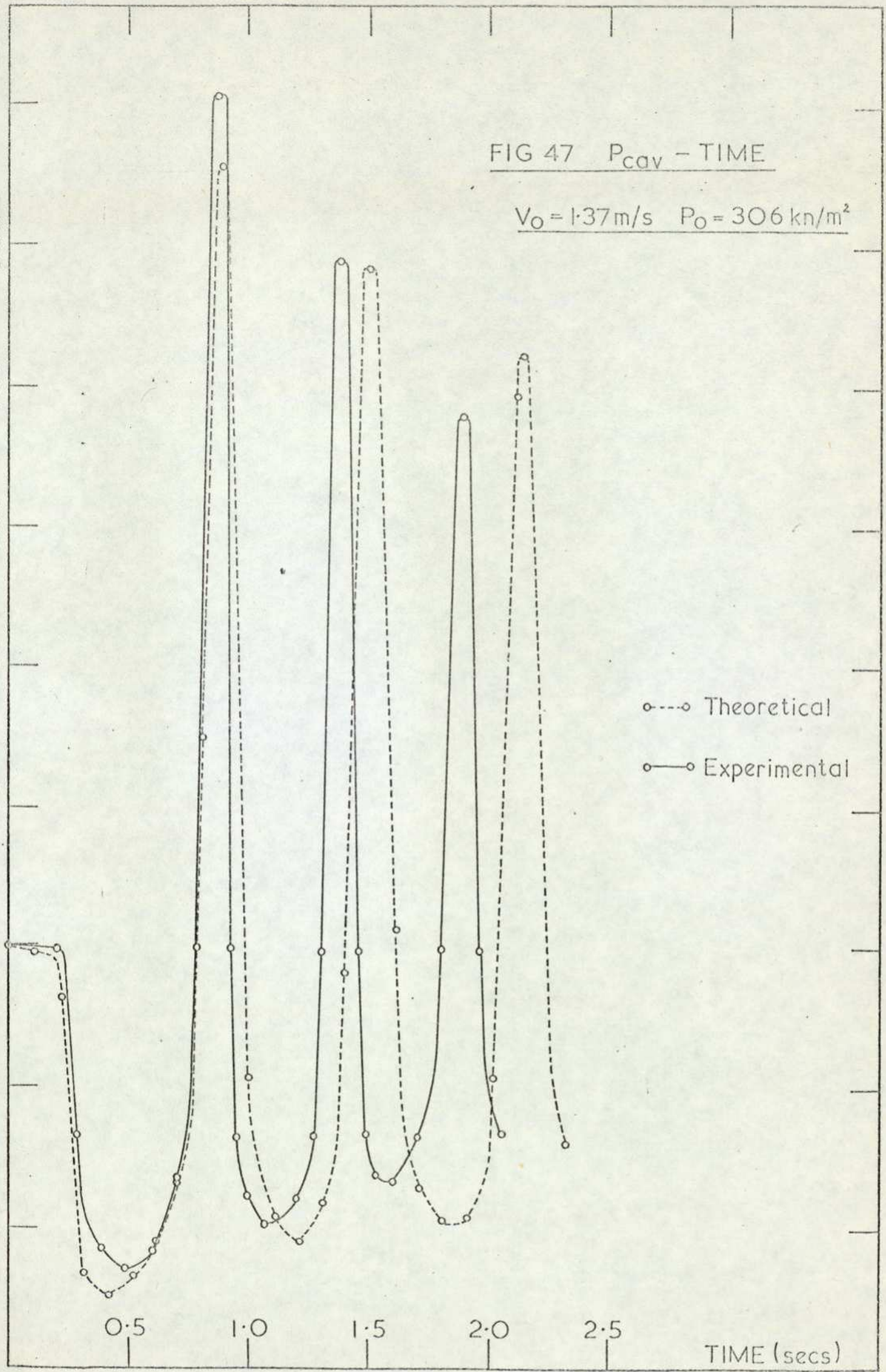


FIG 46 P_{cav} – TIME V_O = 1·37 m/s P_O = 237 kn/m^2


FIG 47 P_{cav} – TIME
V_O = 1·37 m/s P_O = 306 kn/m²
Theoretical
Experimental
0·5
1·0
1·5
2·0
2·5
TIME (secs)

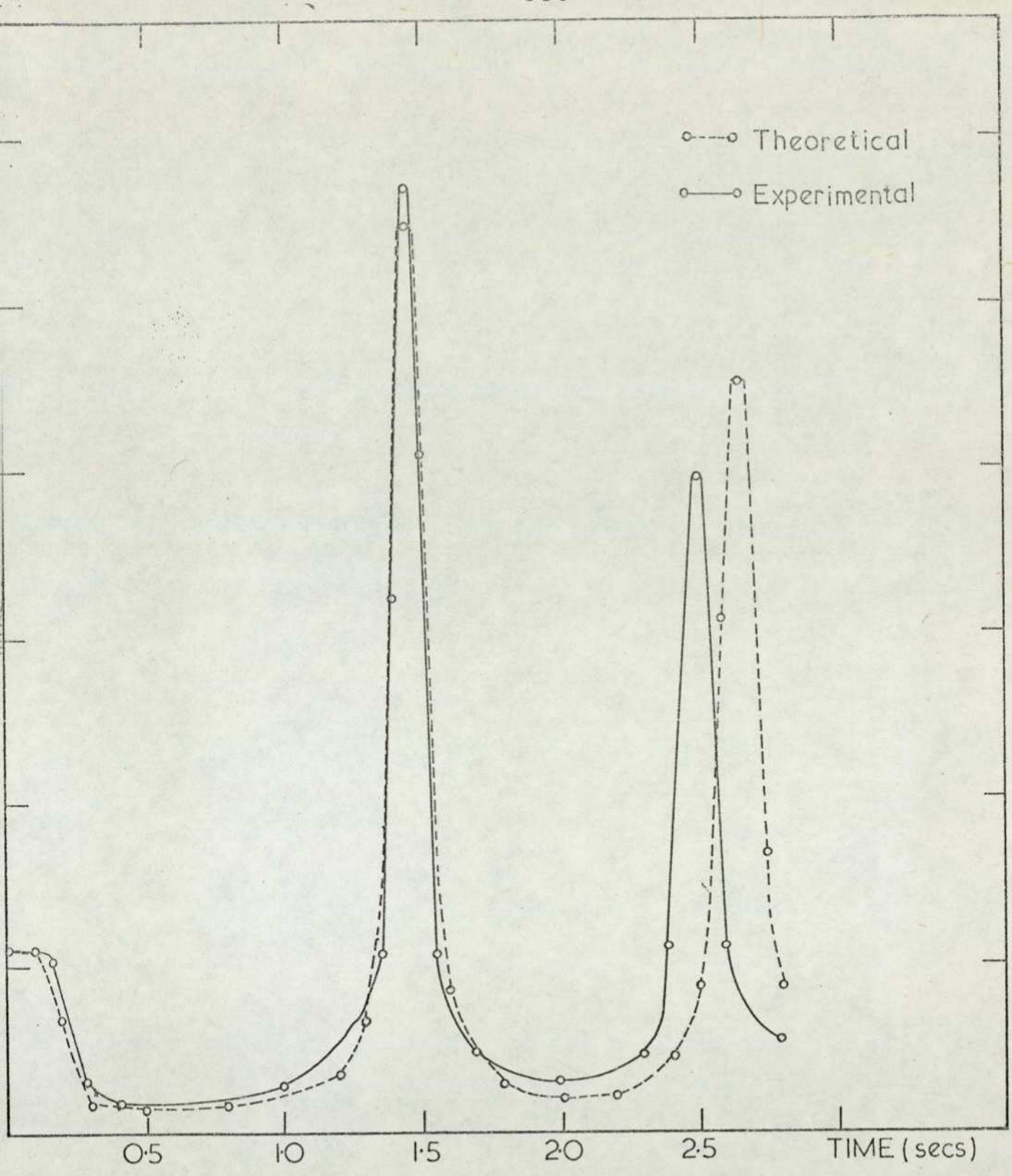


FIG 48 P_{cav} – TIME $V_o = 1{\cdot}99$ m/s $P_o = 237$ kn/m^2

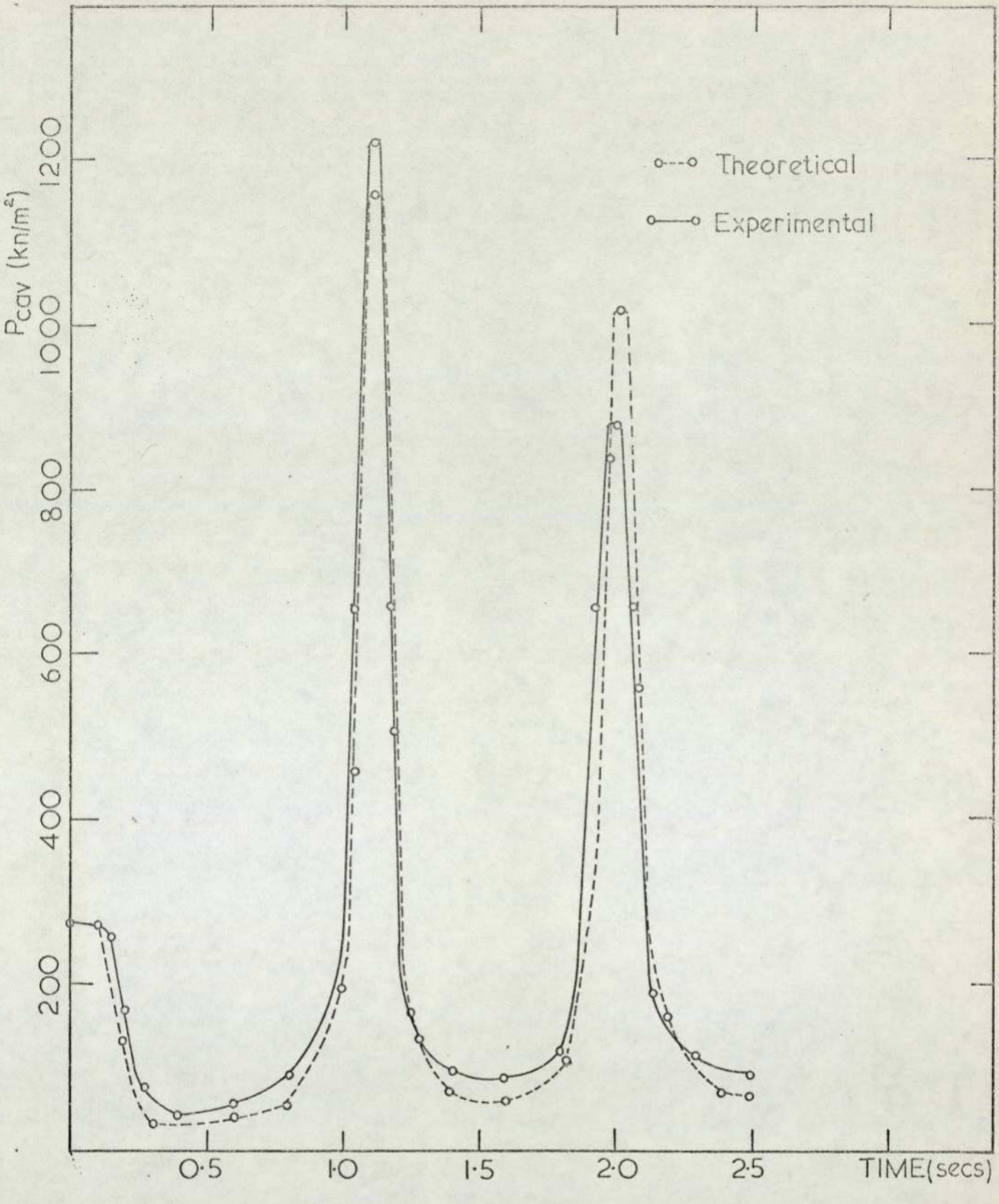


FIG 49 P_{cav} –TIME V_o=1·99 m/s P_o=306 kn/m²

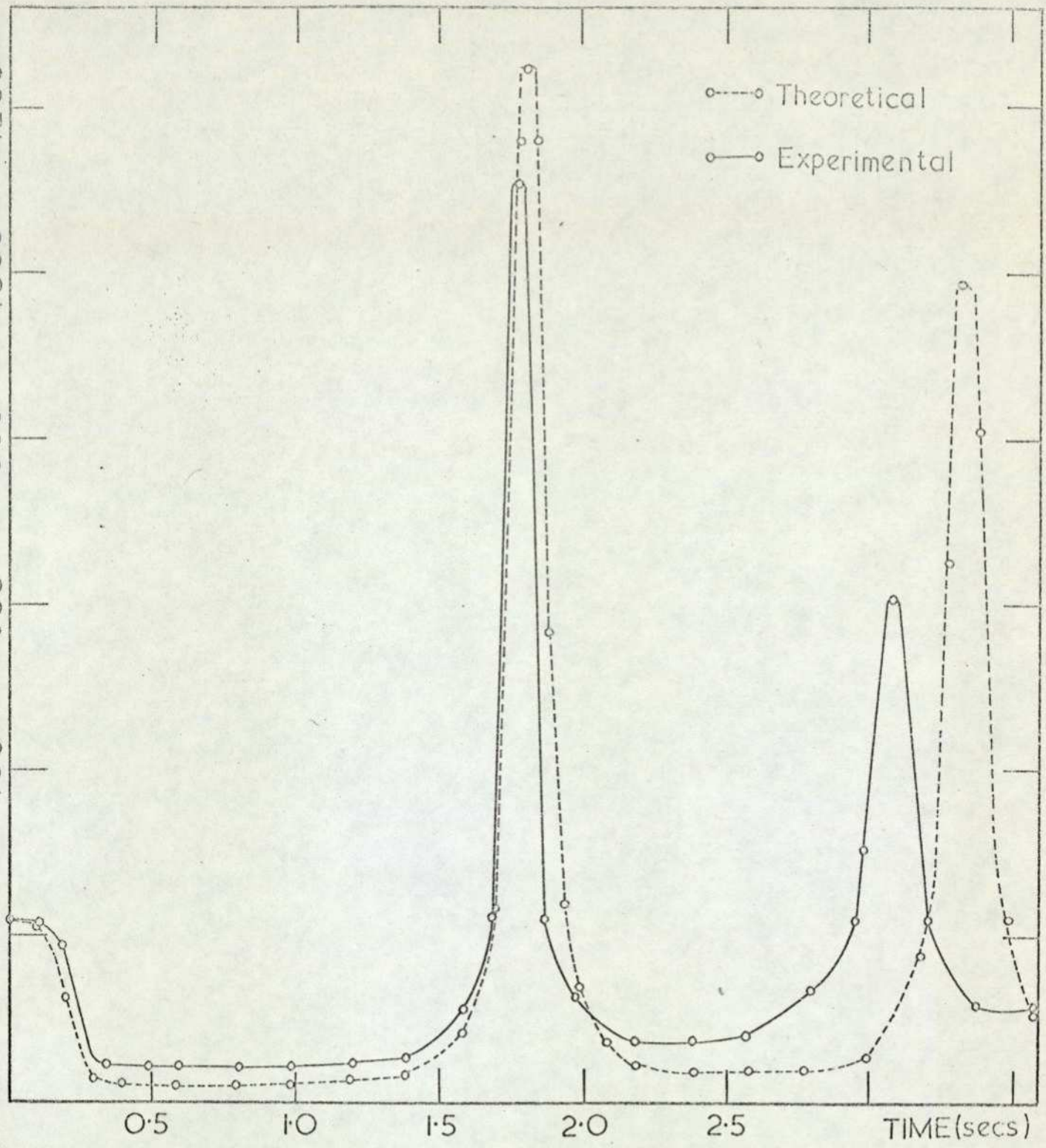


FIG 50 P_{cav} - TIME $V_o = 2{\cdot}38$ m/s $P_o = 237$ kn/m^2

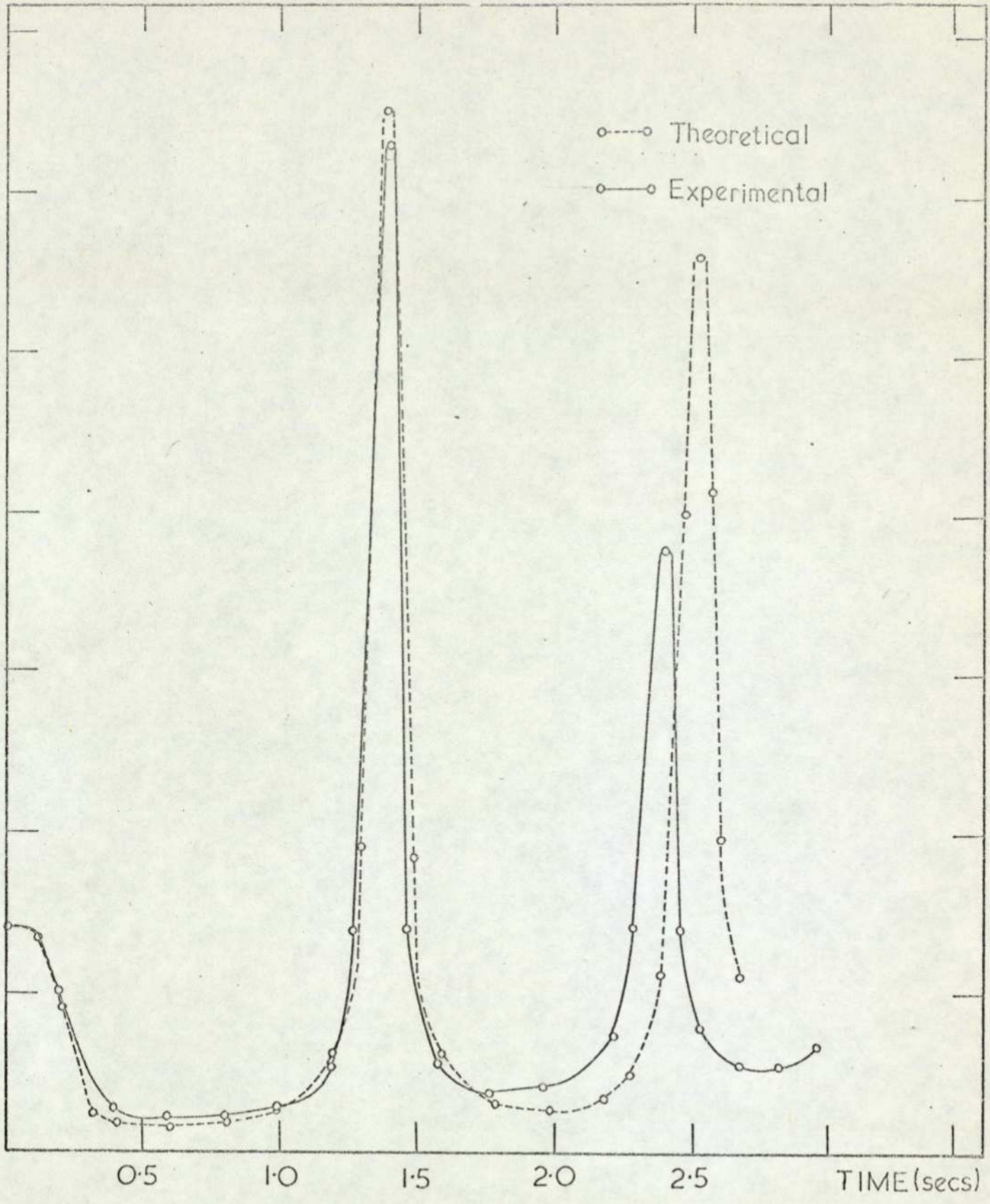


FIG 51 P_{cav} -TIME $V_0 = 2{\cdot}38$ m/s $P_0 = 306$ kn/m^2

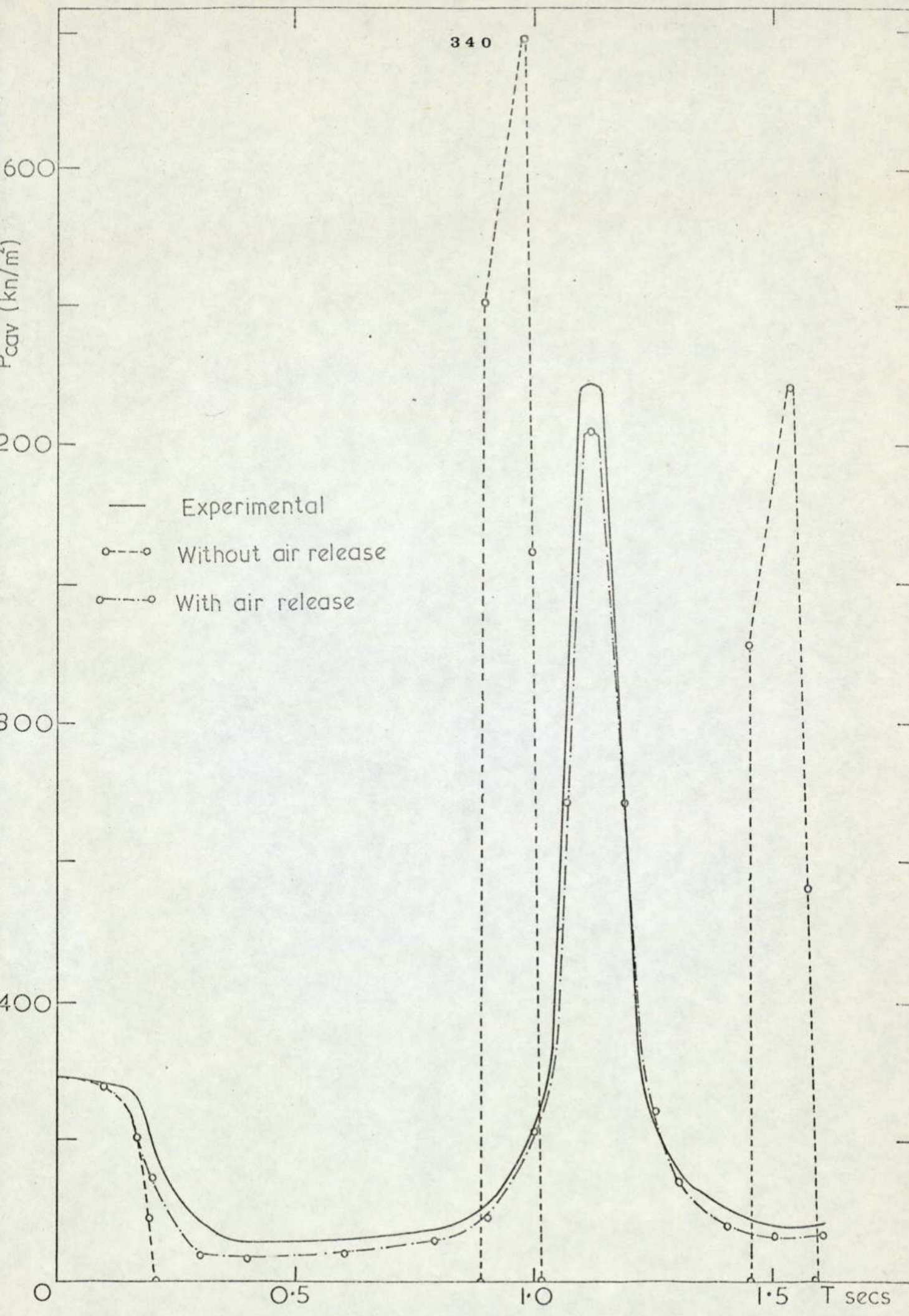


FIG 52 COMPARISON OF EXPERIMENTAL RESULTS WITH OUTPUT OF PROGRAMS PTP1 & PTP3

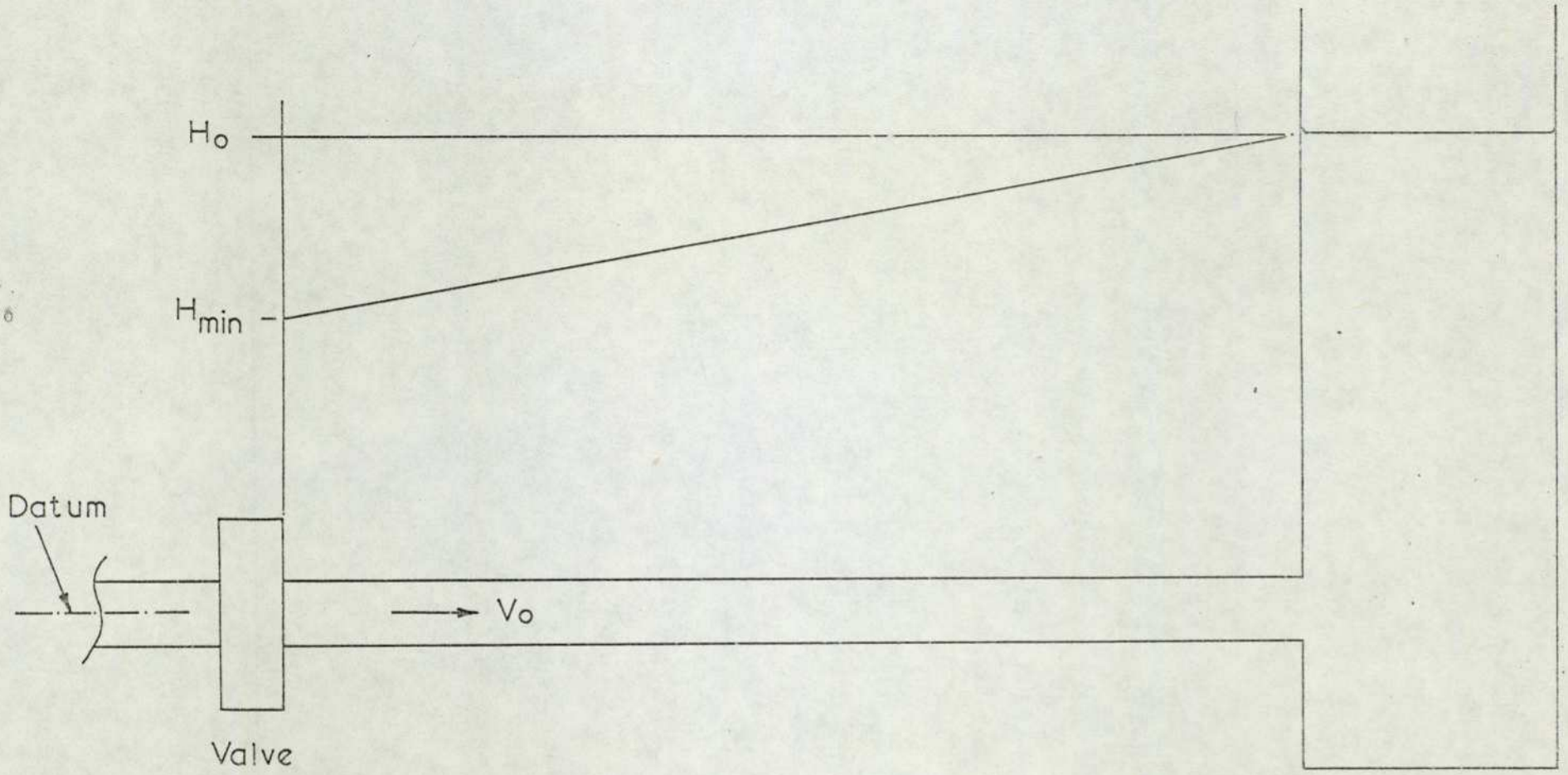


FIG 53 DEFINITION OF VALVE STROKING PARAMETERS

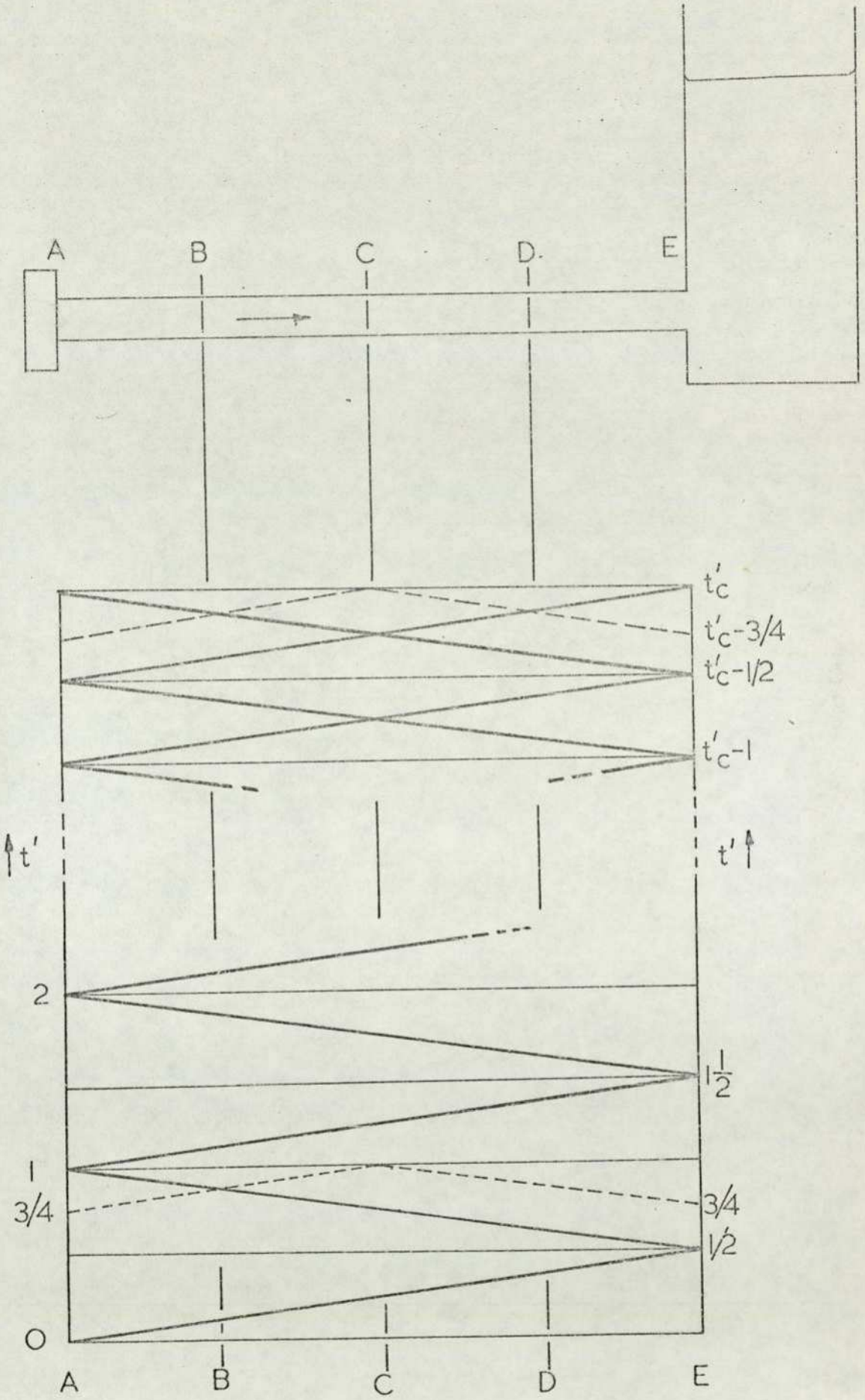


FIG 54 WAVE DIAGRAM USED IN GRAPHICAL ANALYSIS OF VALVE STROKING

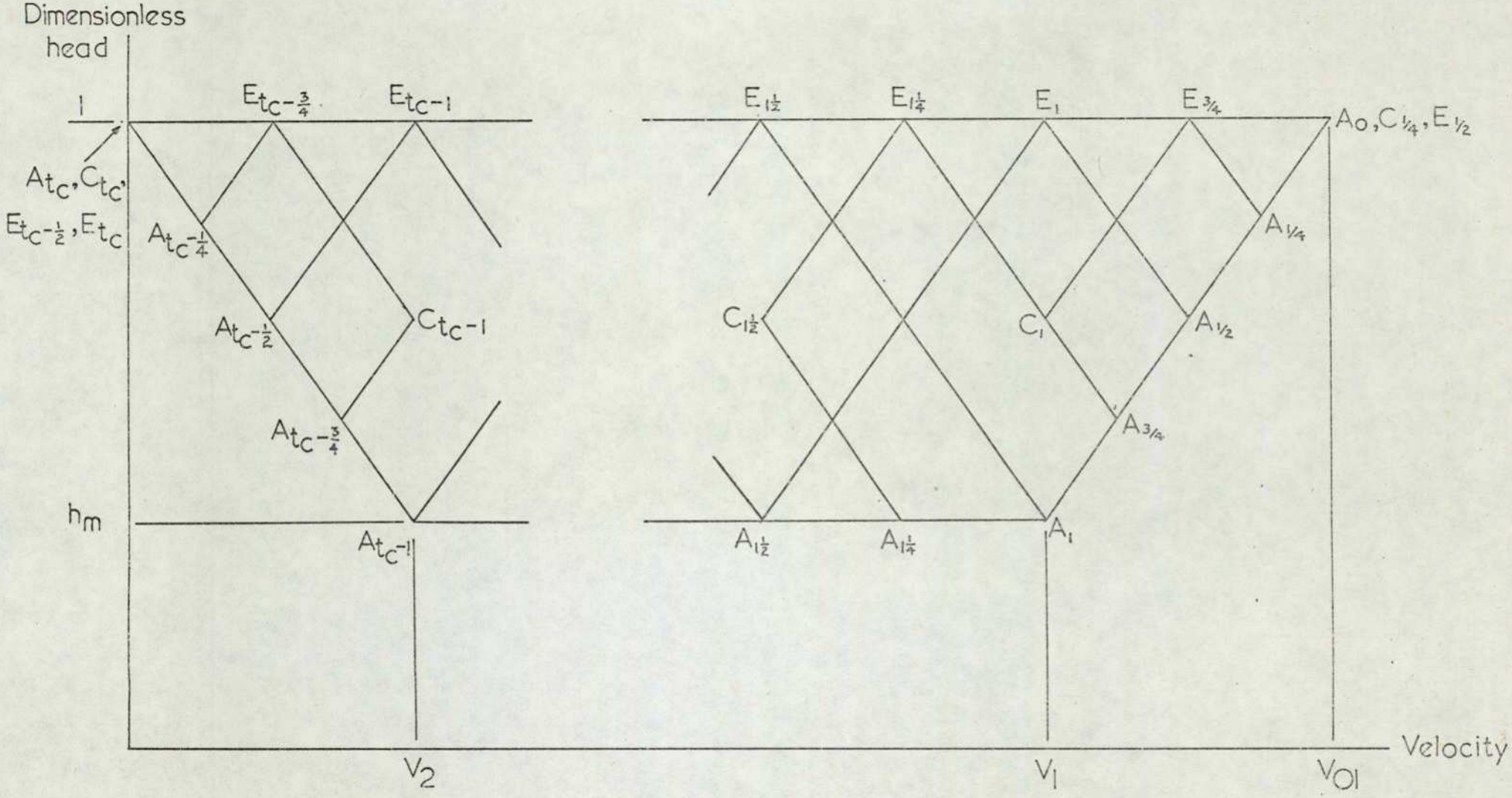


FIG 55 GRAPHICAL ANALYSIS OF FRICTIONLESS VALVE STROKING

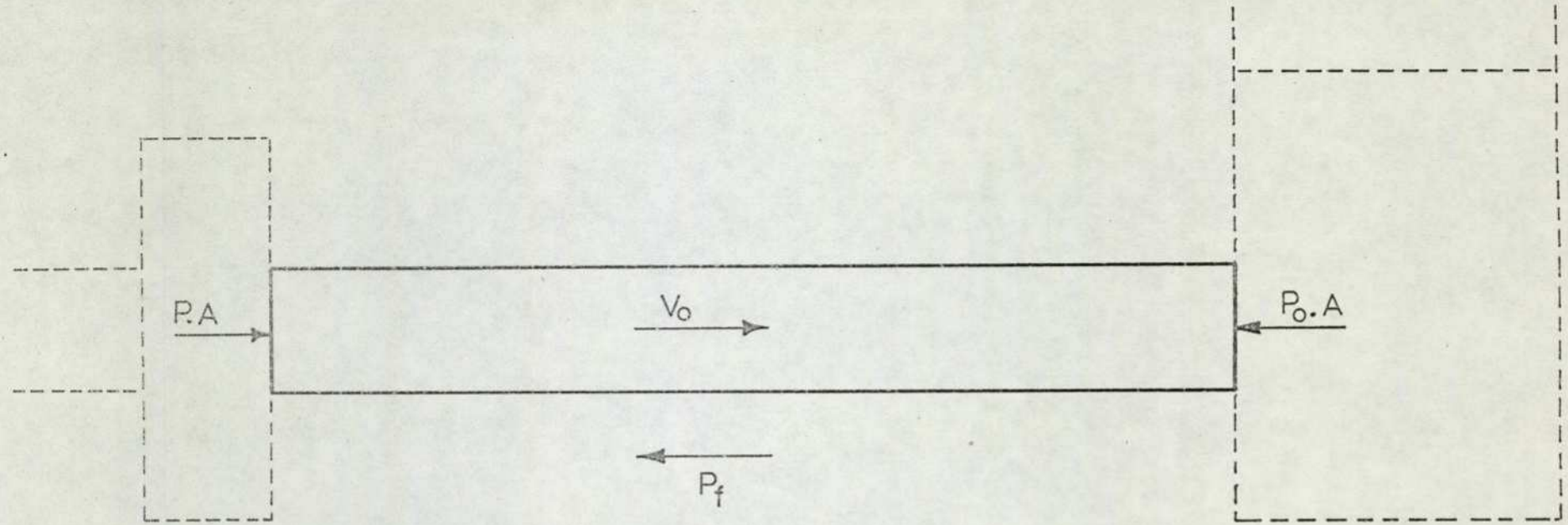


FIG 56 FREE BODY DIAGRAM OF INCOMPRESSIBLE COLUMN

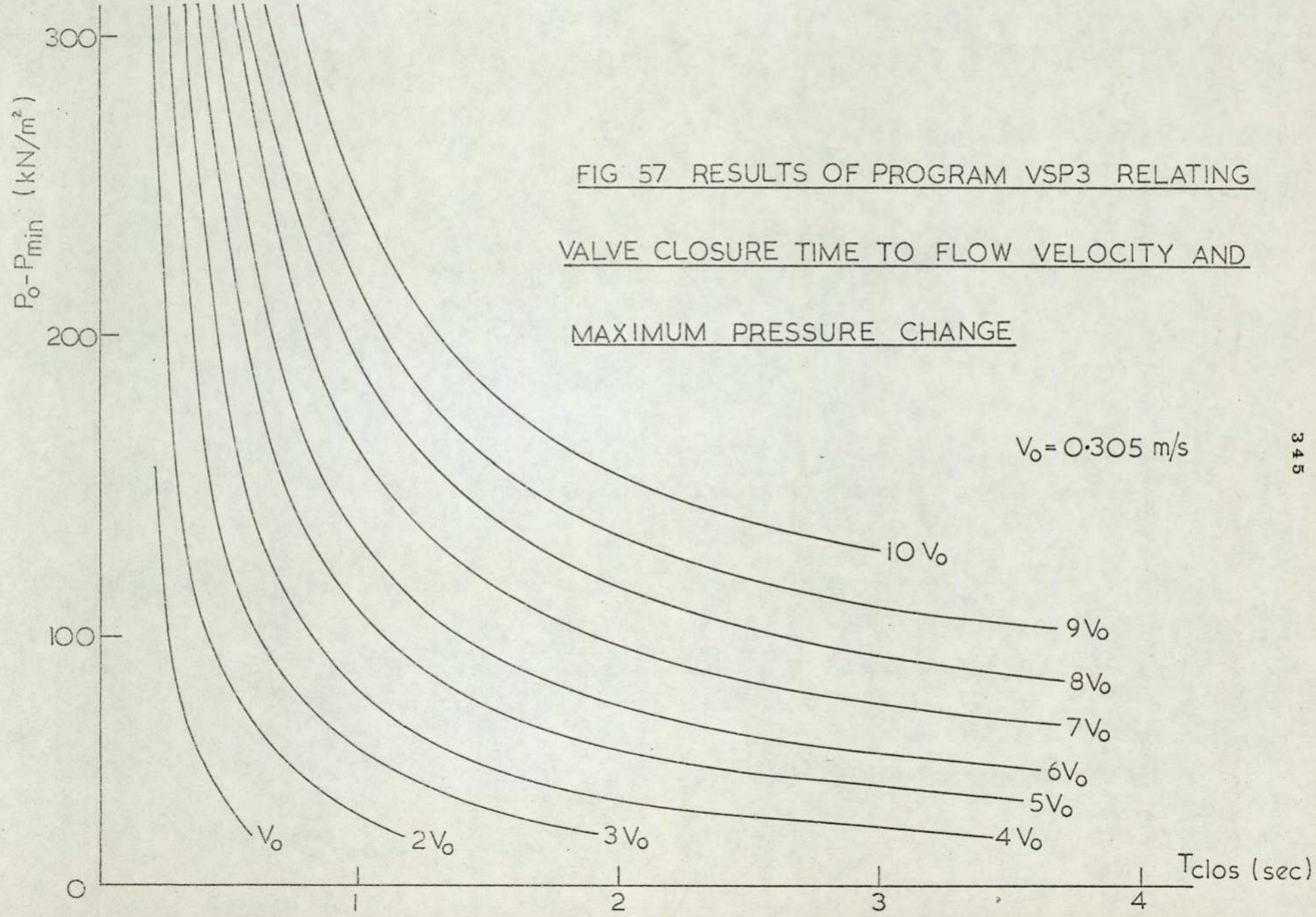


FIG 57 RESULTS OF PROGRAM VSP3 RELATING VALVE CLOSURE TIME TO FLOW VELOCITY AND MAXIMUM PRESSURE CHANGE

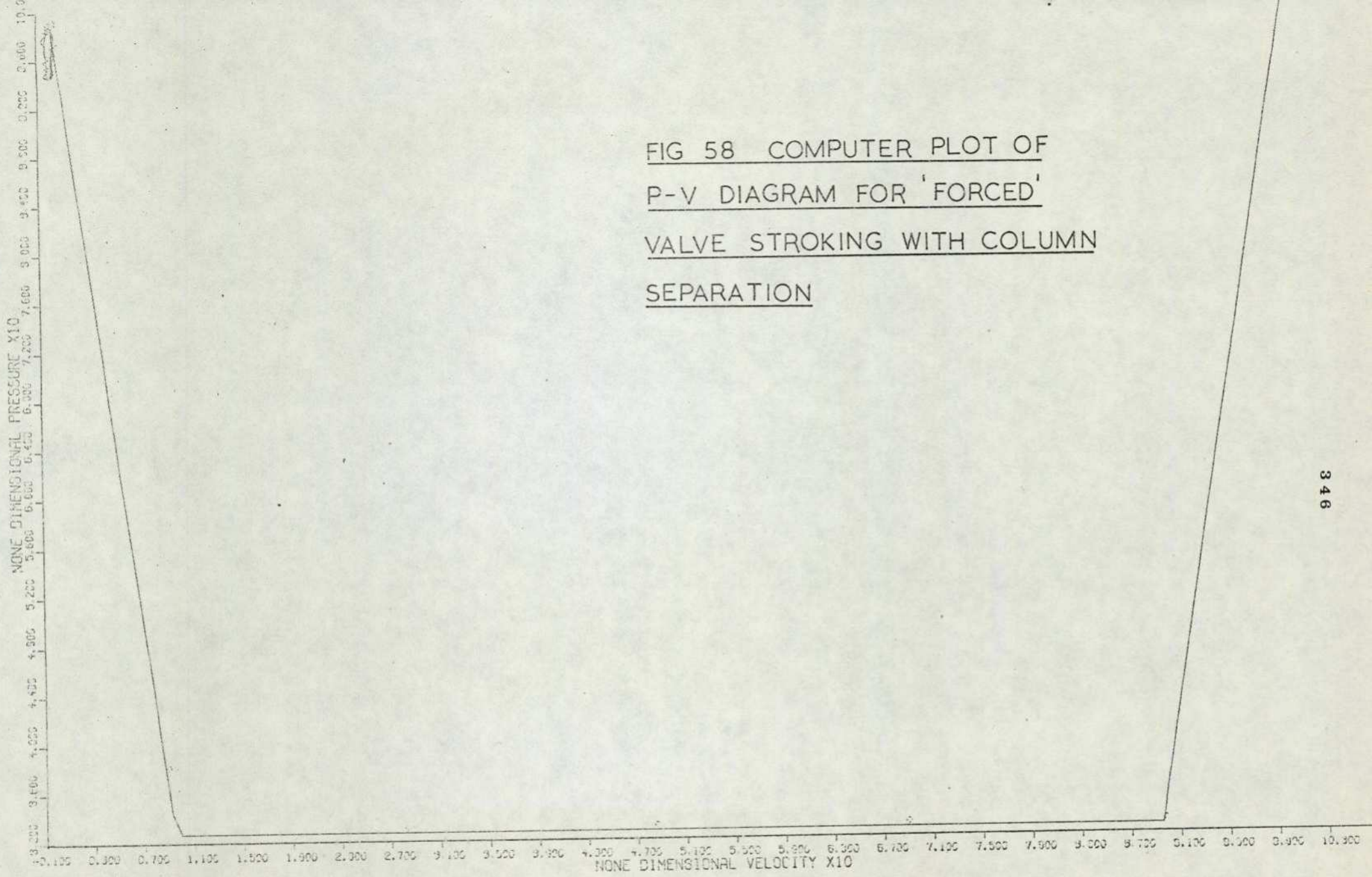
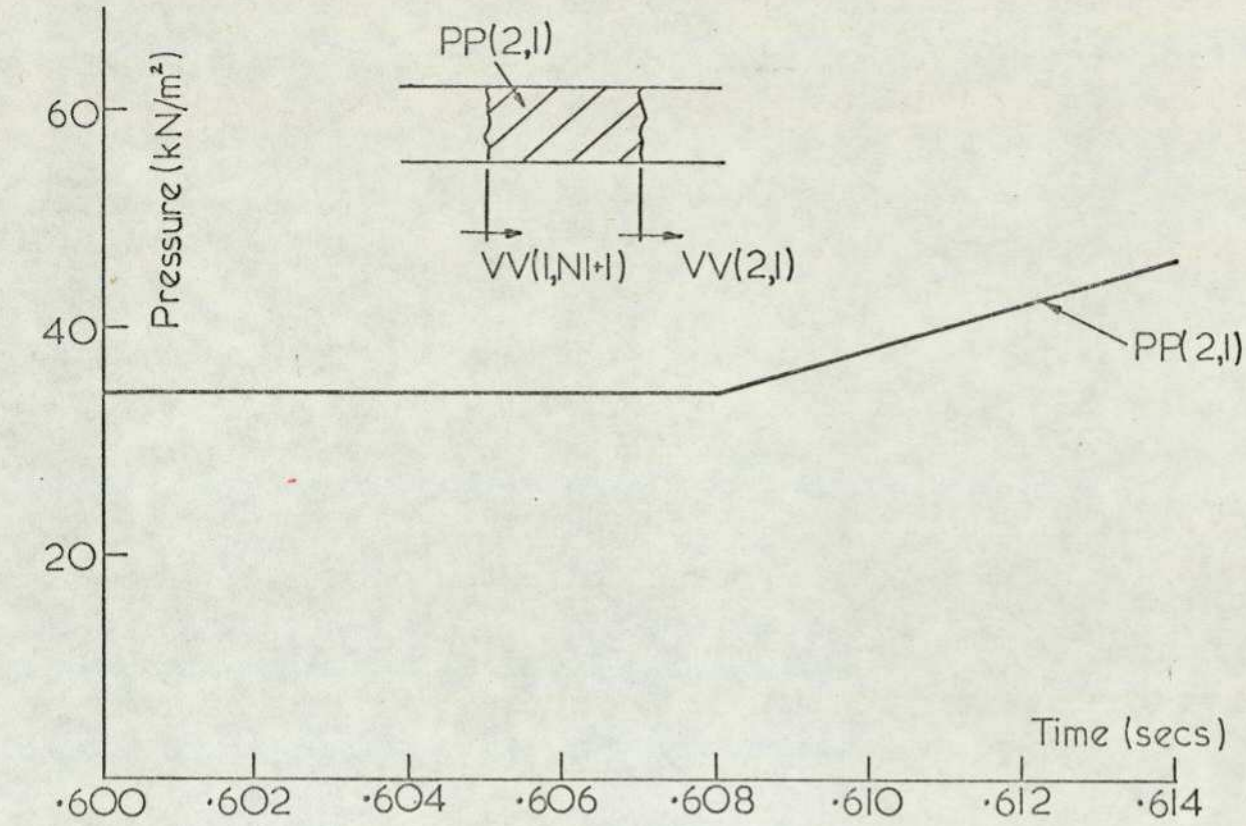


FIG 58 COMPUTER PLOT OF P-V DIAGRAM FOR 'FORCED' VALVE STROKING WITH COLUMN SEPARATION



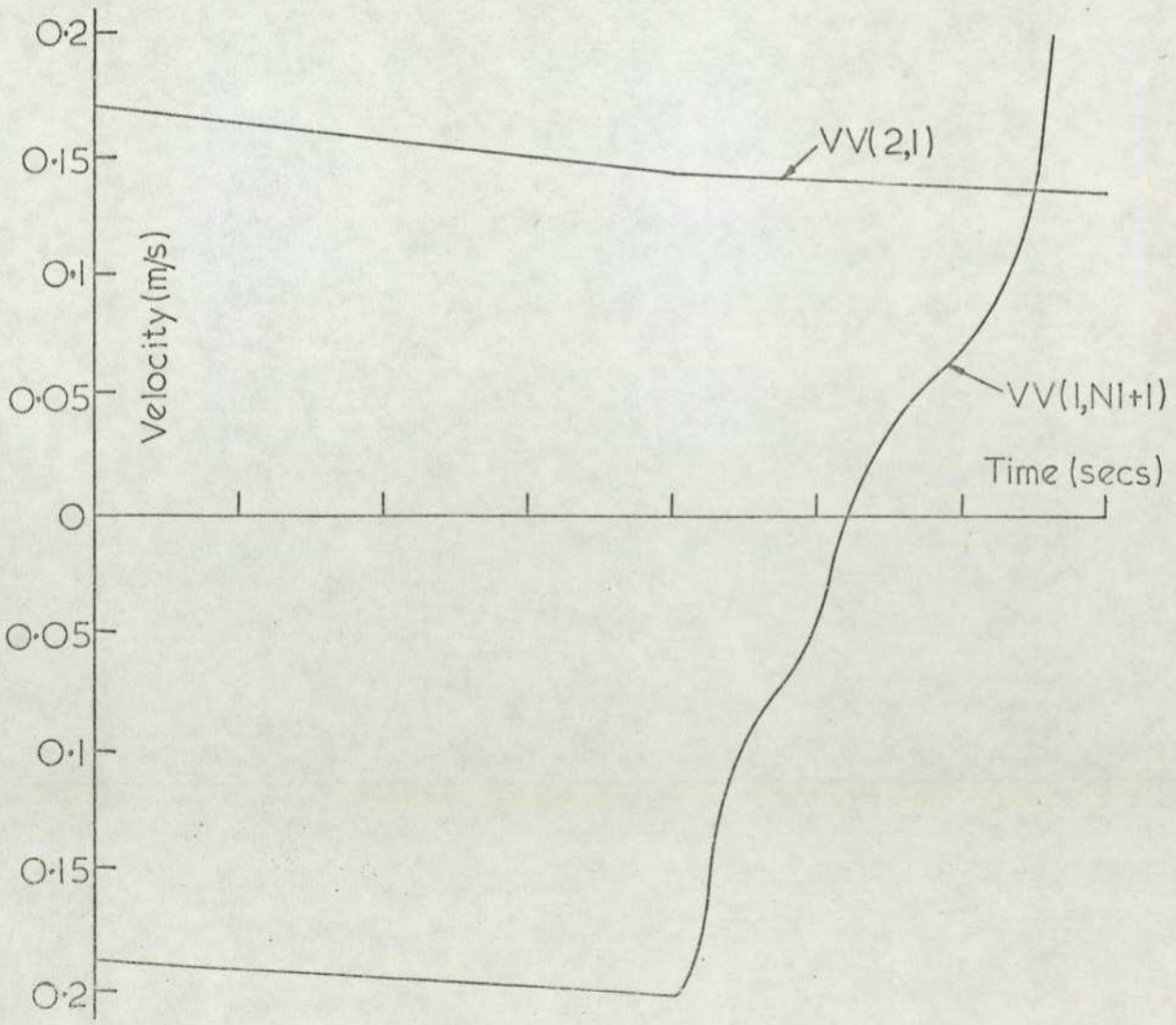


FIG 59 CAVITY INTERFACE VELOCITIES TO PRODUCE PHASE 3 OF IDEAL VALVE STROKING

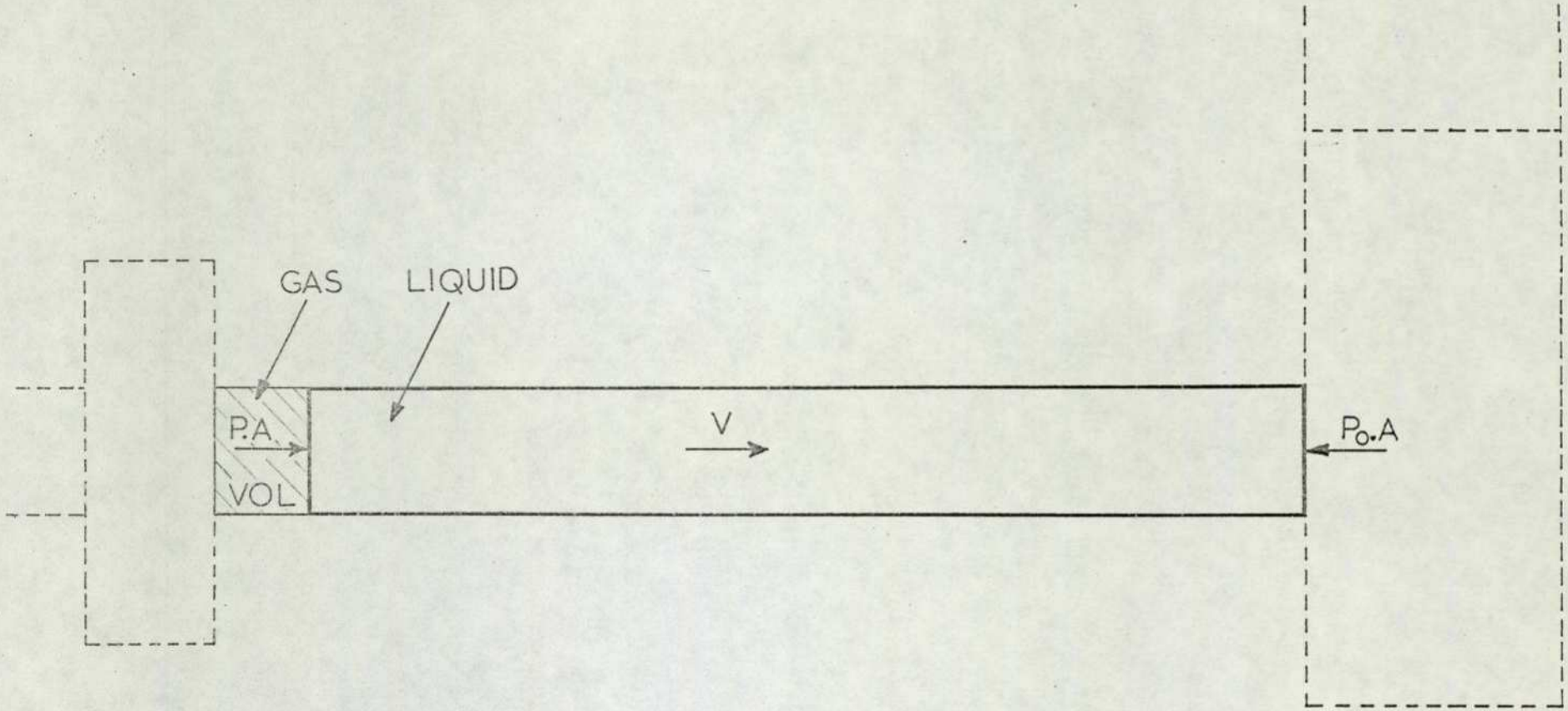


FIG 60 ASSUMED SYSTEM FOR PROPOSED VALVE STROKING METHOD No. 1

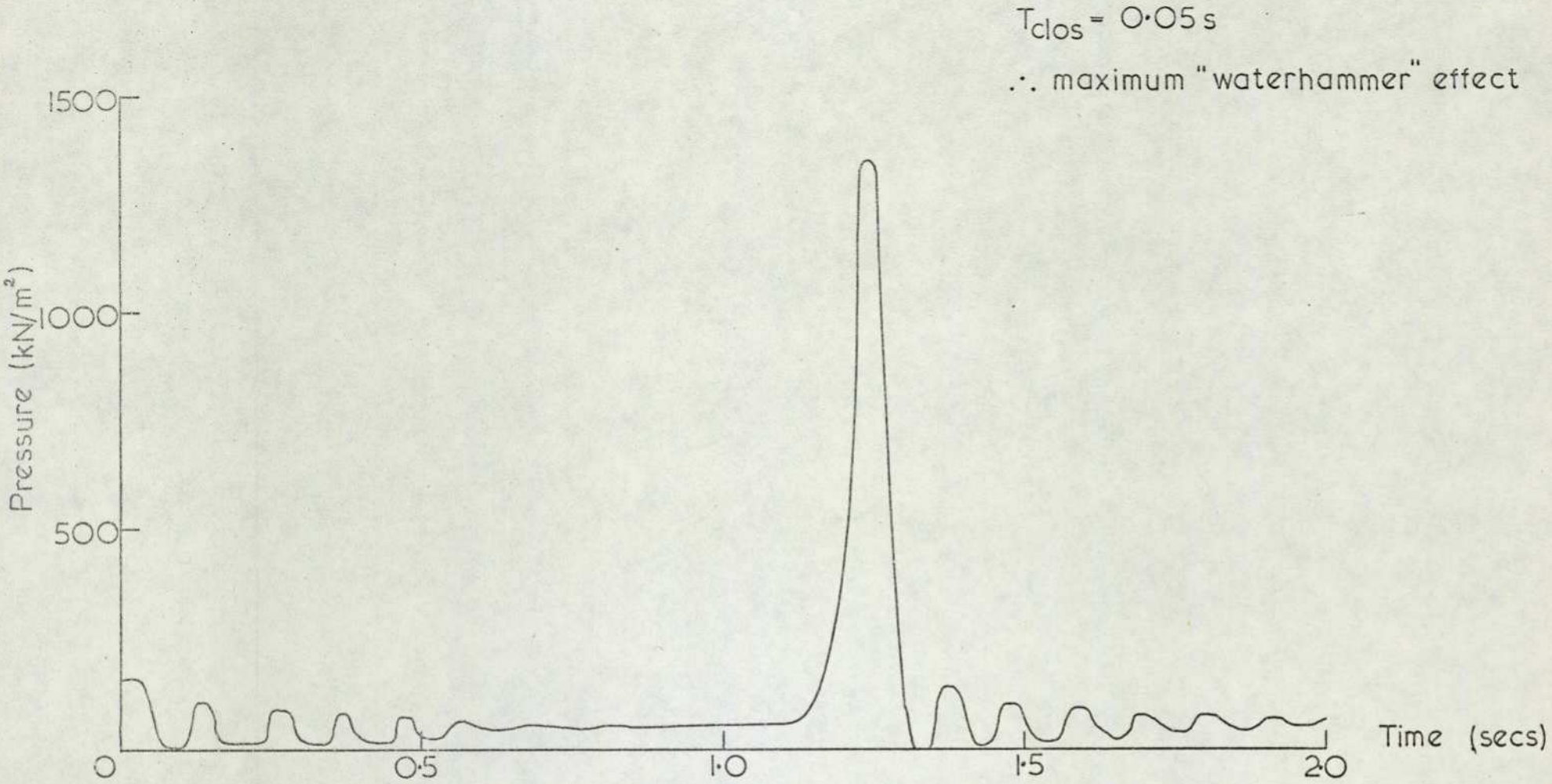


FIG 61 PRESSURE PREDICTED AT A POINT 32 m FROM THE VALVE FOLLOWING RAPID CLOSURE, SHOWING TRANSIENTS DUE TO BOTH "WATERHAMMER" AND MASS OSCILLATION EFFECTS

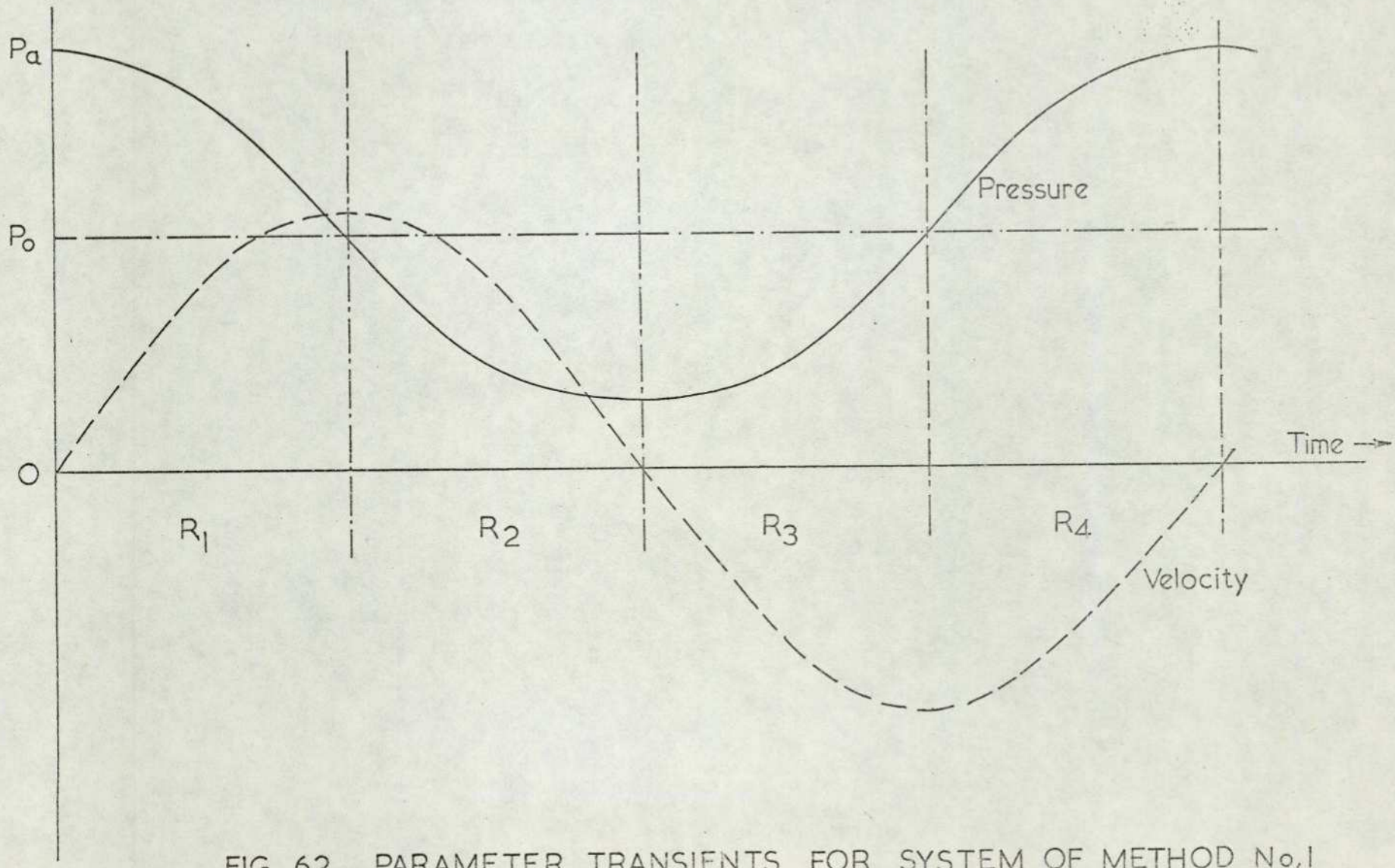


FIG 62 PARAMETER TRANSIENTS FOR SYSTEM OF METHOD No.1

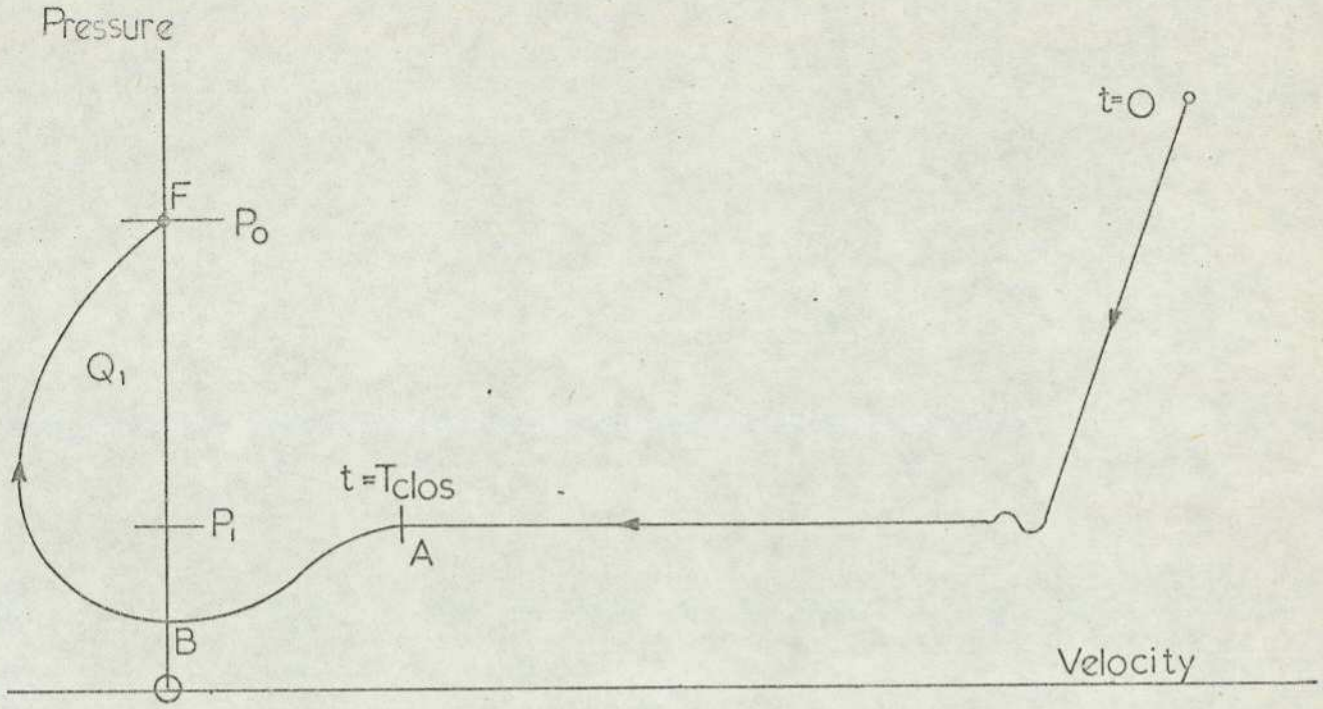


FIG 63 DESIRED TRAJECTORY FOR METHOD I

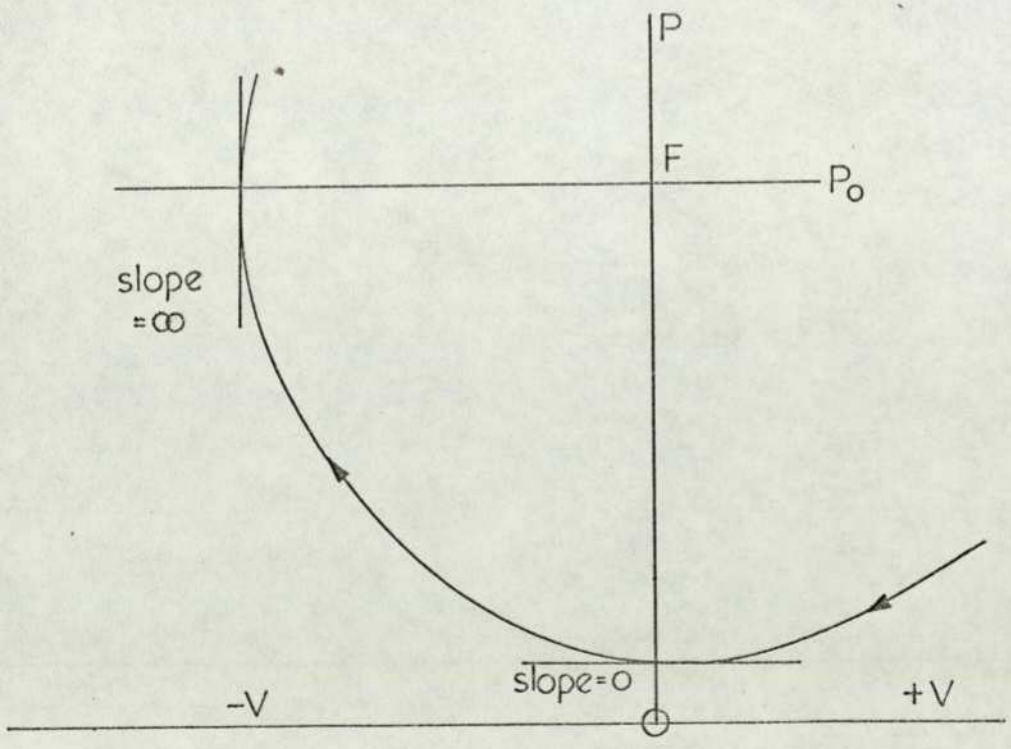


FIG 64 LIMITATIONS ON P-V LOCUS

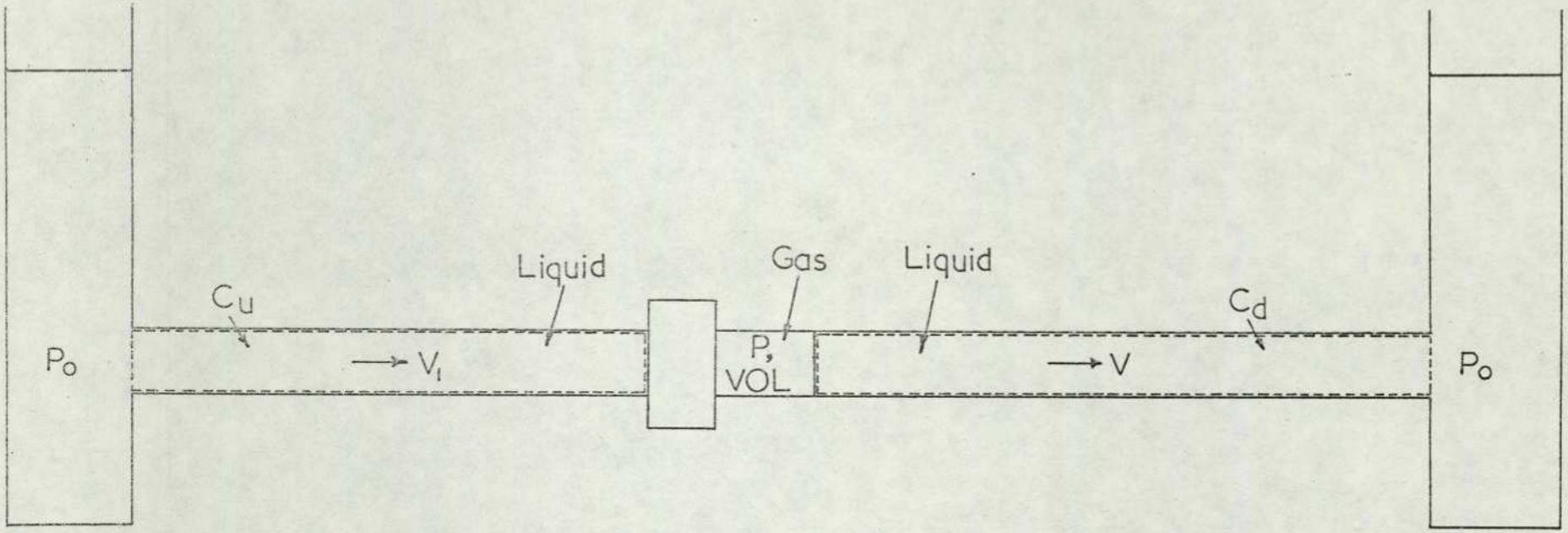


FIG 65 ASSUMED SYSTEM FOR PROPOSED VALVE STROKING METHOD No. 2

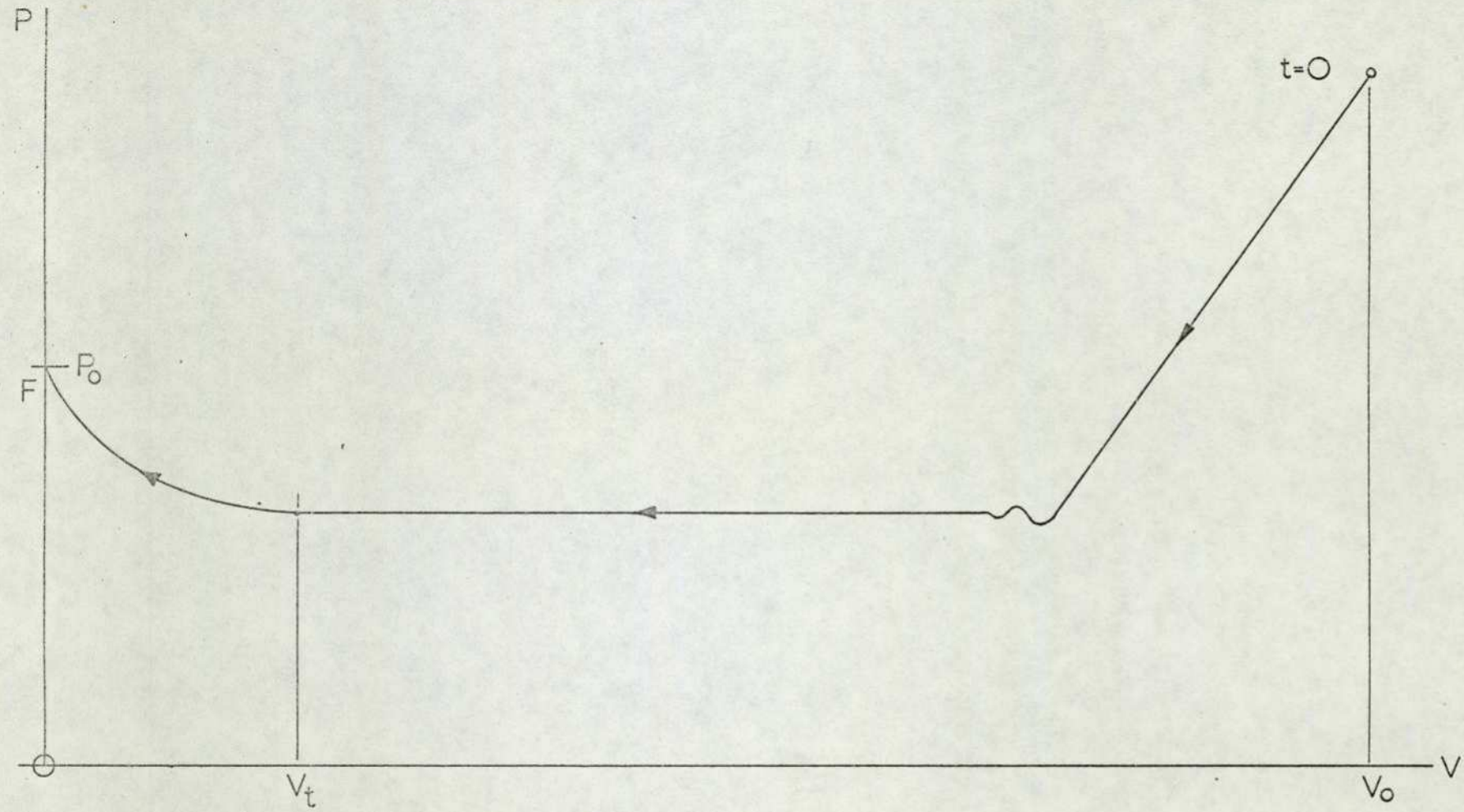


FIG 66 DESIRED P-V TRAJECTORY FOR METHOD No. 2

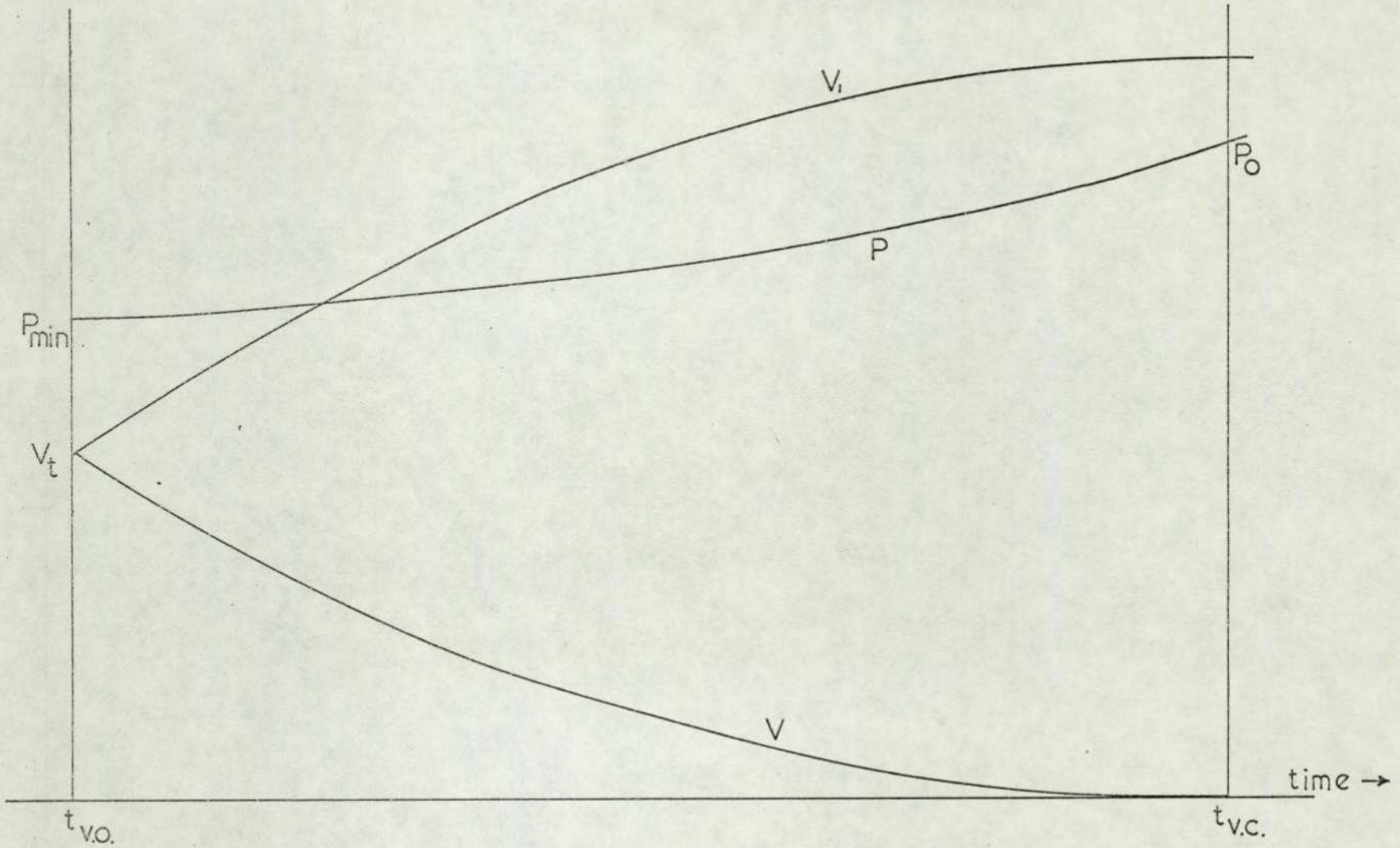


FIG 67 PRESSURE & VELOCITY VARIATION WITH TIME FOR METHOD 2

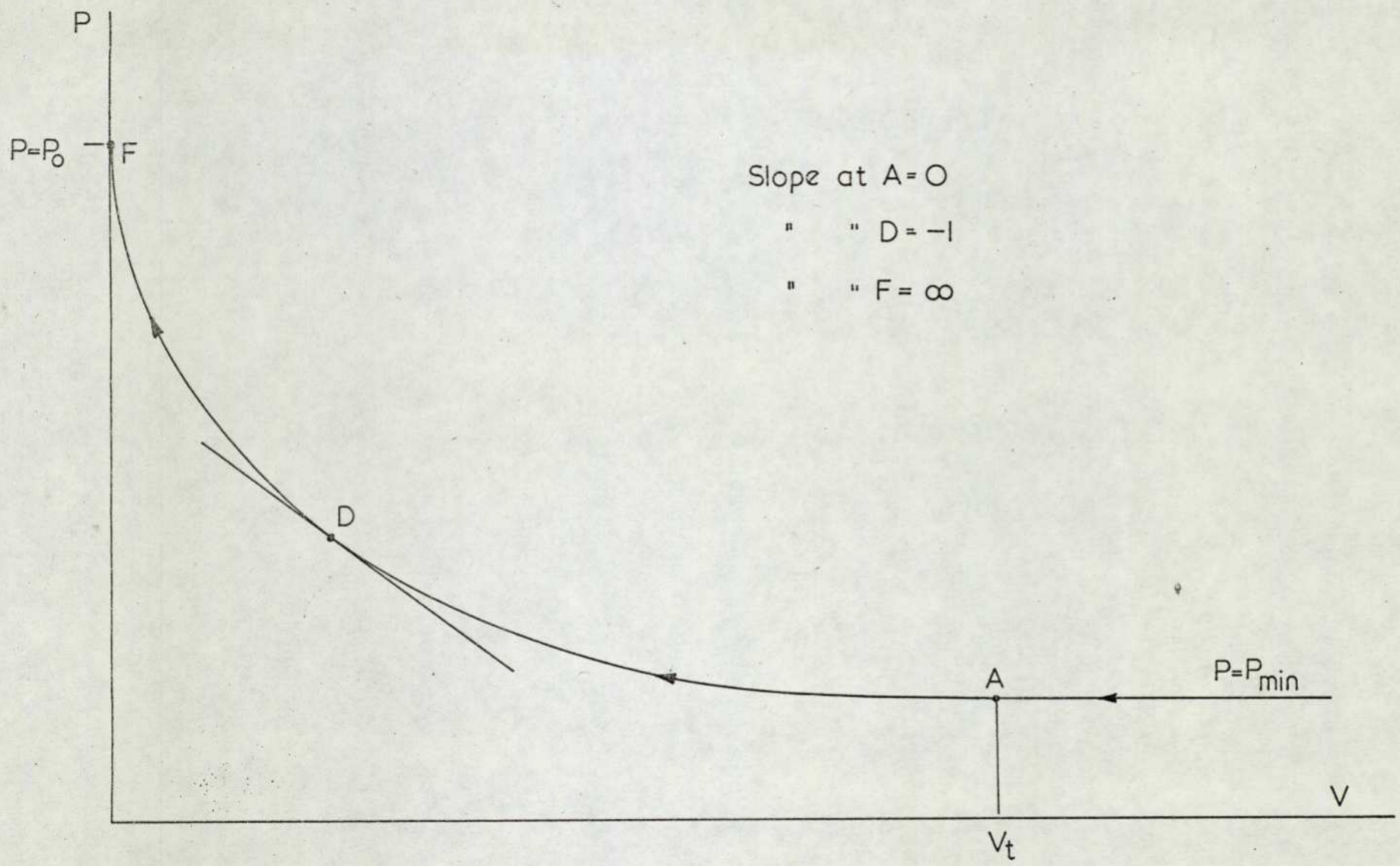


FIG 68 INTEGRATION PATH FOR EQUATION 64

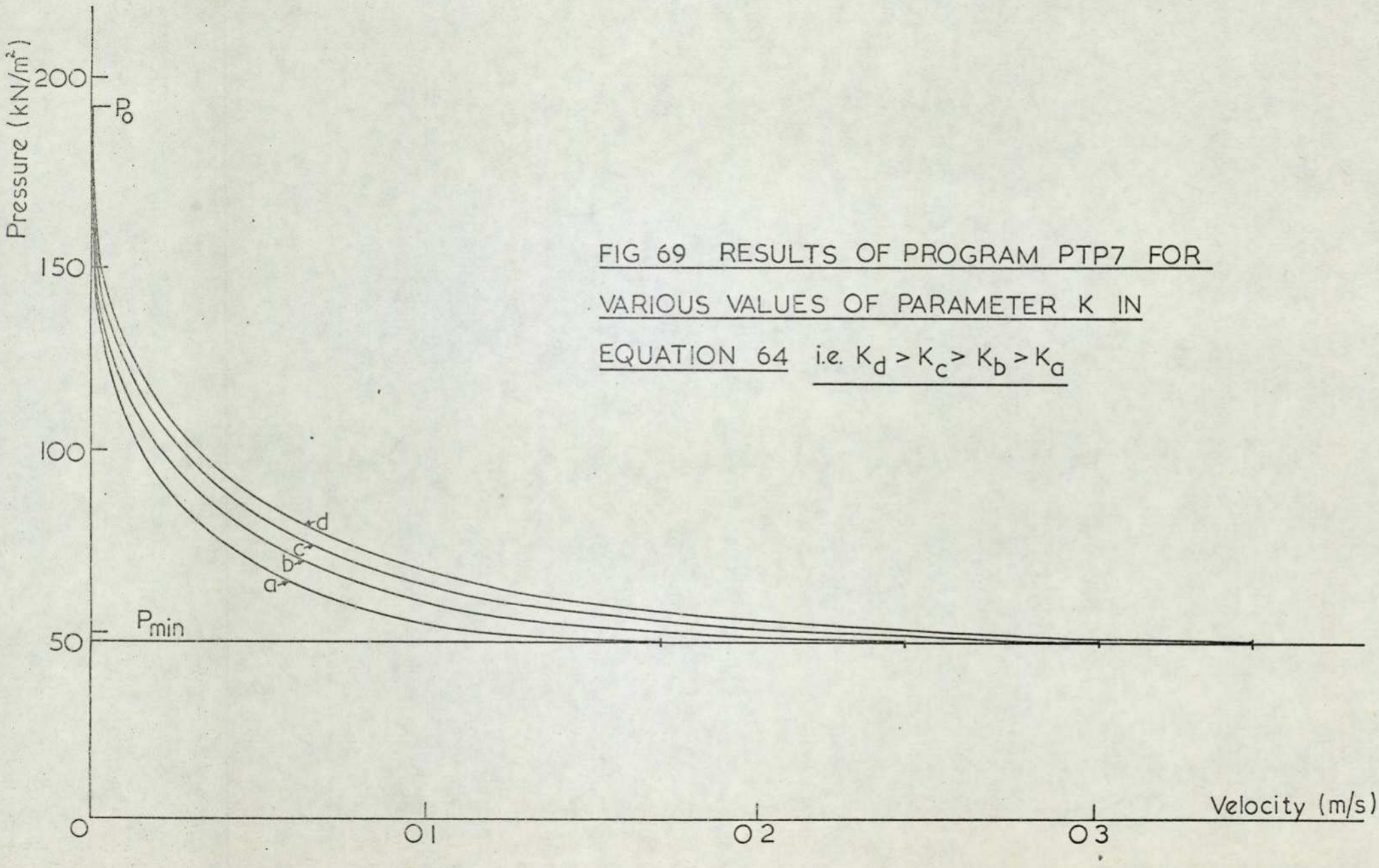
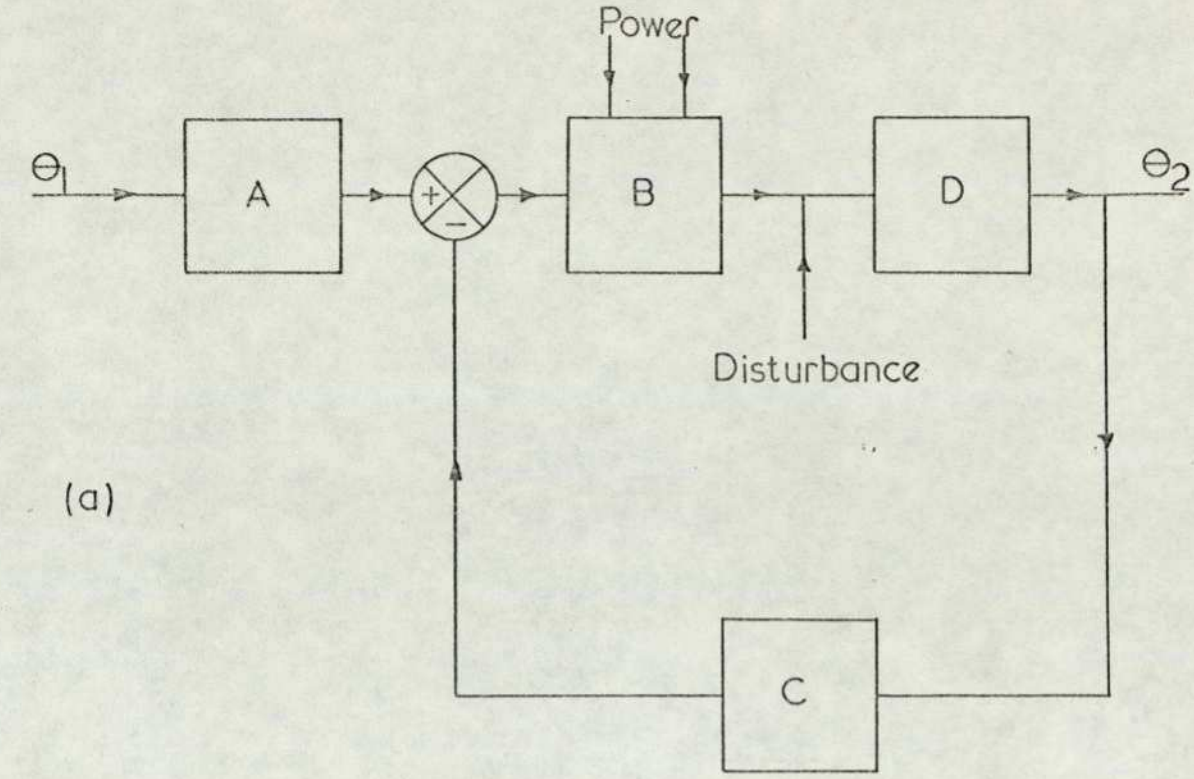
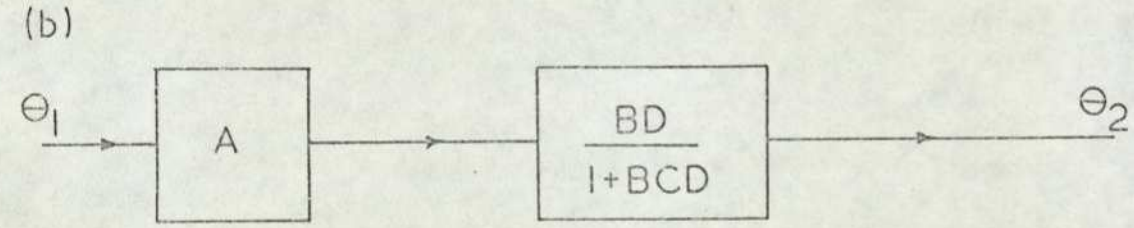


FIG 69 RESULTS OF PROGRAM PTP7 FOR VARIOUS VALUES OF PARAMETER K IN EQUATION 64 i.e. $K_d > K_c > K_b > K_a$





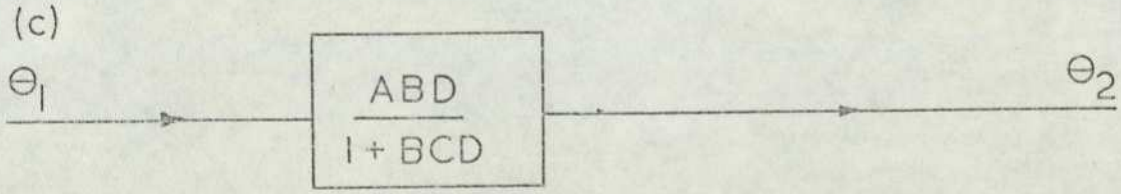


FIG 70 REDUCTION OF BASIC FEEDBACK SERVO

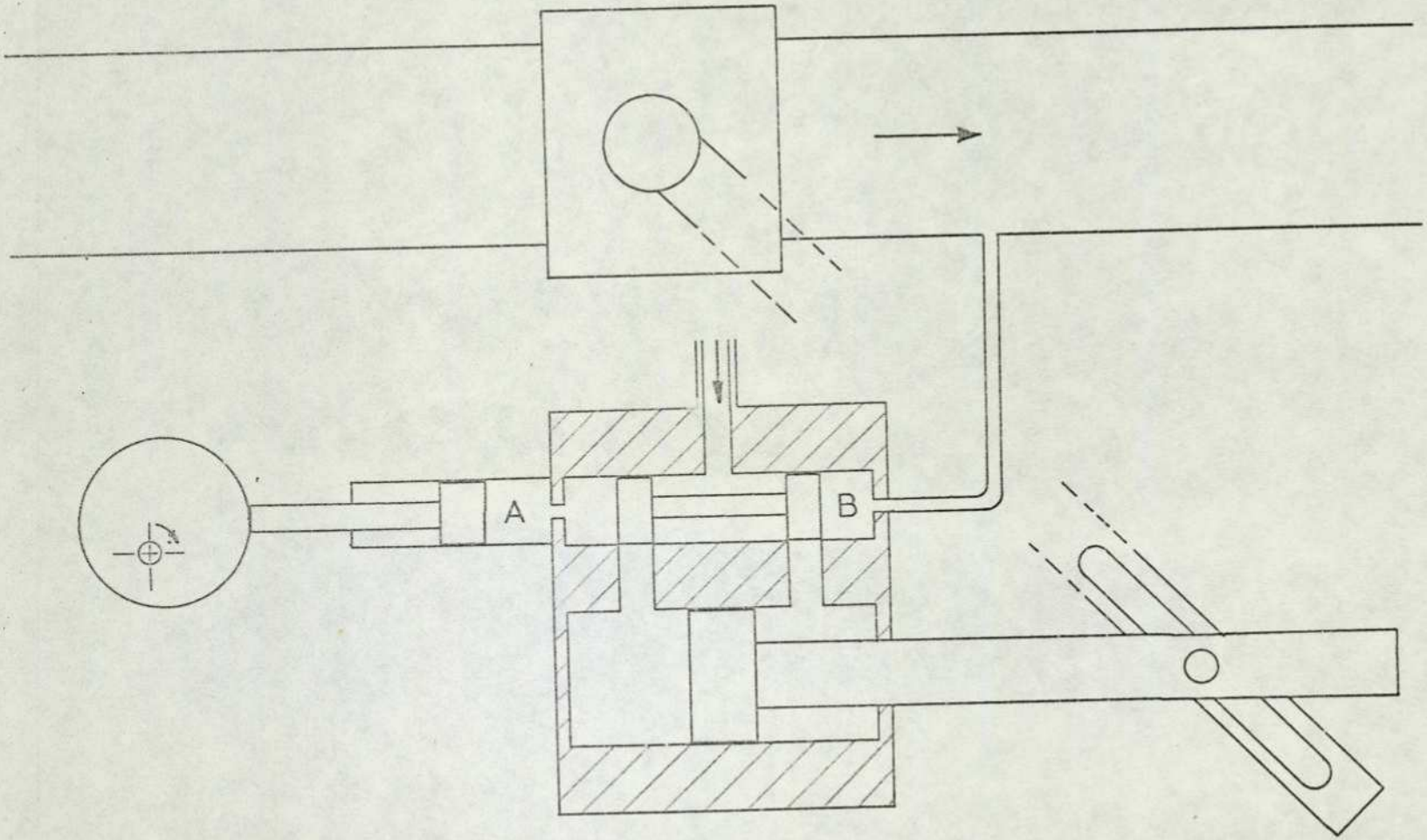


FIG 71 SIMPLE CLOSED LOOP PRESSURE CONTROL SYSTEM

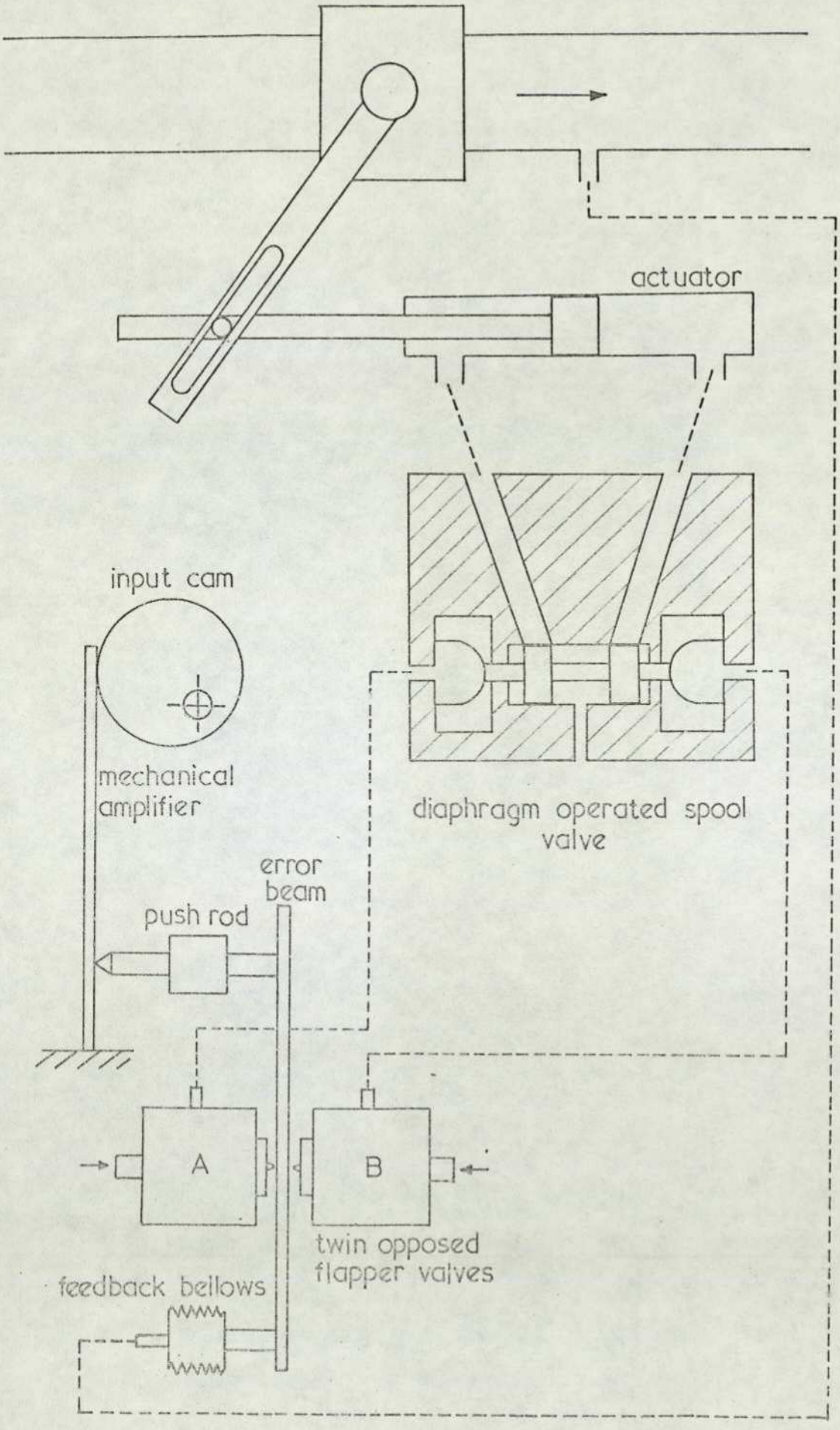


FIG 72 PNEUMATIC/MECHANICAL FEEDBACK CONTROL SYSTEM

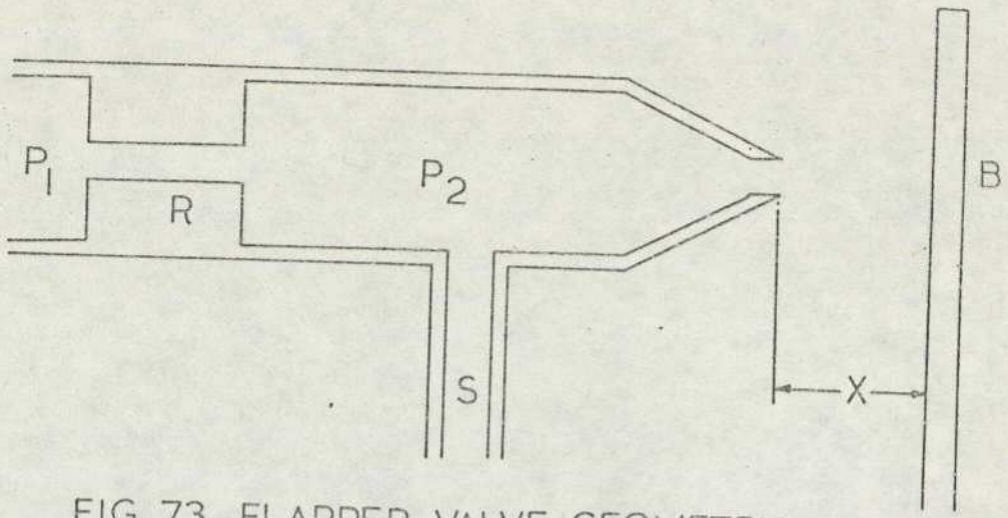


FIG 73 FLAPPER VALVE GEOMETRY

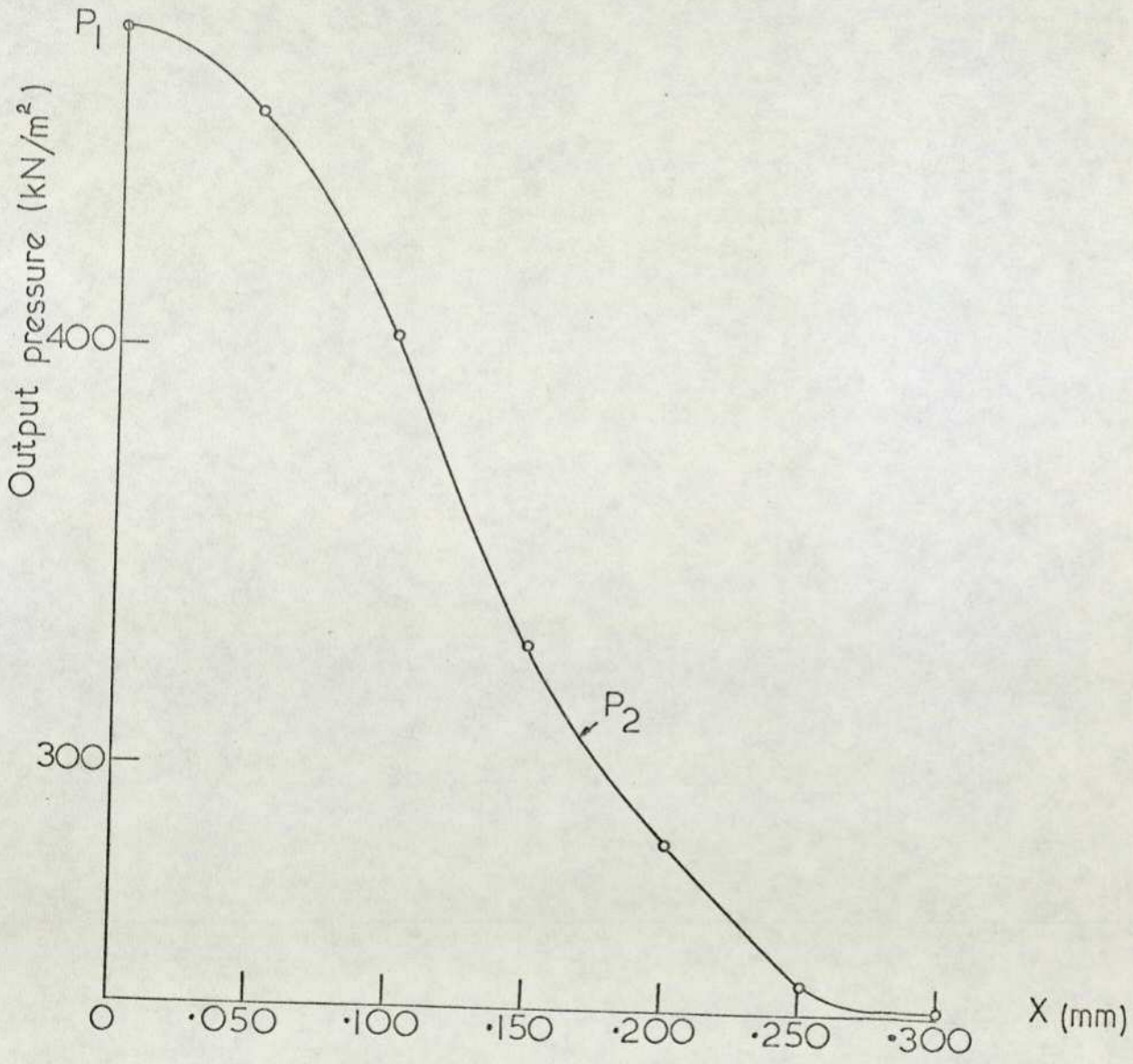


FIG 74 STATIC PERFORMANCE OF FLAPPER VALVE

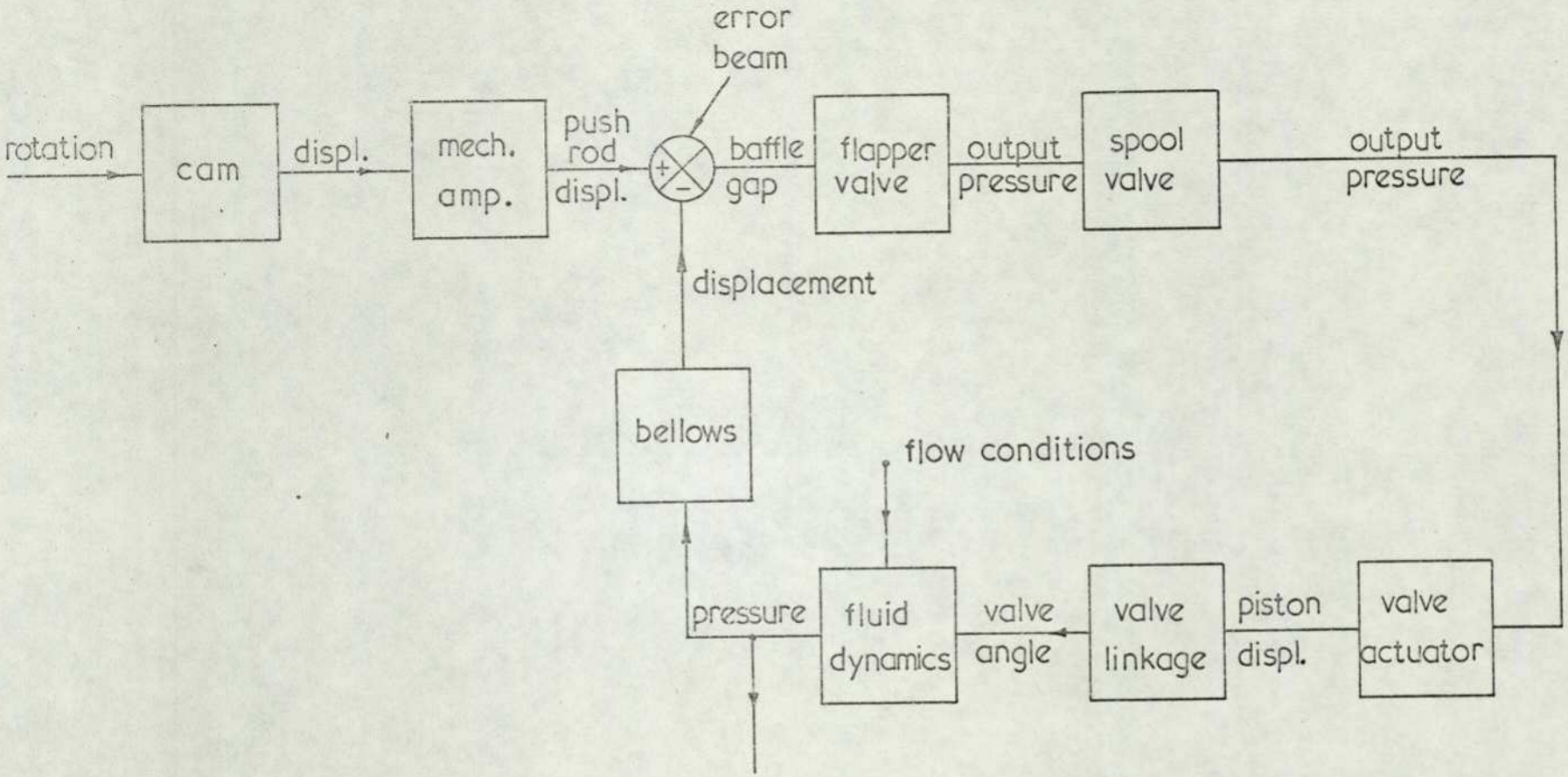


FIG 75 BLOCK DIAGRAM OF PNEUMATIC/MECHANICAL SERVO SYSTEM

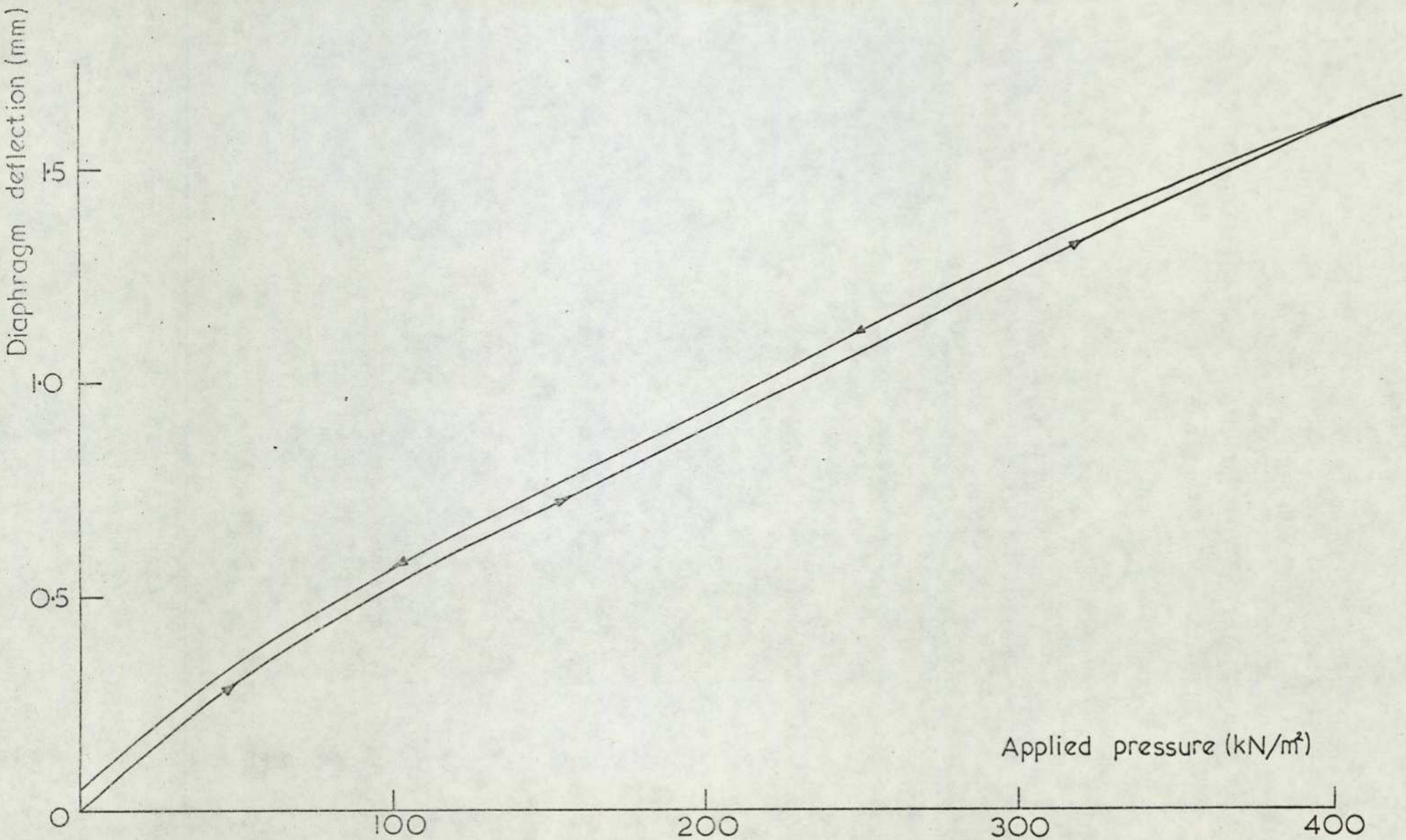


FIG 76 EXPERIMENTAL CHARACTERISTICS OF MUNRO METAL BELLOWS

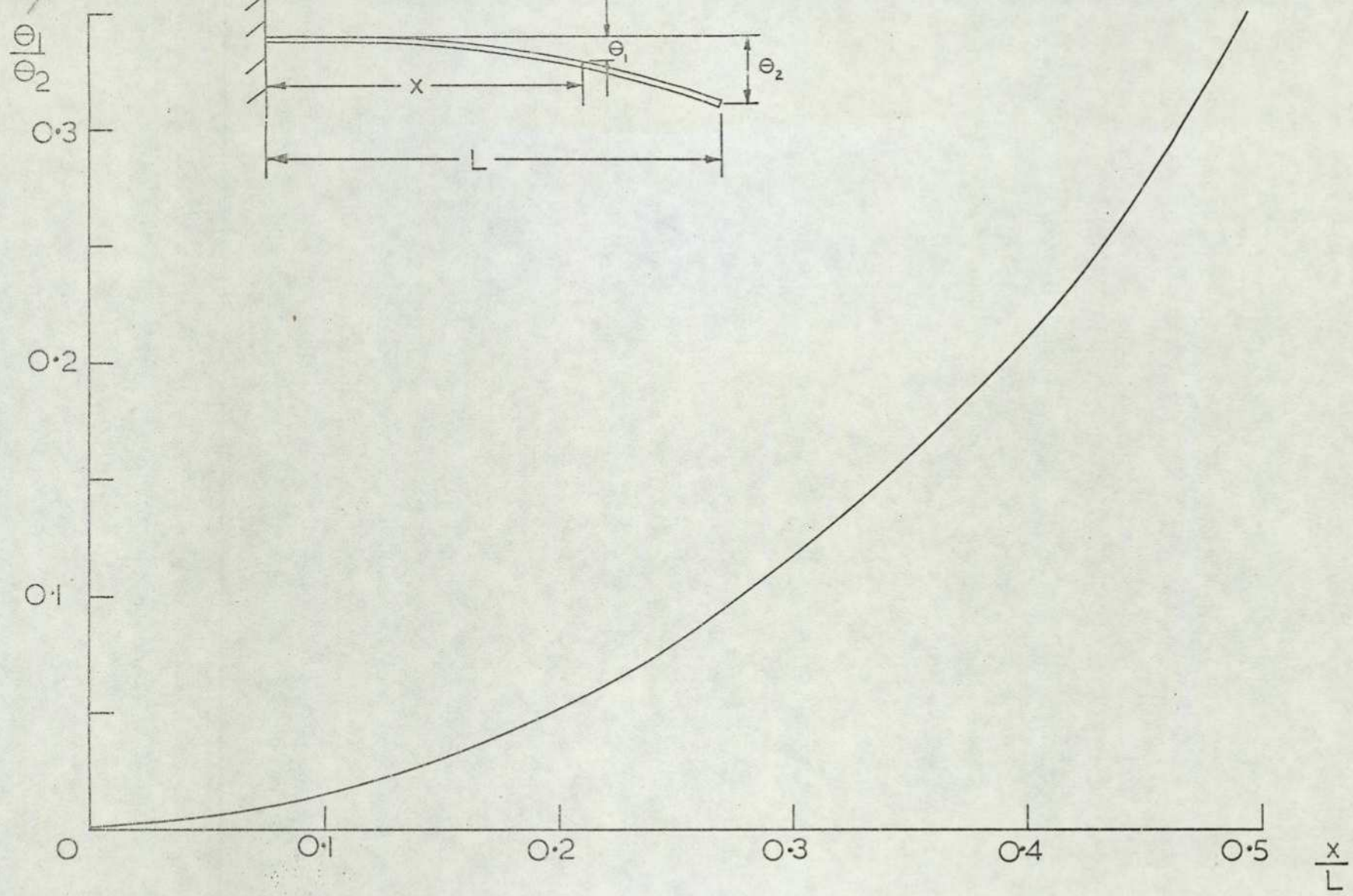


FIG 77 AMPLIFICATION CHARACTERISTICS FOR A BUILT IN BEAM

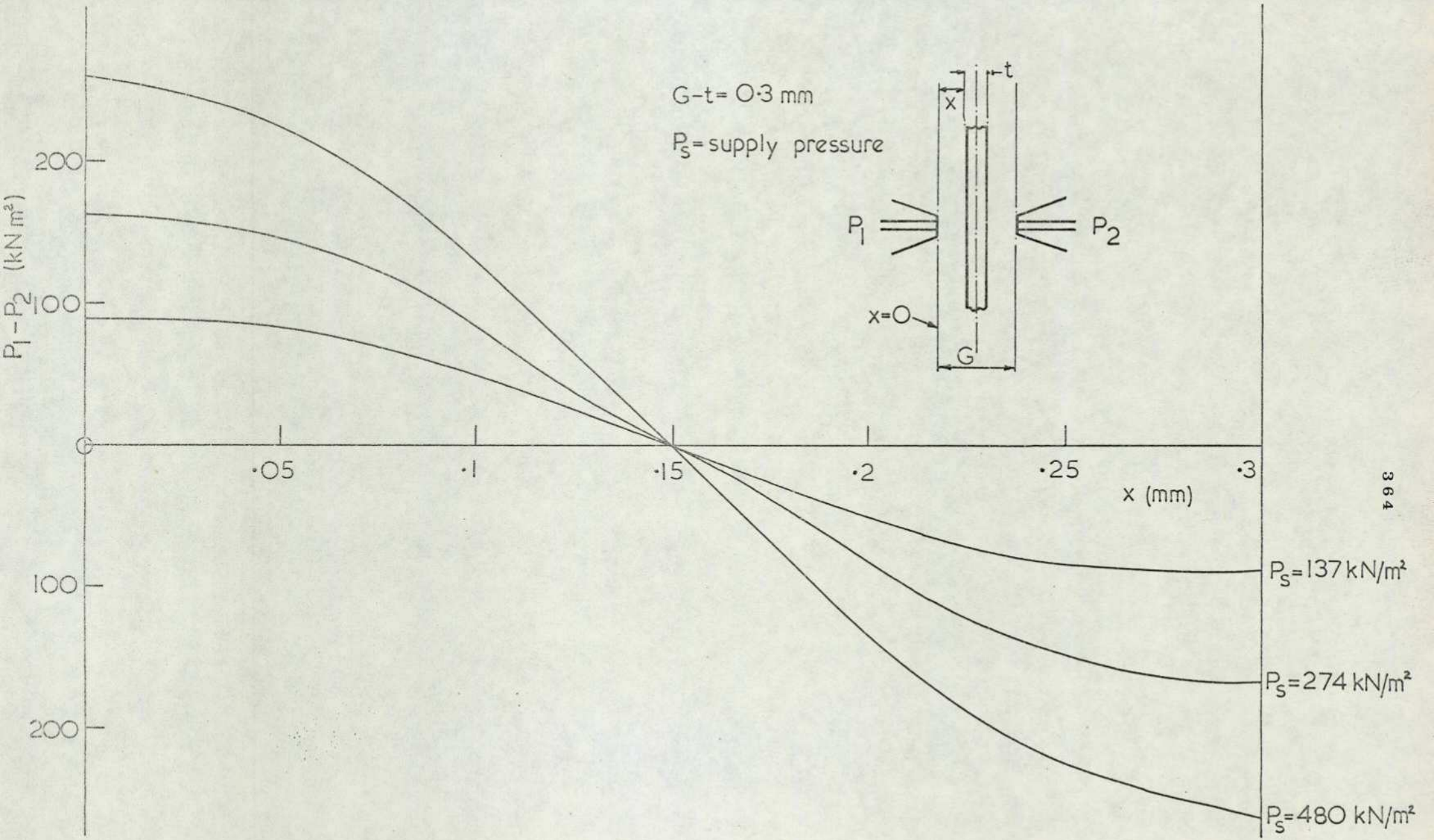
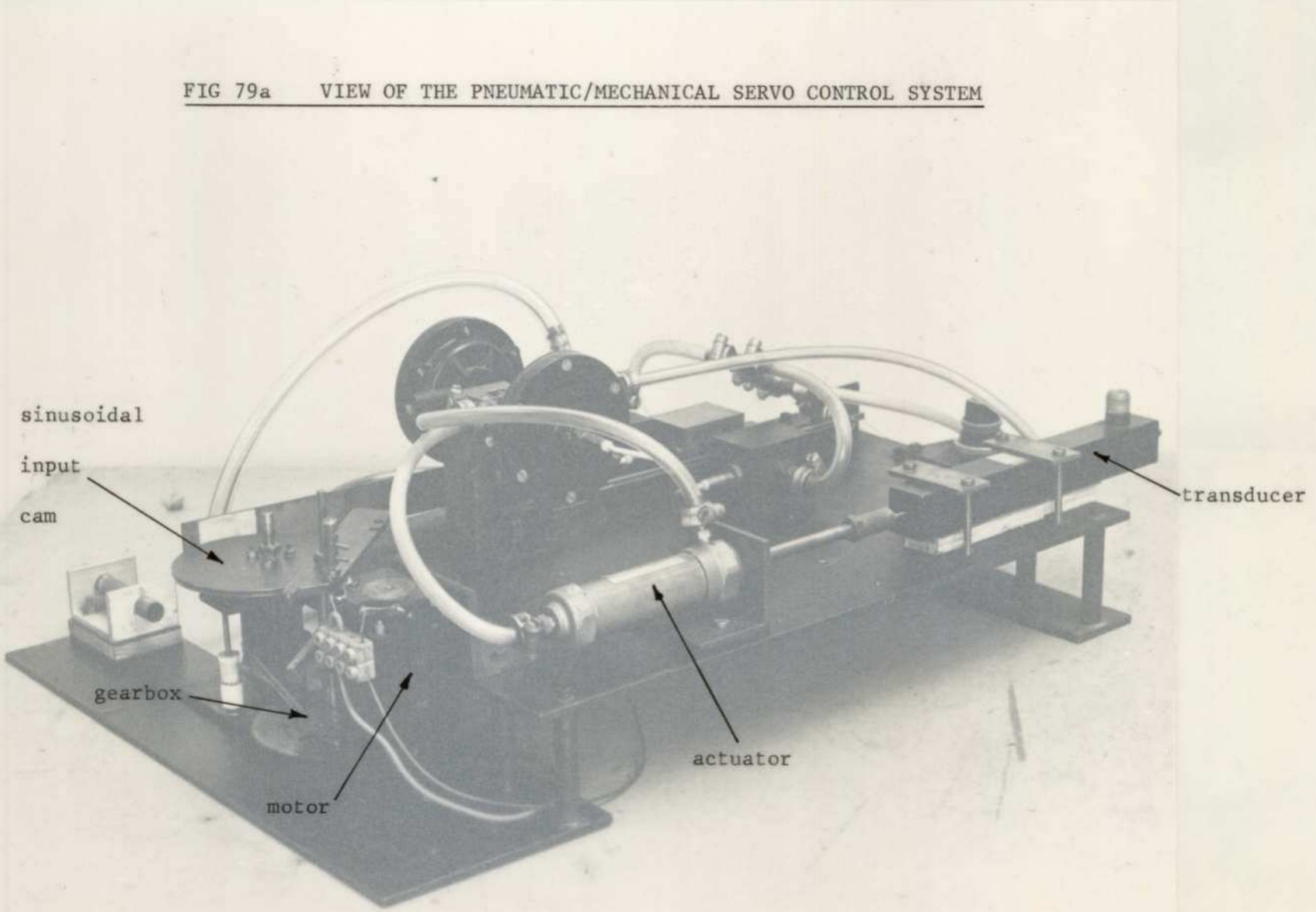


FIG 78 EXPERIMENTAL CHARACTERISTICS OF OPPOSED FLAPPER VALVES

FIG 79a VIEW OF THE PNEUMATIC/MECHANICAL SERVO CONTROL SYSTEM



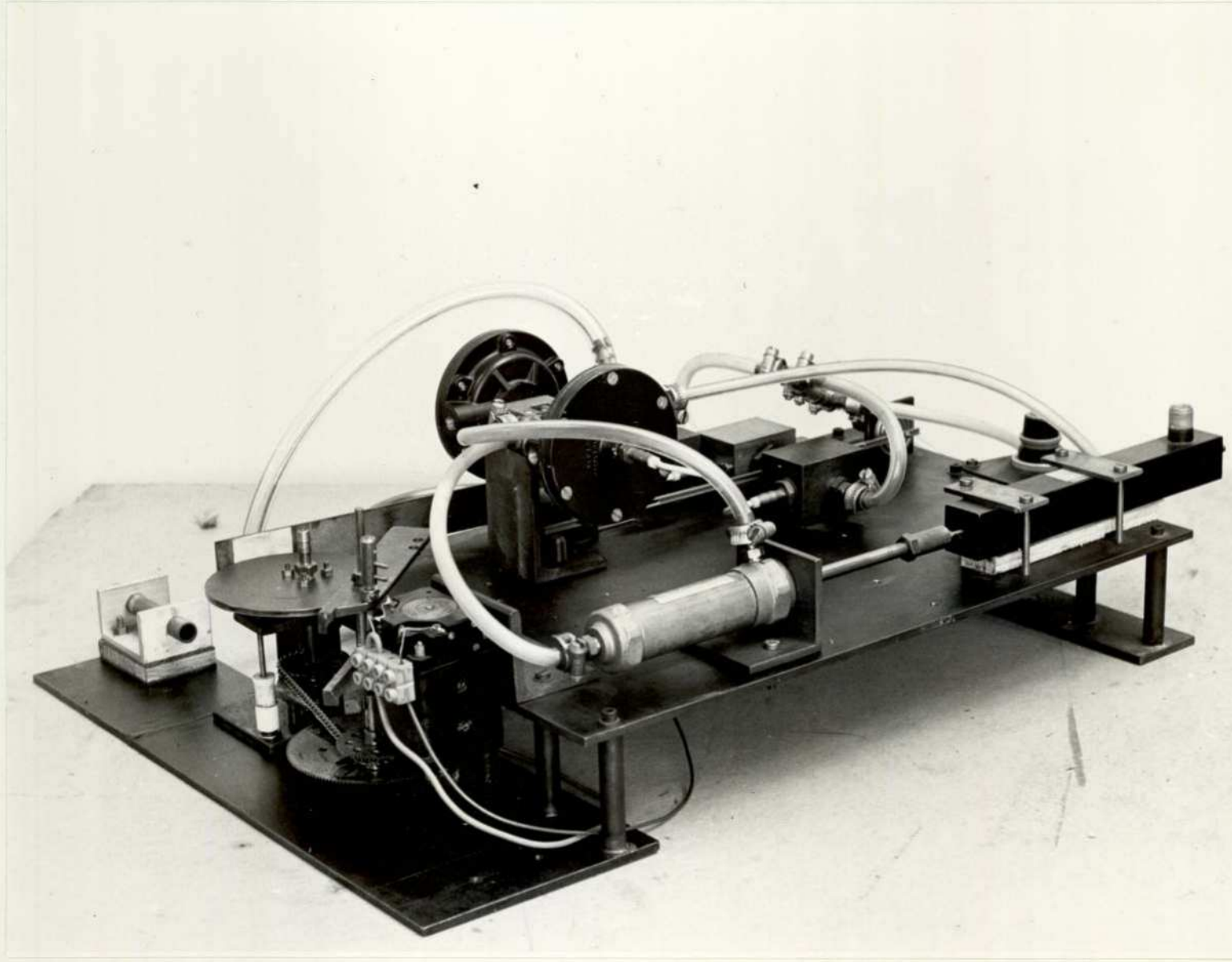
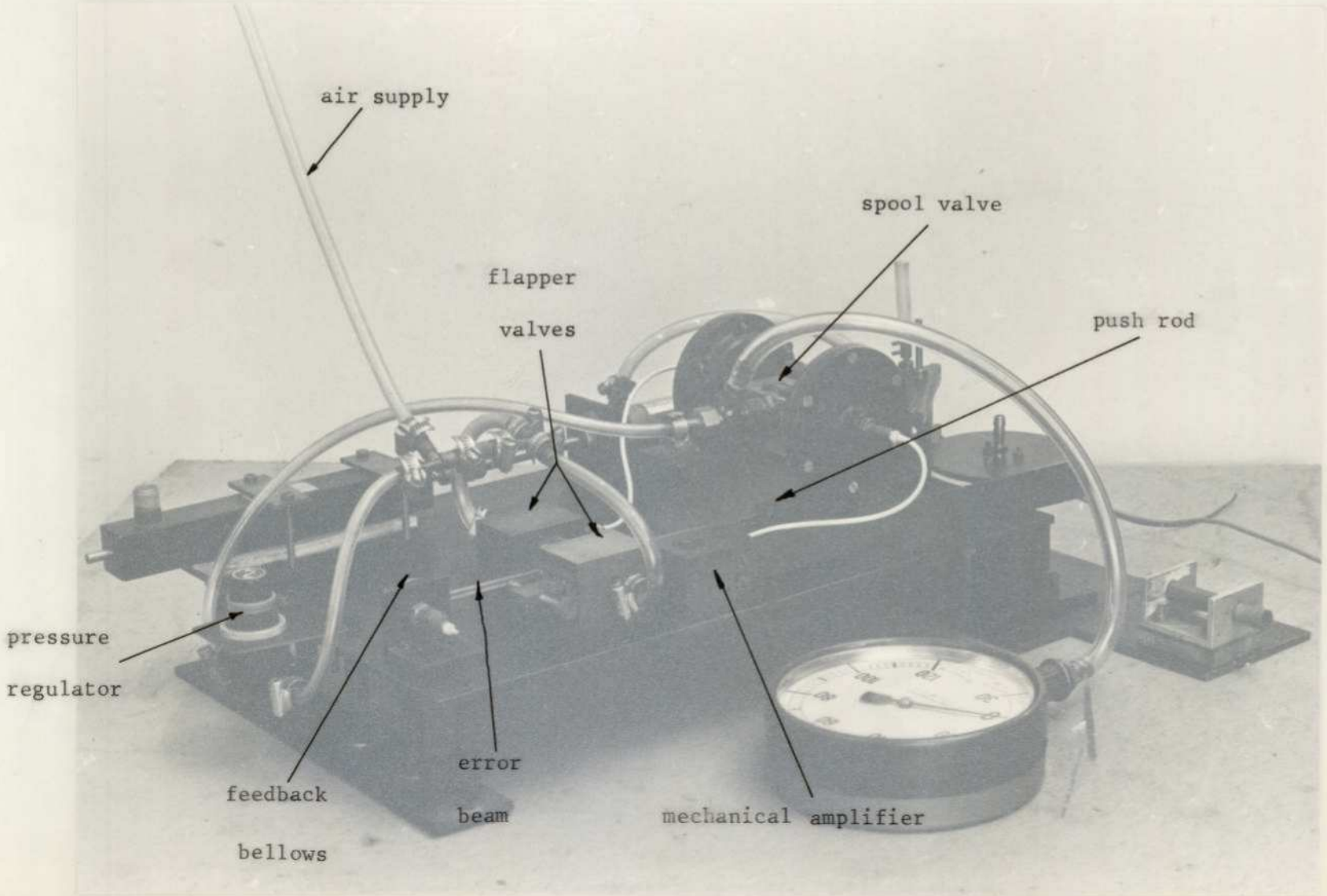
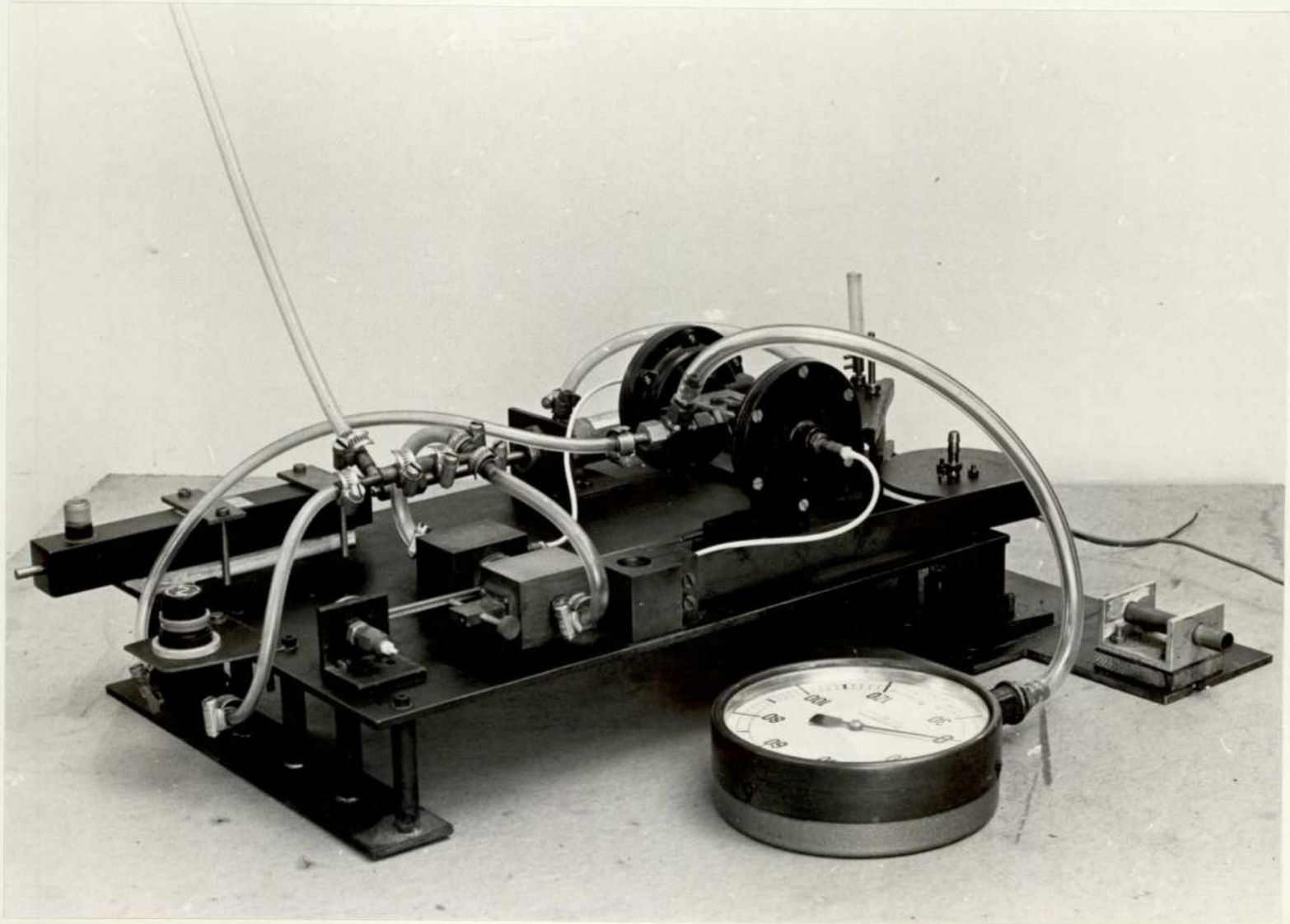


FIG 79b VIEW OF THE PNEUMATIC/MECHANICAL SERVO CONTROL SYSTEM





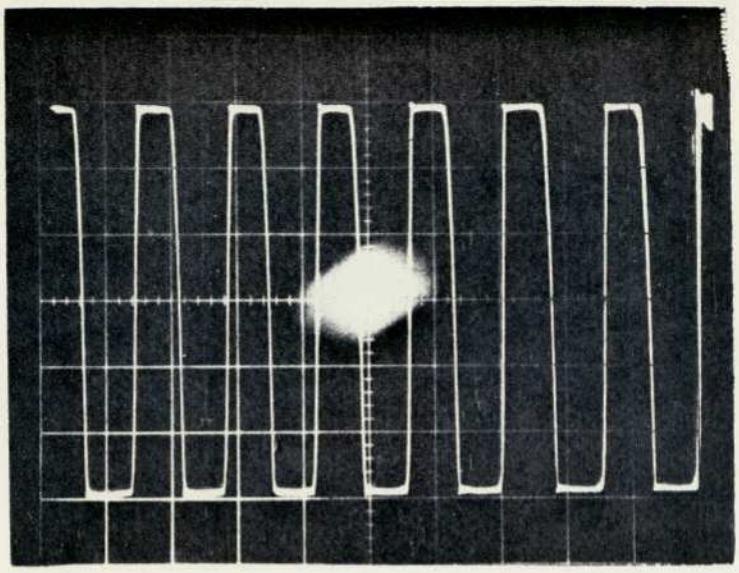


FIG 80 SERVO TEST FOR ω=0·693 Hz

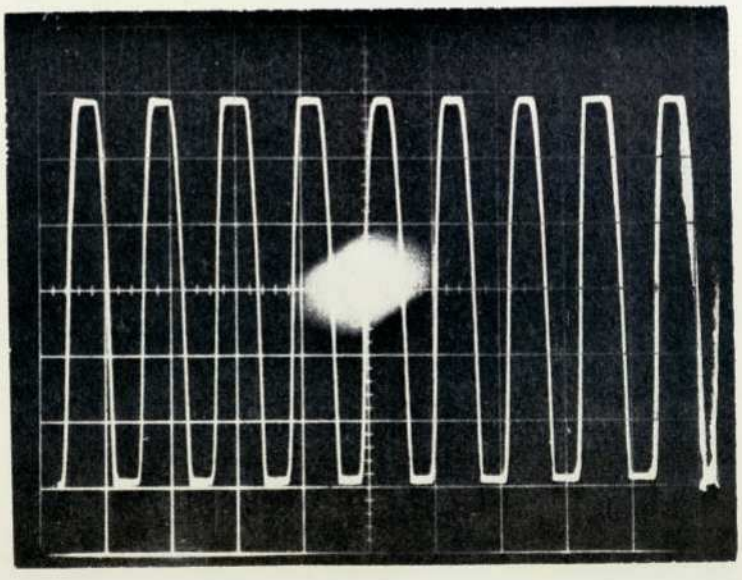


FIG 81 SERVO TEST FOR ω=0·880 Hz

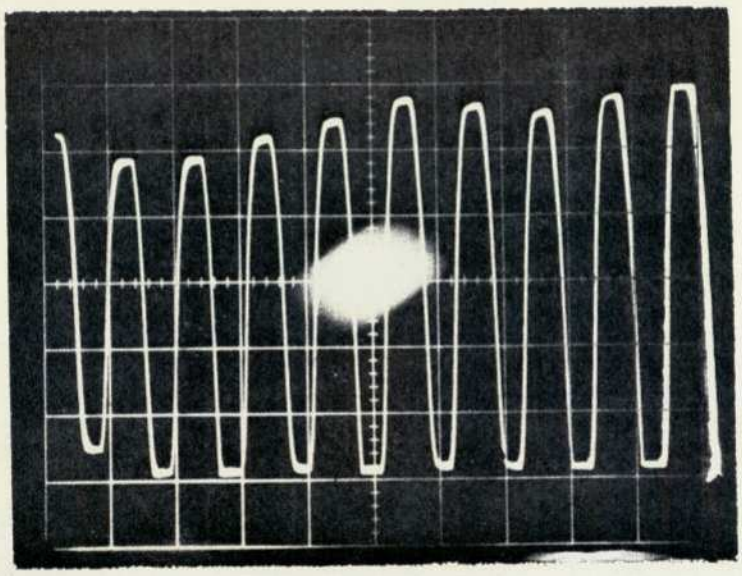


FIG 82 SERVO TEST FOR ω=0·930 Hz

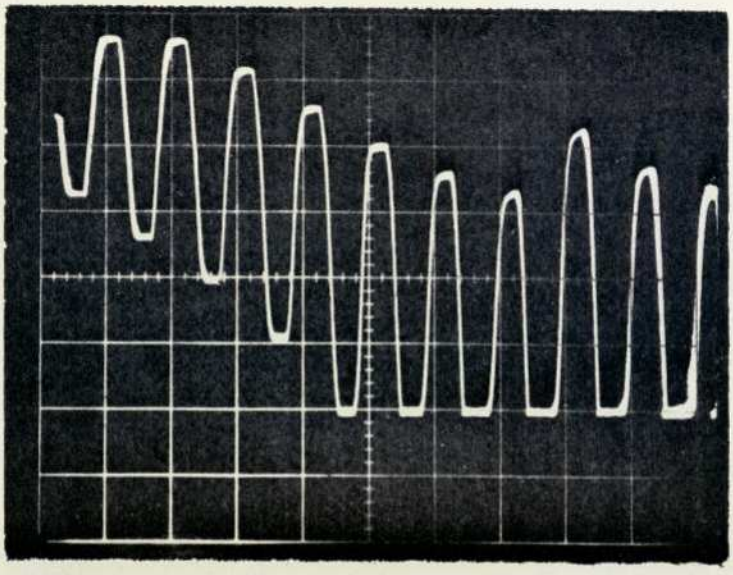


FIG 83 SERVO TEST FOR ω=0·978 Hz

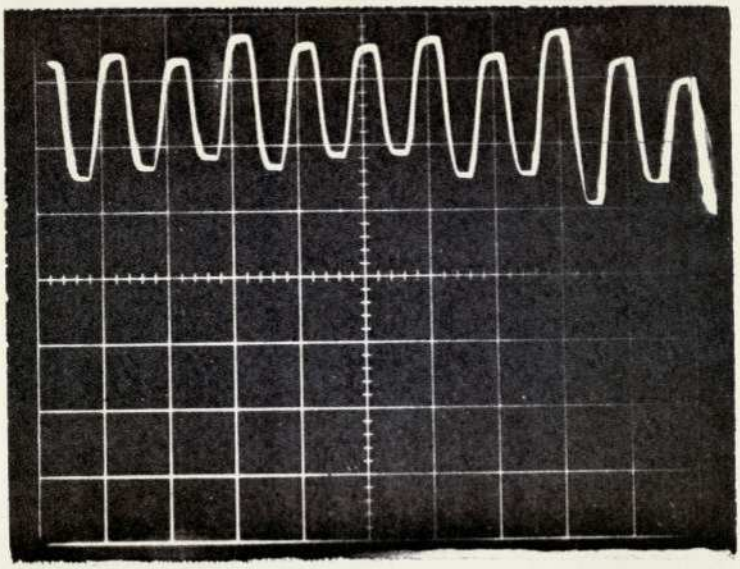
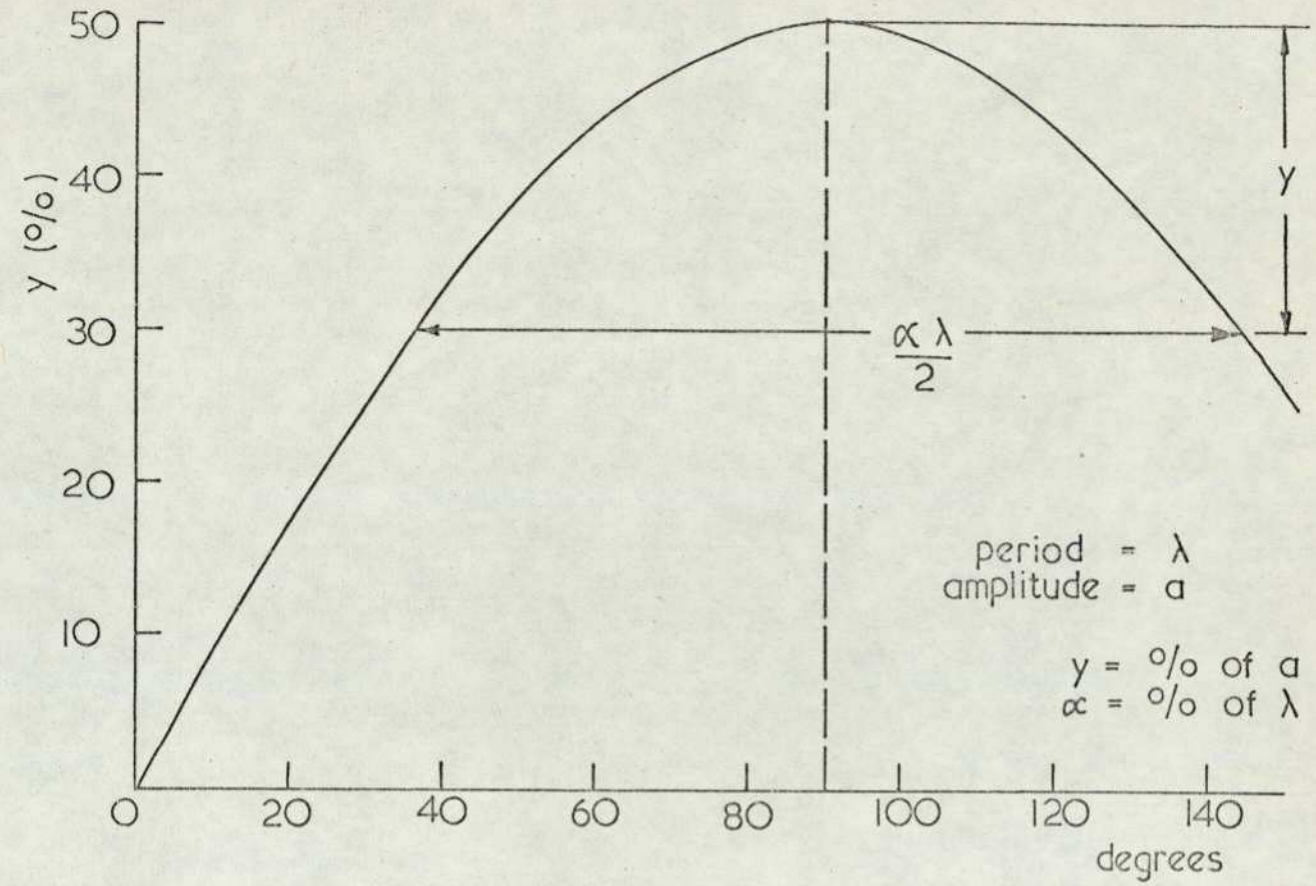


FIG 84 SERVO TEST FOR ω=1·035 Hz



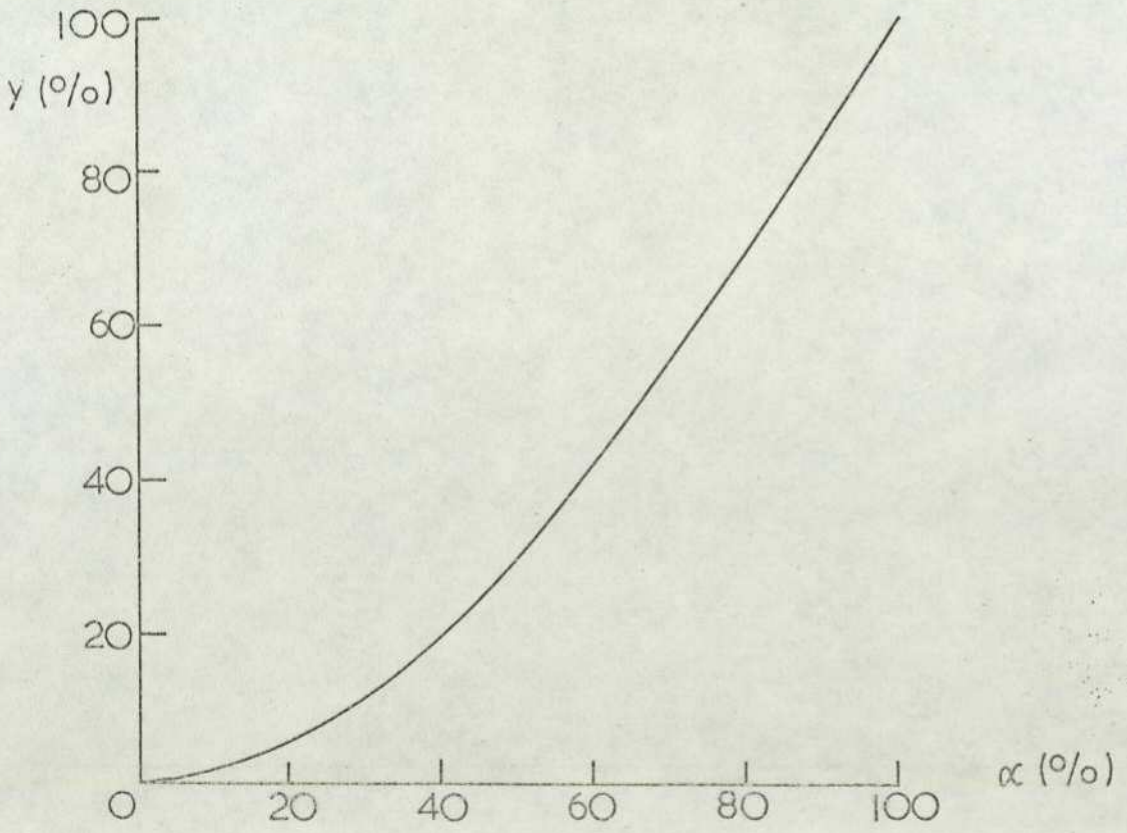


FIG 85 FUNCTIONS USED TO DETERMINE THE TOTAL AMPLITUDE OF CLIPPED SINE WAVES

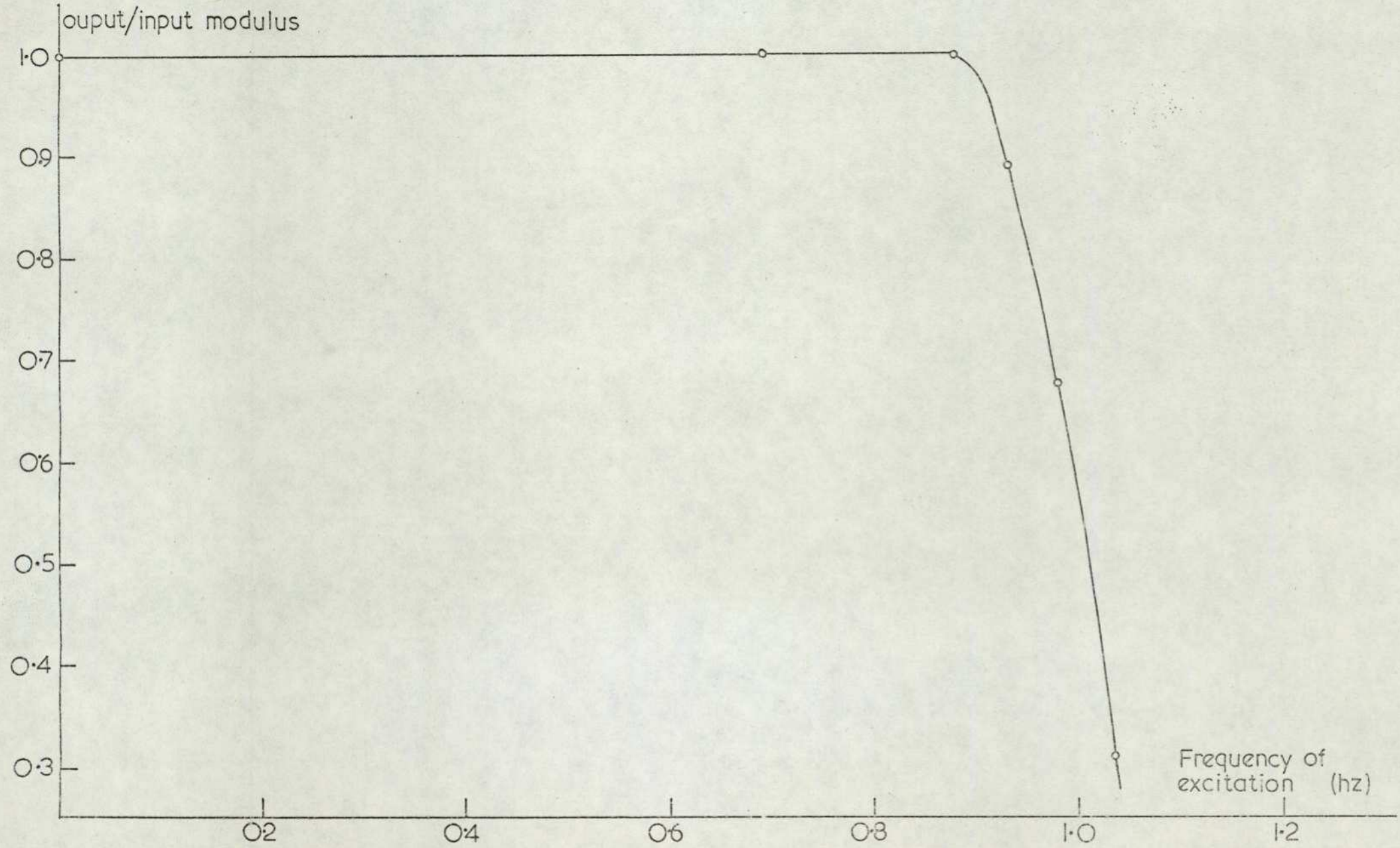


FIG 86 OPEN LOOP FREQUENCY RESPONSE OF PNEUMATIC SERVOMECHANISM

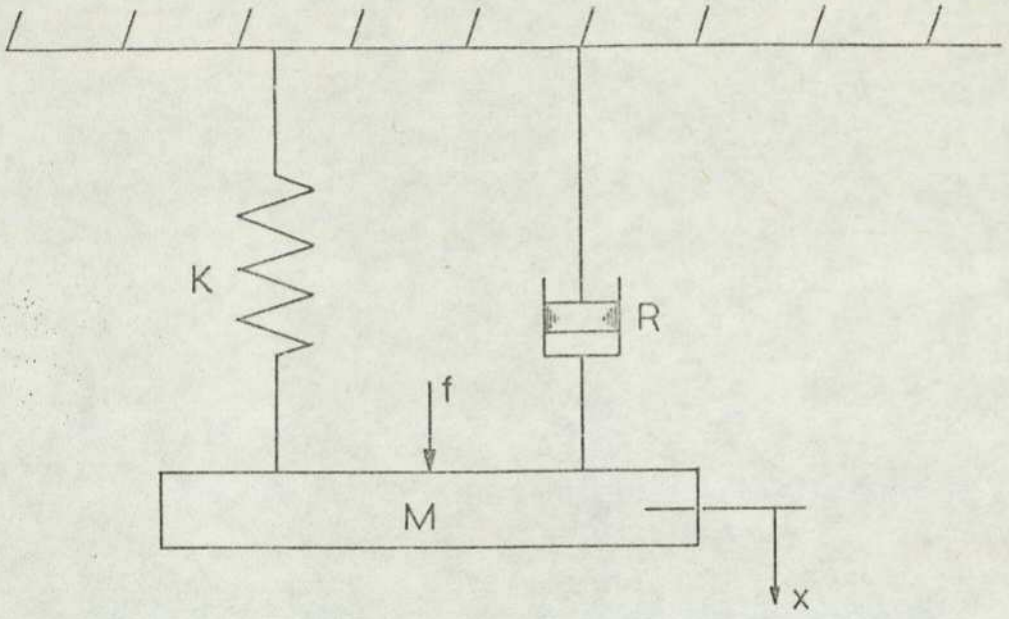


FIG 87 MECHANICAL SUSPENSION

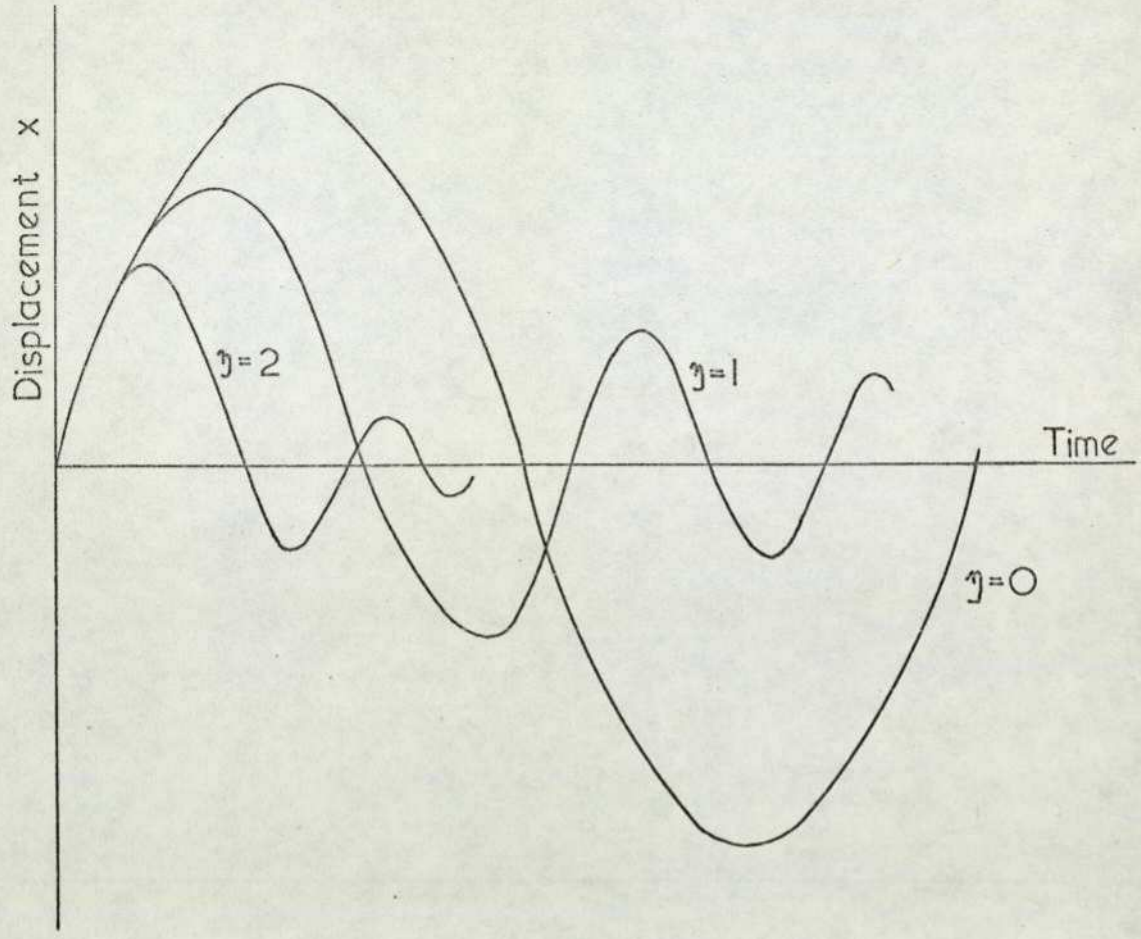


FIG 88 RESPONSE OF MECHANICAL SYSTEM FOR VARIABLE DAMPING FACTOR

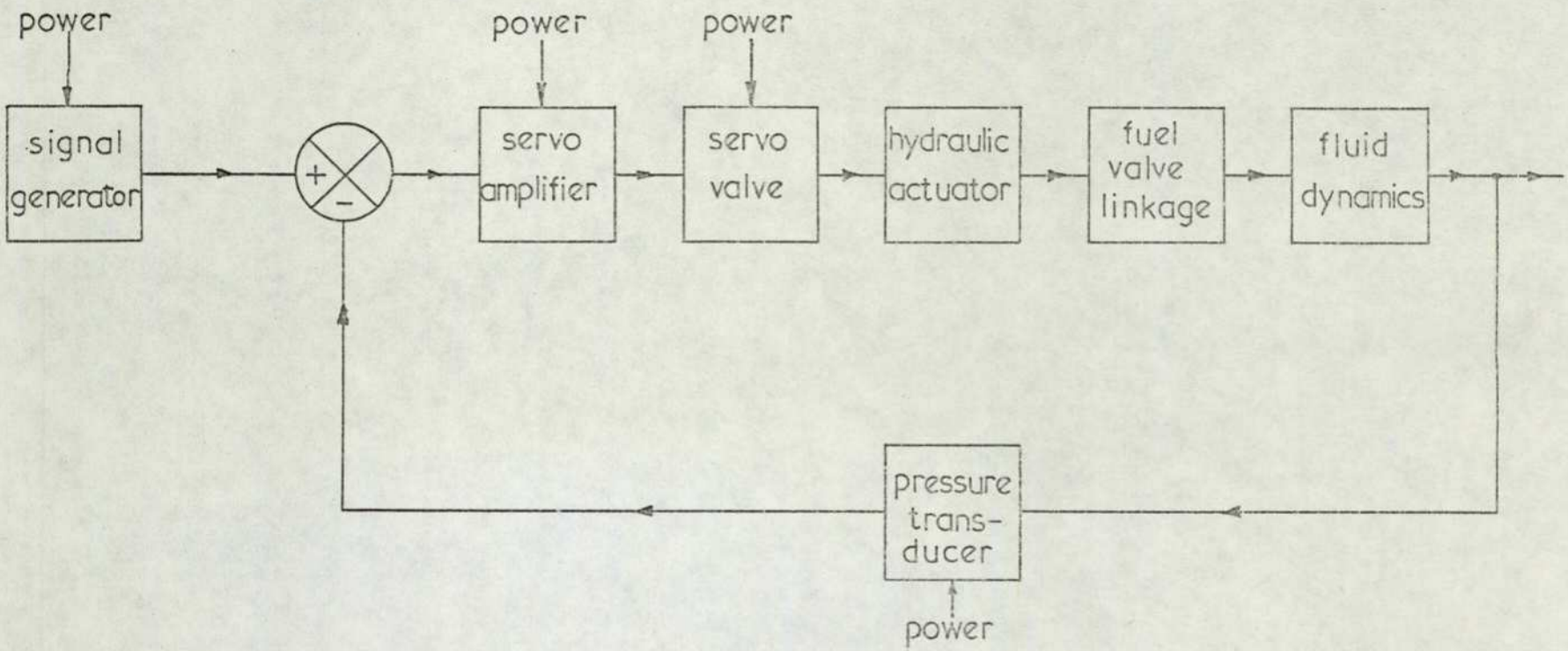


FIG 89 ELECTRO-HYDRAULIC PRESSURE CONTROL SERVO SYSTEM

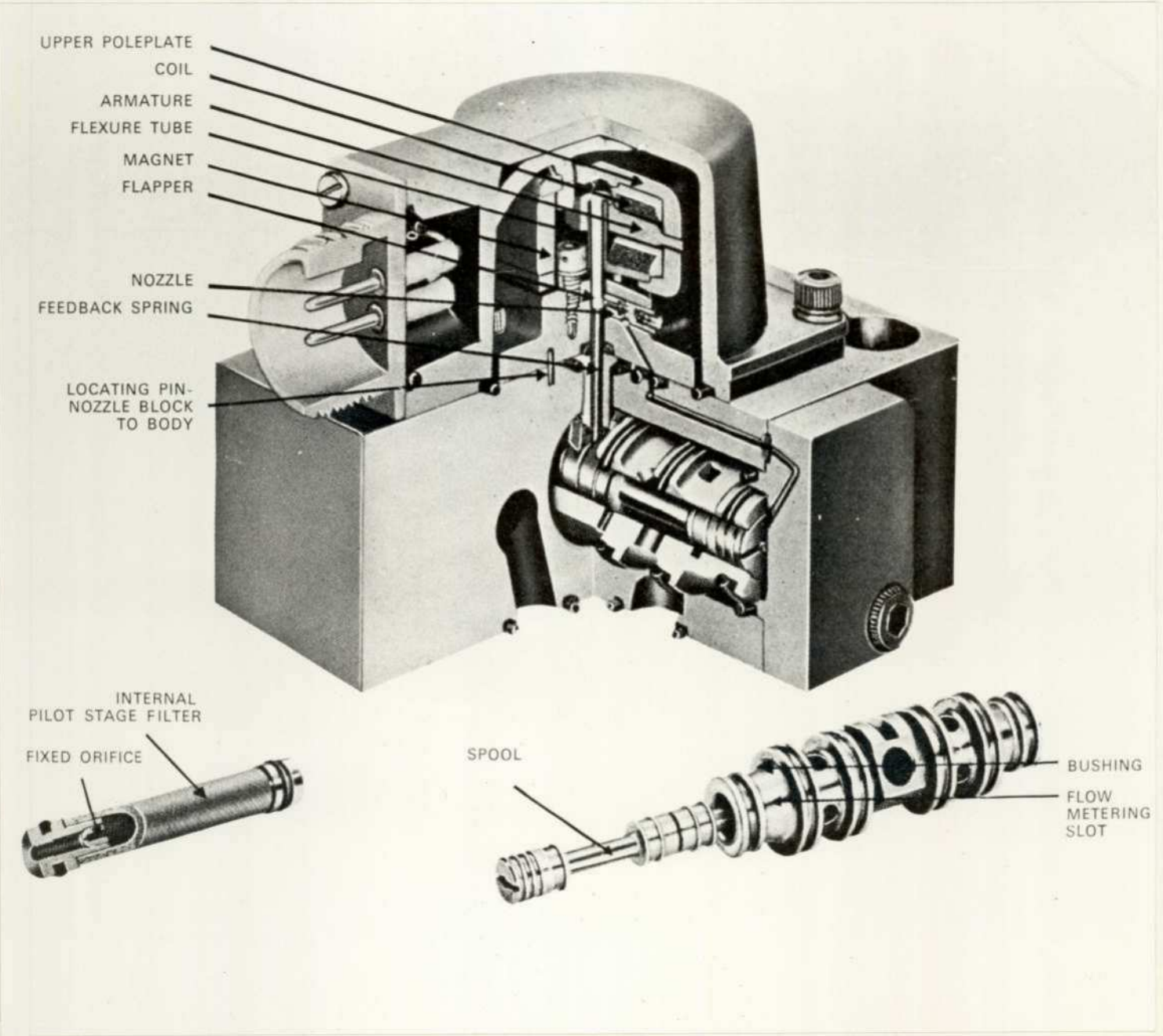


FIG 90 CUTAWAY VIEW OF DOWTY ELECTROHYDRAULIC SERVO VALVE

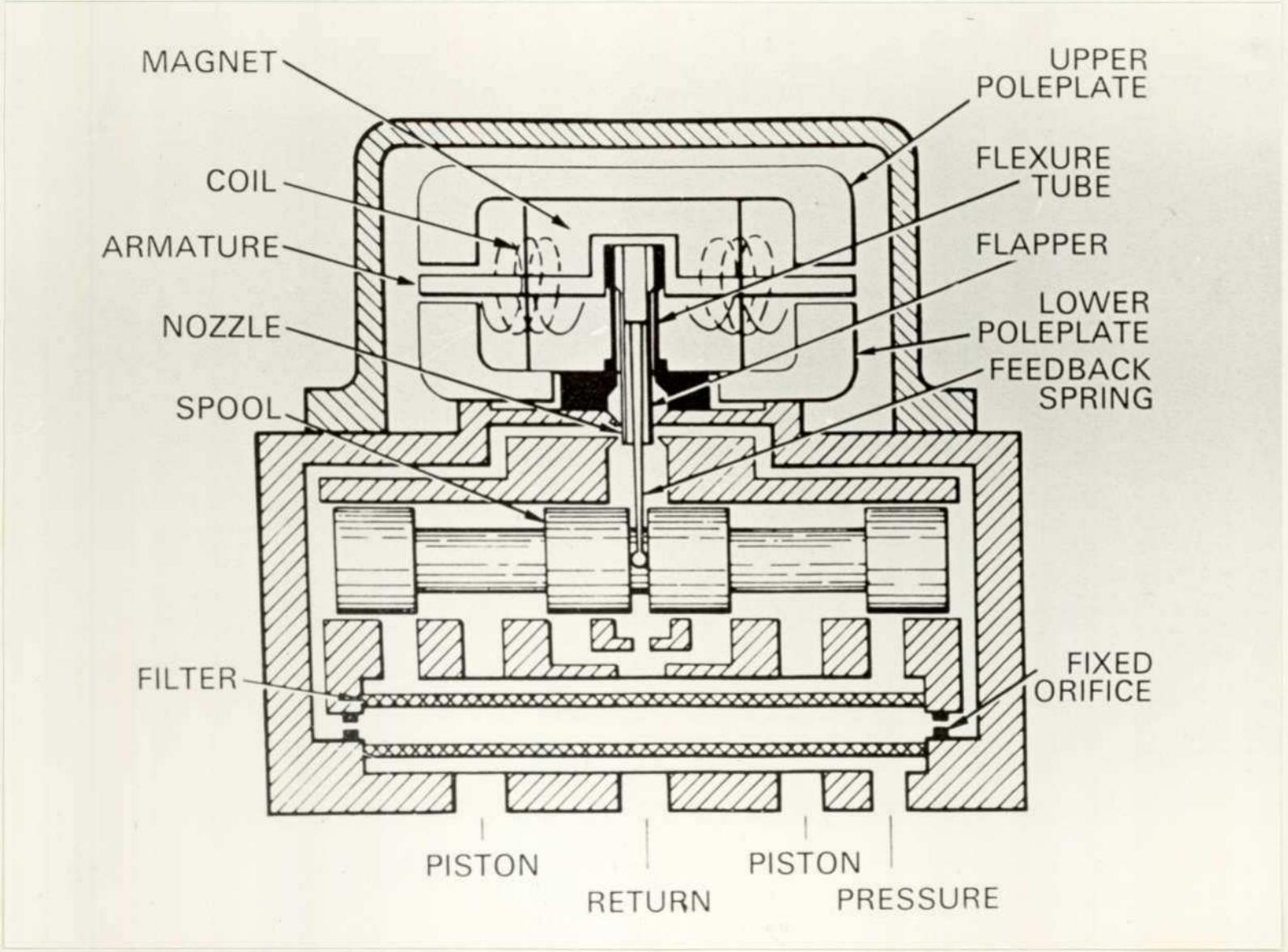
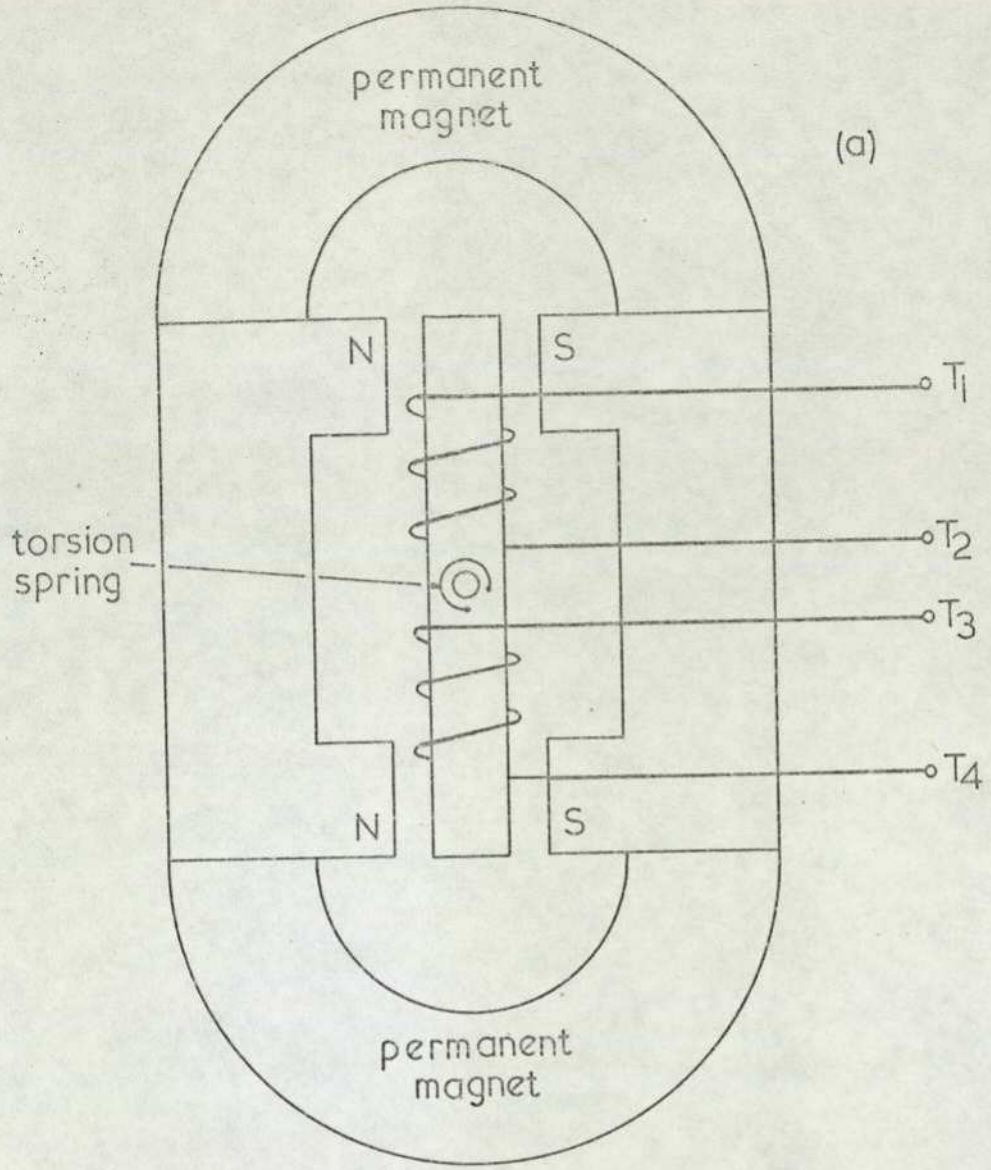
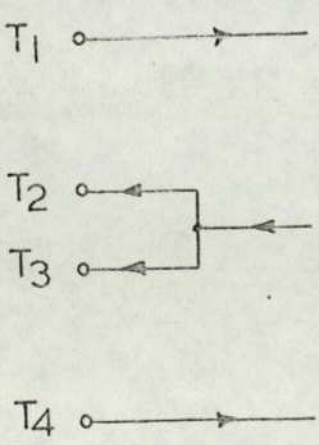


FIG 91 FUNCTIONAL DIAGRAM OF DOWTY SERVO VALVE



(b) push pull



(c) series

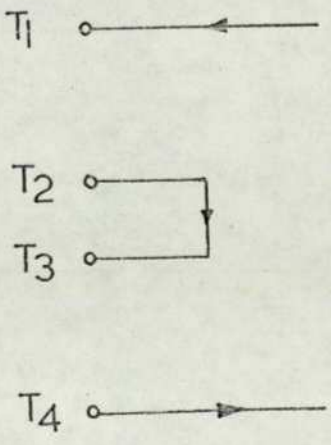


FIG 92 SERVO VALVE TORQUE MOTOR & CONNECTIONS

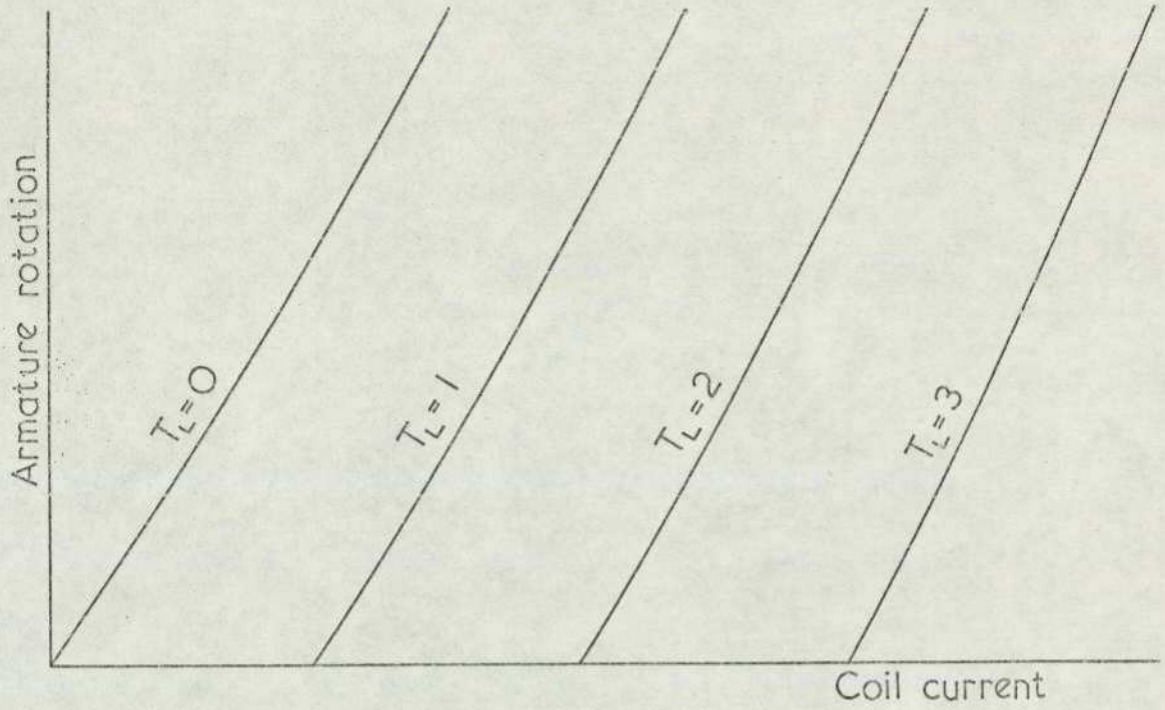


FIG 93 TORQUE MOTOR CHARACTERISTICS FOR VARIABLE TORSION SPRING STIFFNESS T_L

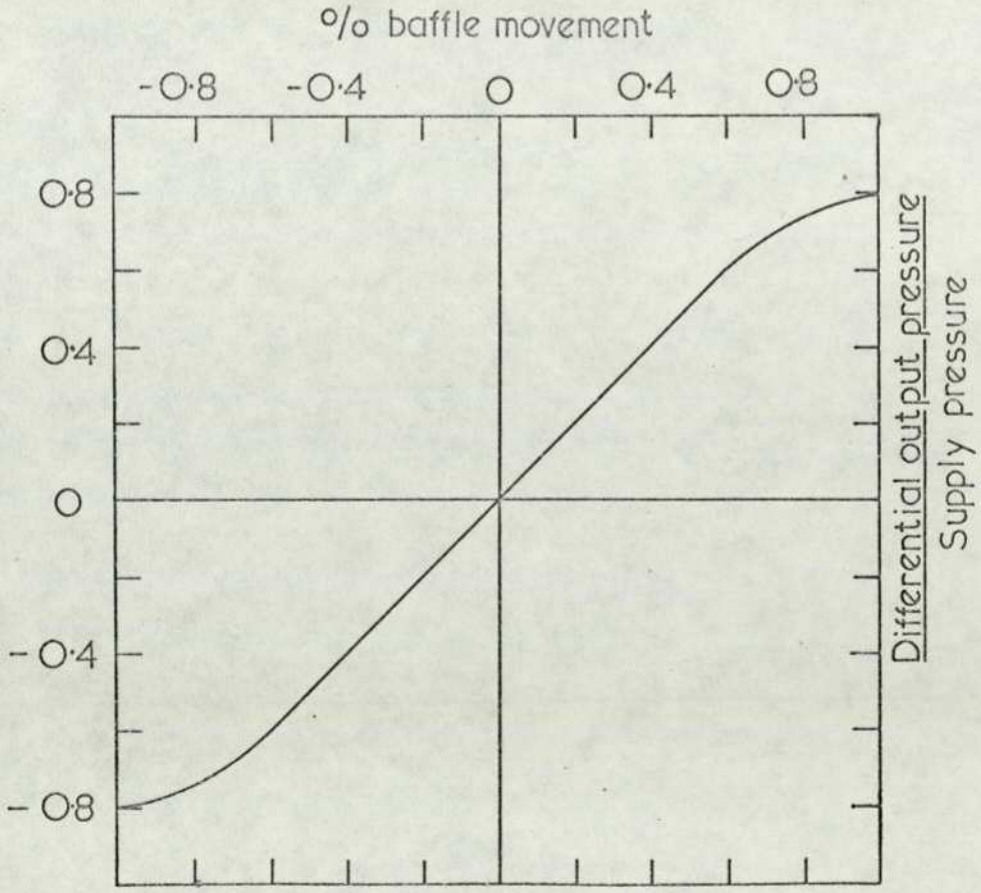


FIG 94 SERVO VALVE BAFFLE CHARACTERISTIC

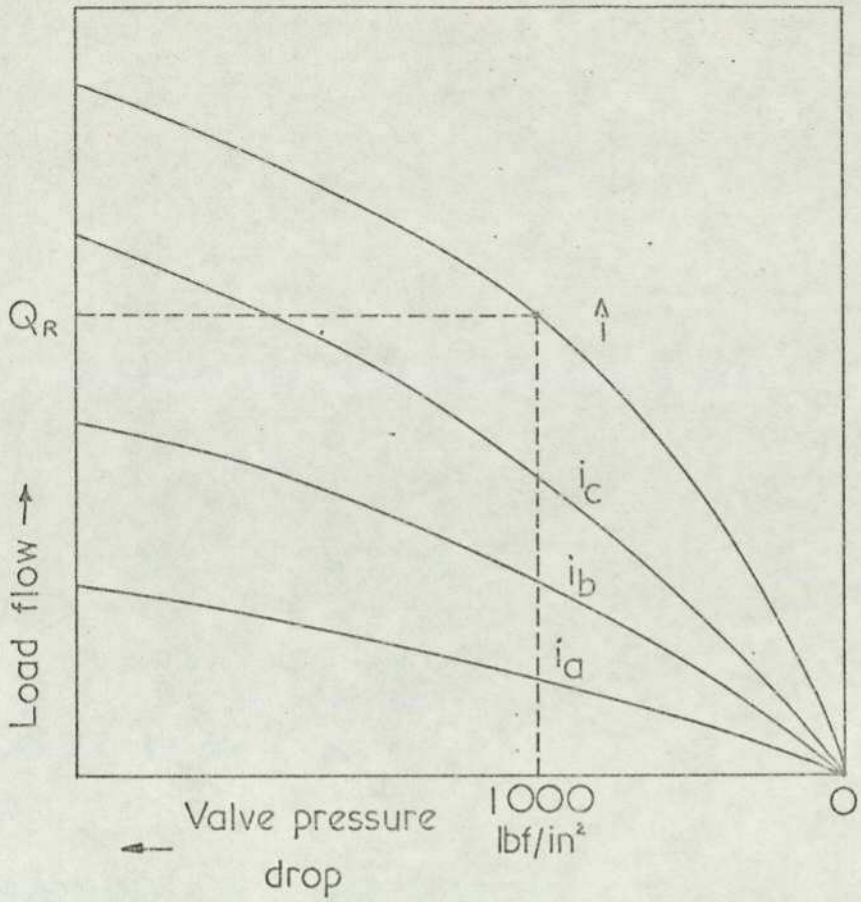
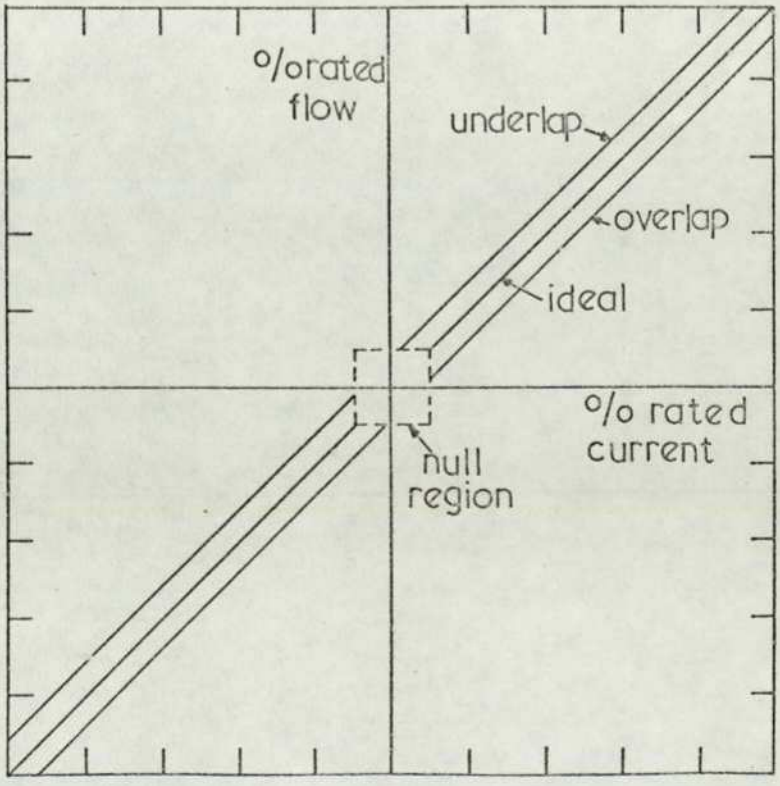


FIG 95 FLOW PRESSURE DROP FOR SERVO VALVE



For details of null region see Fig 97

FIG 96 FLOW GAIN OF SERVO VALVE

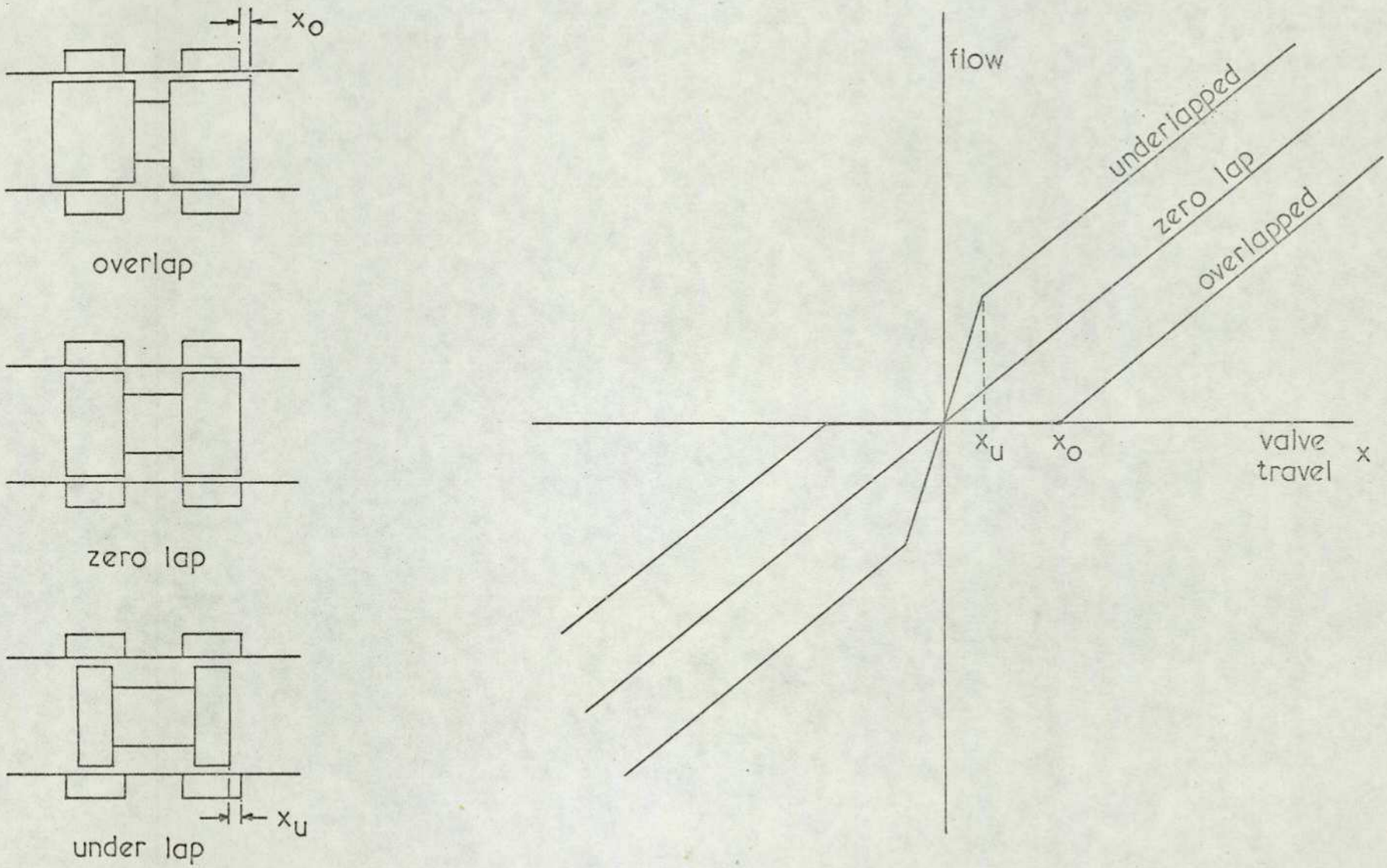


FIG 97 EFFECT OF SPOOL LAP ON SERVO VALVE FLOW GAIN IN THE NULL REGION

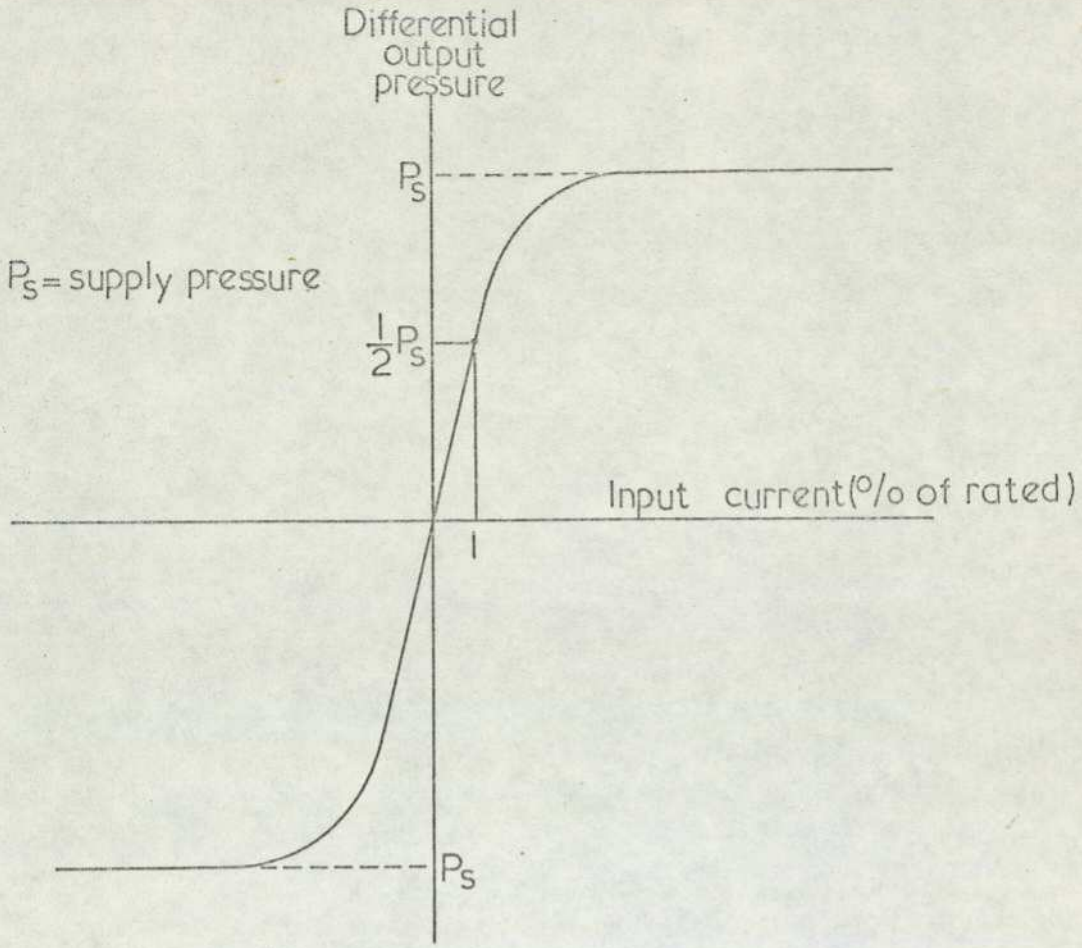


FIG 98 PRESSURE GAIN FOR BLOCKED LOAD

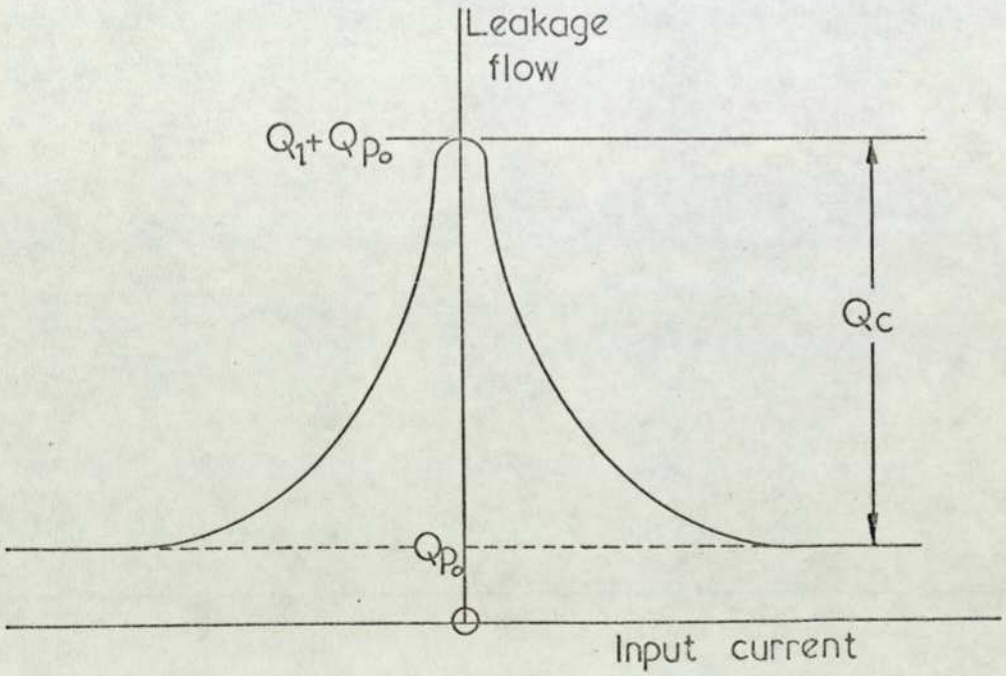


FIG 99 SERVO VALVE LEAKAGE CURVE

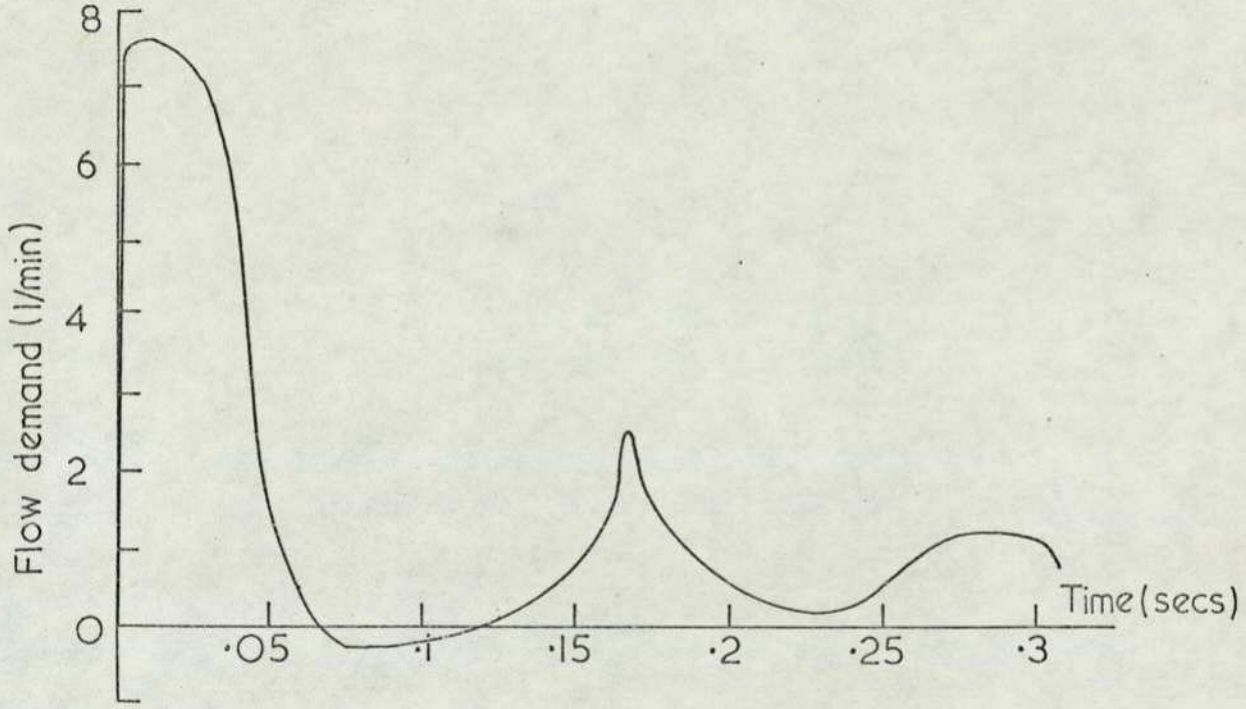


FIG 100 FLOW-TIME PREDICTED BY PROGRAM VSP2

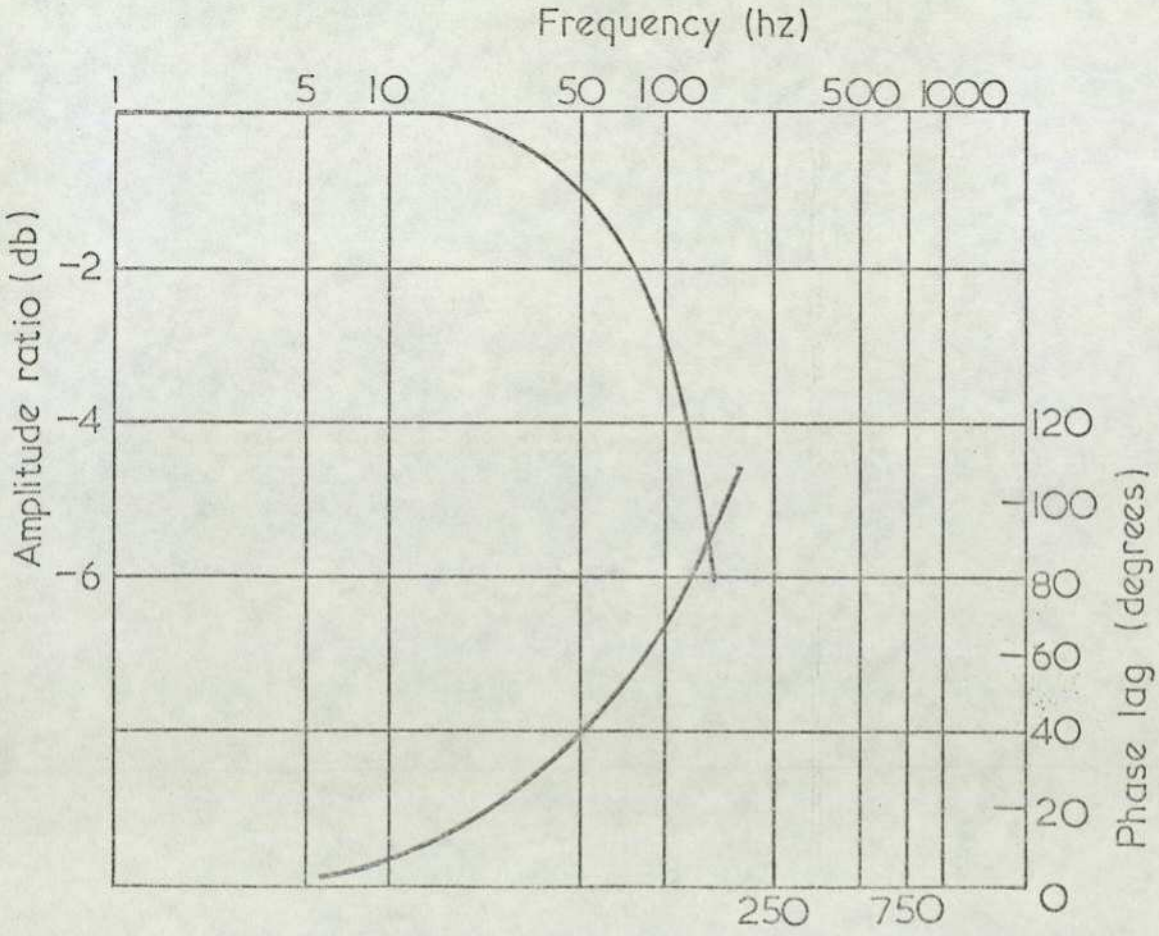


FIG 101 BODE DIAGRAM FOR DOWTY 4551.262 SERIES SERVO VALVE

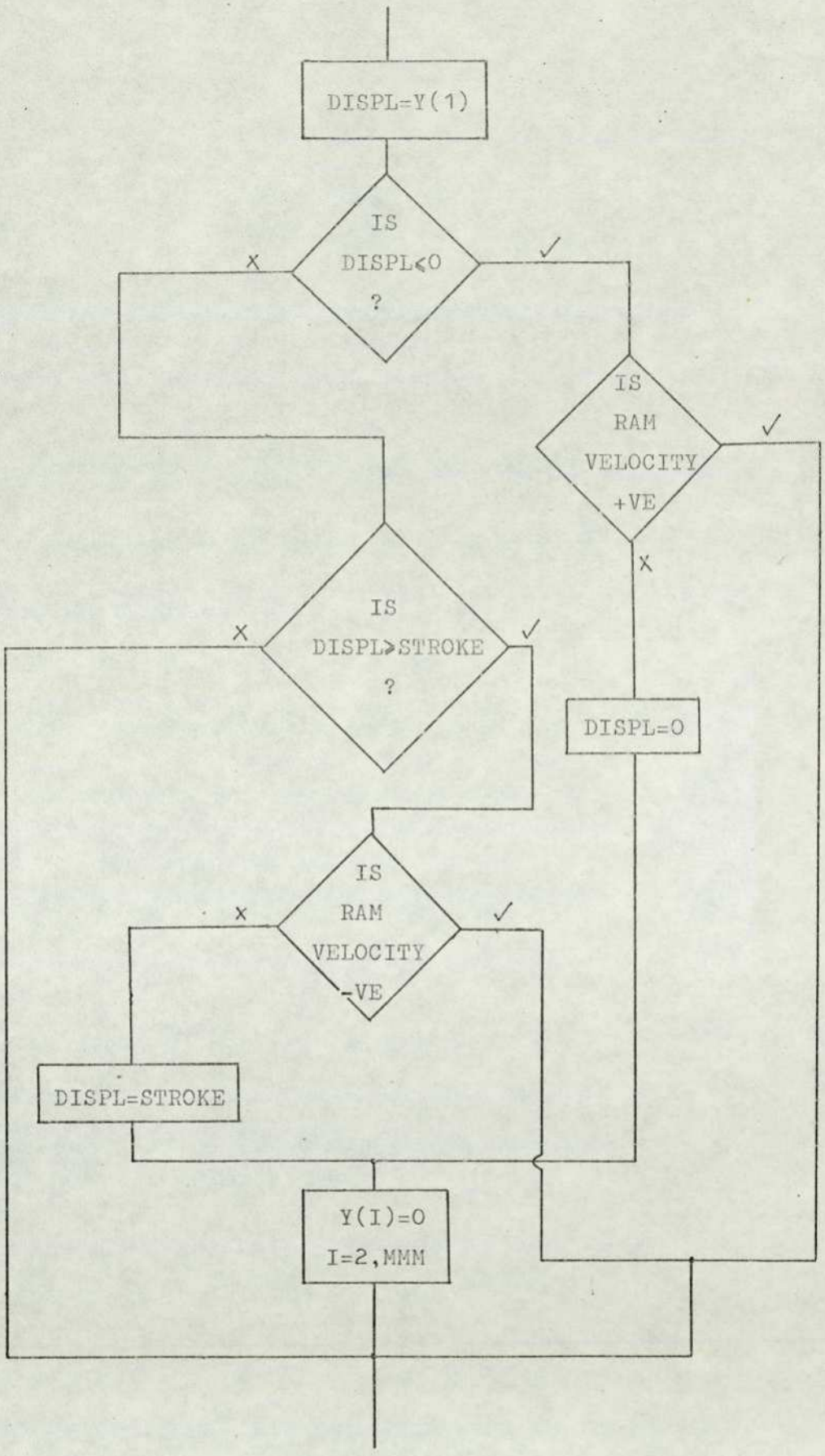
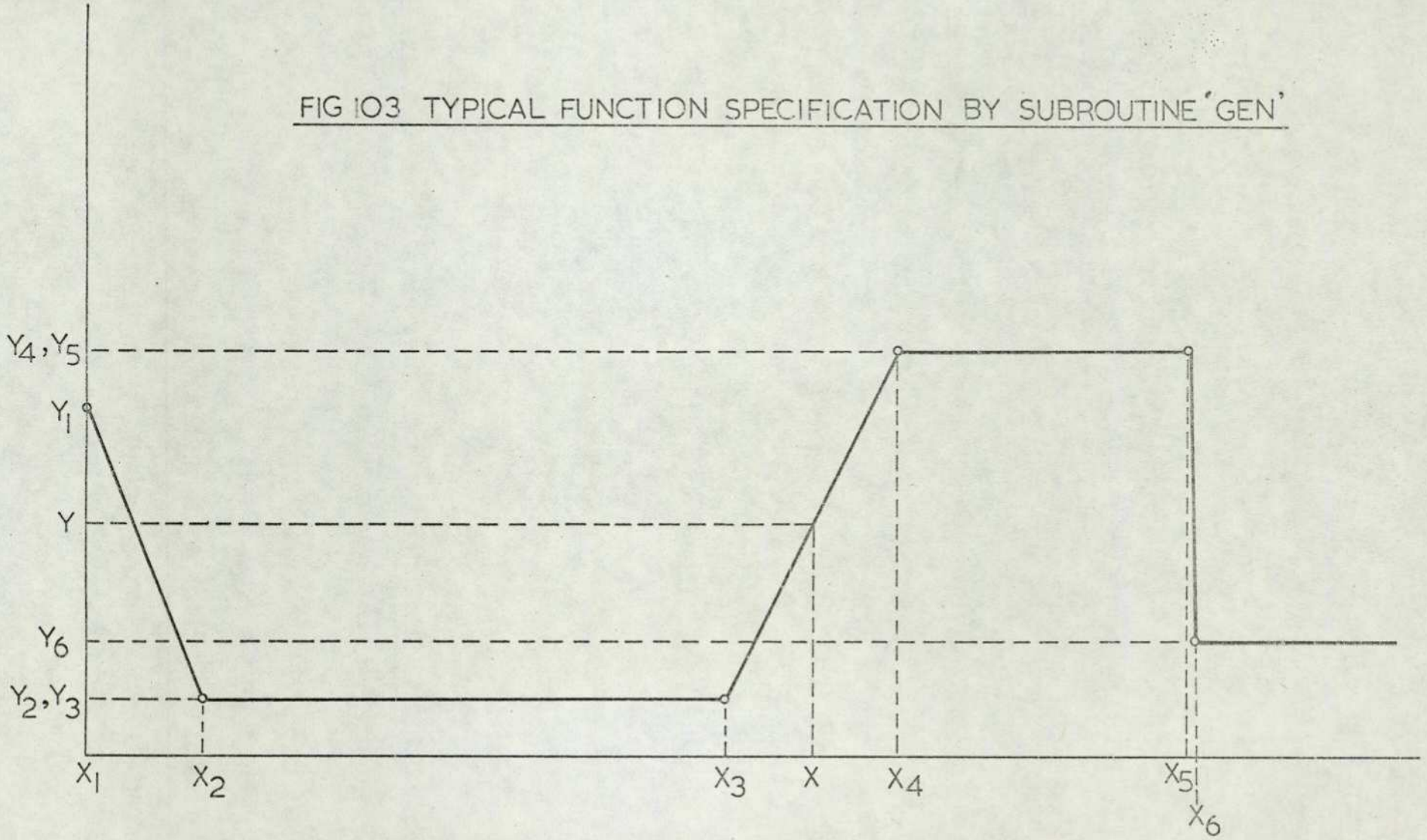


FIG 102 FLOW DIAGRAM FOR 'DISPL' IN PROGRAM VSP2

FIG 103 TYPICAL FUNCTION SPECIFICATION BY SUBROUTINE 'GEN'



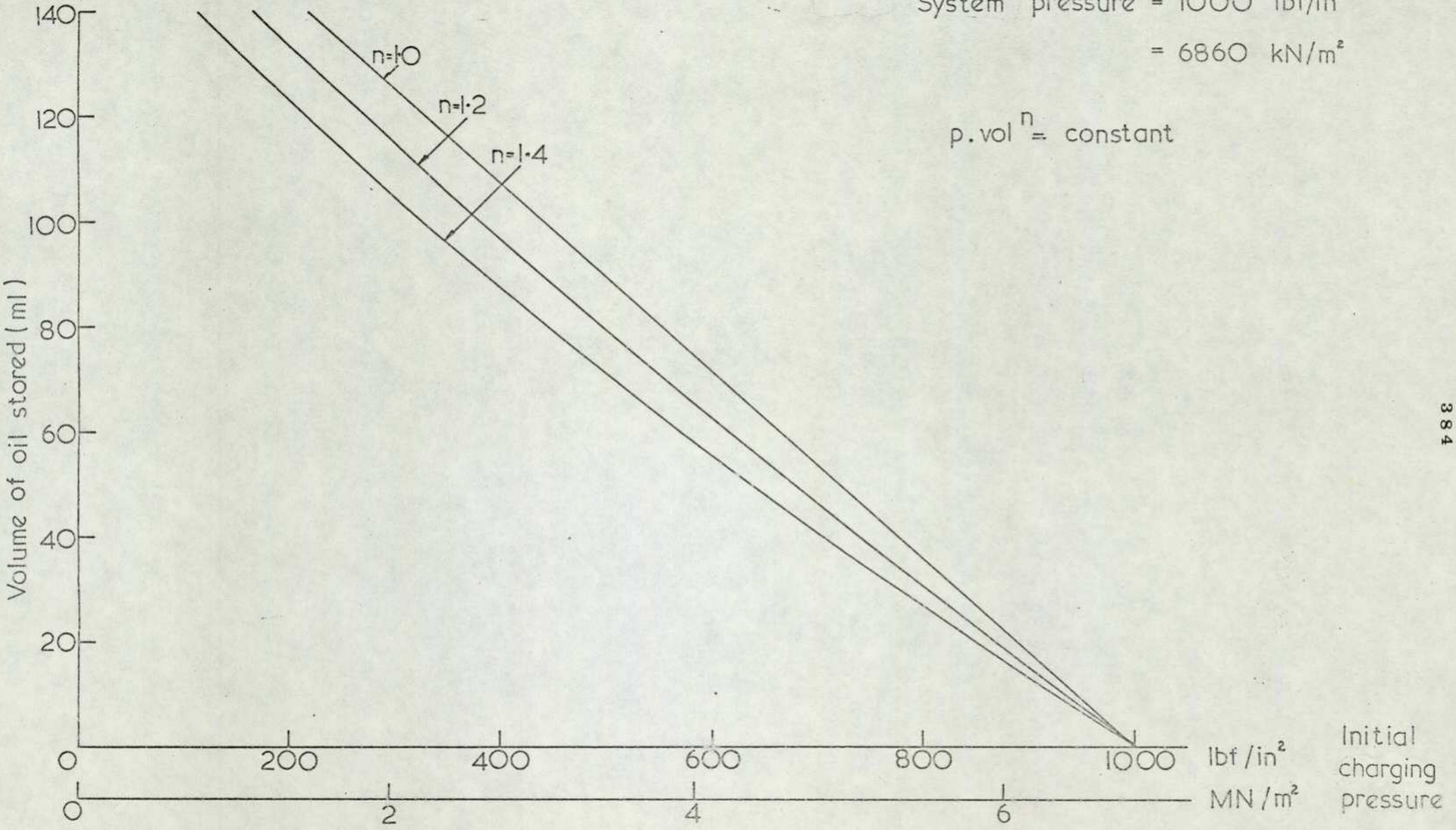


FIG 104 ACCUMULATOR CHART – H.P. RANGE

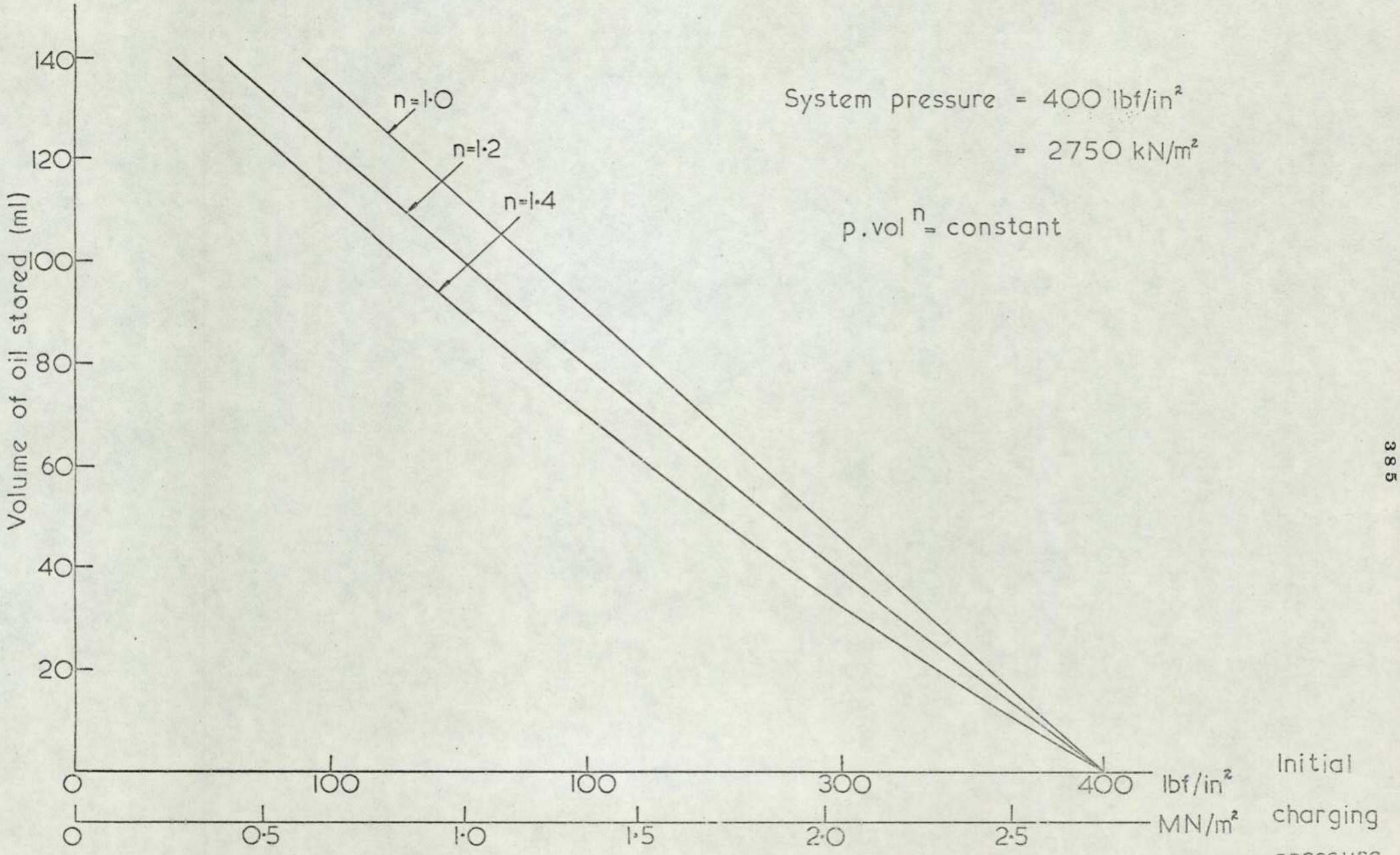


FIG 105 ACCUMULATOR CHART - L.P. RANGE

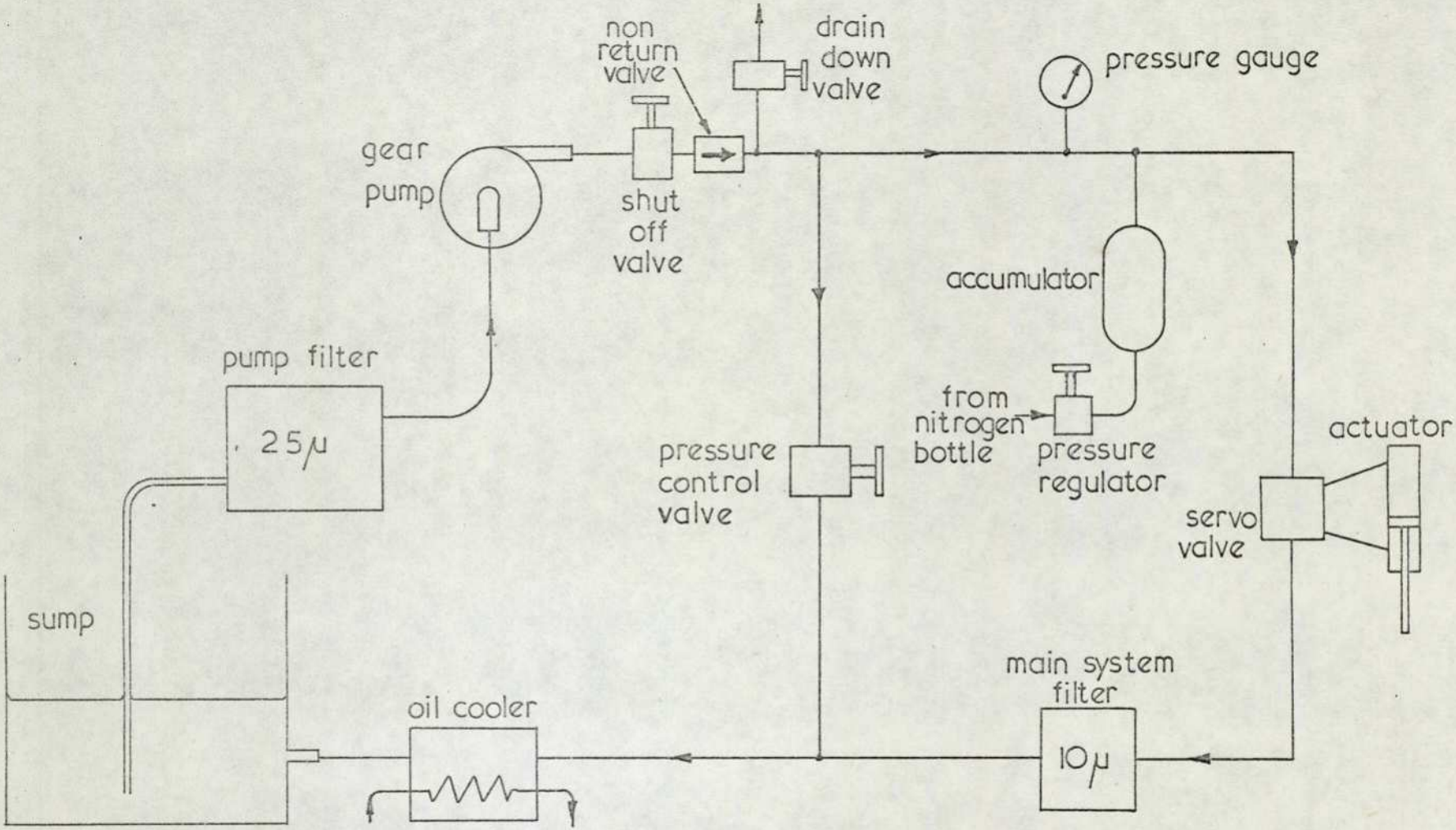


FIG 106 SCHEMATIC DIAGRAM OF HYDRAULIC CIRCUIT

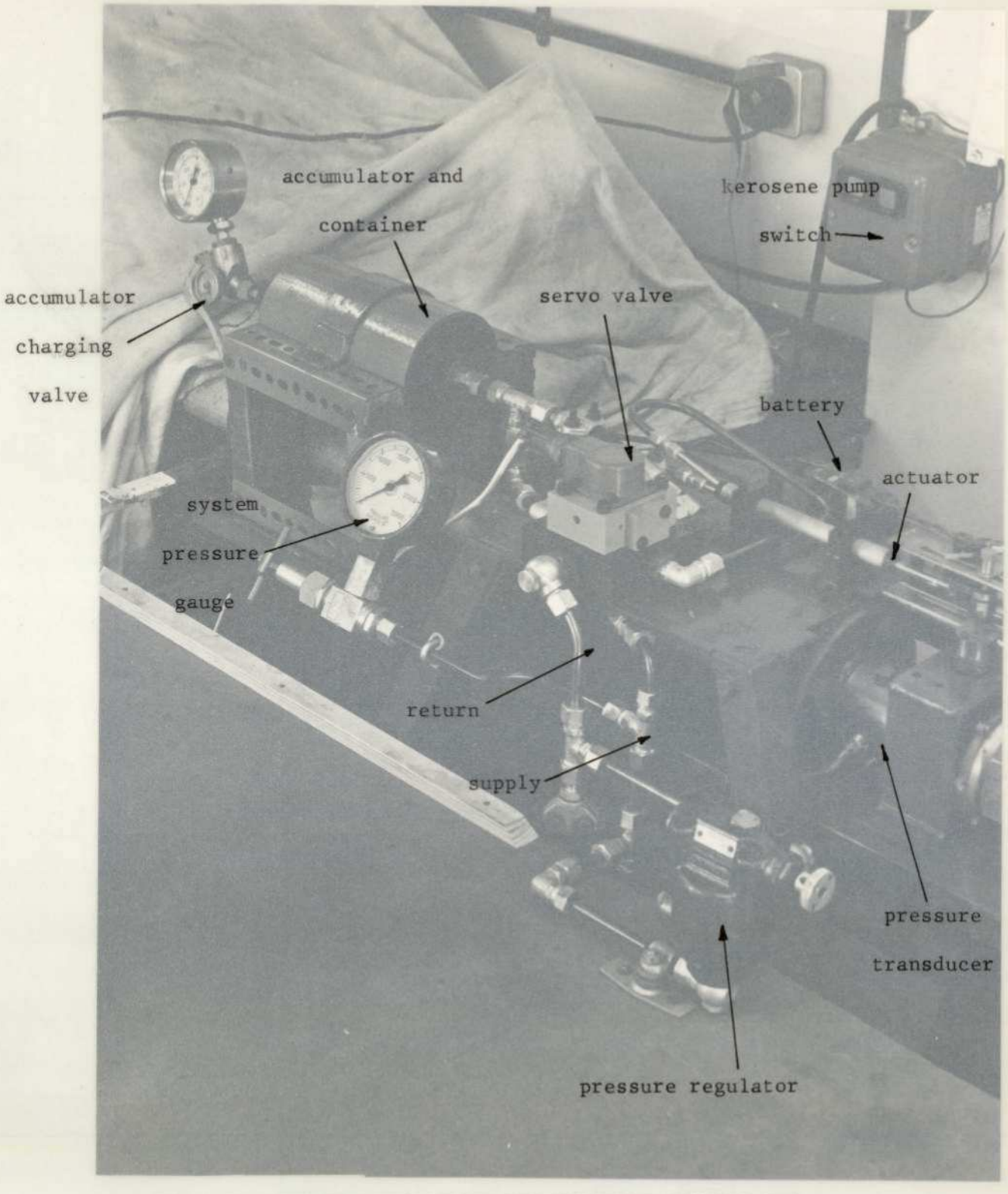


FIG 107 VIEW OF SERVO VALVE INSTALLATION SHOWING THE HYDRAULIC ACTUATOR AND VALVE LINKAGE

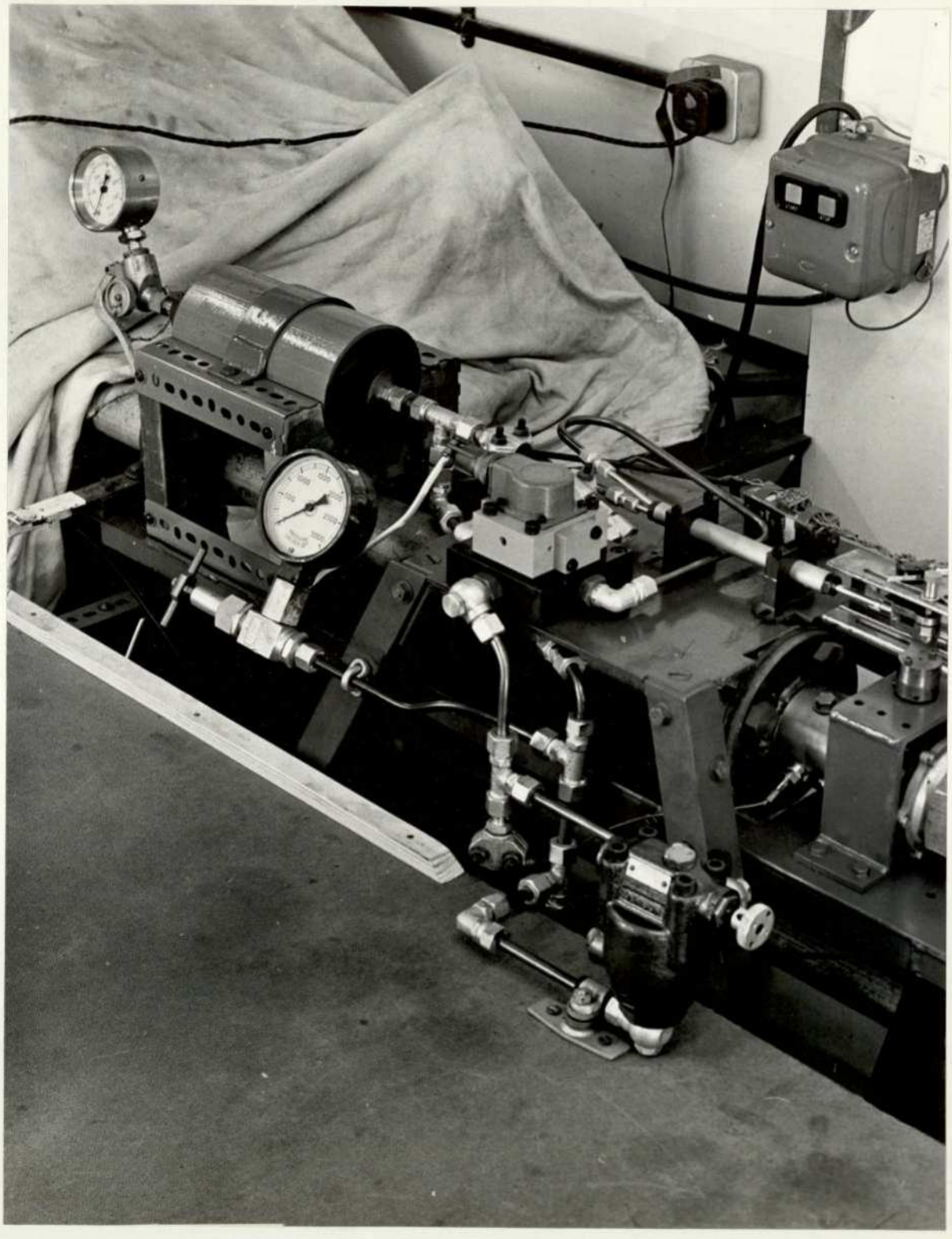
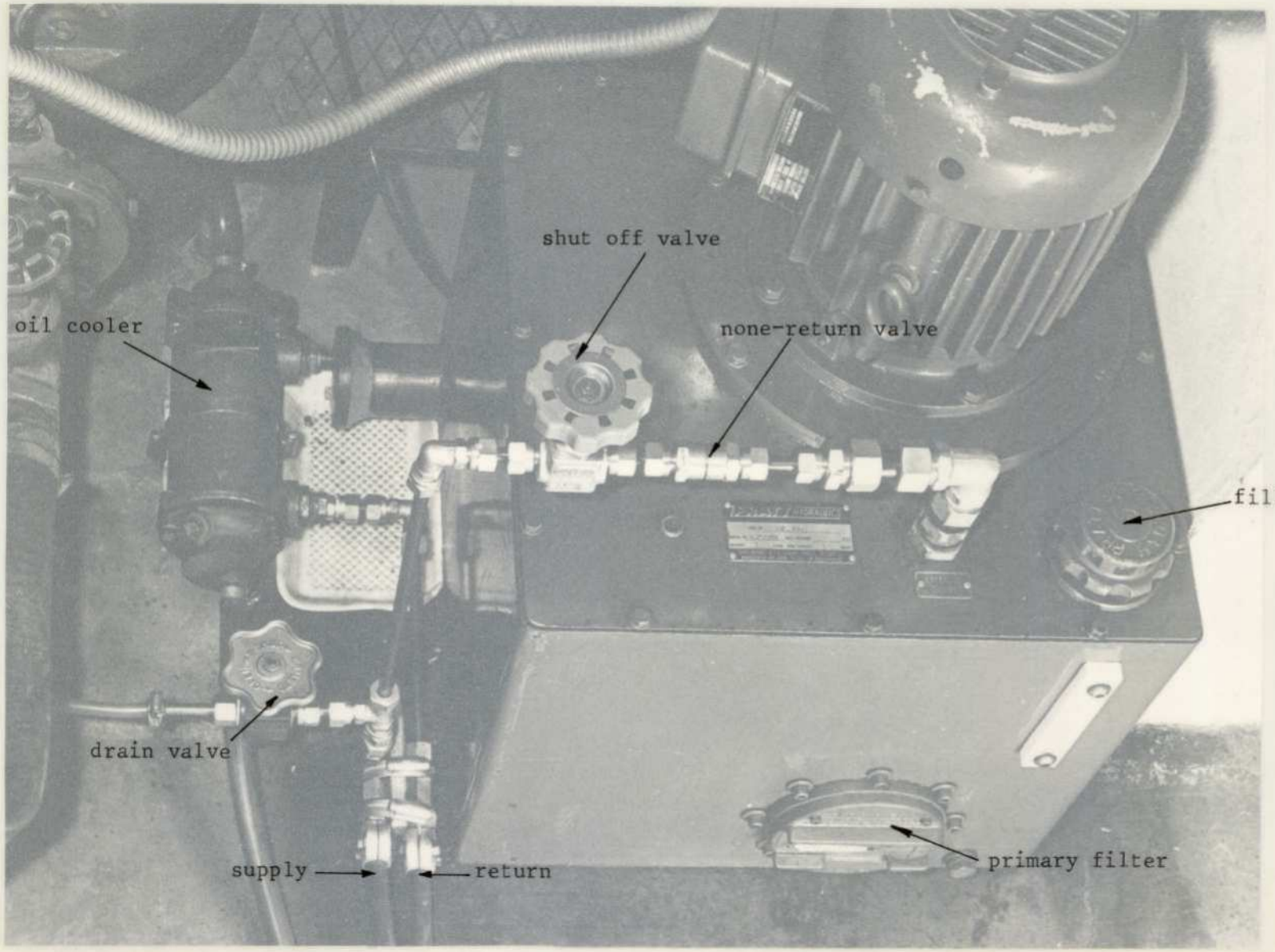
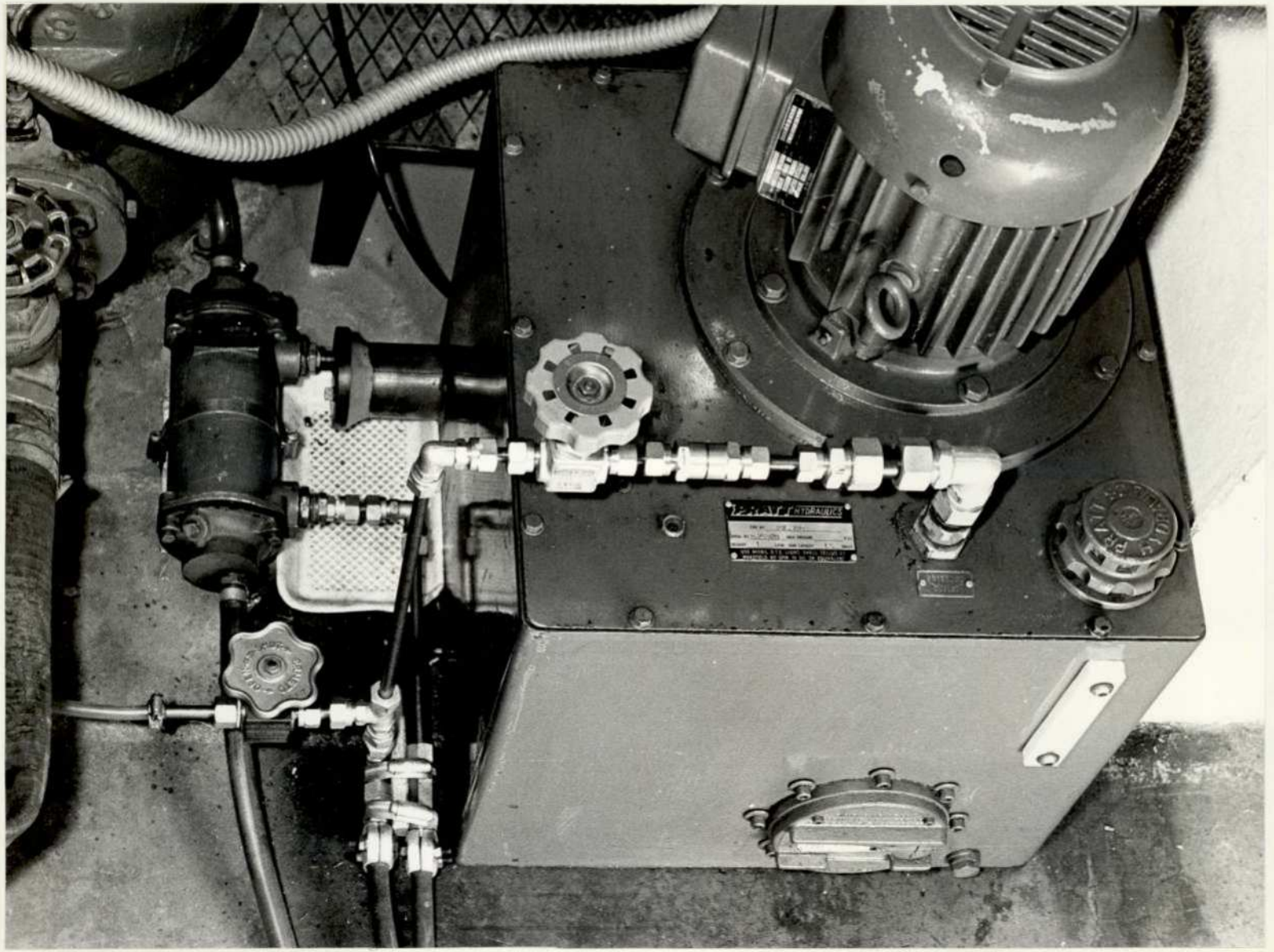


FIG 108 VIEW OF HYDRAULIC POWER SUPPLY AND ANCILLIARY EQUIPMENT





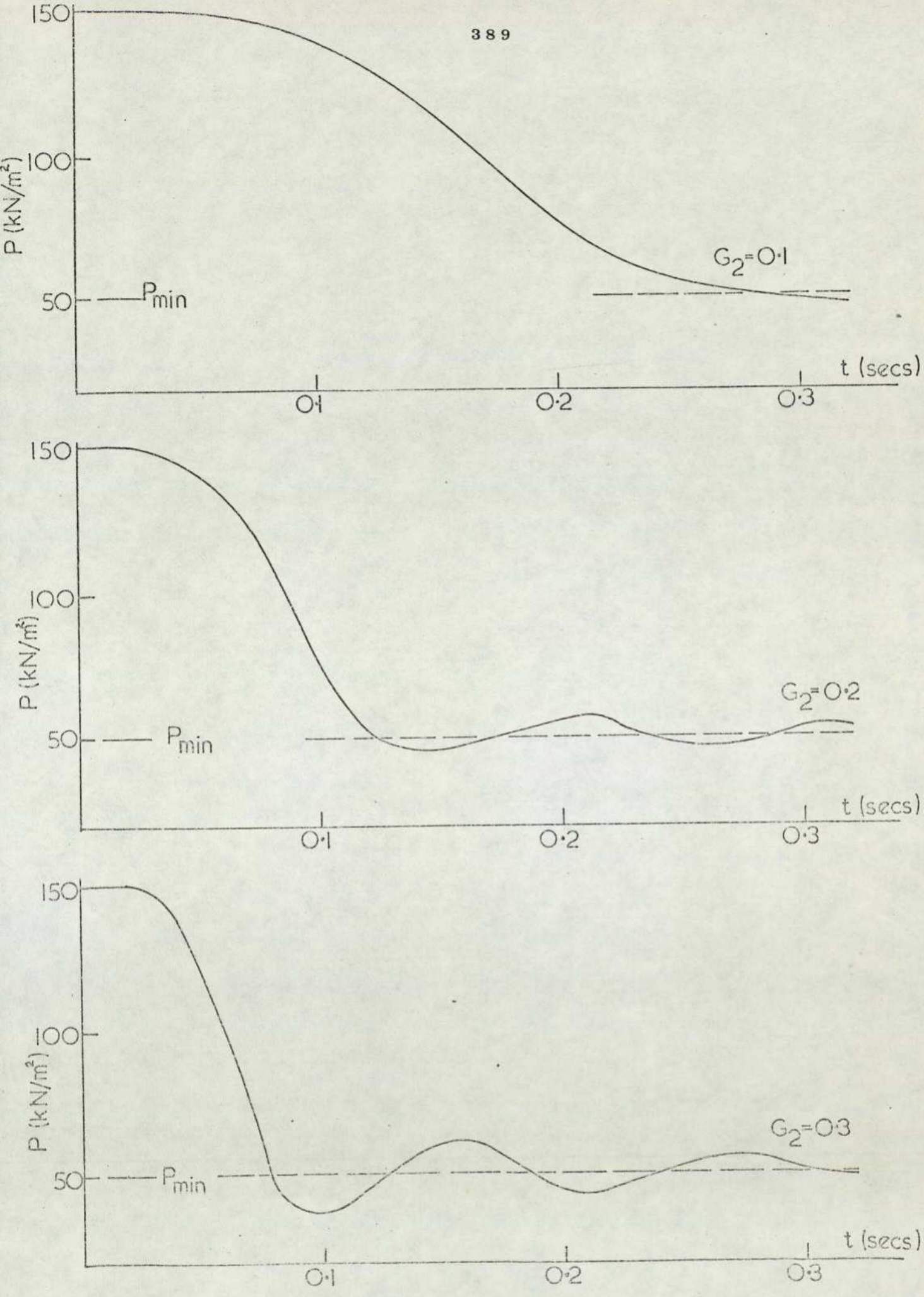


FIG 109 SERVO PERFORMANCE FOR VARIABLE LOOP GAIN

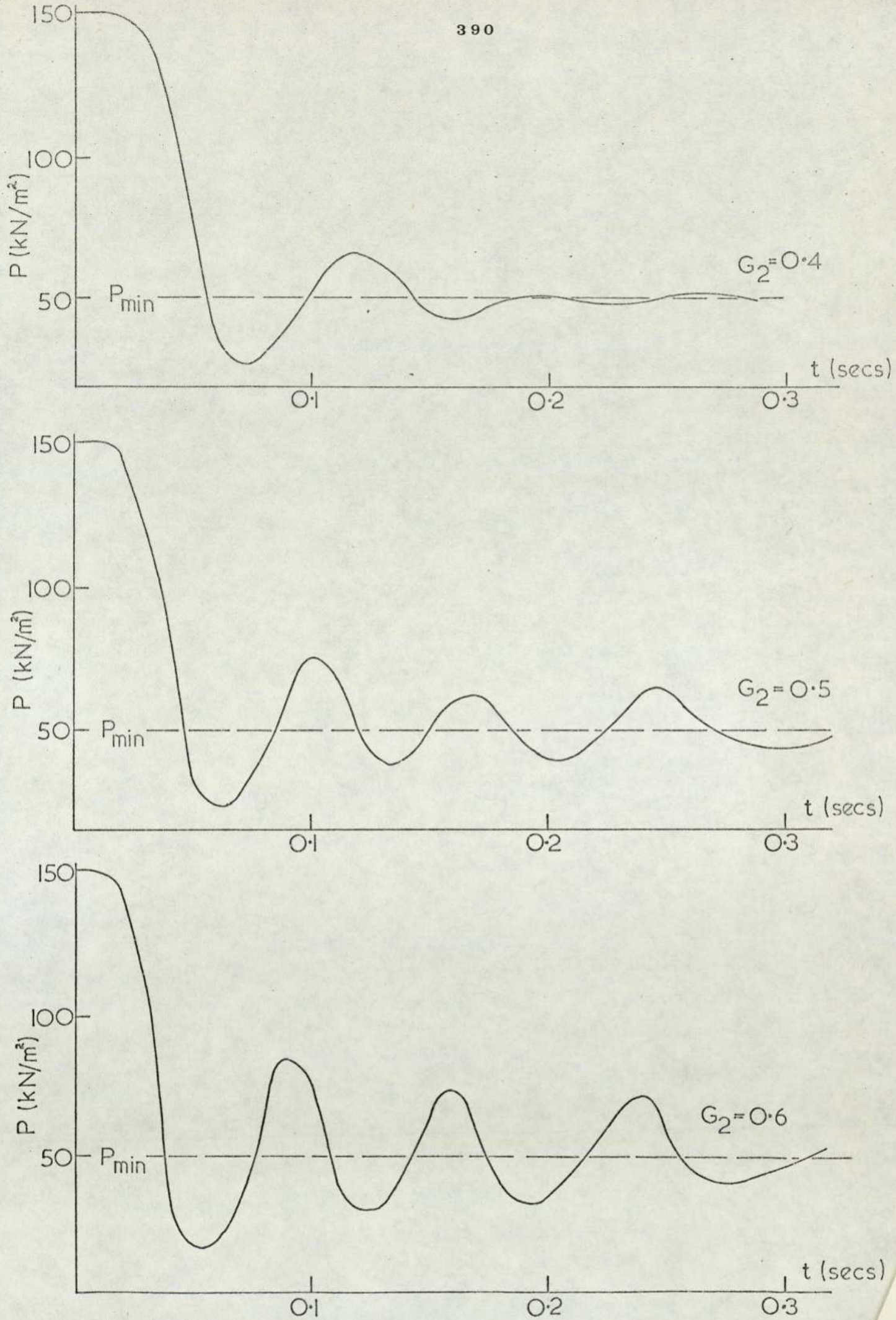


FIG 109 CONTINUED

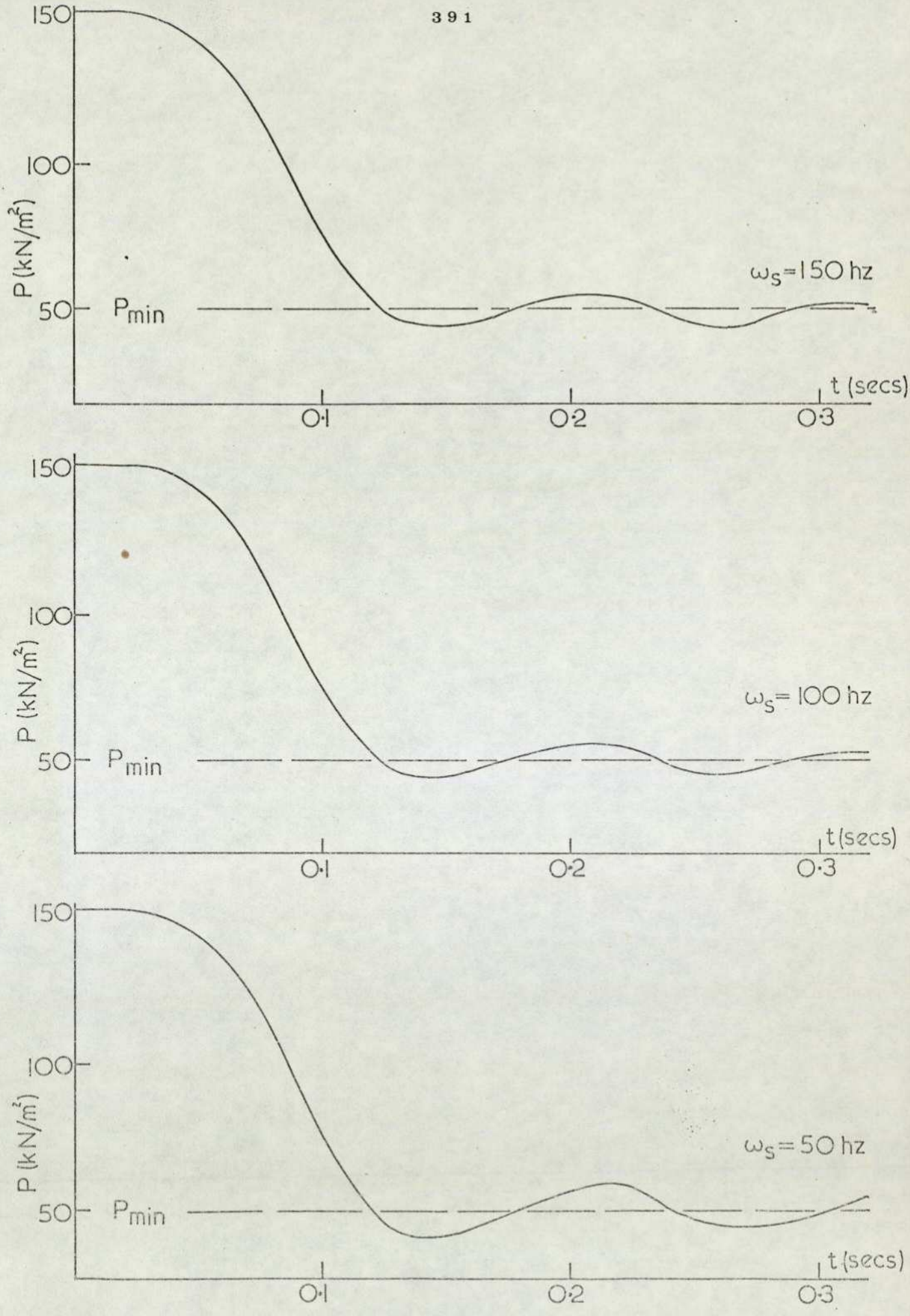


FIG 110 CONTROL SYSTEM PERFORMANCE FOR VARIABLE SERVO VALVE BANDWIDTH

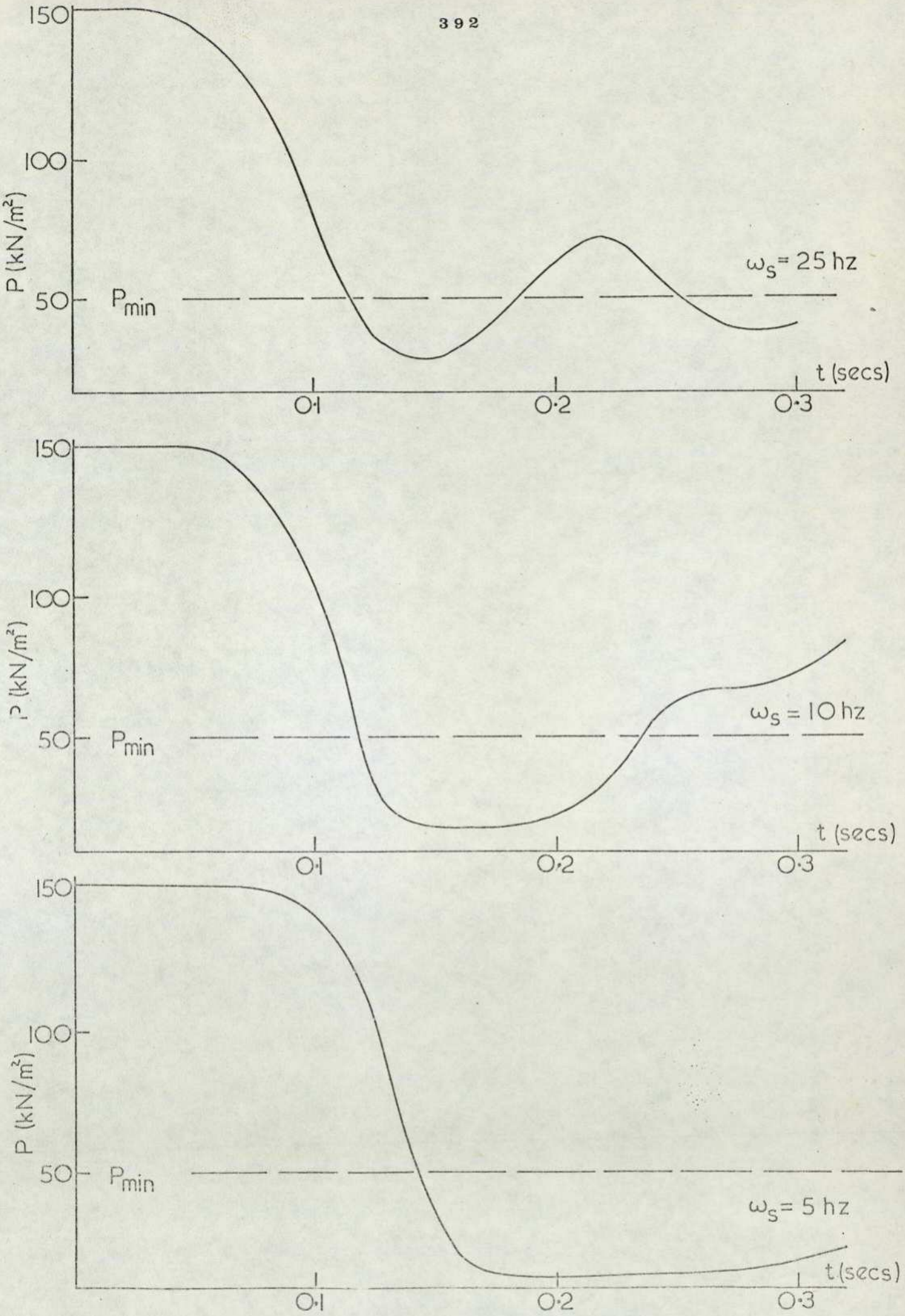


FIG 110 CONTINUED

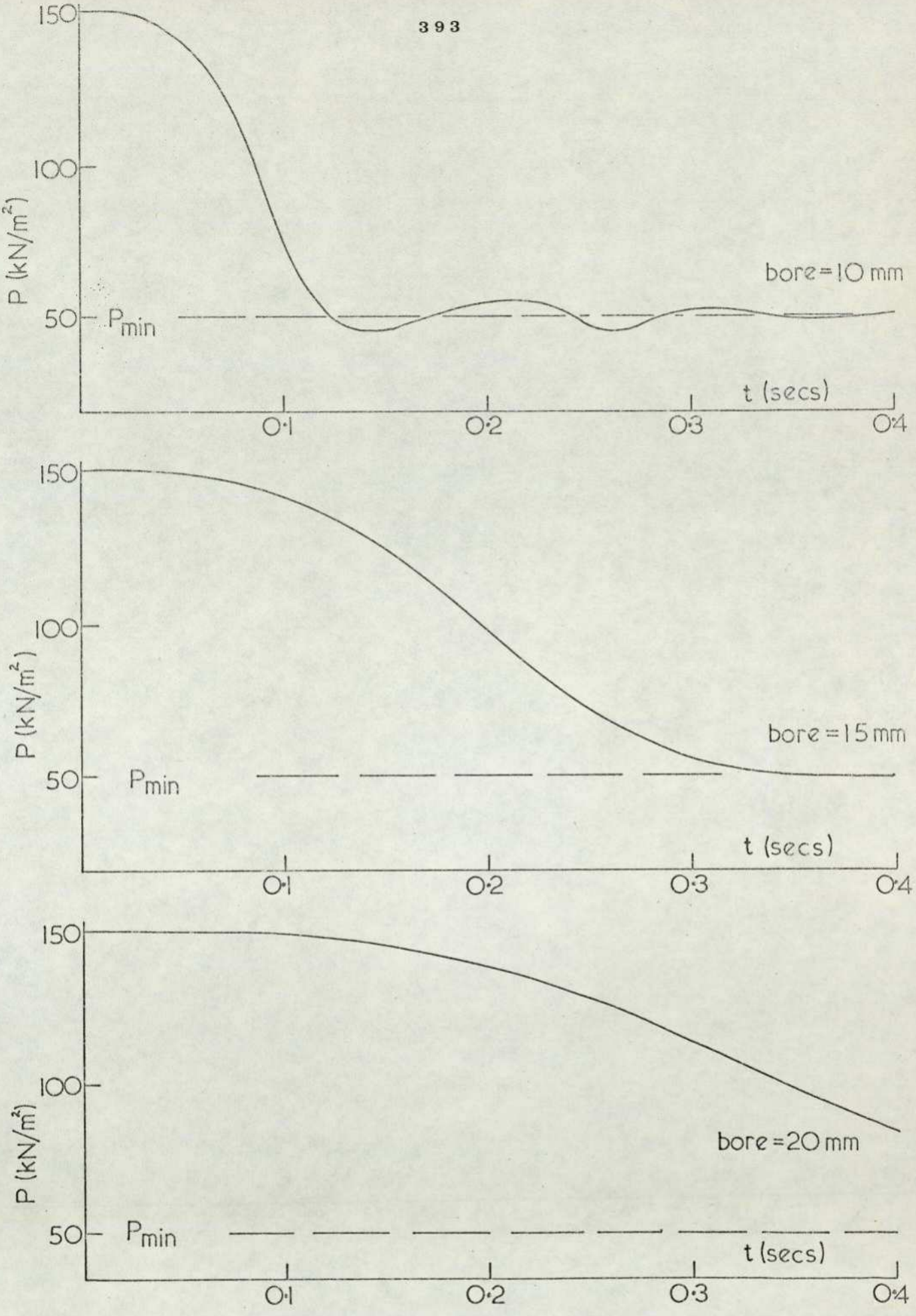


FIG 111 CONTROL SYSTEM PERFORMANCE FOR VARIABLE ACTUATOR BORE DIAMETER

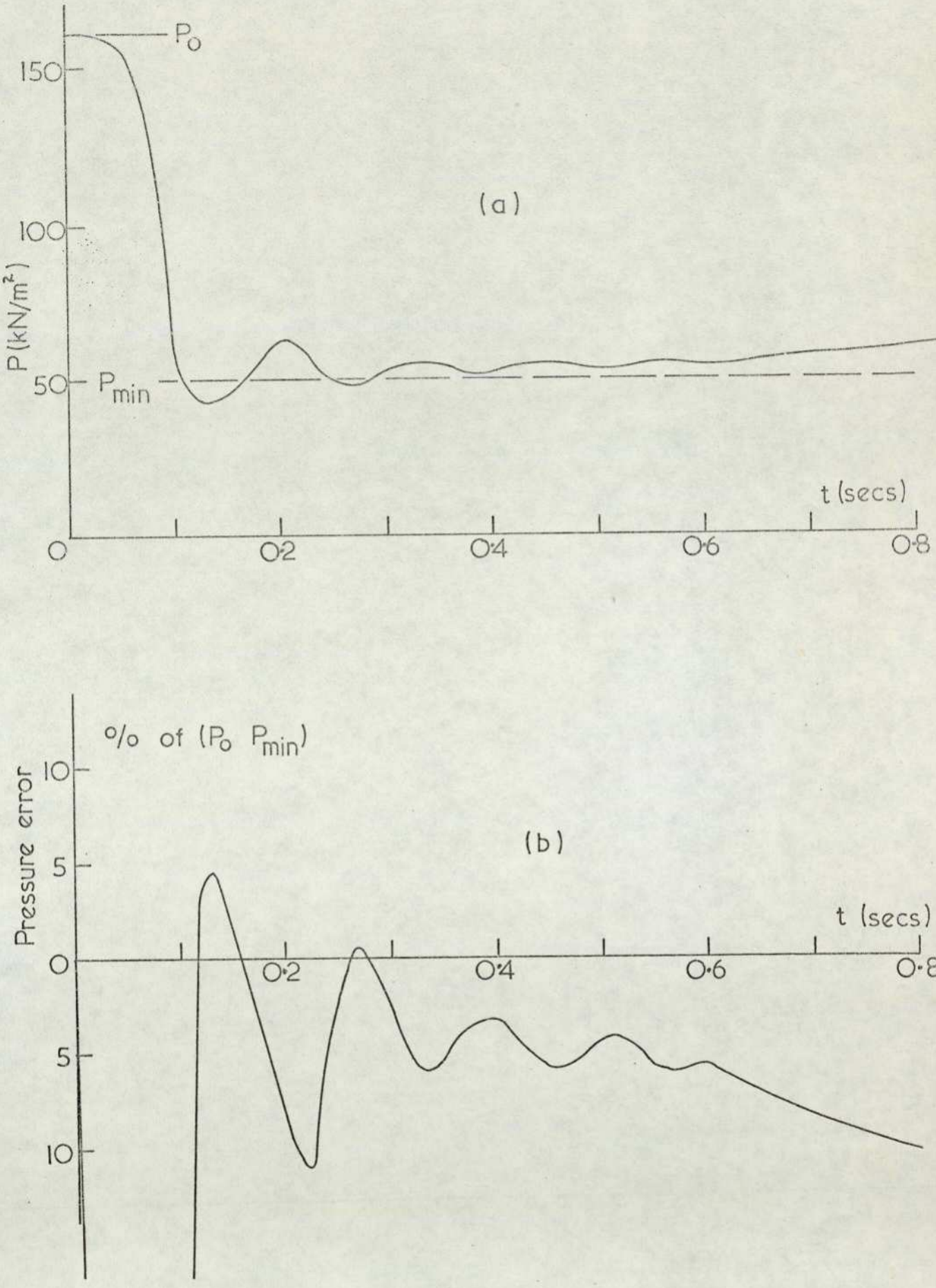


FIG 112 REPRESENTATIVE CONTROL LOOP PARAMETERS AS FORECAST BY PROGRAM VSP2

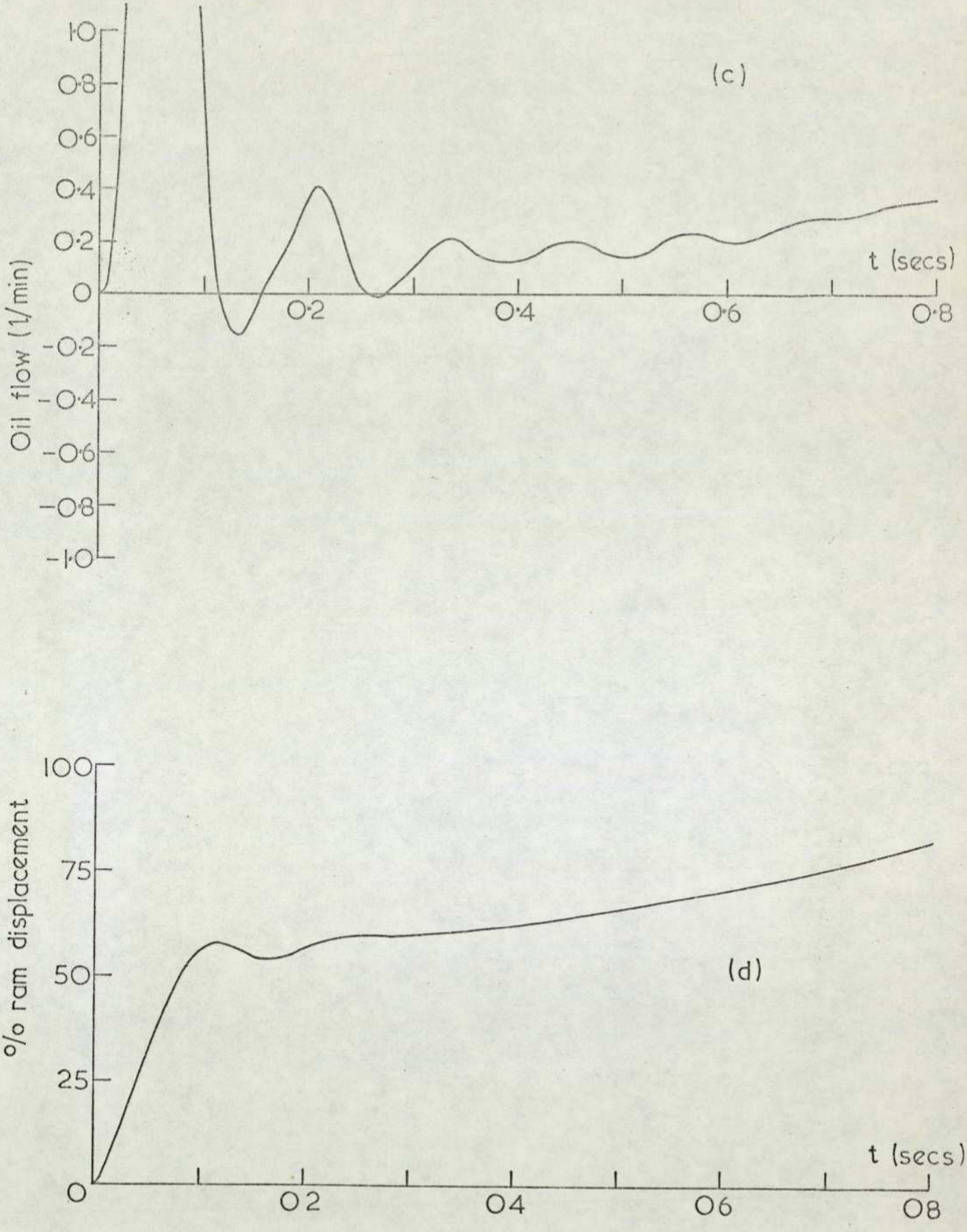
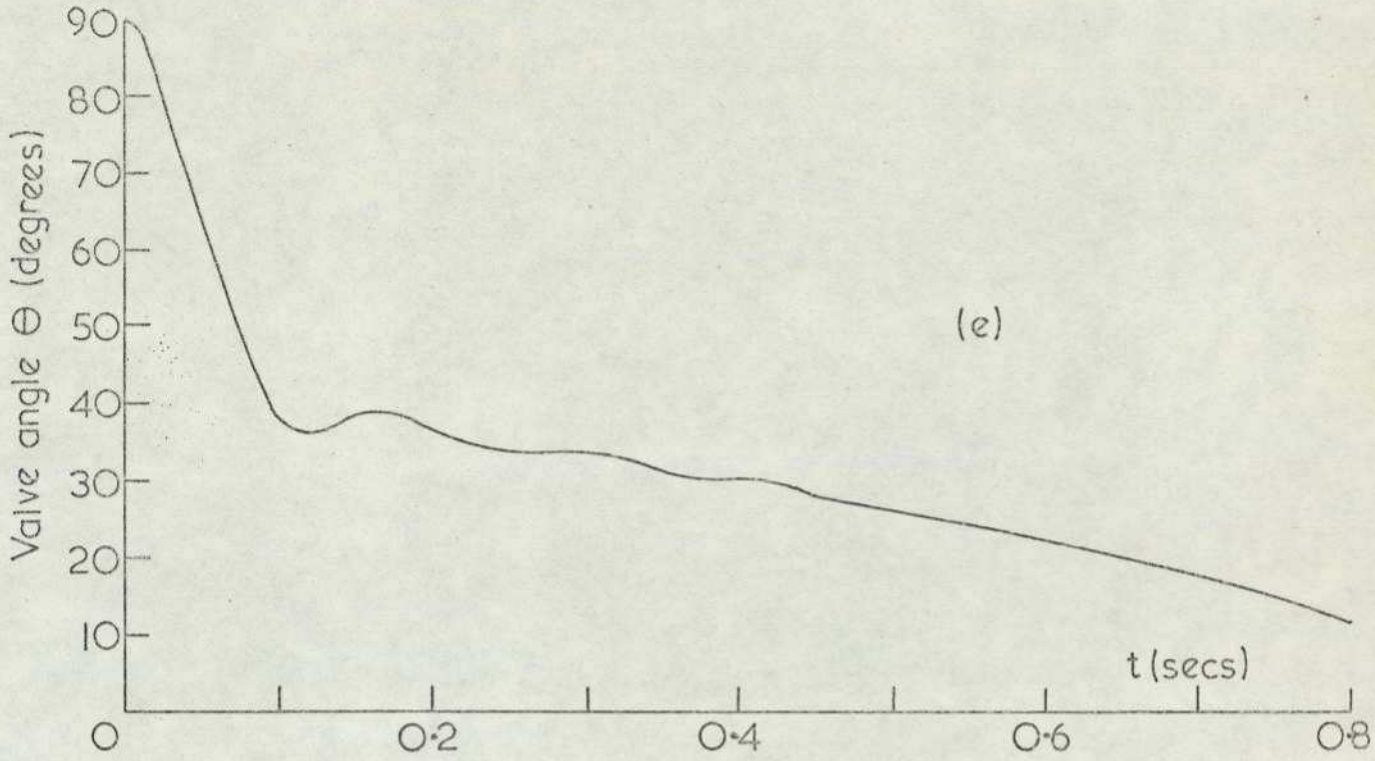


FIG 112 CONTINUED



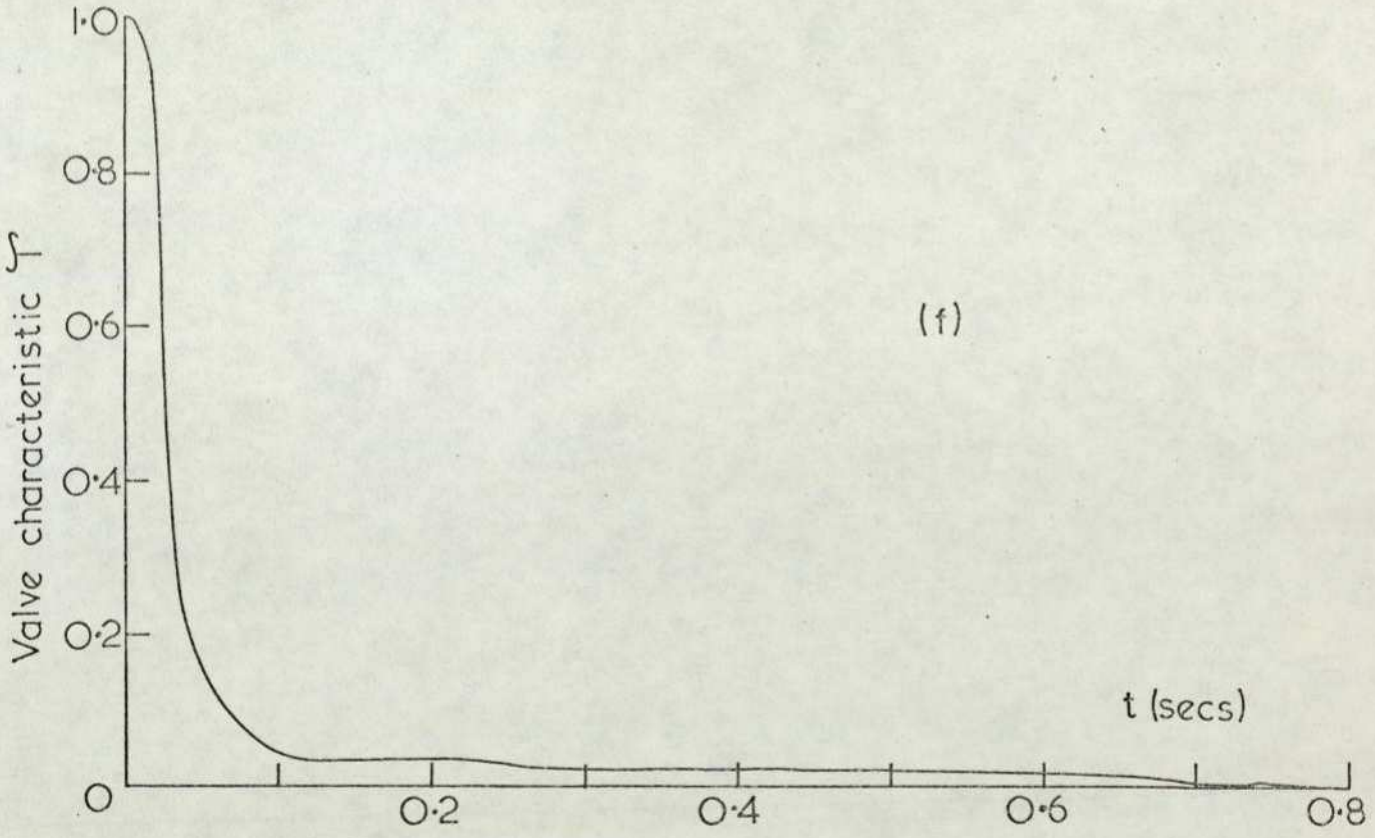


FIG 112 CONTINUED

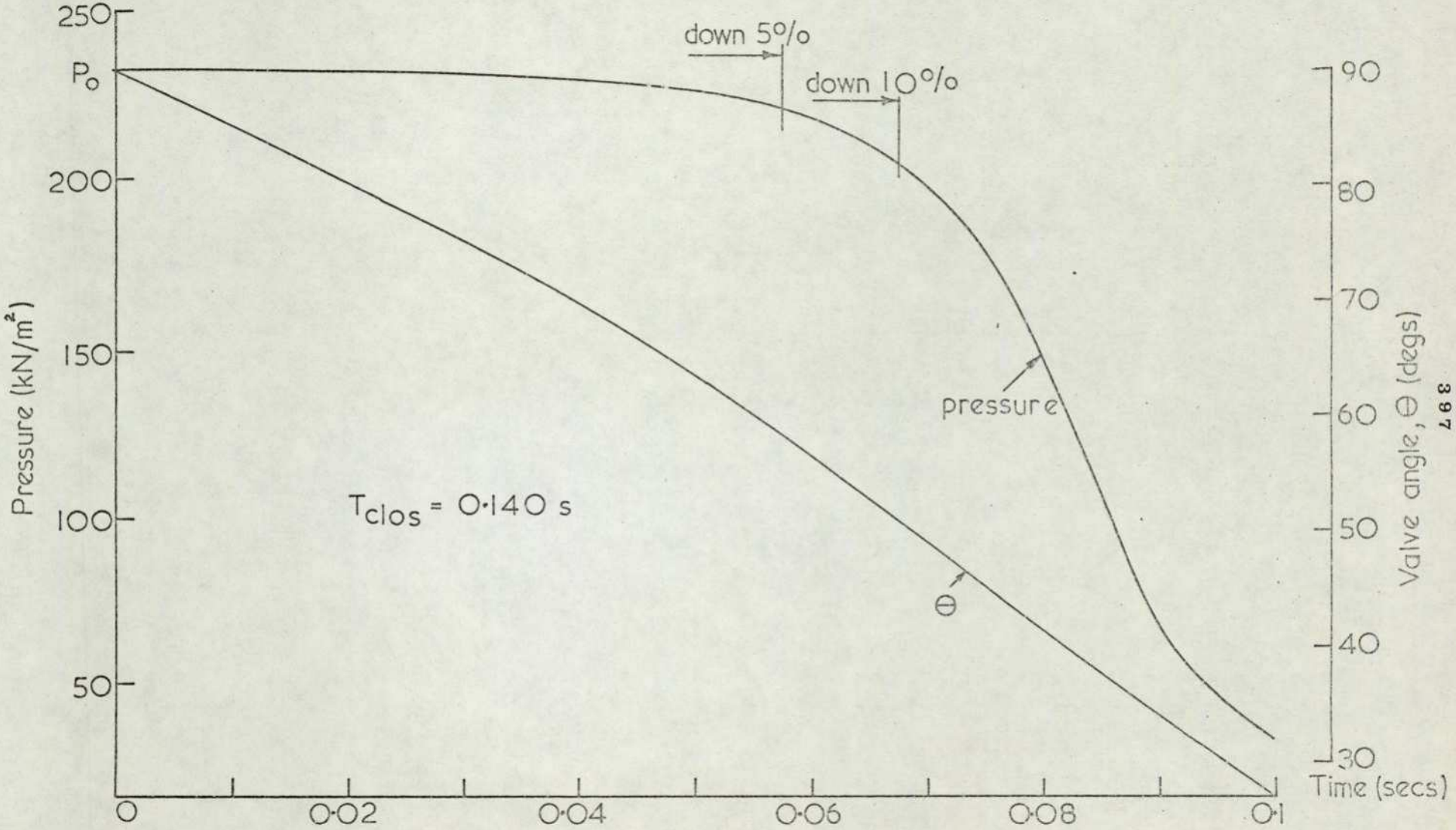


FIG 113 PREDICTED RATE OF PRESSURE DROP FOR LINEAR CLOSURE

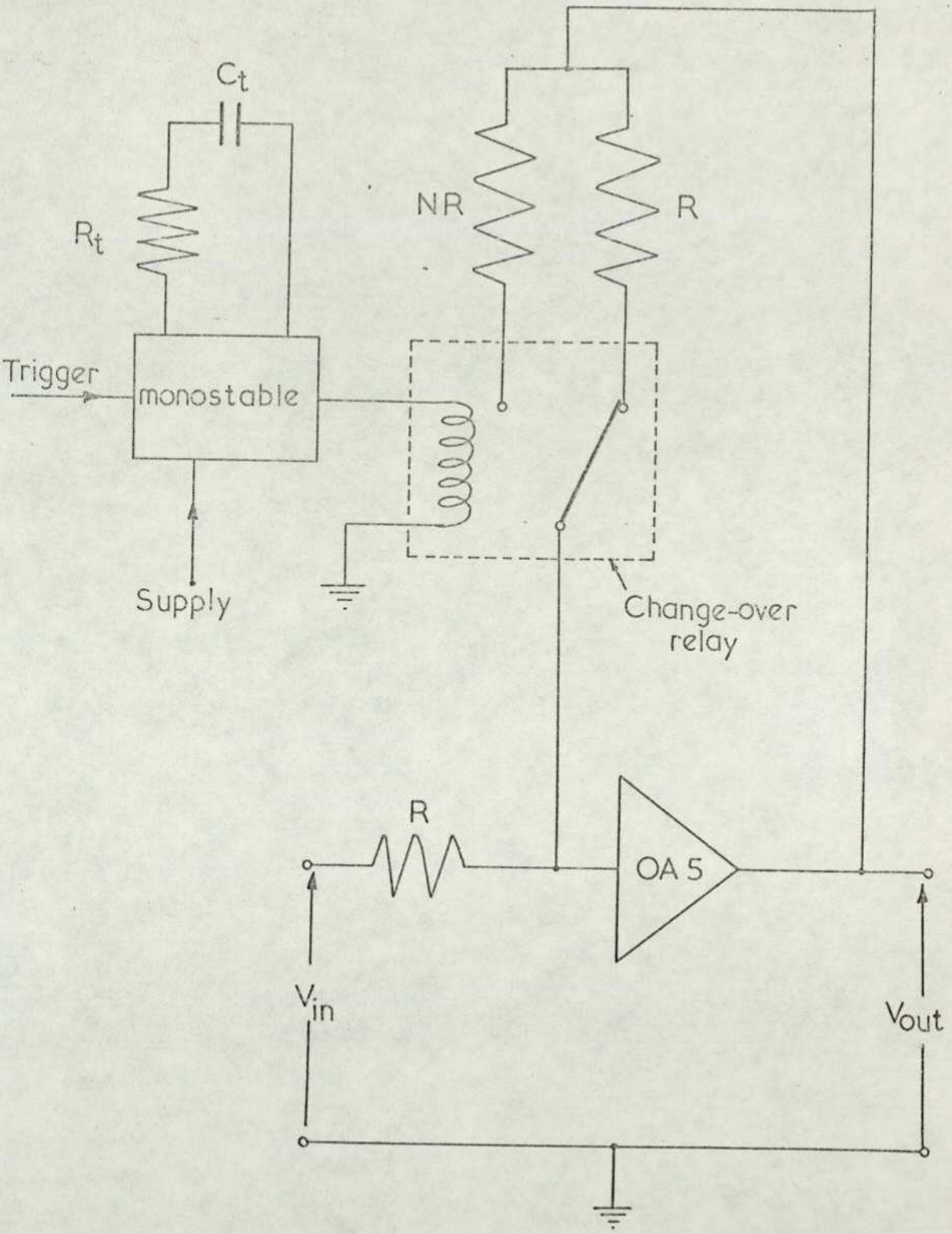


FIG 114 SUGGESTED METHOD FOR GAIN SWITCHING THE SERVO AMPLIFIER BY A FACTOR N

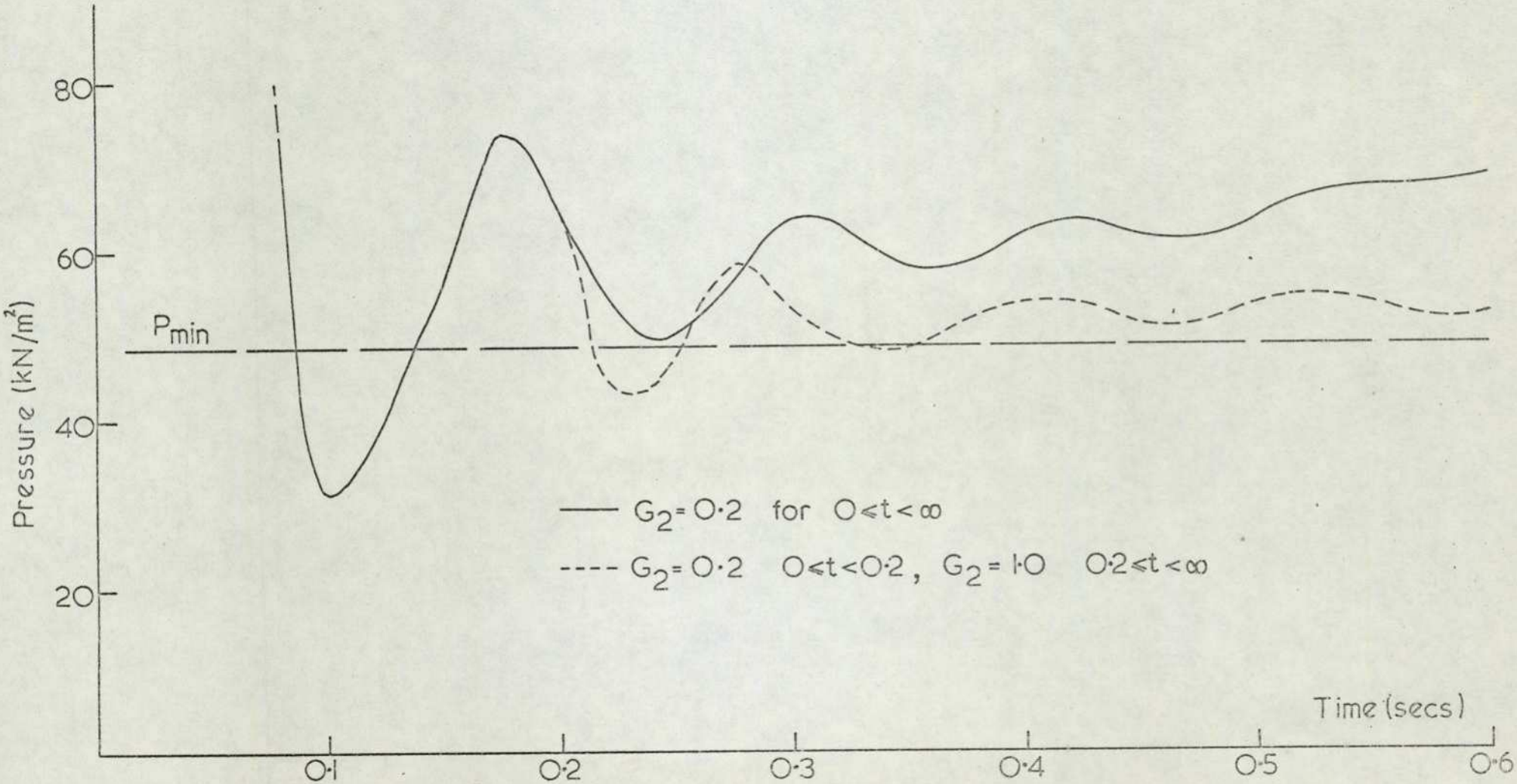


FIG 115 EFFECT OF GAIN SWITCHING ON PRESSURE CONTROL SYSTEM

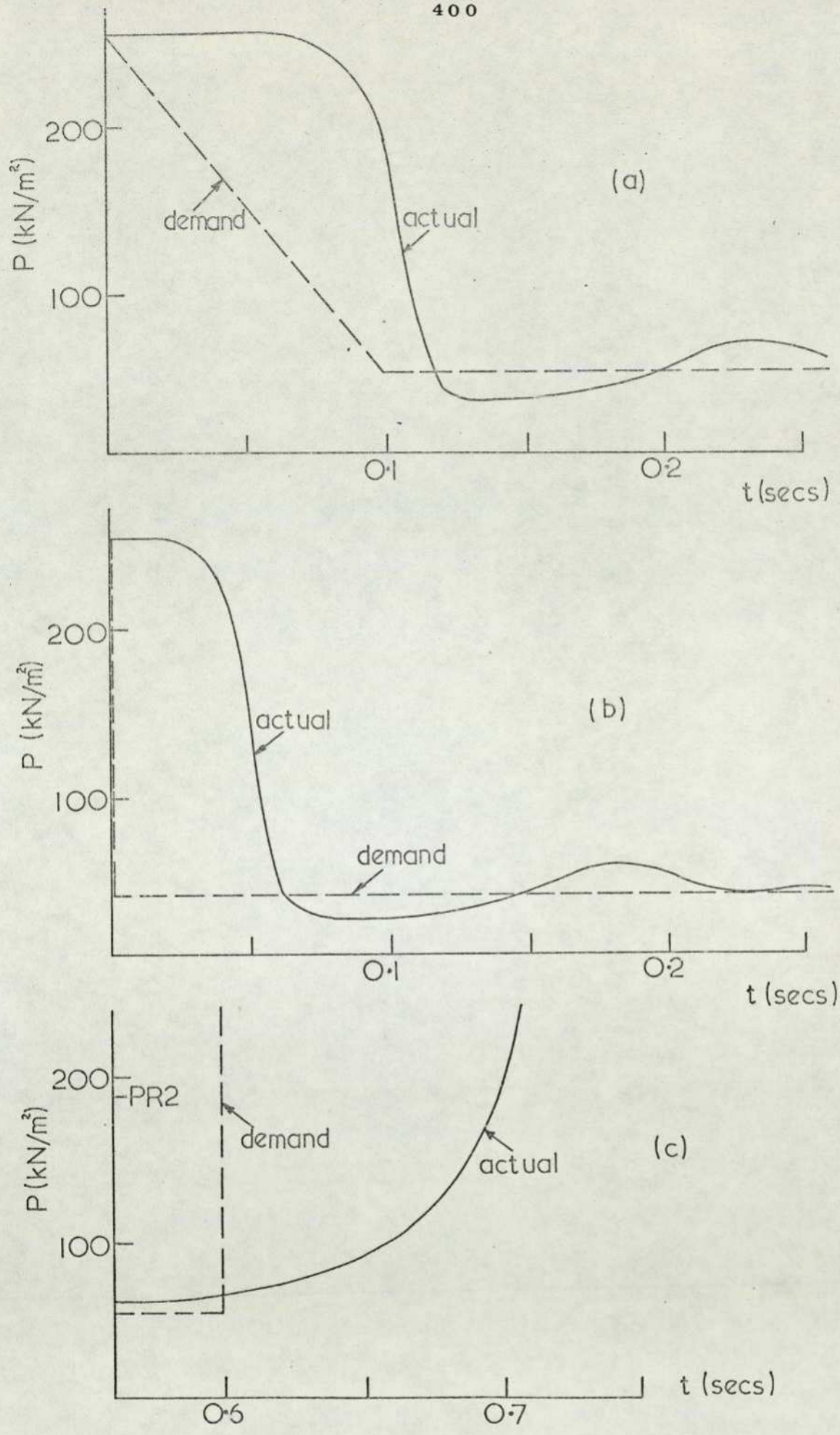


FIG 116 RESPONSE OF SYSTEM TO VARIOUS INPUTS

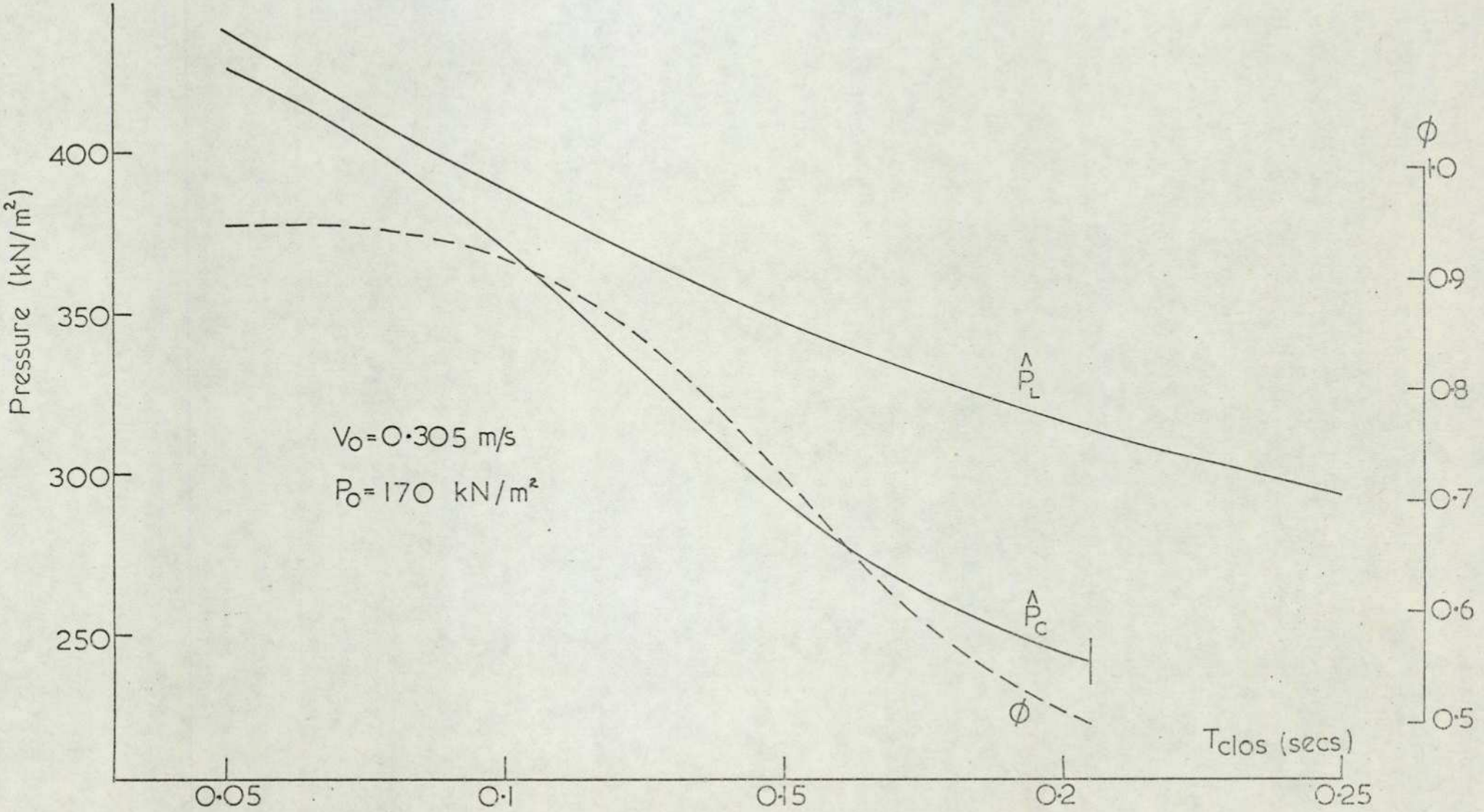


FIG 117 METHOD No. 3 FOR G_2 = 0·2 & P_{min} = 34·3 kN/m²

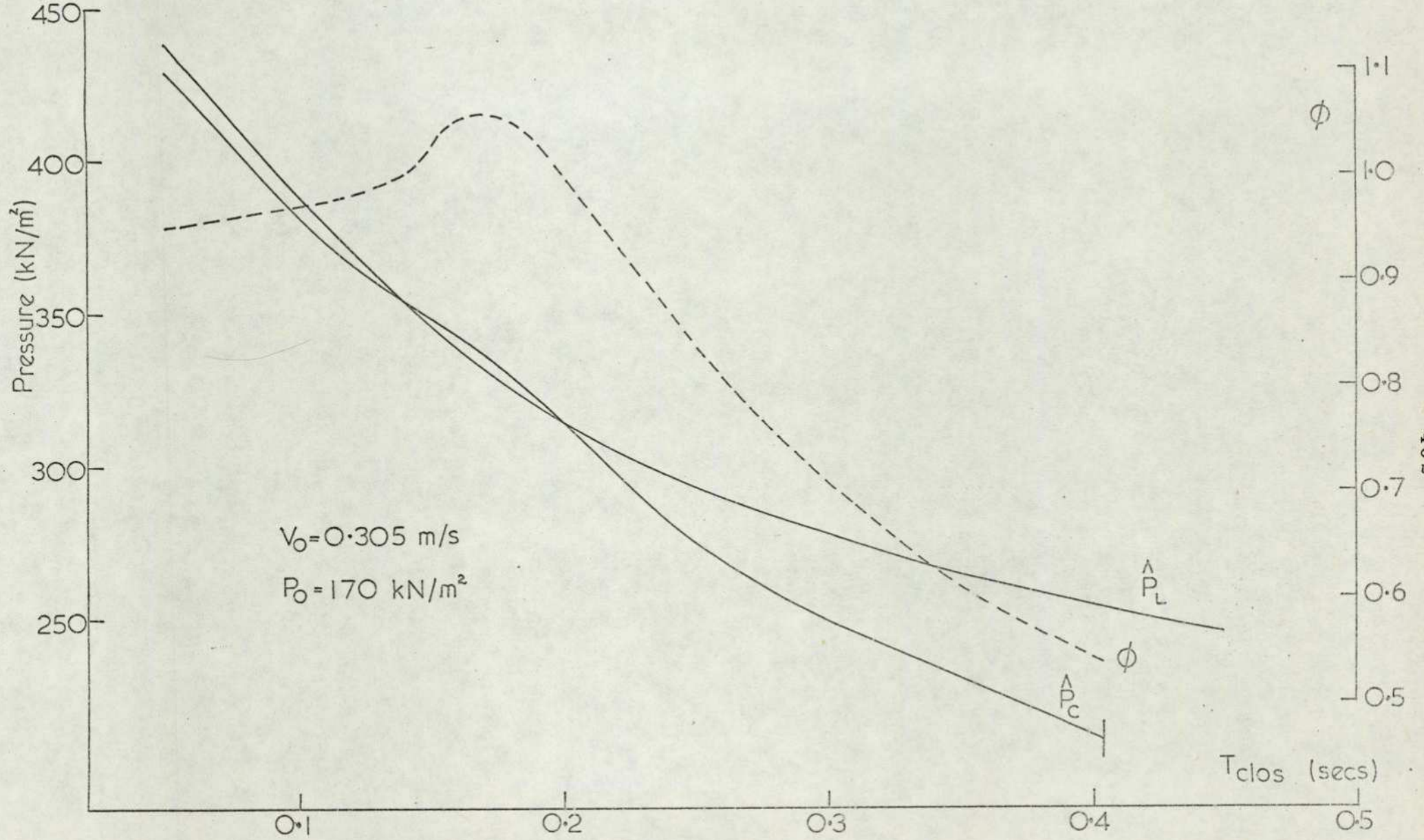


FIG 118 METHOD No. 3 FOR $G_2 = 0{\cdot}2$ & $P_{min} = 103$ kN/m²

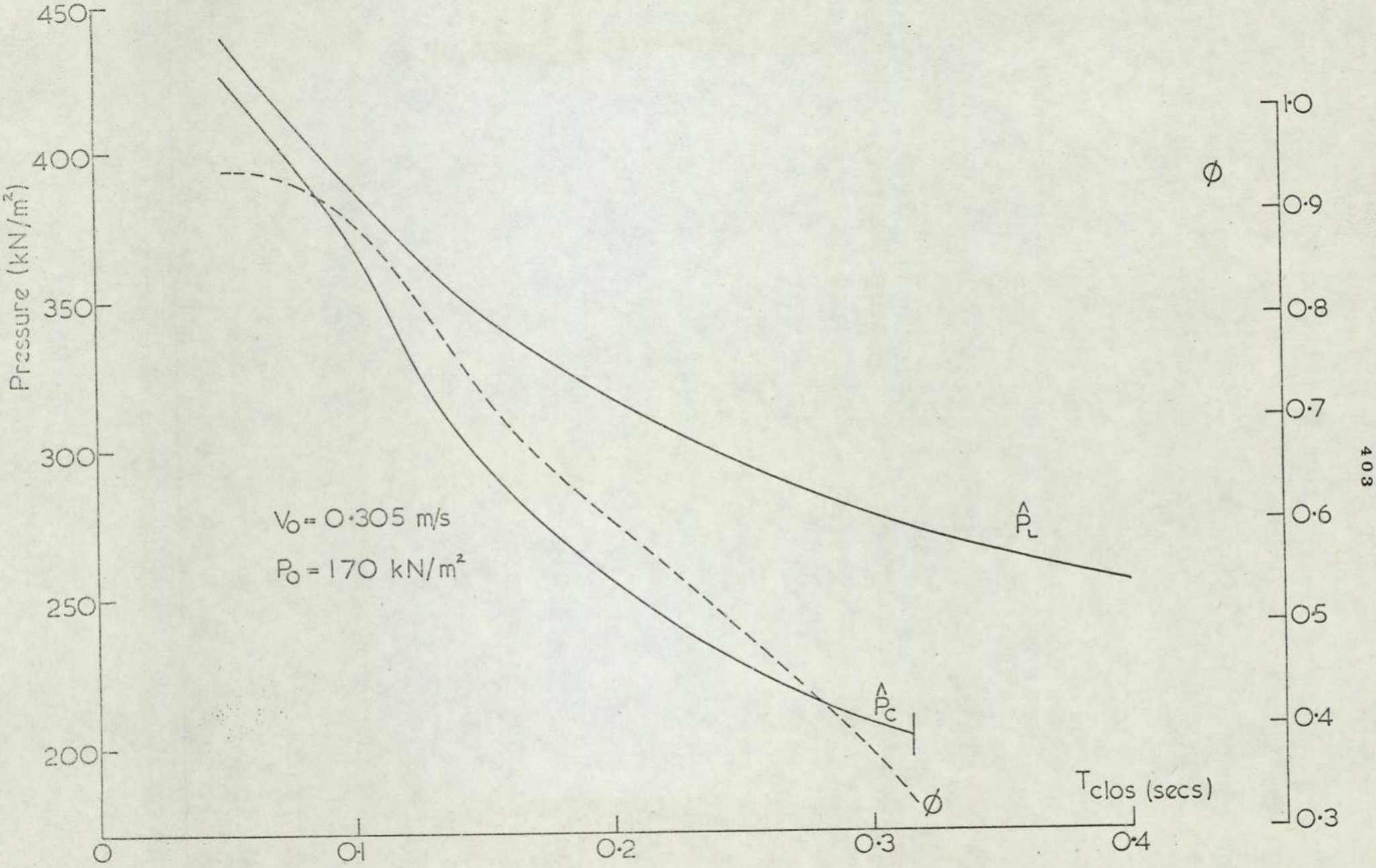


FIG 119 METHOD No. 3 FOR G_2=0·6 & P_{min}=103 kN/m²

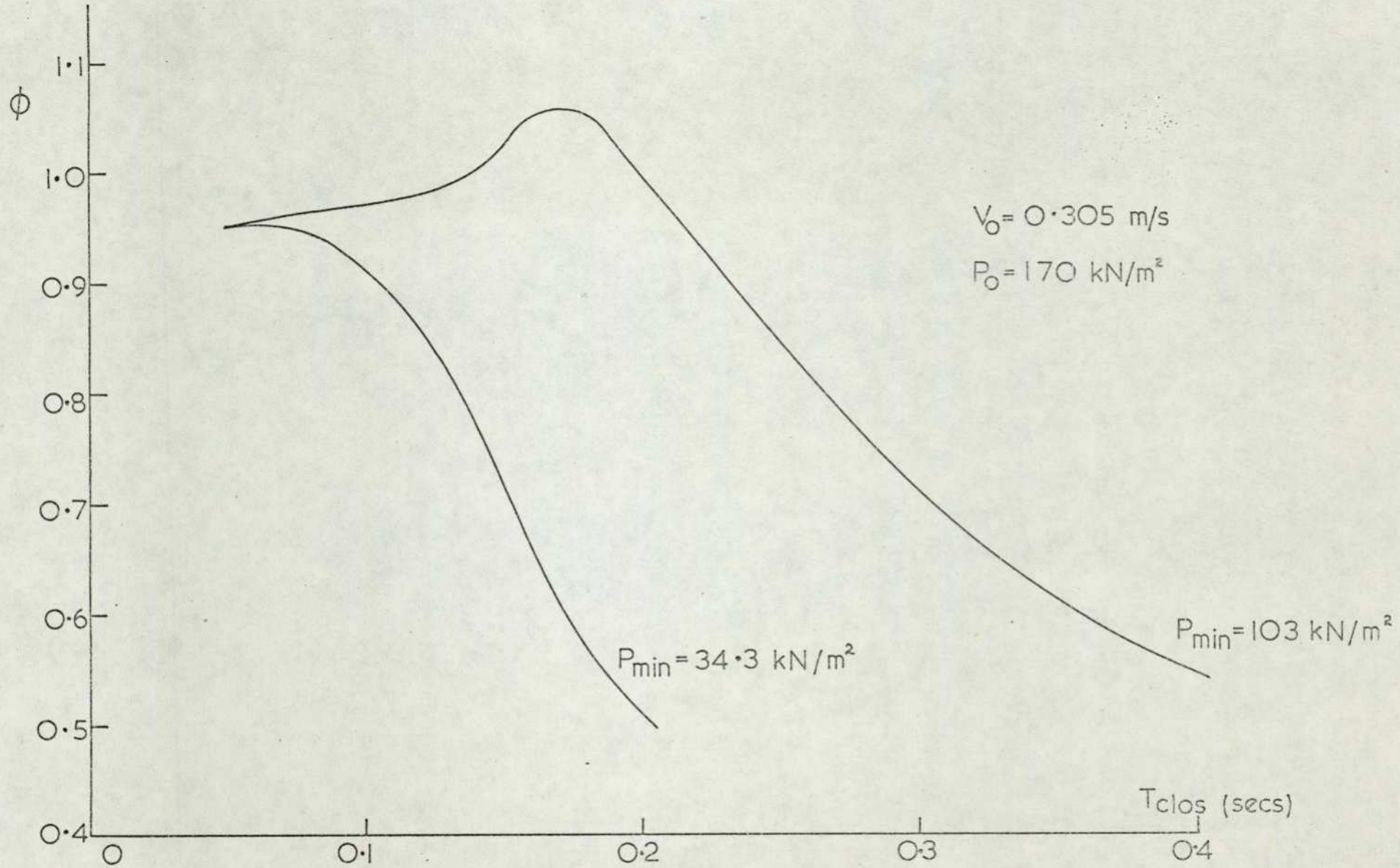


FIG 120 PREDICTED EFFECT ON Ø OF VARYING P_{min} ONLY

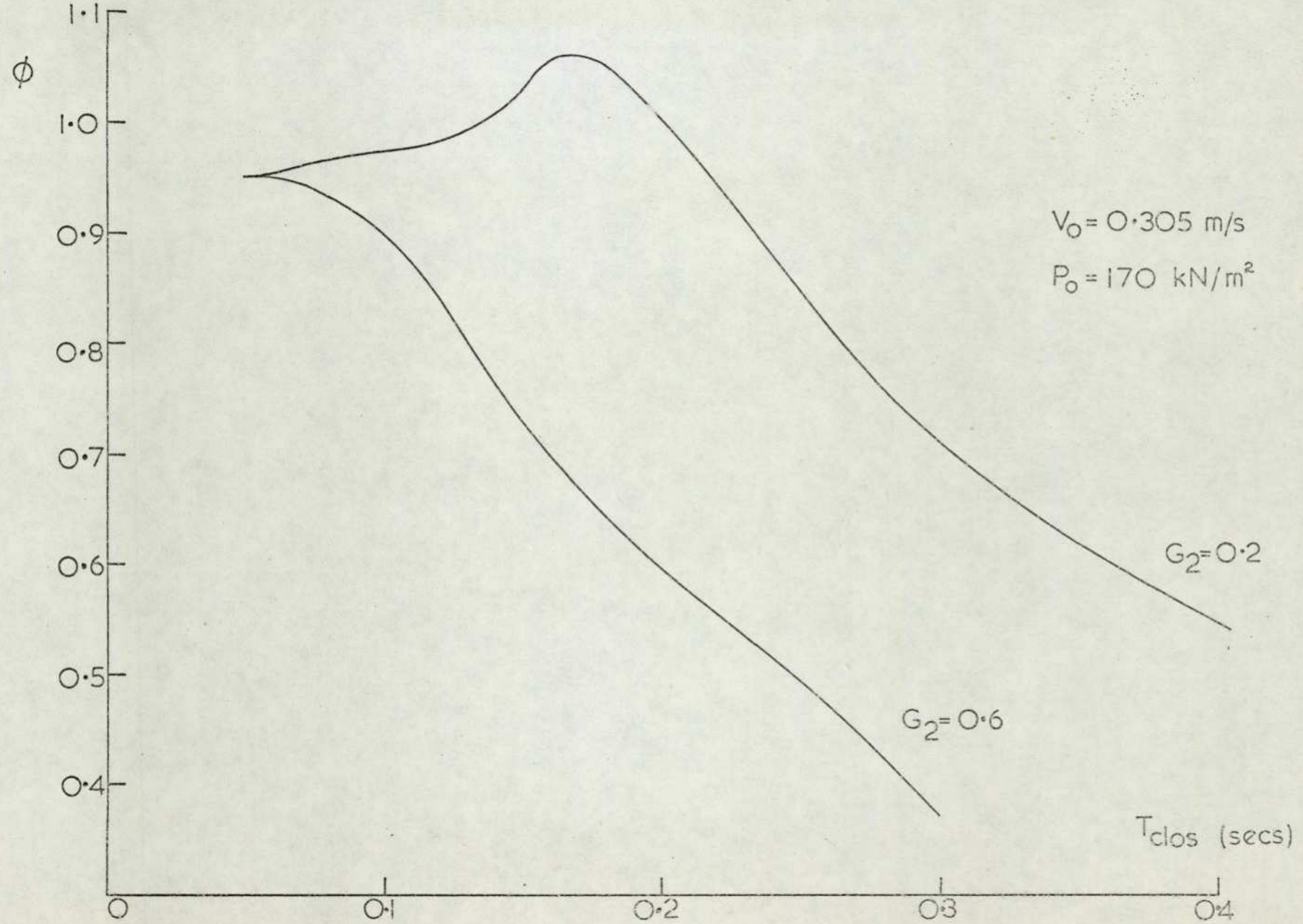


FIG 121 PREDICTED EFFECT ON Φ OF VARYING G_2 ONLY

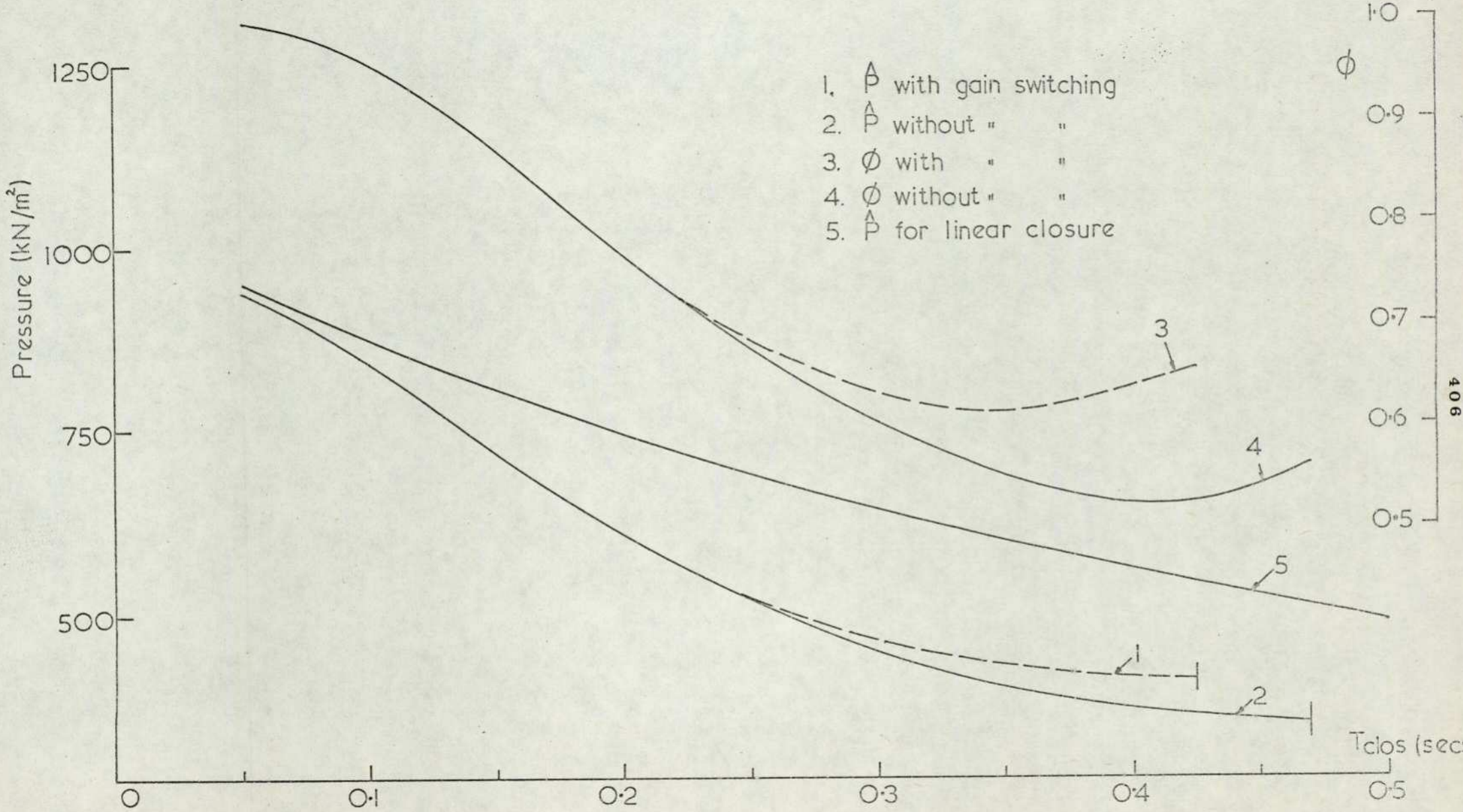


FIG 122 PREDICTED EFFECT OF GAIN SWITCHING ON METHOD No. 3

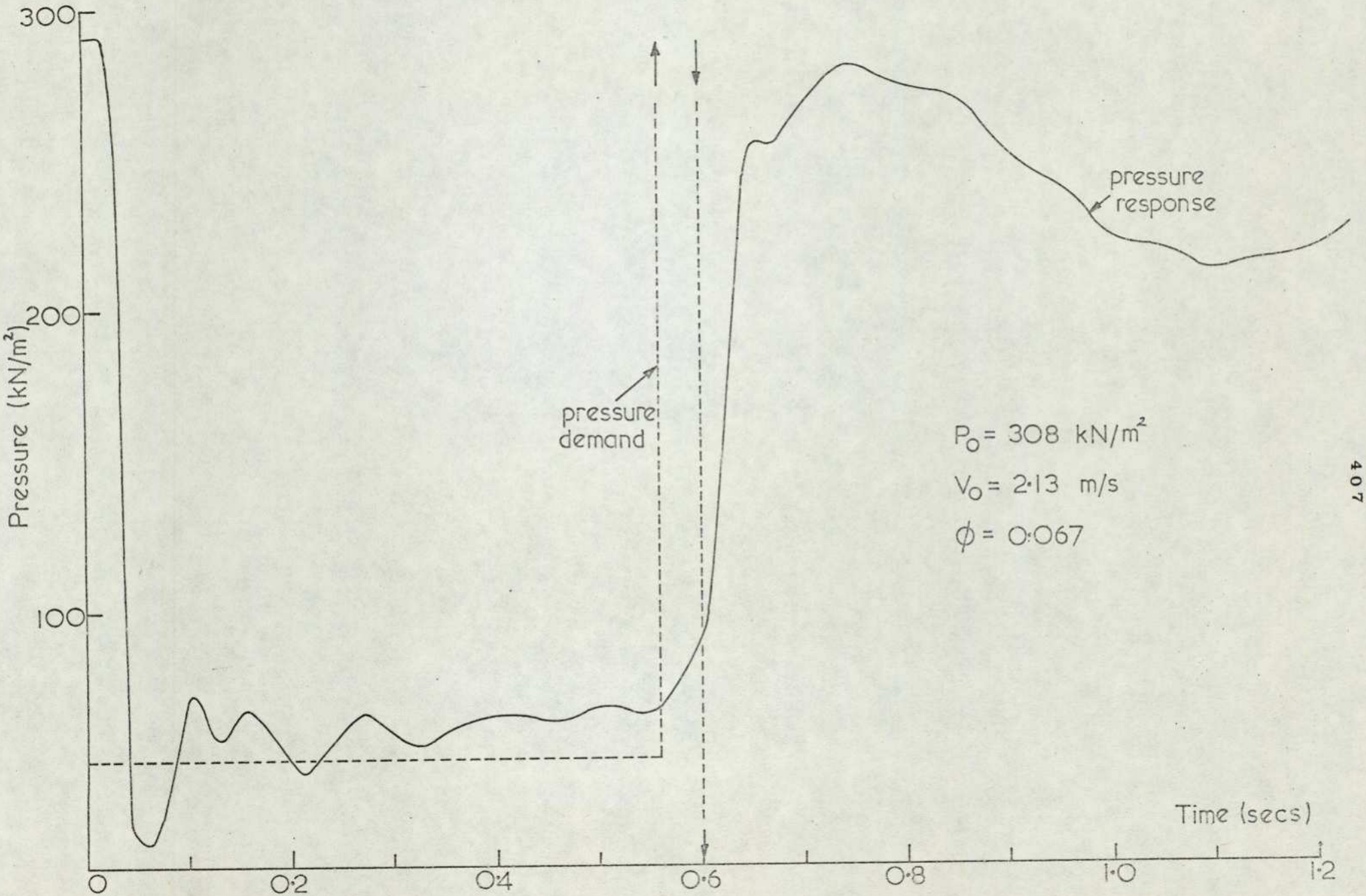


FIG 123 PRESSURE TIME FOR METHOD No. 2 AS PREDICTED BY VSP2

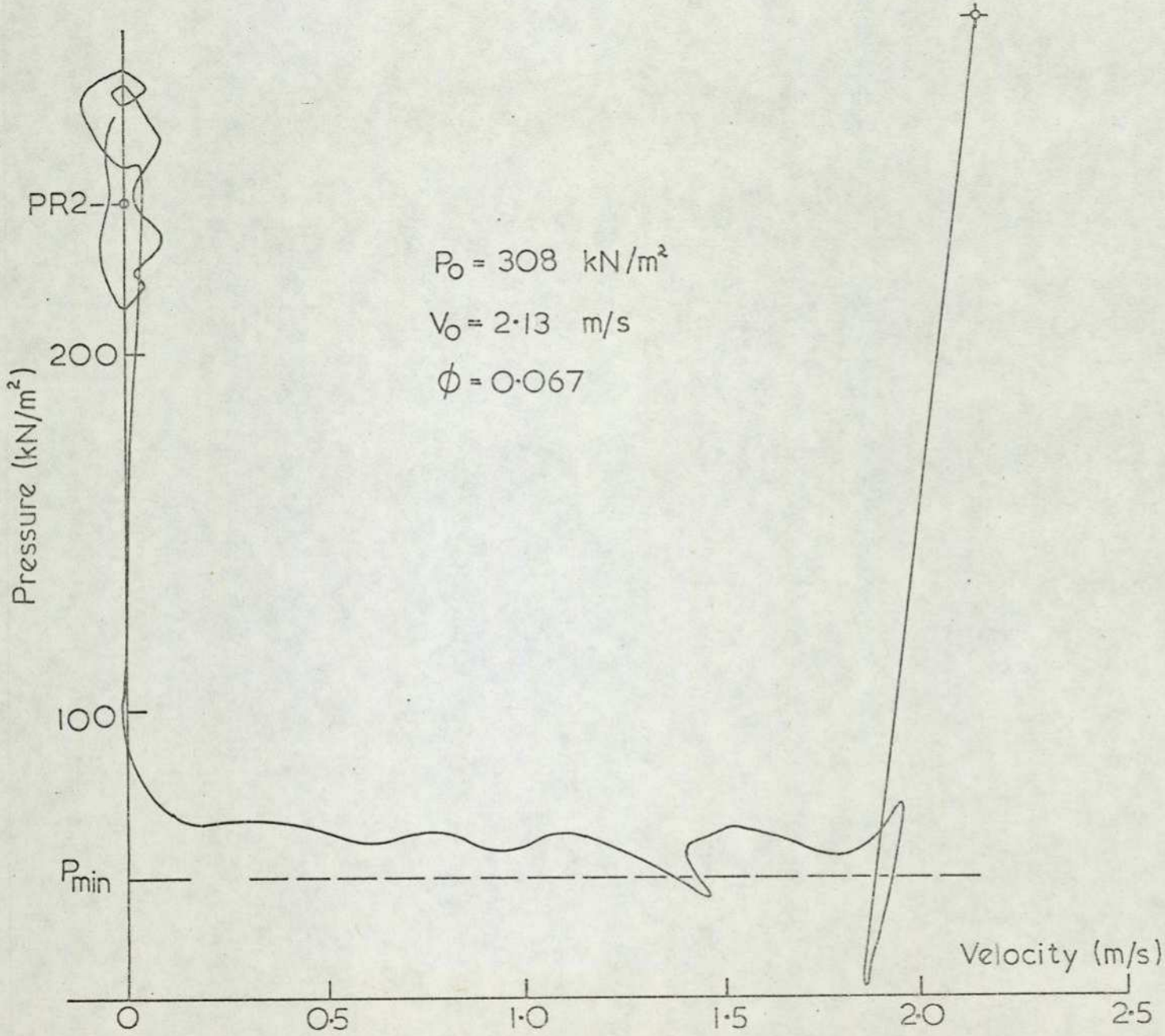


FIG 124 PRESSURE-VELOCITY DIAGRAM FOR METHOD No. 2 (AS PREDICTED)

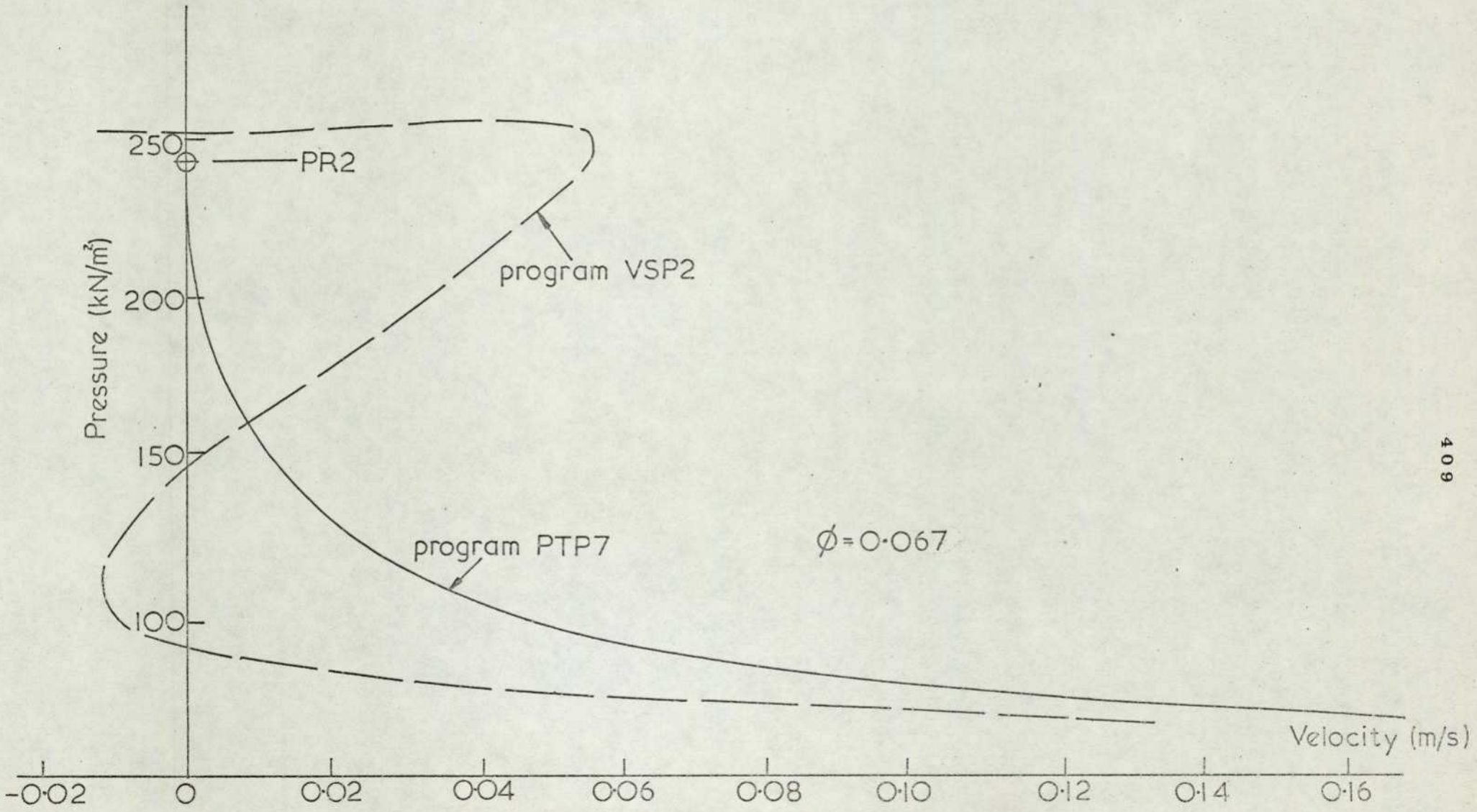


FIG 125 THEORETICAL INVESTIGATION OF METHOD No. 2

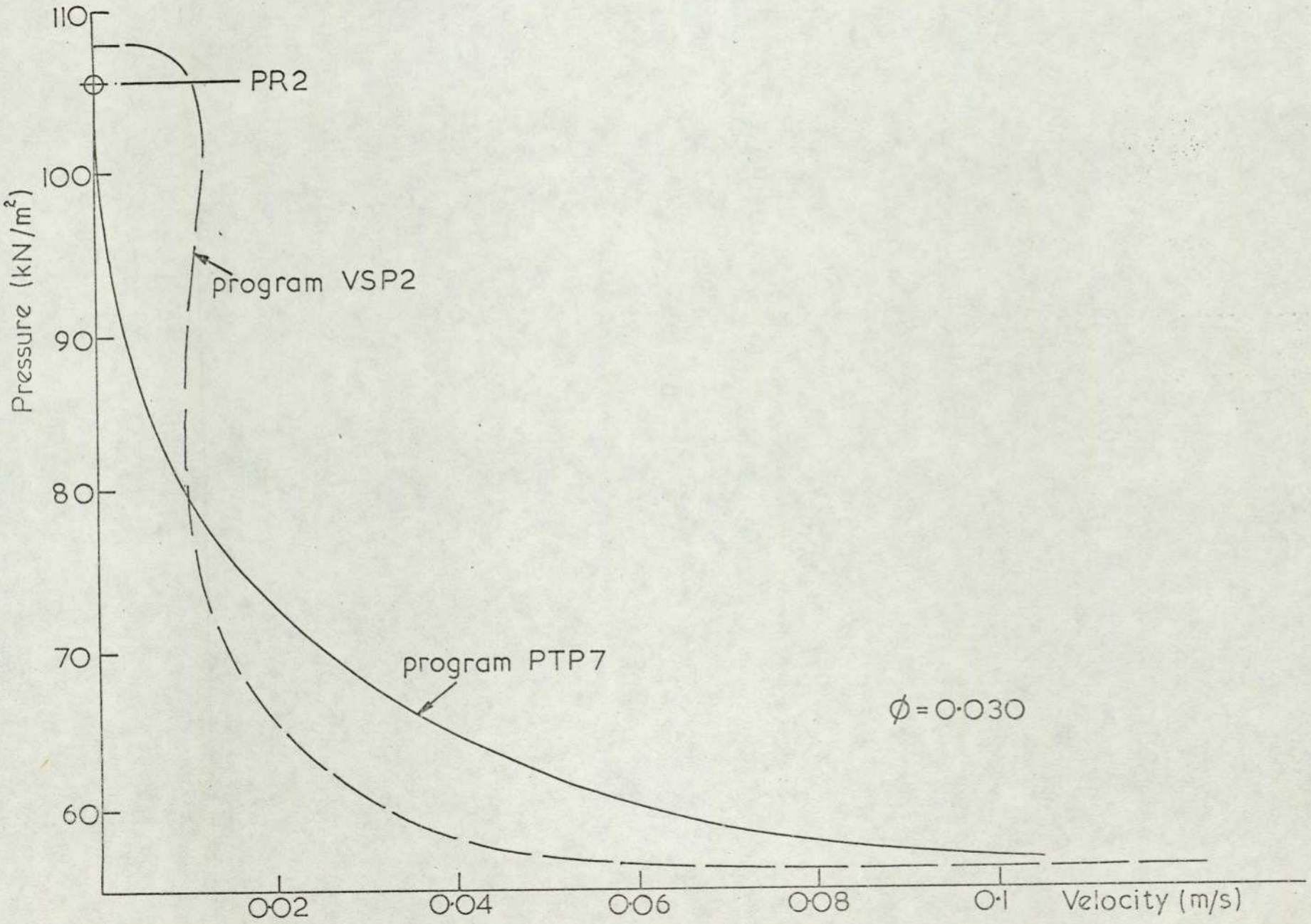


FIG 126 THEORETICAL INVESTIGATION OF METHOD No. 2

EXPERIMENTAL WORK-PRESENTATION OF RESULTS

For an explanation of figs 127-192 reference should be made to table 5, which defines the flow cases encountered: table 6 for the photographically recorded results and table 7 for the results recorded directly from the oscilloscope.

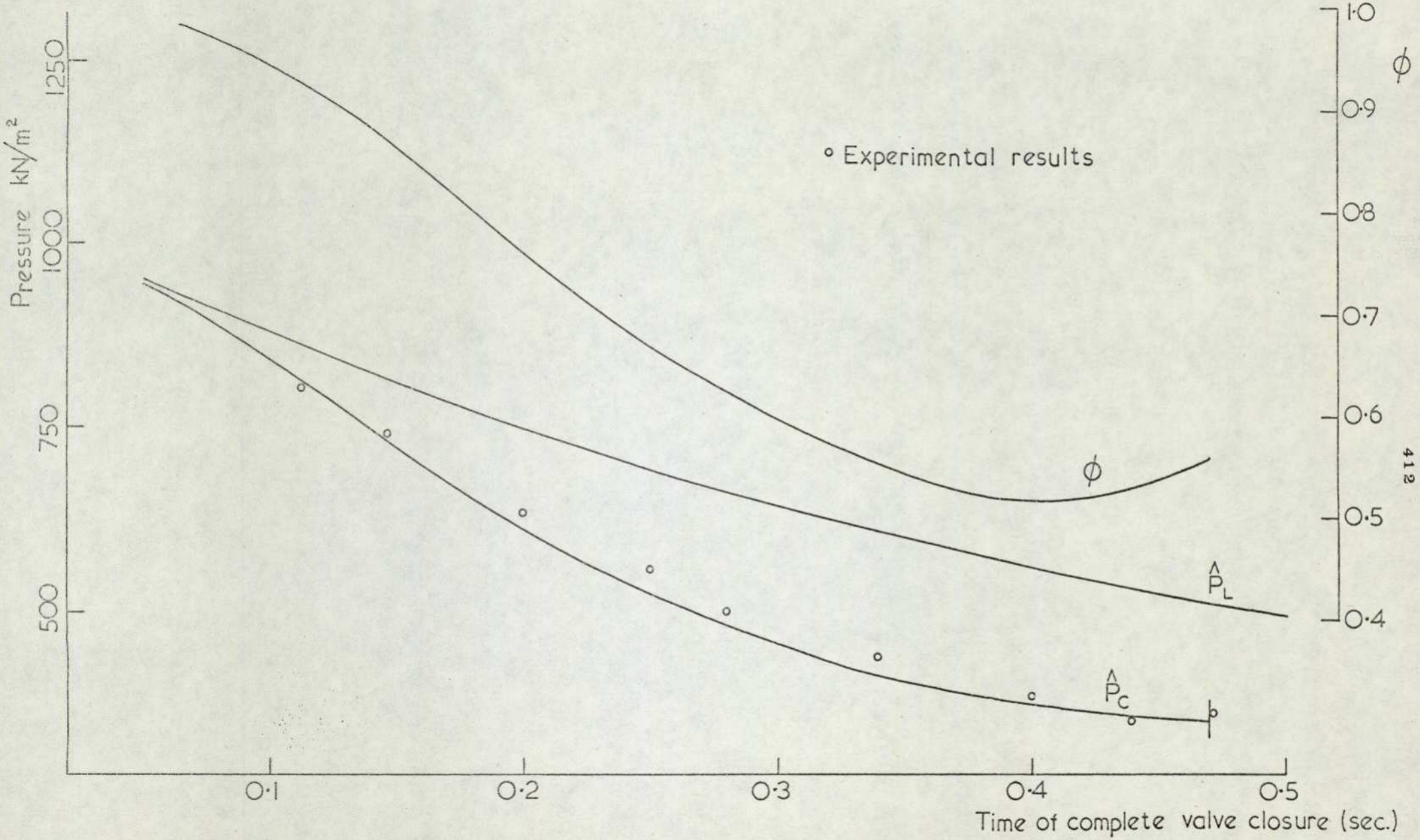


FIG 127 SUMMARY OF RESULTS - TEST CASE No.1

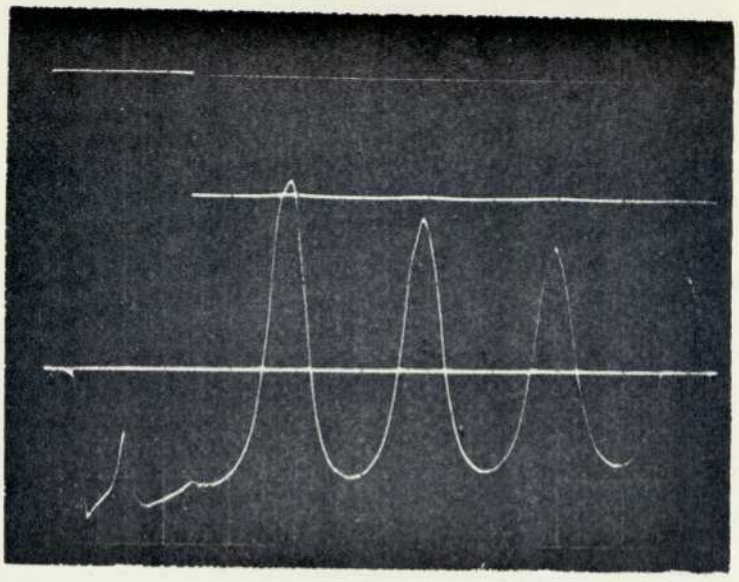


FIG 128

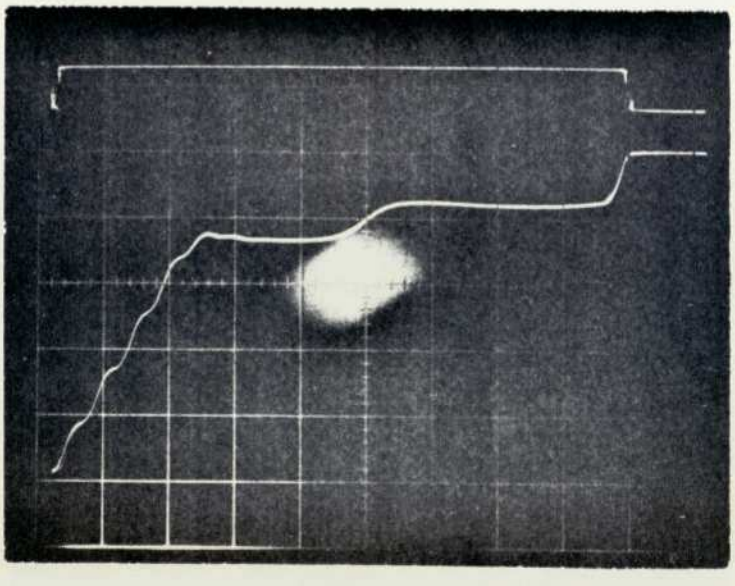


FIG 129

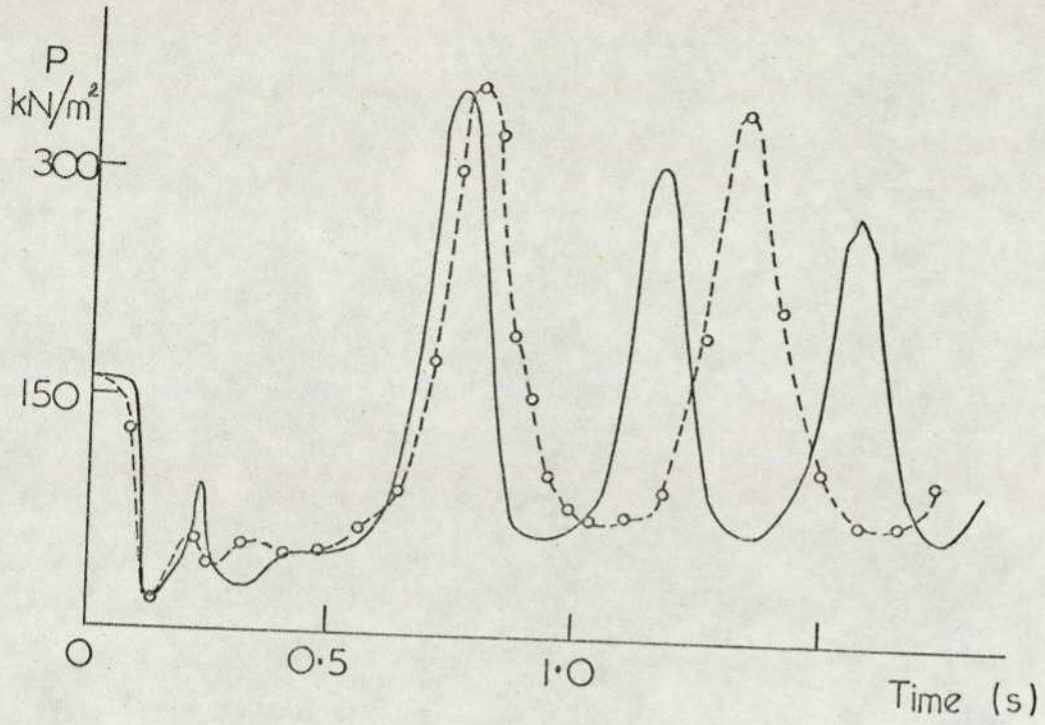


FIG 130

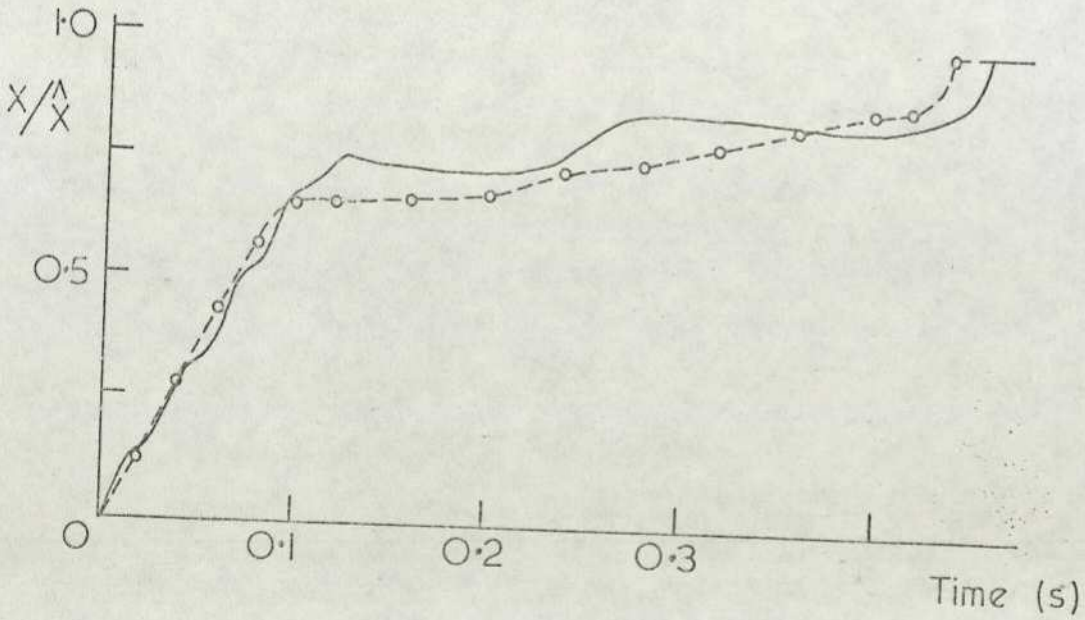


FIG 131

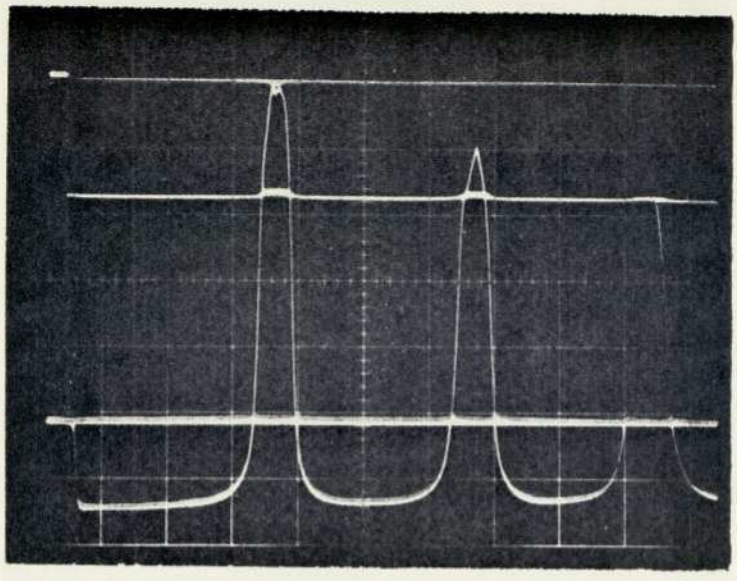


FIG 132

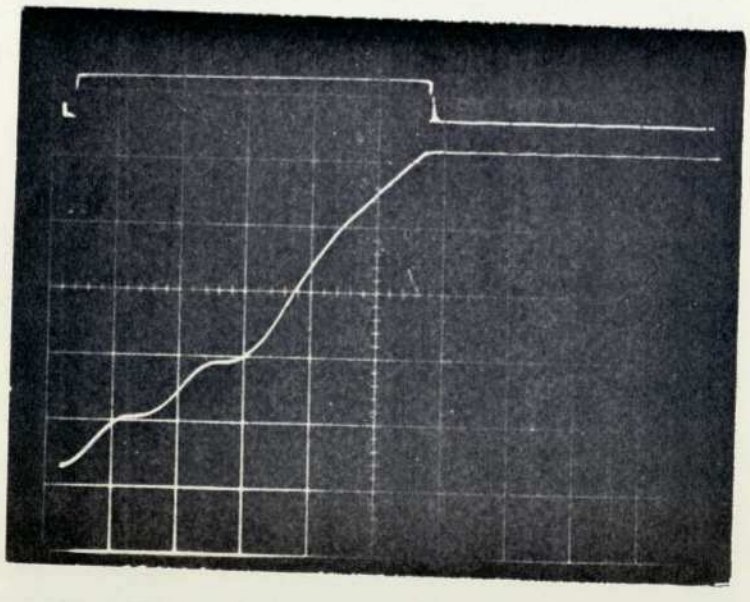


FIG 133

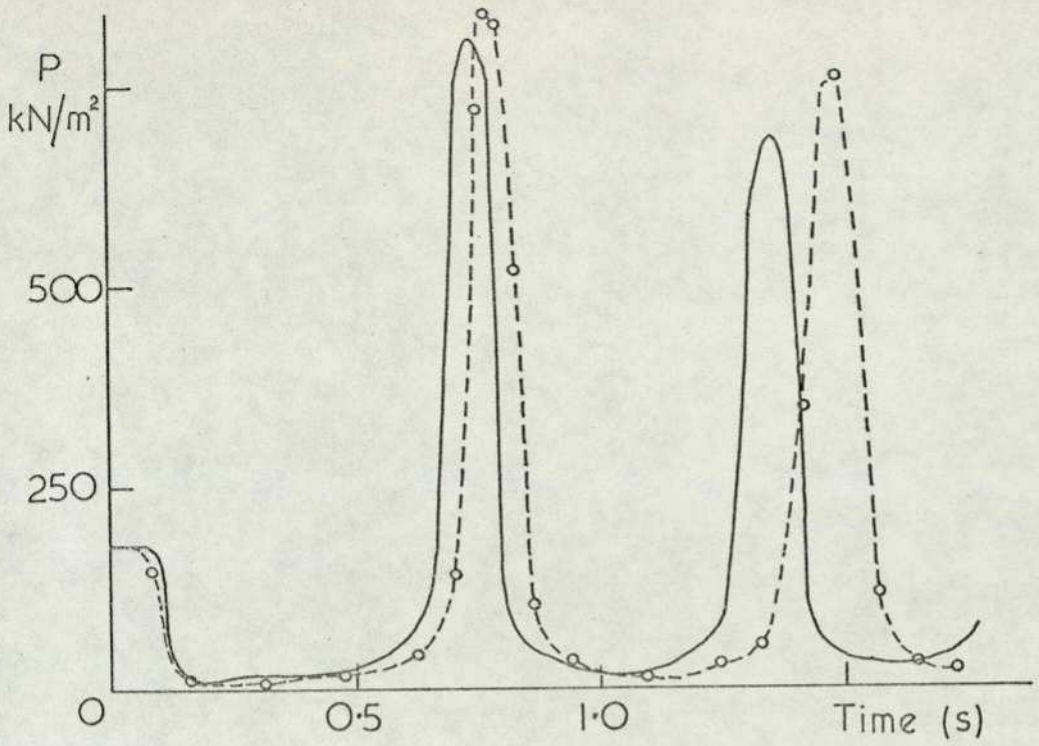


FIG 134

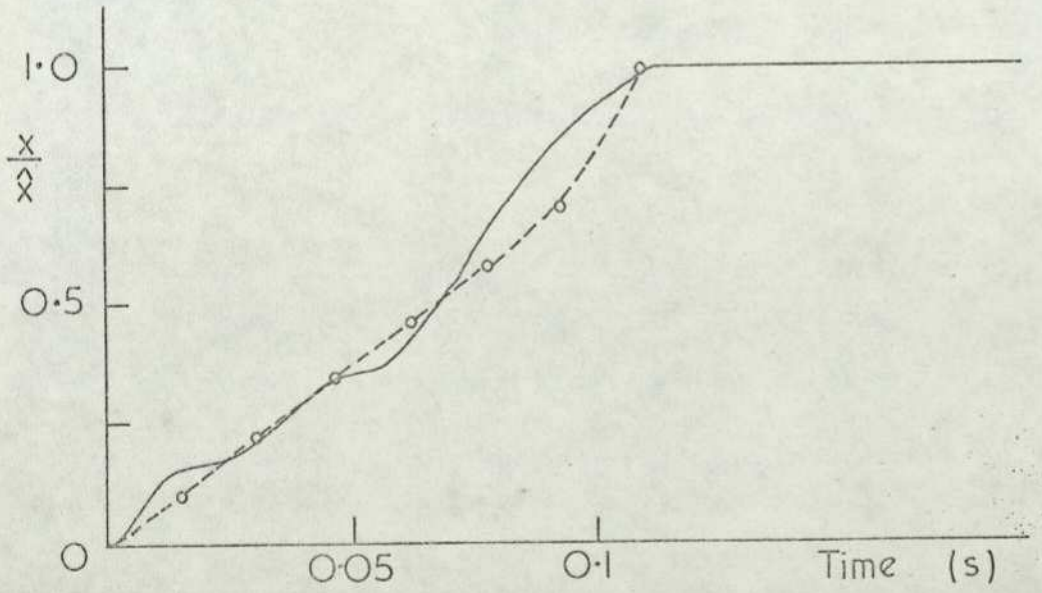


FIG 135

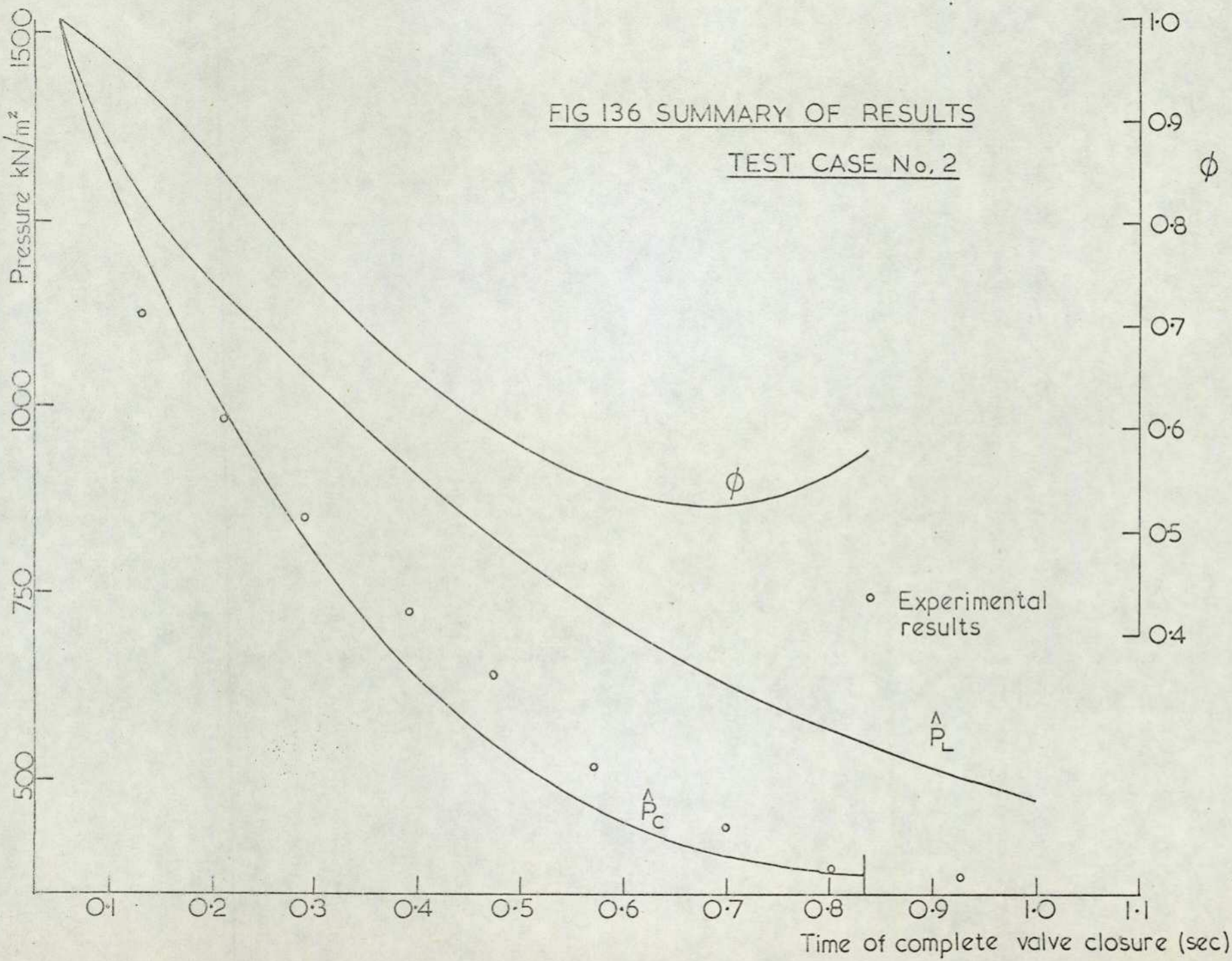


FIG 136 SUMMARY OF RESULTS

TEST CASE No. 2

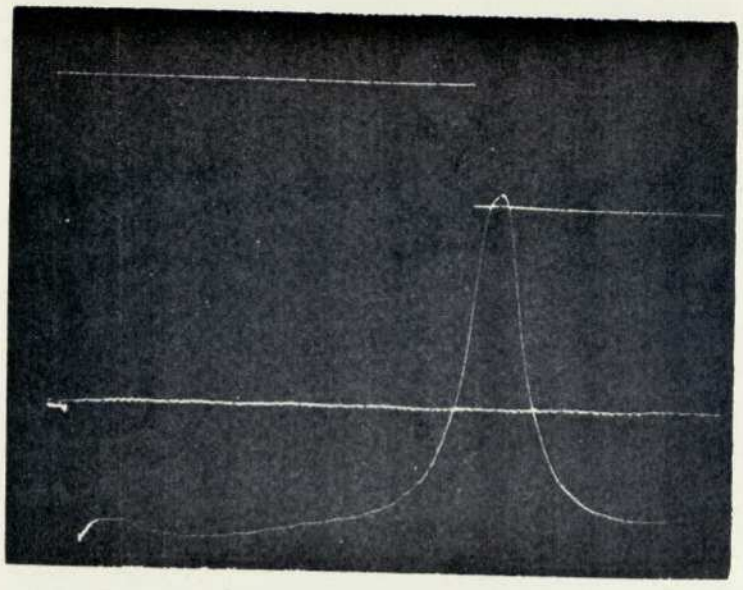


FIG 137

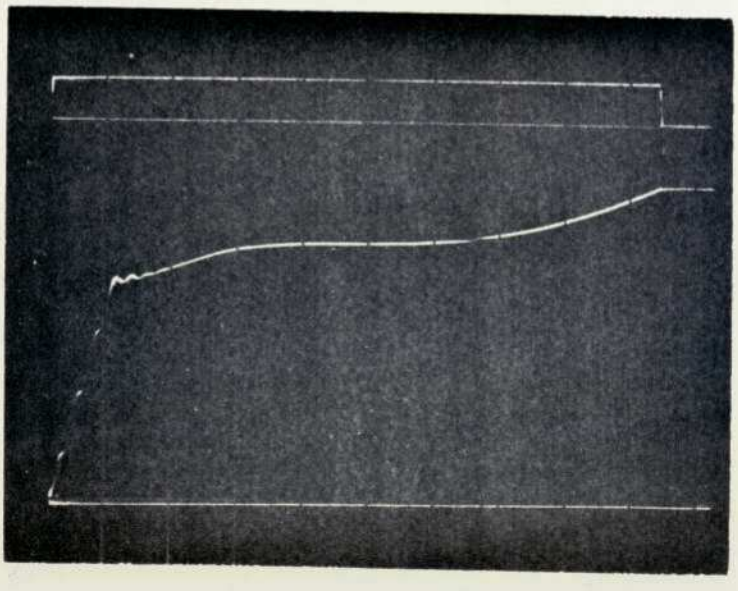


FIG 138

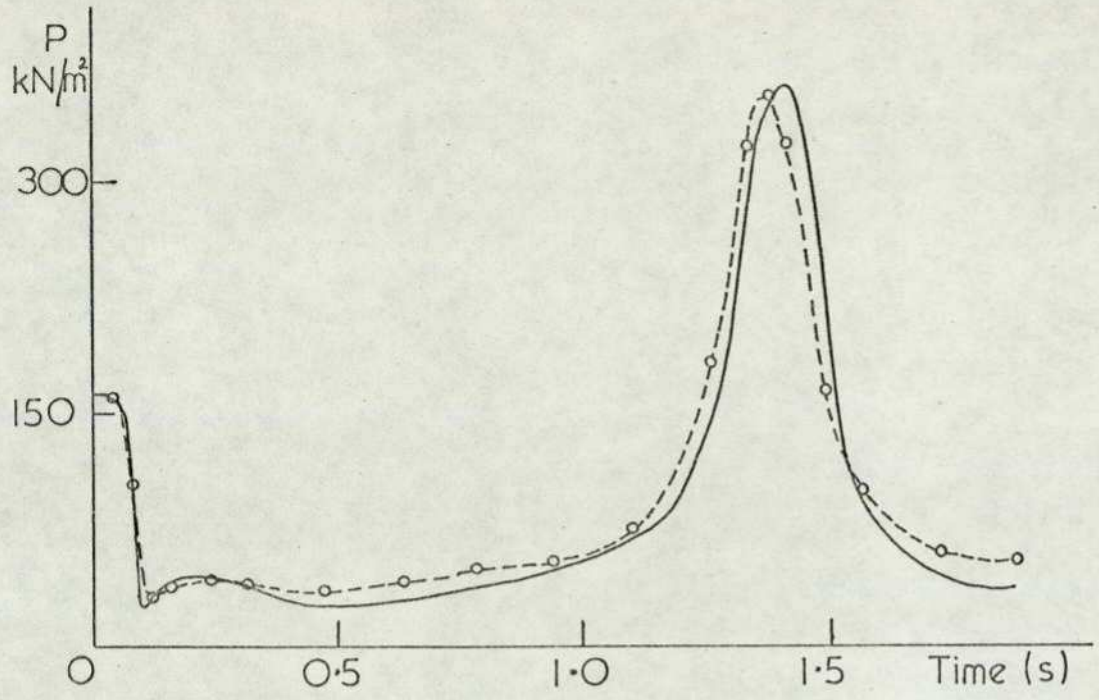


FIG 139

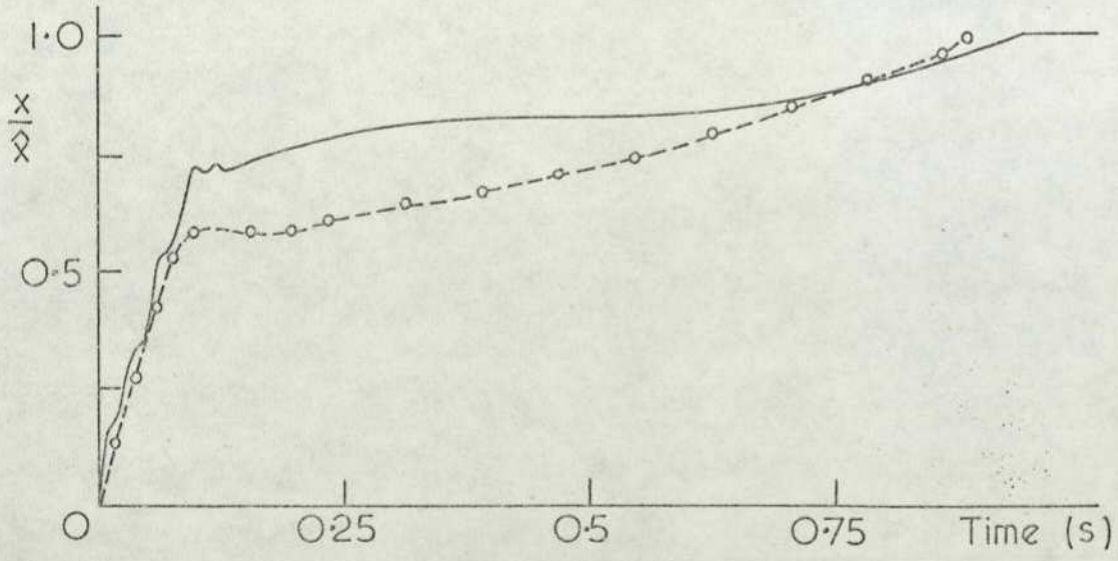


FIG 140

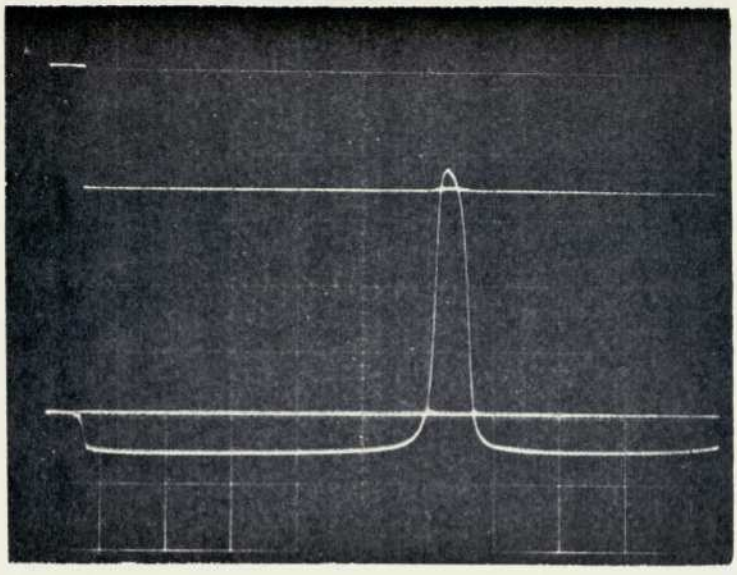


FIG 141

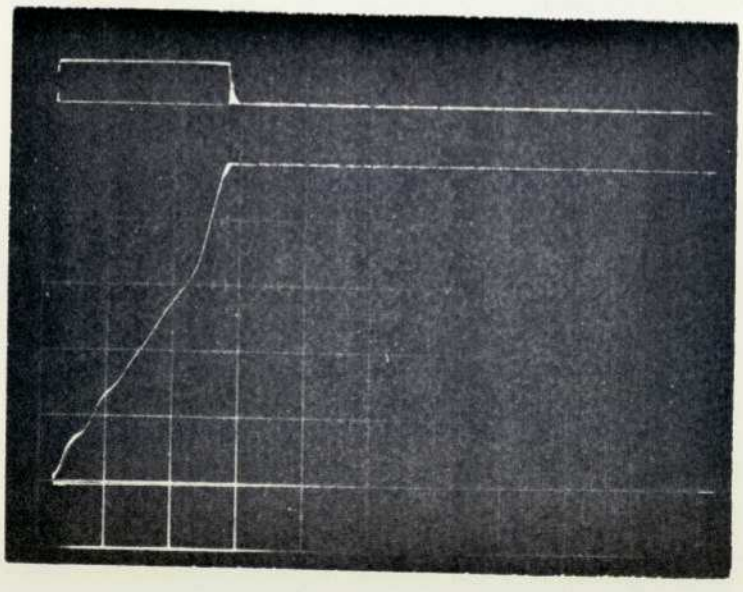


FIG 142

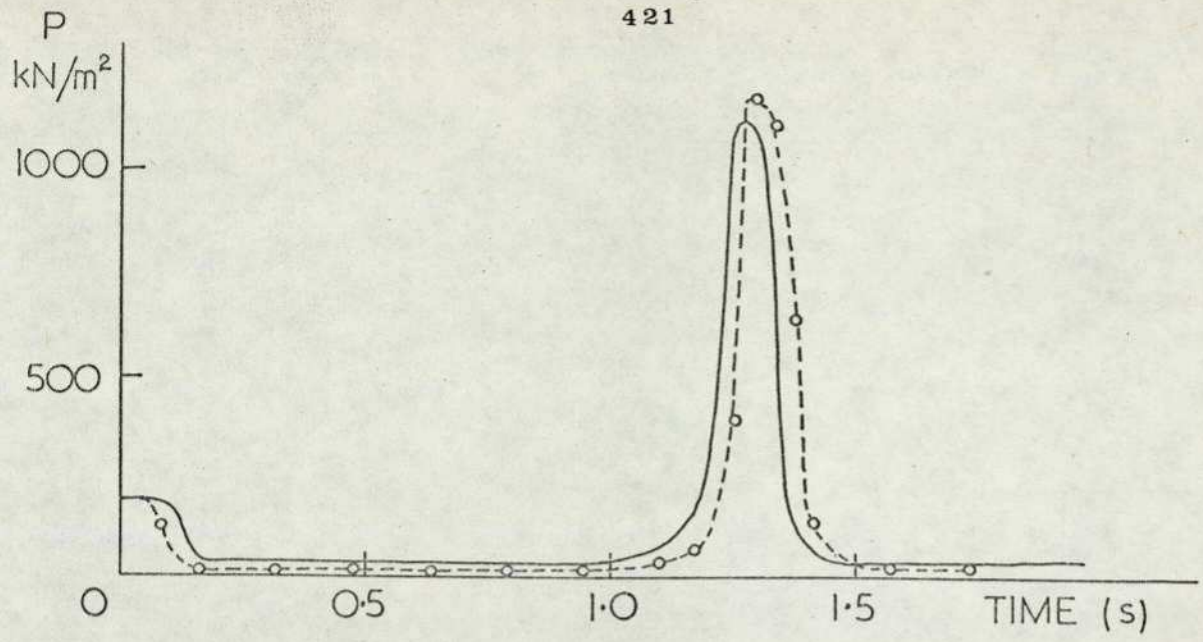


FIG 143

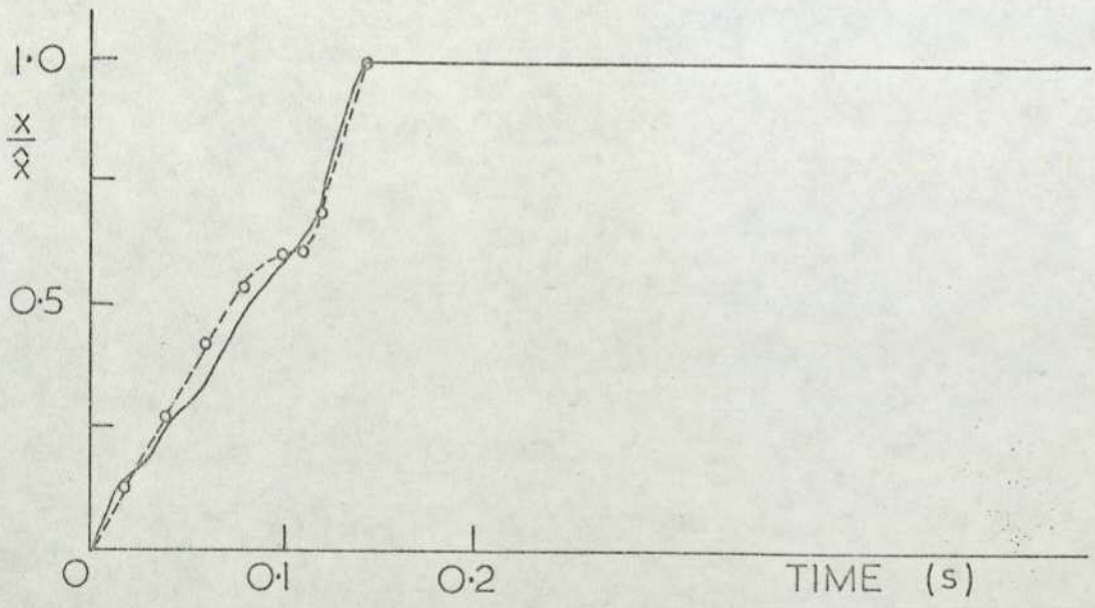


FIG 144

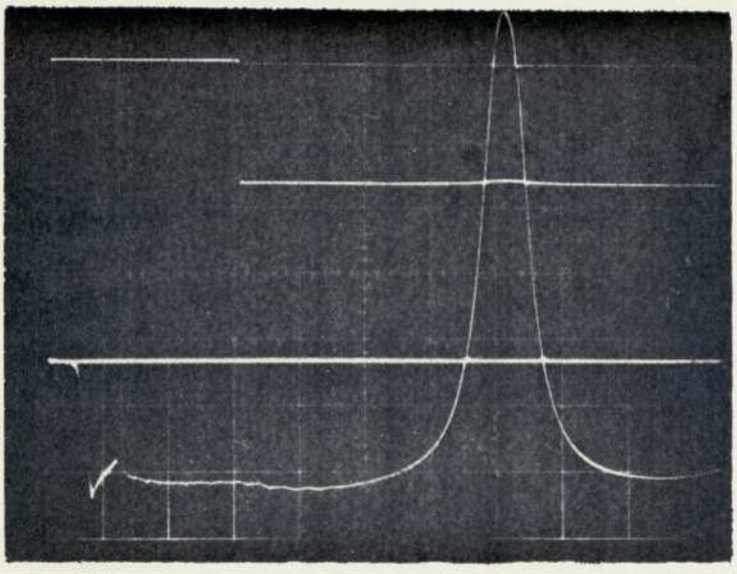


FIG 145

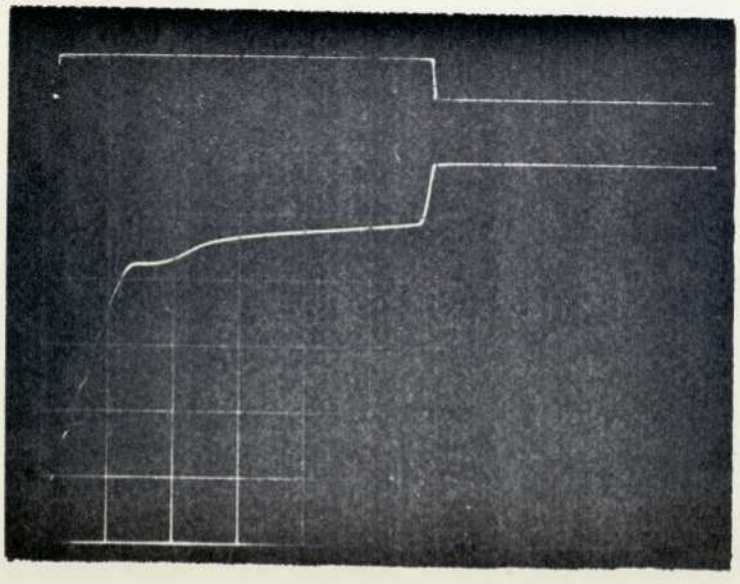


FIG 146

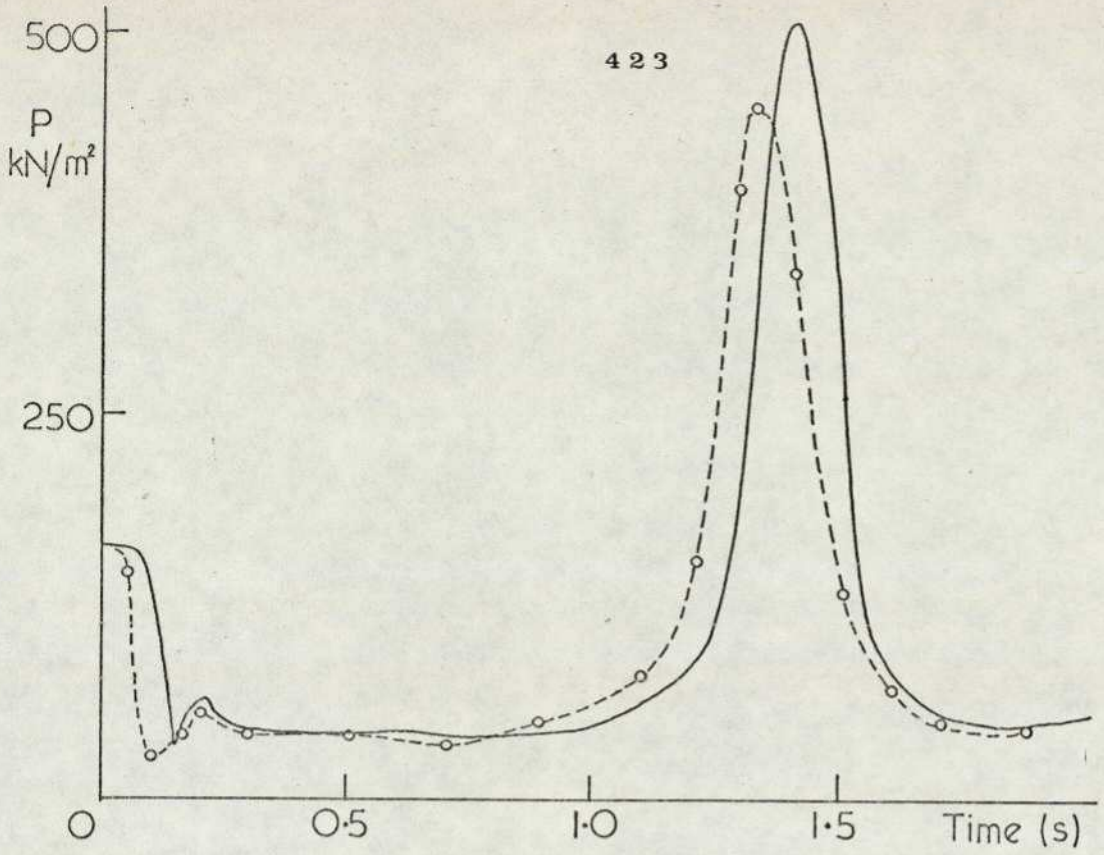


FIG 147

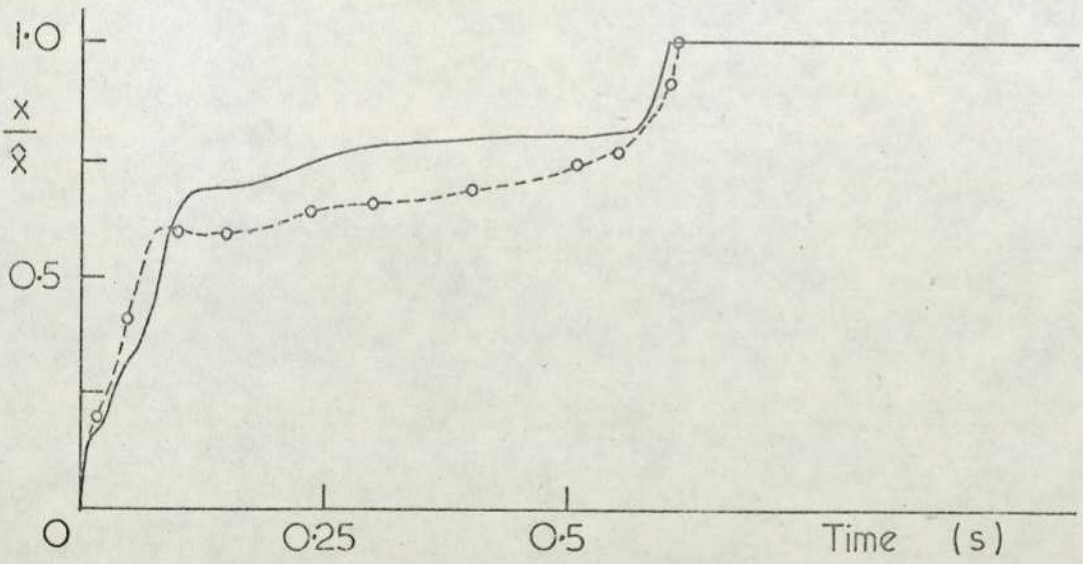


FIG 148

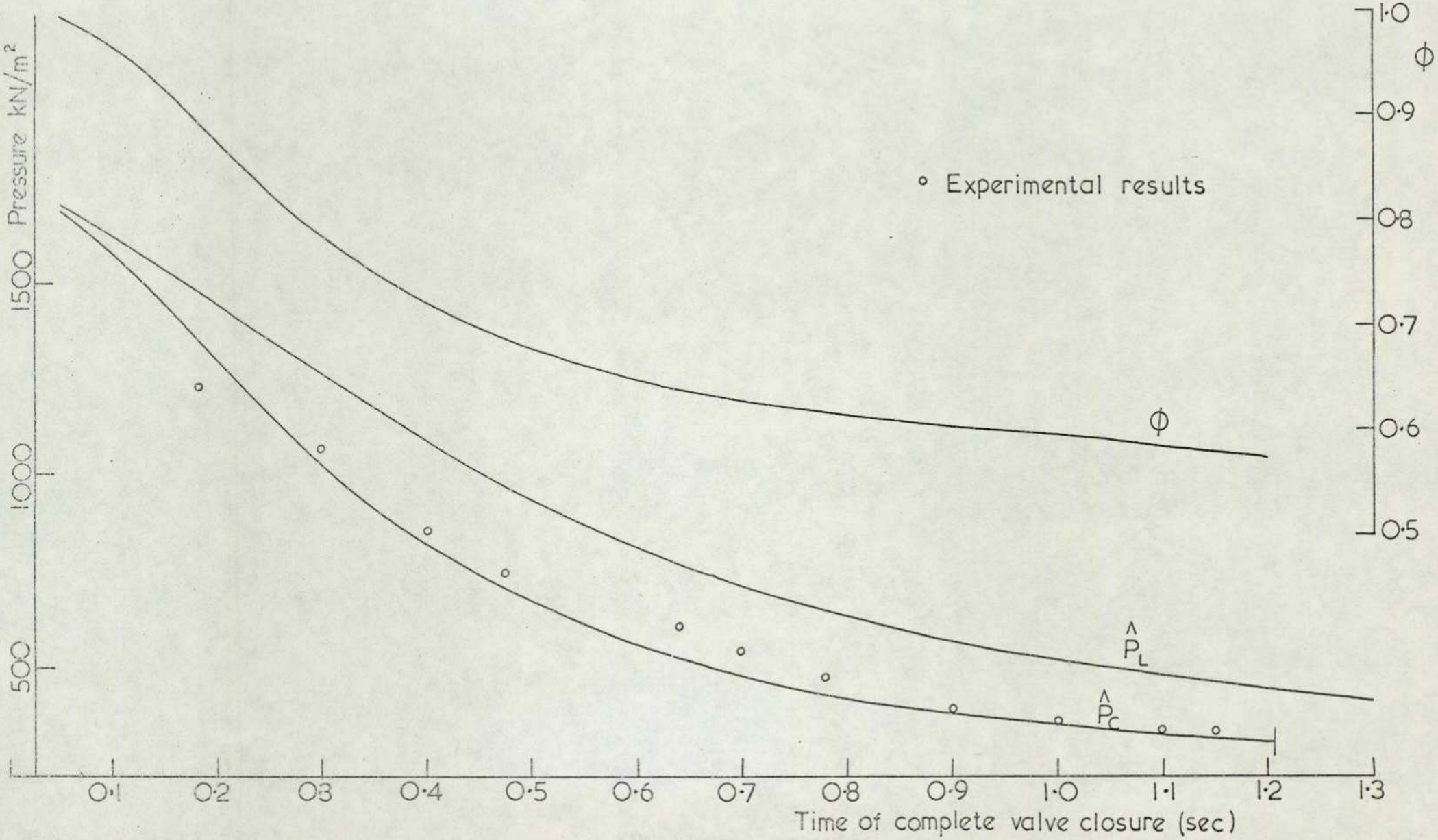


FIG 149 SUMMARY OF RESULTS - TEST CASE No. 3

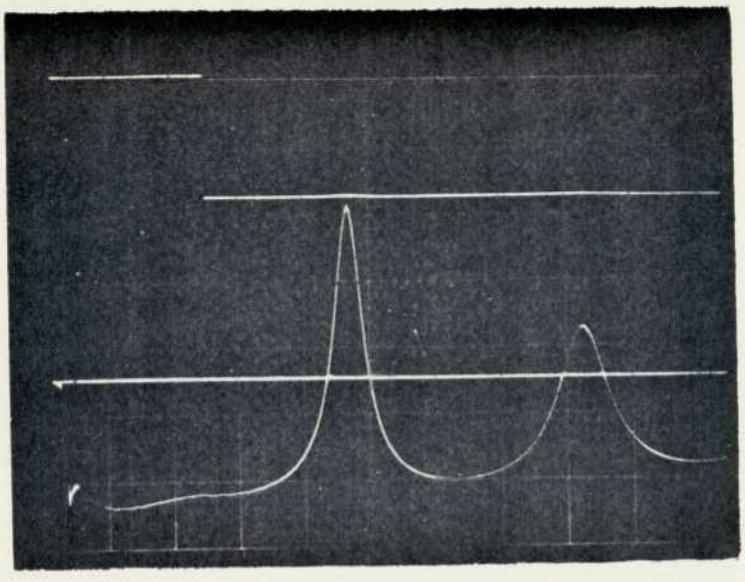


FIG 150

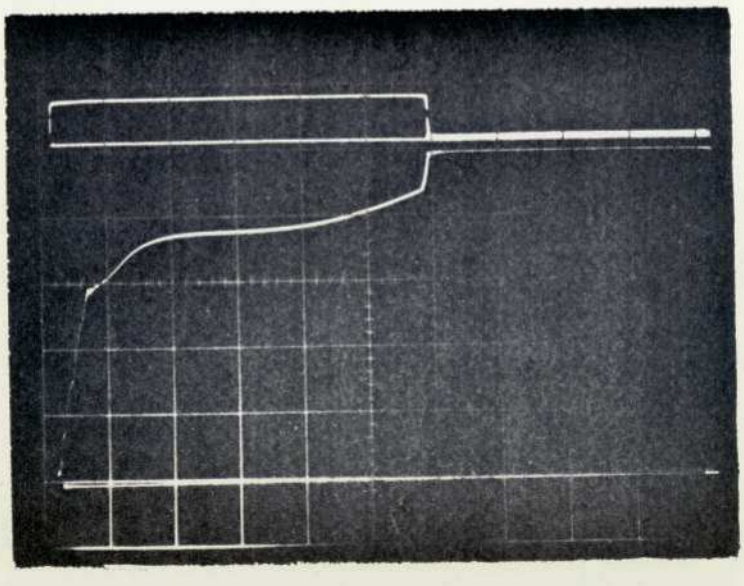


FIG 151

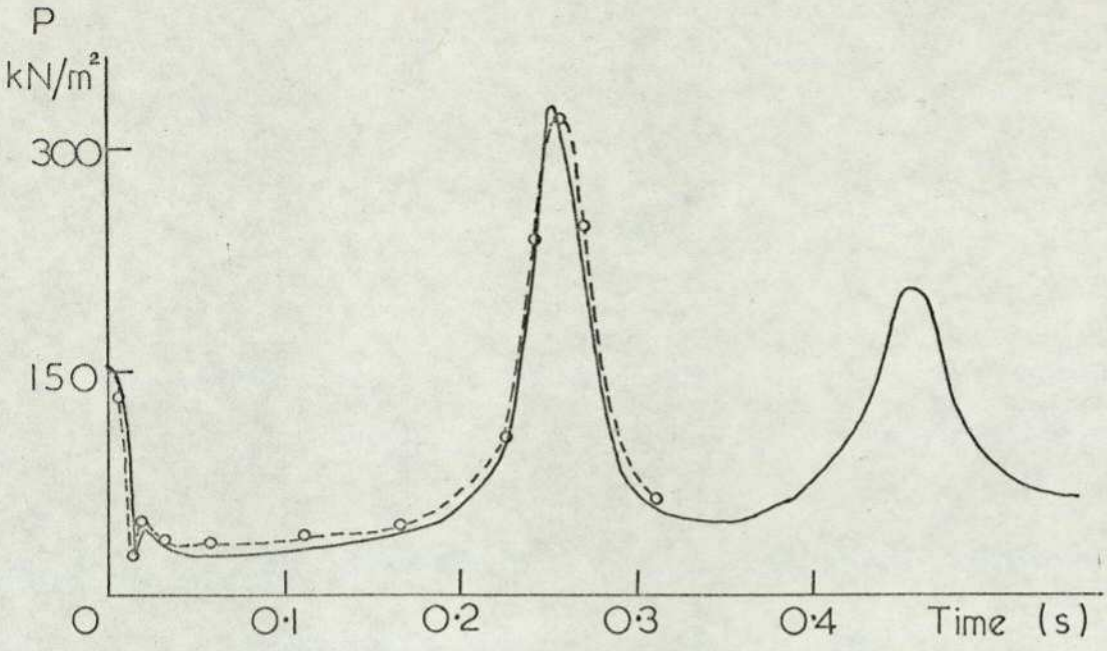


FIG 152

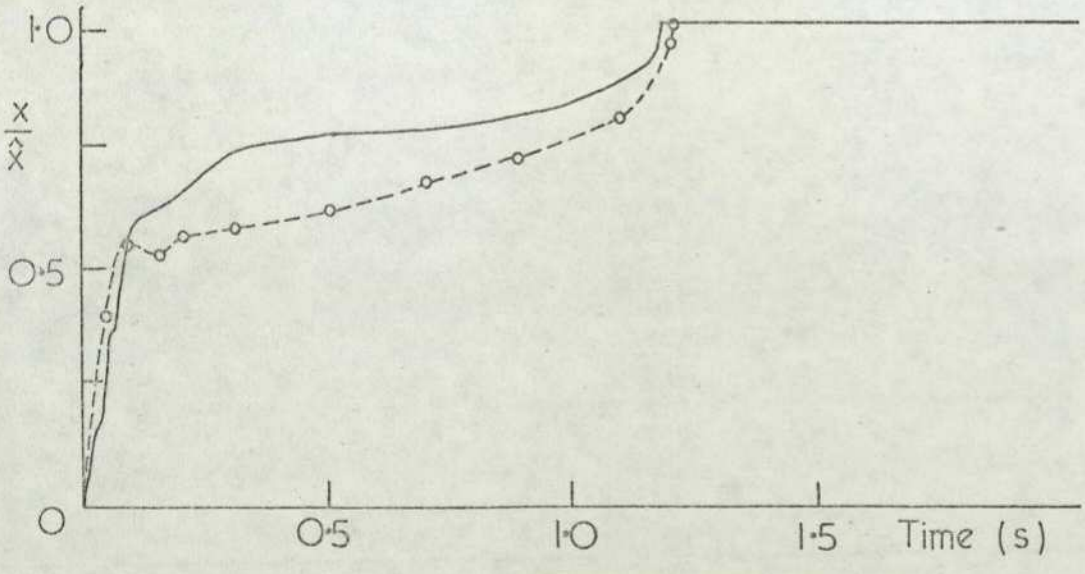


FIG 153

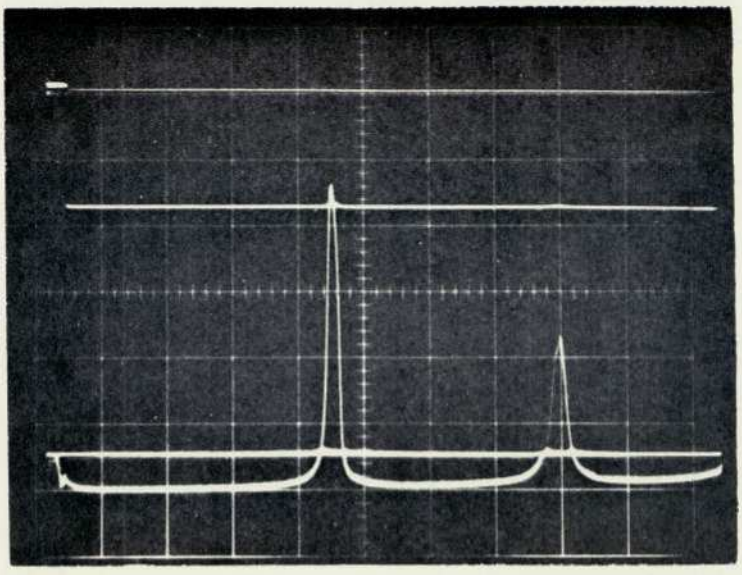


FIG 154

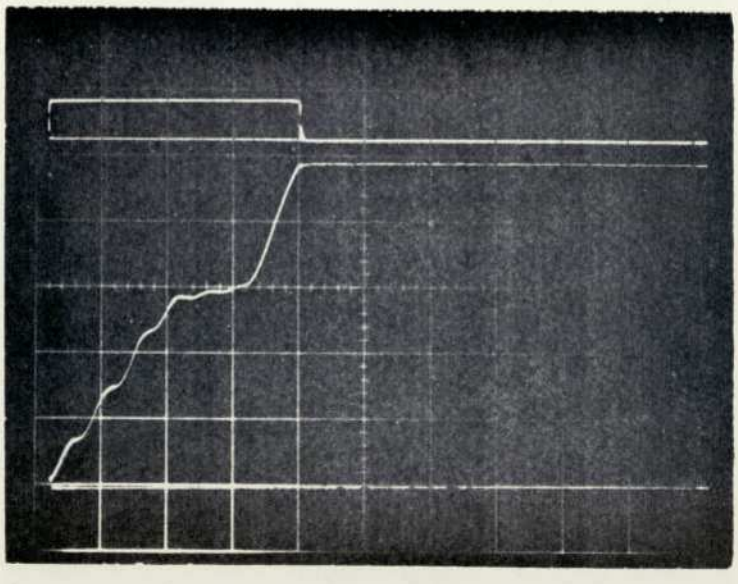


FIG 155

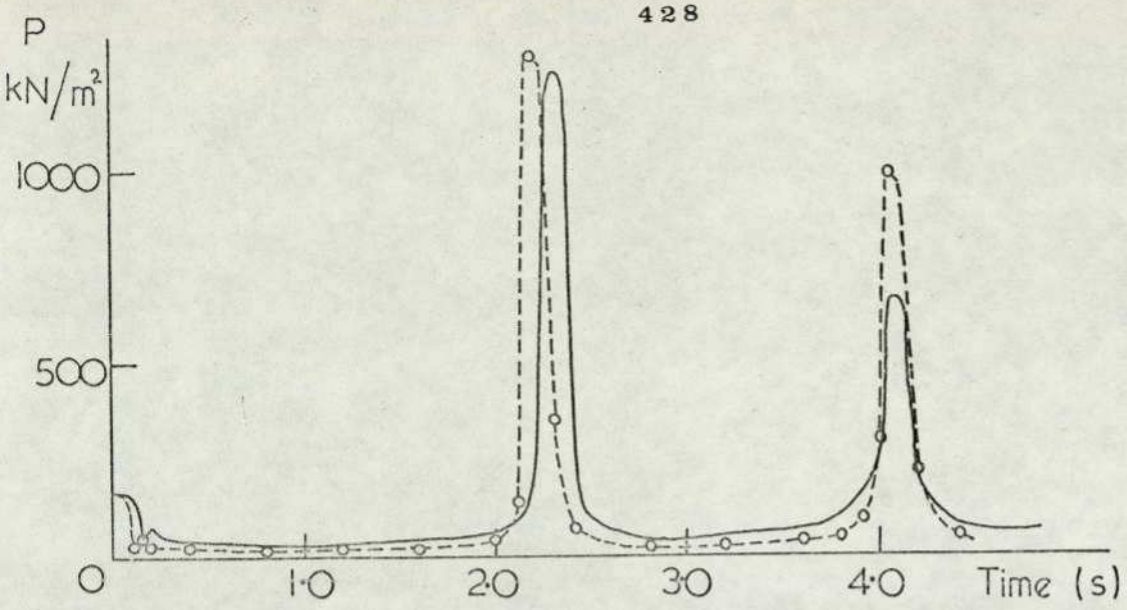


FIG 156

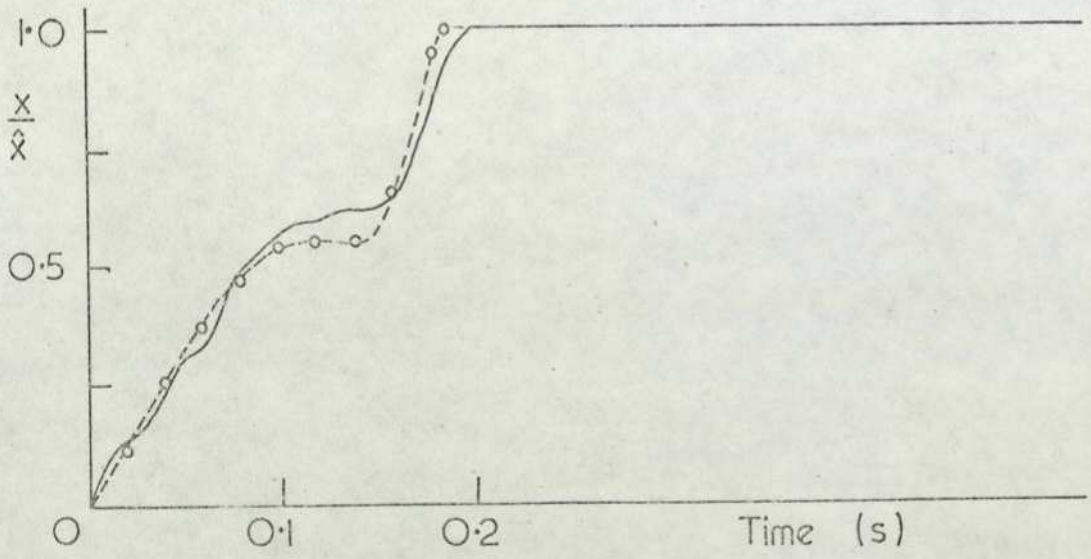


FIG 157

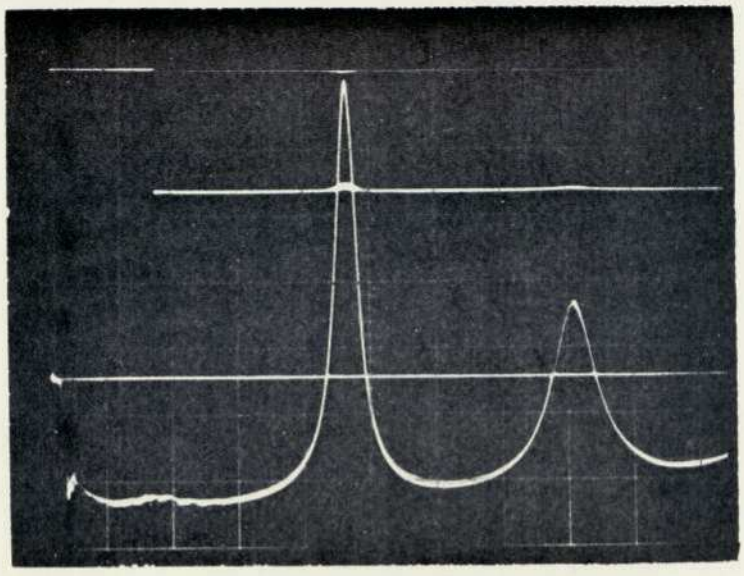


FIG 158

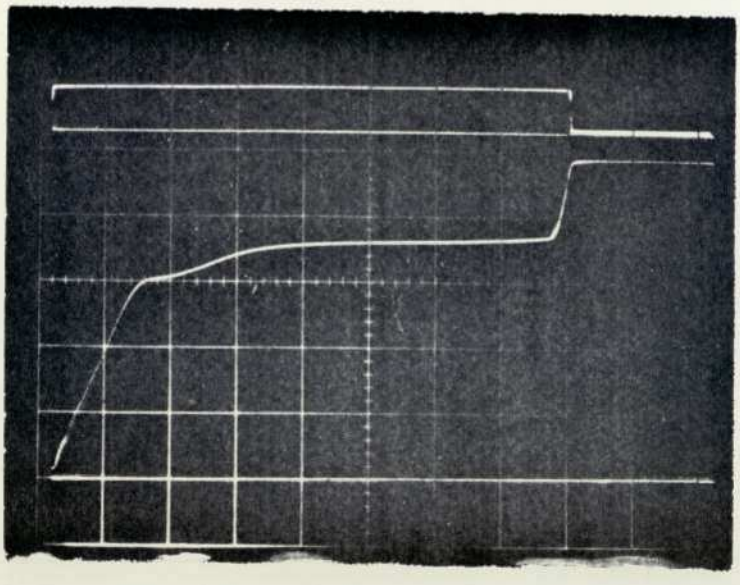


FIG 159

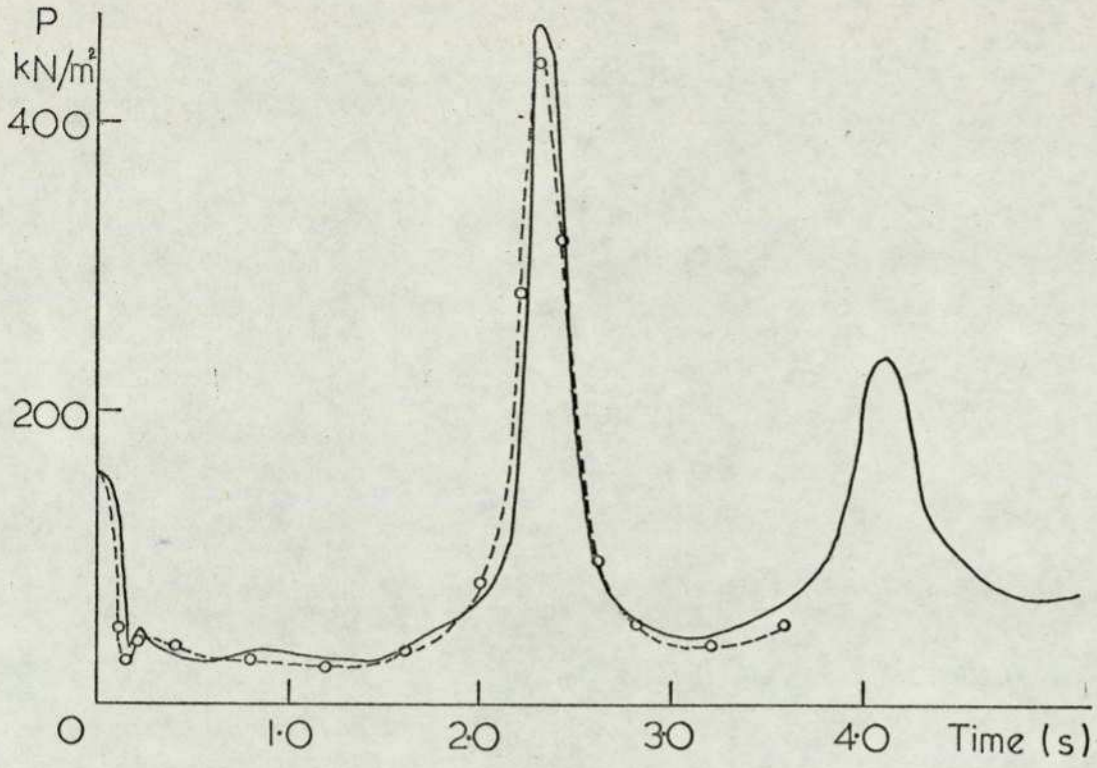


FIG 160

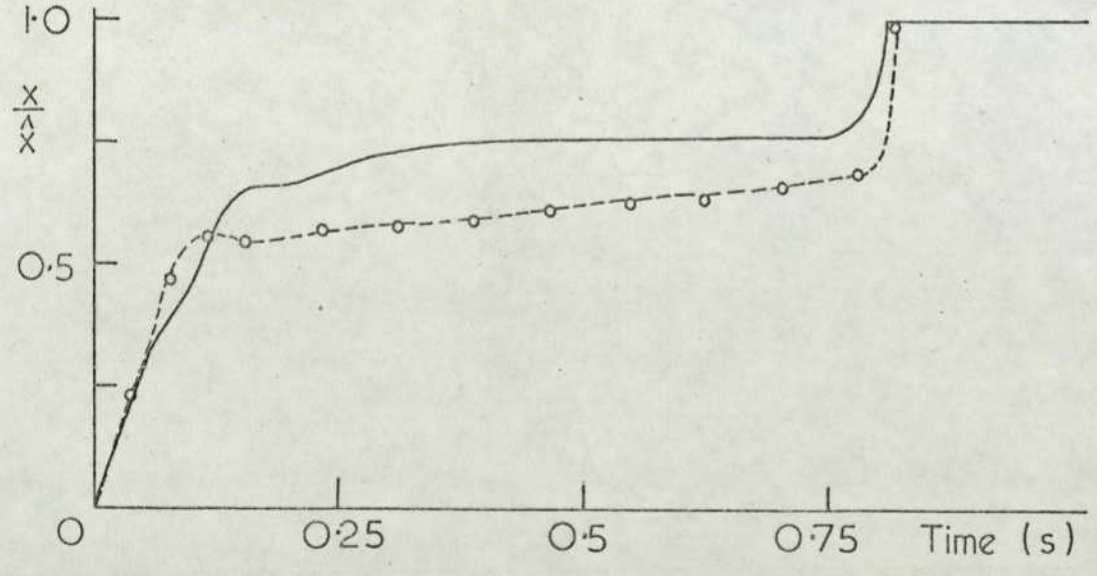


FIG 161

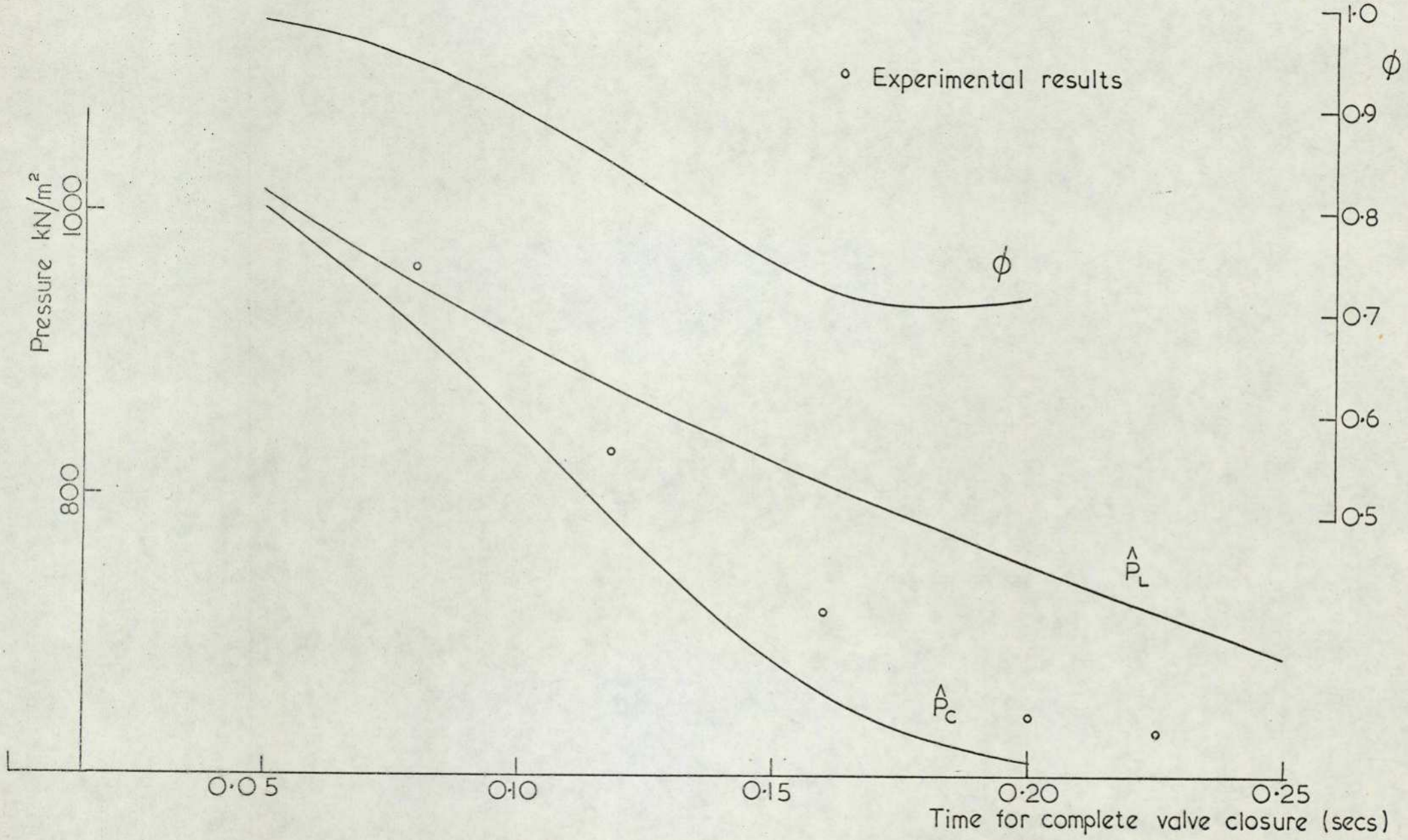


FIG 162 SUMMARY OF RESULTS - TEST CASE No. 4

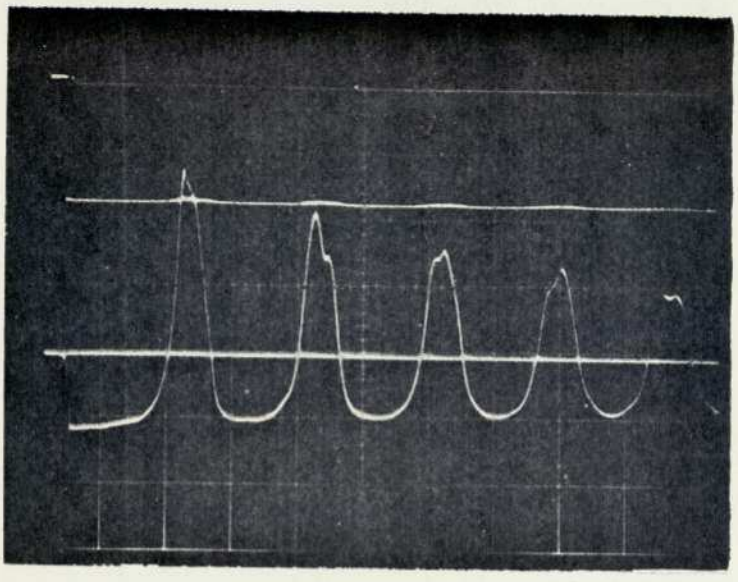


FIG 163

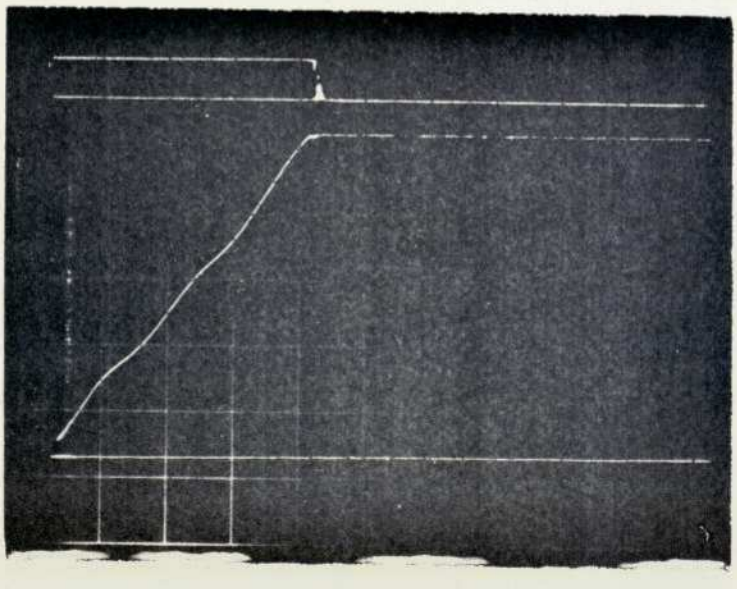


FIG 164

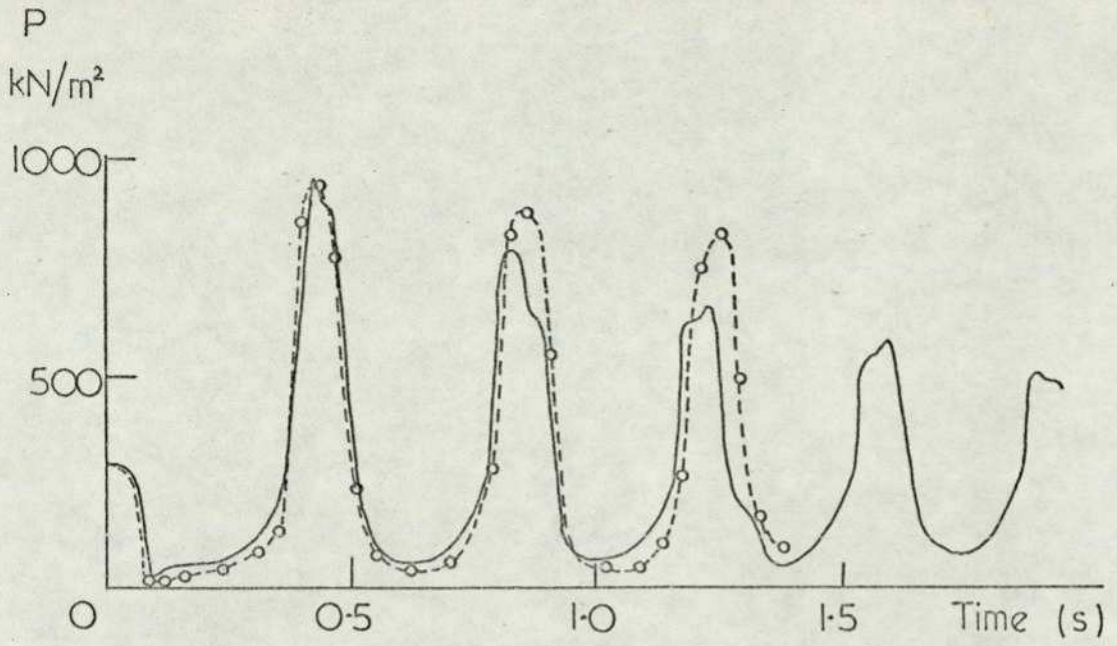


FIG 165

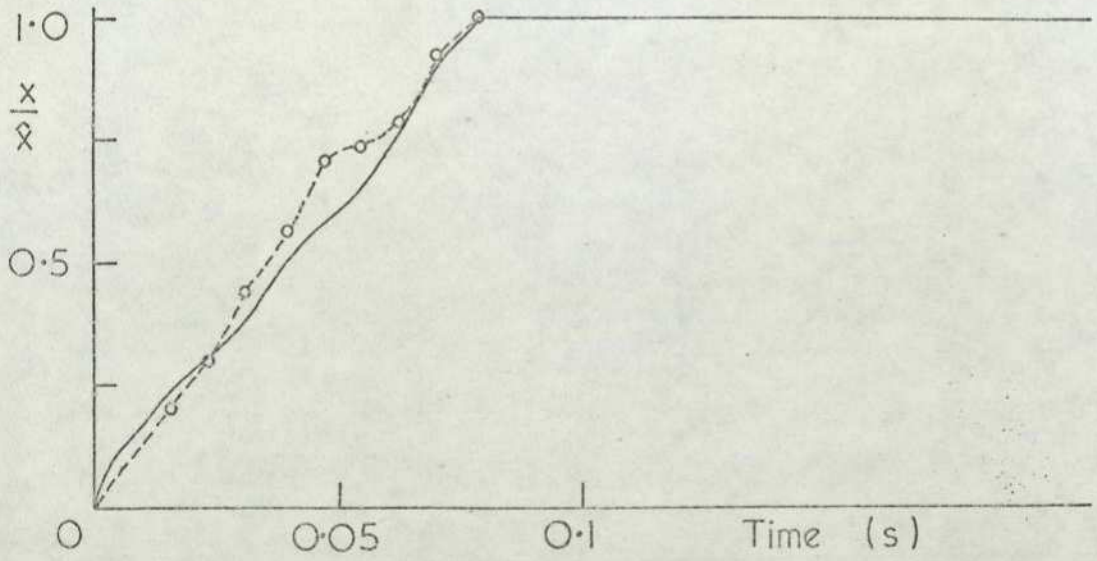


FIG 166

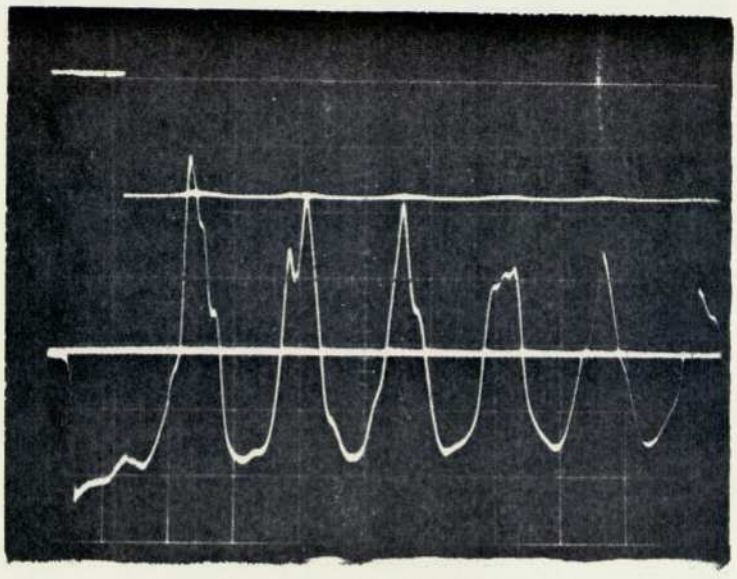


FIG 167

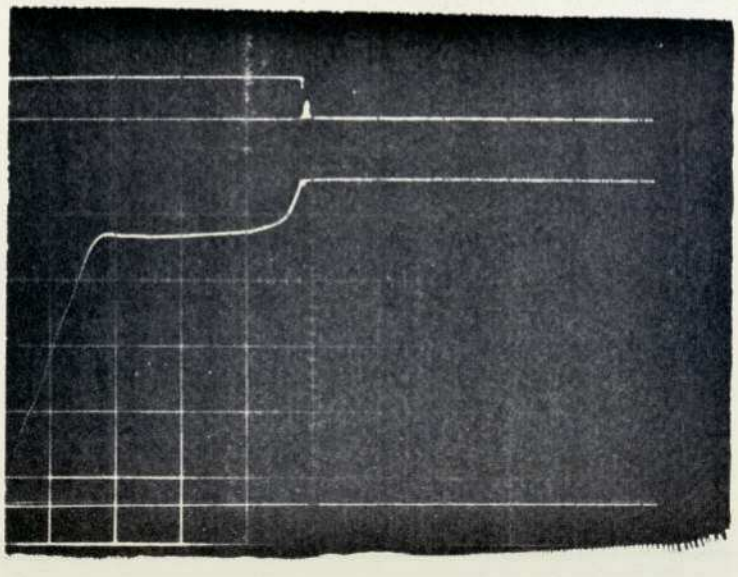


FIG 168

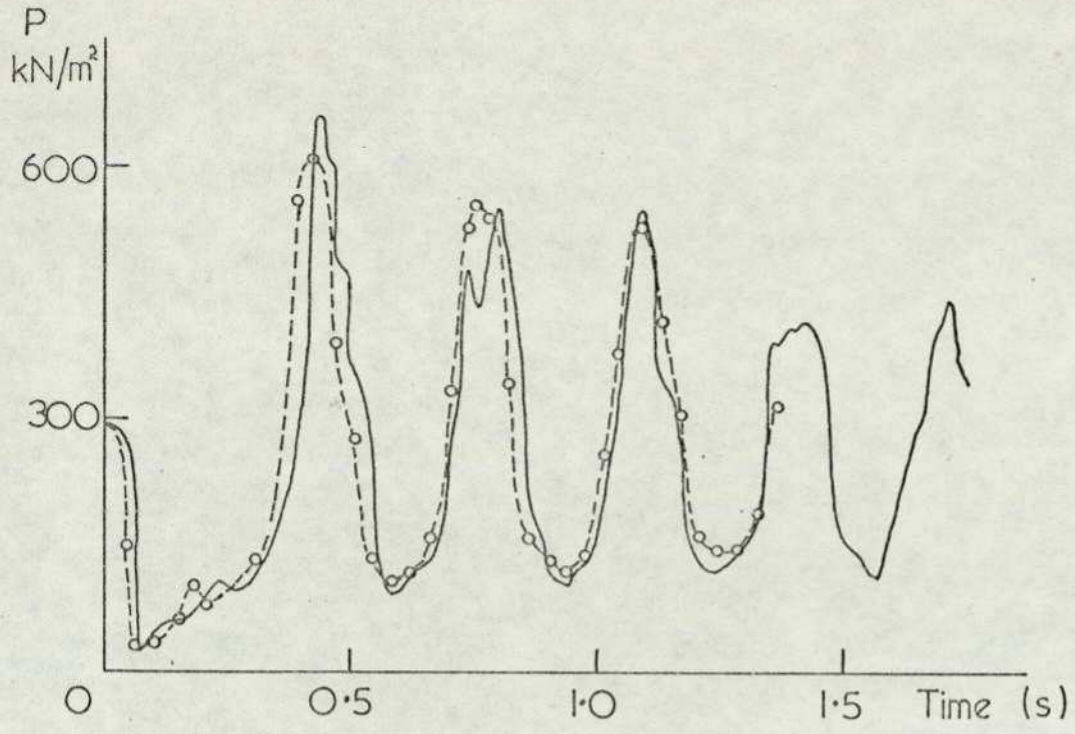


FIG 169

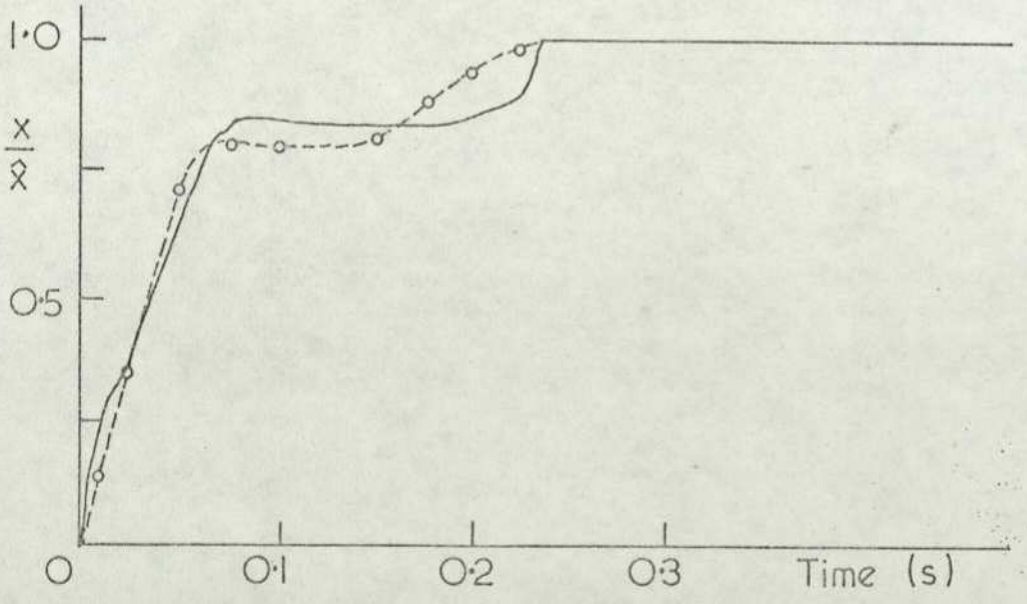
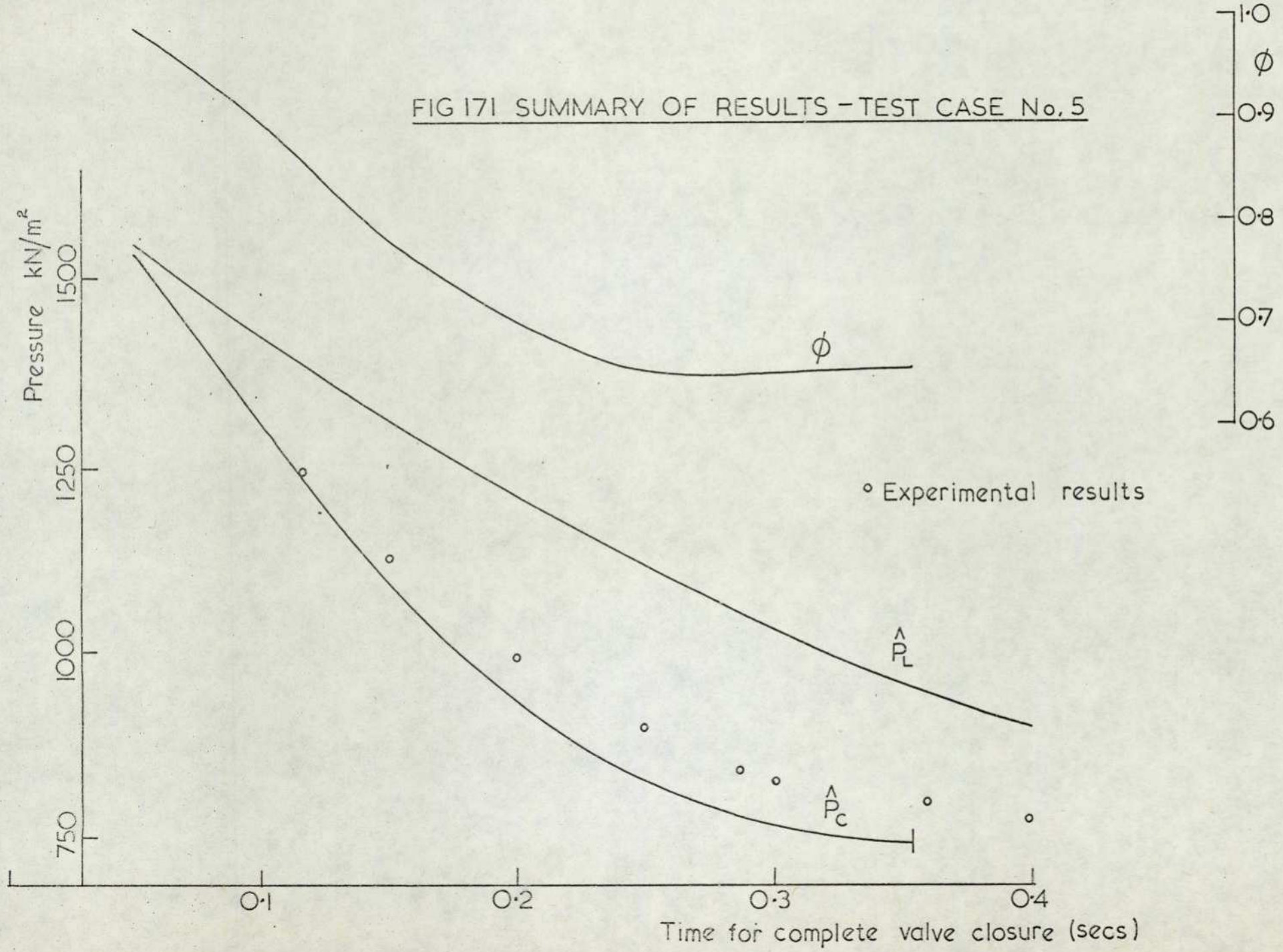


FIG 170

FIG 171 SUMMARY OF RESULTS – TEST CASE No. 5



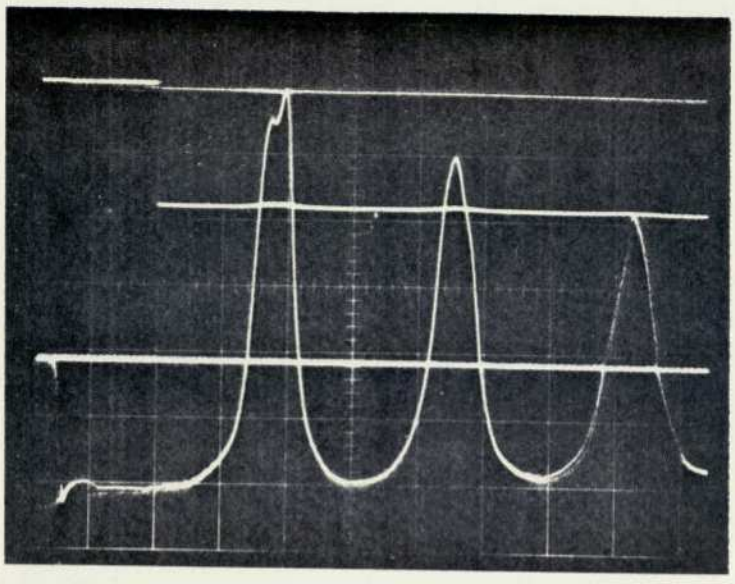


FIG 172

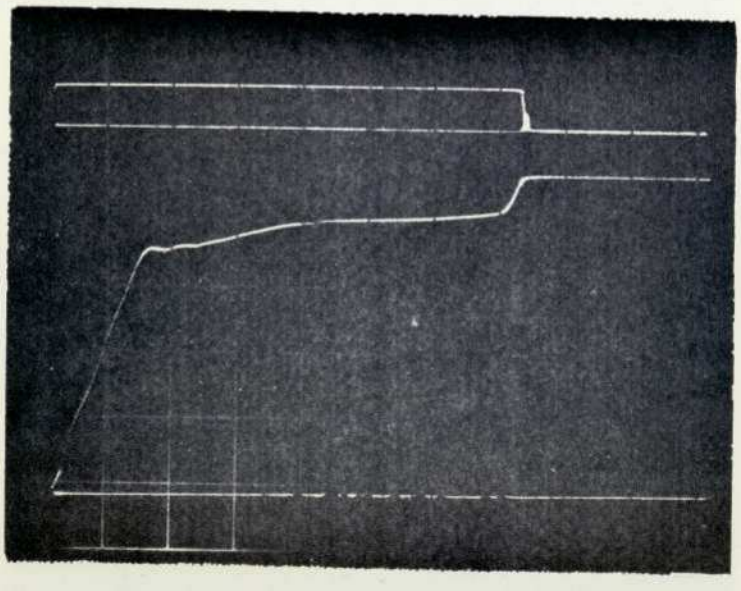


FIG 173

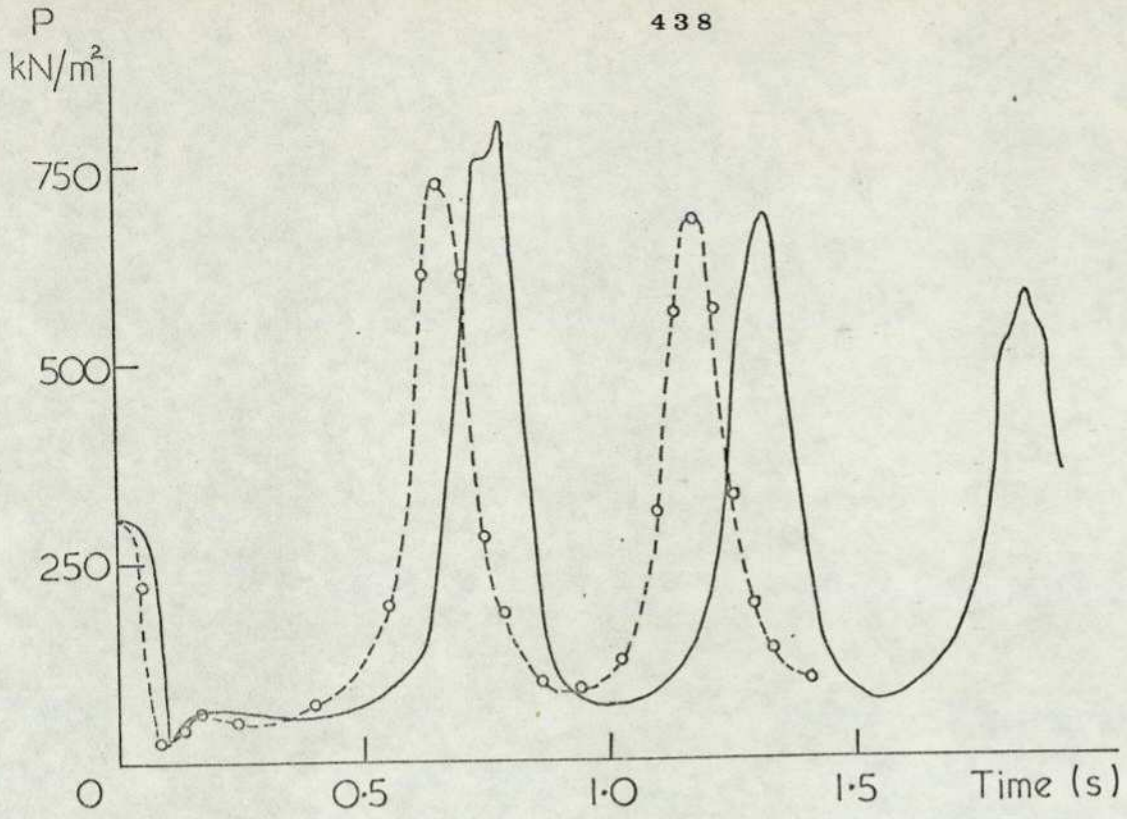


FIG 174

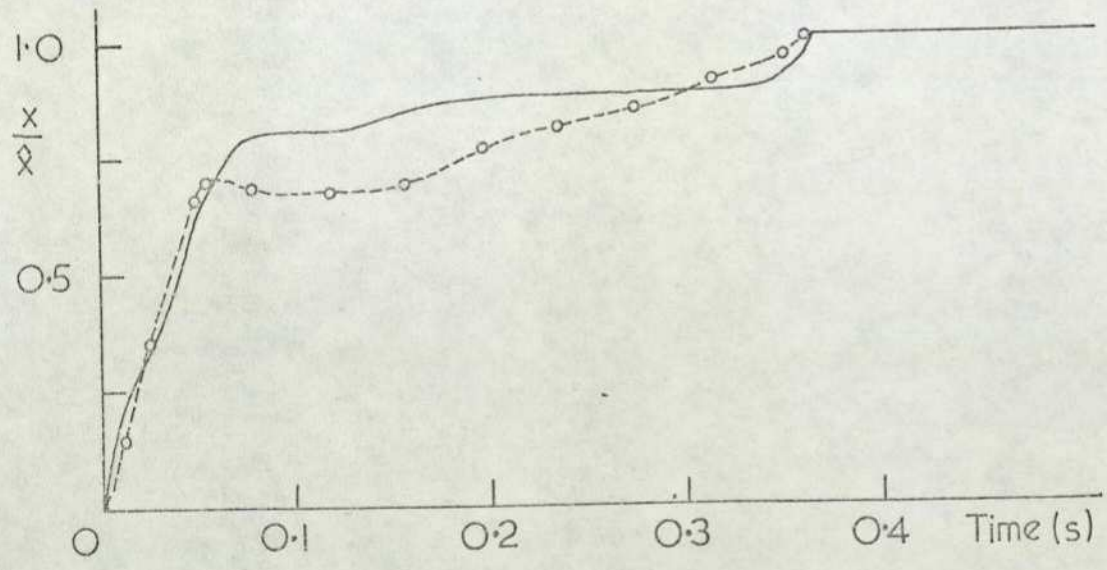


FIG 175

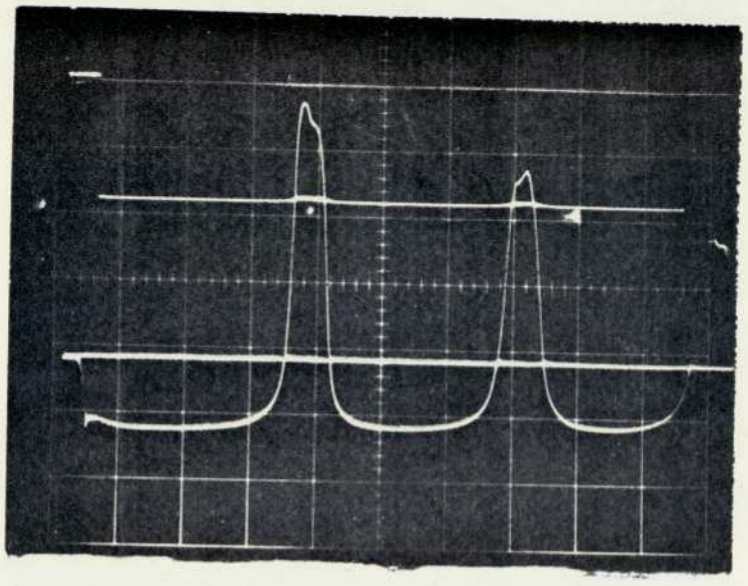


FIG 176

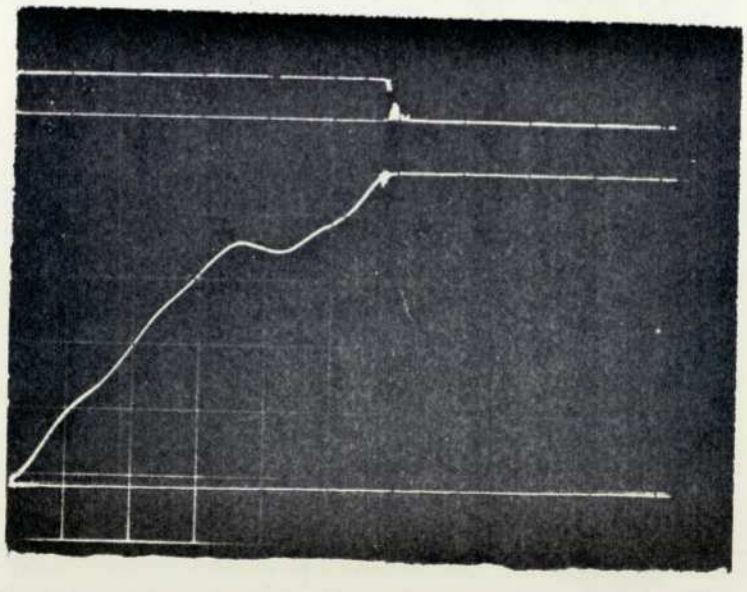


FIG 177

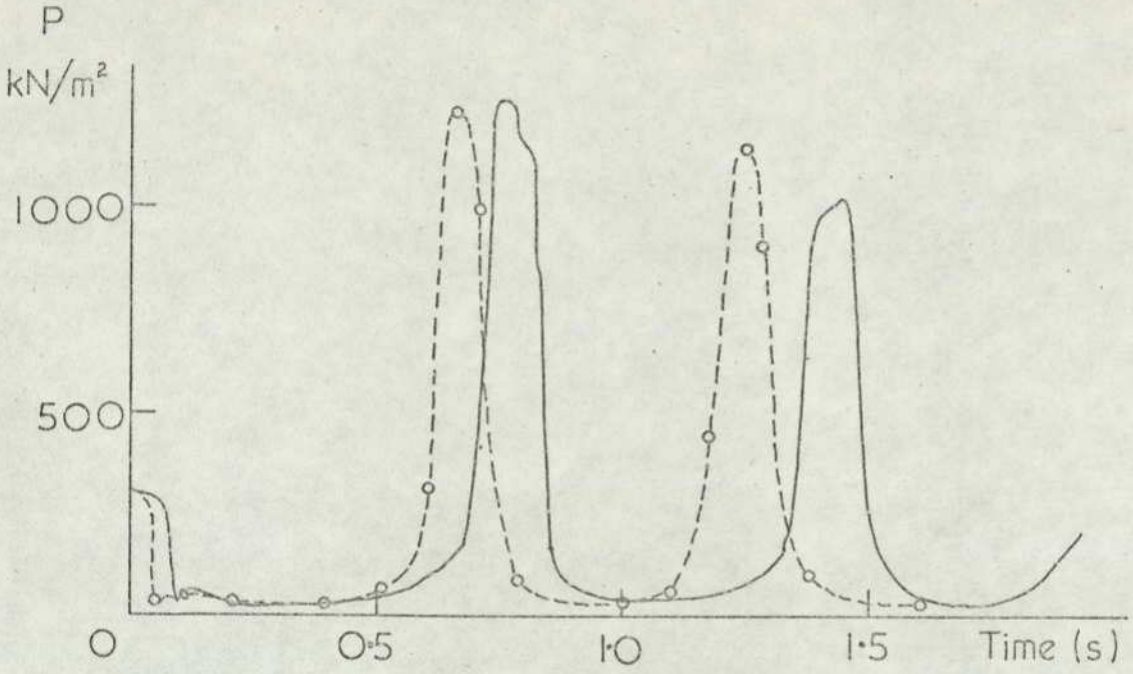


FIG 178

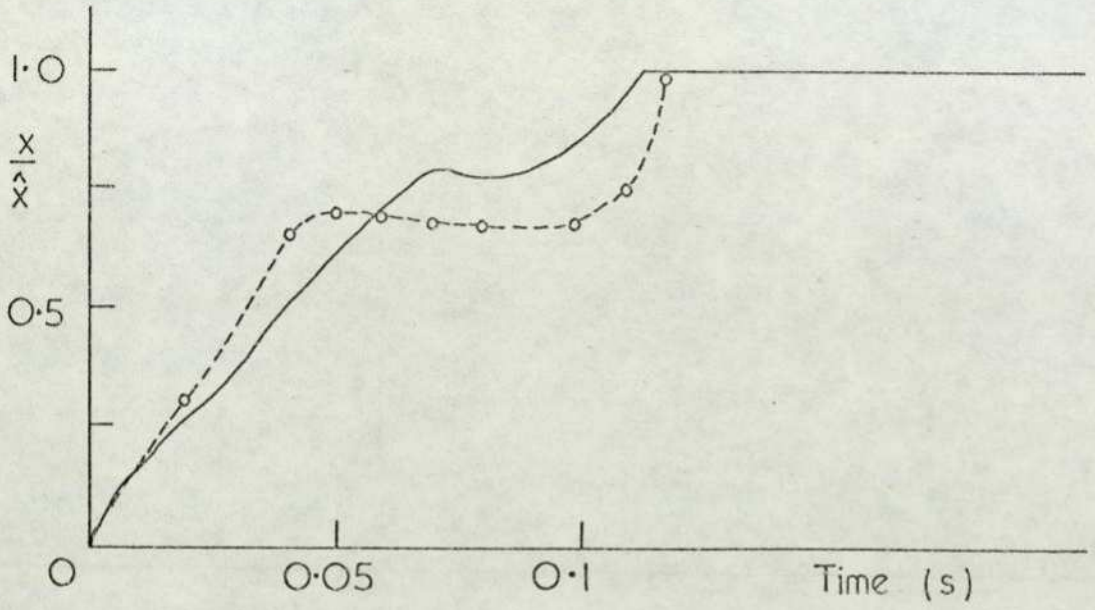


FIG 179

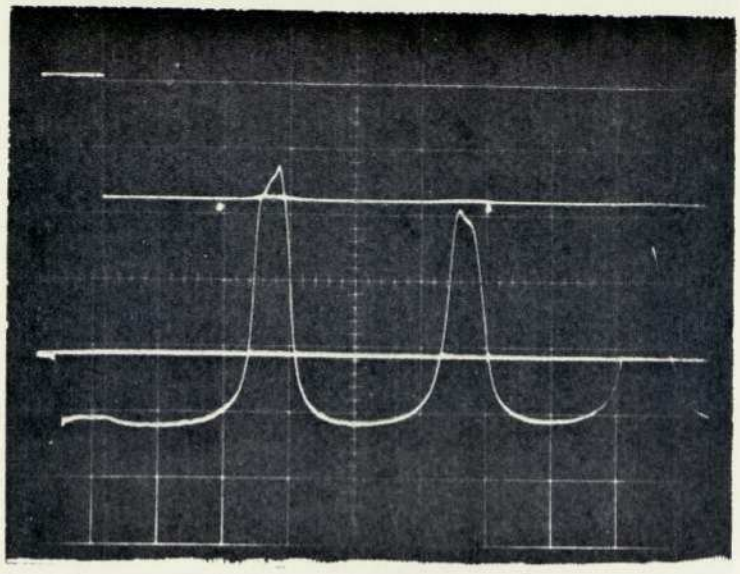


FIG 180

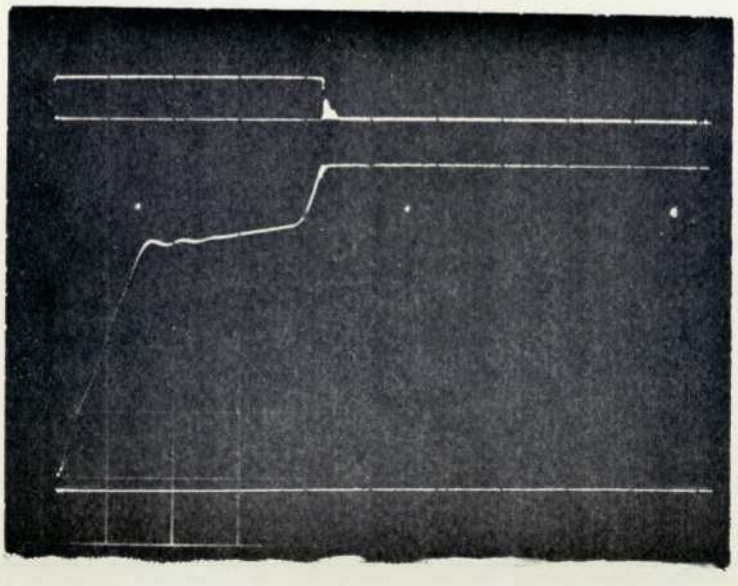


FIG 181

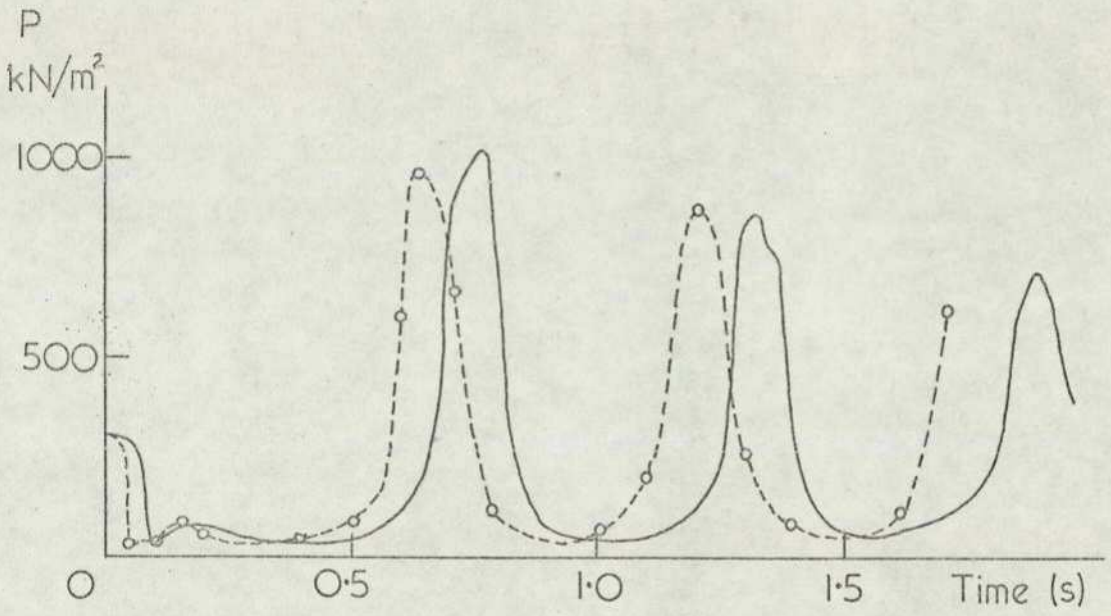


FIG 182

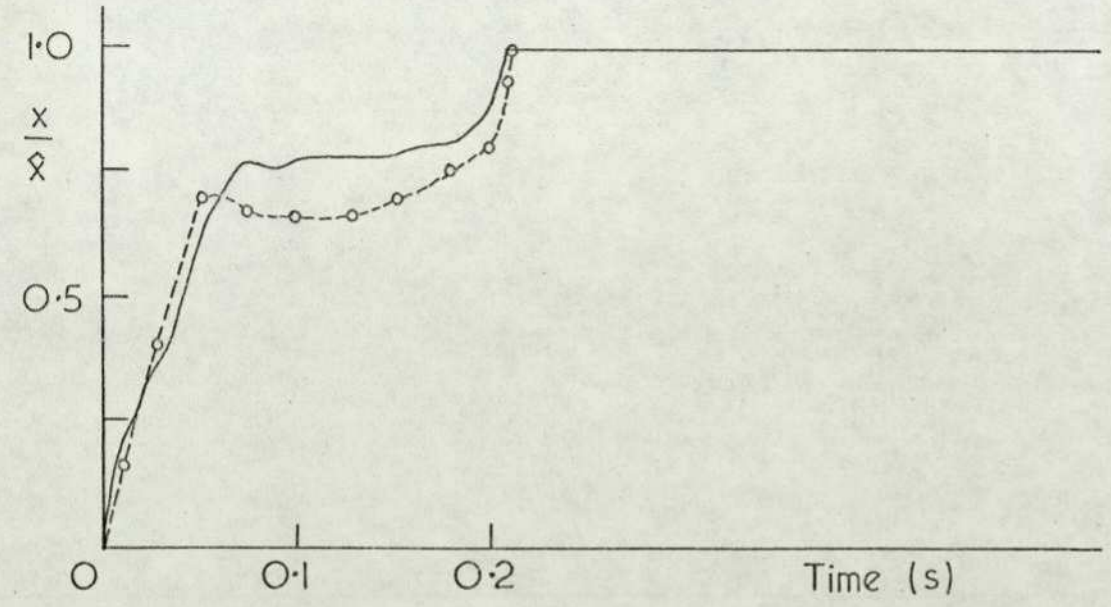
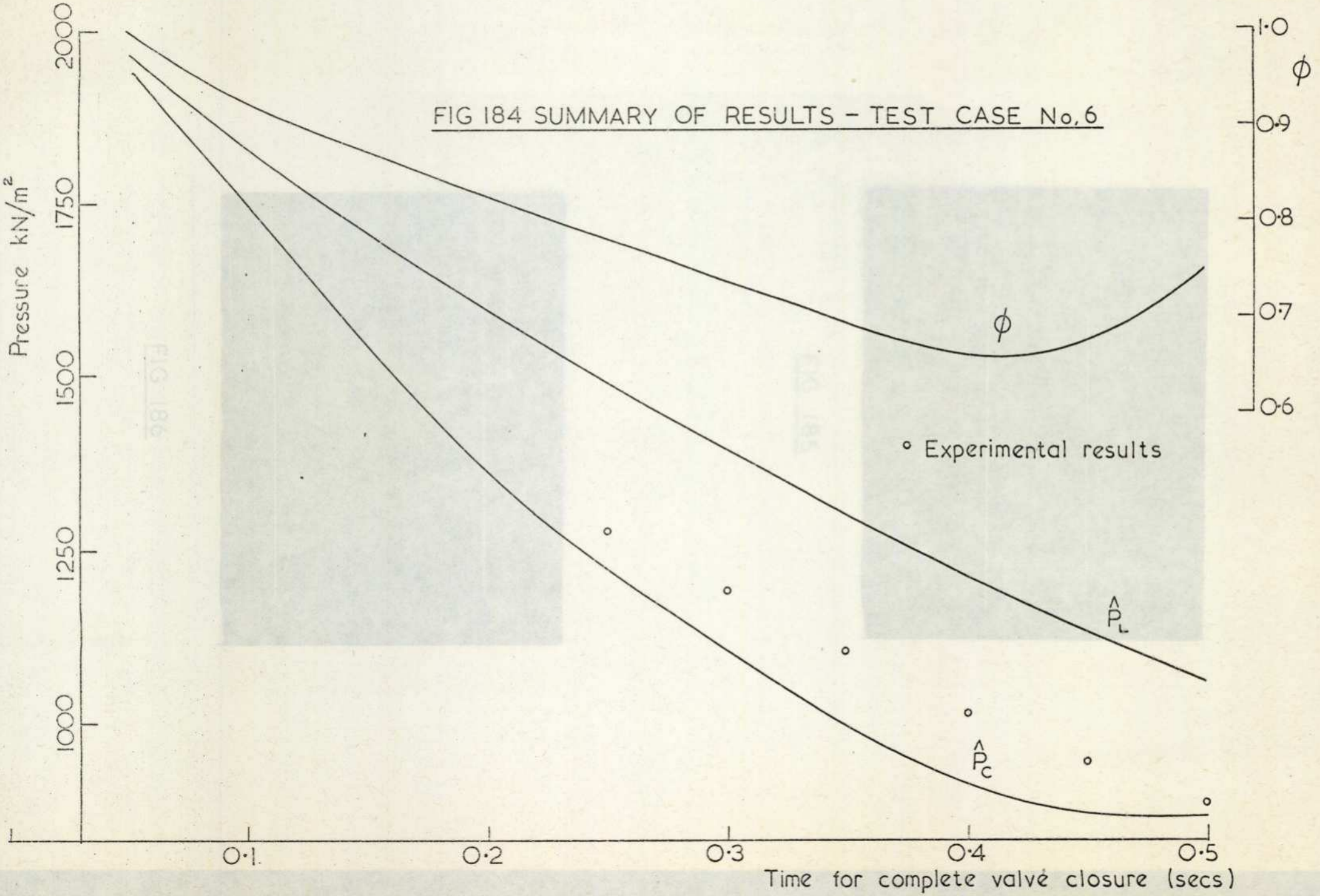


FIG 183


FIG 184 SUMMARY OF RESULTS – TEST CASE No. 6
Pressure kN/m²
2000
1750
1500
1250
1000
1·0
0·9
0·8
0·7
0·6
ϕ
ϕ
° Experimental results
$\hat{P}_L$
$\hat{P}_C$
0·1
0·2
0·3
0·4
0·5
Time for complete valve closure (secs)

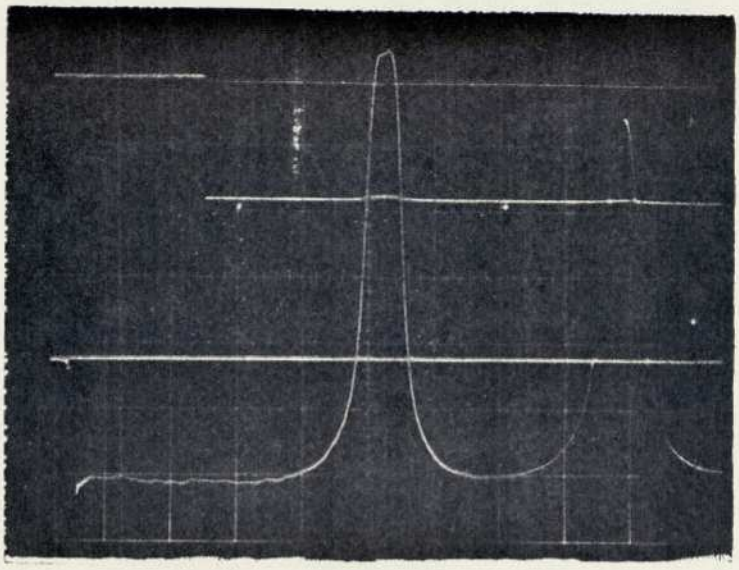


FIG 185

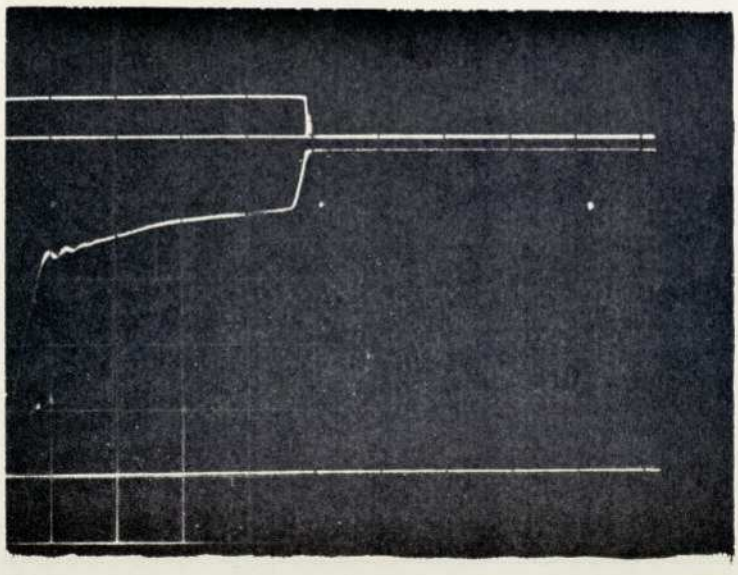


FIG 186

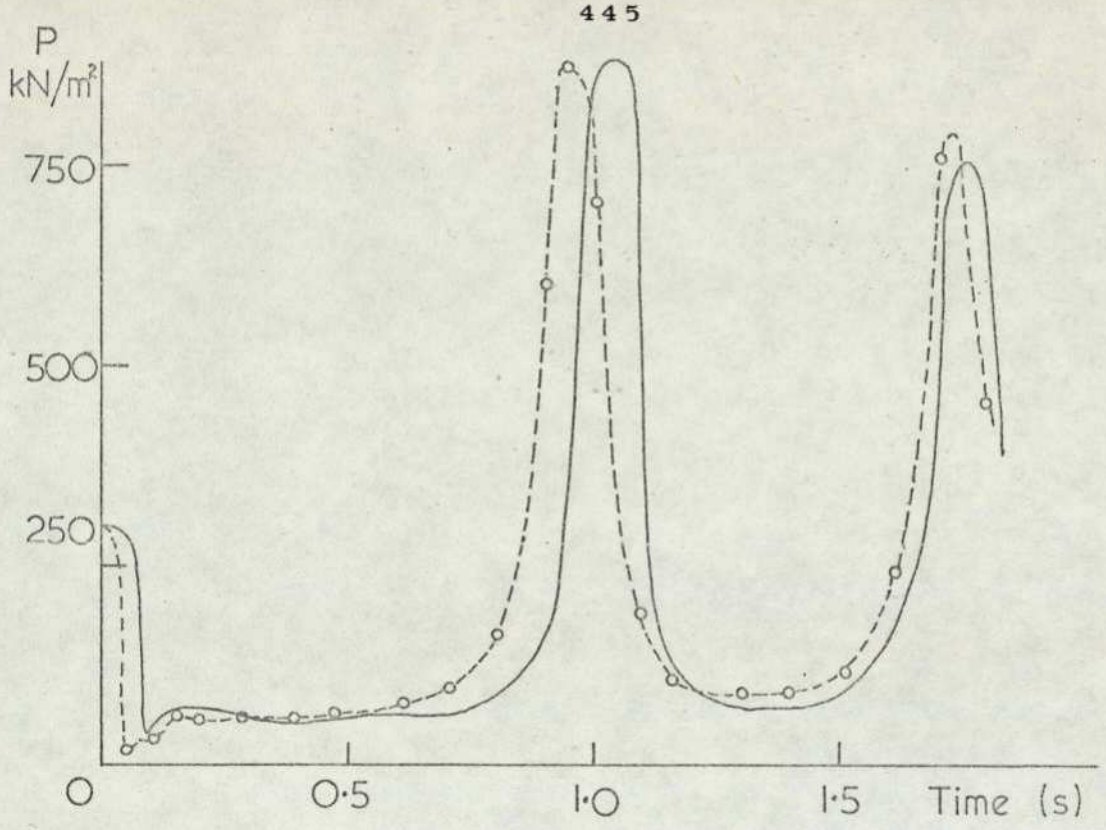


FIG 187

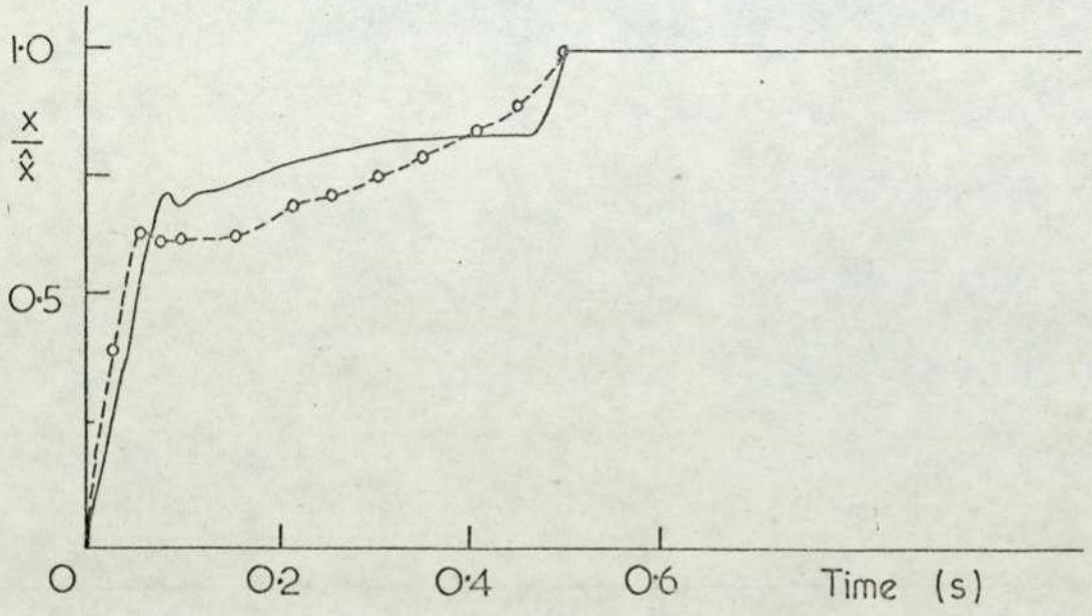


FIG 188

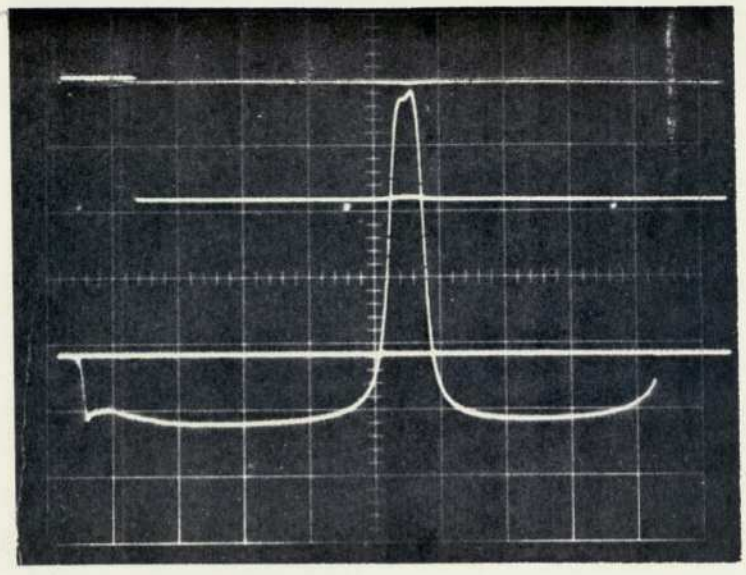


FIG 189

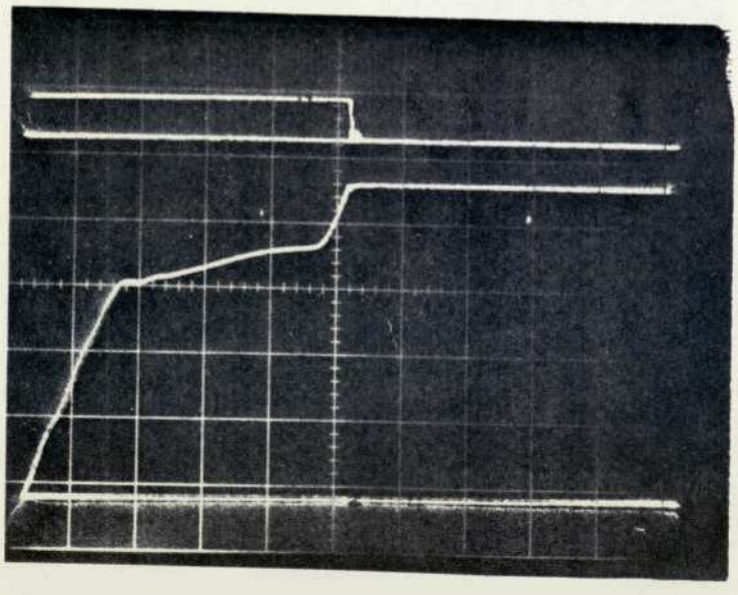


FIG 190

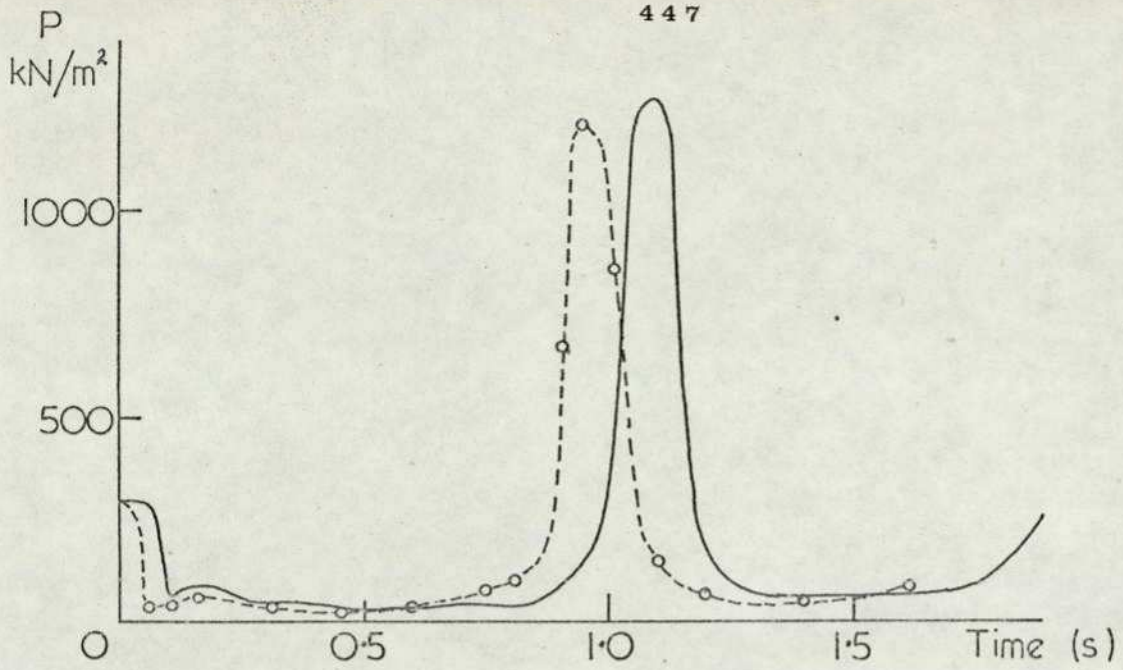


FIG 191

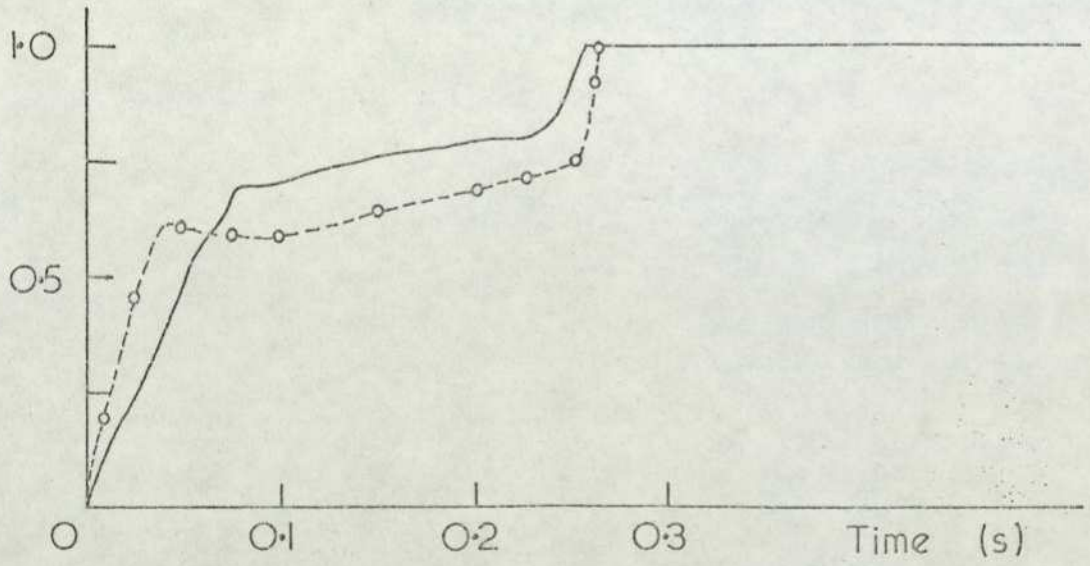


FIG 192

EXPERIMENTAL WORK-PRESENTATION OF RESULTS

Figs 193-198 shows the variation in transient pressure for different values of the minimum demanded pressure P_{min}. The values of P_{min} in each case is given in the table below.

Fig No.	P_{min} (KN/m^2)	P_c (KN/m^2)
193	34.3	780
194	51.4	750
195	68.6	625
196	85.6	545
197	103.0	795
198	120.0	850

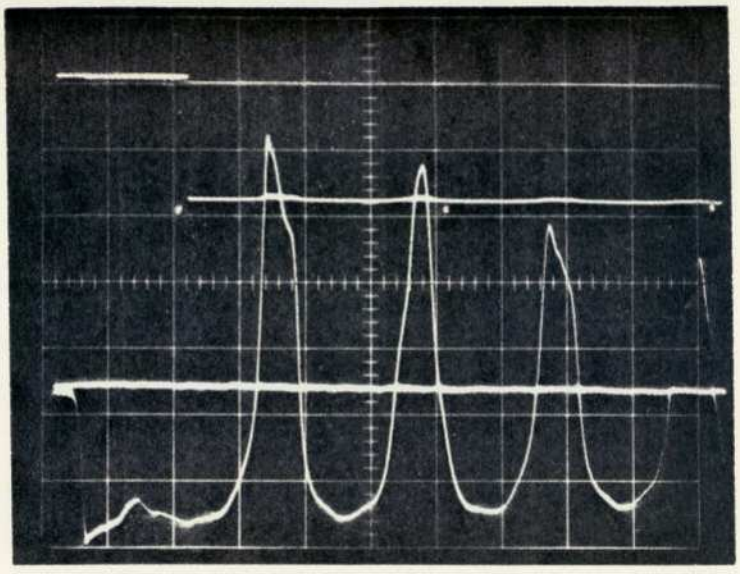


FIG 193

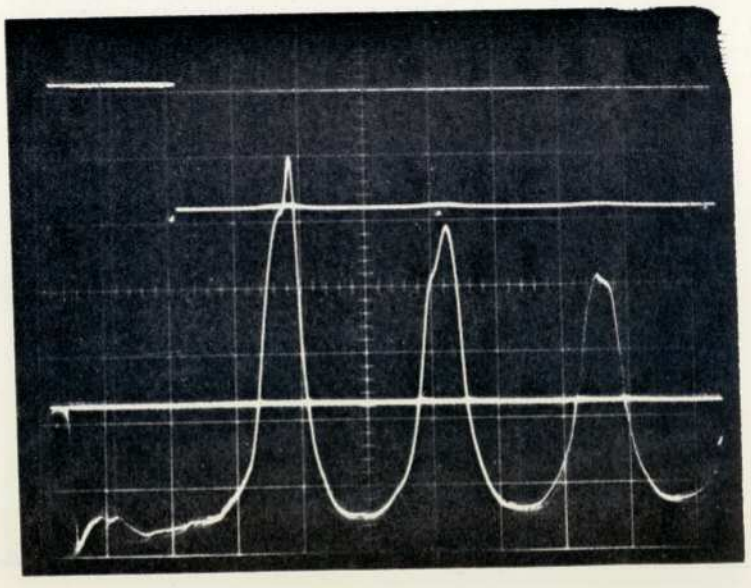


FIG 194

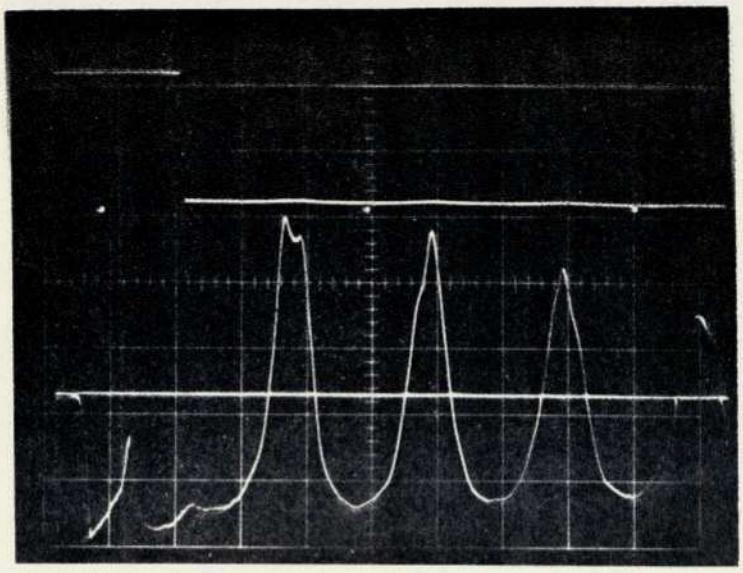


FIG 195

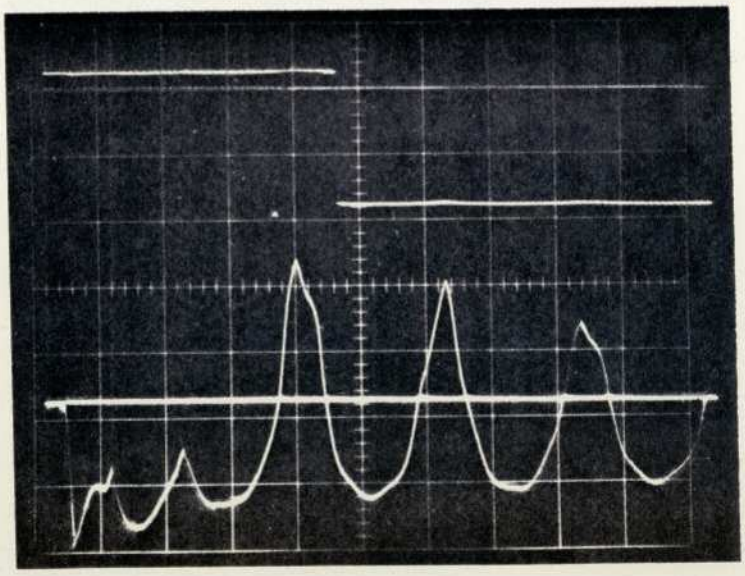


FIG 196

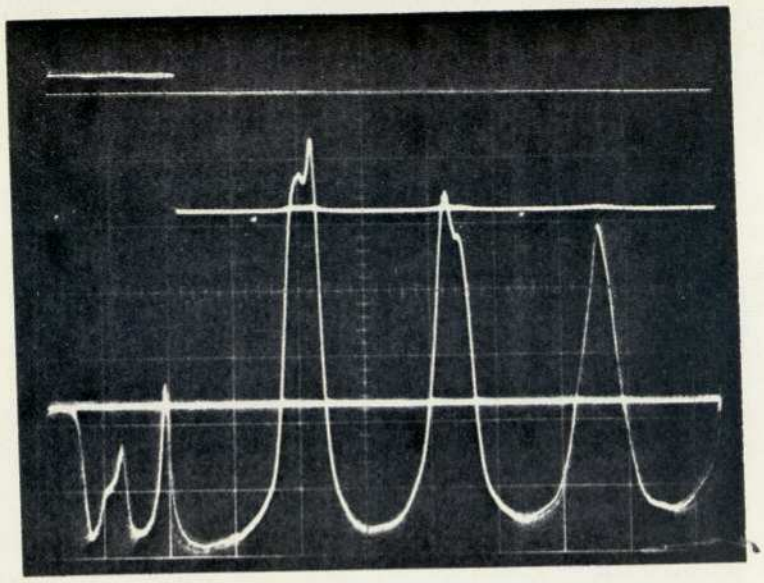


FIG 197

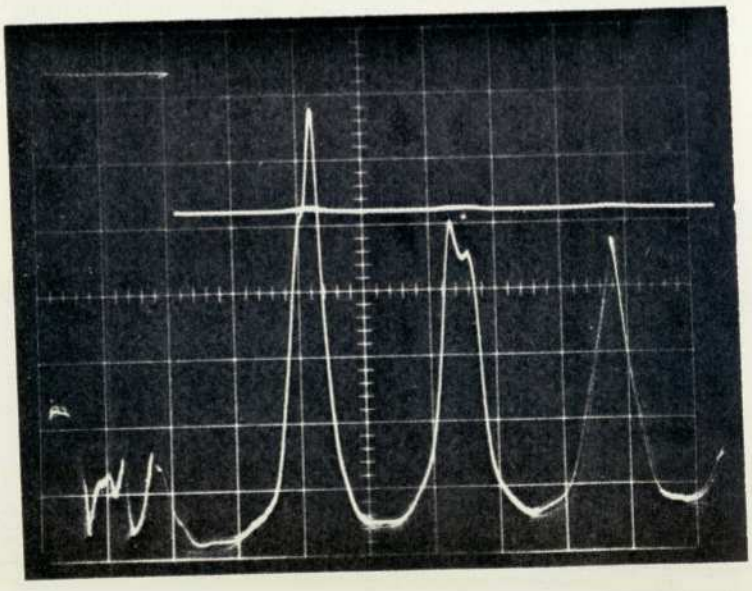


FIG 198

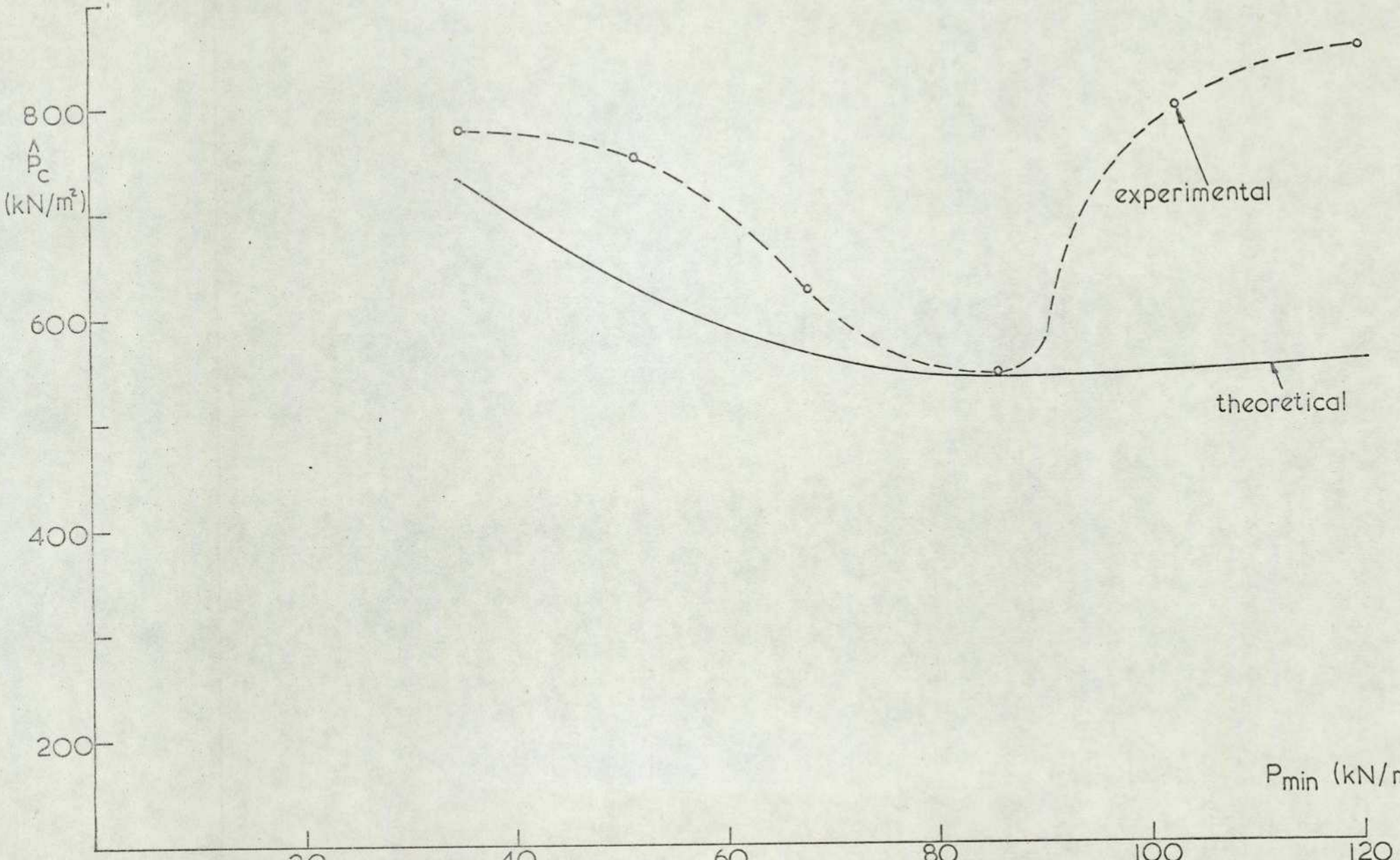


FIG 199 EFFECT OF CHANGING P_{min} ON MAX. SYSTEM PRESSURE

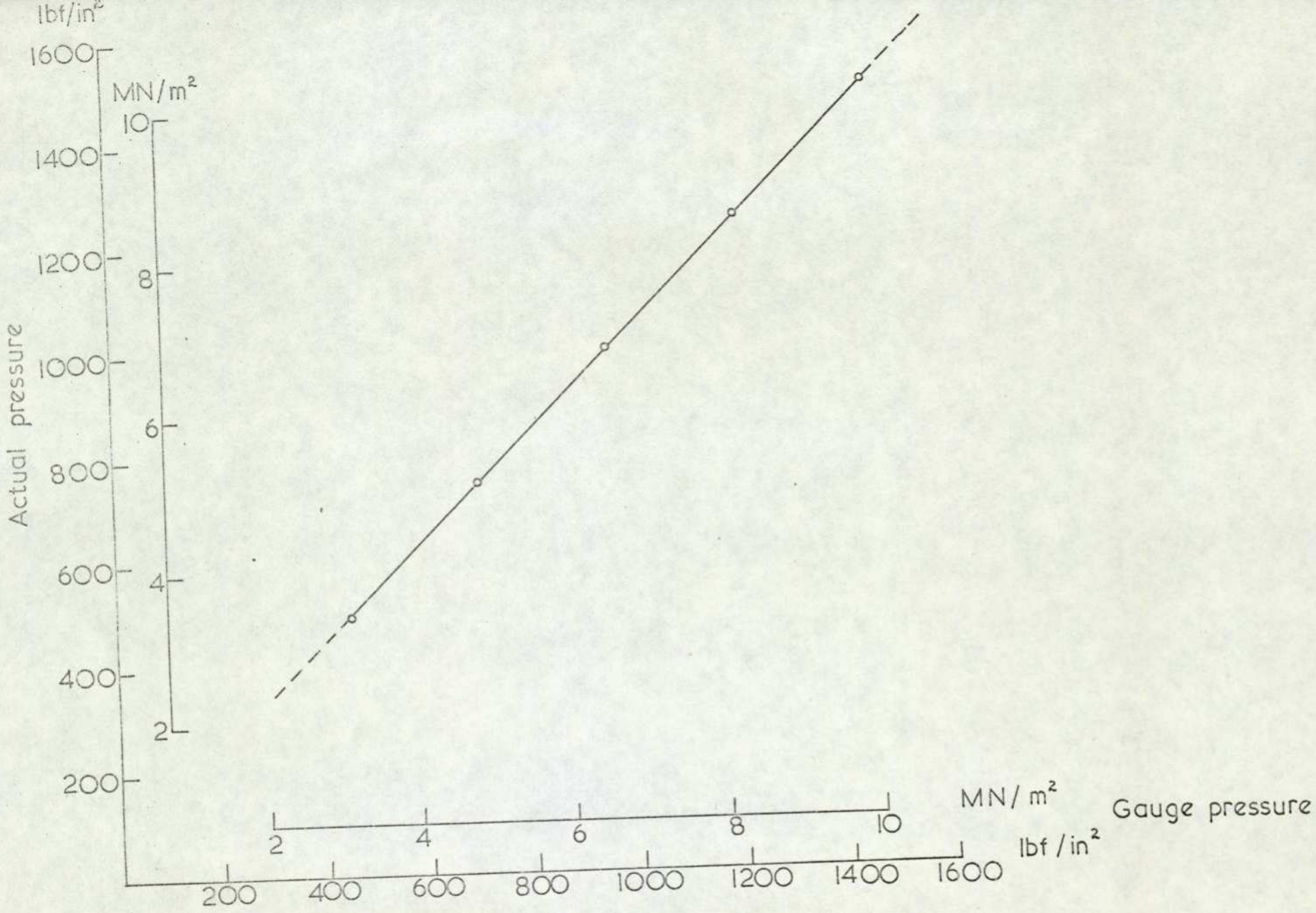
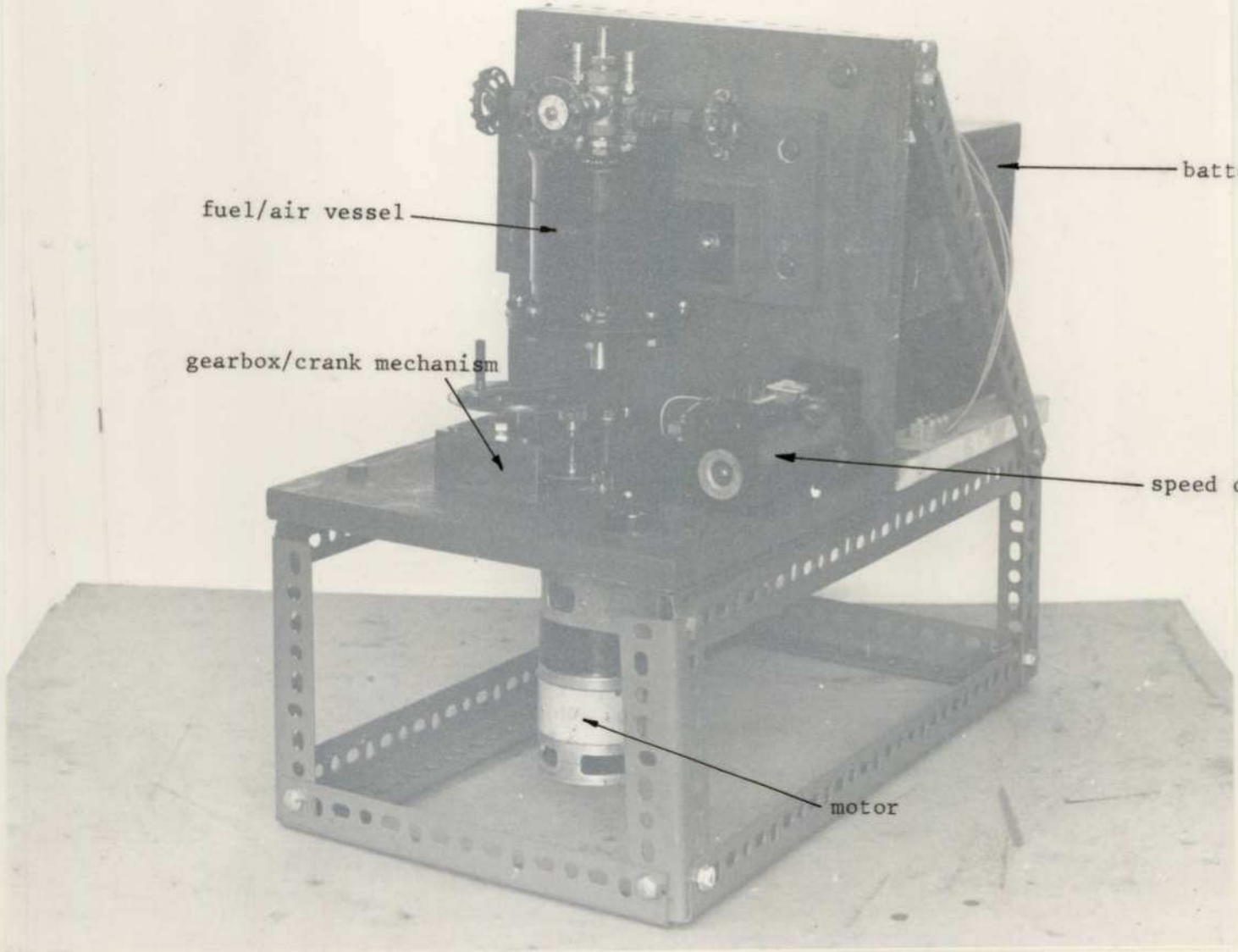


FIG 200 SERVO SYSTEM PRESSURE CALIBRATION CHART

FIG 201 VIEW OF TRANSIENT AIR RELEASE EQUIPMENT



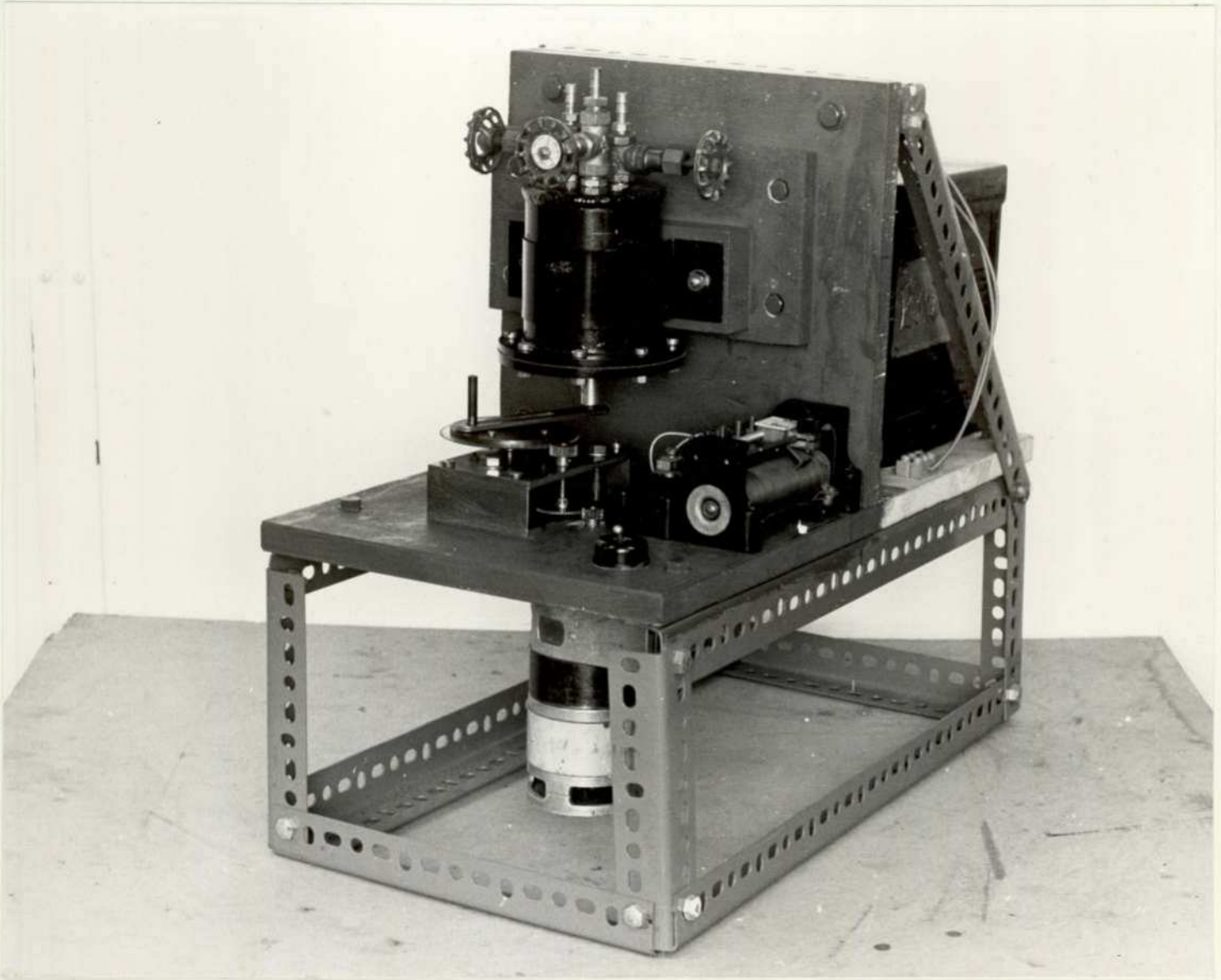
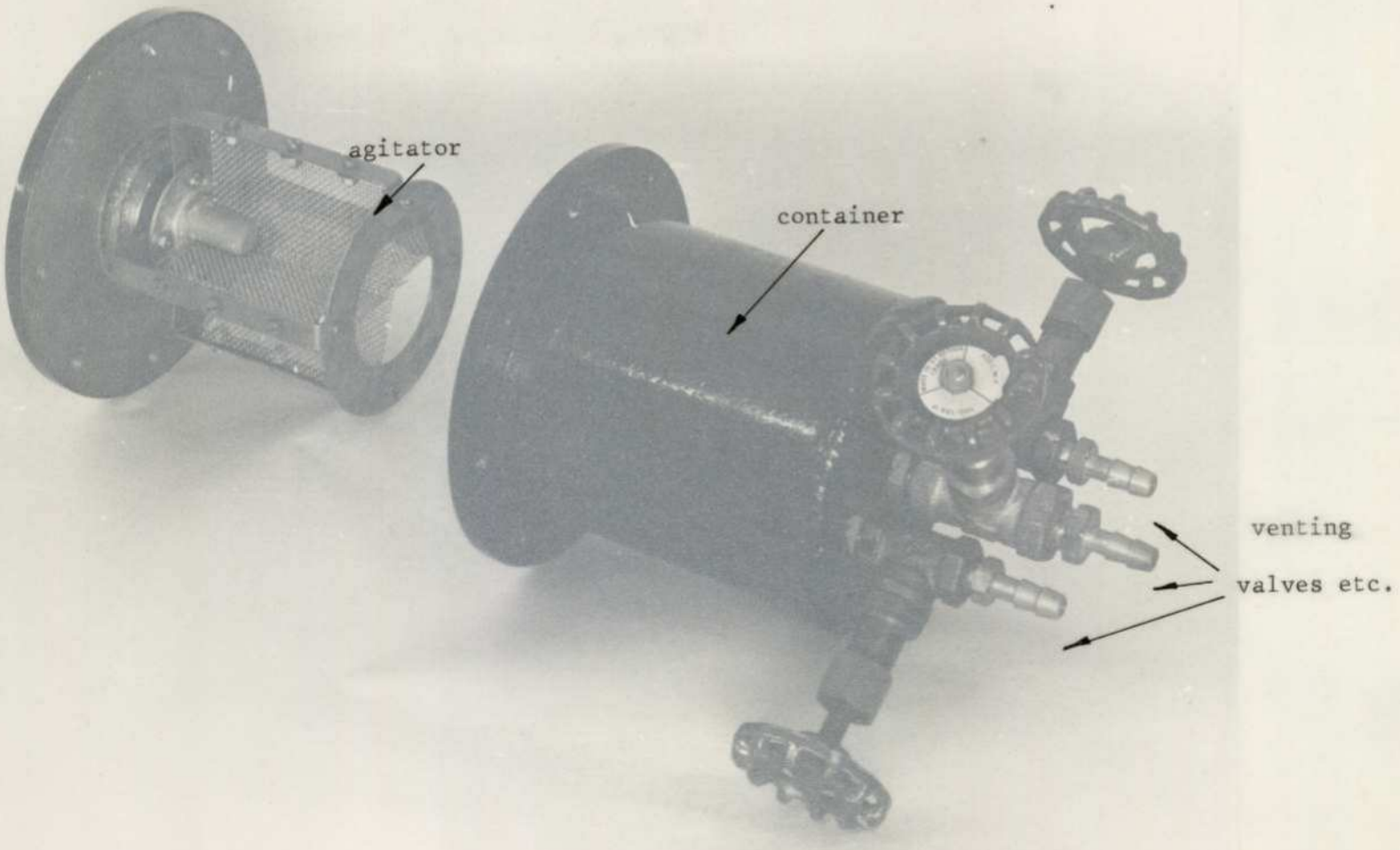
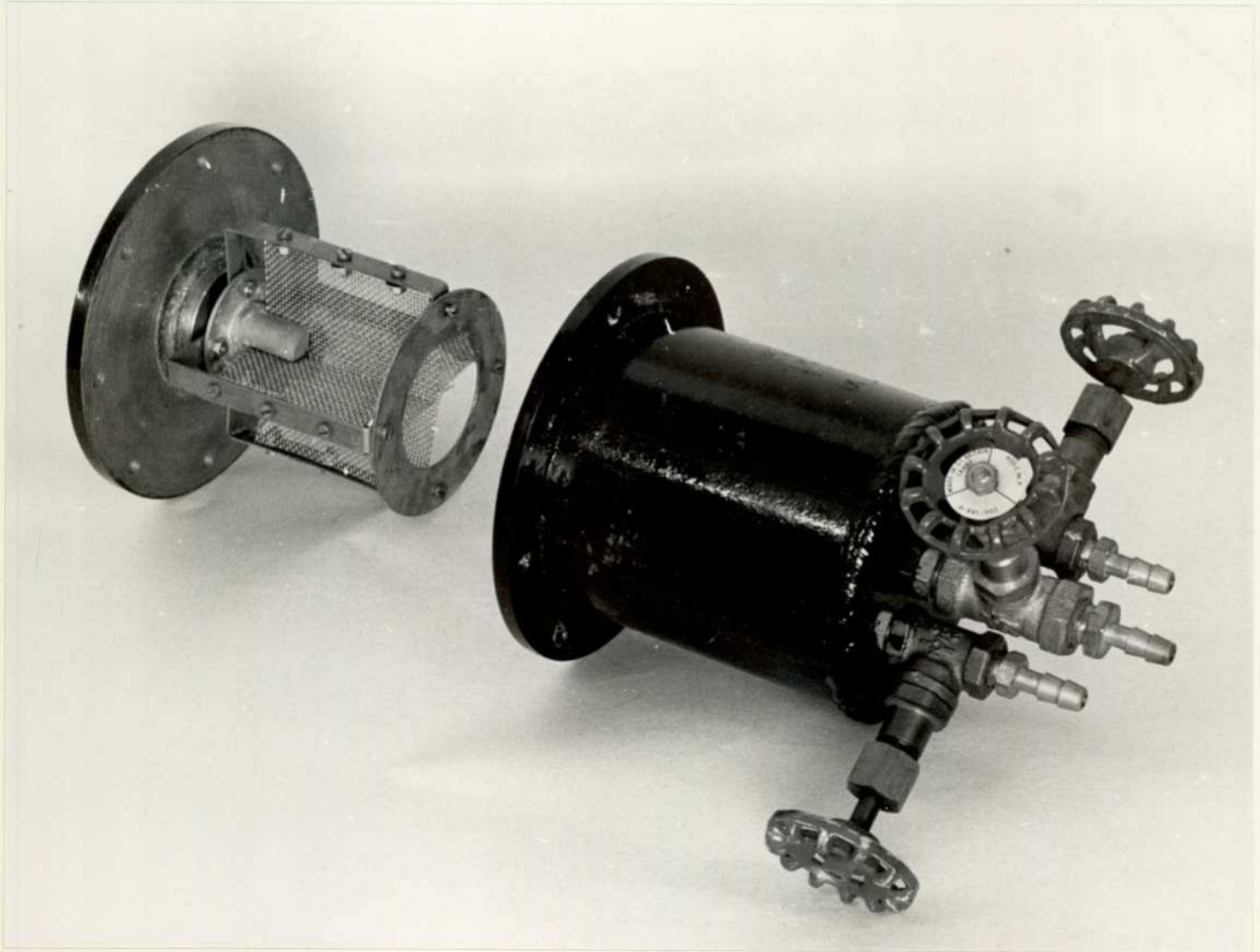


FIG 202 VIEW OF AGITATOR AND CONTAINER OF THE TRANSIENT AIR RELEASE EQUIPMENT





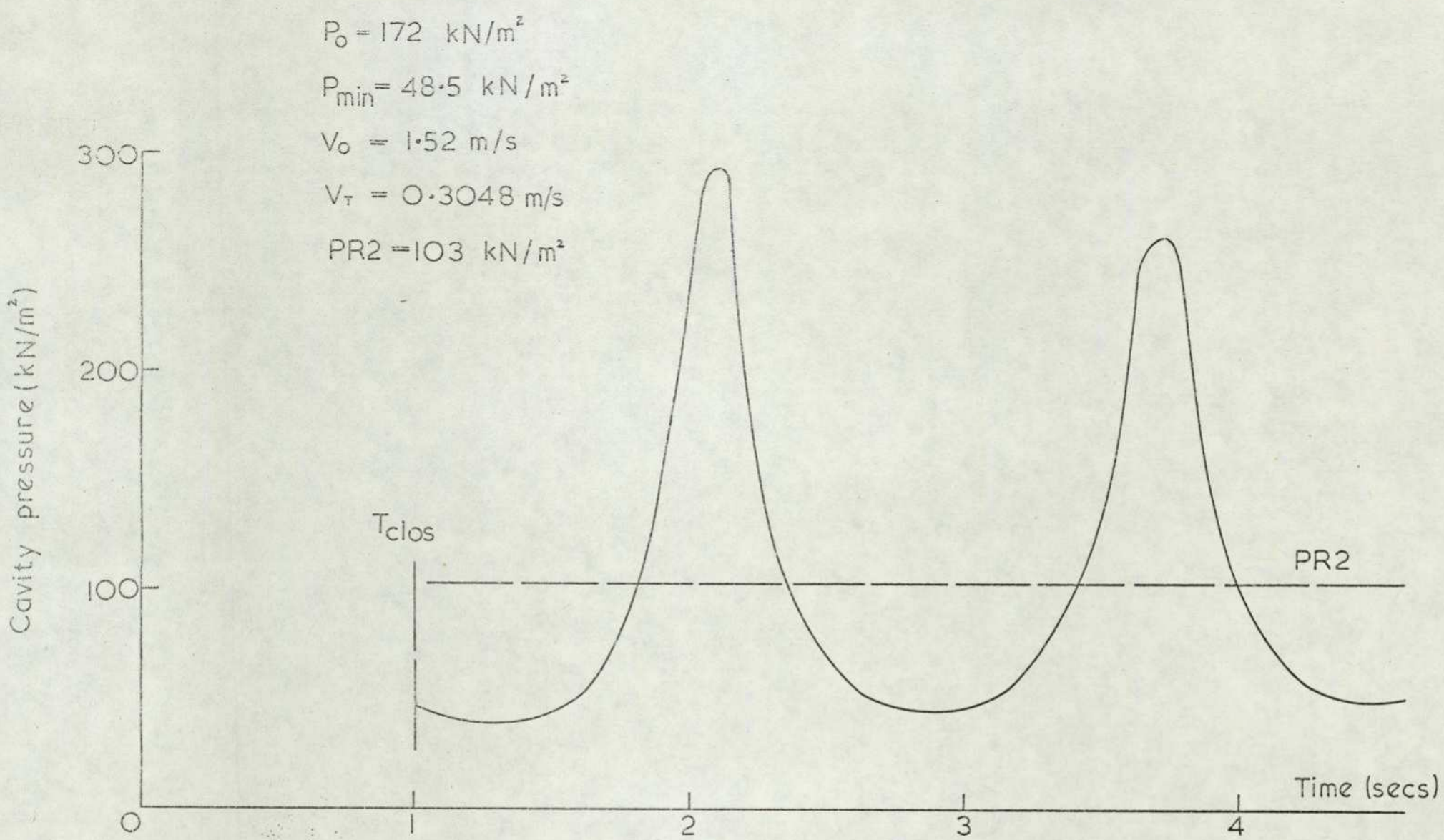


FIG 203 TYPICAL OUTPUT OF PROGRAM PTP6

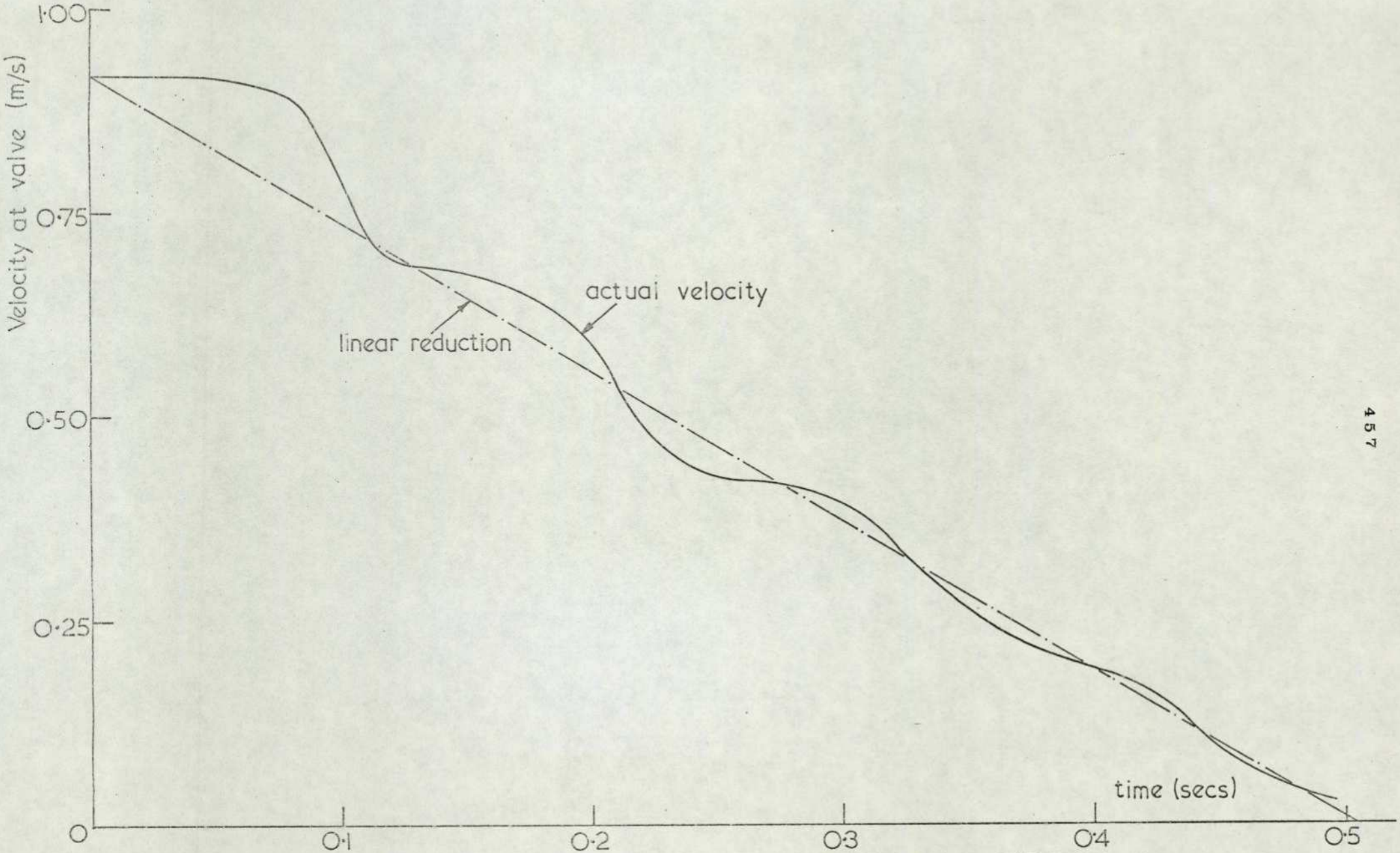


FIG 204 FLOW REDUCTION PREDICTED FOR V.S. METHOD 3

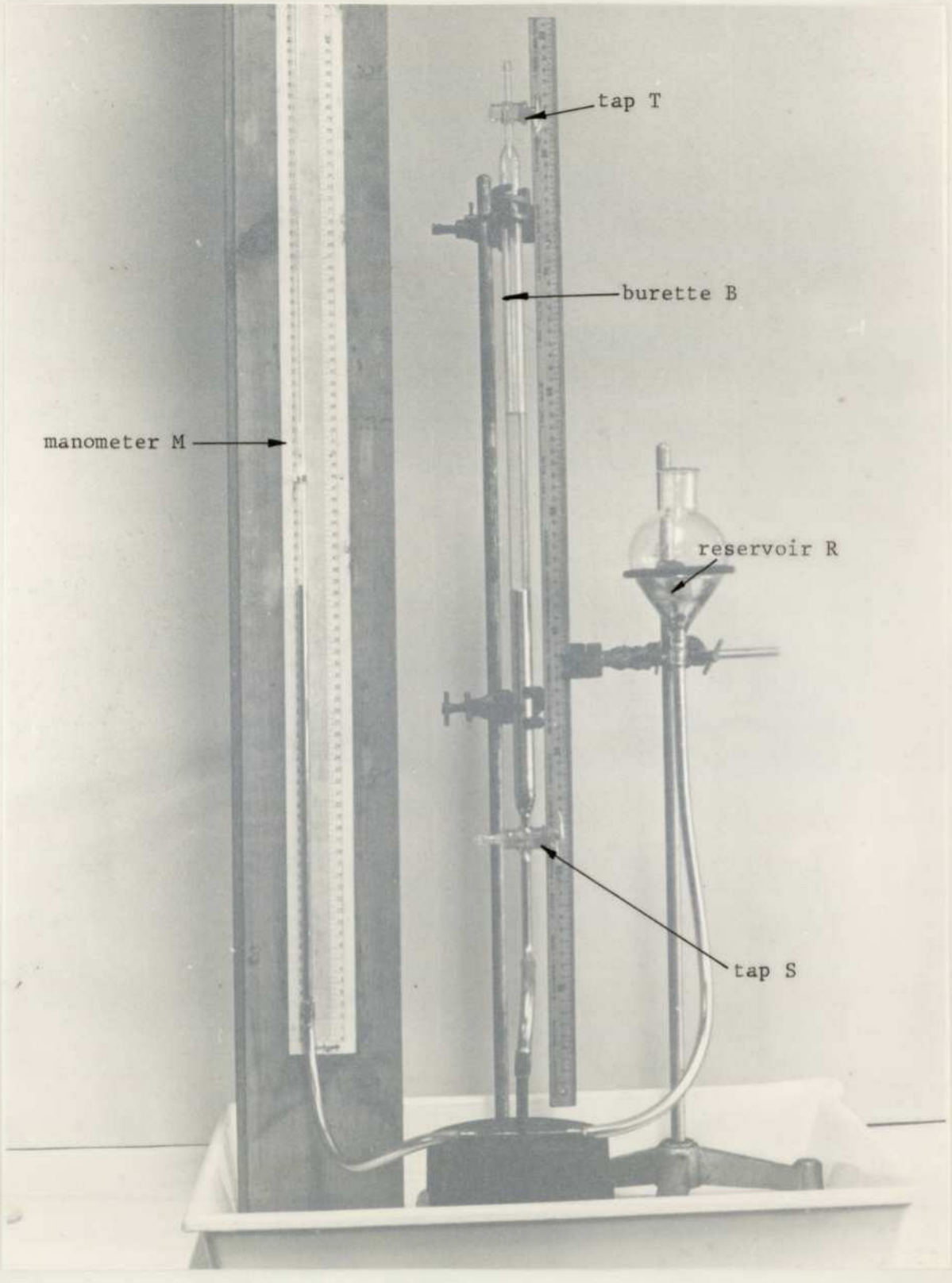


FIG 205 VIEW OF STEADY STATE AIR RELEASE EQUIPMENT

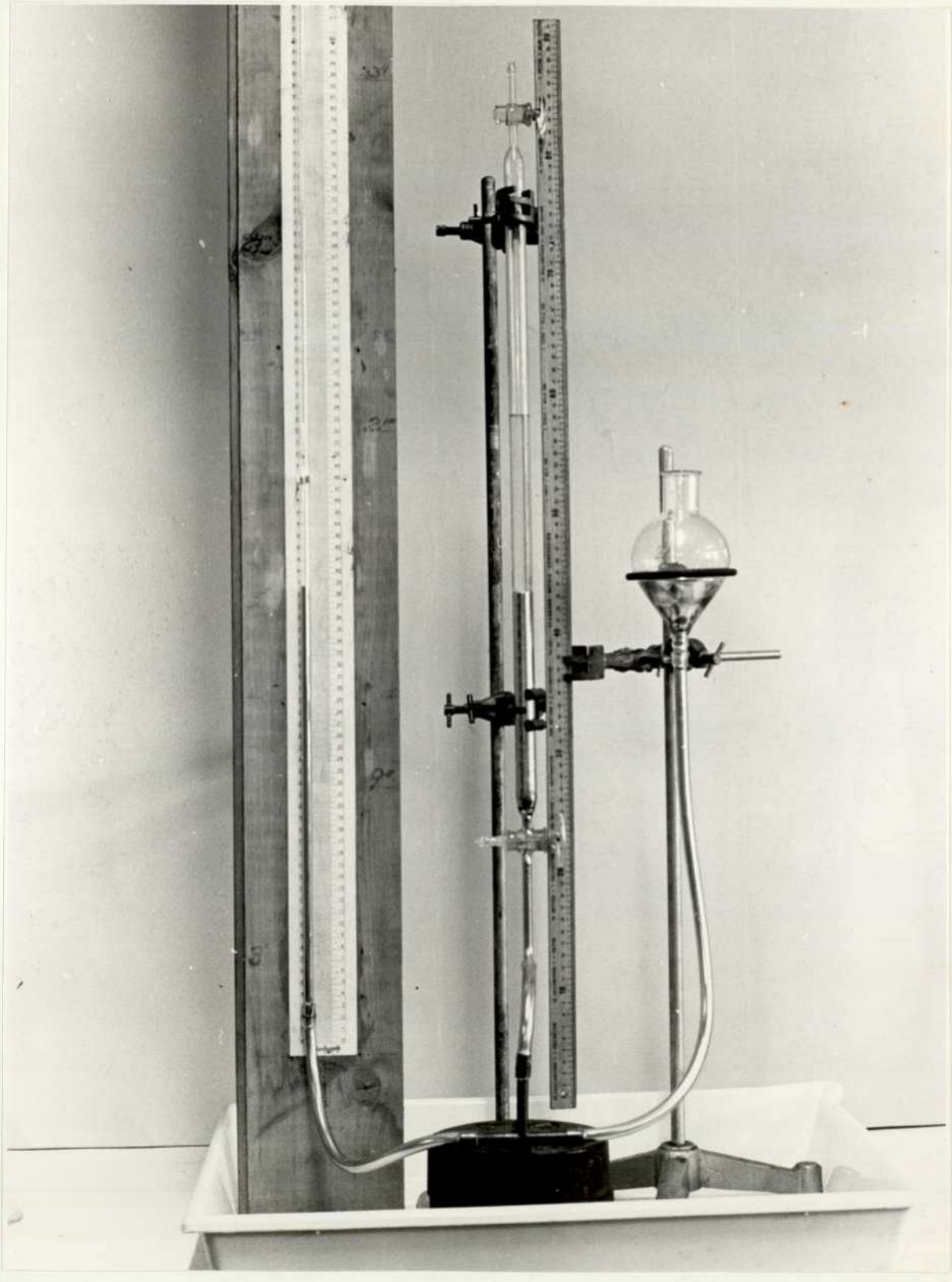
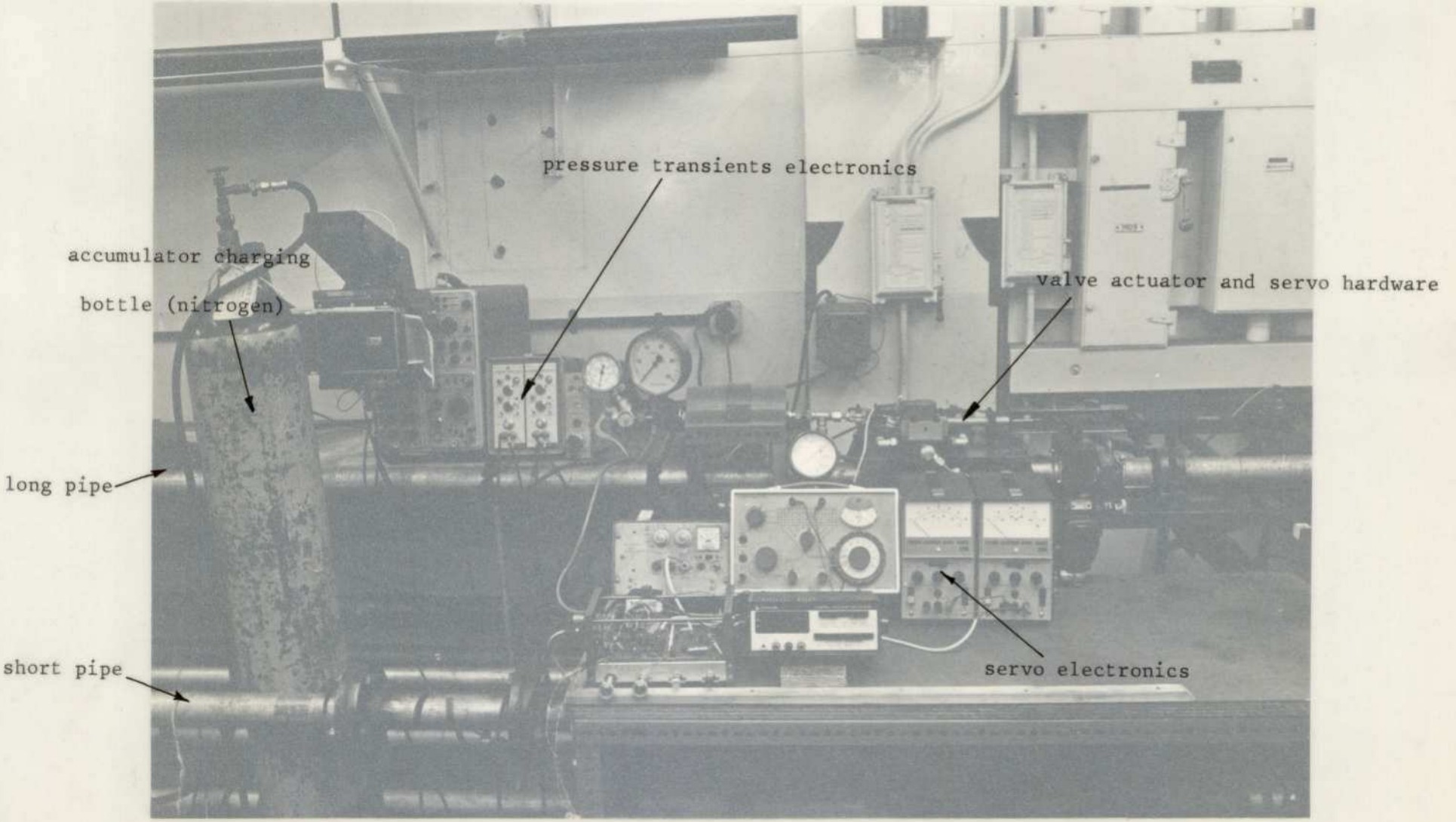


FIG 206 GENERAL VIEW OF RIG OPERATING AREA



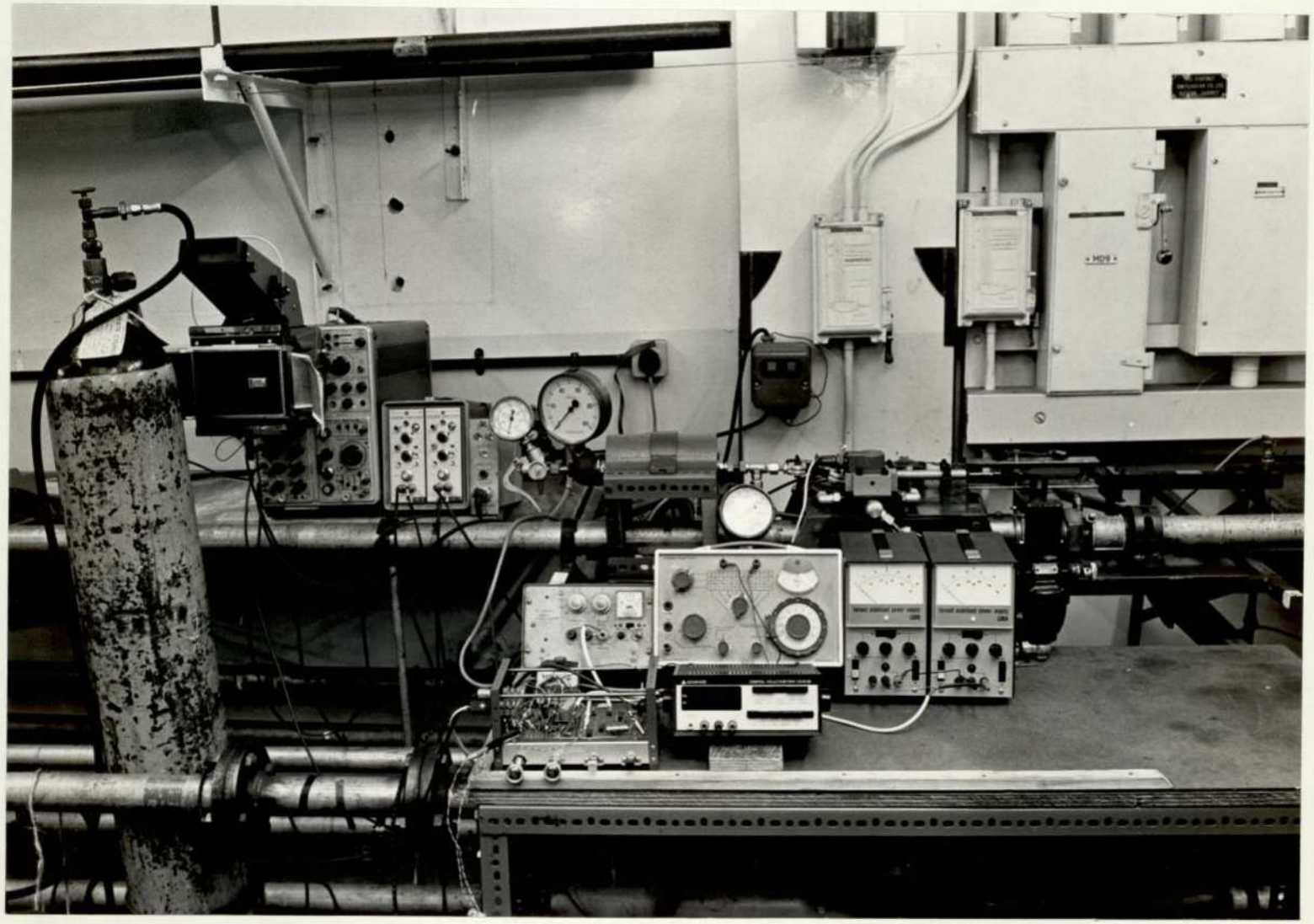
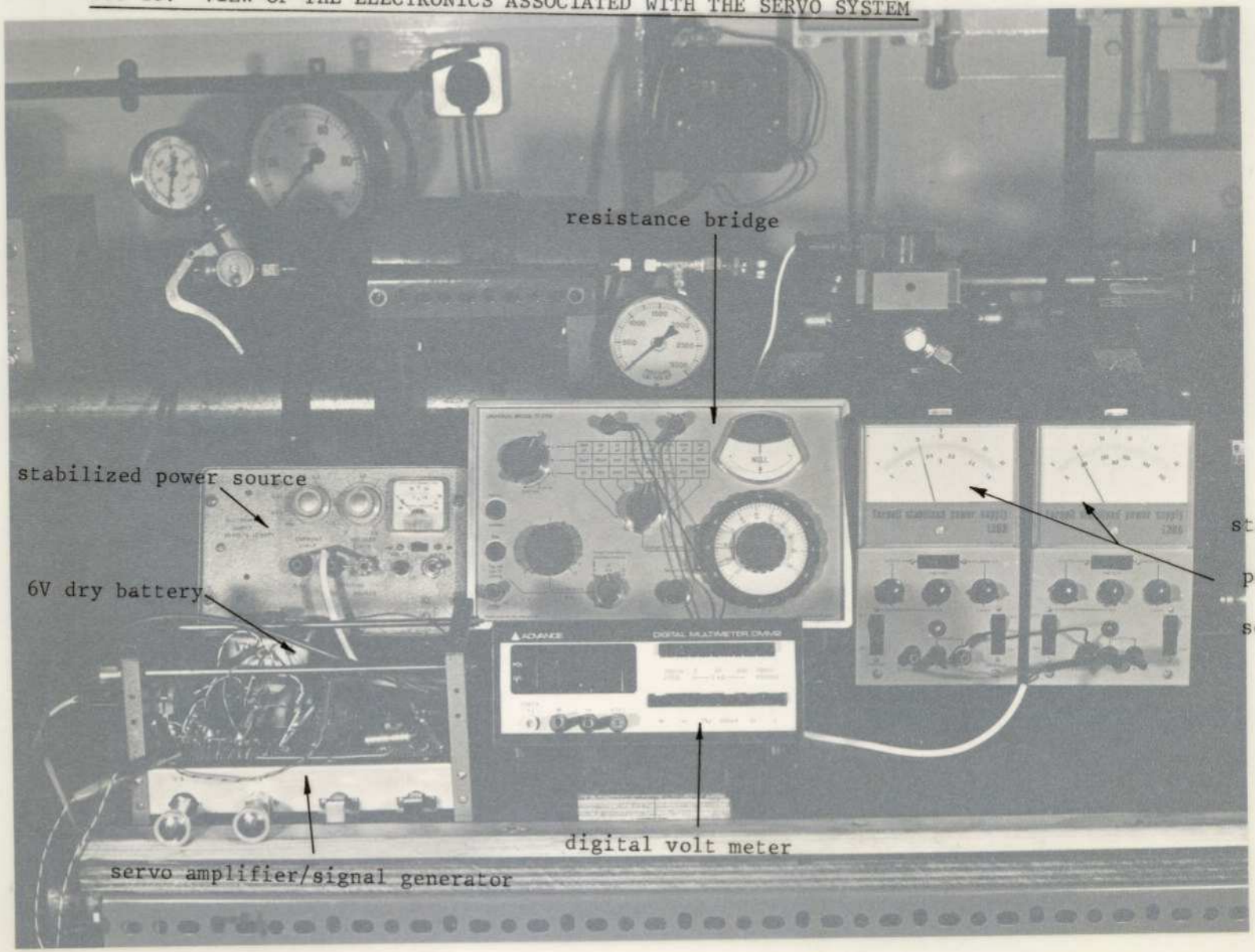
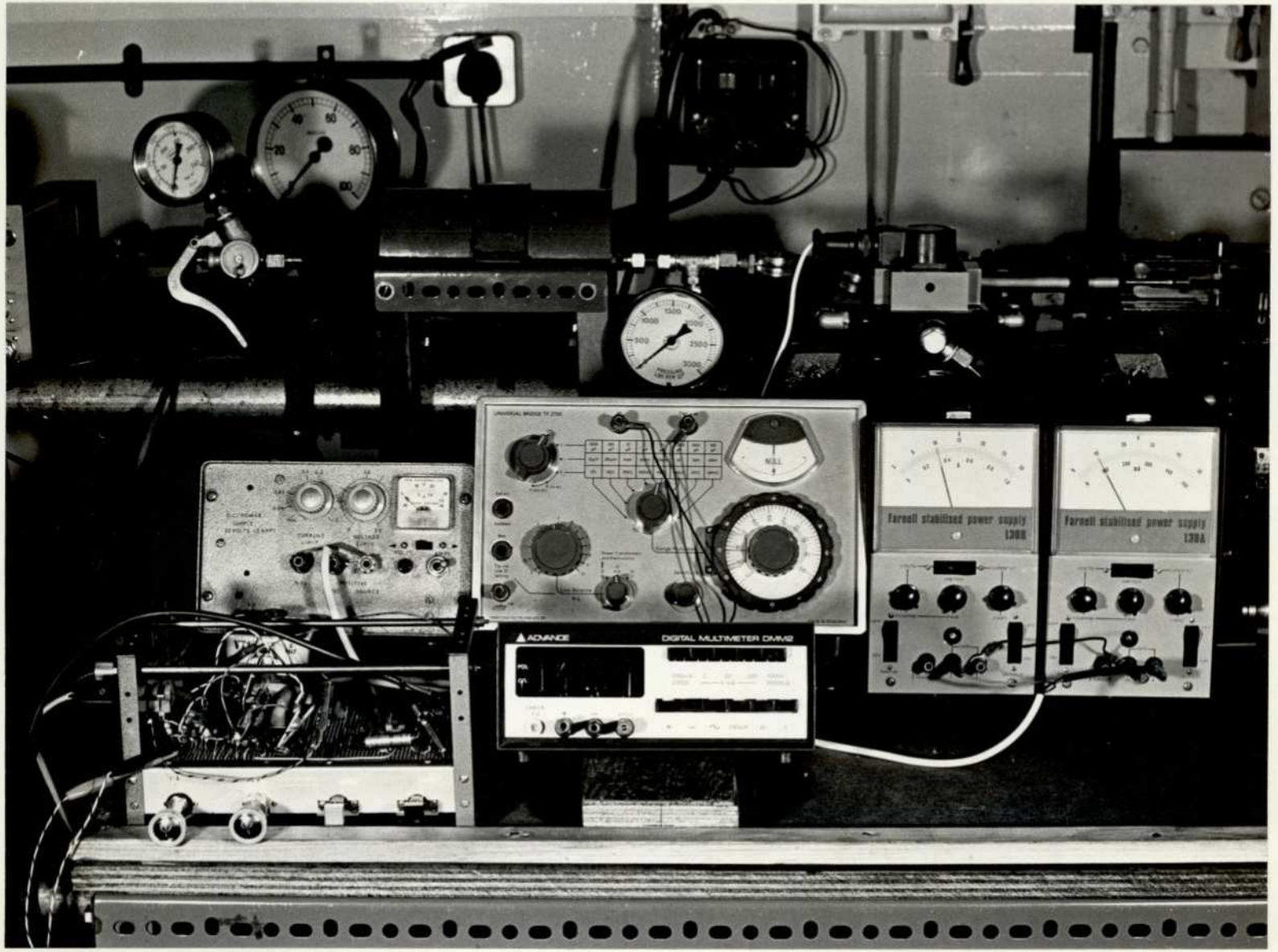


FIG 207 VIEW OF THE ELECTRONICS ASSOCIATED WITH THE SERVO SYSTEM




Farnell stabilised power supply
L30B
Farnell stabilised power supply
L30A
ADVANCE
DIGITAL MULTIMETER DMM2

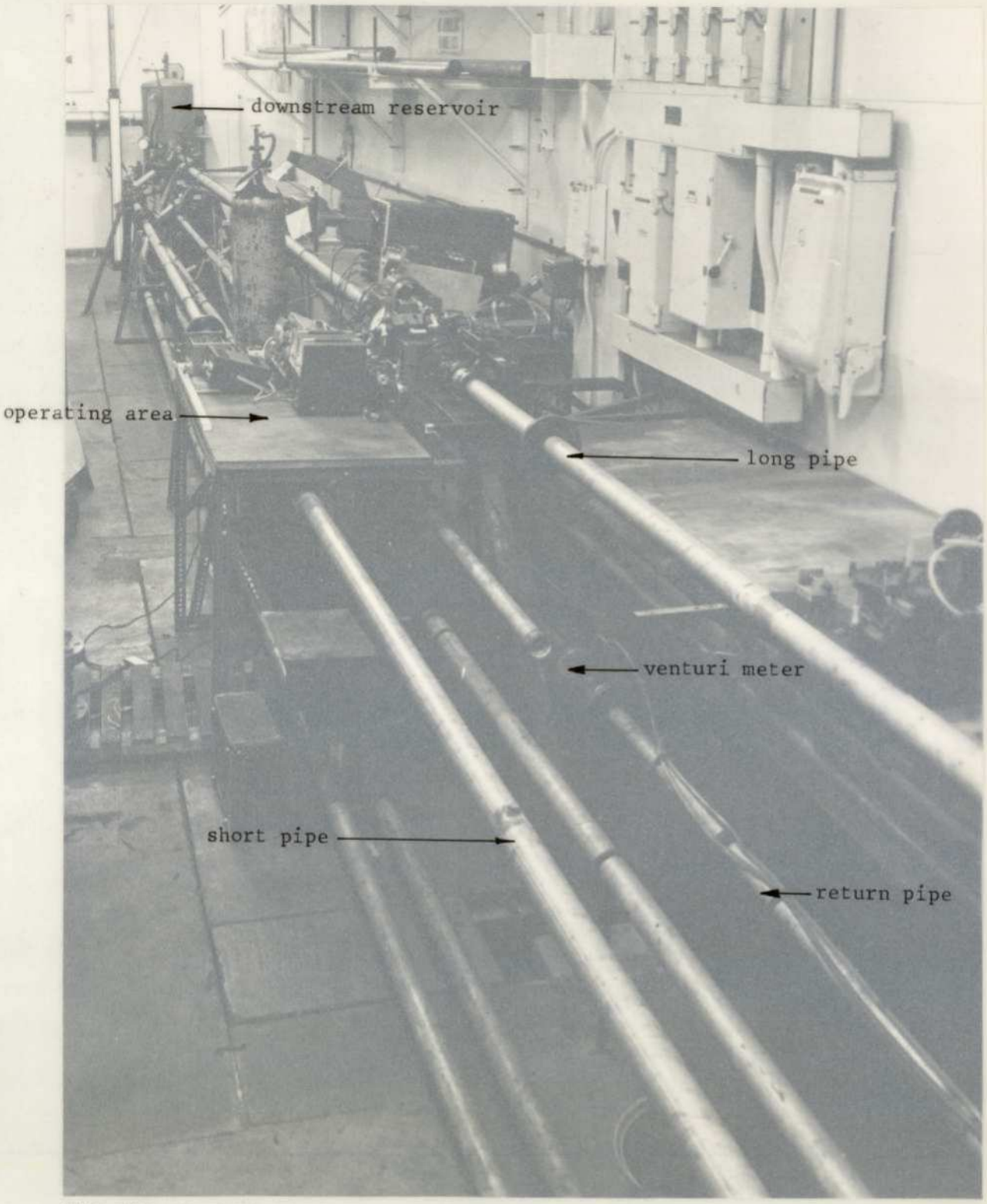


FIG 208 GENERAL VIEW OF TEST RIG LOOKING TOWARDS THE DOWNSTREAM END

FOR FIG 209 SEE FIG 38

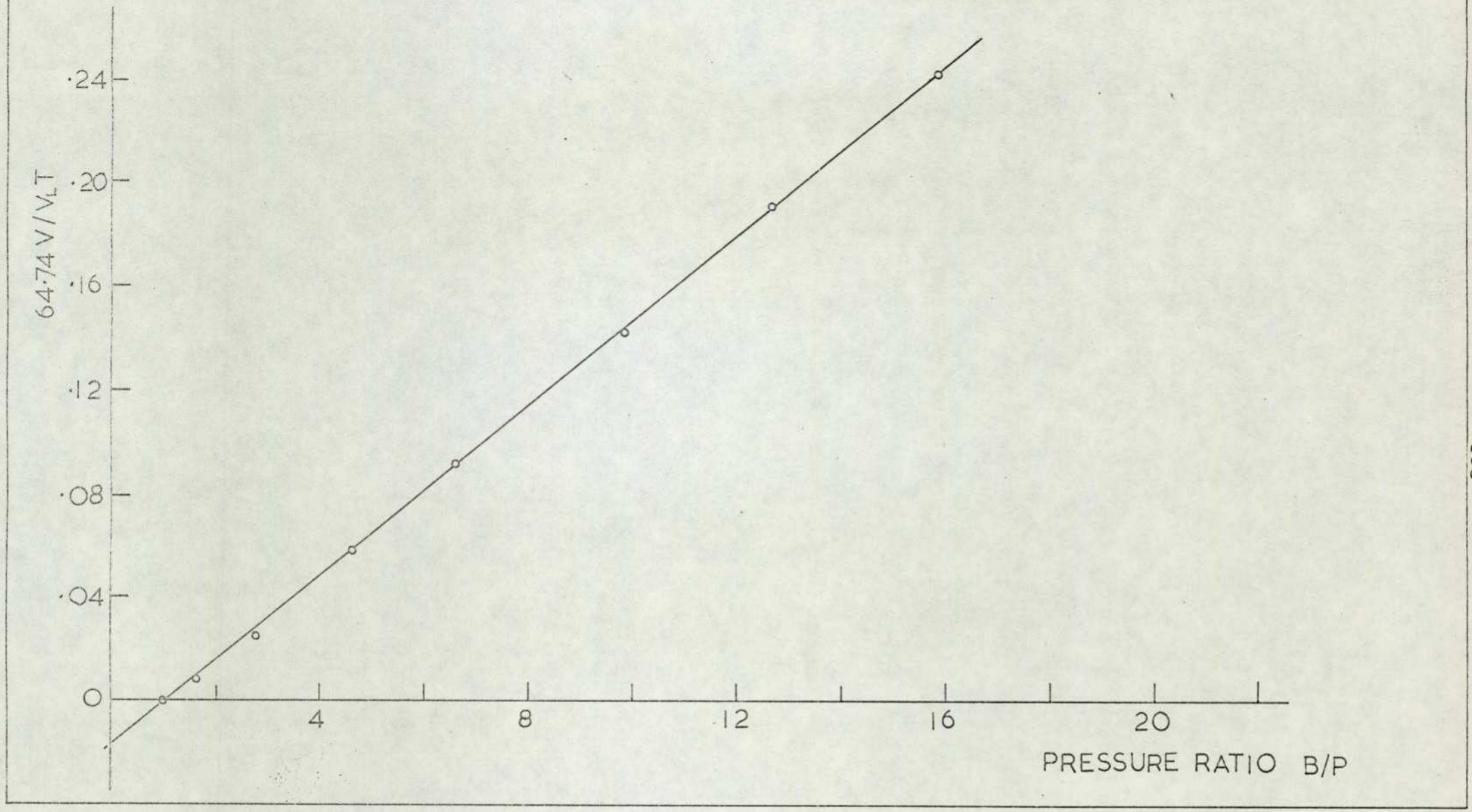


FIG 210 DETEMINATION OF SOLBILITY COEFFICIENT FOR SATURATION TIME = 100 MINS.

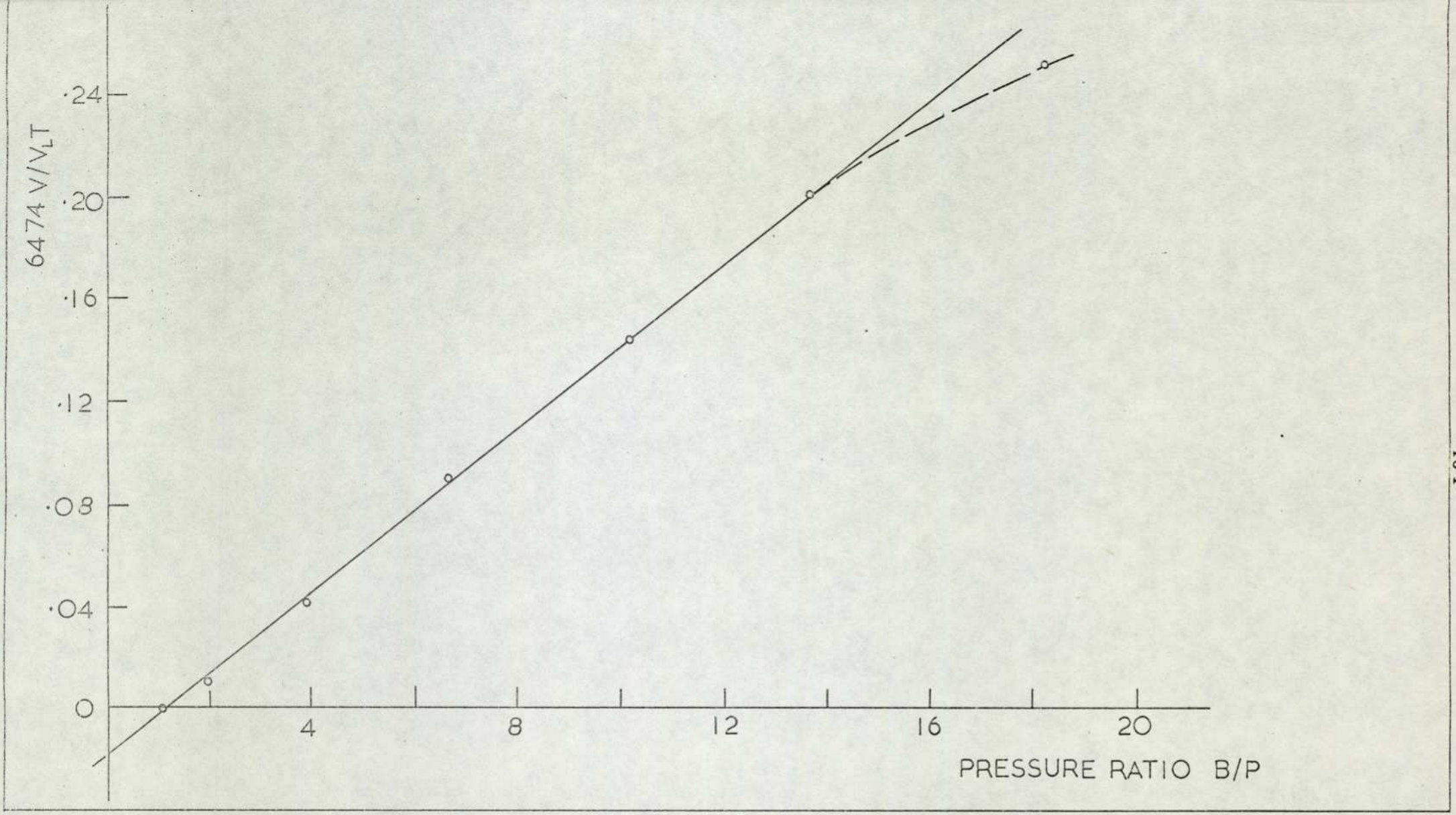


FIG 211 DETERMINATION OF SOLUBILITY COEFFICIENT FOR SATURATION

TIME = 15 MINS.

TABLE 1 TEST 1

V_o Flow vel ft/s	P_1 U/S air Pressure Cms Hg	h_1 U/S static head "kerosene	P_2 D/S air pressure "Hg	h_2 D/S static head cms kerosene	P_1 Pressure drop across valve cms Ker.	P corrected for pipe dia. cms Ht	R_e Reynolds No. x 10^4	P_2 Press. drop in U/S pipe cms Hg	P_3 Press drop in d/s pipe cms Hg	$P_1 + P_2 + P_3$ cms Hg	P_v cms Hg
7.70	111.6	9.8	18.9	12.4	-52.7	0.476	7.12	3.48	41.5	45.26	9.6
5.90	111.2	9.5	27.6	17.4	-29.3	0.288	5.45	2.21	26.4	28.90	6.4
4.05	111.2	9.0	35.8	23.1	-14.6	0.134	3.74	1.14	13.6	14.87	3.2
3.20	111.2	8.8	38.5	24.1	-10.5	0.076	2.96	0.75	8.95	9.78	1.7
0.00	111.2	/	/	/	0.0	0.0	0.0	0.0	0.0	0.0	0.0
1	2	3	4	5	6	7	8	9	10	11	12

TABLE 2 TEST 2

θ°	venturi man ht in hg	Δ Pressure drop across valve cms ker.	V ft/sec	ΔP drop across valve cms Ker.	ΔP corrected for venturi height	$\frac{\Delta P_o}{\Delta P}$	$\frac{\Delta P_o}{\Delta P}$	$\frac{V}{V_o}$	γ
90	11.75	-5.4	6.65	-5.4	2.64	1.00	1.0	1.000	1.0
85	11.75	-5.0	6.65	-5.0	3.00	0.88	0.937	1.000	0.937
80	11.75	2.5	6.65	2.5	8.25	0.312	0.562	1.000	0.562
75	11.65	34.1	6.60	34.1	42.10	0.0627	0.250	0.992	0.248
70	11.45	66.1	6.55	66.1	74.1	0.0356	0.189	0.985	0.187
65	11.40	84.9	6.55	84.9	92.9	0.0284	0.168	0.985	0.165
60	11.25	8.9*	6.50	151.0	159.0	0.0166	0.129	0.978	0.126
55	10.70	14.0*	6.30	238.0	246.0	0.0108	0.104	0.947	0.0985
50	10.00	22.2*	6.15	377.0	385.0	0.00686	0.0829	0.925	0.0766
45	8.8	33.2*	5.75	565.0	573.0	0.00461	0.0680	0.865	0.0588
40	7.3	47.9*	5.20	813.0	821.0	0.00322	0.0568	0.783	0.0445
35	5.5	64.8*	4.50	1100.0	1108.0	0.00238	0.0488	0.677	0.0330

* Switch to mercury man; diff. in Hg heights.

TABLE 3

Test Performed	7.9.71.
Ambient temperature	22.1°C
Fuel saturation time	100 mins
Volume of wire cage	0.15 ml
Initial volume of fuel	26.0 ml
Final volume of fuel	25.9 ml

Reading on Manometer Scale cm. Hg.	Reading on Burette Scale cm. Hg.	Cavity Volume ml	Cavity Pressure cm. Hg.	$\frac{B}{P}$	$\frac{64.74V}{V_L.T}$
100.0	46.3	0.0	76.0	1.00	0.00000
69.4	45.4	1.7	46.3	1.64	0.00797
43.8	43.2	5.4	27.1	2.80	0.02530
37.6	40.6	10.1	19.3	3.94	0.04740
24.7	35.4	19.6	11.6	6.55	0.09200
15.0	29.5	30.5	7.8	9.87	0.14300
7.5	23.8	41.0	6.0	12.65	0.19200
0.5	18.0	51.8	4.8	15.85	0.24300

TABLE 4

Test Performed	9.9.71
Ambient temperature	21.0°C
Fuel saturation time	15 mins
Volume of wire cage	0.15 ml
Initial volume of fuel	25.8 ml
Final volume of fuel	25.7 ml

Reading on Manometer Scale cm. Hg.	Reading on Burette Scale cm. Hg.	Cavity Volume ml	Cavity Pressure cm. Hg.	$\frac{B}{P}$	$\frac{64.74V}{V_L.T}$
100.7	46.3	0.0	76.0	1.00	0.0000
63.8	45.1	2.1	40.3	1.89	0.0100
39.6	41.4	8.8	19.8	3.84	0.0419
25.6	35.9	18.8	11.3	6.73	0.0895
15.5	29.6	30.4	7.5	10.15	0.1450
7.2	23.2	42.1	5.6	13.56	0.2010
0.2	17.4	52.7	4.2	18.10	0.2510

Table 5 Summary of test cases considered for the second stage of experimental work

Test case no.	P_o kN/m^2	V_o m/s	P_{min} kN/m^2
1	170.0	0.915	34.3
2	170.0	1.525	34.3
3	170.0	2.130	34.3
4	308.0	0.915	34.3
5	308.0	1.525	34.3
6	308.0	2.130	34.3

Table 6 List of results for the experimental investigation of Valve Stroking Method No. 3

Fig No.	Test case No.	Title or remarks	T_{clos} secs	$\hat{P}_c$ kN/m^2	Pressure scale kN/m /cm	Time scale sec/cm
127	1	summary	/	/	/	/
128	1	P-t, E	0.430	348	/	0.200
129	1	x-t, E	0.430	/	/	0.050
130	1	P-t, ET	0.430	348	49.7	0.159
131	1	x-t, ET	0.430	/	/	0.040
132	1	P-t, E	0.105	800	/	0.200
133	1	x-t, E	0.105	/	/	0.020
134	1	P-t, ET	0.105	800	96.5	0.159
135	1	x-t, ET	0.105	/	/	0.016
136	2	summary	/	/	/	/
137	2	P-t, E	0.930	366	/	0.200
138	2	x-t, E	0.930	/	/	0.100
139	2	P-t, ET	0.930	366	50.1	0.159
140	2	x-t, ET	0.930	/	/	0.079
141	2	P-t, E	0.130	1118	/	0.200
142	2	x-t, E	0.130	/	/	0.050
143	2	P-t, ET	0.130	1118	186.0	0.159
144	2	x-t, ET	0.130	/	/	0.040
145	2	P-t, E	0.570	510	/	0.200
146	2	x-t, E	0.570	/	/	0.100
147	2	P-t, ET	0.570	510	50.5	0.159
148	2	x-t, ET	0.570	/	/	0.079
149	3	summary	/	/	/	/
150	3	P-t, E	1.140	331	/	0.500
151	3	x-t, E	1.140	/	/	0.200
152	3	P-t, ET	1.140	331	52.0	0.400
153	3	x-t, ET	1.140	/	/	0.159

154	3	P-t, E	0.180	1220	/	0.500
155	3	x-t, E	0.180	/	/	0.050
156	3	P-t, ET	0.180	1220	194.0	0.400
157	3	x-t, ET	0.180	/	/	0.040
158	3	P-t, E	0.780	461	/	0.500
159	3	x-t, E	0.780	/	/	0.100
160	3	P-t, ET	0.780	461	53.0	0.400
161	3	x-t, ET	0.780	/	/	0.079
162	4	summary	/	/	/	/
163	4	P-t, E	0.080	965	/	0.200
164	4	x-t, E	0.080	/	/	0.020
165	4	P-t, ET	0.080	965	182.0	0.159
166	4	x-t, ET	0.080	/	/	0.016
167	4	P-t, E	0.225	648	/	0.200
168	4	x-t, E	0.225	/	/	0.050
169	4	P-t, ET	0.225	648	90.0	0.159
170	4	x-t, ET	0.225	/	/	0.040
171	5	summary	/	/	/	/
172	5	P-t, E	0.360	793	/	0.200
173	5	x-t, E	0.360	/	/	0.050
174	5	P-t, ET	0.360	793	96.1	0.159
175	5	x-t, ET	0.360	/	/	0.040
176	5	P-t, E	0.114	1249	/	0.200
177	5	x-t, E	0.114	/	/	0.020
178	5	P-t, ET	0.114	1249	186.5	0.159
179	5	x-t, ET	0.114	/	/	0.016
180	5	P-t, E	0.205	993	/	0.200
181	5	x-t, E	0.205	/	/	0.050
182	5	P-t, ET	0.205	993	187.5	0.159
183	5	x-t, ET	0.205	/	/	0.040
184	6	summary	/	/	/	/
185	6	P-t, E	0.500	876	/	0.200

186	6	x-t, E	0.500	/	/	0.100
187	6	P-t, ET	0.500	876	95.3	0.159
188	6	x-t, ET	0.500	/	/	0.079
189	6	P-t, E	0.250	1270	/	0.200
190	6	x-t, E	0.250	/	/	0.050
191	6	P-t, ET	0.250	1270	188.0	0.159
192	6	x-t, ET	0.250	/	/	0.040

x ..... Displacement of hydraulic actuator piston

P ..... Cavity pressure

E ..... Figure displaying experimental result only

ET ..... Figure comparing experimental and theoretical results

Table 7 Summary of results measured directly from the oscilloscope screen

Test case no.	T_{clos} secs	$\hat{P}_c$ kN/m^2	Test case no.	T_{clos} secs	$\hat{P}_c$ kN/m^2
1	0.147	734	3	0.700	535
1	0.200	624	3	0.900	377
1	0.250	548	3	1.000	343
1	0.280	494	3	1.100	328
1	0.340	432	4	0.119	835
1	0.400	377	4	0.160	726
1	0.472	357	4	0.200	658
2	0.210	974	5	0.150	1125
2	0.290	844	5	0.250	891
2	0.390	721	5	0.287	836
2	0.475	638	5	0.300	823
2	0.700	431	5	0.400	775
2	0.800	377	6	0.300	1185
3	0.300	1033	6	0.350	1095
3	0.400	835	6	0.400	1005
3	0.475	740	6	0.450	939
3	0.640	596			

Table 8 Determination of acoustic velocity

Ambient temperature = 15.5°C

Distance between pressure transducers = 10.53 m

Test No.	Wave travel time secs	Test No.	Wave travel time secs
1	0.0086	6	0.0086
2	0.0087	7	0.0085
3	0.0087	8	0.0086
4	0.0086	9	0.0086
5	0.0085	10	0.0086

Average wave travel time = 0.0086 secs

APPENDIX 1 - MEASUREMENT OF AIR RELEASE FROM KEROSENE

The air saturation apparatus consisted of a glass flask, with a single exit pipe near the bottom, into which a sample of about 200 ml of kerosene was poured. A glass pipe was placed with its lower end submerged in the kerosene and its upper end open to the atmosphere. A second glass tube had its lower end about 1" above the surface of the kerosene in the flask, its upper end being connected to a vacuum pump. When the pump was started, air was drawn through the liquid causing saturation at atmospheric pressure. The amount of air drawn through the liquid was controlled by including a bleed pipe to the vacuum pump.

The apparatus for measuring the air content is shown in Fig. 205 and consists of a Hempel gas burette B graduated in ml. attached through a T piece to a manometer M and mercury reservoir R. Inside B was a soft iron cage of wire which could be moved up and down by means of a magnet. Samples of kerosene could be introduced through tap T and burette flushed and dried through the three-way tap S.

Procedure

The kerosene was saturated with air for a known period of time in the apparatus described. The apparatus shown in Fig.205 was filled with mercury to the level shown. The exit pipe from the saturation bottle was connected to tap T and the mercury level raised, by raising R, until all the air in the burette and pipe was exhausted through the kerosene. Lowering the mercury reservoir introduced a known quantity of kerosene into the burette. Tap T was then closed. Reservoir R was lowered to a selected level and the kerosene sample agitated with the magnet and wire cage. This was continued until all the air was given off and holding the wire cage in the kerosene with the magnet, the volume of

air, and the two mercury heights were noted. The reservoir was lowered to other levels and the agitation and measurements repeated. At the end of the test, atmospheric pressure and the ambient temperature were noted. The kerosene sample was drained via tap S and air passed through the burette B to dry the walls from kerosene. The test was repeated with a sample of kerosene which had been saturated with air for a different period, to investigate this effect.

Calculations & Results

Since the kerosene sample contained the wire cage also, the volume of the wire cage had to be found. Thus knowing the diameter of wire used and its original length

$$\text{Vol. of wire} = \frac{\pi.(0.036)^2}{4} 9$$

$$= 9.15.10^{-3} \text{ in}^3$$

$$= \underline{0.150 \text{ ml}}.$$

Now from section, 2.1, the equation relating volume of air (V) released to its pressure (P) is:

$$\frac{64.74V}{T.V_L} = C\left(\frac{B}{P} - 1\right)$$

where

V_L = volume of liquid giving up air,

T = temperature

C = Solubility coefficient (% vol at NTP/mm Hg)

B = Saturation pressure.

Since the experiment was conducted at atmospheric pressure, B = 760 mm of mercury, V_L & T also being known. The procedure was to plot B/P against $\frac{64.74V}{T.V_L}$. The result should be a straight line, if Henry's law holds,

with slope and intercept = C. It was decided to investigate the effect of saturation time on the solubility coefficient and Table 3 gives the results of a test for which the kerosene was saturated for 100 mins. Fig. 210 shows the results plotted and the measured value of solubility coefficient is

C = 0.0162 % vol at NTP/mm of Hg

Table 4 gives the results of a test on a sample saturated for 15 mins, these being plotted in Fig. 211 From this graph

C = 0.0159 % vol at NTP/mm of Hg.

The final point in Fig. 211 was thought to be the result of experimental error, however repeated tests still showed a deviation from a straight line indicating a possible incompatability with the Henry's Law assumption for liquids which are not aerated for sufficiently long periods. However for the purposes of this report the effect was ignored and a value for the solubility coefficient assumed to be

C = 0.0160 % vol at NTP/mm of Hg.

Appendix 2 Solution of Boundary Condition Equations

2a. While the Valve is Closing

The equations of set 1 are:

$$VV(1,N1+1) = X_1 - X_2\, PP(1,N1+1) \qquad A2.1$$

$$VV(2,1) = X_3 + X_4\, PP(2,1) \qquad A2.2$$

$$VOL_G = \alpha' \left\{ P_0/PP(2,1) - 1 \right\} \qquad A2.3$$

$$VOL_T = VOL_{T-1} + \beta \left(VOL_G - VOL_{T-1} \right) \qquad A2.4$$

$$VOL_T = VOL_{T-1} + 1/2\ A.Dt \left\{ VV(2,1) + V(2,1) - V(1,N1+1) - VV(1,N1+1) \right\} \qquad A2.5$$

$$\Upsilon = \frac{VV(1,N1+1)}{V_0} \sqrt{\frac{\Delta P_0}{PP(1,N1+1) - PP(2,1)}} \qquad A2.6$$

$$VOL_{F,T} = VOL_{F,T-1} + A\,Dt\ V(1,N1+1) \qquad A2.7$$

Squaring A2.6 gives

$$\frac{\Upsilon^2 V_0^2}{\Delta P_0} \left\{ PP(1,N1+1) - PP(2,1) \right\} = VV(1,N1+1)^2$$

Putting $\Upsilon^2 V_0^2 / \Delta P_0 = X_6$ and substituting A2.1

$$X_6 \left\{ \frac{X_1 - VV(1,N1+1)}{X_2} - PP(2,1) \right\} = VV(1,N1+1)^2$$

$$\frac{X_6 X_1}{X_2} - \frac{X_6}{X_2} VV(1,N1+1) - X_6 PP(2,1) = VV(1,N1+1)^2$$

If $X_6 X_1 / X_2 = X_7$ and $X_6 / X_2 = X_8$

$$VV(1,N1+1)^2 + X_8 VV(1,N1+1) + X_6 PP(2,1) - X_7 = 0$$

Putting $X_9 = {}^1/_2 X_8$

$$VV(1,N1+1) = -X_9 + \sqrt{X_9^2 + X_7 - X_6 PP(2,1)} \qquad \text{A2.8}$$

Substituting A2.8 and A2.2 into A2.5 we get:

$$VOL_T = VOL_{T-1} + {}^1/_2 A Dt \left\{ X_3 + X_4 PP(2,1) + V(2,1) - V(1,N1+1) + X_9 - \sqrt{X_9^2 + X_7 - X_6 PP(2,1)} \right\} \qquad \text{A2.9}$$

From A2.3 and A2.4 we get

$$VOL_T = VOL_{T-1} + \gamma \{ P_0 / PP(2,1) - 1 \} - \beta VOL_{T-1} PP(2,1) \qquad \text{A2.10}$$

Where $\gamma = \alpha' \beta$

Now equating A2.9 and A2.10

$$\tfrac{1}{2}\,A\,Dt\left\{X_3 + X_4\,PP(2,1) + V(2,1) - V(1,N1+1) + X_9 - \sqrt{X_9^2 + X_7 - X_6\,PP(2,1)}\right\}$$
$$= \left\{\gamma P_0 - \gamma\,PP(2,1) - \beta\,VOL_{T-1}\,PP(2,1)\right\} / PP(2,1)$$

$$A_1\left\{X_3 + V(2,1) + V(1,N1+1) + X_9\right\} PP(2,1) + A_1 X_4\,PP(2,1)^2$$
$$- A_1\,PP(2,1)\sqrt{A_5 - X_6\,PP(2,1)} = \gamma P_0 - \gamma\,PP(2,1) - \beta\,VOL_{T-1}\,PP(2,1)$$

Which is of the form $f(x) = 0$

$$A_2\,PP(2,1)^2 + A_3\,PP(2,1) + A_4 - A_1\,PP(2,1)\sqrt{A_5 - X_6\,PP(2,1)} = 0$$

A2.11

Where

$A_1 = \tfrac{1}{2}\,A\,Dt$

$A_2 = A_1 X_4$

$A_3 = A_1(X_3 + V(2,1) - V(1,N1+1) + X_9) + \gamma + \beta\,VOL_{T-1}$

$A_4 = -\gamma P_0$

$A_5 = X_9^2 + X_7$

And if $A_6 = A_5 - X_6\,PP(2,1)$ which is, of course, unknown

then

$$f'(x) = 2A_2\,PP(2,1) + A_3 - A_1\left\{\frac{PP(2,1)\left[-\tfrac{1}{2}X_6\right]}{\sqrt{A_5 - X_6\,PP(2,1)}} + \sqrt{A_5 - X_6\,PP(2,1)}\right\}$$

$$= 2\,A_2\,PP(2,1) + A_3 - A_1\left\{\frac{A_6 - \tfrac{1}{2}\,X_6\,PP(2,1)}{\sqrt{A_6}}\right\} \qquad \text{A2.12}$$

From this point, Newton's iterative proceedure is used namely

$$x_{n+1} = x_n - f(x_n)/f'(x_n) \qquad \text{A2.13}$$

An initial value of PP(2,1) is guessed using a linear interpolation from the previous two values. This enables A6 to be calculated and a new value of PP(2,1) found from A2.13 where f(x) and f'(x) are given by A2.11 and A2.12 respectively. The iteration continues until sufficient accuracy is achieved.

2b. When the valve is closed, air release continuing

The proceedure in 2a could still be followed by just putting V(1,N1+1) = 0 but it is more efficient to write an alternative proceedure as the resulting equation is of a quadratic form, the iteration being avoided. Set 2 may be written:

$$VV(2,1) = X_3 + X_4\, PP(2,1) \qquad \text{A2.14}$$

$$VOL_T = VOL_{T-1} + \tfrac{1}{2} A\, DL \left\{ VV(2,1) + V(2,1) \right\} \qquad \text{A2.15}$$

$$VOL_4 = \alpha' \left\{ P_0 / PP(2,1) - 1 \right\} \qquad \text{A2.16}$$

$$VOL_T = VOL_{T-1} + \beta \left(VOL_4 - VOL_{T-1} \right) \qquad \text{A2.17}$$

Substituting A2.14 into A2.15, and A2.16 into A2.17 gives

$$VOL_T = VOL_{T-1} + \tfrac{1}{2} A\, DL \left\{ X_3 + X_4 PP(2,1) + V(2,1) \right\}$$

$$= VOL_{T-1} + \gamma \left\{ P_0 / PP(2,1) - 1 \right\} - \beta\, VOL_{T-1}$$

Or using the rotation in Appendix 2a

$$A_1 \left\{ X_3 + V(2,1) \right\} PP(2,1) + A_1 X_4\, PP(2,1)^2 = \gamma P_0 - \gamma\, PP(2,1) - \beta\, VOL_{T-1}\, PP(2,1)$$

Putting

$$A_7 = A_1 X_4 \qquad A_8 = A_1 \left\{ X_3 + V(2,1) \right\} + \gamma + \beta \, VOL_{T-1}$$

$$\therefore \; A_7 \, PP(2,1)^2 + A_8 \, PP(2,1) + A_4 = 0$$

$$\therefore \quad PP(2,1) = \frac{-A_8 + \sqrt{A_8^2 - 4 A_7 A_8}}{2 A_7}$$

2c. Valve closed, air release ceased.

Set 3 is given by:

$$PP(2,1)\ [VOL_T]^n = RTM \qquad A2.18$$

$$VV(2,1) = X_3 + X_4\ PP(2,1) \qquad A2.19$$

$$VOL_T = VOL_{T-1} + \tfrac{1}{2}\ A\ DL \left\{ VV(2,1) + V(2,1) \right\} \qquad A2.20$$

From A2.18

$$VOL_T = \left\{ RTM / PP(2,1) \right\}^{1/n} \qquad A2.21$$

Substituting A2.19 into A2.20 and equating to A2.21 gives:

$$RTM / PP(2,1) = \left\{ VOL_{T-1} + A_1 \left[X_3 + V(2,1) + X_4\ PP(2,1) \right] \right\}^n$$

$$\text{or} \quad PP(2,1) = RTM \Big/ \left\{ VOL_{T-1} + A_1 \left[X_3 + V(2,1) + X_4 PP(2,1) \right] \right\}^n \qquad A2.22$$

which is of the form $x = f(x)$ or $x_n = f(x_{n-1})$. The proceedure being that the guessed value of PP(2,1) is substituted into the R.H.S of A2.22 to derive a new value. Again the process is repeated until the required degree of accuracy is achieved.

2d. Cavity collapse while the valve is still closing.

Set 4 is given by:

$$PP(2,1)\left[VOL_T\right]^n = RTM \qquad \text{A2.23}$$

$$\Upsilon = \frac{VV(1,N1+1)}{V_0}\sqrt{\frac{\Delta P_0}{PP(1,N1+1) - PP(2,1)}} \qquad \text{A2.24}$$

$$VV(1,N1+1) = X_1 - X_2\, PP(1,N1+1) \qquad \text{A2.25}$$

$$VV(2,1) = X_3 + X_4\, PP(2,1) \qquad \text{A2.26}$$

$$VOL_T = VOL_{T-1} + \tfrac{1}{2} A\, DT \left\{VV(2,1) + V(2,1) - VV(1,N1+1) - V(1,N1+1)\right\} \qquad \text{A2.27}$$

These equations are solved by an iterative proceedure mainly due to the non-linear nature of equation A2.23. A linearly interpolated guess (PG) is first made of PP(2,1). Now from A2.24 and A2.25 we can obtain in a process identical to that shown in appendix 2a:

$$VV(1,N1+1)^2 + X_8\, VV(1,N1+1) + X_6\, PP(2,1) - X_7 = 0$$

Thus an estimated value of PP(2,1) enables the above quadratic to be solved for $VV(1,N1+1)^*$, and from A2.23 and A2.27 we get:

$$PP(2,1) = RTM \Big/ \left\{VOL_T + \tfrac{1}{2} A\, DT \left[X_3 + X_4 PG + V(2,1) - V(1,N1+1) - VV(1,N1+1)^*\right]\right\}^n$$

enabling the iteration process to be initiated

2e. Valve closing - No separated flow (program PTP3)

The set from which a solution is obtained is:

$$VV(1,N1+1) = X_1 - X_2\, PP(1,N1+1) \qquad \text{A2.28}$$

$$VV(2,1) = X_3 + X_4\, PP(2,1) \qquad \text{A2.29}$$

$$\Upsilon = \frac{VV(1,N1+1)}{V_0}\sqrt{\frac{\Delta P_0}{PP(1,N1+1) - PP(2,1)}} \qquad \text{A2.30}$$

$$VV(1,N1+1) = VV(2,1) \qquad \text{A2.31}$$

Squaring A2.30 gives

$$\Upsilon^2 V_0^2 \left\{ PP(1,N1+1) - PP(2,1) \right\} / \Delta P_0 = VV(1,N1+1)^2$$

Substituting in A2.28, A2.29 and A2.31 gives

$$\frac{X_5}{X_2}\left\{ X_1 - X_3 + X_4\, PP(2,1) \right\} - \left[X_3 + X_4\, PP(2,1) \right] = X_3^2$$

$$+ X_4^2\, PP(2,1)^2 + 2 X_3 X_4\, PP(2,1)$$

$$X_4^2\, PP(2,1)^2 + PP(2,1)\left\{ 2 X_3 X_4 + X_5 (1 + X_4/X_2) \right\} + X_3^2$$

$$+ X_5 (X_3 - X_1)/X_2$$

$$X_6\, PP(2,1)^2 + X_7\, PP(2,1) + X_8 = 0$$

where

$$X_5 = \rho^2 V_0^2 / \Delta P_0$$

$$X_6 = X_4^2$$

$$X_7 = 2X_3X_4 + X_5 (1 + X_4/X_2)$$

$$X_8 = X_3^2 + X_5 (X_3 - X_1)/X_2$$

Thus

$$PP(2,1) = \frac{-X_7 + \sqrt{X_7^2 - 4X_6X_8}}{2X_6}$$

Appendix 3 Program description and listing

The following nomenclature includes some of the more important parameters used in the program PTP1. The same notation will also cover programs PTP2-PTP5. Parameters not to be found in this list may be in the list at the beginning of the memorandum, as those parameters are not listed here.

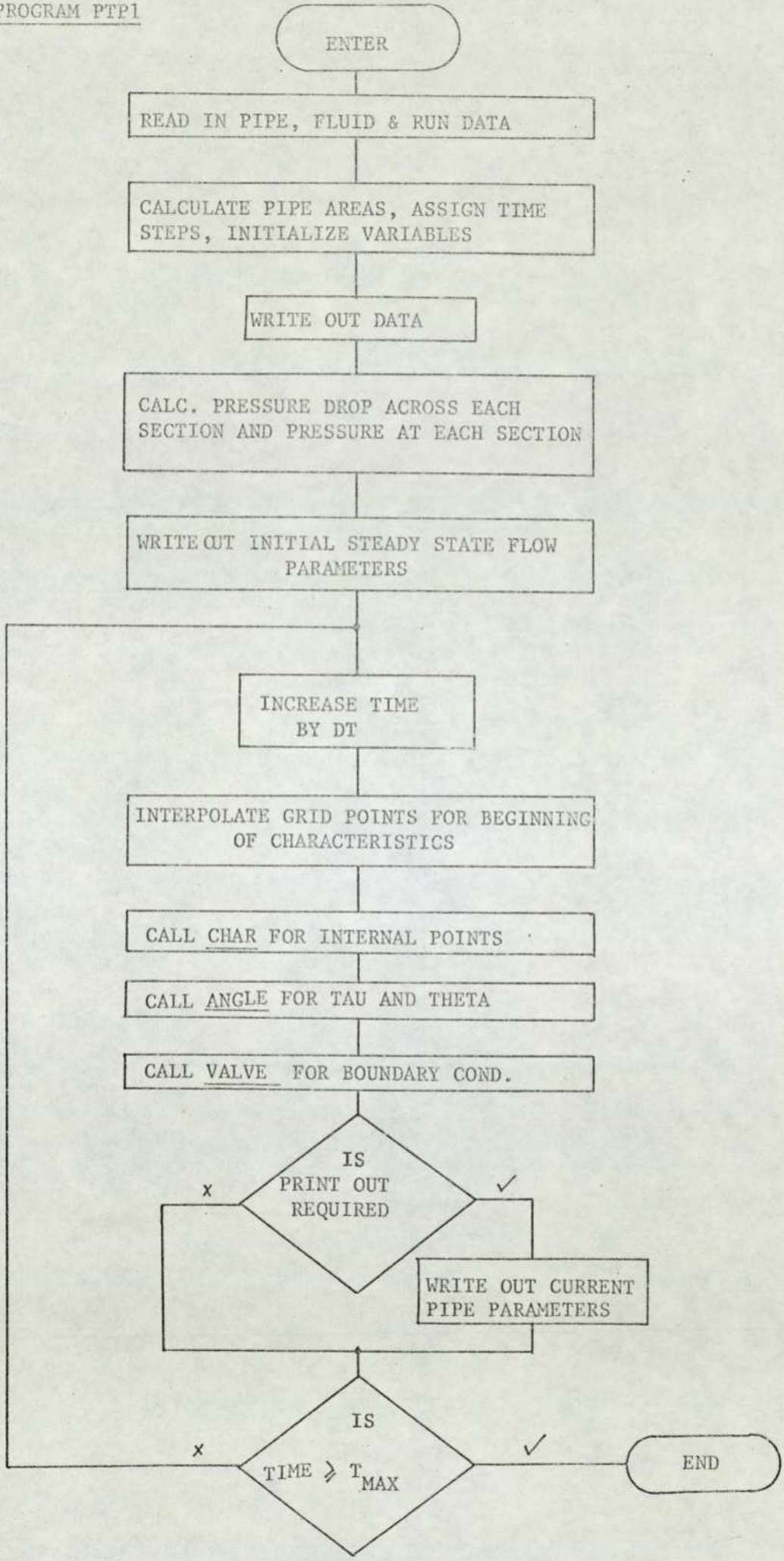
A1 - A8	Constants used in VALVE
AP	Array storing scaled values of array P in lbf/in^2 units.
DPO	Steady state pressure drop across ball valve
DP1	" " " " disc "
DT	Time step
FDR	Friction drop per characteristic length
FF,Z	Friction factor
FRAC1	Time constant of air release (see Chapter 2)
F1U, F1D	Friction terms in equation 14
GMRM	Grid mesh ratio = DT/DX
ICOUNT	Number of steps after which output printing occurs
ITCOUNT	Number of iterations required by a numerical procedure to converge to a specified accuracy.
KINVIS (real)	Kinematic viscosity of fluid
KONST3	$1 - \exp(-\alpha \Delta t)$ - see Chapter 4.
MARKER	Indicates which section of VALVE the control was switched to
N	Number of pipe sections
OFFSET	See fig. 14
PG	Linearly interpolated value of P
PHI	See fig. 14
PL	Pipe length

PLL	PP(2, 1) at time t = t - 2DT
POWER	Cavity process index
PR1	Upstream reservoir pressure (constant)
PR2	Downstream " " "
PSAT	Kerosene/air saturation pressure
RADIUS	See fig 14
REN	Reynolds Number
RHO	Fluid density
RTM	A constant proportional to the mass of gas in the cavity
SOLC	Solubility coefficient
STROKE	See fig. 14
TA	Absolute ambient temperature
TAMB	Ambient temperature (^{o}F)
TANG	Array storing values of θ for increments of γ
TAU1	Valve characteristic
TCLOS	Valve closure time
THETA	Valve angle at time t
THETAO	Initial valve angle (see fig. 14)
TMAX	Maximum run time (model time)
TRANS	Transitional Reynolds Number
TRAT	Linear degree of valve closure
V_o	Initial steady state flow velocity
VOLCON	Volume of fuel considered to release air
VOLT	Volume of cavity at time t
VOLTS	Scaled version of VOLT
VOLTM1	Value of VOLT at t = t - DT
VOLTIN	Steady state cavity volume (= VOL_G)
X1 - X9	Constants used in VALVE
Y1 - Y3	" " " CHAR

In a typical computer run, the variables supplied as input were assigned the following values:

KINVIS	=	0.000194 m/s^2	OFFSET	=	0.0508 m
TRANS	=	2300.0	RADIUS	=	0.0508 m
RHO	=	814.954 Kg/m^3	STROKE	=	0.116 m
PL(1)	=	5.486 m	N(1)	=	4
PL(2)	=	65.53 m	N(2)	=	20
C	=	1219.2 m/s	TCLOS	=	variable
D	=	0.0508 m	SOLC	=	0.016 vol at NTP /unit of P
TAMB	=	60.0 ^{o}F	TMAX	=	5.0 sec
PR1	=	variable	FRAC1	=	0.2 sec^{-1}
VO(1)	=	variable			

MASTER SEG. PROGRAM PTP1

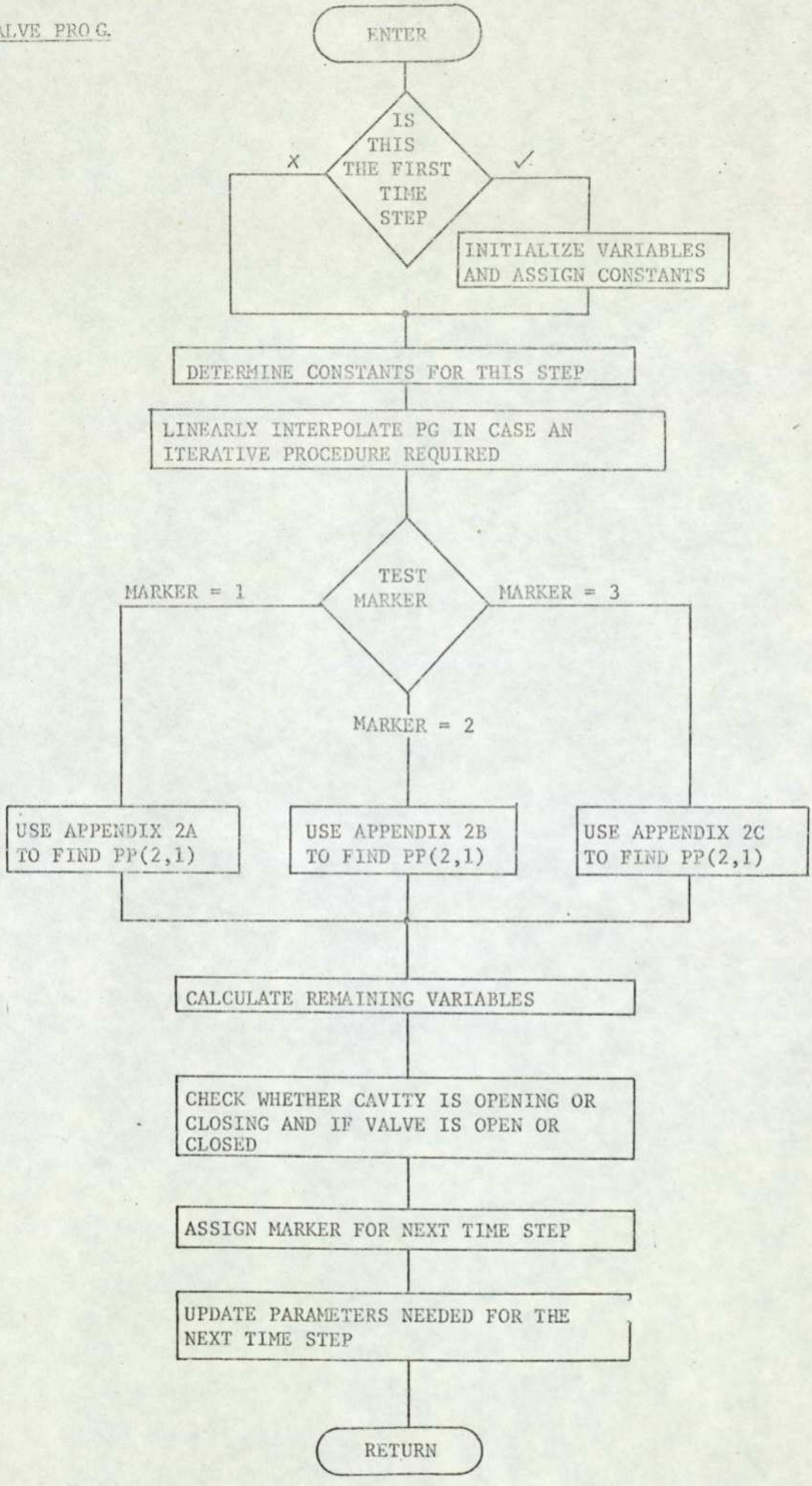


```
      MASTER PTP1
      REAL KINVIS
      DIMENSION TANG( 31),A(2),D(2),V(2,21),P(2,21),VV(2,21),PP(2,21),
     1  C(2),DT(2),PL(2),N(2),V0(2),AP(2,21),GMRN(2),DTF(2),VU(2,21),
     2  PU(2,21),VD(2,21),PD(2,21),F1U(2,21),F1D(2,21)
      COMMON/BL2/RHO,N,DT,TIME,A,C,TAMB,SOLC,TCLOS,FRAC1,VOLT,DP0,
     1TAU1,ITCOUNT,VAP,MARKER,RTM,D,TRANS,KINVIS
      EQUIVALENCE(V(2,V0(2)),(DT2,DT(2)),(N1,N(1)),(N2,N(2))
      READ(1,100) KINVIS,TRANS,RHO,PL(1),PL(2),C(1),D(1)
      READ(1,104) TAMB,OFFSET,RADIUS,STROKE,N(1),N(2)
      READ(1,101) TCLOS
      READ(1,101) SOLC,TMAX,FRAC1
      READ(1,101) PR1,V0(1)
      READ(1,105) (TANG(JB), JB=1,30)
      PRS=PR1
      D(2)=D(1)
      C(2)=C(1)
      V0(2)=V0(1)
      WRITE(2,202)TRANS,RHO,KINVIS,PL(1),PL(2),C(1),C(2),D(1),D(2),V0(1
     1),V0(2),PRS,TCLOS,TMAX,SOLC,TAMB,FRAC1,N1,N2
      ICH=1
      CALL CHANGE(KINVIS,RHO,PL,C,D,OFFSET,RADIUS,STROKE,SOLC,PR1,V0,
     1  VOLTS,V,AP,ICH)
      WRITE(2,202)TRANS,RHO,KINVIS,PL(1),PL(2),C(1),C(2),D(1),D(2),V0(1
     1),V0(2),PRS,TCLOS,TMAX,SOLC,TAMB,FRAC1,N1,N2
      PR1=PR1*144.0
      DO 1 I=1,2
      D(I)=D(I)/12.0
      A(I)=3.1417*(D(I)**2)/4.0
      DT(I)=0.001
      GMRN(I)=DT(I)*N(I)/PL(I)
1     CONTINUE
      DP1=5.11*V02*V02
      DP2=0.224*V02*V02
      PR1=PR1-DP1
      DP=DP2/144.0
      DP0=DP
      ICOUNT=5
      TRAT=0.0
      VOLT=0.0
      J1=N(1)+1
      J2=N(2)+1
      J3=N(2)
      TIME=0.0
      VAP=0.2*144.0
      DO 23 I=1,2
      REN=ABS(V0(I))*D(I)/KINVIS
      FF=0.079/(REN**0.25)
      FDR=2.0*RHO*FF*PL(I)*(V0(I)**2)/(D(I)*N(I))
      AA=0.
      J=N(I)+1
      DO 23 K=1,J
```

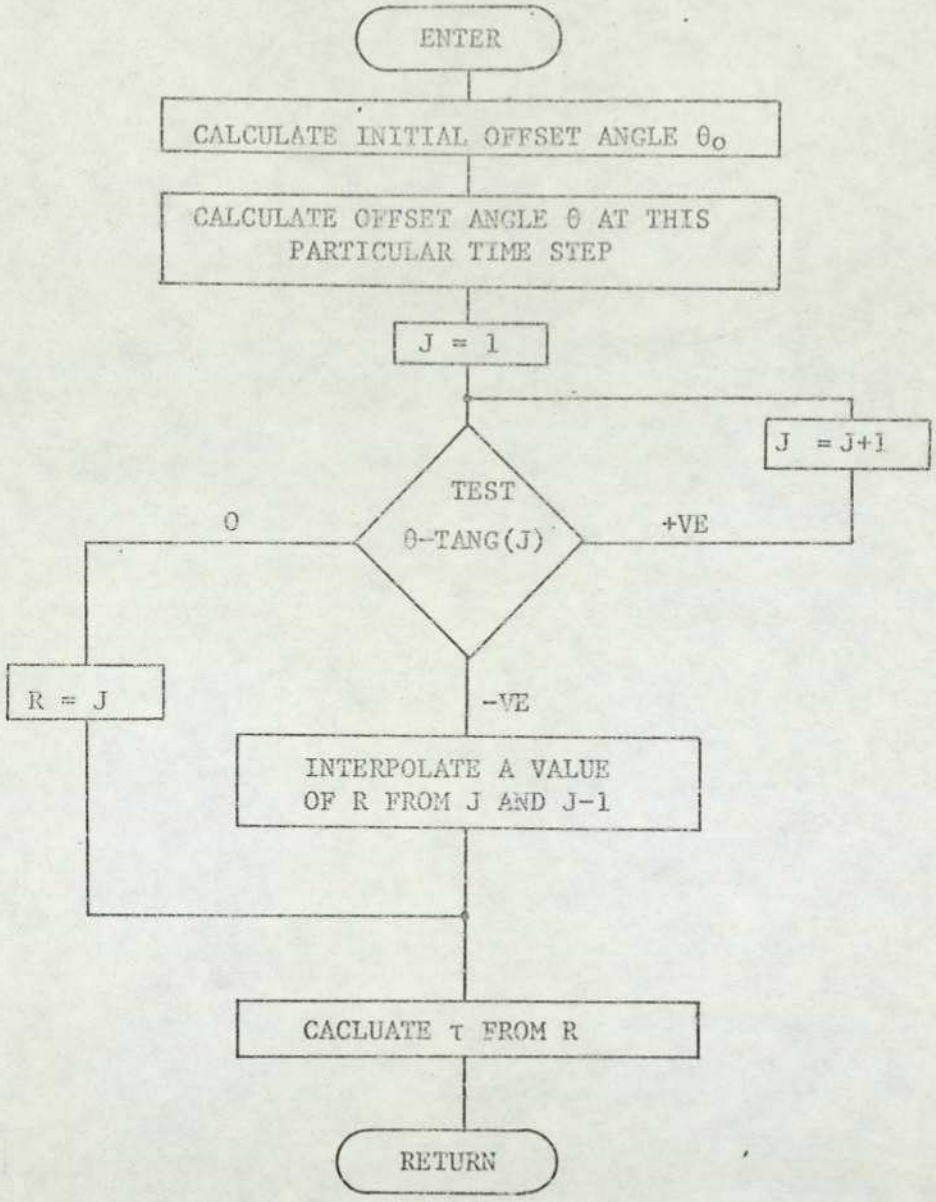
```
      V(I,K)=V0(I)
      XR=PR1
      IF(I.EQ. 2)XR=P(1,N1+1)-(DP*144.0)
      AA=AA+1.0
      P(I,K)=XR-(AA-1.0)*FDR
      AP(I,K)=P(I,K)/144.0
   23 CONTINUE
      PR2=P(2,N2+1)
      CALL ANGLE(OFFSET,RADIUS,STROKE,TRAT,TANG,THETA,TAU1,DT2)
      L1=N2/5
      WRITE(2,200)
      ICH=2
      CALL CHANGE(KINVIS,RHO,PL,C,D,OFFSET,RADIUS,STROKE,SOLC,PR1,V0,
     1  VOLTS,V,AP,ICH)
      WRITE(2,201) TIME,TAU1,THETA,VOLT,(V(1,I),I=1,J1,1), (V(2,I),I=1,
     1  J2,L1),ITCOUNT,   MARKER,(AP(1,I),I=1,J1,1),(AP(2,I),I=1,J2,L1)
      ICH=3
      CALL CHANGE(KINVIS,RHO,PL,C,D,OFFSET,RADIUS,STROKE,SOLC,PR1,V0,
     1  VOLTS,V,AP,ICH)
    8 TIME=TIME+DT(2)
      TRAT=TIME/TCLOS
      VD(1,N1+1)=0.0
      PD(1,N1+1)=0.0
      VU(1,1)=0.0
      PU(1,1)=0.0
      VU(2,1)=0.0
      PU(2,1)=0.0
      VD(2,N2+1)=0.0
      PD(2,N2+1)=0.0
      L4=1
      IF(TIME .GT. (TCLOS-0.000001)) L4=2
      DO 61 J=L4,2
      KT=N(J)+1
      DO 60 I=2,KT
      VU(J,I)=V(J,I)+GMRM(J)*C(J)*(V(J,I-1)-V(J,I))
      PU(J,I)=P(J,I)+GMRM(J)*C(J)*(P(J,I-1)-P(J,I))
   60 CONTINUE
      KS=N(J)
      DO 61 I=1,KS
      VD(J,I)=V(J,I)+GMRM(J)*C(J)*(V(J,I+1)-V(J,I))
      PD(J,I)=P(J,I)+GMRM(J)*C(J)*(P(J,I+1)-P(J,I))
   61 CONTINUE
      CALL CHAR(VU,PU,F1U,PD,VD,F1D,VV,PP,PR1,PR2)
      IF(TIME .GT. (TCLOS-0.00001)) GOTO 13
      CALL ANGLE(OFFSET,RADIUS,STROKE,TRAT,TANG,THETA,TAU1,DT2)
      GOTO 4
   13 TAU1=0.0
      V(1,N1+1)=0.0
    4 CALL VALVE(V0,V,P,VV,PP,VU,PU,VD,PD,F1U,F1D)
      DO 7 I=L4,2
      J=N(I)+1
      DO 7 K=1,J
```

```
      V(I,K)=VV(I,K)
      P(I,K)=PP(I,K)
      AP(I,K)=PP(I,K)/144.0
    7 CONTINUE
      ICOUNT=ICOUNT-1
      IF(ICOUNT .NE. 0) GOTO 9
      ICOUNT=5
      ICH=2
      CALL CHANGE(KINVIS,RHO,PL,C,D,OFFSET,RADIUS,STROKE,SOLC,PR1,V0,
     1  VOLTS,V,AP,ICH)
      VOLT=VOLT*0.093
      IF(TIME .GT. (TCLOS-0.000001)) GOTO 16
      GOTO 17
   16 VOLTS=VOLT*1000.0
      WRITE(2,205) TIME,ITCOUNT,MARKER,VOLTS,(V(2,I),I=1,J2,L1),(AP(2,I)
     1    ,I=1,J2,L1)
      GOTO 5
   17 WRITE(2,201) TIME,TAU1,THETA,VOLT,(V(1,I),I=1,J1,1), (V(2,I),I=1,
     1  J2,L1),ITCOUNT,   MARKER,(AP(1,I),I=1,J1,1),(AP(2,I),I=1,J2,L1)
    5 ICH=3
      CALL CHANGE(KINVIS,RHO,PL,C,D,OFFSET,RADIUS,STROKE,SOLC,PR1,V0,
     1  VOLTS,V,AP,ICH)
      VOLT=VOLT/0.093
    9 IF(TIME .LT. TMAX) GOTO 8
  100 FORMAT(F10.7,6F10.5)
  101 FORMAT(3F10.2)
  104 FORMAT(4F10.2,215)
  105 FORMAT(10F6.2)
  200 FORMAT(1H1///,1X,4HTIME,5X,3HTAU,5X,5HTHETA,4X,3HVOL,20X,
     1    8HUPSTREAM,15X,5HVALVE,20X,10HDOWNSTREAM)
  201 FORMAT(/,1X,F6.4,2X,F6.4,4X,F6.2,1X,F6.3,5X,3HV=,5F7.3,
     1   3X,6F7.3,/,2(5X,I5),17X,2HP=,5F7.1,4X,6F7.1)
  202 FORMAT(/,9F13.7,/,/,8F13.7,214)
  205 FORMAT(/,1X,F6.4,213,F6.2,2X,2HV=,6F7.3,2X,2HP=,6F7.2)
      STOP
```

SUBROUTINE VALVE PROG.
PTP1



SUBROUTINE ANGLE

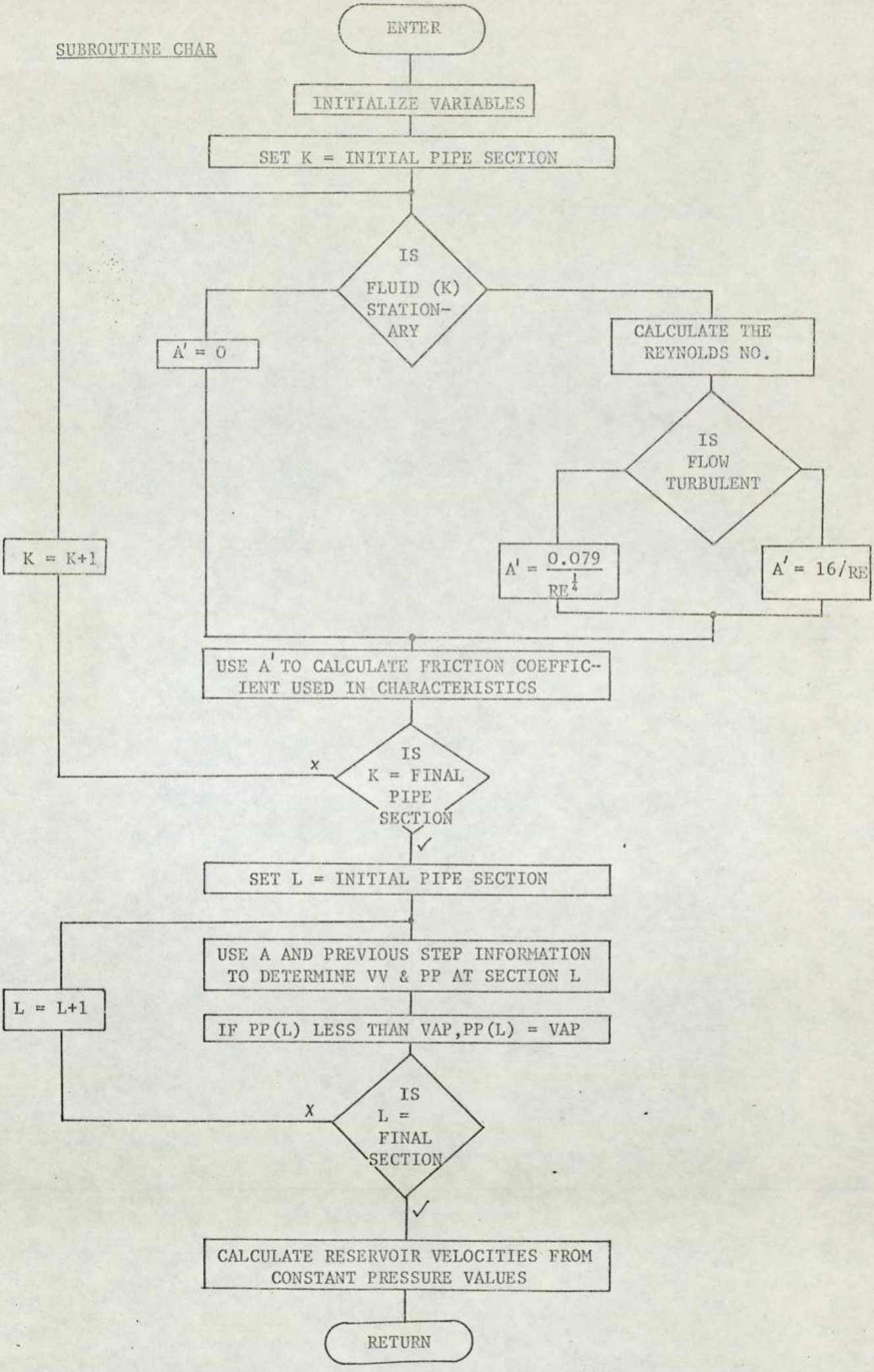


```
      SUBROUTINE VALVE(V0,V,P,VV,PP,VU,PU,VD,PD,F1U,F1D)
      REAL KINVIS,KONST3
      DIMENSION A(2),C(2),DT(2),N(2),V0(2),V(2,21),P(2,21),VV(2,21),
     1  PP(2,21),VU(2,21),PU(2,21),VD(2,21),PD(2,21),F1U(2,21),F1D(2,21)
     2 ,TANG(31),D(2)
      COMMON/BL2/RHO,N,DT,TIME,A,C,TAMB,SOLC,TCLOS,FRAC1,VOLT,DP0,
     1TAU1,ITCOUNT,VAP,MARKER,RTM,D,TRANS,KINVIS
      EQUIVALENCE (N1,N(1)),(N2,N(2))
      ITCOUNT=0
      RR=DT(2)+0.000001
      IF(TIME .GT. RR) GOTO 18
      VOLTM1=0.0
      FRAC1=0.2
      KONST3=1.0-EXP(-0.693*DT(2)/FRAC1)
      POWER=1.4
      MARKER=1
      PLL=P(2,1)
      VOLCONT=0.0
      PL=0.00005
      TA=TAMB*460.0
      PSAT=P(2,1)
   18 CONTINUE
      VOLCON=VOLCONT+A(2)*DT(2)*V(1,N1+1)
      X1=VU(1,N1+1)+F1U(1,N1+1)*VU(1,N1+1)*ABS(VU(1,N1+1))+PU(1,N1+1)/
     1   (RHO*C(1))
      X2=1.0/(RHO*C(1))
      X3=VD(2,1)-F1D(2,1)*VD(2,1)*ABS(VD(2,1))-PD(2,1)/(RHO*C(2))
      X4=1.0/(RHO*C(2))
      X6=((TAU1*V0(2))**2)/(DP0*144.0)
      X7=X6*X1/X2
      X8=X6/X2
      X9=0.5*X8
      ALPHA=VOLCON*SOLC*TA/23.21
      BETA=KONST3
      GAMMA=ALPHA*BETA
      A1=0.5*A(2)*DT(2)
      A2=A1*X4
      A3=A1*(X3+V(2,1)-V(1,N1+1)+X9)+GAMMA*BETA*VOLTM1
      A4=-GAMMA*PSAT
      A5=X9*X9+X7
      PG=P(2,1)-(PLL-P(2,1))
      PLIN=PG
      IF((MARKER .EQ. 1) .AND. (TAU1 .LT. 0.000005)) MARKER=2
      GOTO(3,4,6),MARKER
    3 IF(TIME .LT. (3.0*DT(2))) PG=0.999995*P(2,1)
    1 ITCOUNT=ITCOUNT+1
      A6=A5-X6*PG
      FX=A2*PG*PG +A3*PG +A4 -A1*PG*SQRT(A6)
      FXD=2.0*A2*PG +A3 -A1*((A6-0.5*X6*PG)/SQRT(A6))
      PN=PG-FX/FXD
      PERROR=ABS((PN-PG)/PG)
      PG=PN
```

```
      IF(PERROR-PL) 2,2,1
4     ITCOUNT=88
      A7=A1*X4
      A8=A1*(X3+V(2,1))+GAMMA+BETA*VOLTM1
      PG=(-A8+SQRT(A8*A8-4.0*A7*A4))/(2.0*A7)
      RTM=P(2,1)*(VOLTM1**POWER)
      GOTO 2
6     PN=RTM/((VOLTM1+A1*(X3+X4*PG+V(2,1)))**POWER)
      PG=PN
      IF((ABS((PN-PG)/PG)) .LT. PL) GOTO 2
      ITCOUNT=ITCOUNT+1
      GOTO 6
2     PP(2,1)=PG
      VV(2,1)=X3+X4*PP(2,1)
      VV(1,N1+1)=-X9+SQRT(A5-X6*PP(2,1))
      PP(1,N1+1)=(X1-VV(1,N1+1))/X2
      VOLT=VOLTM1+A1*(VV(2,1)+V(2,1)-VV(1,N1+1)-V(1,N1+1))
      VOLTIN=ALPHA*(PSAT/PP(2,1)-1.0)
      M2=0
      IF(VOLTIN .LT. VOLTM1) M2=1
      IF((MARKER .EQ. 2) .AND. (M2 .EQ. 1)) MARKER=3
      VOLCONT=VOLCON
      PLL=P(2,1)
      VOLTM1=VOLT
      RETURN
```

```
      SUBROUTINE ANGLE(OFFSET,RADIUS,STROKE,TRAT,TANG,THETA,TAU1,DT2)
      DIMENSION TANG(31)
      PI=3.14159265
      THETA0=ATAN(OFFSET/RADIUS)
      PHI=ATAN((OFFSET-(TRAT*STROKE))/RADIUS)
      THETA=90.0-180.0*(THETA0-PHI)/PI
      J=1
      IF(THETA .LT. 0.0) THETA=0.0
4     IF(THETA-TANG(J)) 1,2,3
3     J=J+1
      GOTO 4
2     K=J
      K=31
      GOTO 5
1     K=J-1
      R=K+(THETA-TANG(K))/(TANG(J)-TANG(K))
5     CONTINUE
      TAU1=(R+10.0)/20.0
      IF(K .LT. 11) TAU1=(R+1.0)/220.0
      RETURN
```

SUBROUTINE CHAR



```
      SUBROUTINE CHAR(VU,PU,F1U,PD,VD,F1D,VV,PP,PR1,PR2)
      REAL KINVIS
      DIMENSION N(2),C(2),VU(2,21),PU(2,21),F1U(2,21),PD(2,21),VD(2,21),
     1  F1D(2,21),VV(2,21),PP(2,21),D(2),DT(2),A(2)
      COMMON/BL2/RHO,N,DT,TIME,A,C,TAMB,SOLC,TCLOS,FRAC1,VOLT,DP0,
     1TAU1,ITCOUNT,VAP,MARKER,RTM,D,TRANS,KINVIS
      Y1=D(2)/KINVIS
      Y2=1.0/(RHO*C(2))
      Y3=2.0*DT(2)/D(2)
      L4=1
      IF(TIME .GT. (TCLOS-0.00001)) L4=2
      DO 6 I=L4,2
      DO 6 J=1,2
      DO 6 K=1,N(I)+1
      X=VD(I,K)
      IF(J .EQ. 1) X=VU(I,K)
      IF(X) 7,8,7
    8 Z=0.0
      GOTO 9
    7 RE=ABS(X)*Y1
      IF(RE-TRANS) 10,11,11
   10 Z=16.0/RE
      GOTO 9
   11 Z=0.079/(RE**0.25)
    9 IF(J-1) 12,12,13
   12 F1U(I,K)=Z*Y3
      GOTO 6
   13 F1D(I,K)=Z*Y3
    6 CONTINUE
      DO 3 I=L4,2
      JA=N(I)
      DO 5 L=2,JA
      VV(I,L)=0.5*(VU(I,L)+VD(I,L)+Y2*(PU(I,L)-PD(I,L)) -(F1U(I,L)*VU(I,
     1L)*ABS(VU(I,L))+F1D(I,L)*VD(I,L)*ABS(VD(I,L))))
      PP(I,L)=0.5*((PU(I,L)+PD(I,L)+(VU(I,L)-VD(I,L))/Y2) -(F1U(I,L)
     1  *VU(I,L)*ABS(VU(I,L))-F1D(I,L)*VD(I,L)*ABS(VD(I,L)))/Y2)
      IF(PP(I,L) .LT. VAP) PP(I,L)=VAP
    5 CONTINUE
      IF (I-1) 1,1,2
    1 PP(1,1) = PR1
      VV(1,1)=VD(1,1)+Y2*(PR1-PD(1,1))-F1D(1,1)*VD(1,1)*ABS(VD(1,1))
      GOTO 3
    2 PP(2,N(2)+1)=PR2
      VV(2,N(2)+1)=VU(2,N(2)+1)-Y2*(PR2-PU(2,N(2)+1))-F1U(2,N(2)+1)
     1  *VU(2,N(2)+1)*ABS(VD(2,N(2)+1))
    3 CONTINUE
      RETURN
```

```
      SUBROUTINE CHANGE(KINVIS,RHO,PL,C,D,OFFSET,RADIUS,STROKE,SOLC,
     1  PR1,V0,VOLTS,V,AP,ICH)
      REAL KINVIS
      DIMENSION PL(2),C(2),D(2),V0(2),V(2,21),AP(2,21)
      GOTO (1,2,3), ICH
    1 KINVIS=KINVIS*0.0929
      RHO=RHO*0.062428/32.2
      OFFSET=OFFSET*39.3701
      RADIUS=RADIUS*39.3701
      STROKE=STROKE*39.3701
      SOLC=SOLC/(144.0*0.0193)
      PR1=PR1*0.145
      PMIN=PMIN*0.145
      DO 5 I=1,2
      PL(I)=PL(I)*3.28084
      C(I)=C(I)*3.28084
      D(I)=D(I)*39.3701
    5 V0(I)=V0(I)*3.28084
      GOTO 4
    2 CONTINUE
      DO 6 I=1,2
      DO 6 J=1,21
      V(I,J)=V(I,J)*0.3048
    6 AP(I,J)=AP(I,J)*6.895
      GOTO 4
    3 CONTINUE
      DO 7 I=1,2
      DO 7 J=1,21
      V(I,J)=V(I,J)/0.3048
    7 AP(I,J)=AP(I,J)/6.895
    4 RETURN
```

DATA

```
0.000194 2300.0      814.954      5.486     65.532  1219.2          0.0508
 60.0        0.0508     0.0508     0.1016      4    20
  0.4
  0.0160     9.0        0.2
169.5        2.14
00.00  7.50 15.00 22.50 27.00 30.50 33.50 35.50 39.50 40.00
41.50 55.00 64.00 71.20 75.00 77.20 78.25 79.00 79.40 79.70
80.00 80.50 81.00 81.30 81.60 82.00 82.70 84.00 86.00 90.00
```

```
      MASTER PTP2
      REAL KINVIS
      DIMENSION TANG( 31),A(2),D(2),V(2,21),P(2,21),VV(2,21),PP(2,21),
     1  C(2),DT(2),PL(2),N(2),V0(2),AP(2,21),GMRM(2),DTF(2),VU(2,21),
     2  PU(2,21),VD(2,21),PD(2,21),F1U(2,21),F1D(2,21),PSAVE(250)
      COMMON/BL2/RHO,N,DT,TIME,A,C,TAMB,SOLC,TCLOS,FRAC1,VOLT,DP0,
     1TAU1,ITCOUNT,VAP,MARKER,RTM,D,TRANS,KINVIS
      EQUIVALENCE(V02,V0(2)),(DT2,DT(2)),(N1,N(1)),(N2,N(2))
      READ(1,100) KINVIS,TRANS,RHO,PL(1),PL(2),C(1),D(1)
      READ(1,104) TAMB,OFFSET,RADIUS,STROKE,N(1),N(2)
      READ(1,101) TCLOS
      READ(1,101) SOLC,TMAX,FRAC1
      TMAX=2.5
      READ(1,101) PR1,V0(1)
      READ(1,105) (TANG(JB), JB=1,30)
      PRS=PR1
      D(2)=D(1)
      C(2)=C(1)
      V0(2)=V0(1)
      WRITE(2,202)TRANS,RHO,KINVIS,PL(1),PL(2),C(1),C(2),D(1),D(2),V0(1
     1),V0(2),PRS,TCLOS,TMAX,SOLC,TAMB,FRAC1,N1,N2
      ICH=1
      CALL CHANGE(KINVIS,RHO,PL,C,D,OFFSET,RADIUS,STROKE,SOLC,PR1,V0,
     1  VOLTS,V,AP,ICH)
      WRITE(2,202)TRANS,RHO,KINVIS,PL(1),PL(2),C(1),C(2),D(1),D(2),V0(1
     1),V0(2),PRS,TCLOS,TMAX,SOLC,TAMB,FRAC1,N1,N2
      PR1=PR1*144.0
      DO 1 I=1,2
      D(I)=D(I)/12.0
      A(I)=3.1417*(D(I)**2)/4.0
      DT(I)=0.001
      GMRM(I)=DT(I)*N(I)/PL(I)
1     CONTINUE
      ICOUNT=10
      JKL=0
      ICI=50
      AICI=ICI*DT2
      PGM=1500.0
      PGS=PGM/12.0
      PMAX=0.0
      DP1=5.11*V02*V02
      DP2=0.224*V02*V02
      PR1=PR1-DP1
      DP=DP2/144.0
      DP0=DP
      TRAT=0.0
      VOLT=0.0
      J1=N(1)+1
      J2=N(2)+1
      J3=N(2)
      TIME=0.0
      VAP=0.2*144.0
```

```
      DO 23 I=1,2
      REN=ABS(V0(I))*D(I)/KINVIS
      FF=0.079/(REN**0.25)
      FDR=2.0*RHO*FF*PL(I)*(V0(I)**2)/(D(I)*N(I))
      AA=0
      J=N(I)+1
      DO 23 K=1,J
      V(I,K)=V0(I)
      XR=PR1
      IF(I.EQ.2)XR=P(1,N1+1)-(DP*144.0)
      AA=AA+1.0
      P(I,K)=XR-(AA-1.0)*FDR
      AP(I,K)=P(I,K)/144.0
   23 CONTINUE
      PR2=P(2,N2+1)
      CALL ANGLE(OFFSET,RADIUS,STROKE,TRAT,TANG,THETA,TAU1,DT2)
      L1=4
      WRITE(2,200)
      ICH=2
      CALL CHANGE(KINVIS,RHO,PL,C,D,OFFSET,RADIUS,STROKE,SOLC,PR1,V0,
     1  VOLTS,V,AP,ICH)
      WRITE(2,201) TIME,TAU1,THETA,VOLT,(V(1,I),I=1,J1,1), (V(2,I),I=1,
     1  J2,L1),ITCOUNT,   MARKER,(AP(1,I),I=1,J1,1),(AP(2,I),I=1,J2,L1)
      ICH=3
      CALL CHANGE(KINVIS,RHO,PL,C,D,OFFSET,RADIUS,STROKE,SOLC,PR1,V0,
     1  VOLTS,V,AP,ICH)
    8 TIME=TIME+DT(2)
      TRAT=TIME/TCLOS
      VD(1,N1+1)=0.0
      PD(1,N1+1)=0.0
      VU(1,1)=0.0
      PU(1,1)=0.0
      VU(2,1)=0.0
      PU(2,1)=0.0
      VD(2,N2+1)=0.0
      PD(2,N2+1)=0.0
      L4=1
      IF(TIME .GT. (TCLOS-0.000001)) L4=2
      DO 61 J=L4,2
      KT=N(J)+1
      DO 60 I=2,KT
      VU(J,I)=V(J,I)+GMRM(J)*C(J)*(V(J,I-1)-V(J,I))
      PU(J,I)=P(J,I)+GMRM(J)*C(J)*(P(J,I-1)-P(J,I))
   60 CONTINUE
      KS=N(J)
      DO 61 I=1,KS
      VD(J,I)=V(J,I)+GMRM(J)*C(J)*(V(J,I+1)-V(J,I))
      PD(J,I)=P(J,I)+GMRM(J)*C(J)*(P(J,I+1)-P(J,I))
   61 CONTINUE
      CALL CHAR(VU,PU,F1U,PD,VD,F1D,VV,PP,PR1,PR2)
      IF(TIME .GT. (TCLOS-0.00001)) GOTO 10
      CALL ANGLE(OFFSET,RADIUS,STROKE,TRAT,TANG,THETA,TAU1,DT2)
```

```
      GOTO 4
   13 TAU1=0.0
      V(1,N1+1)=0.0
    4 CALL VALVE(V0,V,P,VV,PP,V0,P0,VD,PD,P10,P1D)
      IF(PP(2,1) .GT. PMAX) PMAX=PP(2,1)
      ICI=ICI-1
      IF(ICI .NE. 0) GOTO 50
      JKL=JKL+1
      IF(JKL .GT. 250) GOTO 50
      PSAVE(JKL)=PP(2,1)*6.895/144.0
      ICI=50
   50 CONTINUE
      DO 7 I=L4,2
      J=N(I)+1
      DO 7 K=1,J
      V(I,K)=VV(I,K)
      P(I,K)=PP(I,K)
      AP(I,K)=PP(I,K)/144.0
    7 CONTINUE
      ICOUNT=ICOUNT+1
      IF(ICOUNT .NE. 0) GOTO 9
      ICOUNT=10
      ICH=2
      CALL CHANGE(KINVIS,RHO,PL,C,D,OFFSET,RADIUS,STROKE,SOLC,PR1,V0,
     1  VOLTS,V,AP,ICH)
      VOLT=VOLT*0.093
      IF(TIME .GT. (TCLOS-0.000001)) GOTO 16
      GOTO 17
   16 VOLTS=VOLT*1000.0
      WRITE(2,205) TIME,ITCOUNT,MARKER,VOLTS,(V(2,I),I=1,J2,L1),(AP(2,I)
     1    ,I=1,J2,L1)
      GOTO 5
   17 WRITE(2,201) TIME,TAU1,THETA,VOLT,(V(1,I),I=1,J1,1), (V(2,I),I=1,
     1  J2,L1),ITCOUNT,   MARKER,(AP(1,I),I=1,J1,1),(AP(2,I),I=1,J2,L1)
    5 ICH=3
      CALL CHANGE(KINVIS,RHO,PL,C,D,OFFSET,RADIUS,STROKE,SOLC,PR1,V0,
     1  VOLTS,V,AP,ICH)
      VOLT=VOLT/0.093
    9 IF(TIME .LT. TMAX) GOTO 8
      V02=V02*0.3048
      PMAX=PMAX*6.895/144.0
      CALL PLOT(PSAVE,PGM,PRS,V02,TCLOS,AICI,PGS,PMAX,TMAX)
  100 FORMAT(F10.7,6F10.5)
  101 FORMAT(3F10.5)
  104 FORMAT(4F10.5,2I5)
  105 FORMAT(10F6.2)
  200 FORMAT(1H1///,1X,4HTIME,5X,3HTAU,5X,5HTHETA,4X,3HVOL,20X,
     1    8HUPSTREAM,15X,5HVALVE,20X,10HDOWNSTREAM)
  201 FORMAT(/,1X,F6.4,2X,F6.4,4X,F6.2,1X,F6.3,5X,3HV=,5F7.3,
     1  3X,6F7.3,/,2(5X,I5),17X,2HP=,5F7.1,4X,6F7.1)
  202 FORMAT(/,9F13.7,/,8F13.7,2I4)
  205 FORMAT(/,1X,F6.4,2I3,F6.2,2X,2HV=,6F7.3,2X,2HP=,6F7.2)
```

```
      SUBROUTINE PLOT(X,XMAX,A,B,C,D,E,F,G)
      REAL LINE
      DIMENSION X(250),LINE(120)
      DATA DOT,STAR,BLANK/1H.,1H*,1H /
      WRITE(2,200) A,B,C,D,E,F
      DO 1 J=1,120
    1 LINE(J)=DOT
      WRITE(2,201) LINE
      DO 2 J=1,120
    2 LINE(J)=BLANK
      LINE(1)=DOT
      DO 3 K=1,250
      J=120.0*X(K)/XMAX
      LINE(J)=STAR
      WRITE(2,201) LINE
      LINE(J)=BLANK
      LINE(1)=DOT
    3 CONTINUE
  200 FORMAT(1H1,/,10X,19HINITIAL PRESSURE = ,F5.1,10X,19HINITIAL VELOCI
     1TY = ,F5.2,10X,21HVALVE CLOSURE TIME = ,F5.3,//,10X,13HTIME SCALE
     2= ,F5.3,2X,10HSECS/SPACE,3X,17HPRESSURE SCALE = ,F5.1,2X,
     3 12HKN/M.SQ/INCH,4X,16HPEAK PRESSURE = ,F6.1,1X,7HKN/M.SQ,/)
  201 FORMAT(1H ,120A1)
      RETURN
```

```
      PROGRAM  PTP3

      SUBROUTINE VALVE(V0,V,P,VV,PP,VU,PU,VD,PD,F1U,F1D)
      REAL KINVIS,KONST3
      DIMENSION A(2),C(2),DT(2),N(2),V0(2),V(2,21),P(2,21),VV(2,21),
     1  PP(2,21),VU(2,21),PU(2,21),VD(2,21),PD(2,21),F1U(2,21),F1D(2,21)
     2 ,TANG(31),D(2)
      COMMON/BL2/RHO,N,DT,TIME,A,C,TAMB,SOLC,TCLOS,FRAC1,VOLT,DP0,
     1TAU1,ITCOUNT,VAP,MARKER,RTM,D,TRANS,KINVIS
      EQUIVALENCE (N1,N(1)),(N2,N(2))
      IF(TIME .LT. (DT(2)*0.00001)) VOLTM1=0.0
      VAPP=VAP*0.01
      X1=VU(1,N1+1)*F1U(1,N1+1)*VU(1,N1+1)*ABS(VU(1,N1+1))+PU(1,N1+1)/
     1    (RHO*C(1))
      X2=1.0/(RHO*C(1))
      X3=VD(2,1)-F1D(2,1)*VD(2,1)*ABS(VD(2,1))-PD(2,1)/(RHO*C(2))
      X4=1.0/(RHO*C(2))
      IF(TIME .GT. (TCLOS*0.000001)) GOTO 1
      X5=((TAU1*V0(2))**2)/(DP0*144.0)
      X6=X4*X4
      X7=2.0*X3*X4 +X5*(1.0+X4/X2)
      X8=X3*X3 +X5*(X3-X1)/X2
      PP(2,1)=(-X7+SQRT(X7*X7-4.0*X6*X8))/(2.0*X6)
      VV(2,1)=X3+X4*PP(2,1)
      MARKER=2
      GOTO 2
3     PP(2,1)=VAP
      MARKER=3
      VV(2,1)=X3+X4*PP(2,1)
      X9=X5*X1/X2
      X10=X5/X2
      X11=X10/2.0
      VV(1,N1+1)=-X11+SQRT(X11*X11+X9-X5*PP(2,1))
      PP(1,N1+1)=(X1-VV(1,N1+1))/X2
      VOLT=VOLTM1+0.5*A(2)*DT(2)*(VV(2,1)+V(2,1)-VV(1,N1+1)-V(1,N1+1))
      IF(VOLT .LT. 0.0) VOLT=0.0
      VOLTM1=VOLT
      GOTO 4
6     FACT=(VAP-P(2,1))/(PP(2,1)-P(2,1))
      IF(L3 .EQ. 0) GOTO 4
      MARKER=6
      TIME=TIME-DT(2)*(1.0-FACT)
      L4=1
      IF(TAU1 .LT. 0.0001) L4=2
      DO 7 I=L4,2
      DO 7 J=1,N(I)+1
      VV(I,J)=V(I,J)+FACT*(VV(I,J)-V(I,J))
7     PP(I,J)=P(I,J)+FACT*(PP(I,J)-P(I,J))
      GOTO 4
1     VV(2,1)=0.0
      PP(2,1)=-X3/X4
      MARKER=1
2     VV(1,N1+1)=VV(2,1)
      PP(1,N(1)+1)=(X1-VV(1,N1+1))/X2
      IF((PP(2,1).LT.VAPP) .AND. (P(2,1).LT.VAPP)) GOTO 3
      IF(VOLT.GT.0.0) GOTO 3
      IF(((P(2,1).GT.VAPP).AND.(PP(2,1).LT.VAPP)).OR.((P(2,1).LT.VAPP)
     1  .AND. (PP(2,1) .GT. VAPP))) GOTO 6
4     L3=MARKER
      RETURN
```

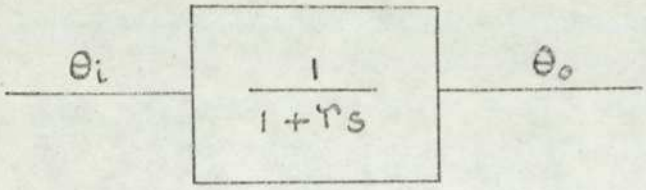
```
      MASTER PTP4
      REAL KINVIS
      DIMENSION TANG( 31),A(2),D(2),V(2,21),P(2,21),VV(2,21),PP(2,21),
     1  C(2),DT(2),PL(2),N(2),V0(2),AP(2,21),GMRM(2),DTF(2),VU(2,21),
     2  PU(2,21),VD(2,21),PD(2,21),F1U(2,21),F1D(2,21)
      COMMON/BL2/RHO,N,DT,TIME,A,C,TAMB,SOLC,TCLOS,FRAC1,VOLT,DP0,
     1TAU1,ITCOUNT,VAP,MARKER,RTM,D,TRANS,KINVIS,DVOL,DTS
      EQUIVALENCE(V02,V0(2)),(DT2,DT(2)),(N1,N(1)),(N2,N(2))
      READ(1,100) KINVIS,TRANS,RHO,PL(1),PL(2),C(1),D(1)
      READ(1,104) TAMB,OFFSET,RADIUS,STROKE,N(1),N(2)
      READ(1,101) TCLOS
      TCLOS=0.1
      READ(1,101) SOLC,TMAX,FRAC1
      READ(1,101) PR1,V0(1)
      READ(1,105) (TANG(JB), JB=1,30)
      PRS=PR1
      D(2)=D(1)
      C(2)=C(1)
      V0(2)=V0(1)
      WRITE(2,202)TRANS,RHO,KINVIS,PL(1),PL(2),C(1),C(2),D(1),D(2),V0(1
     1),V0(2),PRS,TCLOS,TMAX,SOLC,TAMB,FRAC1,N1,N2
      ICH=1
      CALL CHANGE(KINVIS,RHO,PL,C,D,OFFSET,RADIUS,STROKE,SOLC,PR1,V0,
     1  VOLTS,V,AP,ICH)
      WRITE(2,202)TRANS,RHO,KINVIS,PL(1),PL(2),C(1),C(2),D(1),D(2),V0(1
     1),V0(2),PRS,TCLOS,TMAX,SOLC,TAMB,FRAC1,N1,N2
      PR1=PR1*144.0
      DO 1 I=1,2
      D(I)=D(I)/12.0
      A(I)=3.1417*(D(I)**2)/4.0
      DT(I)=0.001
      GMRM(I)=DT(I)*N(I)/PL(I)
1     CONTINUE
      ICOUNT=5
      ISTEP=1
      DP1=5.11*V02*V02
      DP2=0.224*V02*V02
      PR1=PR1-DP1
      DP=DP2/144.0
      DP0=DP
      TRAT=0.0
      VOLT=0.0
      DVOL=0.0
      J1=N(1)+1
      J2=N(2)+1
      J3=N(2)
      TIME=0.0
      VAP=0.2*144.0
      DO 23 I=1,2
      REN=ABS(V0(I))*D(I)/KINVIS
      FF=0.079/(REN**0.25)
      FDR=2.0*RHO*FF*PL(I)*(V0(I)**2)/(D(I)*N(I))
```

```
      AA=0
      J=N(I)+1
      DO 23 K=1,J
      V(I,K)=V0(I)
      XR=PR1
      IF(I.EQ. 2)XR=P(1,N1+1)-(DP*144.0)
      AA=AA+1.0
      P(I,K)=XR-(AA-1.0)*FDR
      AP(I,K)=P(I,K)/144.0
   23 CONTINUE
      PR2=P(2,N2+1)
      CALL ANGLE(OFFSET,RADIUS,STROKE,TRAT,TANG,THETA,TAU1,DT2)
      L1=N2/5
      WRITE(2,200)
      ICH=2
      CALL CHANGE(KINVIS,RHO,PL,C,D,OFFSET,RADIUS,STROKE,SOLC,PR1,V0,
     1  VOLTS,V,AP,ICH)
      WRITE(2,201) TIME,TAU1,THETA,VOLT,(V(1,I),I=1,J1,1), (V(2,I),I=1,
     1  J2,L1),ITCOUNT,   MARKER,(AP(1,I),I=1,J1,1),(AP(2,I),I=1,J2,L1)
      ICH=3
      CALL CHANGE(KINVIS,RHO,PL,C,D,OFFSET,RADIUS,STROKE,SOLC,PR1,V0,
     1  VOLTS,V,AP,ICH)
      VD(1,N1+1)=0.0
      PD(1,N1+1)=0.0
      VU(1,1)=0.0
      PU(1,1)=0.0
      VU(2,1)=0.0
      PU(2,1)=0.0
      VD(2,N2+1)=0.0
      PD(2,N2+1)=0.0
    8 TIME=TIME+DT(2)
      TRAT=TIME/TCLOS
      IF(P(2,1) .GT. 7200) GOTO 11
      DIV=5.0
      GMRM1=GMRM(2)
      GMRM2=GMRM(2)/DIV
      IF((TIME .GT. TCLOS) .AND. (DVOL .GT. 0.34)) GOTO 11
      GOTO 10
   11 TIME=TIME-DT(2)
      MARKER=3
      DTS=DT(2)/DIV
      ISTEP=5
    3 TIME=TIME+DTS
      GMRM(2)=GMRM2
   10 L4=1
      IF(TIME .GT. (TCLOS-0.000001)) L4=2
      DO 61 J=L4,2
      KT=N(J)+1
      DO 60 I=2,KT
      VU(J,I)=V(J,I)+GMRM(J)*C(J)*(V(J,I-1)-V(J,I))
      PU(J,I)=P(J,I)+GMRM(J)*C(J)*(P(J,I-1)-P(J,I))
   60 CONTINUE
```

```
      KS=N(J)
      DO 61 I=1,KS
      VD(J,I)=V(J,I)+GMRM(J)*C(J)*(V(J,I+1)-V(J,I))
      PD(J,I)=P(J,I)+GMRM(J)*C(J)*(P(J,I+1)-P(J,I))
   61 CONTINUE
      CALL CHAR(VU,PU,F1U,PD,VD,F1D,VV,PP,PR1,PR2)
      IF(TIME .GT. (TCLOS-0.00001)) GOTO 13
      CALL ANGLE(OFFSET,RADIUS,STROKE,TRAT,TANG,THETA,TAU1,DT2)
      GOTO 4
   13 TAU1=0.0
      V(1,N1+1)=0.0
    4 CALL VALVE(VU,V,P,VV,PP,VU,PU,VD,PD,F1U,F1D)
      DO 7 I=L4,2
      J=N(I)+1
      DO 7 K=1,J
      V(I,K)=VV(I,K)
      P(I,K)=PP(I,K)
      AP(I,K)=PP(I,K)/144.0
    7 CONTINUE
      ISTEP=ISTEP-1
      GMRM(2)=GMRM1
      IF(ISTEP .NE.0) GOTO 3
      DTS=DT2
      ISTEP=1
      ICOUNT=ICOUNT+1
      IF(ICOUNT .NE. 0) GOTO 9
      ICOUNT=5
      ICH=2
      CALL CHANGE(KINVIS,RHO,PL,C,D,OFFSET,RADIUS,STROKE,SOLC,PR1,V0,
     1  VOLTS,V,AP,ICH)
      VOLT=VOLT*0.093
      IF(TIME .GT. (TCLOS-0.000001)) GOTO 16
      GOTO 17
   16 VOLTS=VOLT*1000.0
      WRITE(2,205) TIME,ITCOUNT,MARKER,VOLTS,(V(2,I),I=1,J2,L1),(AP(2,I)
     1    ,I=1,J2,L1)
      GOTO 5
   17 WRITE(2,201) TIME,TAU1,THETA,VOLT,(V(1,I),I=1,J1,1), (V(2,I),I=1,
     1  J2,L1),ITCOUNT,   MARKER,(AP(1,I),I=1,J1,1),(AP(2,I),I=1,J2,L1)
    5 ICH=3
      CALL CHANGE(KINVIS,RHO,PL,C,D,OFFSET,RADIUS,STROKE,SOLC,PR1,V0,
     1  VOLTS,V,AP,ICH)
      VOLT=VOLT/0.093
    9 IF(TIME .LT. TMAX) GOTO 8
  100 FORMAT(F10.7,6F10.5)
  101 FORMAT(3F10.5)
  104 FORMAT(4F10.5,2I5)
  105 FORMAT(10F6.2)
  200 FORMAT(1H1///,1X,4HTIME,5X,3HTAU,5X,5HTHETA,4X,3HVOL,20X,
     1    8HUPSTREAM,15X,5HVALVE,20X,10HDOWNSTREAM)
  201 FORMAT(/,1X,F8.4,2X,F6.4,4X,F6.2,1X,F6.3,5X,3HV=,5F7.3,
     1  3X,6F7.3,/,2(5X,I5),17X,2HP=,5F7.1,4X,6F7.1)
  202 FORMAT(/,9F13.7,/,8F13.7,2I4)
  205 FORMAT(/,1X,F8.4,2I3,F8.2,2X,2HV=,6F7.3,2X,2HP=,6F7.2)
      STOP
```

Appendix 4a Simulation of a first order lag element

This element is simulated in the program VSP2 and is intended to attenuate any high frequency signals generated by the pressure measuring equipment which may de-stabilize the remaining components of the servo system. This element is placed in the feedback path and is given a variable bandwidth denoted by w_1. The element is shown diagramatically below where $\tau = 1/w_1$ and s = the Laplace operator.



i.e. $$\theta_o = \frac{\theta_i}{(1+\tau s)}$$

$$\theta_o + \tau s \theta_o = \theta_i$$

Assuming $s \equiv \frac{d}{dt}$ we may make a first order approximation to the differential namely:

$$\theta_o + \tau(\theta_o - \theta_{o1})/\Delta t = \theta_i$$

where θ_{o1} is the value of θ_o at the beginning of the time step Δt and θ_o is the value at the end.

$$\theta_o (1 + \tau/\Delta t) = \theta_i + \theta_{o1} \tau/\Delta t$$

thus: $$\theta_o = (\theta_i + \theta_{o1} \tau/\Delta t)/(1 + \tau/\Delta t)$$

This is the equation used in VSP2 where:

θ_o = FB

θ_{o1} = FBLAST

θ_i = FBIN

$\tau/\Delta t$ = C7

Appendix 4b. Program VSP3

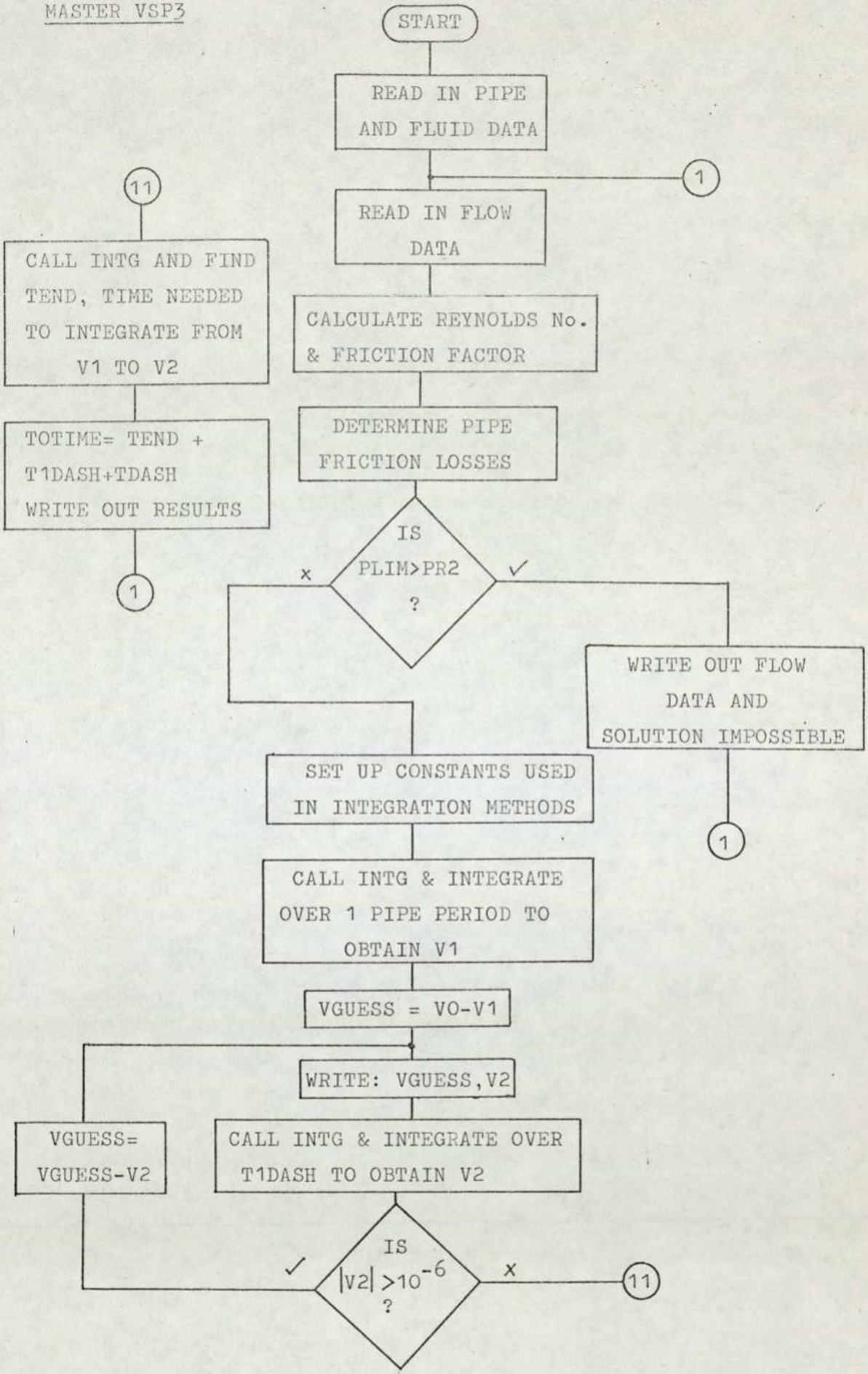
This program is used to determine the overall valve closure time required to close a valve while achieving the objectives of the ideal valve stroking proceedures outlined in section 9. The method is fully described in section 9.2. The master segment begins by reading in the pipe and fluid parameters (usually invariant) followed by a card containing details of the flow conditions in question. After this the Reynolds number is calculated and hence the friction factor, enabling the pressure losses in the upstream and downstream pipes to be determined. Knowing the pressure loss through the valve, a test may be made to check the relative size of PR2 and the minimum control pressure. If the pressure gradient is positive then from the arguments presented in section 9.3 a solution is impossible and the line printer outputs such a message before another data card is read in. Providing a solution does exist, the initial conditions for the first integration are set up. This initial integration is from the initial conditions of $V = V_o$ when $t = 0$ and increments t until $t = t' = 1$ pipe period. The value of the liquid velocity V_1 is determined at the end of this period; the integration being performed in subroutine INTG (see section). The next integration interval from some unknown initial condition of P = PLIM, $V = V_2$, requires the equation of motion of the liquid column to be integrated over a known interval T1DASH such that at the end of the interval P = PR2 and V = 0. The integration is performed in an iterative fashion beginning with a guessed value of V2, executing the integration

and determining how close to zero the final value of the velocity is. The error is added or subtracted (depending on its sign) to the initial guess of V2 enabling a better guess to be made, and the process repeated. Once a solution is found, the velocities at both ends of phase 1 and phase 2 are known and the equation of motion may be integrated between the two velocity limits to determine the overall time required to decelerate the liquid column from one velocity to the other. Thus the valve closure time is the sum of the times of the three individual phases of flow retardation. The results are printed out together with the initial flow conditions to which they refer.

Parameter list

COEF	V squared friction coeficient for downstream pipe
COEF1	" " " " " upstream "
L	Downstream pipe length
PO	Initial upstream reservoir pressure
PL1	Upstream pipe length
PLIM	Minimum control pressure
PLOSS	Downstream pipe pressure loss
PLOSS1	Upstream " " "
PR2	Downstream reservoir pressure
PV	Initial steady state valve pressure
TO1	Inital interval time
TO2	Final " "
T1DASH	Integration interval for final phase
TDASH	" ' " initial " (= 1 pipe period)
TOTIME	Total valve closure time
VO1	Initial interval velocity
VO2	Final " "
VO	Initial steady state fluid velocity
VGUESS	Guessed value of velocity of integration iteration
VPD	Initial valve pressure drop
VMIN	Final steady state fluid velocity

MASTER VSP3


START
READ IN PIPE AND FLUID DATA
1
READ IN FLOW DATA
CALCULATE REYNOLDS No. & FRICTION FACTOR
DETERMINE PIPE FRICTION LOSSES
IS PLIM>PR2 ?
x
✓
WRITE OUT FLOW DATA AND SOLUTION IMPOSSIBLE
1
SET UP CONSTANTS USED IN INTEGRATION METHODS
CALL INTG & INTEGRATE OVER 1 PIPE PERIOD TO OBTAIN V1
VGUESS = VO-V1
WRITE: VGUESS, V2
CALL INTG & INTEGRATE OVER T1DASH TO OBTAIN V2
IS |V2| >10^-6 ?
✓
x
11
VGUESS= VGUESS-V2
11
CALL INTG AND FIND TEND, TIME NEEDED TO INTEGRATE FROM V1 TO V2
TOTIME= TEND + T1DASH+TDASH
WRITE OUT RESULTS
1

```
      MASTER VSP3
      REAL L,KINVIS
      READ(1,101) L,C,RHO,DIA,KINVIS,PL1,VPD
      C=C*1000.0
    1 READ(1,102) P0,V0,PLIM
      VMIN=0.0
      P0=P0*144.0
      PLIM=PLIM*144.0
      REN=(ABS(V0*DIA))/KINVIS
      FRICTF=0.079/(REN**0.25)
      COEF=(2.0*RHO*FRICTF*L)/DIA
      COEF1=2.0*RHO*FRICTF*PL1/DIA
      PLOSS=COEF*(V0**2)
      PLOSS1=COEF1*V0*V0
      TDASH=(2.0*L)/C
      A=1.0/(RHO*L)
      PV=P0-PLOSS1-VPD*144.0
      PR2=PV-PLOSS
      IF(PLIM .GT. PR2) GOTO 4
      T1DASH=TDASH*(PR2-PLIM)/(P0-PLIM)
      B=PV
      F=PLIM
      D=PR2-PLIM
      CC=(PV-PLIM)/(PV*TDASH)
      CD=(PLIM-PR2)/(PLIM*T1DASH)
      E=COEF
      ZD=DIA/KINVIS
      ZE=2.0*RHO*L/DIA
      T01=0.0
      T02=T1DASH
      V01=V0
      V02=0.0
      STEP=0.001
      I=1
      CALL INTG(I,T01,V01,STEP,TDASH,V1,A,B,CC,ZD,ZE,PR2)
      VGUESS=V0-V1
      V2=0.0
    8 CONTINUE
      T02=0.0
      WRITE(2,200) VGUESS,V2
      V02=VGUESS
      CALL INTG(I,T02,V02,STEP,T1DASH,V2,A,F,CD,ZD,ZE,PR2)
      V2A=ABS(V2)
      IF(V2A .LT. 0.000001) GOTO 11
      VGUESS=VGUESS-V2
      GOTO 8
   11 CONTINUE
      V2=VGUESS
      IF(V2 .GT. V1) GOTO 4
      T03=0.0
      V1D=V1
      V2D=V2
```

```
      I=3
      CALL INTG(I,T03,V1D,STEP,TEND,V2D,A,F,CC,ZD,,E,PR2)
      TOTIME=TEND+TDASH+T1DASH
      P0=P0/144.0
      PV=PV/144.0
      PLIM=PLIM/144.0
      WRITE(2,201) P0,PV,V0,PLIM,TOTIME,V1,V2
      GOTO 7
    4 CONTINUE
      PV=PV/144.0
      P0=P0/144.0
      PLIM=PLIM/144.0
      WRITE(2,202) P0,PV,V0,PLIM
    7 CONTINUE
      GOTO 1
  101 FORMAT(7F10.5)
  102 FORMAT(3F10.5)
  200 FORMAT(2F10.5)
  201 FORMAT(//,5X,4HP0 =,F5.1,5X,4HPV =,F5.1,5X,4HV0 =,F5.2,5X,6HPLIM =
     1,F5.2,5X,12HTOTAL TIME =,F5.3,5X,4HV1 =,F5.3,5X,4HV2 =,F5.3)
  202 FORMAT(//,5X,4HP0 =,F5.1,5X,4HPV =,F5.1,5X,4HV0 =,F5.2,5X,6HPLIM =
     1,F5.2,5X,19HSOLUTION IMPOSSIBLE)
      STOP
```

```
      SUBROUTINE INTG(I,XN,YN,D,XEND,YEND,ZA,ZB,ZC,ZD,ZE,PR2)
      GIVF(X,Y,COEF)=ZA*(ZB*(1.0-ZC*X)-PR2-COEF*Y*Y)
      GIVG(Y,COEF)=ZA*(ZB-PR2-COEF*Y*Y)
      DD=0.5*D
    1 X=XN
      Y=YN
      RE=ABS(Y)*ZD
      COEF=0.079/(RE**0.25)
      IF(RE .LT. 2300.0) COEF=16.0/RE
      COEF=COEF*ZE
      J=1
    2 Z=GIVF(X,Y,COEF)
      IF(I .EQ. 3) Z=GIVG(Y,COEF)
      GOTO(3,4,5,6),J
    3 C1=D*Z
      X=XN+DD
      Y=YN+(C1/2)
      J=2
      GOTO 2
    4 C2=D*Z
      Y=YN+(C2/2)
      J=3
      GOTO2
    5 C3=D*Z
      X=XN+D
      Y=YN+C3
      J=4
      GOTO 2
    6 XN=X
      C4=D*Z
      YN=YN+(C1+2*(C2+C3)+C4)/6
      IF(I-2) 7,8,10
    7 IF(XN-XEND) 1,9,9
    8 IF(XEND-XN) 1,9,9
   10 IF(YEND-YN) 1,9,9
    9 CONTINUE
      XEND=XN
      YEND=YN
      RETURN
```

DATA

```
215.000000   4,000000   1,55        0.166667  0.000018 18.000000  0.180000
  50.0          6.0        45.0
  50.0          6.0        40.0
  50.0          6.0        35.0
  50.0          6.0        30.0
  50.0          6.0        25.0
  50.0          6.0        20.0
  50.0          6.0        15.0
  50.0          6.0        10.0
  50.0          6.0         5.0
  50.0          7.0         5.0
  50.0          7.0        10.0
  50.0          7.0        15.0
  50.0          7.0        20.0
  50.0          7.0        25.0
  50.0          7.0        30.0
  50.0          7.0        35.0
  50.0          7.0        40.0
  50.0          7.0        45.0
  50.0          8.0        45.0
  50.0          8.0        40.0
  50.0          8.0        35.0
  50.0          8.0        30.0
  50.0          8.0        25.0
  50.0          8.0        20.0
  50.0          8.0        15.0
  50.0          8.0        10.0
  50.0          8.0         5.0
  50.0          9.0        45.0
  50.0          9.0         5.0
  50.0          9.0        10.0
  50.0          9.0        15.0
  50.0          9.0        20.0
  50.0          9.0        25.0
  50.0          9.0        30.0
  50.0          9.0        35.0
  50.0          9.0        40.0
  50.0         10.0        45.0
  50.0         10.0        40.0
  50.0         10.0        35.0
  50.0         10.0        30.0
  50.0         10.0        25.0
  50.0         10.0        20.0
  50.0         10.0        15.0
  50.0         10.0        10.0
  50.0         10.0         5.0
  50.0          1.0        45.0
  50.0          1.0        40.0
  50.0          1.0        35.0
  50.0          1.0        30.0
  50.0          1.0        25.0
  50.0          1.0        20.0
```

50.0	1.0	15.0
50.0	1.0	10.0
50.0	1.0	5.0
50.0	2.0	45.0
50.0	2.0	40.0
50.0	2.0	35.0
50.0	2.0	30.0
50.0	2.0	25.0
50.0	2.0	20.0
50.0	2.0	15.0
50.0	2.0	10.0
50.0	2.0	5.0
50.0	3.0	45.0
50.0	3.0	40.0
50.0	3.0	35.0
50.0	3.0	30.0
50.0	3.0	25.0
50.0	3.0	20.0
50.0	3.0	15.0
50.0	3.0	10.0
50.0	3.0	5.0
50.0	4.0	45.0
50.0	4.0	40.0
50.0	4.0	35.0
50.0	4.0	30.0
50.0	4.0	25.0
50.0	4.0	20.0
50.0	4.0	15.0
50.0	4.0	10.0
50.0	4.0	5.0
50.0	5.0	45.0
50.0	5.0	40.0
50.0	5.0	35.0
50.0	5.0	30.0
50.0	5.0	25.0
50.0	5.0	20.0
50.0	5.0	15.0
50.0	5.0	10.0

Appendix 5 Program PTP6

The object of this program is to simulate the system shown in fig. 60 and to illustrate the type of pressure fluctuations encountered after valve closure is complete assuming equations apply to the system. To achieve this, an estimation of the amount of air released from the kerosene has to be made involving approximations about the pressure and flow variations during valve closure. These assumptions may seem extreme, but it should be remembered that the chief purpose of the program lies in the events occuring after valve closure and those preceeding this only serve to set up the initial conditions.

The program begins by reading in two data cards. The first is a list of variables which define the initial flow conditions in terms of the kerosene saturation pressure, the initial flow velocity, the final flow velocity at valve closure (which may not be zero) , the minimum control pressure and the pressure of the downstream reservoir. The second data card lists the parameters associated with the fluid and pipe geometry. The next section converts the data to British units. If the program is to be used entirely in British units, these cards may be omitted and the data specified in the same system. Then the initial conditions for subroutine INTG are set up and when called the subroutine evaluates the time taken for the velocity to fall from the initial to final values. This time is thus the valve closure time TCL and is written out on the line printer. In calculating this time it is assumed that the minimum control pressure PMIN is achieved instantaniously and

that the column is subject to a decelerating pressure difference of PR2 - PMIN across its ends. Knowing the time taken to close the valve, it may be assumed that this also gives the interval over which air release occurs. Also, assuming that the velocity reduction is linear with time, the amount of fuel to give up air in a time dt is:

$$dV_{OLCON} = A V \, dt$$

and since $V = V_0 - (V_0 - V_T) t / TCL$

we get $dV_{OLCON} = A \left\{ V_0 - (V_0 - V_T) t / TCL \right\} dt$

Hence we may integrate over the valve closure interval to obtain the total amount of fuel passing through the valve

$$VOLCON = \int_0^{TCL} dV_{OLCON} = A \int_0^{TCL} \left\{ V_0 - (V_0 - V_T) t / TCL \right\} dt$$

$$= A \left\{ V_0 t - (V_0 - V_T) t^2 / 2 TCL \right\}_0^{TCL}$$

$$= A \left\{ V_0 \, TCL - \tfrac{1}{2} (V_0 - V_T) TCL \right\}$$

$$\therefore VOLCON = \tfrac{1}{2} A \, TCL \, (V_0 + V_T)$$

Thus VOL_0, the volume of the cavity at the end of the valve closure time may be found, enabling the equation

$$PMIN \times (VOL_0)^{\gamma} = CONSTANT$$

to determine the constant for subsequent cavity processes.

This completes the initial section of the program and provides the initial conditions for the second section. TIME is assigned the value of TCL and is incremented by the time step in the statement labelled 1. Then, using the pressure and velocity of the previous time step, the differential equation of motion of the liquid column is integrated over one time interval to determine the velocity at the end of the interval. Frictional effects are based on the velocity at the beginning of the interval, as is the pressure assumed to exist within the cavity. The integration is performed in the subroutine INTG. Once the velocity is known, the cavity volume and hence the cavity pressure may be determined. The results are not printed out every time step, the variable ICOUNT determining how many steps are performed before the results are printed. The output variables are: time(secs), cavity volume (m^3), cavity pressure (kN/m^3), and velocity of the liquid column (m/s). The program then returns to statement 1 and increases TIME by another step unless the value of TIME after printing out is greater than TMAX in which case the program is terminated.

Subroutine INTG

This subroutine is used often in the research reported and solves equations of the form:

$$dy/dx = f(x,y)$$

over an interval of either x or y by using a Runge-Kutta numerical integration proceedure. The actual proceedure is a piece of standard mathematics and need not be described here except to say that the function 'f' above is defined in the function statement:

GIVF(X,Y) = ...

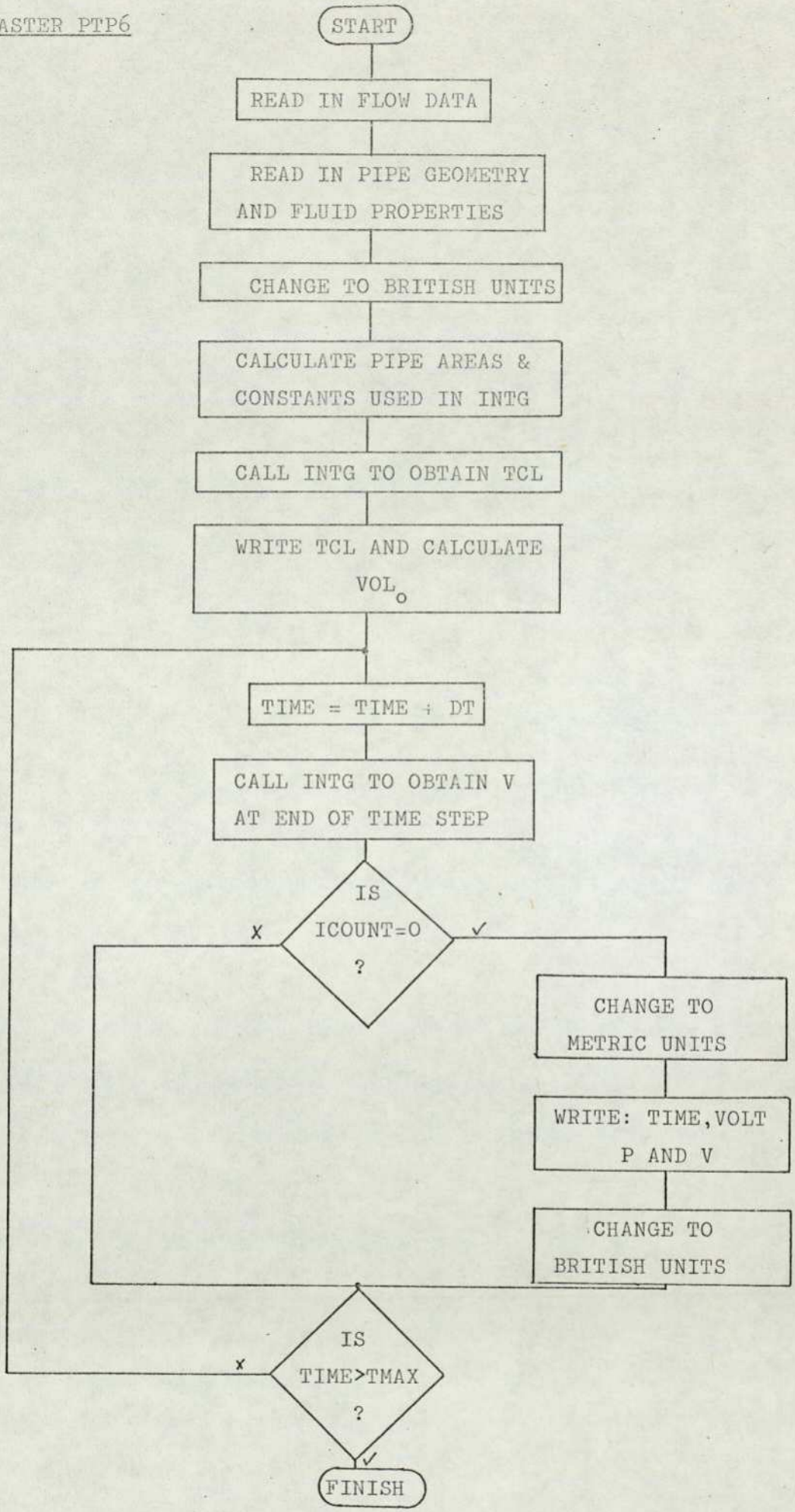
Also, the last character I in the subroutine declaration statement defines whether an integration over x or y is required. Thus:

I = 1 Integration over a region of x is required

I = 2 Integration over a region of y is required

The majority of parameters used in PTP6 are defined in appendix 3. In the next few pages, a flow chart, program listing and representative print-out are presented for program PTP6.

MASTER PTP6


START
READ IN FLOW DATA
READ IN PIPE GEOMETRY AND FLUID PROPERTIES
CHANGE TO BRITISH UNITS
CALCULATE PIPE AREAS & CONSTANTS USED IN INTG
CALL INTG TO OBTAIN TCL
WRITE TCL AND CALCULATE VOL$_o$
TIME = TIME + DT
CALL INTG TO OBTAIN V AT END OF TIME STEP
IS ICOUNT=0 ?
X
✓
CHANGE TO METRIC UNITS
WRITE: TIME, VOLT P AND V
CHANGE TO BRITISH UNITS
IS TIME>TMAX ?
x
✓
FINISH

```
      MASTER PTP6
      READ(1,100) PSAT,PMIN,V0,PR2,VT
      READ(1,100) GAMMA,RHO,DIA,PL1,TMAX,CINVIS,FRACC1,TAMB,SOLC
      PSAT=PSAT*144.0/6.895
      PMIN=PMIN*144.0/6.895
      PR2=PR2*144.0/6.895
      V0=V0/0.3048
      VT=VT/0.3048
      RHO=RHO*0.062428/32.2
      DIA=DIA/0.3048
      PL1=PL1/0.3048
      CINVIS=CINVIS*0.0929
      SOLC=SOLC/(144.0*0.0193)
      PLAST=0.0
      PI=3.1415926
      AREA=PI*DIA*DIA*0.25
      DT1=0.0005
      DT2=0.001
      C1=1.0/(RHO*PL1)
      C2=DIA/CINVIS
      C3=2.0*RHO*PL1/DIA
      VTS=VT
      TIME=0.0
      TLAST=TIME
      PCAV=PMIN
      V=V0
      ICOUNT=1
      U=V
      CALL INTG(TLAST,U,DT2,TCL,VT,C1,C2,C3,PCAV,PR2,1)
      WRITE(2,203) TCL
      WRITE(2,202)
      TIME=TCL
      P1=(-0.693*TCL)/FRAC1
      C4=1.0-EXP(P1)
      VOLCON=0.5*AREA*TCL*(V0+VT)
      X10=VOLCON*(TAMB+460.0)*SOLC/23.21
      VOLTINF=X10*(PSAT/PMIN-1.0)
      VOL0=C4*VOLTINF
      V=V0
      VOLT=VOL0
      VOLTM1=VOL0
      CONST=PCAV*(VOLT**GAMMA)
      V0=VTS
1     TIME=TIME+DT1
      V0D=V0
      TIMED=TIME
      CALL INTG(TLAST,V0D,DT1,TIMED,V,C1,C2,C3,PCAV,PR2,2)
      VOLT=VOLTM1+0.5*AREA*DT1*(V+V0)
      PCAV=CONST/(VOLT**GAMMA)
      TLAST=TIME
      V0=V
      VOLTM1=VOLT
```

```
      ICOUNT=ICOUNT-1
      IF(ICOUNT .NE. 0) GOTO 1
      ICOUNT=20
      VOLT=VOLT*0.093
      PCAVS=PCAV*5.595/144.0
      V=V*0.3048
      WRITE(2,200) TIME,VOLT,PCAVS,V
      VOLT=VOLT/0.093
      V=V/0.3048
      IF(TIME .LT. TMAX) GOTO 1
100   FORMAT(100F0.0)
200   FORMAT(4(5X,F10.5))
202   FORMAT(//,10X,4HTIME,10X,6HVOLUME,9X,4HPCAV,8X,8HVELOCITY)
203   FORMAT(1H1,//,10X,21HVALVE CLOSURE TIME = ,F9.5)
      STOP
```

```
      SUBROUTINE INTG(XN,YN,D,XEND,YEND,X1,X2,X3,PCAV,PR2,I)
      GIVF(F,Y)=X1*(PCAV-PR2-F*Y*ABS(Y))
      DD=0.5*D
1     X=XN
      Y=YN
      J=1
 2    REN=X2*ABS(Y)
      IF(REN .LT. 0.000001) REN=0.000001
      ACOEF=0.079/(REN**0.25)
      IF(REN.LT.2300.0) ACOEF=16.0/REN
      F=X3*ACOEF
      Z=GIVF(F,Y)
      GOTO(3,4,5,6),J
3     C1=D*Z
      X=XN+DD
      Y=YN+(C1/2)
      J=2
      GOTO 2
4     C2=D*Z
      Y=YN+(C2/2)
      J=3
      GOTO2
5     C3=D*Z
      X=XN+D
      Y=YN+C3
      J=4
      GOTO 2
6     XN=X
      C4=D*Z
      YN=YN+(C1+2*(C2+C3)+C4)/6
      IF(I.EQ.2) GOTO 8
      IF(YN-YEND) 7,7,1
 8    CONTINUE
      IF(XN-XEND) 1,7,7
7     CONTINUE
      XEND=XN
      YEND=YN
      RETURN
```

DATA

```
172.0   46.5   1.52   103.0   0.3048
1.4   814.9   0.0508   65.53   5.0   0.000194   0.2   60.0   0.016
```

Appendix 6 Program PTP7

This program solves either the equation

$$\frac{dP}{dV} = \frac{P^2}{(P_o - P)}\sqrt{2k\left\{\frac{P_o}{P^*} - \frac{P_o}{P} - \log\left(\frac{P}{P^*}\right)\right\}} \qquad A6.1$$

which is of the form

$$dP/dV = f(P)$$

or the inverse equation·

$$\frac{dV}{dP} = \frac{P_o - P}{P^2}\sqrt{\frac{1}{2k\left\{\frac{P_o}{P^*} - \frac{P_o}{P} - \log\left(\frac{P}{P^*}\right)\right\}}} \qquad A6.2$$

which is of the form

$$dV/dP = f(P)$$

where P^*, P_o, and k are constants for any particular solution. Subroutine INTG is ideally suited to handle such equations except that as the initial solution proceeds using P as the independant variable we have $dP/dV = \infty$ at one of the boundary conditions. This condition is that $P = P_o$ when $V = 0$. It is required to determine V at the other boundaty such that at the boundary $P = P^*$. Thus the program begins by integrating "away" from the boundary at which conditions are known by the use of equation A6.2 which gives $dV/dP = 0$ for the initial condition. Since this derivative becomes ∞ as $P \to P^*$, the proceedure uses equation A6.1 after some convenient change over point such as $dV/dP = dP/dV = 1$.

The program begins by reading in the values of P_o, P^* and k (PO, PS and A2 in the program). The data is then converted to the British system of units and various fluid and pipe parameters are defined. A counter, IRUN, is set equal to unity and the necessaty constants used in the integration proceedure are assigned. The marker J indicates the use of either equation A6.1 or A6.2 in the integration: if J = 1 then the integration proceeds with equation A6.2. This equation is used initially

to determine the new value of V for a small step in P. After this is done, in subroutine INTG, a check is made to see whether the new value of P is very near to P^* and if it is the step size of P is reduced, the amount of reduction depending upon the proximity of the two variables. The slope of the integration path is then calculated (dV/dP) and the program writes out a line of results including:

a) The number of the integration step.

b) Value of J (indicating which equation is being integrated)

c) Value of P

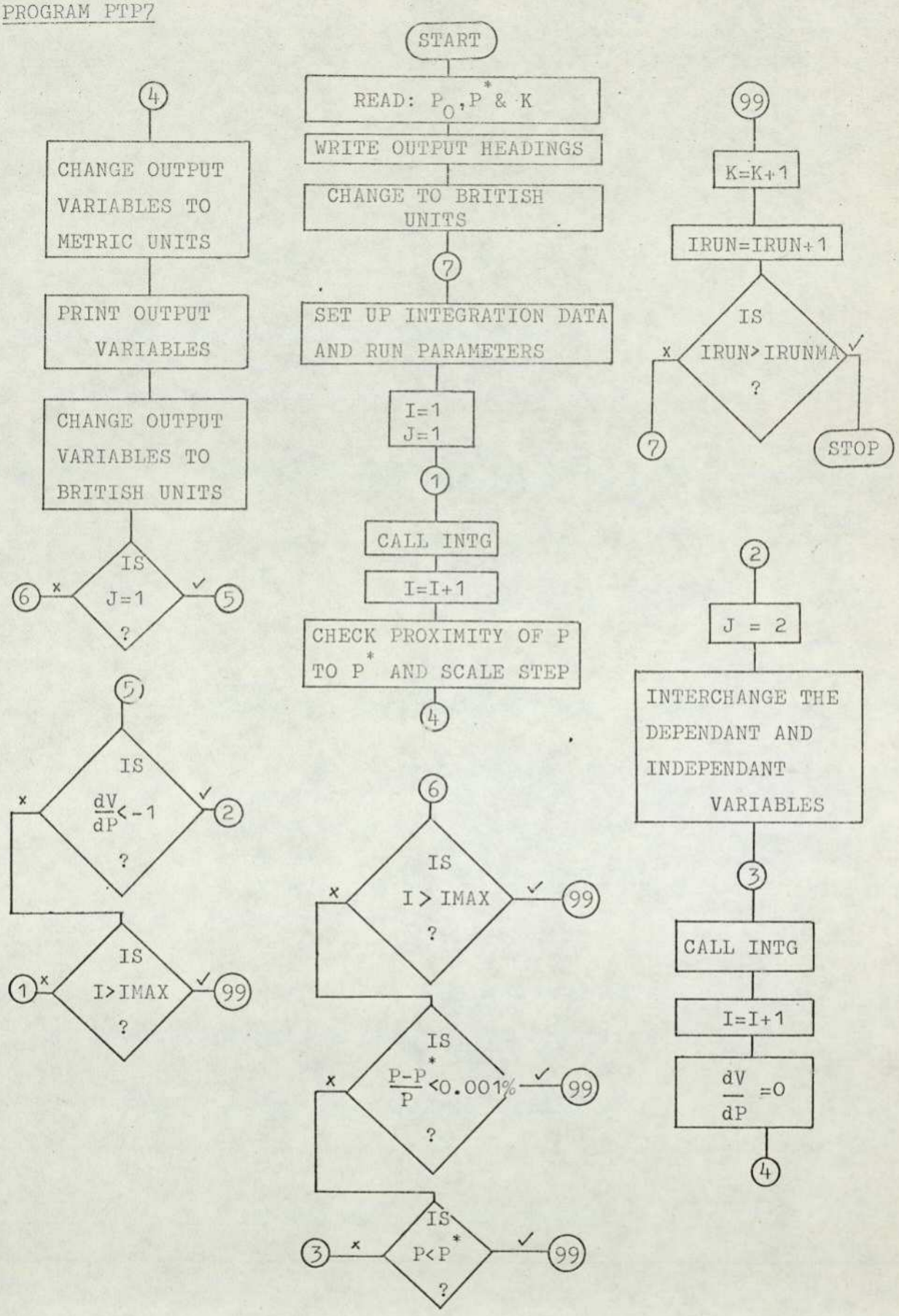
d) Value of V

e) The slope of the integration path

Control is returned to the point before writing occured and a check is made of the value of the slope. If this is greater than -1 then equation A6.2 is used again for the next integration step. If the slope is less than -1, the independant and dependant variables are changed over and equation A6.1 is used. The basic proceedure is repeated i.e. integrating over one step, writing out the results and incrementing the independant variable. The proceedure is halted once P and P^* differ by less than 0.001%.

The constant k in equations A6.1 and A6.2 is generally an unknown quantity although an estimate is usually available. The program repeats the proceedure outlined above for a value of k which is different to the previous value by 1. This is done IRUNMA times, the value of this variable being written in the program and not read in as data. The program will fail if it has to perform more than 1000 integration steps for any single value of k.

PROGRAM PTP7



```
      MASTER PTP7
      READ(1,100) P0,PS,A2
100   FORMAT(3F10,5)
      WRITE(2,201)
201   FORMAT(1H1,/,14X,4HSTEP,1X,4HMARK,2X,8HPRESSURE,2X,8HVELOCITY,
     1  2X,5HSLOPE)
      PS=PS*144,0/6,895
      P0=P0*144,0/6,895
      A2=A2/(6,895*0,3048)
      RHO=1,58
      PL1=18,0
      PL2=215,0
      D=2,0/12,0
      A=3,14159*D*D*0,25
      A1=1,0/(RHO*PL2)
      A3=A
      A4=1,0/(RHO*PL1)
      IRUN=1
    7 XK=A3*(A1+A4)/(A2*A1*A1)
      XN=P0
      YN=0,0
      D=-10,0
      I=0
      IMAX=1000
      IRUNMA=5
      YNM1=0,0
      J=1
    1 CALL INTG(XN,YN,D,XEND,YEND,J,XK,P0,PS)
      I=I+1
      P=XN
      PLAST=P
      V=YN
      PSC=P/144,0
      IF(P,LE,1,01*PS) D=-0,1
      IF(P,LE,1,001*PS) D=-0,01
      IF(P,LE,1,0001*PS) D=-0,001
      DVDP=144,0*(YN-YNM1)/D
      GOTO 4
    5 IF(DVDP,LT,-1,0) GOTO 2
      IF(I,GT,IMAX) GOTO 99
      YNM1=YN
      GOTO 1
    2 J=2
      XN=V
      YN=P
      D=0,01
    3 CALL INTG(XN,YN,D,XEND,YEND,J,XK,P0,PS)
      I=I+1
      V=XN
      P=YN
      PSC=P/144,0
      DVDP=0,0
```

```
      GOTO 4
    6 IF(I,GT,IMAX) GOTO 99
      IF((ABS(PS-P)) ,LT, 0,00001) GOTO 99
      PINT=P-(PLAST-P)
      IF(PINT,LE,PS) GOTO 99
      PLAST=P
      GOTO 3
    4 PSC=PSC*6,895
      V=V*0,3048
      DVDP=DVDP*0,3048/6,895
      WRITE(2,200) I,J,PSC,V,DVDP
  200 FORMAT(/,10X,215,3F10,5)
      PSC=PSC/6,895
      V=V/0,3048
      DVDP=DVDP*6,895/0,3048
      IF(J,EQ,1) GOTO 5
      GOTO 6
   99 A2=A2+1,0
      IRUN=IRUN+1
      IF(IRUN,GT,IRUNMA) GOTO 999
      GOTO 7
  999 STOP
```

```
      SUBROUTINE INTG(XN,YN,D,XEND,YEND,K,XK,P0,PS)
      GIVF(P)=(P0-P)/(P*P*SQRT(2.0*XK*(P0/PS-P0/P-BLOG(P/PS))))
      GIVG(P)=(P*P/(P0-P))*SQRT(2.0*XK*(P0/PS-P0/P-BLOG(P/PS)))
      DD=0.5*D
    1 X=XN
      Y=YN
      J=1
    2 IF(K.EQ.1) Z=GIVF(X)
      IF(K.EQ.2) Z=GIVG(Y)
      Z=-Z
      GOTO(3,4,5,6),J
    3 C1=D*Z
      X=XN+DD
      Y=YN+(C1/2)
      J=2
      GOTO 2
    4 C2=D*Z
      Y=YN+(C2/2)
      J=3
      GOTO2
    5 C3=D*Z
      X=XN+D
      Y=YN+C3
      J=4
      GOTO 2
    6 XN=X
      C4=D*Z
      YN=YN+(C1+2*(C2+C3)+C4)/6
      XEND=XN
      YEND=YN
      RETURN


      FUNCTION BLOG(X)
      Z=(X-1.0)/(X+1.0)
      IF(ABS(Z).GT.0.01) GOTO 1
      Z2=Z*Z
      BLOG=2.0*Z*(1.0+Z2/3.0+Z2*Z2/5.0+Z2*Z2*Z2/7.0)
      GOTO 99
    1 BLOG=ALOG(X)
   99 RETURN
```

DATA

```
135.0       63.0       25.5
```

Appendix 7 Program VSP2

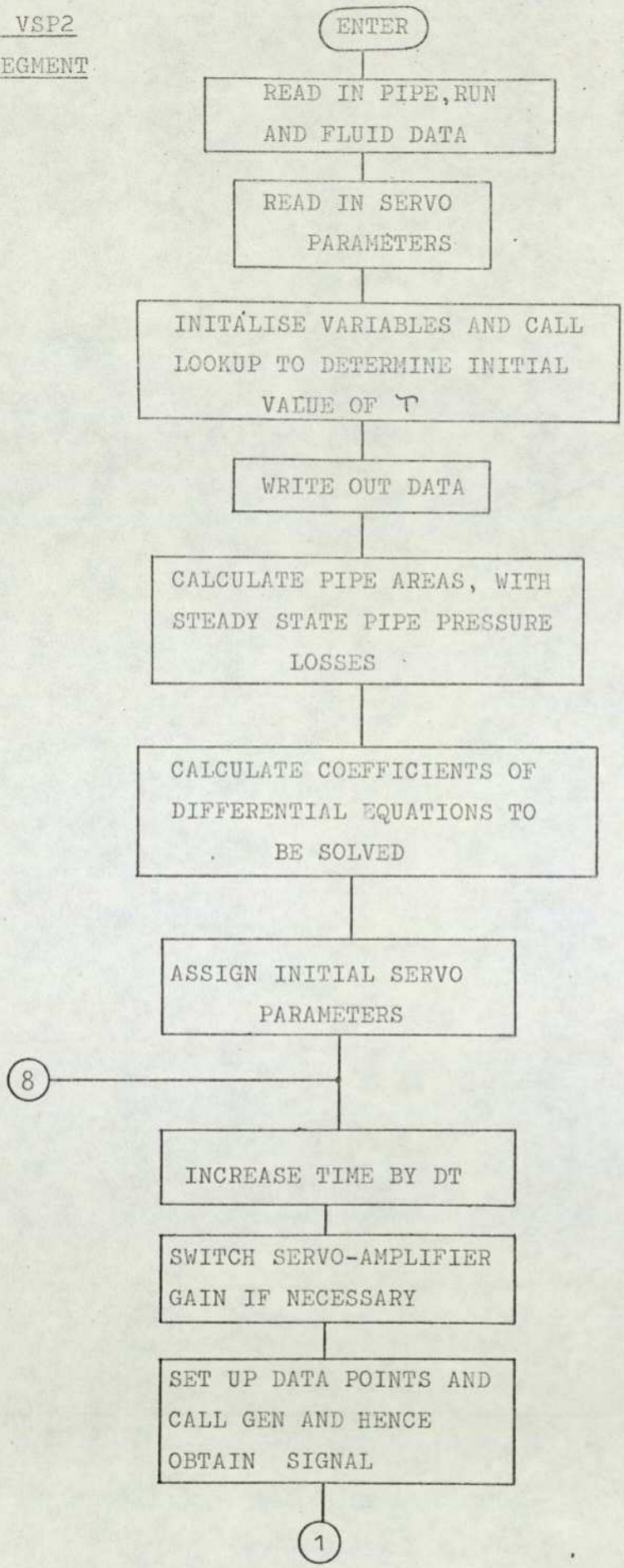
The following list includes some of the more important parameters used in program VSP2. Since this program is essentially an extension of PTP1, reference should also be made to the list provided in appendix 3. The parameters listed here are chiefly associated with the servo aspects of the program.

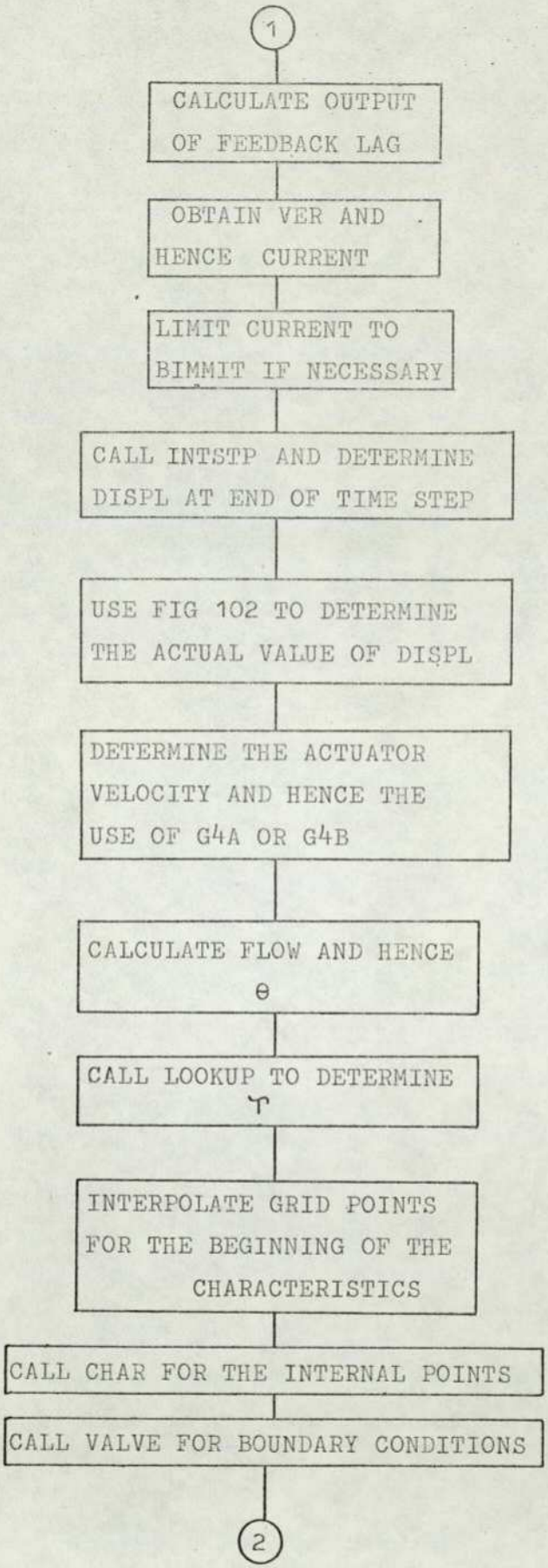
BIMIT	Maximum absolute value of servo amplifier output
C1-C6	Constants used in the differential equations describing the servo valve and hydraulic actuator.
C7	Constant used in simulation of feedback lag (see appendix 4)
CURRENT	Current output of servo amplifier
DISPL	Displacement of actuator at time t
DISLAST	" " " " " $t - \Delta t$
DISL2	" " " " " $t - 2\Delta t$
DXDT	Velocity of actuator piston
F (array)	Time differential of Y (i.e. $F(1) = \dot{Y}(1)$)
FB	Feedback voltage between summing junction and filter
FBLAST	Value of FB at time $t - \Delta t$
FBL2	Value of FB at time $t - 2\Delta t$
FBIN	Voltage output of pressure transducer
FLOW	Oil flow rate from servo-valve
FPG	Formard path gain of servo loop (=G3.G4)
FR1	Cut off frequency of feedback filter
G1	Gain of signal generator
G2	Gain of servo amplifier
G3	Steady state gain of servo valve

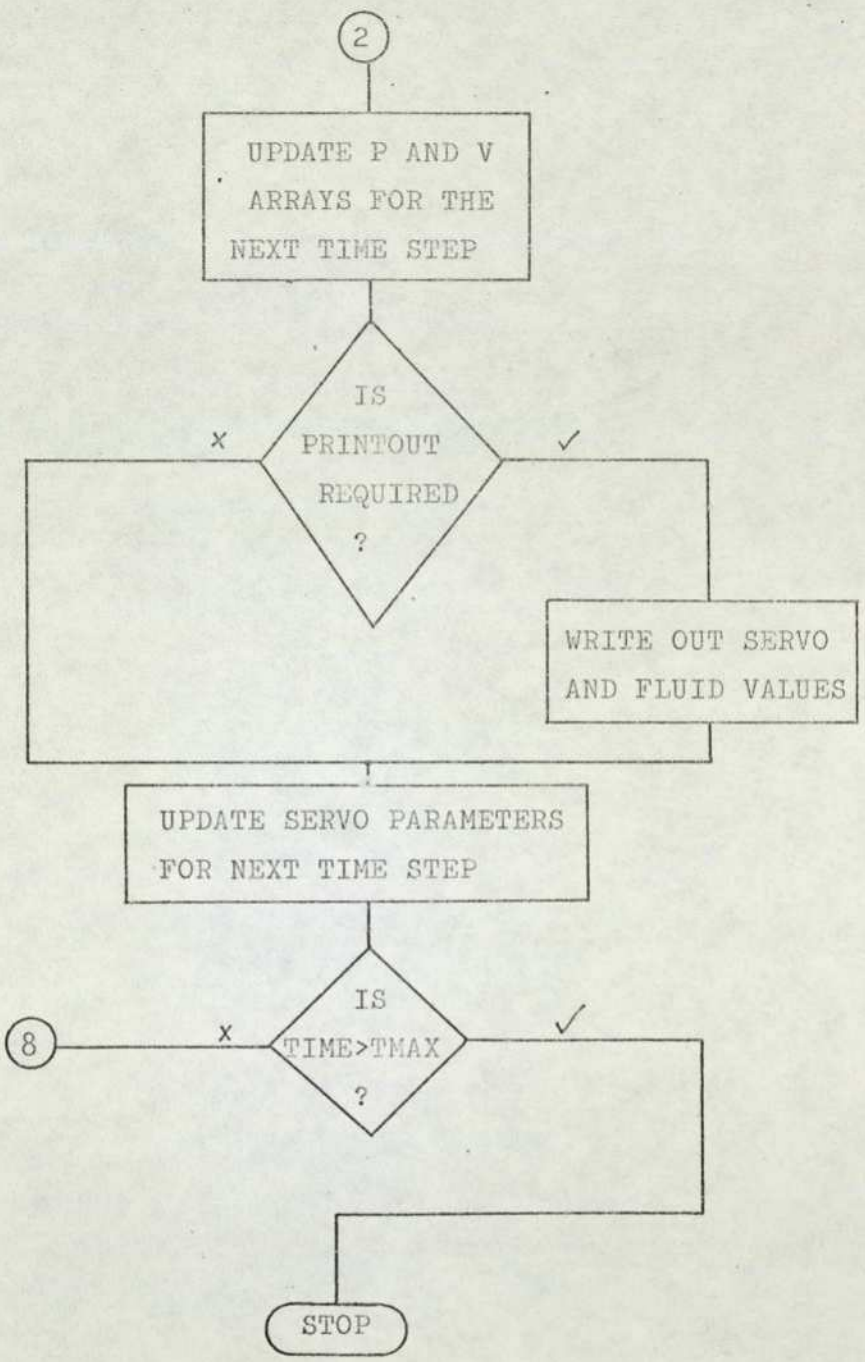
G4	Steady state gain of hydraulic actuator
G4A	Value of G4 when DXDT is positive
G4B	" " " " " " negative
G5	Gain of feedback pressure transducer
HHH	Integration step size of subroutine INTSTP
MMM	Number of first order differential equations in subroutine INTG
POUT	Output pressure of subroutine GEN
QA, QB, QC, QD	Coefficients used in the transfer functions of the servo valve and hydraulic actuator
SIGNAL	Voltage output of signal generator
TG2	Value of G2 after gain switching (if applicable)
VER	Voltage error (output of summing junction)
WA	Natural mechanical frequency of hydraulic actuator
WS	" " " " servo valve
W1	Natural frequency of feedback filter
X1-X6	Input X coordinates of subroutine GEN
XXX	Independant variable (time) in subroutine INTSTP
Y1-Y6	Input Y coordinates of subroutine GEN
Y (array)	Array containing the dummy variables used to reduce the fifth order differential equation described in section 19.2
ZA	Mechanical damping factor of hydraulic actuator
ZS	" " " " servo valve

PROGRAM VSP2

MASTER SEGMENT




1
CALCULATE OUTPUT OF FEEDBACK LAG
OBTAIN VER AND HENCE CURRENT
LIMIT CURRENT TO BIMMIT IF NECESSARY
CALL INTSTP AND DETERMINE DISPL AT END OF TIME STEP
USE FIG 102 TO DETERMINE THE ACTUAL VALUE OF DISPL
DETERMINE THE ACTUATOR VELOCITY AND HENCE THE USE OF G4A OR G4B
CALCULATE FLOW AND HENCE θ
CALL LOOKUP TO DETERMINE ϒ
INTERPOLATE GRID POINTS FOR THE BEGINNING OF THE CHARACTERISTICS
CALL CHAR FOR THE INTERNAL POINTS
CALL VALVE FOR BOUNDARY CONDITIONS
2


2
UPDATE P AND V ARRAYS FOR THE NEXT TIME STEP
IS PRINTOUT REQUIRED ?
X
✓
WRITE OUT SERVO AND FLUID VALUES
UPDATE SERVO PARAMETERS FOR NEXT TIME STEP
IS TIME>TMAX ?
8
X
✓
STOP

```
      MASTER VSP2
      REAL KINVIS
      DIMENSION TANG( 31),A(2),D(2),V(2,21),P(2,21),VV(2,21),PP(2,21),
     1  C(2),DT(2),PL(2),N(2),VO(2),AP(2,21),GMRM(2),DTF(2),VU(2,21),
     2  PU(2,21),VD(2,21),PD(2,21),F1U(2,21),F1D(2,21),X(20),Y(20),Z(20)
      COMMON/BL1/C1,C2,C3,C4,C5,C6,CURRENT,FPG
      COMMON/BL2/RHO,N,DT,TIME,A,C,TAMB,SOLC,TCLOS,FRAC1,VOLT,DP0,
     1TAU1,ITCOUNT,VAP,MARKER,KTM,D,TRANS,KINVIS
      EQUIVALENCE(VO2,VO(2)),(DT2,DT(2)),(N1,N(1)),(N2,N(2))
      EXTERNAL DIFEQN
      READ(1,100) KINVIS,TRANS,RHO,PL(1),PL(2),C(1),D(1)
      READ(1,104) TAMB,OFFSET,RADIUS,STROKE,N(1),N(2)
      READ(1,101) TCLOS
      TCLOS=5.0
      READ(1,101) SOLC,TMAX,FRAC1
      READ(1,101) PR1,VO(1)
      PR1=170.0
      VO(1)=0.915
      READ(1,101) PMIN
      PMIN=34.5
      READ(1,101) THETA
      READ(1,105) (TANG(JB), JB=1,30)
      READ(1,102)G1,G2,G3,G4A,G4B,G5
      READ(1,101) WS,ZS,WA,ZA
      READ(1,101) FR1
      D(2)=D(1)
      C(2)=C(1)
      VO(2)=VO(1)
      SIGNAL=0.0
      VER=0.0
      CURRENT=0.0
      FLOW=0.0
      DISPL=0.0
      SWCH=1.0
      MM=1
      FBLAST=0.0
      DISLAST=0.0
      DISL2=0.0
      FBL2=0.0
      VOLT=0.0
      VOLTS=0.0
      PI=3.14159265
      PRS=PR1
      ITCOUNT=0
      MARKER=0
      FB=0.0
      V(2,1)=VO(1)
      AP(2,1)=0.0
      G2=-G2
      W1=1.0/(2.0*PI*FR1)
      WS=2.0*PI*WS
      WA=2.0*PI*WA
```

```
      TIME=0.0
      CALL LOOKUP(TAU1,TANG,THETA)
      PSI=(THETA-45.0)*PI/180.0
      DISA= TAN(PSI)*RADIUS
      DISPL=OFFSET-DISA
      THETA0=THETA
      J1=N(1)+1
      J2=N(2)+1
      J3=N(2)
      WRITE(2,203) G1,G2,G3,G4A,G4B,G5,WS,ZS,WA,ZA,PMIN,W1
      WRITE(2,202) TRANS,RHO,KINVIS,PL(1),PL(2),C(1),C(2),D(1),D(2),
     1V0(1),V0(2),PRS,TCLOS,TMAX,SOLC,TAMB,FRAC1,N1,N2
      ICH=1
      CALL CHANGE(KINVIS,RHO,PL,C,D,OFFSET,RADIUS,STROKE,SOLC,PR1,V0,
     1PMIN,G1,G3,G4A,G4B,G5,FLOW,DISPL,VOLTS,FB,SIGNAL,V,AP,ICH)
      WRITE(2,203) G1,G2,G3,G4A,G4B,G5,WS,ZS,WA,ZA,PMIN,W1
      WRITE(2,202) TRANS,RHO,KINVIS,PL(1),PL(2),C(1),C(2),D(1),D(2),
     1V0(1),V0(2),PRS,TCLOS,TMAX,SOLC,TAMB,FRAC1,N1,N2
      WRITE(2,200)
      G3=1.0
      G4=G4A
      V02=V0(2)
      PR1=PR1*144.0
      TG2=3.0*G2
      G5=G5/144.0
      DO 1 I=1,2
      D(I)=D(I)/12.0
      A(I)=3.1417*(D(I)**2)/4.0
      DT(I)=0.001
      GMRM(I)=DT(I)*N(I)/PL(I)
1     CONTINUE
      ICOUNT=5
      ICI=50
      DP1=5.11*V02*V02
      DP2=0.224*V02*V02
      PR1=PR1-DP1
      DP=DP2/144.0
      DP0=DP
      VAP=0.2*144.0
      DO 23 I=1,2
      REN=ABS(V0(I))*D(I)/KINVIS
      FF=0.079/(REN**0.25)
      FDR=2.0*RHO*FF*PL(I)*(V0(I)**2)/(D(I)*N(I))
      AA=0
      J=N(I)+1
      DO 23 K=1,J
      V(I,K)=V0(I)
      XR=PR1
      IF(I.EQ. 2)XR=P(1,N1+1)-(DP*144.0)
      AA=AA+1.0
      P(I,K)=XR-(AA-1.0)*FDR
      AP(I,K)=P(I,K)/144.0
```

```
 23 CONTINUE
    PRS=P(2,1)
    L1=N2/5
    MP=3
    MMM=5
    HHH=0.001
    QA=2.0*ZS/WS
    QB=1.0/(WS**2)
    QC=2.0*ZA/WA
    QD=1.0/(WA**2)
    C1=QB*QD
    C2=QB*QC+QA*QD
    C3=QB+QD+QA*QC
    C4=QA+QC
    C5=1.0
    C6=0.0
    PR2=P(2,N2+1)
    P3=PR2/144.0
    XXX=DT(2)
    DO 31 I=1,MMM.
    Y(I)=0.0
 31 CONTINUE
    Y(1)=DISPL
    FBIN=P(2,1)*G5
    FB=FBIN
    FBLAST=FB
    VD(1,N1+1)=0.0
    PD(1,N1+1)=0.0
    VU(1,1)=0.0
    PU(1,1)=0.0
    VU(2,1)=0.0
    PU(2,1)=0.0
    VD(2,N2+1)=0.0
    PD(2,N2+1)=0.0
  8 TIME=TIME+DT(2)
    SIGNAL=P(2,1)*G1/144.0
    FBIN=P(2,1)*G5
    TIMEDAS=TIME
    X1=0.0
    Y1=PMIN
    X2=0.005
    Y2=PMIN
    X3=0.010
    Y3=PMIN
    X4=0.08
    Y4=PMIN
    X5=0.085
    Y5=-100.0
    X6=10.0
    Y6=-100.0
    CALL GEN(X1,Y1,X2,Y2,X3,Y3,X4,Y4,X5,Y5,X6,Y6,TIME,POUT)
    IF((TIME.GT.X4).AND.(AP(2,1).GE.P3)) POUT=-1.0,0.0
```

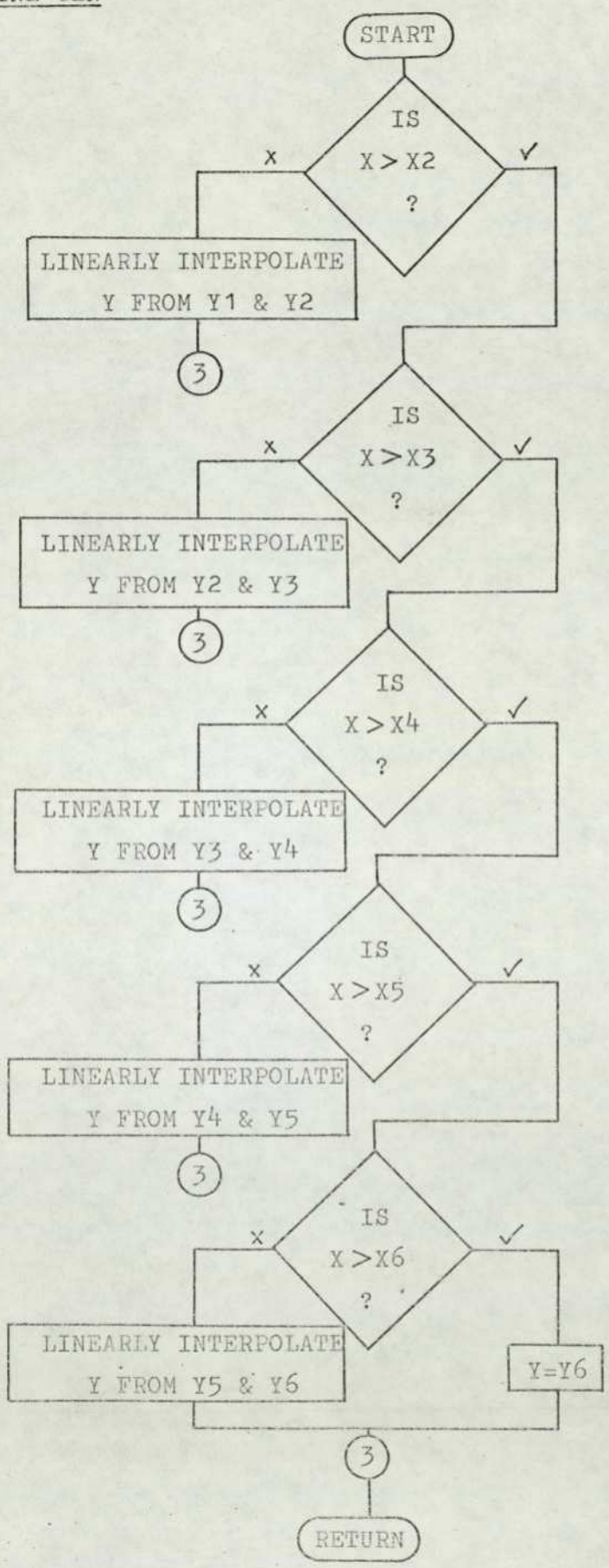
```
      SIGNAL=POUT*G1
      C7=DT(2)/W1
      FB=(FBLAST+ C7*FBIN)/(1,0+C7)
      IF(FR1 ,GT, 990,0) FB=FBIN
      VER=SIGNAL-FB
      CURRENT=G2*VER
      BIMIT=10,0
      IF( CURRENT ,GT, BIMIT) CURRENT=BIMIT
      IF(CURRENT ,LT, -BIMIT) CURRENT=-BIMIT
      FPG=G3*G4
      CALL INTSTP(MMM,HHH,XXX,Y,DIFEQN)
      DISPL=Y(1)
      IF(DISPL,LE,0,0) GOTO 2
      IF(DISPL,GE,STROKE) GOTO 3
      GOTO 5
    2 IF(Y(2),GT,0.0) GOTO 5
      DISPL=0,0
      GOTO 6
    3 IF(Y(2),LT,0.0) GOTO 5
      DISPL=STROKE
    6 DO 10 I=2,MMM
   10 Y(I)=0.0
    5 Y(1)=DISPL
      DXDT=DISPL-DISLAST
      G4=G4A
      IF(DXDT,LT,0.0) G4=G4B
      FLOW=(Y(2)+QC*Y(3)+QD*Y(4))/G4
      ARG2=(OFFSET-DISPL)/RADIUS
      PHID=ATAN(ARG2)
      THETA=180,0*PHID/PI +44,9999
      CALL LOOKUP(TAU1,TANG,THETA)
      IF((TIME,GT,X4),AND,(TAU1,LT,0,0001)) TCLOS=TIME
      L4=1
      IF(TIME ,GT, (TCLOS=0,000001)) L4=2
      DO 61 J=L4,2
      KT=N(J)+1
      DO 60 I=2,KT
      VU(J,I)=V(J,I)+GMRM(J)*C(J)*(V(J,I-1)-V(J,I))
      PU(J,I)=P(J,I)+GMRM(J)*C(J)*(P(J,I-1)-P(J,I))
   60 CONTINUE
      KS=N(J)
      DO 61 I=1,KS
      VD(J,I)=V(J,I)+GMRM(J)*C(J)*(V(J,I+1)-V(J,I))
      PD(J,I)=P(J,I)+GMRM(J)*C(J)*(P(J,I+1)-P(J,I))
   61 CONTINUE
      CALL CHAR(VU,PU,F1U,PD,VD,F1D,VV,PP,PR1,PR2)
      IF(TIME ,GT, (TCLOS=0,00001)) GOTO 13
      GOTO 4
   13 TAU1=0,0
      V(1,N1+1)=0,0
      VV(1,N1+1)=0,0
    4 CALL VALVE(VU,V,P,VV,PP,VD,PU,VD,PD,F1U,F1D)
```

```
      DO 7 I=L4,2
      J=N(I)+1
      DO 7 K=1,J
      V(I,K)=VV(I,K)
      P(I,K)=PP(I,K)
      AP(I,K)=PP(I,K)/144.0
    7 CONTINUE
      VOLTS=VOLT*1000.0
      ICOUNT=ICOUNT-1
      IF(ICOUNT .NE. 0) GOTO 9
      ICOUNT=5
      ICH=2
      CALL CHANGE(KINVIS,RHO,PL,C,D,OFFSET,RADIUS,STROKE,SOLC,PR1,V0,
     1PMIN,G1,G3,G4A,G4B,G5,FLOW,DISPL,VOLTS,FB,SIGNAL,V,AP,ICH)
      IF(TIME .GT. (TCLOS-0.000001)) GOTO 16
      GOTO 17
   16 WRITE(2,205) TIME,ITCOUNT,MARKER,VOLTS,(V(2,I),I=1,J2,L1),(AP(2,I)
     1    ,I=1,J2,L1)
      GOTO15
   17 WRITE(2,201) TIME,SIGNAL,FB,VER,CURRENT,FLOW,DISPL,THETA,TAU1,
     1  VOLTS,V(2,1),V(1,J1),AP(2,1),ITCOUNT,MARKER
   15 ICH=3
      CALL CHANGE(KINVIS,RHO,PL,C,D,OFFSET,RADIUS,STROKE,SOLC,PR1,V0,
     1PMIN,G1,G3,G4A,G4B,G5,FLOW,DISPL,VOLTS,FB,SIGNAL,V,AP,ICH)
    9 DISL2=DISLAST
      FBL2=FBLAST
      DISLAST=DISPL
      FBLAST=FB
      VOLTM1=VOLT
      IF(TMAX-TIME) 99,99,8
  100 FORMAT(F10.7,6F10.5)
  101 FORMAT(6F10.2)
  102 FORMAT(3F10.5,2F10.4,F10.5)
  104 FORMAT(4F10.5,2I5)
  105 FORMAT(10F6.2)
  200 FORMAT(1H1///,6X,4HTIME,3X,6HSIGNAL,3X,3HF/B,4X,5HERROR,4X,
     1    7HCURRENT,3X,4HFLOW,4X,6HTRAVEL,4X,5HTHETA,5X,3HTAU,5X,
     2  6HVOLUME,3X,8HVELOCITY,3X,8HPRESSURE,3X,10HITERATIONS,1X,6HMARKE
     3R)
  201 FORMAT(2X,13F8.3,2I2)
  202 FORMAT(/,9F13.7,/,/,6F13.7,2I4)
  203 FORMAT(//,10X,6F10.4,/,10X,6F10.4)
  205 FORMAT(/,1X,F5.3,2I2,F6.2,    2HV=,6(1X,F7.3),2X,2HP=,6(1X,F7.3))
   99 STOP
```

```
      SUBROUTINE VALVE(V0,V,P,VV,PP,VU,PU,VD,PD,F1U,F1D)
      REAL KINVIS,KONST3
      DIMENSION A(2),C(2),DT(2),N(2),V0(2),V(2,21),P(2,21),VV(2,21),
     1  PP(2,21),VU(2,21),PU(2,21),VD(2,21),PD(2,21),F1U(2,21),F1D(2,21)
     2 ,TANG(31),D(2)
      COMMON/BL2/RHO,N,DT,TIME,A,C,TANB,SOLC,TCLOS,FRAC1,VOLT,DP0,
     1TAU1,ITCOUNT,VAP,MARKER,RTM,D,TRANS,KINVIS
      EQUIVALENCE (N1,N(1)),(N2,N(2))
      ITCOUNT=0
      RR=DT(2)*0.000001
      IF(TIME .GT. RR) GOTO 18
      VOLTM1=0.0
      FRAC1=0.2
      KONST3=1.0-EXP(-0.693*DT(2)/FRAC1)
      POWER=1.4
      MARKER=1
      PLL=P(2,1)
      VOLCONT=0.0
      PL=0.00005
      TA=TAMB*460.0
      PSAT=P(2,1)
18    CONTINUE
      IF(TAU1.LT.0.001) TAU1=0.0
      VOLCON=VOLCONT+A(2)*DT(2)*V(1,N1+1)
      X1=VU(1,N1+1)-F1U(1,N1+1)*VU(1,N1+1)*ABS(VU(1,N1+1))+PU(1,N1+1)/
     1   (RHO*C(1))
      X2=1.0/(RHO*C(1))
      X3=VD(2,1)-F1D(2,1)*VD(2,1)*ABS(VD(2,1))-PD(2,1)/(RHO*C(2))
      X4=1.0/(RHO*C(2))
      X6=((TAU1*V0(2))**2)/(DP0*144.0)
      X7=X6*X1/X2
      X8=X6/X2
      X9=0.5*X8
      ALPHA=VOLCON*SOLC*TA/23.21
      BETA=KONST3
      GAMMA=ALPHA*BETA
      A1=0.5*A(2)*DT(2)
      A2=A1*X4
      A3=A1*(X3+V(2,1)-V(1,N1+1)+X9)+GAMMA*BETA*VOLTM1
      A4=-GAMMA*PSAT
      A5=X9*X9+X7
      PG=P(2,1)-(PLL-P(2,1))
      IF(A5-X6*PG,GE,0.0) GOTO 5
      TAU1=0.0
      GOTO 18
 5    PLIN=PG
      IF((TAU1.GT.0.00001).AND.(M2.EQ.0)) MARKER=1
      IF((TAU1.GT.0.00001).AND.(M2.EQ.1)) MARKER=2
      IF((TAU1.LT.0.00001).AND.(M2.EQ.0)) MARKER=3
      IF((TAU1.LT.0.00001).AND.(M2.EQ.1)) MARKER=4
      IF((TIME.LT.50.0*DT(2)).AND.(PLL/P(2,1).GT.0.995)) MARKER=1
      GOTO (3,6,4,6), MARKER
```

```
3   IF(TIME .LT. (3.0*DT(2))) PG=0.999995*P(2,1)
1   ITCOUNT=ITCOUNT+1
    A6=A5-X6*PG
    FX=A2*PG*PG +A3*PG +A4 -A1*PG*SQRT(A6)
    FXD=2.0*A2*PG +A3 -A1*((A6-0.5*X6*PG)/SQRT(A6))
    PN=PG-FX/FXD
    PERROR=ABS((PN-PG)/PG)
    PG=PN
    IF(PERROR-PL) 2,2,1
4   ITCOUNT=88
    A7=A1*X4
    A8=A1*(X3+V(2,1))+GAMMA+BETA*VOLTM1
    PG=(-A8+SQRT(A8*A8-4.0*A7*A4))/(2.0*A7)
    GOTO 2
6   VG=-X9+SQRT(X9*X9+X7-X6*PG)
    PN=RTM/((VOLTM1+A1*(X3+X4*PG+V(2,1)-V(1,N1+1)-VG))**POWER)
    PERROR=ABS((PN-PG)/PG)
    PG=PN
    IF(PERROR .LT. PL) GOTO 2
    ITCOUNT=ITCOUNT+1
    GOTO 6
2   PP(2,1)=PG
    VV(2,1)=X3+X4*PP(2,1)
    VV(1,N1+1)=-X9+SQRT(A5-X6*PP(2,1))
    PP(1,N1+1)=(X1-VV(1,N1+1))/X2
    VOLT=VOLTM1+A1*(VV(2,1)+V(2,1)-VV(1,N1+1)-V(1,N1+1))
    IF(VOLT.LT.0.0) VOLT=0.0
    VOLTIN=ALPHA*(PSAT/PP(2,1)-1.0)
    M2=0
    IF(VOLTIN .LT. VOLTM1) M2=1
    VOLCONT=VOLCON
    PLL=P(2,1)
    VOL=VOLT
    IF(VOL .LT. 1E-8) VOL=1E-8
    RTM=PP(2,1)*(VOL**POWER)
    VOLTM1=VOLT
    RETURN
```

SUBROUTINE GEN



```
      SUBROUTINE GEN(X1,Y1,X2,Y2,X3,Y3,X4,Y4,X5,Y5,X6,Y6,X,Y)
      IF(X.GT.X2) GOTO 1
      Y=Y1+(X-X1)*(Y2-Y1)/(X2-X1)
      GOTO 3
    1 IF(X.GT.X3) GOTO 2
      Y=Y2+(X-X2)*(Y3-Y2)/(X3-X2)
      GOTO 3
    2 IF(X.GT.X4) GOTO 4
      Y=Y3+(X-X3)*(Y4-Y3)/(X4-X3)
      GOTO 3
    4 IF(X.GT.X5) GOTO 5
      Y=Y4+(X-X4)*(Y5-Y4)/(X5-X4)
      GOTO 3
    5 IF(X.GT.X6) GOTO 6
      Y=Y5+(X-X5)*(Y6-Y5)/(X6-X5)
      GOTO 3
    6 Y=Y6
    3 RETURN
```

```
      SUBROUTINE INTSTP (NN,HH,XX,Y,        EXTERN)
      DIMENSION Y(20),G(20),D(20),Z(20)
      N=NN
      H=HH
      H1=0.5*H
      H2=H/6.
      X=XX
      XHH=X+H1
      XH=X+H
      CALL EXTERN(X,Y,G)
      DO 2 J = 1,N
    2 Z(J)=Y(J)+H1*G(J)
      CALL EXTERN(XHH,Z,D)
      DO 3 J = 1,N
      G(J)=G(J)+2.0*D(J)
    3 Z(J)=Y(J)+H1*D(J)
      CALL EXTERN(XHH,Z,D)
      DO 5 J = 1,N
      G(J)=G(J)+2.0*D(J)
    5 Z(J)=Y(J)+H*D(J)
      CALL EXTERN(XH,Z,D)
      DO 6 J = 1,N
    6 Y(J)=Y(J)+H2*(G(J)+D(J))
      XX=XH
      RETURN
```

```
      SUBROUTINE DIFEQN(X,Y,F)
      DIMENSION Y(20),F(20)
      COMMON/BL1/C1,C2,C3,C4,C5,C6,CURRENT,FPG
      F(1)=Y(2)
      F(2)=Y(3)
      F(3)=Y(4)
      F(4)=Y(5)
      F(5)=(FPG*CURRENT-C2*Y(5)-C3*Y(4)-C4*Y(3)-C5*Y(2)-C6*Y(1))/C1
      RETURN
```

```
      SUBROUTINE LOOKUP(TAU1,TANG,THETA)
      DIMENSION TANG(51)
      J=1
      IF(THETA .GT. 0.000001) GOTO 44
      THETA=0.0
      TAU1=0.0
      GOTO 46
   44 IF(THETA-TANG(J)) 41,42,43
   43 J=J+1
      GOTO44
   42 R=J
      K=51
      GOTO45
   41 K=J-1
      R=K+(THETA-TANG(K))/(TANG(J)-TANG(K))
   45 TAU1=(R-10.0)/20.0
      IF(K .LT. 11). TAU1=(R-1.0)/220.0
   46 RETURN
```

```
      SUBROUTINE CHAR(VU,PU,F1U,PD,VD,F1D,VV,PP,PR1,PR2)
      REAL KINVIS
      DIMENSION N(2),C(2),VU(2,21),PU(2,21),F1U(2,21),PD(2,21),VD(2,21),
     1  F1D(2,21),VV(2,21),PP(2,21),D(2),DT(2),A(2)
      COMMON/BL2/RHO,N,DT,TIME,A,C,TAMB,SOLC,TCLOS,FRAC1,VOLT,DP0,
     1TAU1,ITCOUNT,VAP,MARKER,RTM,D,TRANS,KINVIS
      Y1=D(2)/KINVIS
      Y2=1.0/(RHO*C(2))
      Y3=2.0*DT(2)/D(2)
      L4=1
      IF(TIME .GT. (TCLOS-0.00001)) L4=2
      DO 6 I=L4,2
      DO 6 J=1,2
      DO 6 K=1,N(I)+1
      X=VD(I,K)
      IF(J .EQ. 1) X=VU(I,K)
      IF(X) 7,8,7
    8 Z=0.0
      GOTO 9
    7 RE=ABS(X)*Y1
      IF(RE-TRANS) 10,11,11
   10 Z=16.0/RE
      GOTO 9
   11 Z=0.079/(RE**0.25)
    9 IF(J-1) 12,12,13
   12 F1U(I,K)=Z*Y3
      GOTO 6
   13 F1D(I,K)=Z*Y3
    6 CONTINUE
      DO 3 I=L4,2
      JA=N(I)
      DO 5 L=2,JA
      VV(I,L)=0.5*(VU(I,L)+VD(I,L)+Y2*(PU(I,L)-PD(I,L)) -(F1U(I,L)*VU(I,
     1L)*ABS(VU(I,L))+F1D(I,L)*VD(I,L)*ABS(VD(I,L))))
      PP(I,L)=0.5*((PU(I,L)+PD(I,L)+(VU(I,L)-VD(I,L))/Y2) -(F1U(I,L)
     1  *VU(I,L)*ABS(VU(I,L))-F1D(I,L)*VD(I,L)*ABS(VD(I,L)))/Y2)
      IF(PP(I,L) .LT. VAP) PP(I,L)=VAP
    5 CONTINUE
      IF(I-1) 1,1,2
    1 PP(1,1)=PR1
      VV(1,1)=VD(1,1)+Y2*(PR1-PD(1,1))-F1D(1,1)*VD(1,1)*ABS(VD(1,1))
      GOTO 3
    2 PP(2,N(2)+1)=PR2
      VV(2,N(2)+1)=VU(2,N(2)+1)-Y2*(PR2-PU(2,N(2)+1))-F1U(2,N(2)+1)
     1  *VU(2,N(2)+1)*ABS(VU(2,N(2)+1))
    3 CONTINUE
      RETURN
```

```
      SUBROUTINE CHANGE(KINVIS,RHO,PL,C,D,OFFSET,RADIUS,STROKE,SOLC,PR1,
     1V0,PMIN,G1,G3,G4A,G4B,G5,FLOW,DISPL,VOLTS,FB,SIGNAL,V,AP,ICH)
      REAL KINVIS
      DIMENSION PL(2),C(2),D(2),V0(2),V(2,21),AP(2,21)
      GOTO (1,2,3), ICH
    1 KINVIS=KINVIS*0.0929
      RHO=RHO*0.062428/32.2
      OFFSET=OFFSET*39.3701
      RADIUS=RADIUS*39.3701
      STROKE=STROKE*39.3701
      SOLC=SOLC/(144.0*0.0193)
      PR1=PR1*0.145
      PMIN=PMIN*0.145
      G1=G1/0.145
      G3=G3*5.886*0.1728
      G4A=G4A/1550.0
      G4B=G4B/1550.0
      G5=G5/0.145
      DO 5 I=1,2
      PL(I)=PL(I)*3.28084
      C(I)=C(I)*3.28084
      D(I)=D(I)*39.3701
    5 V0(I)=V0(I)*3.28084
      GOTO 4
    2 FLOW=FLOW*1699.0/1728.0
      SIGNAL=SIGNAL*6.895
      FB=FB*6.895
      VOLTS=VOLTS*0.02832
      DISPL=DISPL*0.0254
      DO 6 I=1,2
      DO 6 J=1,21
      V(I,J)=V(I,J)*0.3048
    6 AP(I,J)=AP(I,J)*6.895
      GOTO 4
    3 FLOW=FLOW*1728.0/1699.0
      SIGNAL=SIGNAL/6.895
      FB=FB/6.895
      VOLTS=VOLTS/0.02832
      DISPL=DISPL/0.0254
      DO 7 I=1,2
      DO 7 J=1,21
      V(I,J)=V(I,J)/0.3048
    7 AP(I,J)=AP(I,J)/6.895
    4 RETURN

      DATA
0.000194 2300.0      814.954      5.486     65.532  1219.2        0.0508
 60.0        0.0508     0.0508     0.1016      4   20
 10.0
  0.0160     9.0        0.2
169.5        2.14
 48.0
 90.0
00.00  7.50 15.00 22.50 27.00 30.50 33.50 35.50 37.50 40.00
41.50 55.00 64.00 71.20 75.00 77.20 78.25 79.00 79.40 79.70
80.00 80.50 81.00 81.30 81.60 82.00 82.70 84.00 86.00 90.00
  0.145      0.2        1.311   12710.0    19040.0       0.145
100.0        0.7      100.0        0.7
999.0
```

Appendix 8 Derivation of the Bode diagram for a dynamic system

It is possible (ref 102) to show that the amplitude and phase of the steady state response of a linear system to a sinusoidal input can be obtained from the Laplace transform of the system by replacing 's' by 'jw' in the differential equation, providing that the initial conditions are zero.

Thus considering as an example the first order system shown in fig A8.1, the equation of motion may be represented by the differential equation:

$$y = ax + \frac{dx}{dt}$$

Providing the initial conditions are zero, the Laplace transform of the equation is

$$Y = (s+a)X \qquad \text{——————} \quad 1$$

For the frequency responce, the input is considered to be sinusoidal i.e.

$$y = E \sin \omega t \qquad \text{——————} \quad 2$$

If equation 1 is re-written and 's' is replaced by 'jw' we obtain:

$$\frac{X}{Y} = \frac{1/a}{1 + j\omega/a} \qquad \text{——————} \quad 3$$

which is of course a vector quantity which may be evaluated in terms of a magnitude and a phase angle. The magnitude of X/Y, and hence of x/y is

$$x/y = \frac{1/a}{\sqrt{1+\omega^2/a^2}} \qquad \text{——————} \quad 4$$

and the phase angle is

$$\psi = \angle x/y = -\tan^{-1} \omega/a \qquad \text{——————} \quad 5$$

If the Laplace transform of equation 2 is substituted into equation 3 and the inverse transform taken, the result is

$$x = \frac{E}{a\sqrt{1+\omega^2/a^2}} \quad \sin(\omega t - \psi)$$

Equations 4 and 5 are used to determine the Bode diagram for the system by plotting the magnitude and phase angle for increasing forcing frequency, w. Note that when w = 0 then x = y/a and as $w \to \infty$ $x \to 0$, illustrating the failure to respond at high frequencies. Also when w = a, $|x/y| = 1/a\sqrt{2}$ and $\psi = -90^{\circ}$. This point is known as the break frequency and sometimes called the bandwidth.

It is usual to plot 20 log|x/y| along the vertical axis as this then has the units of decibels and makes the analysis of complex systems more convenient. When a system is investigated for its response at high frequencies, it is usual to define the bandwidth as the frequency range over which the amplitude ratio does not drop by more than 3db below the zero frequency or D.C. magnitude. The figure of 3db is conventional yet quite arbitary and coresponds to a modulus ratio of 0.707 (see fig. A8.2)

FIG A8.1 1st ORDER SYSTEM

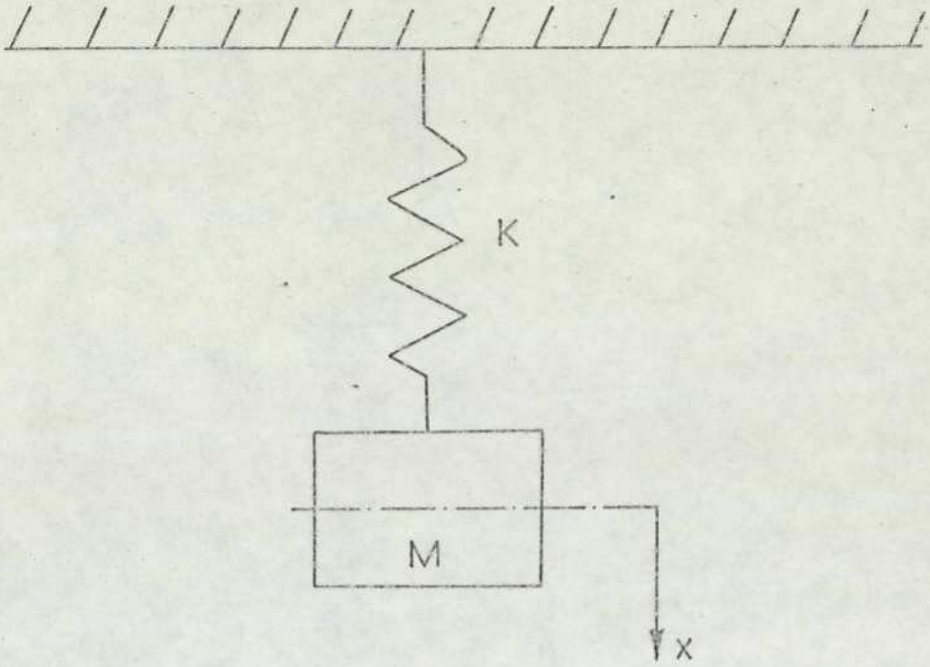
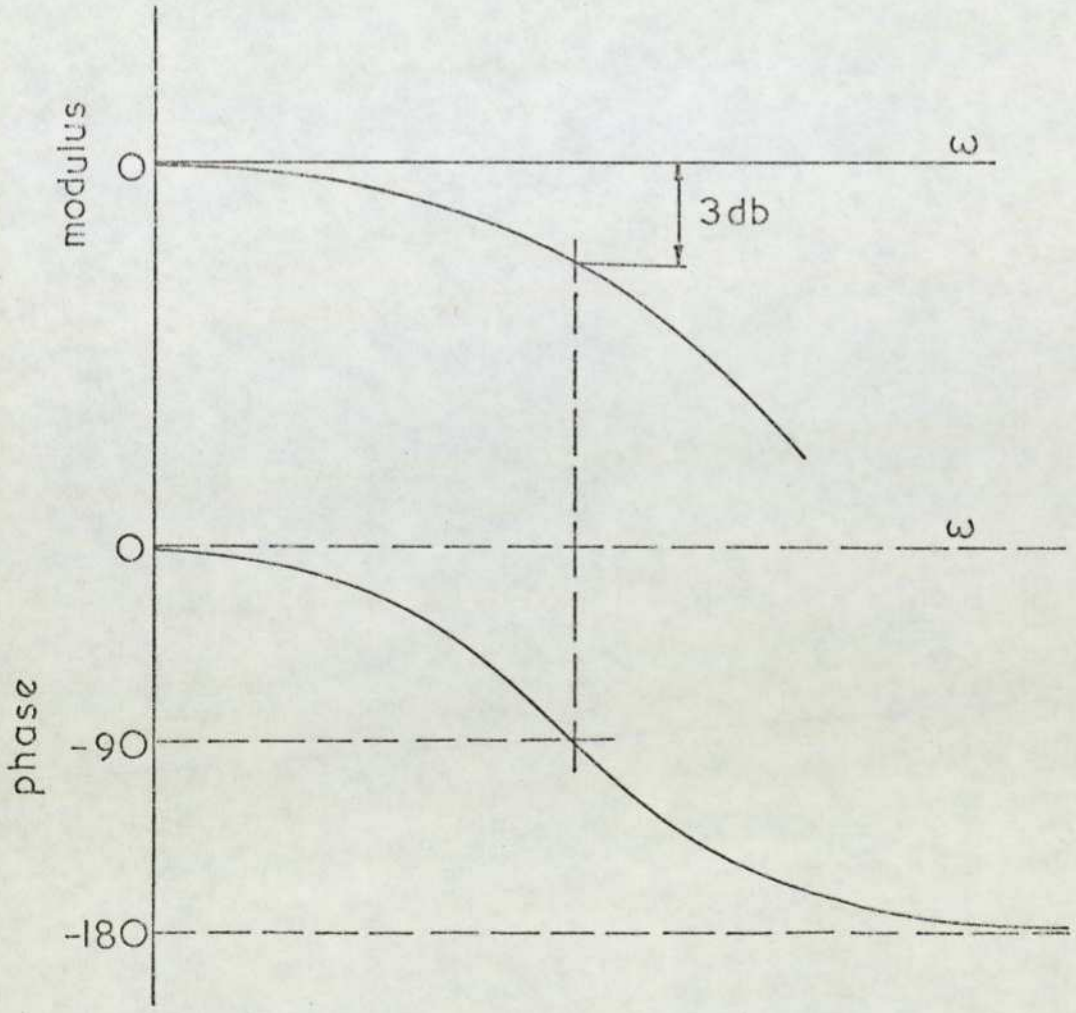


FIG A8.2 BODE DIAGRAM FOR 1st ORDER SYSTEM



APPENDIX 9

The Design, Construction and Testing of a Servo Amplifier and Signal Generator

M.R. Driels

SUMMARY

The purpose of this report is to discuss the development of a servo-amplifier and signal generator as used on a closed loop pressure control system. It deals with both practical and theoretical aspects of gain setting and it is hoped that sufficient generality is preserved to make the final design useful in a wide variety of control applications.

CONTENTS

		Page
1.	Introduction	1
2.	Definition of Gain	2
3.	Servo-Amplifier Design	6
4.	Servo-Amplifier Testing - Static and Dynamic	12
5.	Gain Settings	15
6.	Signal Generator Design	18
7.	Conclusions	23
	Acknowledgements	24
	Appendix 1 - Practical Layout	25
	Appendix 2 - Conversion to Metric System	27
	Appendix 3 - Operating/Start Up Procedures	28
	Tables	33
	Figures	35

LIST OF FIGURES

1. Theoretical and Experimental System Paths

2. Steady State Servo-Valve Characteristics

3. Single Input Servo-Amplifier Circuit Diagram

4. Summing Junction and Multi-Input Circuit Diagram

5. Frequency Sensitive Components

6. Effect of Capacitive Compensation on Amplifier Band Width

7. Open Loop Frequency Response of Servo-Amplifier

8. Servo-Amplifier Static Experimental Results

9. Definition of Voltage-Time Functions Required

10. Summing Junction using High-Gain Amplifier

11. Signal Generator Circuit Diagram

12. Diagram of Signal Multiplier

13. Schematic Diagram of Overall System

14. Plan View of Unit Showing Principle Components

15. General View of Unit

LIST OF TABLES

1. Static Analysis of Servo-Amplifier

2. Dynamic Analysis of Servo-Amplifier

NOTATION

C	Capacitance (farads)
f(s)	Dynamic components of servo valve response
G_1	Model servo-amplifier gain (ma/volt)
G_2	Actual servo-amplifier gain (ma/volt)
G_v	Voltage gain (non dimensional)
i	Current (amps)
K	Actual servo valve steady state gain ($in^3/s/ma$)
L	Inductance (Henrys)
P	Pressure (lbf/in^2)
Q	Flow of oil from servo valve
R	Resistance (ohms)
S_1	Model signal generator scaling factor ($volts/lbf/in^2$)
S_2	Actual " " " "
T_1	Model Transducer amplifier gain ($volts/lbf/in^2$)
T_2	Actual " " " " "
V,E	Voltage
W	Frequency (sec^{-1})
X	Impedance of frequency sensitive components (ohms)

1. INTRODUCTION

In applications utilizing closed loop control of systems, one of the most important group of components are those comprising the error detector, signal generator (or driving function) and servo amplifier. Since for most systems these items will usually have fewer design constraints imposed upon them than other items, such as prime movers, it is difficult for manufacturers to cater for all of the requirements of a customer. Thus the construction of such items is usually left to the user.

The purpose of this report is to describe the design, construction and testing of various items used in a particular control system, although it is hoped that generality is preserved and the components may be used for many other applications. The work is divided into two main groups: the first dealing with the summing junction/servo amplifier unit and the second with a signal generator which provides a series of step functions of variable amplitude and duration. Before practical circuit design is considered however, a re-assessment of the definition of 'gain' is given since an amplifier gain derived theoretically is not always the 'best' value.

Since the electrohydraulic servo value is specified completely by the manufacturers in terms of the British system of units, it was found convenient to adopt this system for the remainder of the analysis. Following the report are appendices which contain a description of the actual unit constructed to assist users with its operation. Also a conversion table is given which allows the various gains derived to be expressed in both British and Metric systems of units.

2. GAIN - EXPERIMENTAL AND THEORETICAL CONSIDERATIONS

The system for which this unit was designed is an electro-hydraulic pressure control system. It is required to control the pressure at a certain point in a fluid which is flowing through a valve. The pressure time history is derived electronically in the signal generator (see Fig. 1). The actual pressure is measured with a quartz crystal pressure transducer which, in conjunction with its charge amplifier, provides a voltage signal proportional to the recorded pressure. An error or summing unit subtracts these signals and the resultant voltage is the input to the servo amplifier thus producing a closed loop system. This unit should provide a current proportional to, and in phase with, the input voltage. This is because the power unit, an electro-hydraulic servo valve, is current driven. The output of this unit is considered to be a flow of hydraulic oil proportional to the input current.

Obviously there are more components in the system but as far as the work recorded here is concerned, these are all that it is necessary to consider. A computer model was available of the overall system and all of the theoretical values of gain were pre-determined. It was recognised that various practical restraints would probably require that certain gains, such as T_2 and S_2 would be changed from one particular fluid flow case to another and so to preserve uniformity in the theoretical results, it was assumed that no restraints existed. For example, the maximum output of the charge amplifier is $\pm$ 10 v and so T_2 would vary depending upon the actual fluctuation in pressure. If, say, 100 lbf/in^2 was achieved then $T_2 < 0.1$ volts/lbf/in^2 while if 50 lbf/in^2 was achieved then $T_2 < 0.2$ volts/lbf/in^2. In the theoretical model, this type of restraint would only

complicate the task of comparing the overall loop gain for different flow conditions and hence T_1 and S_1 were considered to be 1 volt/lbf/in^2. Similarly the steady state gain of the servo valve was considered to be unity because at the time of writing the model, no servo valve had been selected. This means that the overall loop gain was controlled in the model by the value of the servo amplifier gain G_1, which enables a ready loop gain comparison to be made.

However, it is obvious from the practical constraints mentioned in the previous paragraph that some form of comparison is needed when the gain of the actual servo amplifier is determined, knowing the required theoretical gain. Further complications arise when a practical servo amplifier is considered. Such an amplifier will have a certain current or voltage saturation limit and this may well affect the overall system performance. This will be demonstrated in the following analysis.

To compare the path gains we assume that the system is linear and that the overall transfer function from pressure to flow of oil is the same i.e.

$$T_1 G_1 = T_2 G_2 K \qquad \text{defined in Figure 1.}$$

and $$S_1 G_1 = S_2 G_2 K$$

$$\therefore \quad \frac{G_2}{G_1} = \frac{T_1}{T_2 K} = \frac{S_1}{S_2 K}$$

and since $S_1 = T_1 = 1$ volt/lbf/in^2

$$\frac{G_2}{G_1} = \frac{1}{T_2 K} = \frac{1}{S_2 K} \qquad \ldots\ (1)$$

So we could begin by making the same assumptions for the rig as for the model i.e.

$$T_2 = S_2 = 1 \text{ volt/lbf/in}^2$$

Now in practice the steady state servo valve is shown in Fig. 2 giving

$$\hat{Q} = 10.0 \text{ in}^3/\text{s} \quad \text{and} \quad \hat{i} = 7.5 \text{ ma}$$

$$\therefore \quad K = \frac{10}{7.5} = \frac{4}{3} \text{ in}^3/\text{s per ma.}$$

and it is found that for most cases considered

$$G_1 = -0.2 \text{ ma/volt}$$

thus substituting into (1) above, the actual amplifier gain G_2 is:

$$G_2 = \frac{G_1}{S_2 K} = \frac{0.2 \; 1 \; 3}{4} = 0.15 \text{ ma/volt}$$

It is a worthwhile exercise to check that both model and rig are the same at this point. Suppose that there exists a pressure demand from the signal generator of 10 lbf/in^2 and a feedback or measured pressure of 6 lbf/in^2 then we have

$$Q_{\text{model}} = (10 \; S_1 - 6 \; T_1) \; G_1 = 0.2 \; (10-6) = 0.8 \text{ in}^3/\text{s}$$

$$Q_{\text{rig}} = (10 \; S_2 - 6 \; T_2) \; G_2 K = \frac{0.15.4}{3} \; (10 - 6) = 0.8 \text{ in}^3/\text{s}$$

so the two systems are identical. However, since the linear input of G_2 is limited to $\pm$ 10 v then the output of G_2 will be 1.5 ma (from Fig. 2). Thus the servo valve will provide, at maximum, only 20% of its full flow capability. Since this flow of oil goes to a ram, or actuator, then the transfer function may be written for this component as

$$\frac{dx}{dt} = \frac{1Q}{A}$$

where x = displacement of ram

A = cross-sectional area of ram.

It will be appreciated that the frequency response of the ram, or the speed with which the ram may be moved from one extreme position to the other extreme position and back again, is proportional to dx/dt and hence Q. Also it is generally true that in such systems the ram limits the overall system response because it is the slowest moving component. Thus it is most important that if the overall system performance is not to be degraded, then the maximum value of Q when the amplifier is saturated should be as large as possible i.e. the largest that the servo valve can provide. In this case the value is

$$\hat{Q} = 10.0 \text{ in}^3/\text{s}$$

Thus the best design criteria is that when the servo amplifier is saturated, the servo valve delivers its maximum flow of oil.

Up to this point, the servo amplifier has only been considered in terms of a current to voltage gain. However, it will also have a voltage to voltage gain which will be determined by the input and output impedances. Thus if the voltage gain is G_v then

$$V_{out} = G_v \times V_{in}$$

and since saturation occurs when $V_{out} = \pm 10v$

then $$\hat{V}_{in} = \frac{10}{G_v} \text{ for linear operation.}$$

The above argument is just to introduce the idea of amplifier saturation and voltage gain. The significance of the ideas is best demonstrated practically when the amplifier performance is discussed in detail.

3. SERVO AMPLIFIER DESIGN

The circuit diagram for the amplifier may be found in several books and a representative form is shown in Fig. 3. Since the operational amplifier has a gain of the order 10^7 and the maximum output is 10 v then the input may be considered as a 'virtual earth'. Thus the amplifier equation becomes

$$i_s + i_f = 0$$

or

$$\frac{V_s}{R_s} = \frac{-V_f}{R_{18}}$$

If we consider initially the d.c. analysis of the amplifier then

$$i_c = 0$$

and

$$i_f = i_L - i_e$$

Similarly for d.c. signals the impedance of the servo valve coils is simply the resistance of the coils

$$\therefore \quad V_L = i_L R_L$$

and

$$V_f = V_o - V_L$$

$$= V_o - i_L R_L$$

also

$$V_f = i_e R_{19} = i_f R_{18}$$

$$= R_{18} (i_L - i_e)$$

$$V_f = R_{18} \left(\frac{V_o - V_f}{R_L} - \frac{V_f}{R_{19}} \right)$$

$$\therefore \quad V_f = \frac{V_o R_{18}}{R_L} - V_f \frac{R_{18}}{R_L} - V_f \frac{R_{18}}{R_{19}}$$

$$V_f \left(1 + \frac{R_{18}}{R_L} + \frac{R_{18}}{R_{19}}\right) = V_o \frac{R_{18}}{R_L}$$

$$\text{and} \quad V_f = V_o \frac{R_{18}}{R_L \left(1 + \frac{R_{18}}{R_L} + \frac{R_{18}}{R_{19}}\right)}$$

also since $$\frac{V_s}{R_s} = \frac{-V_f}{R_{18}}$$

$$\frac{V_s}{R_s} = \frac{-V_o}{R_L + R_{18} + \frac{R_{18} R_L}{R_{19}}}$$

$$\therefore \quad V_o = -V_s \frac{R_L + R_{18} + R_{18} R_L / R_{19}}{R_s} \qquad \ldots (2)$$

and since $$i_L = \frac{V_o - V_f}{R_L} = \frac{V_o}{R_L} \left(1 - \frac{V_f}{V_o}\right)$$

$$= \frac{V_o}{R_L} \left(1 - \frac{1}{\frac{R_L}{R_{18}} + \frac{R_L}{R_{19}} + 1}\right)$$

$$i_L = \frac{-V_s}{R_s R_L}\left[R_L + R_{18} + \frac{R_{18}R_L}{R_{19}} - R_{18}\right]$$

$$\therefore \quad i_L = -V_s\left(\frac{1}{R_s} + \frac{R_{18}}{R_s R_{19}}\right) \qquad \ldots (3)$$

This is of the form

$$i_L = -G_2 V_s \qquad \text{(current gain)} \qquad \ldots (4)$$

where $$G_2 = \frac{1}{R_s} + \frac{R_{18}}{R_s R_{19}}$$

and the gain may be varied by the potentiometer R_{19}; equation (2) may also be re-written as

$$V_o = -V_s G_v \qquad \text{(voltage gain)} \qquad \ldots (5)$$

where $$G_v = \frac{R_L + R_{18} + R_{18}R_L/R_{19}}{R_s}$$

when the amplifier is saturated $V_o = 10v$

$$\therefore \quad V_s = \frac{-10}{G_v}$$

and substituting in (4) gives

$$i_L = \frac{10G_2}{G_v} \qquad \ldots (6)$$

Since both G_2 and G_v are dependent only on R_{19} if the other resistances are fixed, then equation (6) predicts that i_L will have a maximum value and from the arguments of section 2, this value should equal 7.5 ma. This is because when the amplifier saturates, we require maximum flow rate and this occurs, from Fig. 2, when the coil current is 7.5 ma. Thus from equation (6)

$$G_2 = \frac{7.5\ G_v}{10} \quad \text{ma/volt}$$

which implies that the servo amplifier gain G_2 has two independent, conflicting values. One is determined by practical considerations and one by theoretical. It is possible, however, to comply with the practical requirements and determine the specified gain, and to adjust the overall loop gain by changing the values of S_2 and T_2 (Fig. 1) to comply with theoretical demands. It is this principle that is used in this particular application. Since both G_2 and G_v above are functions of R_{19} only we have

$$f\ (R_{19}) = 0.75\ g\ (R_{19})$$

This equation could be solved for R_{19} which would then determine both G_2 and G_v. However, it is recognised that circuit components are subject to manufacturing errors (typical resistors are $\pm$ 20%) and so the investigation is best continued once the circuit has been constructed. The results of the amplifier tests are given in a later section.

The summing junction is considered next, and the operational amplifier used for the servo amplifier is also used in the summing circuit. For simplicity the preceeding analysis assumed a single input to the operational amplifier but the circuit shown in Fig. 4 now shows multiple inputs. The purpose of operational amplifier OA2 and its feedback resistor R_f is simply to invert the polarity of the input voltages. Since point P in Fig. 4 is a virtual earth the multiple input arrangement may be related to the single input by

$$i_{12} - i_{13} = i_s$$

$$\frac{V_{12}}{R_{12}} - \frac{V_{13}}{R_{13}} - \frac{V_{14}}{R_{14}} = \frac{V_s}{R_s}$$

suppose $R_{12} = R_{13} = R_s = R_{14}$

then $V_s = V_{12} - V_{13} - V_{14}$

Thus the voltage V_s appearing in equations (4) and (5) may be considered to be simply the difference or error voltage between the desired value, V_{12} and the feedback value $(V_{13} + V_{14})$. The necessity for a D.C. signal to be added to the feedback transducer signal is a result of the type of transducer used. For steady conditions in the fluid pipeline it is required that the transducer produces a voltage proportional to the pressure in the pipe. However, this particular transducer reads zero voltage at any steady conditions so that the voltage output is always a fixed voltage away from the true signal. For example if the steady state voltage is P_o then the transducer should read $P_{ox}\ T_2$ volts. However, since it reads 0 volts a d.c. voltage equal to $P_o\ T_2$ is added to it. For this purpose, the + 6v d.c. supply and potentiometer are used.

3.1 Dynamic Analysis

The frequency sensitive components of the amplifier and servo valve are shown on Fig. 5a. If the capacitor was not in the circuit the phasor diagram would be as shown in Fig. 5b. Note that as the frequency of the input voltage V_o increases then the impedance of the inductance increases and the resultant voltage becomes more out of phase with reference to the current. This means that the ratio of the in-phase voltage to the input voltage decreases as shown in Fig. 6a. This circuit has a bandwidth of only B_1 rad/s. However, if the circuit includes a capacitor then resonance will occur as shown by Fig. 6b. This occurs when the current in the combined

circuit of fig. 5a is in phase with the applied voltage. The phasor diagram for an A.C. supply is shown in fig. 5c and resosonance occurs when $\emptyset \rightarrow 0$.

i.e. when

$$i_{r + \ell} \sin \theta = i_{cap}$$

now from the R - L circuit

$$\text{Tan } \theta = \frac{V_L}{V_R} = \frac{iWL}{iR} = \frac{WL}{R}$$

and by Pythagoras' theorum

$$\text{Sin } \theta = \frac{WL}{\sqrt{R^2 + W^2L^2}}$$

and since $i_{r + \ell} = \frac{V_o}{\sqrt{R^2 + W^2L^2}}$ and $i_{cap} = V_o WC$

we get for the resonant condition:

$$\frac{\frac{V_o WL}{(R^2 + W^2L^2)}}{} = WCV_o$$

i.e. $$C = \frac{L}{(R^2 + W^2L^2)}$$

It may easily be shown that the break point of the attenuating circuit of just resistance - inductance is given by

$$W_1 = R/L$$

Thus if we arrange to set the resonating frequency of the R-C-L circuit at a value of about 1.5 W_1 we get

$$W_1 = 1.5R/L = 1.5.400/2 = 300 \text{ rad/s}$$

Hence $C = \frac{2}{160000 + 90000.4} = 3.8 \ \mu F$

A standard capacitance of 3.2 μF was used for the compensation circuit.

4. AMPLIFIER TESTING

The circuit shown in Fig. 2 was constructed. Note that the other inputs to the operational amplifiers are the non-inverting inputs and these have to be connected to earth to maintain a constant temperature coefficient for the amplifier.

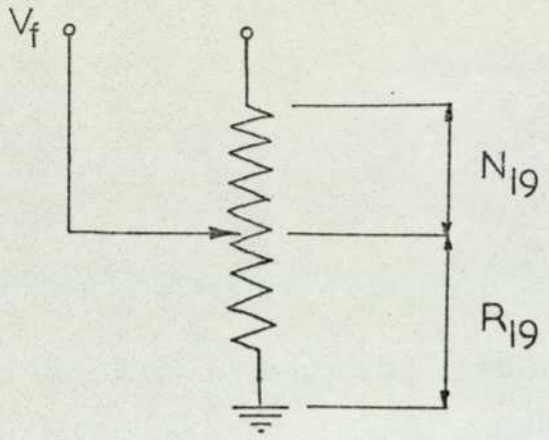
Dynamic Testing

The input to the non-inverting terminal of the amplifier was connected to a Venner TSA625 signal generator and the output voltage across the 420 Ω output resistor was measured. The amplitude of the input sine wave and of the output sine wave were measured on an oscilloscope and the attenuation of the output signal noted for increasing frequency. A Bode diagram was plotted for the amplifier and this is shown in Fig. 7. The bandwidth is defined as the frequency at which the output/input ratio drops 3 db from its D.C. value and this appears to be 47 KHz. Considering the bandwidth of the servo valve as 200 Hz the dynamic behaviour of the amplifier seems adequate. The table of results for this experiment is given in Table 1. Note that the high frequency attenuation is a result of the lag due to the operational amplifier only.

Static Testing

It was shown in Section 3 equations 4, 5 and 6 that the current gain, voltage gain and output current were all dependent upon R_{19}. This resistance is a potentiometer and to quote values of R_{19} accurately it would be necessary to isolate this potentiometer from the remainder of the circuit which is an impractical thing to do. For this reason, the open circuit portion of the potentiometer is measured and is designated N_{19}.

(See Figure below).



The procedure is to apply a voltage to the non-inverting terminal to the servo amplifier and measure the output voltage across the load resistor. The input voltage is increased until the amplifier saturates hence the output voltage remains constant for increasing input voltage. The maximum saturating input voltage is recorded along with the output voltage across the load resistor, and the value of N_{19}. N_{19} is changed and the process repeated. The table of results shown in Table 2 gives the complete set of figures obtained. All voltages were measured with a D.V.M. The analysis is as follows:

Since R_L = 420 Ω and V_L is measured then

$$i_L = V_L/R_L$$

and if the amplifier saturates at 10v and $\hat{V}_s$ is measured then

$$G_v = 10/\hat{V}_s$$

also

$$G_2 = i_L/\hat{V}_s$$

The three parameters above, along with $\hat{V}_s$ are plotted in Fig. 8.

Summing Junction Test

This test included both the summing junction and servo amplifier units. A value was chosen for N_{19} on Fig. 8 and a known voltage applied to the non-inverting and inverting terminal to the summing junction. For example + 6v was applied to T_1 and + 3 volts applied to T_2 while N_{19} = 720 Ω. This means that the input voltage = + 6 - 3 = + 3 volts. Also for this value of N_{19} the servo amplifier gain G_2 = 2.1 ma/volt. The maximum input voltage is 4.5 but as only 3 volts should be going in, the amplifier should not be saturated. Thus the output current should be 3 x 2.1 = 6.3 ma and the recorded voltage across the 420 Ω resistance, 2.67 volts. When the system was switched on the D.V.M. recorded 2.79 volts. When the + 6 volts was removed the output voltage should be -2.67v and -2.68 was recorded. The different values probably result from inaccuracies in setting the + 6 and + 3 voltages but it was concluded that the summing junction and amplifier operated within a sufficiently accurate envelope.

5. GAIN SETTINGS

It may be seen from Fig. 8 that a value of N_{19} of 435 Ω gives a value of G_2 = 1.38 ma/volt and $\hat{i}_L$ = 7.5 ma. This is the ideal condition with regard to the analysis of Section 2 since amplifier saturation is associated with maximum current delivery to the servo valve and will thus protect it from overload conditions as well as providing maximum flow of oil. Note that the maximum input voltage is 5.4 volts.

From equation 1

$$T_2 = S_2$$

and

$$\frac{T_1}{T_2} = \frac{KG_2}{G_1} = \frac{4\ 1.38}{3\ 0.2}$$

$$\therefore\ T_2 = 0.109 \text{ volts/lbf/in}^2 \quad (= S_2)$$

This means that the maximum recorded pressure passed by the charge amplifier is that pressure corresponding to 10 volts i.e.

$$\hat{P} = \frac{10}{0.109} \simeq 92 \text{ lbf/in}^2$$

Once again it is good practice to check one case in particular, the one considered before where the demand was for 10 lbf/in^2 and the feedback was 6 lbf/in^2.

Hence

$$Q_{model} = (10S_1 - 6T_1)\ G_1 = 0.2\ (10-6) = 0.8 \text{ in}^3/\text{s}$$

$$Q_{rig} = (10S_2 - 6T_2)\ G_2K = \frac{4.138}{3}\ (10.0.109 - 6.0.109)$$

$$= 0.8 \text{ in}^3/\text{s}$$

and the servo loops are identical once more.

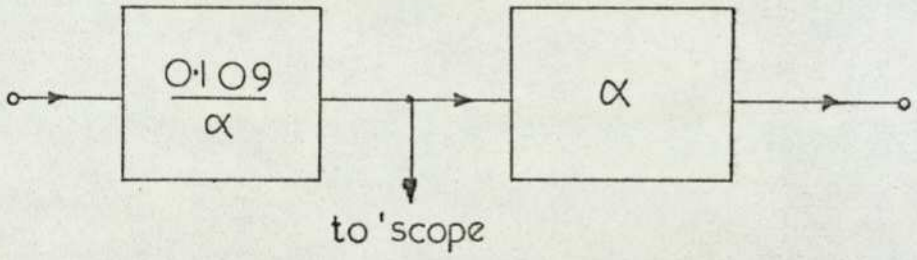
Note that this value of T_2 = 0.109 volts/lbf/in^2 may bring about a practical difficulty. Since the maximum output of the charge amplifier is

$\pm$ 10v, a maximum pressure of 10/0.109 or 92 lbf/in^2 may be recorded by the transducer and charge amplifier. In some circumstances it may be necessary to observe pressures in excess of this figure. This implies a contradiction in the use of the pressure signal for the dual purposes of

(a) Observing the pressure-time signal on an oscilloscope

(b) Using the pressure-time signal as an integral part of a closed loop control system.

This apparent contradiction is resolved by realising that only the overall transfer function, or gain of the amplifier needs to be 0.109 and this may be split up into two units of different gain as shown below



The first unit is the charge amplifier which has a gain determined by α . Suppose α = 2 then the gain of the charge amplifier is 0.0545 volts/ lbf/in^2 which for a $\pm$ 10v output signal allows a maximum reading of 184 lbf/in^2. This will provide sufficient range for most of the pressures encountered to be observed. Thus a lead may be taken from the charge amplifier output to the oscilloscope for observation purposes. Now, to comply with the control function, a second unit is required which will multiply the charge amplifier output by 2 to restore the overall gain to 0.109 volts/lbf/in^2.

The construction of this second unit is shown in Fig. 12 and employs a simple operational amplifier with resistive feedback. When using the

non-inverting input of the amplifier, the gain is no longer simply the ratio of the feedback and input resistances. It may be shown that

$$\frac{V_{out}}{V_{in}} = \frac{R_D + R_B}{R_D}$$

where R_D and R_B are given the values shown in Fig. 12. This multiplier unit is located in the control loop between the charge amplifier and signal inverter. Thus to comply with the notation shown in Fig. 4, the output of the multiplier is labelled V_{13}. A functional layout of the overall system is shown in Fig. 14.

6. SIGNAL GENERATOR

The purpose of the signal generator is to drive the servo system in both closed and open loop fashion. It is required to control the pressure in the flowing liquid in the vicinity of a valve to a value which is typically 5 lbf/in^2. The servo system then maintains the pressure at this value for a specified interval at the end of which one of two operations is needed.

1. To close the valve as quickly as possible
2. To open the valve as quickly as possible and after another specified interval, to close it rapidly.

Now since the signal to the servo amplifier is the difference between the desired value and achieved value it would be convenient if the feedback loop could be disconnected when either of processes 1 or 2 above was implemented. This is because to drive the servo in one direction the feedback loop is not only not required but may degrade the performance of such an operation. All that is really required is that the signal generator supplies a voltage large enough to saturate the servo amplifier in either a positive or negative mode depending upon whether it is desired to open or close the valve. If however the feedback signal should also register a large signal then the difference between the two large signals may not be sufficient to saturate the amplifier and hence operate the actuator with maximum speed. This problem is discussed in a later section.

Thus the resultant voltage functions are those shown in Fig. 9, V_1 being the control level of about 5 psi and the two large $\pm$ 10v steps are those which will effectively operate the system in open loop mode. Typical range of values of T_1 is from 0.05 secs to 1.00 secs while T_2 is in the region of 1.2 secs. Before complete circuit is described, a brief introduction to some of the major components may be instructive.

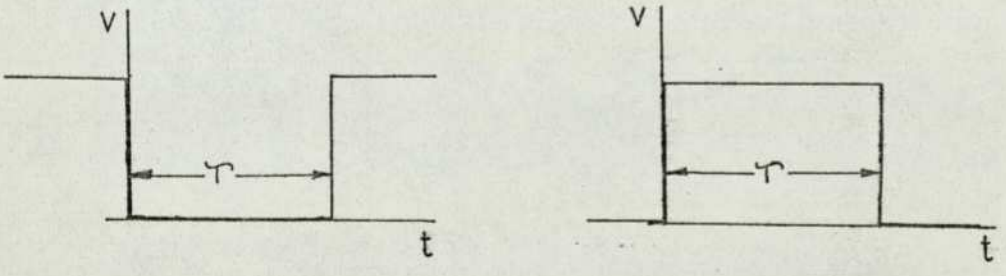
NAND Logic Gate

This may be thought of as simply a "black box" which performs the logic NAND function. It has two inputs and a single output: the relationship between the inputs and output being summarised in the following truth table.

INPUT A	INPUT B	OUTPUT
0	0	1
1	0	1
0	1	1
1	1	0

Monostable

The monostable is a pulse generating circuit which provides a square wave pulse of pre-determined duration once the circuit is triggered by some external means. The pulse is either from a supply voltage down to earth or from earth up to a supply voltage as shown below



a b

When in open circuit monostables tend to give square pulses as shown above but when loaded significantly the pulses have finite slopes and rounded corners. The monostables used in this circuit are SGS 7400's

The interval of the pulse is determined by the values of a resistance-capacitance circuit coupled to the monostable. The manufacturers quote the following formulaefor determining the duration, r

$$r = 0.64\ R\ (C + 20)$$

where r = pulse duration in nano seconds

R = circuit external resistance in KΩ

C = circuit external capacitance in pf

Thus typically R = 10K, C = 100 μf

$$r = 0.64 \quad 10.0 \quad 100.0 \quad 10^{6}$$

$$= 640 \quad 10^{6} \quad 10^{-9} \text{ secs}$$

$$r = 0.64 \text{ secs}$$

Since the monostables will be used in the determination of the signal step duration and this has to be variable in the range 0.05s → 1.00 secs, the required intervals were produced in the following manner. R was variable in the region 10K → 15K so for C = 10 μf

$$r = 0.64 \quad 10 \quad 10 \quad 10^{6} \quad 10^{-9} = 0.064\text{s}$$

and when R = 15K r = 0.096s

R is now returned to 10K and a 14.0 μf capacitor replaces the 10 μf and thus provides a time interval in the range 0.090s → 0.135s. Thus by using capacitors of value 10, 14, 21, 31, 46, 68, 100 and 150, the full range of time intervals was made available. The switching from one capacitor to another is achieved by a two pole 12 position switch.

Summing Junction

This circuit was discussed briefly in an earlier Section and the complete summing junction is re-drawn in Fig. 10. It can easily be shown that

$$E_o = -\left[\frac{R_f}{R_1} E_1 + \frac{R_f}{R_2} E_2 + \frac{R_f}{R_3} E_3\right] \quad \ldots (7)$$

Function Generator Circuit

The circuit is shown in Fig. 11. The power supplies of $\pm$ 6v are available from dry batteries while the operational amplifier supply is from a stabilised source. The circuit is triggered into operation by means of switch S_1. Before S_1 is closed, S_{1c} connects the input to the operational amplifier to earth and hence since there is no input, there is no output. Once the switch is closed, S_{1a}, S_{1b} and S_{1c} are all closed simultaneously and the monostables are triggered by grounding the input. Thus the top path to the summing junction is registering a voltage V_1 depending upon the setting of the first potentiometer P_1. The next path begins with monostable M_1. This is arranged so as to give a positive going pulse (type b on page 19). Thus there is an input into NAND gate N_2. Since the other input is always connected to a supply voltage, it too has a signal and from the truth table, there is no output thus the reed relay RR_1 remains open and results in no voltage being applied to the second path of the summing junction. The last path begins with monostable M_2 which gives type 'a' pulse (on page 19) when triggered. Thus immediately after triggering there is zero output from M_2. This means that there is a single input to N_3 which must have an output. This puts a signal in both inputs of N_4 and thus has no output. Hence as in the second path, the third path has no output immediately after triggering. Thus from equation (7)

$$V_o = +V_1 \frac{1000}{500} = +2V_1$$

This state continues until the duration of M_1 expires (it is arranged to expire before that of M_2) which results in the disappearance of one of the inputs to N_2. Thus N_2 now has an output which is of sufficient power to

close the relay RR_1. This connects a negative voltage to the second path of the summing junction. The value of this voltage again depends upon the setting of a potentiometer, this time P_2. The third path still has no signal on it, so

$$V_o = V_1 \frac{1000}{500} + V_2 \frac{1000}{20}$$

$$\therefore \quad V_o = 2V_1 + 50V_2$$

Finally the interval of M_2 has elapsed and N_3 now has 2 inputs resulting in no output from N_3. N_4 has one input and hence has an output which closes reed relay RR_2. This connects a positive voltage to the third path of the summing junction, the value of the voltage being determined by P_3. Thus

$$V_o = 2V_1 + 50V_2 - 50V_3$$

if $V_1 \simeq \frac{1}{2}$ volt, $V_2 \simeq 1$ volt and $V_3 \simeq 2$ volts then from the moment of switching S_1 the output waveform is that which is required. Note that both V_2 and V_3 are sufficiently large to saturate the 10 volt limit of the operational amplifier, the value of the controlled pressure being determined by V_1.

The other waveform is obtained by switching S_2. This changes the polarity of the supply to the relay RR_1 and isolates monostable M_2 from gate N_3. This makes the third path inoperative over all the operation interval. The procedure is the same as before except that the second path now has a positive voltage signal registered once the pulse interval of M_1 has elapsed. The summing junction reversed the sign and this then follows the requirement for the second waveform.

7. CONCLUSIONS

It is hoped that the design of the servo amplifier will provide a component capable of driving a wide variety of motors and other servo components. The quality of components and power requirements of the operational amplifier will depend upon the particular application intended but these items are not expensive even at higher power levels (1.0 watts). Although it should be realised that a stabilised power source was available to supply the operational amplifiers, the cost of the remainder of the servo amplifier was of the order of £3 which compares favourably with the price of £75 quoted by a manufacture even though the latter does contain its own voltage regulation unit.

The function generator described will probably not be so generally useful but the design was included in this report since it does constitute an important class of generator. There is no theoretical limit to the number of stages included in the summing junction so it is possible to extend the design to one which provides a long series of step functions of variable magnitude.

ACKNOWLEDGEMENTS

The author wishes to express his sincere thanks to Mr. D. Ginn, Department of Mechanical Engineering and Dr. J. Missen, Department of Physics. Without their help the design and construction of the units described would not have been possible.

APPENDIX 1

The signal generator and servo amplifier are in the form of two PCB's mounted on a common chassis. The chassis end plates contain two jack plug sockets for the pressure feedback signal and the servo amplifier output. The PCB nearest the jack plug sockets is the servo amplifier, the other being the signal generator. The leads in the unit are colour-coded and a listing of the principle connections is given below.

(a) Power Supplies

1. Magnitude is ± 10V D.C. from two voltage source units.
2. Brown lead → red plug in right hand voltage source.
3. Yellow/green lead → black plug in right hand voltage source.
4. Blue lead → black plug in left hand voltage source.
5. Connecting wire from red plug left hand unit to black plug on right hand unit.

(b) Pressure Feedback

1. Oscilloscope connections are (a) grey wire → black terminal
   (b) white wire → red terminal
2. Input to inverter is yellow/black wire with clip, automatically earthed.

(c) Servo Amplifier Leads

Output leads both have clips and are grey/black and pink/black.

(d) Signal Generator Leads

Output is red/green with reference to any earth pin.

A photograph of the PCB layout is given in Fig. 14 showing the position of principle components and controls.

The values of resistances not quoted in the text are

$R_{b1} = 0.5\ M\Omega$

$R_{18} = 1.0\ M\Omega$

$R_f = 1.0\ M\Omega$

$R_{12} = R_{13} = R_{14} = 1.0\ M\Omega$

$R_{b2} = 0.3\ M\Omega$

APPENDIX 2

Conversion to Metric Quantities

Parameters involved in this conversion are:

S_1, S_2, T_1, T_2 and K.

The table below gives the values of these quantities along with the derived British Unit values.

Parameter	Value in British System	Value in Metric System
S_1	0.109 V/lbf/in^2	0.0158 V/Kn/M^2
S_2	0.109 V/lbf/in^2	0.0158 V/Kn/M^2
T_1	0.109 V/lbf/in^2	0.0158 V/Kn/M^2
T_2	0.109 V/lbf/in^2	0.0158 V/Kn/M^2
K	1.334 in^3/s/ma	1.30 litres/min

APPENDIX 3

Operating Procedure for Signal Generator/Servo Amplifier Unit

1. Check that both of the stabilised power supply units are connected up correctly, and switch on mains supply.
2. Switch on Digital Volt Meter (D.V.M.)
3. Set the voltage output from the stabilised power supply to be exactly $\pm$ 10V using the digital volt meter.
4. Connect up the 6V dry battery.
5. Measure the E.M.F. of the battery using the D.V.M.
6. Connect up the third stabilised power source by joining the blue lead to the blue terminal, brown lead to the white terminal. Switch on mains supply to this unit.
7. Set the voltage output of the third power source to that of the E.M.F. of the dry battery using the D.V.M.
8. Plug in the pressure feedback and servo amplifier jack plugs.
9. Connect the signal generator output to one channel of a storage oscilloscope.
10. Connect resistance N_{19} to the Universal Bridge by use of the two black wires coming from R_{19}.
11. Set N_{19} to the required value (typically 435 Ω) and lock the adjusting potentiometer.
12. Switch off the Universal Bridge.
13. Switch in the electronics unit to the power supplies.
14. Switch on oscilloscope and set in "trigger" mode.
15. Adjust the capacitance switch C and potentiometer P_6 to produce a pulse of maximum duration.

16. Connect D.V.M. between signal generator output and earth and set level 1 by means of potentiometer P_1. The voltage output will depend upon the minimum pressure required and the value of T_2.
17. Check the polarity of the D.V.M. reading by using the oscilloscope to display the actual pulse.

Checking Voltage Multiplier

18. Connect the 1½ volt dry battery between the earth pin and the voltage multiplier input terminal.
19. Measure exactly this battery's E.M.F. using the D.V.M.
20. Measure the output voltage and adjust potentiometer P_7 until the gain of the multiplier is exactly that required.
21. Remove test battery from the input, and the D.V.M.

Checking Signal Inverter

22. Connect D.V.M. between earth and output terminal of inverting amplifier.
23. Adjust potentiometer P_3 until the D.V.M. reads a voltage equivalent to the steady state pressure at the transducer. This requires the use of the scaling factor and a knowledge of the pressure at the transducer.
24. Remove the D.V.M. leads.

Final Connecting-Up

25. Connect "pressure feedback" lead to multiplier input.
26. Connect signal generator output lead to non-inverting input to the servo amplifier.
27. Re-check the inverter output to be a voltage equivalent to the steady state pressure at the transducer.

28. Connect the servo amplifier output (V_f end) to the pink/black lead, and the two grey/black wires together.

29. Select the position of switch S_2 to the mode of operation required.

30. Using the oscilloscope in triggered/storage mode, select the capacitance switch setting and potentiometer P_6 to provide a pulse of required interval.

31. The system should be ready for operation by depressing switch S_1.

KEY TO FIGURE 14

1. Earth Pin
2. Second interval potentiometer (T_2 in Fig. 9) P_8.
3. First " " (T_1 in Fig. 9) P_6.
4. Four dual input Nand gates.
5. Signal generator output.
6. Operational amplifier used in signal generator, OA3.
7. Input resistances to OA3.
8. Reed relay controlling the switching of the second interval.
9. " " " " " " first "
10. Voltage multiplier output lead.
11. Servo amplifier unit output lead (Op. Amp. end).
12. Capacitors used in frequency compensation of servo amplifier.
13. Non-inverting input pin to servo amplifier.
14. Principle operational amplifier used in servo amplifier.
15. Servo amplifier null adjustment.
16. Pressure feedback input jack plug socket.
17. Servo amplifier output pin (V_f end).
18. Signal inverter output lead.
19. Signal inverter operational amplifier.
20. Null adjustment of signal inverter.
21. Servo amplifier jack plug output socket.
22. Series of capacitors used to set the second interval (T_2 in Fig. 9).
23. Wire from multiplier output to signal inverter input.
24. Multiplier output pin.
25. Potentiometer P_7 to adjust the gain of the voltage multiplier.
26. Input pin to voltage multiplier.

27. Voltage multiplier op. amp. null adjustment potentiometer.

28. Voltage multiplier operational amplifier.

29. Second interval monostable in signal generator.

30. First " " " " "

31. Capacitor used to set the first interval (T_1 in Fig. 9).

TABLE 1 - RESULTS OF STATIC ANALYSIS OF SERVO AMPLIFIER

Value of Resistance N_{19} Ω	Maximum linear Supply Voltage Volts V_s	Voltage across 420 Ω Load Resistance Volts V_L
1020	2.80	5.71
820	4.15	4.48
620	4.85	3.66
420	5.45	3.10
220	5.95	2.68
24	6.25	2.37

Summing Junction Test

N_{19} = 720 Ω

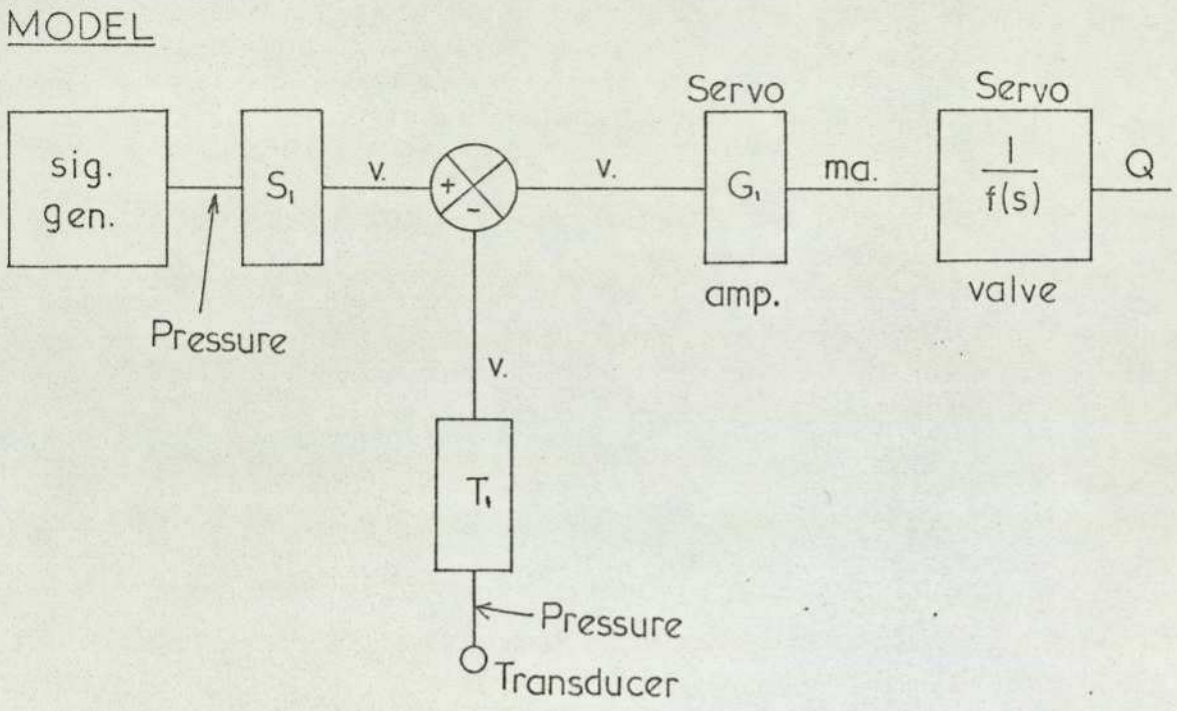
(a) Inputs 1. + 6v)
) Output V_L = 2.79v
2. - 3v)

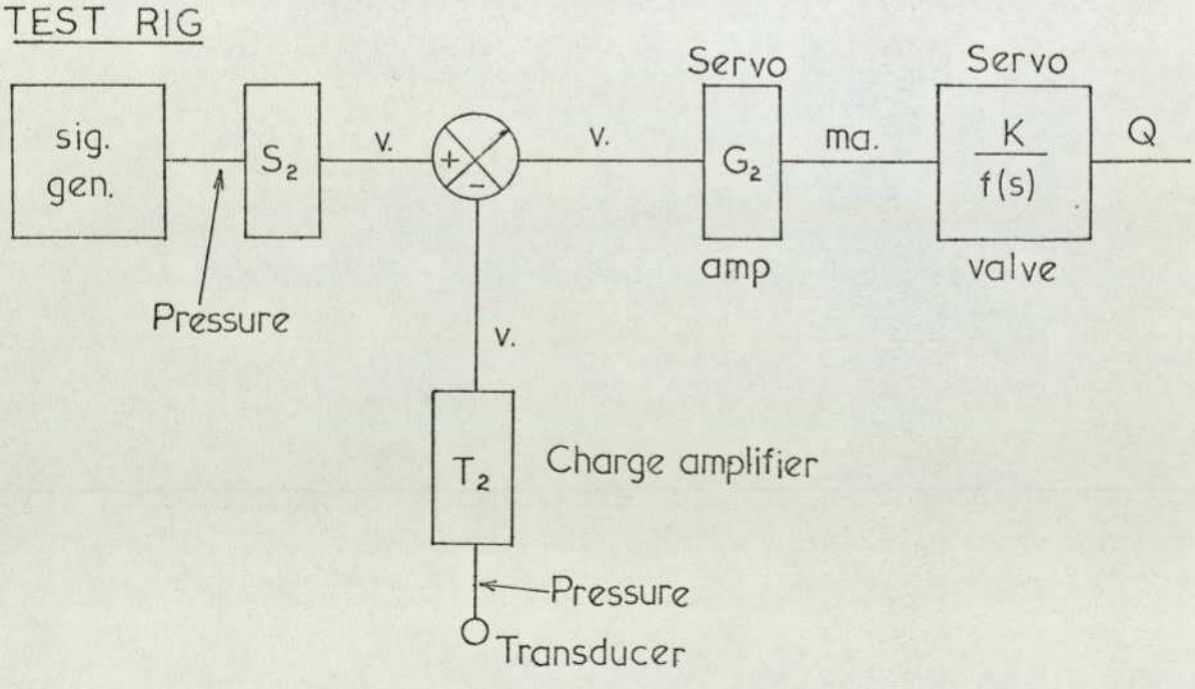
(b) Inputs 1. 0v)
) Output V_L = -2.68v
2. -3v)

TABLE 2 - RESULTS OF DYNAMIC ANALYSIS OF SERVO AMPLIFIER

Signal Frequency Hz	Input Amplitude volts	Output Amplitude volts
10	7.6	9.2
70	7.6	9.2
100	7.6	9.2
700	7.6	8.0
1000	7.6	7.8
7000	7.6	8.2
10000	7.5	8.6
13000	7.6	9.2
16000	7.6	9.4
17000	7.6	9.6
18000	7.6	10.0
19000	7.6	10.2
20000	7.6	10.8
22000	7.6	11.0
24000	7.6	11.6
25000	7.6	12.2
26000	7.6	11.8
28000	7.6	11.2
30000	7.6	10.4
35000	7.6	8.8
40000	7.6	7.9
60000	7.6	5.2
70000	8.0	4.4
100000	7.9	2.9
700000	7.4	0.205

FIG. 1 RELATIONSHIP BETWEEN THEORETICAL AND ACTUAL SYSTEM PATHS





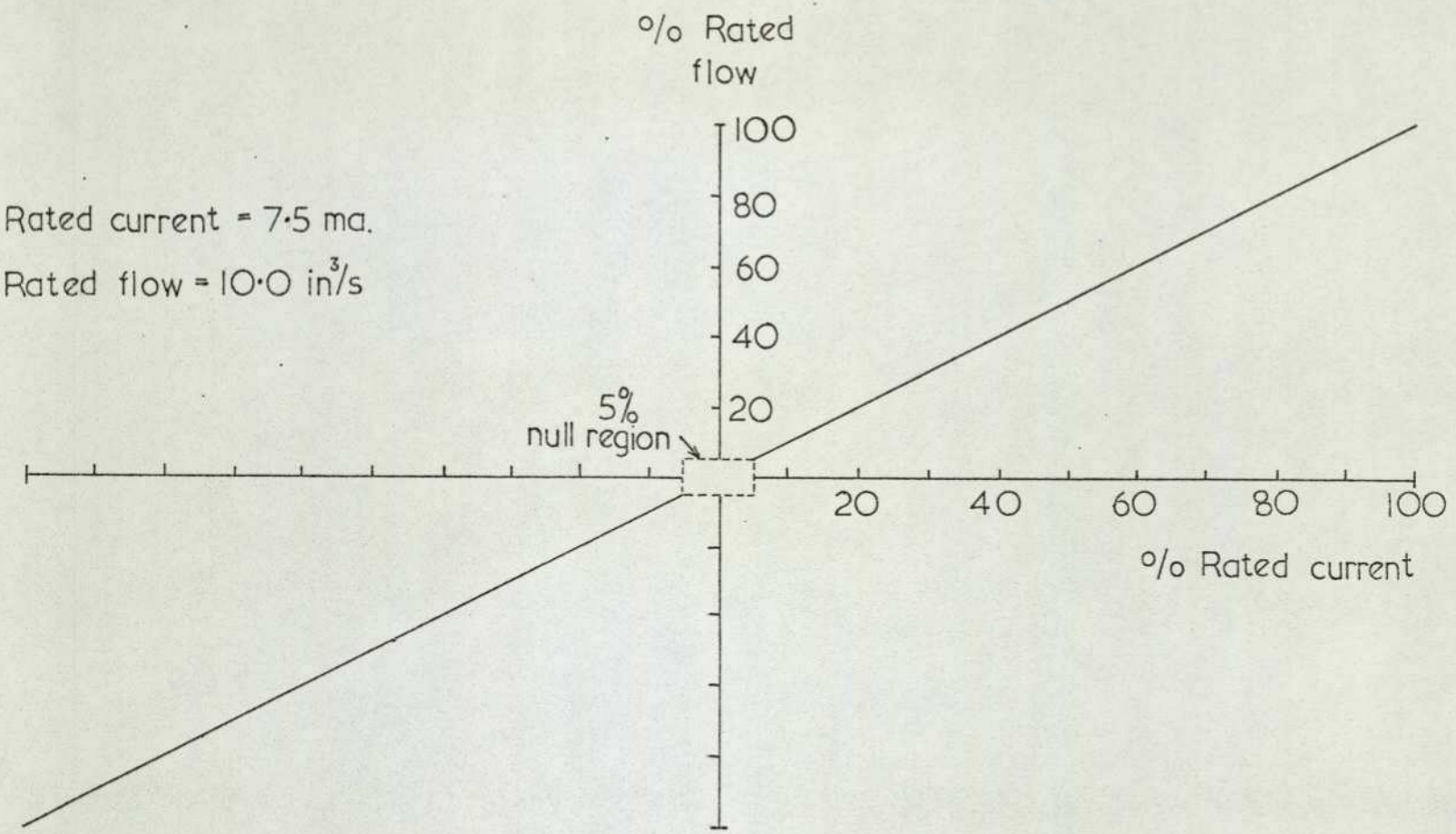


FIG. 2 STEADY STATE CHARACTERISTICS OF SERVO VALVE

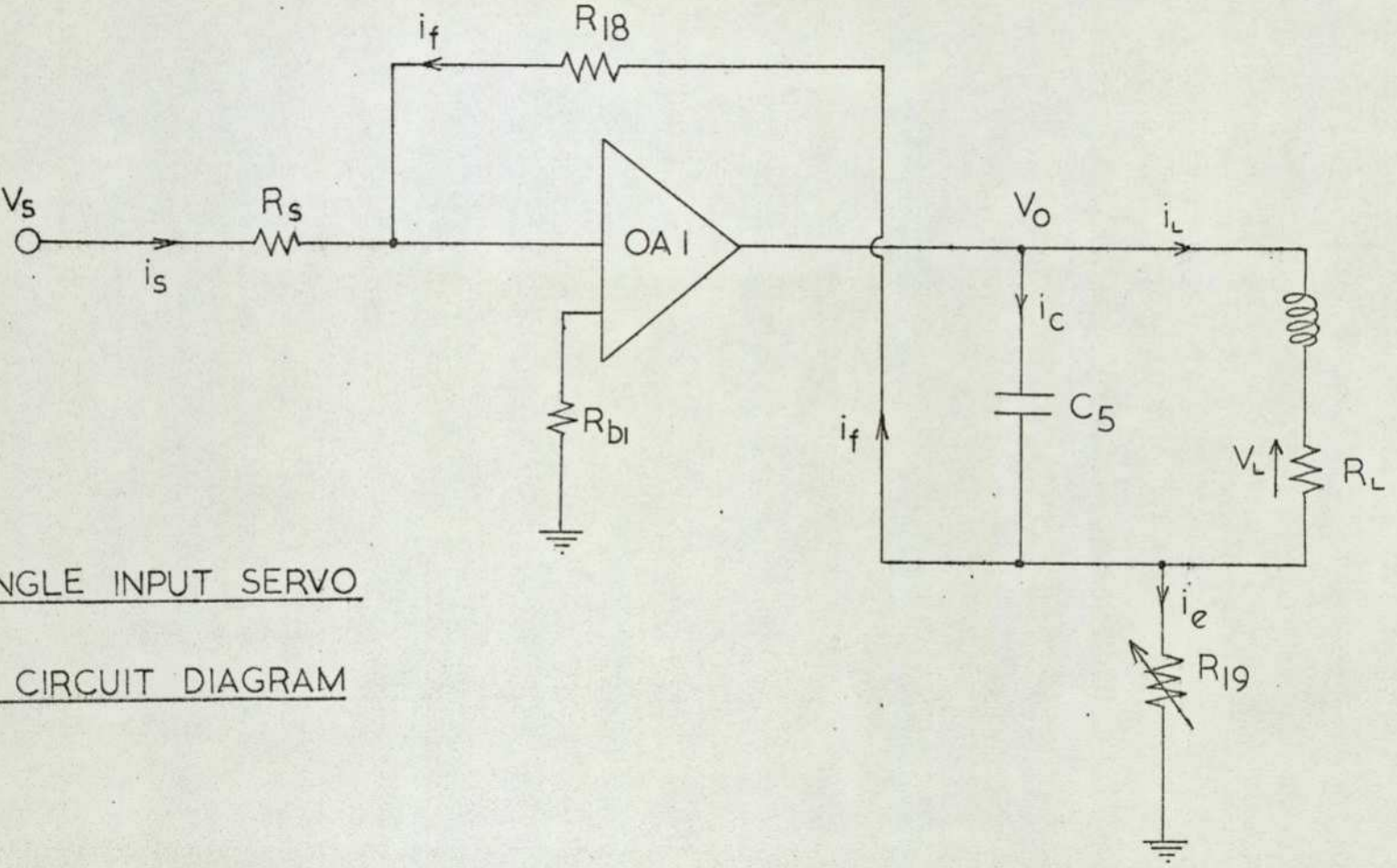


FIG. 3 SINGLE INPUT SERVO

AMPLIFIER CIRCUIT DIAGRAM

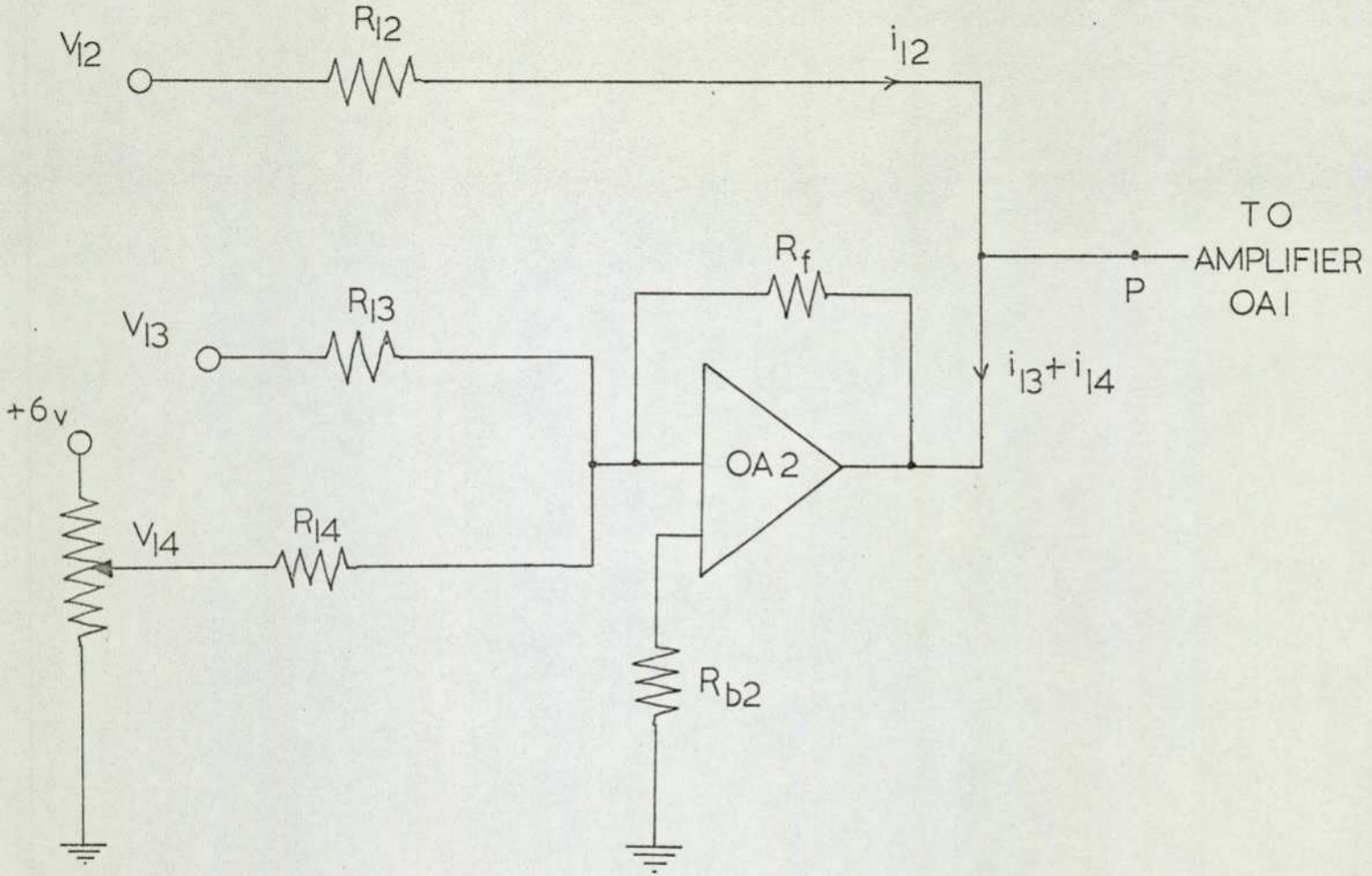


FIG.4 SUMMING JUNCTION & MULTIPLE INPUTS TO SERVO AMPLIFIER

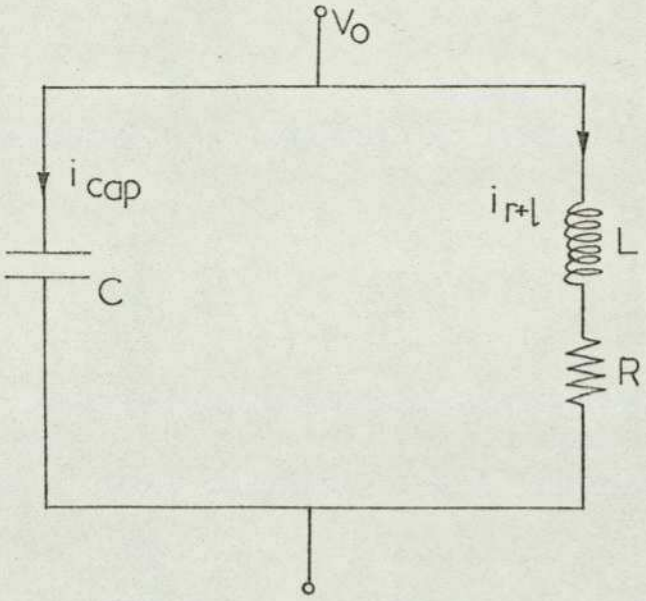


FIG. 5a

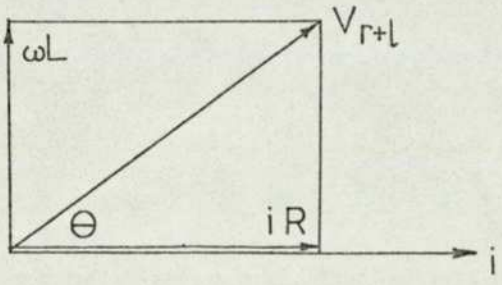


FIG. 5b

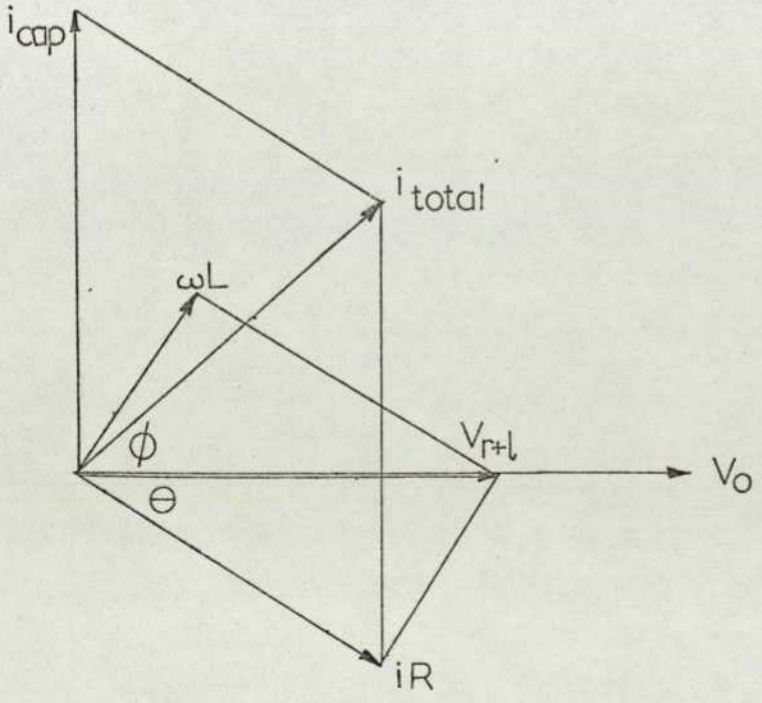
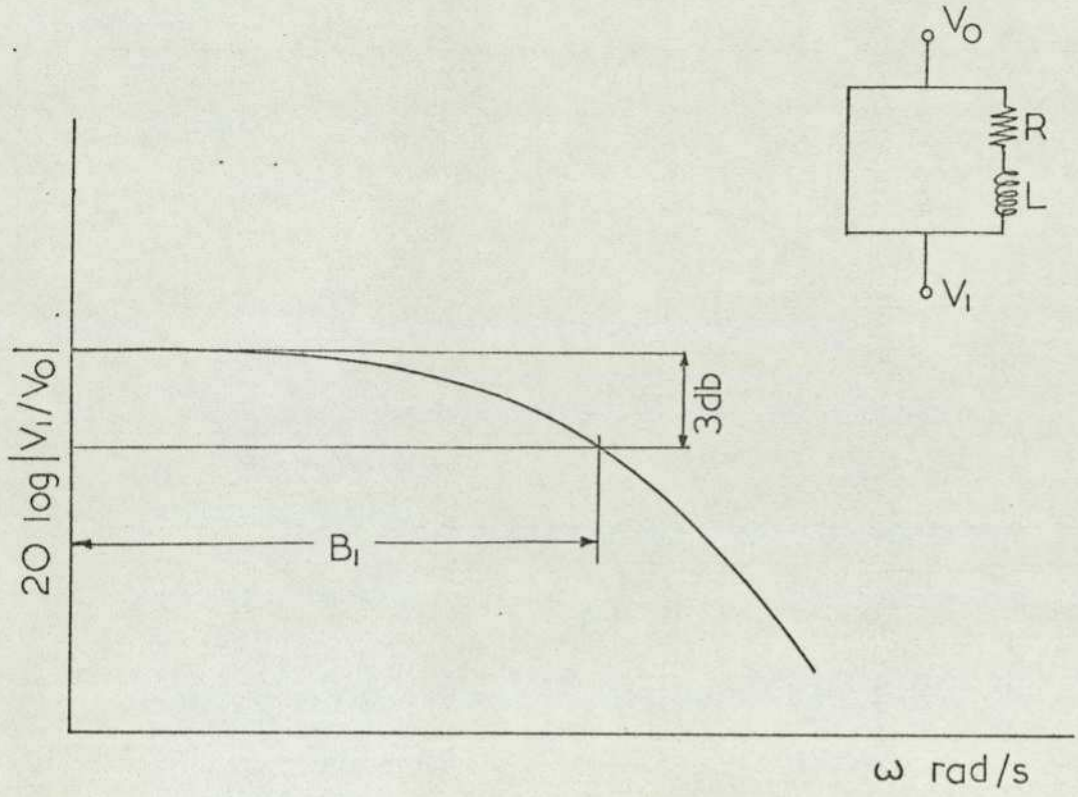


FIG. 5c

FIG 5 FREQUENCY ANALYSIS



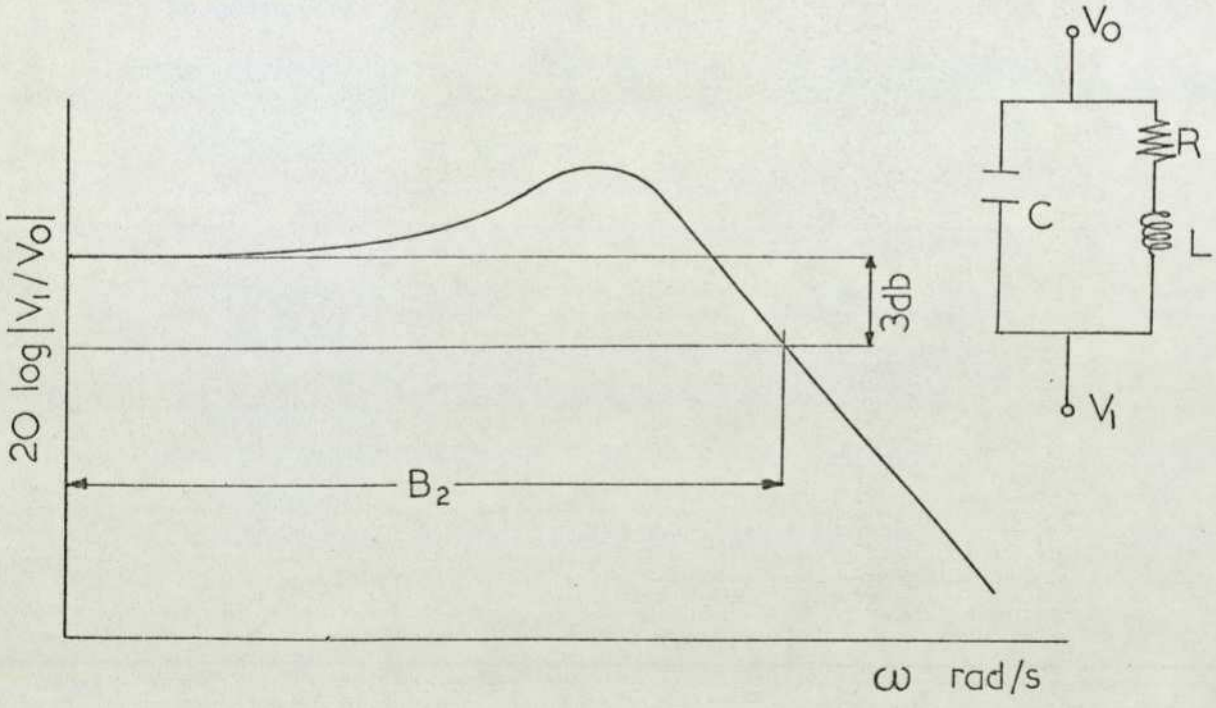


FIG 6. EFFECT OF CAPACITIVE COMPENSATION ON SYSTEM BANDWIDTH

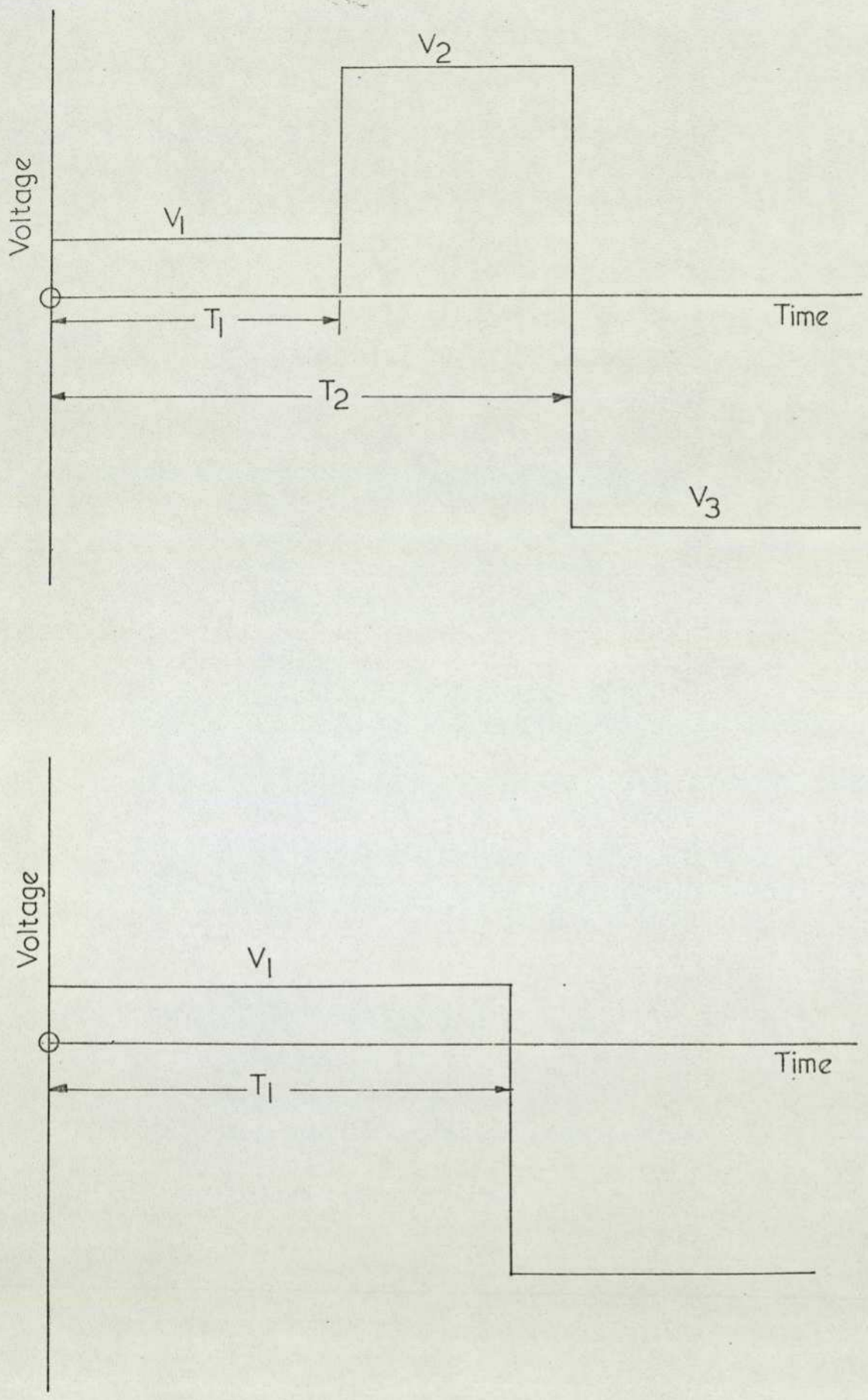
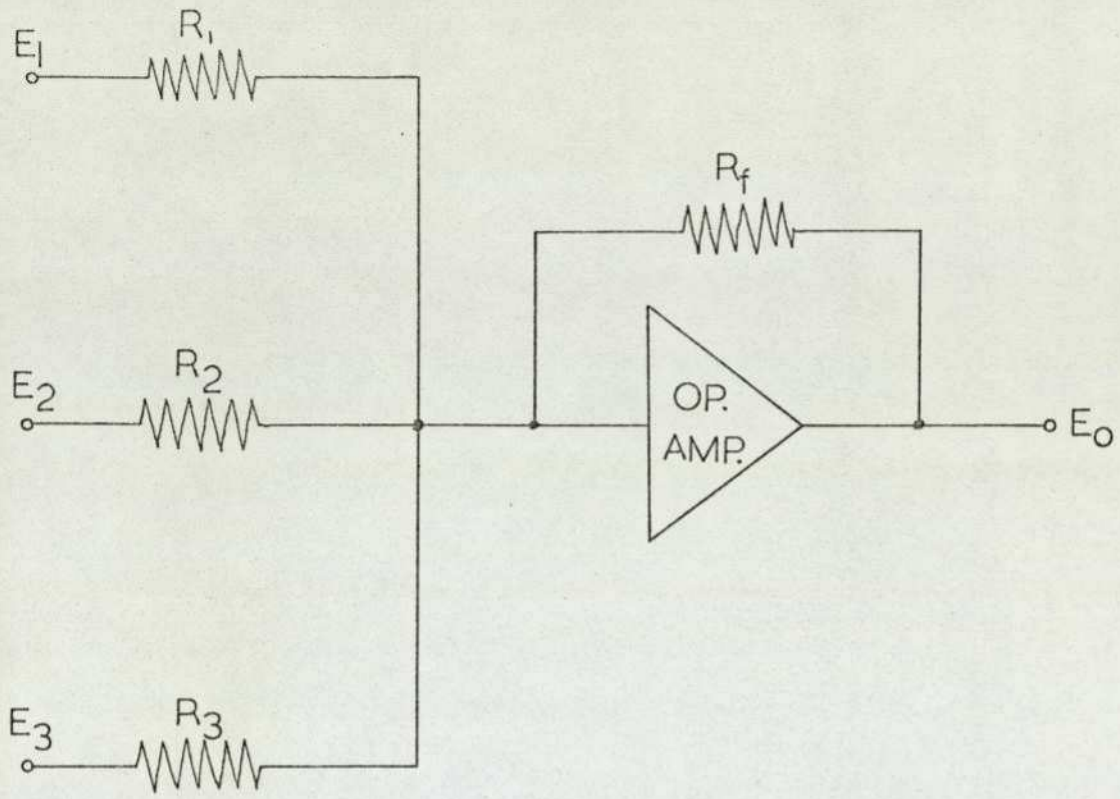


FIG. 9 TYPES OF VOLTAGE-TIME FUNCTIONS TO BE PROVIDED BY THE SIGNAL GENERATOR.



$$E_o = -\left[\frac{R_f}{R_1} E_1 + \frac{R_f}{R_2} E_2 + \frac{R_f}{R_3} E_3\right]$$

FIG.10 SUMMING JUNCTION USING A HIGH GAIN OPERATIONAL AMPLIFIER

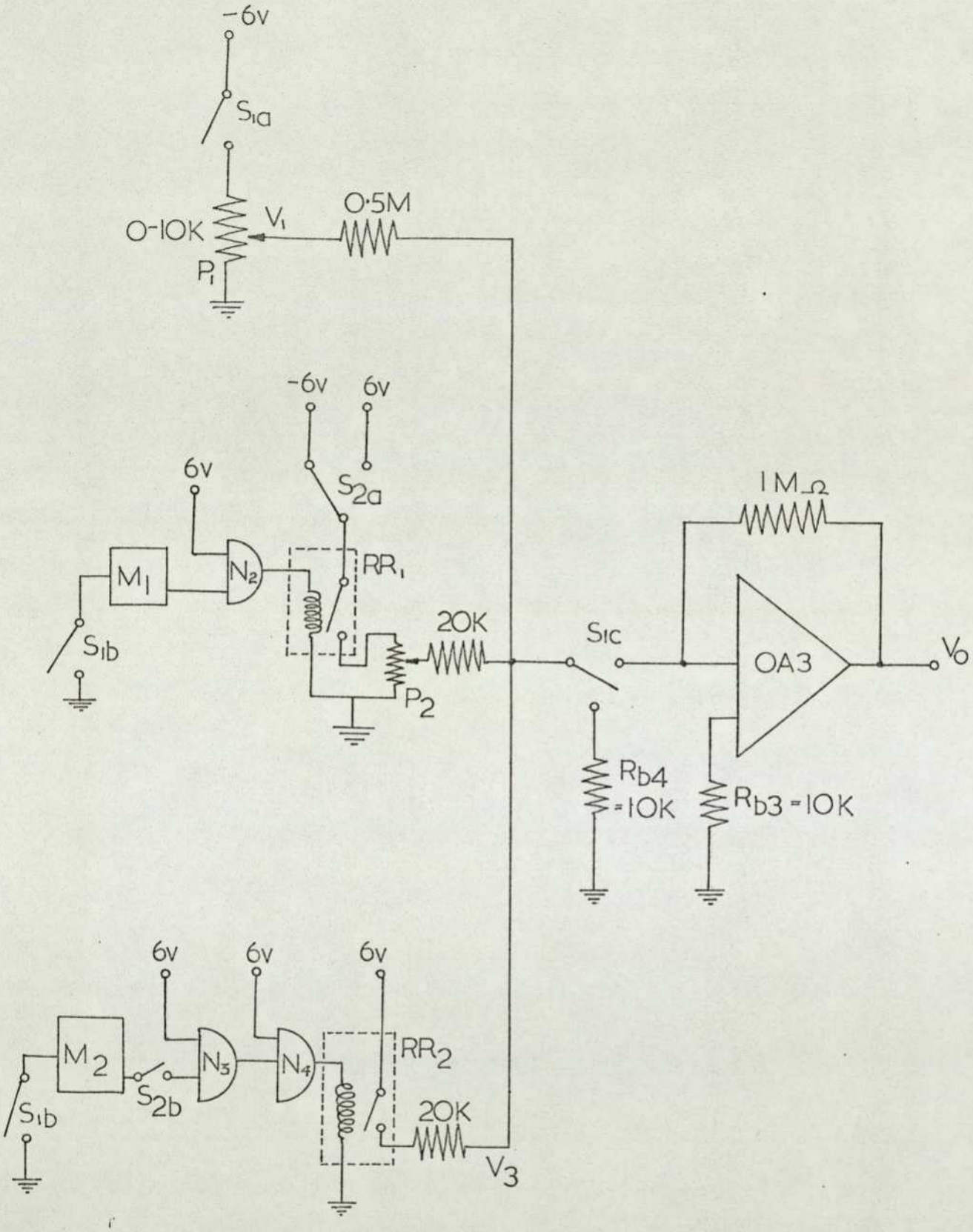


FIG. 11 SIGNAL GENERATOR CIRCUIT DIAGRAM

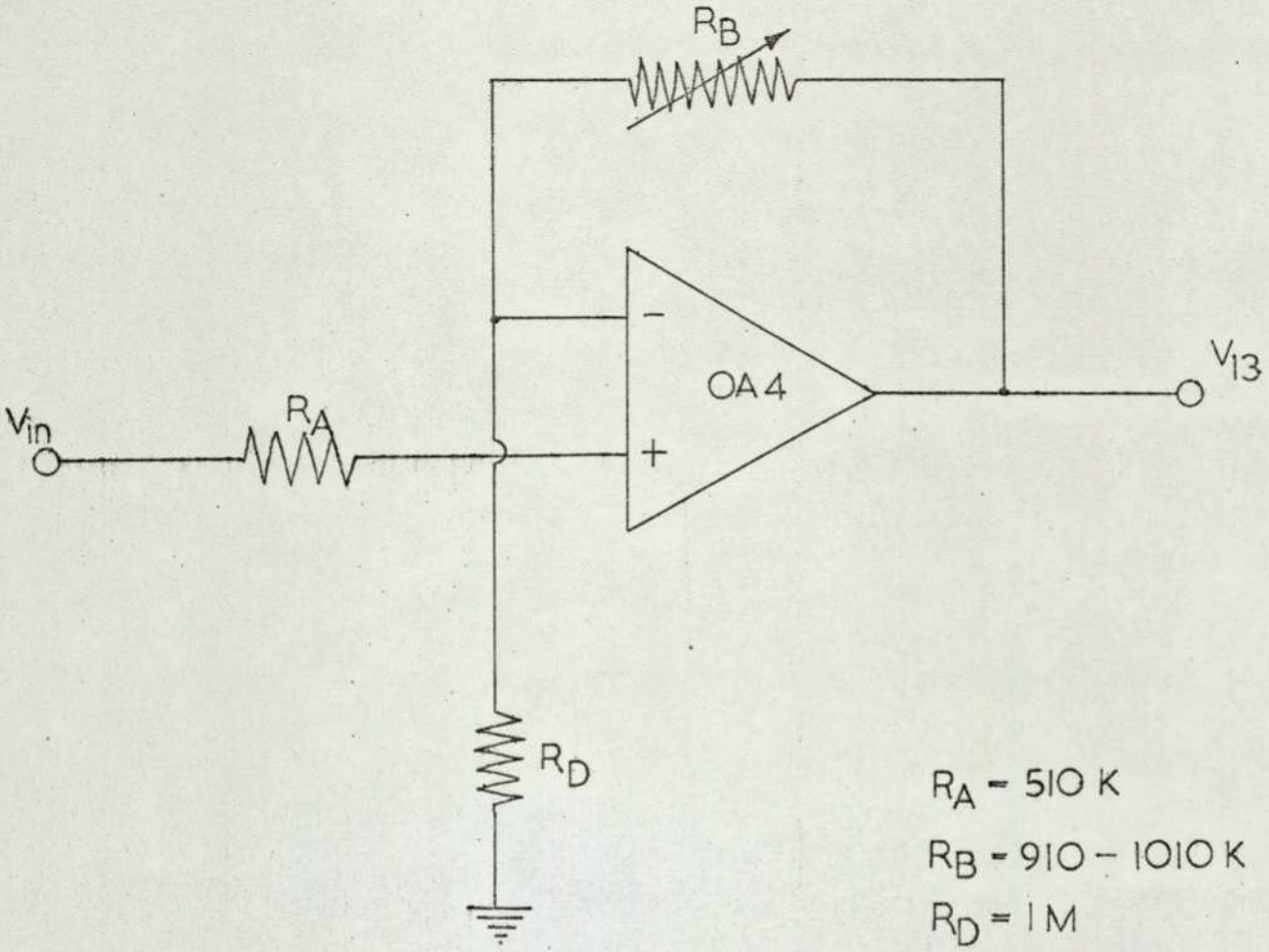


FIG. 12 VOLTAGE MULTIPLIER

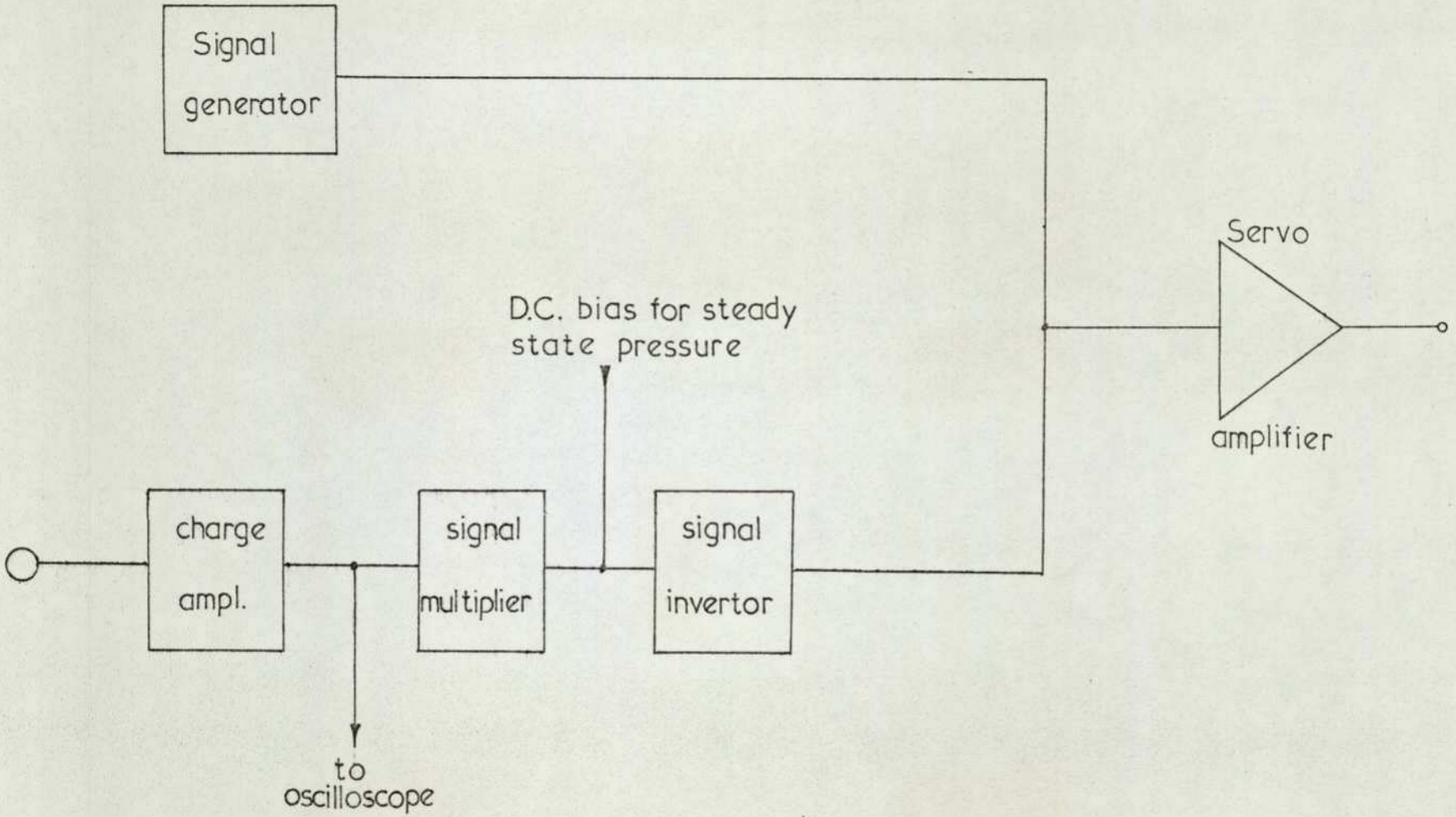


FIG. 13 SCHEMATIC DIAGRAM OF OVERALL SYSTEM

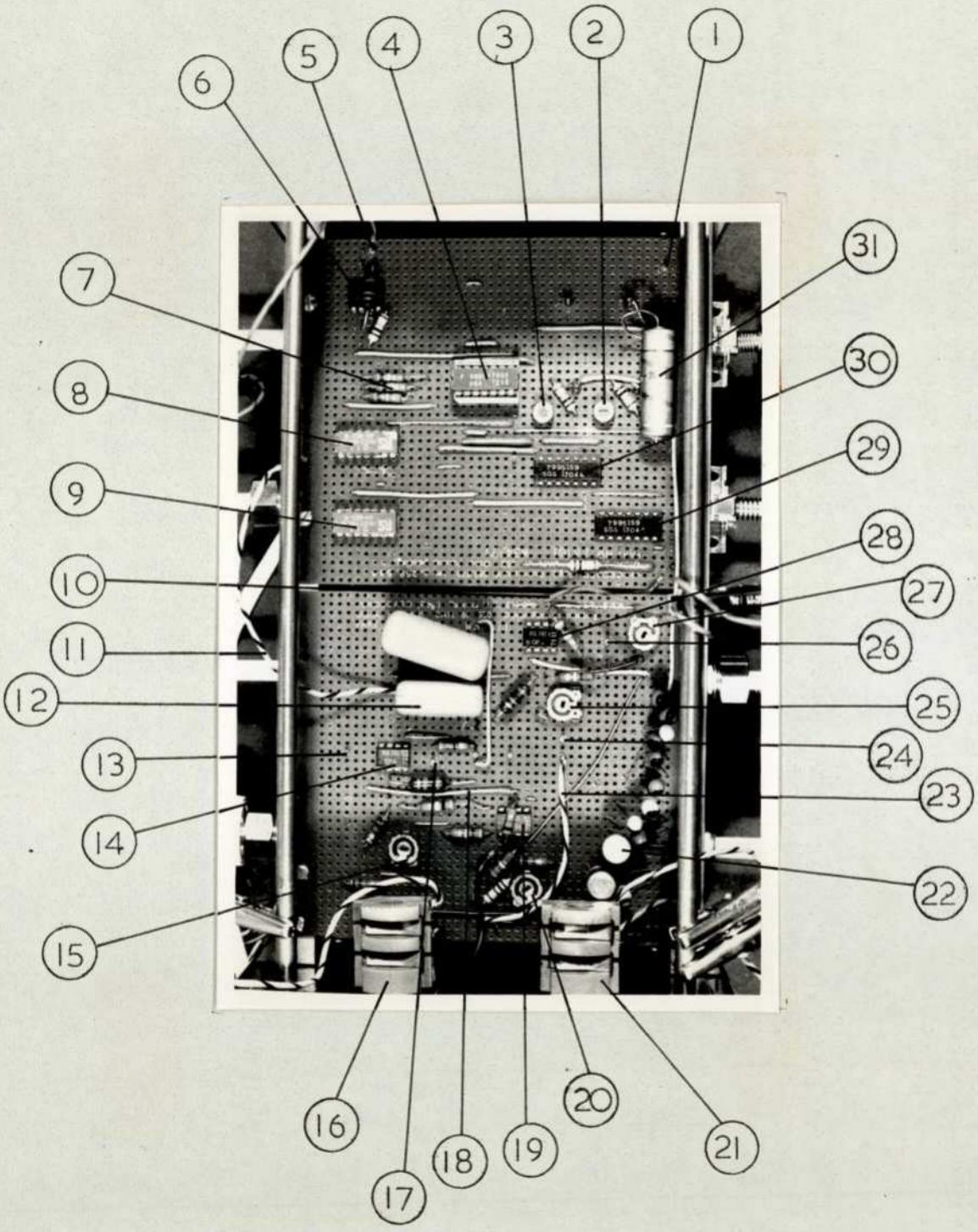


FIG. 14 PLAN VIEW OF COMPLETED UNIT

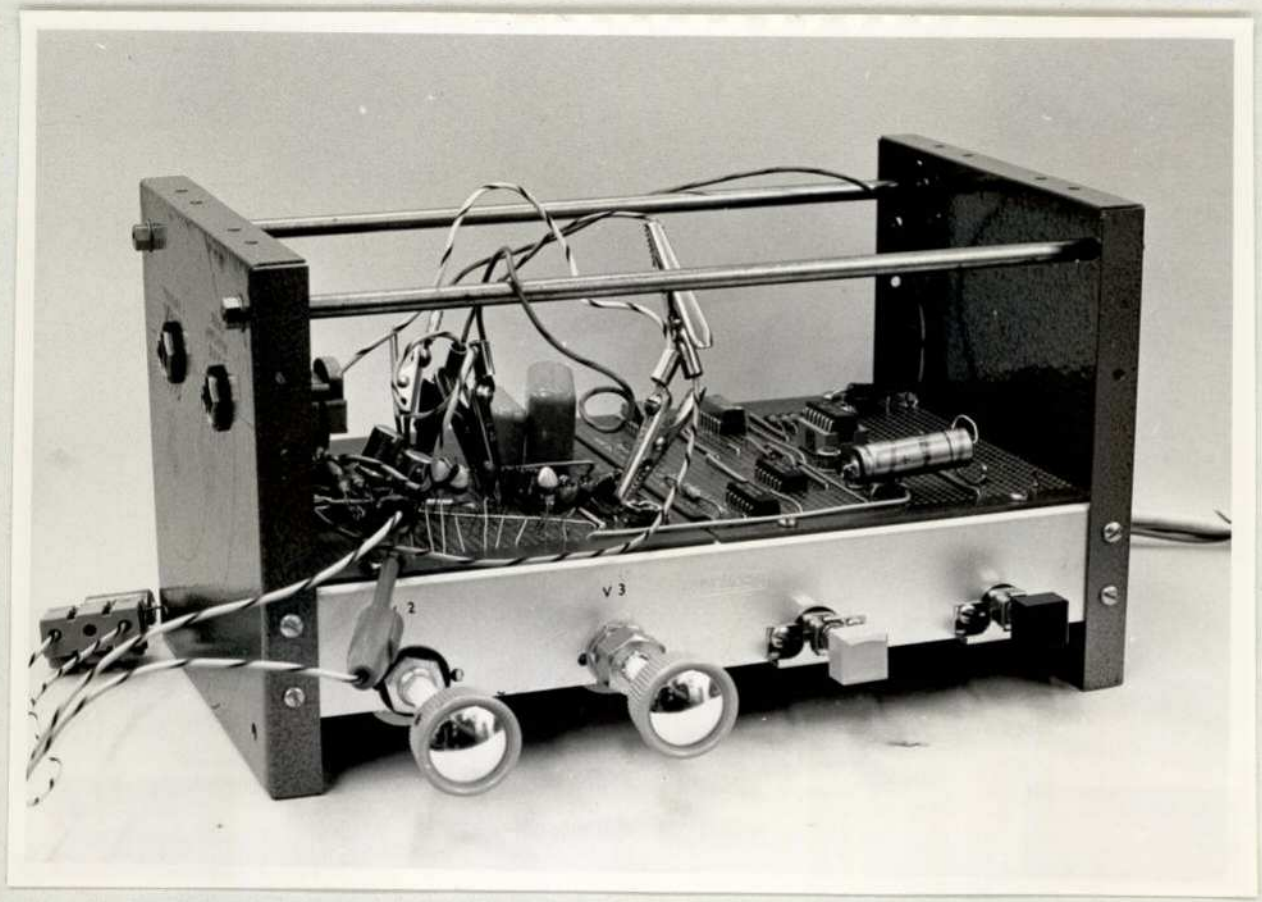


FIG 15 GENERAL VIEW OF COMPLETED UNIT